Lecture Notes in Networks and Systems 512

Marcelo Zambrano Vizuete
Miguel Botto-Tobar
Angela Diaz Cadena
Ana Zambrano Vizuete *Editors*

I+D for Smart Cities and Industry

Proceedings of RITAM 2021

Springer

Lecture Notes in Networks and Systems

Volume 512

Series Editor

Janusz Kacprzyk, Systems Research Institute, Polish Academy of Sciences, Warsaw, Poland

Advisory Editors

Fernando Gomide, Department of Computer Engineering and Automation—DCA, School of Electrical and Computer Engineering—FEEC, University of Campinas—UNICAMP, São Paulo, Brazil

Okyay Kaynak, Department of Electrical and Electronic Engineering, Bogazici University, Istanbul, Turkey

Derong Liu, Department of Electrical and Computer Engineering, University of Illinois at Chicago, Chicago, USA
Institute of Automation, Chinese Academy of Sciences, Beijing, China

Witold Pedrycz, Department of Electrical and Computer Engineering, University of Alberta, Alberta, Canada
Systems Research Institute, Polish Academy of Sciences, Warsaw, Poland

Marios M. Polycarpou, Department of Electrical and Computer Engineering, KIOS Research Center for Intelligent Systems and Networks, University of Cyprus, Nicosia, Cyprus

Imre J. Rudas, Óbuda University, Budapest, Hungary

Jun Wang, Department of Computer Science, City University of Hong Kong, Kowloon, Hong Kong

The series "Lecture Notes in Networks and Systems" publishes the latest developments in Networks and Systems—quickly, informally and with high quality. Original research reported in proceedings and post-proceedings represents the core of LNNS.

Volumes published in LNNS embrace all aspects and subfields of, as well as new challenges in, Networks and Systems.

The series contains proceedings and edited volumes in systems and networks, spanning the areas of Cyber-Physical Systems, Autonomous Systems, Sensor Networks, Control Systems, Energy Systems, Automotive Systems, Biological Systems, Vehicular Networking and Connected Vehicles, Aerospace Systems, Automation, Manufacturing, Smart Grids, Nonlinear Systems, Power Systems, Robotics, Social Systems, Economic Systems and other. Of particular value to both the contributors and the readership are the short publication timeframe and the world-wide distribution and exposure which enable both a wide and rapid dissemination of research output.

The series covers the theory, applications, and perspectives on the state of the art and future developments relevant to systems and networks, decision making, control, complex processes and related areas, as embedded in the fields of interdisciplinary and applied sciences, engineering, computer science, physics, economics, social, and life sciences, as well as the paradigms and methodologies behind them.

Indexed by SCOPUS, INSPEC, WTI Frankfurt eG, zbMATH, SCImago.

All books published in the series are submitted for consideration in Web of Science.

For proposals from Asia please contact Aninda Bose (aninda.bose@springer.com).

More information about this series at https://link.springer.com/bookseries/15179

Marcelo Zambrano Vizuete ·
Miguel Botto-Tobar · Angela Diaz Cadena ·
Ana Zambrano Vizuete
Editors

I+D for Smart Cities and Industry

Proceedings of RITAM 2021

Springer

Editors
Marcelo Zambrano Vizuete
Universidad Técnica del Norte
Ibarra, Ecuador

Miguel Botto-Tobar
Eindhoven University of Technology
Eindhoven, The Netherlands

Angela Diaz Cadena
Universitat de Valencia
València, Spain

Ana Zambrano Vizuete
Escuela Politécnica Nacional
Quito, Ecuador

ISSN 2367-3370 ISSN 2367-3389 (electronic)
Lecture Notes in Networks and Systems
ISBN 978-3-031-11294-2 ISBN 978-3-031-11295-9 (eBook)
https://doi.org/10.1007/978-3-031-11295-9

© The Editor(s) (if applicable) and The Author(s), under exclusive license
to Springer Nature Switzerland AG 2023
This work is subject to copyright. All rights are solely and exclusively licensed by the Publisher, whether the whole or part of the material is concerned, specifically the rights of translation, reprinting, reuse of illustrations, recitation, broadcasting, reproduction on microfilms or in any other physical way, and transmission or information storage and retrieval, electronic adaptation, computer software, or by similar or dissimilar methodology now known or hereafter developed.
The use of general descriptive names, registered names, trademarks, service marks, etc. in this publication does not imply, even in the absence of a specific statement, that such names are exempt from the relevant protective laws and regulations and therefore free for general use.
The publisher, the authors, and the editors are safe to assume that the advice and information in this book are believed to be true and accurate at the date of publication. Neither the publisher nor the authors or the editors give a warranty, expressed or implied, with respect to the material contained herein or for any errors or omissions that may have been made. The publisher remains neutral with regard to jurisdictional claims in published maps and institutional affiliations.

This Springer imprint is published by the registered company Springer Nature Switzerland AG
The registered company address is: Gewerbestrasse 11, 6330 Cham, Switzerland

Preface

The Second International Conference on Technological Research-RITAM 2021 was held virtually on October 27–29, 2021. It aimed to provide a forum for discussion and the dissemination of results from R&D projects that have been developed both within and outside of Ecuador over the last few years. RITAM 2021 was jointly supported and co-organized by the RITAM Research Network (Instituto Superior Tecnológico Sucre, Instituto Superior Universitario Central Técnico, Instituto Superior de Turismo y Patrimonio YAVIRAC, Instituto Superior Tecnológico Luis Napoleón Dillon, Conservatorio Superior Nacional de Música, Instituto Superior Tecnológico Luis A Martínez, Instituto Superior Tecnológico Paulo Emilio Macías, Instituto Superior Tecnológico La Maná, Instituto Superior Tecnológico Luis A Martínez Agronómico, Instituto Tecnológico Superior Loja, Instituto Superior Tecnológico Primero de Mayo, Instituto Superior Pedagógico Intercultural Bilingüe Jaime Roldós Aguilera, Instituto Superior Tecnológico Cotacachi, Instituto Superior Tecnológico Alfonso Herrera), and GDEON. The content of this volume is related to the following subjects:

– Communication
– Electronic and Control
– Energy and Materials
– Technology Trends

RITAM 2021 received 107 submissions written in English by 428 authors coming from 12 different countries. All these papers were peer-reviewed by the RITAM 2021 Program Committee consisting of 63 high-quality researchers. To assure a high-quality and thoughtful review process, we assigned each paper at least three reviewers. Based on the peer reviews, 25 full papers were accepted, resulting in an 23% acceptance rate, which was within our goal of less than 40%.

We would like to express our sincere gratitude to the invited speakers for their inspirational talks, to the authors for submitting their work to this conference, and to the reviewers for sharing their experience during the selection process.

October 2021

Marcelo Zambrano Vizuete
Miguel Botto-Tobar
Angela Diaz Cadena
Ana Zambrano Vizuete

Organization

General Chair

Marcelo Zambrano V.	Universidad Técnica del Norte, Ecuador

Editorial Committee

Marcelo Zambrano V.	Universidad Técnica del Norte, Ecuador
Miguel Botto-Tobar	Eindhoven University of Technology, The Netherlands
Ángela Díaz Cadena	Universitat de Valencia, Spain
Ana Zambrano V.	Escuela Politécnica Nacional, Ecuador

Publication Chairs

Marcelo Zambrano V.	Universidad Técnica del Norte, Ecuador
Miguel Botto-Tobar	Eindhoven University of Technology, The Netherlands

Organizing Committee

Marcelo Zambrano V.	Universidad Técnica del Norte, Ecuador
Alejandra Sarzosa Villarroel	Instituto Superior Tecnológico Sucre, Ecuador
Ricardo Rosero Yugsi	Instituto Superior Tecnológico Sucre, Ecuador
Sandra Díaz Castro	Instituto Superior Tecnológico Sucre, Ecuador
Ricardo Chicaiza	Instituto Superior Tecnológico Sucre, Ecuador
Marcelo Enríquez Sánchez	Instituto Superior Tecnológico Sucre, Ecuador
Edison Meneses Torres	Instituto Superior Tecnológico Sucre, Ecuador
Pamela Ramírez Herrería	Instituto Superior Tecnológico Sucre, Ecuador

Steering Committee

Santiago Illescas Correa	Instituto Superior Tecnológico Sucre, Ecuador
José Luis Flores	Instituto Superior Tecnológico Central Técnico, Ecuador
Iván Borja	Instituto Superior Tecnológico Yavirac, Ecuador
Engels Monteros Tello	Conservatorio Superior Nacional de Música, Ecuador

Program Committee

Marcelo Zambrano	Universidad Técnica del Norte, Ecuador
Ana Zambrano	Escuela Politécnica Nacional, Ecuador
Miguel Botto-Tobar	Eindhoven University of Technology, The Netherlands
Doris Macías	Universidad Laica Eloy Alfaro, Ecuador
Francisco Pérez	Universidad Politécnica de Valencia, Spain
Javier Hingant	Universidad Politécnica de Valencia, Spain
Alberto García	Universidad Politécnica de Valencia, Spain
Víctor Garrido	Universidad Politécnica de Valencia, Spain
Javier Prado	Universidad Técnica Federico Santa María, Chile
Diego Paredes	Universidad de Saragoza, Spain
Henry Díaz	Universidad Técnica del Norte, Ecuador
Ángela Díaz Cadena	Universitat de Valencia, Spain
Jhonny Barrera	Universidad Nacional de la Plata, Argentina
Marco Heredia	Universidad Politécnica de Madrid, Spain
Daniel Ripalda	Universidad Nacional de la Plata, Argentina
Francesc Wilhelmi	Centre Tecnològic de Telecomunicacions de Catalunya, Spain
Ricardo Rosero	Instituto Superior Tecnológico Sucre, Ecuador
Santiago Vidal	Universidad Nacional del Centro de la Provincia de Buenos Aires, Argentina
Jhenny Cayambe	Pontificia Universidad Católica del Ecuador Sede Ibarra, Ecuador
Santiago Ushiña	Likatelec, Ecuador
Jack Vidal	Instituto Superior Tecnológico Sucre, Ecuador
Alejandra Sarzosa	Instituto Superior Tecnológico Sucre, Ecuador
Fabricio Tipantocta	Instituto Superior Tecnológico Sucre, Ecuador
Homero Torres	Instituto Superior Tecnológico Sucre, Ecuador
Anabel Portero	Instituto Superior Tecnológico Sucre, Ecuador
Leandro Bezerra De Lima	Universidad Federal de Mato Grosso Do Sul, Brasil
Andrea Carolina Flores	Embraer Defensa y Seguridad, Brasil
Elmer Levano Huamaccto	Universidad Federal Do Parana, Brasil
Ari Lazzarotti	Universidad Federal de Goiás, Brasil

Ellen Synthia Fernandes de Oliveira	Universidad Federal de Goiás, Brasil
Fernanda Cruvinel Pimentel	Universidad Federal de Goiás, Brasil
Pablo Minango	Universidad Estatal de Campinas, Brasil
Danny De La Cruz	Universidad de las Fuerzas Armadas EPE, Ecuador
Johana Tobar Quevedo	Universidad de las Fuerzas Armadas EPE, Ecuador
Angel Jaramillo	Universidad de las Américas, Ecuador
Holger Aníbal Capa Santos	CACES, Ecuador
Alonso Estrada Cuzcano	Universidad Nacional Mayor de San Marcos, Ecuador
Mariana Lima Bandeira	Universidad Andina Simón Bolivar, Ecuador
Norma Molina	Universidad Israel, Ecuador
Elfio Pérez	Universidad Indoamérica, Ecuador
Alfredo Rodriguez Guzmán	Cedepro Ecuador, Ecuador
Diana Portelles Cobas	Cedepro Ecuador, Ecuador
Lorena Chulde Obando	Instituto Superior de Turismo y Patrimonio YAVIRAC, Ecuador
Francisco Estrella Sotomayo	Instituto Superior de Turismo y Patrimonio YAVIRAC, Ecuador
Diego Yánez Flores	Instituto Superior de Turismo y Patrimonio YAVIRAC, Ecuador
Cristina Pérez Rico	Escuela Politécnica Nacional, Ecuador
Mauricio Rosero	Instituto Superior Tecnológico Sucre, Ecuador
Edgar Maya	Universidad Técnica del Norte, Ecuador
Mauricio Domínguez	Universidad Técnica del Norte, Ecuador
Darwin Aguilar	Universidad de las Fuerzas Armadas ESPE, Ecuador
Sergio Montes	Universidad de las Fuerzas Armadas ESPE, Ecuador
Darwin Noroña	Instituto Superior Tecnológico Sucre, Ecuador
Miguel Granja	Universidad Internacional del Ecuador, Ecuador
Marcelo Flores	Universidad Politécnica Salesiana, Ecuador
Diego Vizuete	Instituto Superior Tecnológico Sucre, Ecuador
Fabián Granda Bustan	Instituto Superior de Turismo y Patrimonio YAVIRAC, Ecuador
María Guacho Tipan	Instituto Superior de Turismo y Patrimonio YAVIRAC, Ecuador
Rafael Carrera Zurita	Instituto Superior de Turismo y Patrimonio YAVIRAC, Ecuador
Néstor Xavier Maya Izurieta	Instituto Superior Universitario Central Técnico, Ecuador
José Beltrán Ruiz	Instituto Superior Universitario Central Técnico, Ecuador

Daniel Barzallo Nuñez — Instituto Superior Universitario Central Técnico, Ecuador

David Basantes Montero — Instituto Superior Universitario Central Técnico, Ecuador

Organizing Institutions

Contents

Communications

Identification of a MIMO Twin Rotor System Using an Artificial Neural Network Trained by PSO

Mauricio Toscano[1,2](✉), William Montalvo[1,2], Cristina Bastidas[1,2], and Eddye Lino[1,2]

[1] Universidad Politécnica Salesiana, UPS, 170146 Quito, Ecuador
estoscanoa@est.ups.edu.ec, wmontalvo@ups.edu.ec, cbastidas@istct.edu.ec, elino@tes.edu.ec

[2] Instituto Superior Universitario Central Técnico, ISUCT, 170146 Quito, Ecuador

Abstract. Twin Rotor Mimo System (TRMS) is a dynamic system with multiple inputs and multiple nonlinear outputs that simulates the action of a helicopter, in this type of system there is a complexity at the time of describing the operation through a transfer function with conventional methods, due to the development of mathematics. For the identification of this type of systems there are alternative methods such as artificial intelligence, specifically Artificial Neural Networks (ANN). The nonlinear autoregressive network with exogenous inputs (NARX) allows modeling nonlinear dynamic systems because it takes prior values of inputs and outputs in different layers. The weights of this network were improved by particle swarm optimization (PSO), as these were considered as particles to find their best position within the search space. For this identification, a data set relating the input to the output of the TRMS at a given time was used through the MATLAB software with its Neural Network Time Series app library and it was obtained as a result that the output signal of the equipment was similar to the estimated output signal of the neural network, optimizing the computational cost and the training time. The algorithm that was developed has the versatility to identify the response of linear systems.

Keywords: NARX · PSO · TRMS

1 Introduction

The identification of systems is based on the experimental collection of input and output data at a given time, i.e. for each signal $u(k{*}T)$ where (T) is the sampling time and which generates a response $y(k{*}T)$, and from these data the dynamic model of the plant is obtained [1]. A fundamental part of obtaining an equation that describes the operation is to determine the type of excitation of the plant in which all the devices preferably act under normal operating conditions in order to obtain an accurate model [2, 3].

© The Author(s), under exclusive license to Springer Nature Switzerland AG 2023
M. Zambrano Vizuete et al. (Eds.): RITAM 2021, LNNS 512, pp. 3–14, 2023.
https://doi.org/10.1007/978-3-031-11295-9_1

TRMS is a Dynamic MIMO system [4], for the identification of this type of equipment, a series of complex techniques are contemplated that allow the description of indeterminate plants or systems by means of a mathematical model [5] and to describe their actual operation within a process or application through the collection of data on inputs and outputs. With the development in the area of artificial intelligence, optimization algorithms and neural networks have become an option for the identification of control systems [6].

According to research by [7], the authors propose an identification of the TRMS by means of a hybrid configuration, between PSO and differential evolution as a training method of a feed-forward neural network combined with back propagation as a global search operator of the weights to be optimized, obtaining as a result that the DEPB algorithm (differential evolution back propagation) [8] performs better in convergence and finding the mean squared error, compared to heuristic algorithms such as PSO.

TRMS identification using dynamic neural networks, especially Recurrent High Order Neural Network (RHONN), is a technique that has satisfactory results because it guarantees the exponential convergence trend of the identification error to zero [9]. In the identification of a 02 DOF robotic arm using an IDMN Neural network optimized by PSO, in which the parameters of a Fuzzy controller *Ke* and *Kde* are calculated obtaining a model that is not affected by extreme changes in the operating environment [10].

In another type of methodology for the identification of TRMS described by [11], the author performs two types of identifications, the first one is developed taking into account the system in one degree of freedom (DOF), that is to say, he divides it into SISO systems. The second method is performed considering two degrees of freedom (MIMO system). The difficulty in the identification procedure of the system of two inputs and two outputs is aggravated by the presence of cross couplings between the planes of motion, in the comparison made between the two methods concludes that it is better to treat the MIMO system as several SISO systems to avoid having complex systems, however, it has been observed that the nonlinear model is only slightly better than the linear model of 1 DOF but with the application of a controller, this difference can be eliminated.

In the development of an unmanned helicopter system, the identification of the system dynamics represents an important technical requirement for the simulation study, design and implementation of controllers. Due to the complex characteristics of the equipment dynamics and the difficulty of directly calculating the system parameters, obtaining a mathematical model has been a difficult task in the development of unmanned aerial vehicles (UAV), according to the solution proposed by [12]. The use of the NARX network was a good alternative in terms of model efficiency but a problem was encountered when taking into account the effect of cross-coupling between the states of the two rotors, therefore a hybrid MODE-NARX network trained by back propagation was used, the estimation provides up to 55% improvement in model accuracy.

In the identification of a system for energy consumption of educational buildings [13]. The computational cost is high because it uses up to 150 particles and 250 iterations with an error of 33.94%, to reduce this percentage increase the number of iterations.

In the research of [14], uses a NARX network for the identification of a gyro-stabilized platform, the main problem that the system has is the noise, in which two tests are made, the first one trains the NARX network with the inputs and outputs without eliminating the noise, the second experiment uses a filtering of the signals with which they manage to increase the accuracy of the identifier from 7 to 23 times with respect to the first experiment.

In this research, what was obtained was the identification of a TRMS 33-220, through the real values of the equipment in a certain time, using the data acquisition interface in unstable conditions, these data were entered into the Neural Network Series App. and the NARX library was used, the training weights of this network were optimized using the PSO algorithm, replacing the weights calculated in the tool by those generated in the optimization algorithm.

2 Methodology

The identification of MIMO models can be done by considering them as SISO subsystems, which provides flexibility in the choice of the system order in each case. In this way, the best fit can be chosen. On the other hand, by using MIMO identification, compact models can be obtained directly, but there are difficulties in obtaining a good fit for all modes at the same time [15, 16]. The results of this methodology make it possible to obtain compact models that facilitate the description of a system by means of a mathematical equation [17].

According to the above, to simplify the identification, the model can be treated as two linear rotor models with two linear couplings between them. Therefore, 4 linear models have to be identified: two for the main dynamic trajectory from $u1$ to φ and from $u2$ to φ and cross-coupling dynamic trajectories from $u1$ to Ψ and from $u2$ to Ψ [4].

The identification of the Twin Rotor MIMO System 33-220 will be based on the structure of Fig. 1, for the elaboration of this research.

2.1 System Data Acquisition

The real data of the system was taken through the equipment's own software, which is a function in Simulink, which generates a control signal u [4], and at the output is the angle θ of the Main Rotor with respect to the vertical axis in radians.

Figure 2 and Fig. 3 show the plots of the Main rotor and Tail rotor control signals, all real-time simulations are performed with a sampling time of $Ts = 0.001\ [s]$. However, because the dynamic response of the plant is relatively slow, the identification is carried out with the sampling time of $Ts = 0.1\ [s]$. The number of data vectors u, y is of order $1*1000$. The data were entered into the MATLAB tool as inputs and outputs of the NARX network.

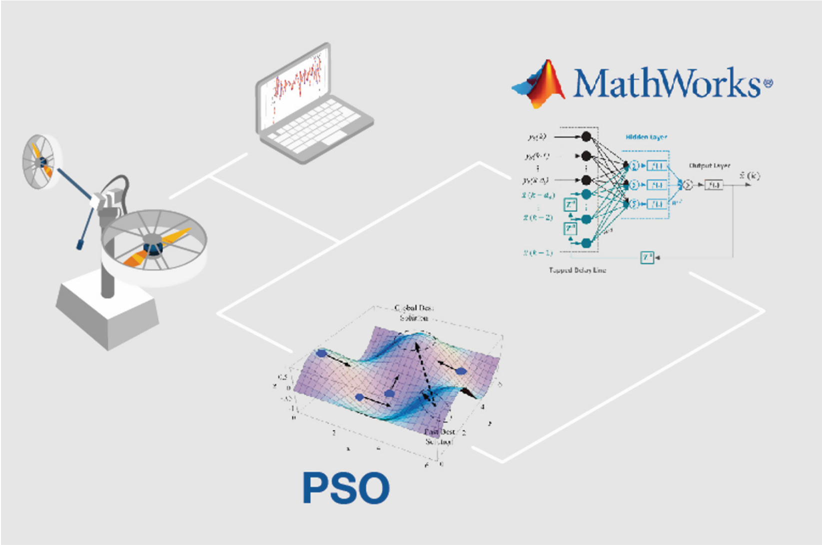

Fig. 1. TRMS identification model

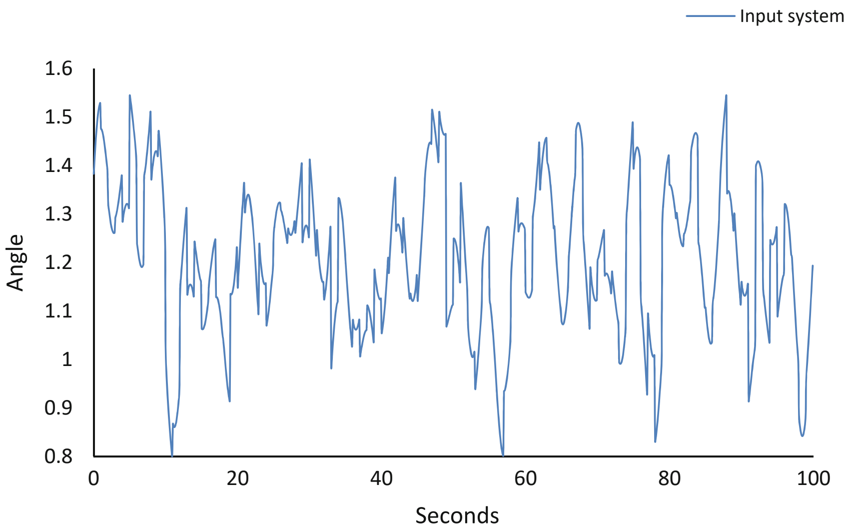

Fig. 2. Input signal Main Rotor

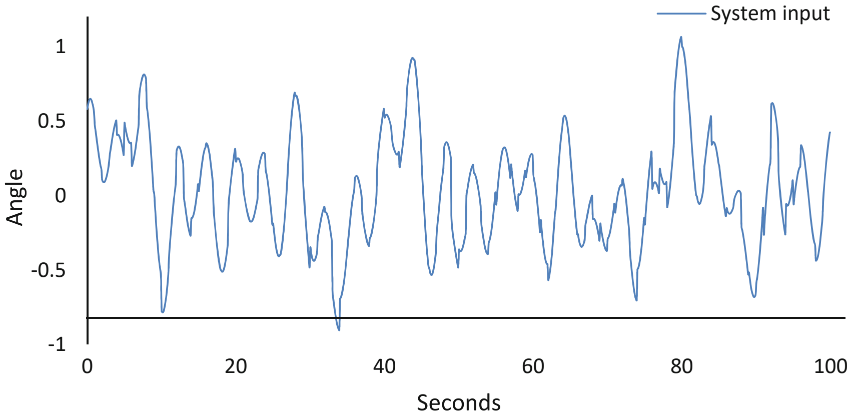

Fig. 3. Input signal Tail Rotor

2.2 Implementation

The MATLAB® *ntstool* (Neural Time Series) library allows the use of the NARX network, the input data for training are the input u and the output y of the equipment in the form of vectors, the hidden neurons and the number of delays are defined to have an estimated output.

The code that is generated presents some design values, which are detailed in Table 1, column one represents the variables that are generated at the time of running the training of the NARX network using the ntstool library, column two (matrix) indicates the order of the matrices that are generated depending on the number of layers and delays of the network, finally column three with the name PSO Variables, are the matrices with the new values of the weights and biases generated by the optimization with PSO that will be replaced in the NARX network for the identification of the system.

The PSO algorithm described in the pseudocode by [18], it is necessary to assign the number of particles, the value of **c1** and **c2,** the limits of the velocities and the iterations to generate the values of the matrices and replace the design data, assigning to the NARX network new weights and biases, which optimizes the mean square error function.

Matrix 1 represents the array that the PSO algorithm builds, each element moves three-dimensionally, the dimensions of these matrices will be related to the design data generated in the ntstool library when using the NARX architecture.

$$Weights = \begin{bmatrix} W_{11} & W_{12} & \cdots & W_{1m} \\ W_{21} & W_{22} & \cdots & W_{2m} \\ \vdots & \vdots & \ddots & \vdots \\ W_{n1} & W_{n2} & \cdots & W_{nm} \end{bmatrix} \tag{1}$$

Table 1. Design variables

Variables	Matrix	PSO variables
x1-step1.xoffset	[1*1]	X1STEPoffset
x1-step1.gain	[1*1]	X1STEPgain
x1-step1.ymin	[1*1]	X1STEPymin
x2-step1.xoffset	[1*1]	X2STEPoffset
x2-step1.gain	[1*1]	X2STEPgain
x2-step1.ymin	[1*1]	YSTEPymin
b1	[20*1]	B1
IW1-1	[20*2]	IW1
IW1-2	[20*2]	IW2
b2	[1*1]	B2
LW2-1	[1*20]	IW3
y1-step1.ymin	[1*1]	YSTEPymin
y1-step1.gain	[1*1]	YSTEPgain
y1-step1.xoffset	[1*1]	YSTEPxoffset

3 Results

3.1 Main Rotor Identification

The identification of the Main Rotor was performed with the parameters of Table 2, the graph of the outputs, real vs. estimated are in overlapping, i.e., they have similarity in their behavior as shown in Fig. 4, in Fig. 5 and Fig. 6 the best positions of the group and global particles are observed with an estimation performance in terms of error of *0.026%.*

Table 2. PSO parameters.

Parameters	Values
Hidden layers	20
Delays	2
C1	2
C2	2
Number of particles	100
Iterations	50
Minimum velocity	0.01
Maximum velocity	0.2
Simulation time	99.9
Time intervals	0.1

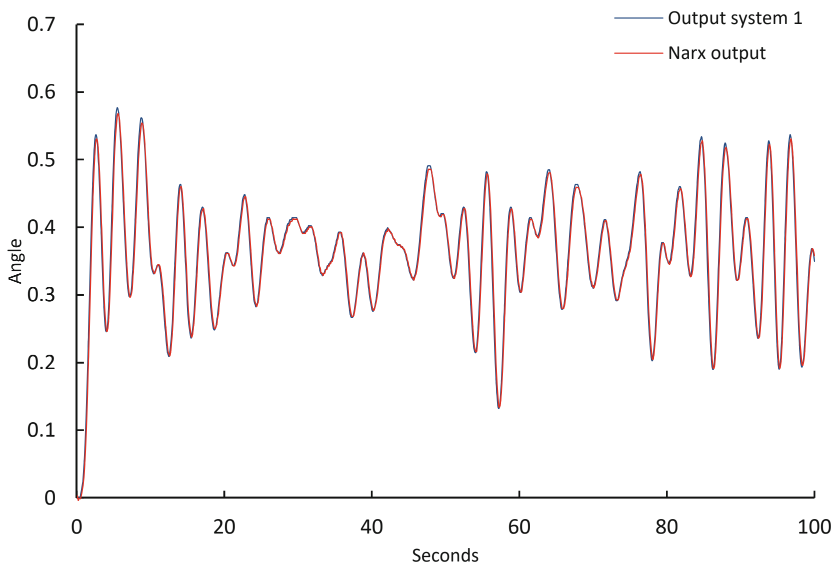

Fig. 4. Main Rotor identification

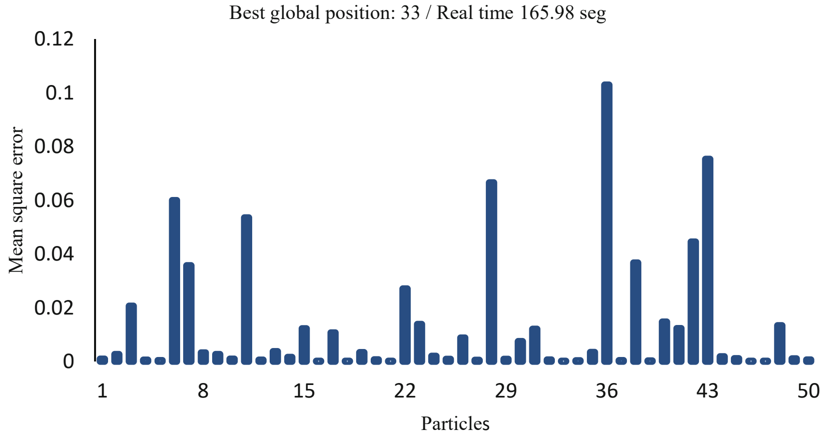

Fig. 5. Error best group position Main Rotor

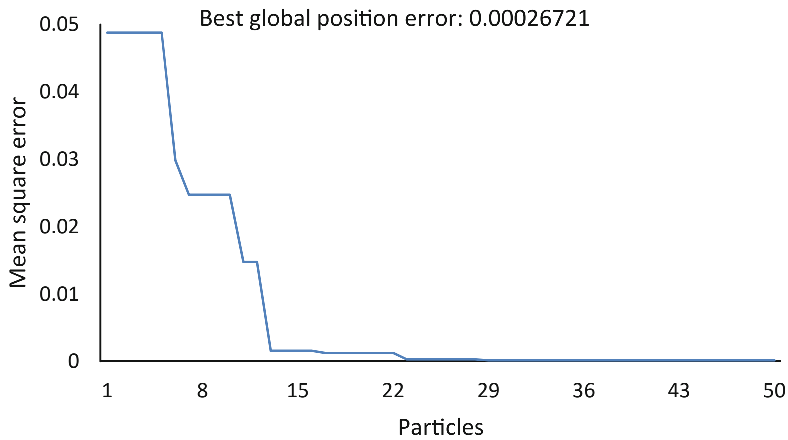

Fig. 6. Mean square error

3.2 Tail Rotor Identification

With the parameters of Table 2, the identification of the Tail Rotor was carried out, the graphic of the outputs, real vs. estimated, is similar, it could be said that they are the same, it is the best estimation that was had in all the tests carried out as shown in Fig. 7, having a performance of the estimation in terms of error of ***0.023%.***

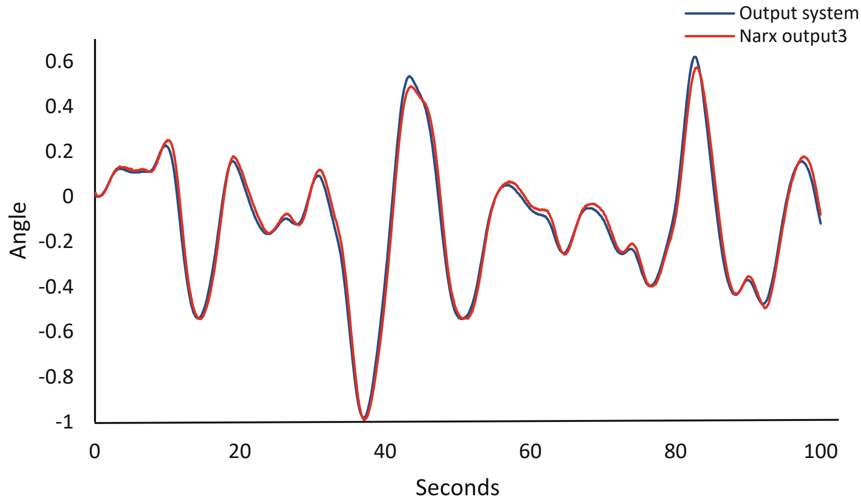

Fig. 7. Tail Rotor identification

4 Discussion

NARX networks optimized by PSO are an option in the modeling of nonlinear dynamic systems, the development of these algorithms allows optimizing the computational cost depending on the complexity of the system.

The results obtained were in accordance with the expectations raised, taking into account that the four SISO subsystems that make up the TRMS were identified and, as seen above, the graphs show an estimate similar to the real output of the equipment, which in comparison with other investigations, the error function is equal to or lower than the real output of the equipment, and that the error function is equal to or lower than the real output of the equipment [19]. Table 3 shows the error percentages of the four identifications performed.

Table 3. Mean square error

Identifications	Error	Percentage
Main rotor	0.000266	0.26%
Tail rotor	0.000239	0.24%
Cross pitch	0.000235	0.24%
Cross yaw	0.000249	0.25%

As part of the validation tests of the methodology, the MATLAB tool IDENT was used, which allows obtaining a transfer function with the input and output data of a system. Figure 8 shows the graphs of the outputs of the transfer function estimation and compares the real output of the system, generating three equations describing the operation of the Main Rotor.

The transfer function described by Eq. 2, obtained by relating the input and output of the Main Rotor to the actual data, was assigned three poles and two zeros with a fit to the estimation data: *83.53%, FPE: 0.0002114, MSE: 0.0002076.*

$$y_{main} = \frac{-1.209s^2 + 6.785s + 1570}{s^3 + 11.58s^2 + 473.4s + 5150} \tag{2}$$

The Eq. 3 represents the transfer function developed with the actual system input data and estimated output of the proposed NARX network, which presents a good fit to the estimation data.: *83.53%, FPE: 0.0002114, MSE: 0.0002076.*

$$YNARX_{output1} = \frac{-0.1209s^2 + 0.6785s + 1.57}{s^3 + 1.158s^2 + 4.734s + 5.15} \tag{3}$$

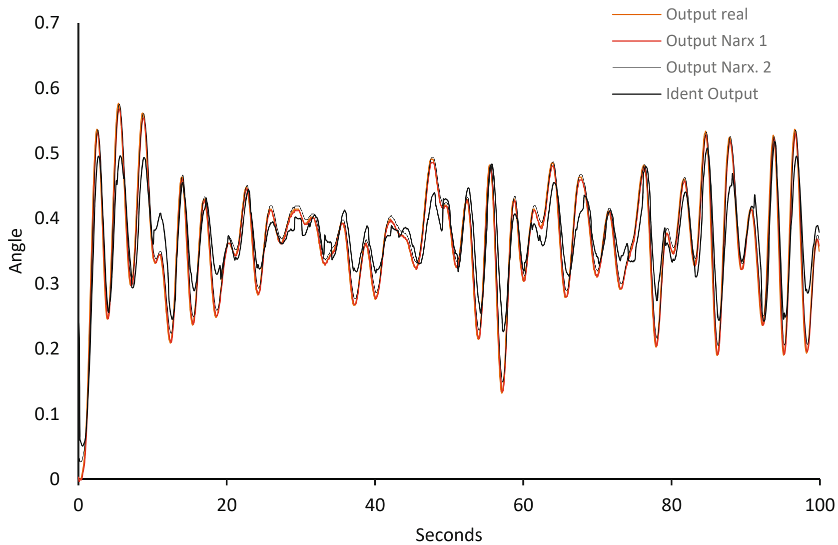

Fig. 8. Transfer function graphs

The transfer function generated in Matlab Ident varies when relating the actual input to the output estimated by the algorithm, this depends on the network training and PSO optimization. Equation 4 shows that the transfer function is different from the previous ones with a fit to the estimation data: *84.15%, FPE: 0.0001675, MSE: 0.0001645*. These data were subsequent to a new training.

$$YNARX_{output1} = \frac{-1.26s^2 - 21.34s + 1257}{s^3 + 9.485s^2 + 471.9s + 4166} \tag{4}$$

Taking into consideration that, in the identification of control systems by means of neural networks, the response as such are the values of the weights of each of the neurons that compose the model after training. In order to have a reference of the validity of the algorithm, it was compared by generating two transfer functions, the first one with the real data of the equipment and the second one with the estimation values of the NARX network by means of the IDENT tool. The results in terms of fit to the estimation data are above *83%* and in reference to other research Works [1] and [19] that obtain models that are estimated from *63%.*

5 Conclusions

The efficiency of the neural networks depends on the number of layers and the iterations in the training, as there is no rule for the assignment of these design values, the selection will depend on the system or the database available. In the case of the identification of the Main Rotor of Fig. 4, it was increased from 20 to 50 hidden layers and from 2 to 4 delays, but the estimation was not as expected, since the mean square error was increased to 1.2%, in consequence, it is necessary to avoid entering in the under and over training zones to have an optimal performance in the execution of a learning algorithm.

Using the Matlab Ident tool, two identifications were performed: *ymain(real)/umain (real)* and *yestimate (NARX)/umain (real),* of which the accuracy of the model is 84.15% and 83.53%, with the difference of 0.63% and it can be concluded that the NARX network trained by PSO successfully identified the system.

In relation to the results of this research, for the identification of the Tail Rotor the iterations can be reduced to 30, but in the case of the Cross Yaw minimum 50 are needed, the assignment of the hidden layers, the delays and iterations will depend on the dynamic characteristics of the system, the more abrupt variations in the output over time, the higher the demand of computer resources to achieve an estimation of the system.

References

1. Miranda, J., Solis, M.: Diseño e implementación de algoritmos de control difuso y PID adaptativo STR para el sistema MIMO de doble rotor 33-220 de Feedback para el laboratorio de control automático de la Universidad Politécnica Salesiana sede Guayaquil automático de la Universid **53**(9), 95 (2018). https://doi.org/10.1017/CBO9781107415324.004
2. Hernández Lopez, Y., Rivas-Perez, R.: Identificación basada en redes neuronales artificiales de un tramo de un canal principal de riego. X Semin. Euro-Latinoamericano Sist. Ing. 17 Conv. Científica Ing. y Arquit, no. July (2014). https://doi.org/10.13140/RG.2.1.3284.3368
3. Urgiles Navarrete, F.A., Ortiz Matos, L.: Estrategia de identificación dinámica no lineal basada en NARX para fuentes de generación distribuida acopladas electrónicamente a micro – redes AC/DC (2020). https://dspace.ups.edu.ec/handle/123456789/18892
4. Feedback: Twin Rotor MIMO Systems Experiments. www.fbk.com
5. Padilla, P.A.: Métodos de Identificación dinámica, no. May (2015)
6. Gil, R.V., Páez, D.G.: Dynamic systems identification using RBF neural networks. RIAI - Rev. Iberoam. Autom. e Inform. Ind. **4**(2), 32–42 (2007). https://doi.org/10.1016/s1697-7912(07)70207-8
7. Subudhi, B., Jena, D.: Nonlinear system identification of a twin rotor MIMO system. In: IEEE Region 10 Annual International Conference Proceedings/TENCON, pp. 1–6 (2009). https://doi.org/10.1109/TENCON.2009.5395966

8. Qu, J., Li, Y., Zhou, J.: Improved differential evolution based BP neural network for prediction of groundwater table. In: 2010 3rd International Symposium on Knowledge Acquisition and Modeling, KAM 2010, pp. 36–39 (2010). https://doi.org/10.1109/KAM.2010.5646232
9. Armenta, C., Bernal, M., Hernandez, F., Villafuerte, R.: Identification-based linear control of a twin rotor MIMO system via dynamical neural networks. In: 2017 14th International Conference on Electrical Engineering, Computing Science and Automatic Control, CCE 2017 (2017). https://doi.org/10.1109/ICEEE.2017.8108829
10. Anh, H.P.H., Phuc, N.H.: Inverse neural MIMO NARX model identification of nonlinear system optimized with PSO. In: Proceedings of the 5th IEEE International Symposium on Electronic Design, Test and Applications, DELTA 2010, pp. 144–149 (2010). https://doi.org/10.1109/DELTA.2010.61
11. Sarvat Mushtaq Ahmad, B.: Modelling and Control of a Twin Rotor MIMO System (2001)
12. Tijani, I.B., Akmeliawati, R., Legowo, A., Budiyono, A.: Nonlinear identification of a small scale unmanned helicopter using optimized NARX network with multiobjective differential evolution. Eng. Appl. Artif. Intell. **33**, 99–115 (2014). https://doi.org/10.1016/j.engappai.2014.04.003
13. Mustapa, R.F., Dahlan, N.Y., Yassin, I.M., Hamizah Mohd Nordin, A., Mahadan, M.E., Mohamad, S.: Particle swarm optimization for NARX-ANN baseline energy modelling in educational buildings. In: Proceedings of the 2019 IEEE International Conference on Automatic Control and Intelligent Systems, I2CACIS 2019, no. June, pp. 19–24 (2019). https://doi.org/10.1109/I2CACIS.2019.8825097
14. Cheng, Z., Xu, J.N., Wu, M., Li, F., Guo, S.L.: Modeling of gyro-stabilized platform based on NARX neural network. In: Proceedings of the 2017 10th International Symposium on Computational Intelligence and Design, ISC 2017, vol. 2018-Janua, pp. 284–288 (2018). https://doi.org/10.1109/ISCID.2017.95
15. Matysko, R.: Theoretical model of the operation parameters regulated by the MIMO and SISO system in a cooling chamber. Int. J. Refrig. **58**, 53–57 (2015). https://doi.org/10.1016/j.ijrefrig.2015.05.020
16. Unneland, K., Perez, T., Egeland, O.: Mimo and SISO identification of radiation force terms for models of marine structures in waves. IFAC Proc. **7**(PART 1), 235–242 (2007). https://doi.org/10.3182/20070919-3-hr-3904.00042
17. Ikhouane, F., Giri, F.: A unified approach for the parametric identification of SISO/MIMO Wiener and Hammerstein systems. J. Franklin Inst. **351**(3), 1717–1727 (2014). https://doi.org/10.1016/j.jfranklin.2013.12.016
18. Brownlee, J.: Jason Brownlee-Clever Algorithms_Nature-Inspired Programming Recipes-LuLu (2011)
19. Liu, H., Song, X.: Nonlinear system identification based on NARX network. In: 2015 10th Asian Control Conference on Emerging Control Techniques for a Sustainable World, ASCC 2015, no. 1 (2015). https://doi.org/10.1109/ASCC.2015.7244449

On-line Monitoring Application for Apparel Manufacturing Purposes: A Low-Cost IoT Approach

Paulina Lara[1](✉), Ximena Vaca[1], and Ivannova Jumbo-Jaramillo[2]

[1] Instituto Superior Tecnológico Carlos Cisneros, Riobamba, Ecuador
{ligia.lara,ximena.vaca}@istcarloscisneros.edu.ec
[2] Sangolquí, Ecuador

Abstract. Think of a sewing machine sending data to the cloud, which technicians monitor at machine manufacturing companies, who then use that information to predict maintenance issues and prevent failures before it happens. This is the evolution of apparel fabrication to Industry 4.0. However, it is unclear how to connect the Internet of Things (IoT) devices with machines for clothing, especially in low-income countries where there is a lot of old and used machinery. Here, a low-cost real-time monitoring application for apparel manufacturing purposes is presented. The system is based on the IoT platform ESP8266 NodeMCU and Google Sheets, and it is used to monitoring the variables: motor temperature, needle bar vibration, and foot pedal force. Expert and beginner operators tested the system while manufacturing an item of unique clothing. The acquired information can be used to develop a predictive maintenance strategy and planning of repairing activities of the machinery. Finally, the data also can be used for qualitative and quantitative production analysis.

Keywords: IoT · Real-time monitoring · Apparel industry · Industry 4.0

1 Introduction

The textile and apparel industry is extremely important in the Ecuadorian economy, represents 5.9% of the industrial sector and contributes close to one percentage point to GDP (0.8%) [1]. There is a common perception that Industry 4.0 is for the engineering and automotive industry and not for labor-oriented apparel manufacturing. However, its potential for future implementation has been evaluated by several companies such as Duerkopp Alder, JUKI and Brother, where the main application of Industry 4.0 in the apparel industry is the resource efficiency and optimization of labors of the machinery and equipment employed in the processes by using Industry 4.0 technologies [2].

IoT systems can distribute data/information and execute in parts autonomously to cyber-physical world events and by triggering processes and formulating services with or without primary human intervention. Some authors use the concept called Industrial

I. Jumbo-Jaramillo—Independent Researcher.

© The Author(s), under exclusive license to Springer Nature Switzerland AG 2023
M. Zambrano Vizuete et al. (Eds.): RITAM 2021, LNNS 512, pp. 15–25, 2023.
https://doi.org/10.1007/978-3-031-11295-9_2

Internet of Things (IIoT) in the application of IoT exclusively for industrial applications [3]. IIoT or IoT identifies manufacturing devices from consumer devices that connect to the internal or industrial networks and the internet, while Industry 4.0 refers to the value of lean, efficient operations and smart manufacturing.

Currently, Ecuador has a low rate of modernization in modern industrial machinery, especially, in the textile and apparel field. Thus, stand out the importance of having a coherent strategy for implementing industry 4.0 in low-income countries, and the need to focus not just on companies but also on creating an eco-system to support the creation of technologies and the need for collaboration within a country and internationally in order to adapt to Industry 4.0 and reach its benefits [4].

The reason for doing this study lies in the need to develop low-cost Industry 4.0 technology by collaborating experts from the garment industry with experts in IoT. As proof of concept, a sensor system has been implemented to monitor the service variables of a sewing machine during garment production. These variables are motor temperature, needle bar vibration, and foot pedal force. The sensor data has been collected in real-time using an IoT NodeMCU and a customized application designed in Google Sheets. The information has then been processed to investigate the performance of the sewing machine when used by expert and beginner personnel. The results will aid in recognizing opportunities for the use of IoT in apparel manufacturing, enabling factories to achieve operational efficiency, optimize production, maintenance planning, and increase worker safety.

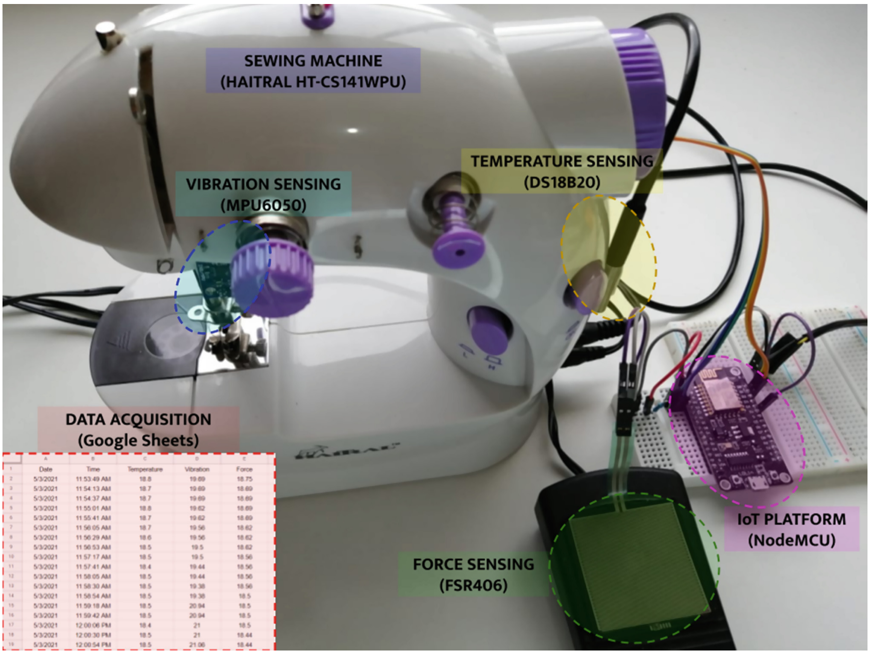

Fig. 1. Configuration scheme of the sewing machine with the IoT devices.

2 Materials and Methods

2.1 Proposed Methodology

The following methodology was proposed in order to study the impact of the application of IoT devices in the apparel industry. A sewing machine (HAITRAL HT-CS141WPU) was used to implement three sensors to monitor the variables: motor temperature, needle bar vibration, and foot pedal force (Fig. 1). The motor temperature was monitored to estimate whether there was overheating from continuous use or misuse of the machine. The sensing of the needle bar vibration offered information to determine patterns of service that can be used for improvement tasks in production and predictive maintenance. Lastly, the pedal force sensor was used to measure the effective time when a worker operates the sewing machine. The three sensors were connected to an ESP8266 NodeMCU platform. After, the information was sent in real-time to a customized Google Sheets application. The evaluation of the IoT technology in the apparel application was carried out using expert and beginner workers.

2.2 Hardware Components

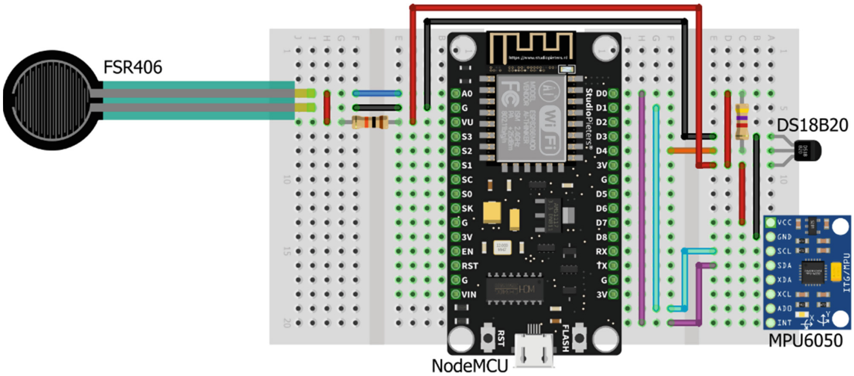

Fig. 2. A breadboard schematic connection of the IoT platform (NodeMCU) and the temperature (DS18B20), vibration (MPU6050) and force (FSR406) sensors.

IoT Platform

A ESP8266 NodeMCU device was used as IoT platform. It has an ESP8266EX Wi-Fi module is a self-contained TCP/IP protocol that can access any Wi-Fi network [5]. The ESP8266 NodeMCU Wi-Fi Module has several advantages, namely: low-cost device, requires minimal external circuitry, low power consumption, robust enough in storing capability, and on-board processing. It allows the integration of different sensors with minimal run time. The connection with the sensors is shown in Fig. 2.

Motor Temperature Sensor

The DS18B20 Digital Thermometer was used as a temperature sensor to monitor the sewing machine's motor heating. This sensor provides 9 to 12-bit (configurable) temperature readings that indicate the temperature of the device. The communication protocol used to send information to/from the DS18B20 is 1-Wire interface so that only one wire (and ground) needs to be connected from the NodeMCU to a DS18B20. The temperature measurement range is −55 to 125 °C.

Needle Bar Vibration Sensor

An MPU6050 module was used to detect the needle bar vibration, in which the tension and movement to make the seam are produced. The MPU6050 is an integrated 6-axis motion tracking device. A 3-axis Gyroscope and 3-axis Accelerometer form it. The accelerometer measures at X, Y and Z axes were used to compute the relative vibration (custom scale 0 to 100 for informative purposes). The NodeMCU can communicate with this module using I2C communication protocol.

Foot Pedal Force Sensor

The measurement of the force produced by the operator on the machine's pedal was carried out with a sensor FSR406 (Interlink Electronics). The sensor, a flexible thin film, is a variable resistor that varies with force. The greater the force applied, the lower its resistance. The measurement range was adapted using a voltage divider to keep a tailored human control range of 0 to 100 when the sensor is pressed with the operator's foot.

2.3 Software Design

To collect the data acquired by the sensors and the IoT platform NodeMCU, a google sheet was prepared to receive data from the IoT device by creating a Google Script to tie the sheet to the IoT device. The sampling time used to collect the data from each sensor was 100 ms. Under every Google Sheet document, it was possible to create multiple sheets, to save information collected from each operator. Due to the considerable amount of noise produced by the electrical elements and the vibration of the sewing machine, a median filter was implemented to filtering the sensors' signals.

2.4 Evaluation of the IoT Concept

For the evaluation of the proposed design, the following approach was used:

1) A garment was chosen to be manufactured with the sewing machine without using the IoT platform. This garment was a t-shirt for an infant from 4 to 6 years old. Using the same garment for information sampling helps to standardize the experiment. Figure 3 shows the pattern of the t-shirt and the seams that must be executed to shape the garment.
2) Five expert workers and five beginners carried out the task of making the children's t-shirt. The actual manufacturing times were timed. That is, exclusively the intervals used to manufacture the ten seams. These times were used to update the program in Google Sheets for online monitoring.

3) The fastest (expert) and slowest (beginner) operators were chosen to make the t-shirt for testing the IoT platform connected to the sewing machine.
4) The fastest operator manufactured the shirt with the IoT platform connected to the sewing machine. The data was collected and processed in order to obtain the "behavior" of the operator and the sewing machine during the actual manufacturing periods.
5) Idem 4, but with the beginner operator.

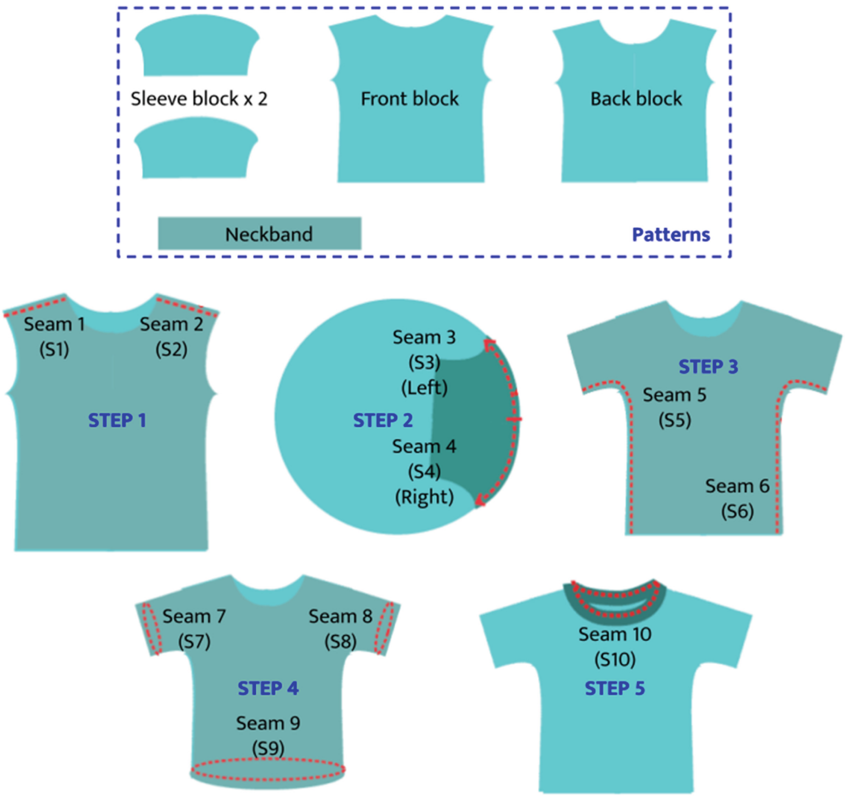

Fig. 3. Child t-shirt pattern and the fabrication steps. Each step can contain one or more seams.

3 Results and Discussions

3.1 Comparison Between Expert and Beginner Operators

Figure 4 shows the time used by the expert and beginner groups to complete each seam (10 in total). As expected, experts spend less time manufacturing the seams. The S10 seam was the longest for both groups. Another feature to highlight is a difference between seams of the same shape and length, for example, S3 and S4. These measurements are the starting point to evaluate the proposed IoT system and can be used for time and motion studies to improve productivity in the apparel industry.

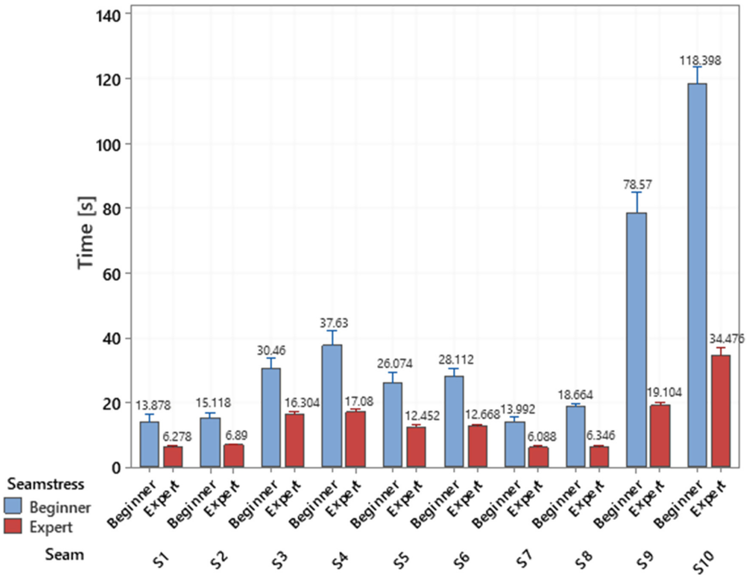

Fig. 4. Evaluation of the manufacturing intervals of each seam of the children's t-shirt for experts and beginners. The displayed value corresponds to the average of each group.

3.2 Motor Temperature Measurement

Figures 5 and 6 represent the evolution of the motor's temperature when the t-shirt was manufactured by an expert and a beginner, respectively. The t-shirt fabrication by the expert is more continuous, and the effective manufacturing time does not exceed 14 s. In this expert manufacturing cycle, a maximum temperature of around 33 °C is detected and occurs at the S9 seam. On the other hand, it takes the beginner approximately 42 s to complete the making of the t-shirt (effective time). The maximum temperature, in this case, is 38 °C, and it occurs in the S10 seam. The temperature increase is more sustained in the case of the beginner because the service time of the sewing machine is longer, so being the temperature, and the tendency is asymptotic. An excessive increase in temperature may indicate an overheating of the motor, which may be a malfunction in the sewing machine. Establishing a statistical control system, for example, control charts, can help plan predictive maintenance, which is cheaper than corrective maintenance.

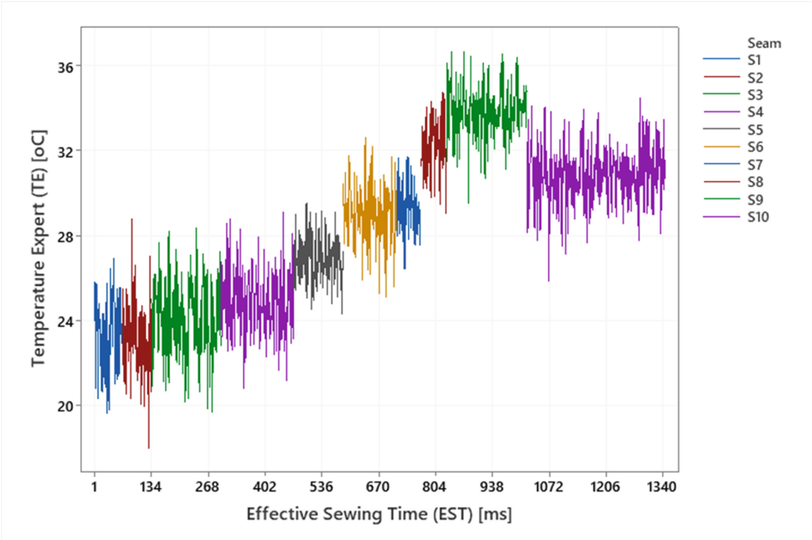

Fig. 5. Evolution of the temperature of the sewing machine's motor during the making of the children's t-shirt by an expert. Only the effective manufacturing intervals for each seam are shown.

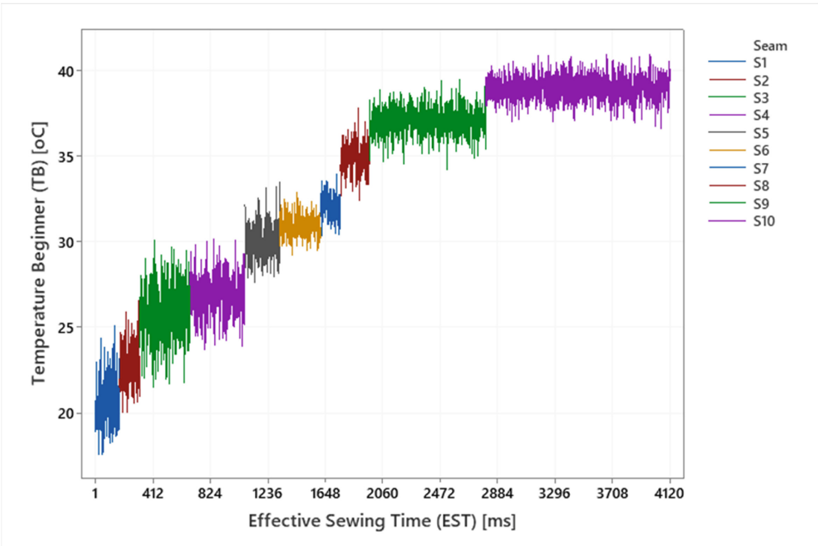

Fig. 6. Evolution of the temperature of the sewing machine's motor during the making of the children's t-shirt by a beginner. Only the effective manufacturing intervals for each seam are shown.

3.3 Needle Bar Vibration Measurement

Vibration measurement of the needle bar is indicated in Fig. 7 (expert) and Fig. 8 (beginner) during the manufacture of the t-shirt. The measurements obtained with the MPU6050 module were systematized to get a normalized value from 0 to 100 (called Relative Expert Vibration) to identify patterns faster for machine operators or users with non-instrumentation backgrounds. In the case of the expert, an average working frequency was 3.2 rad/s. For the beginner, the average frequency was 2.4 rad/s. These values were quite challenging to identify due to interference from accelerated needle bar movement when the sewing machine is working. Although the filtering (median filter) of the measured signals helps determine the behavior of the needle bar, it is necessary to look for another measurement system to detect vibration in a better way. Measuring vibration on machinery is very valuable for planning predictive maintenance tasks.

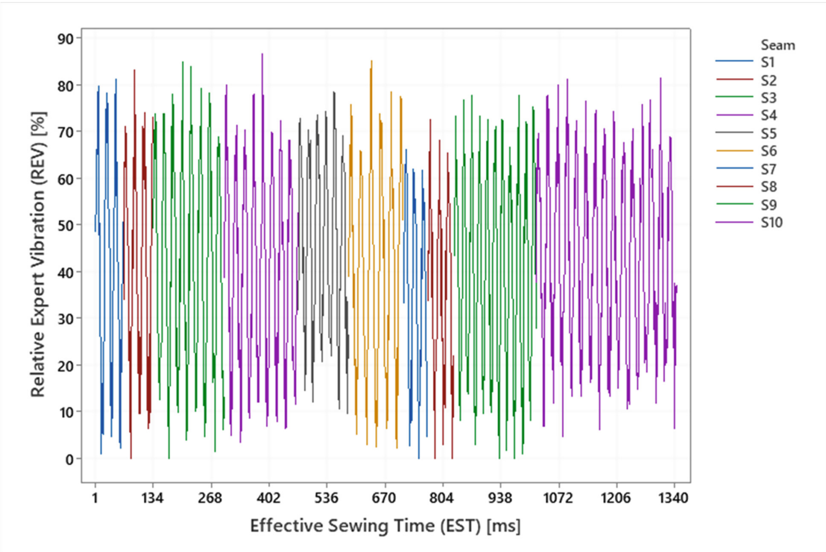

Fig. 7. Vibration measures of the needle bar during the fabrication of the children's t-shirt by an expert. Only the effective manufacturing intervals for each seam are shown.

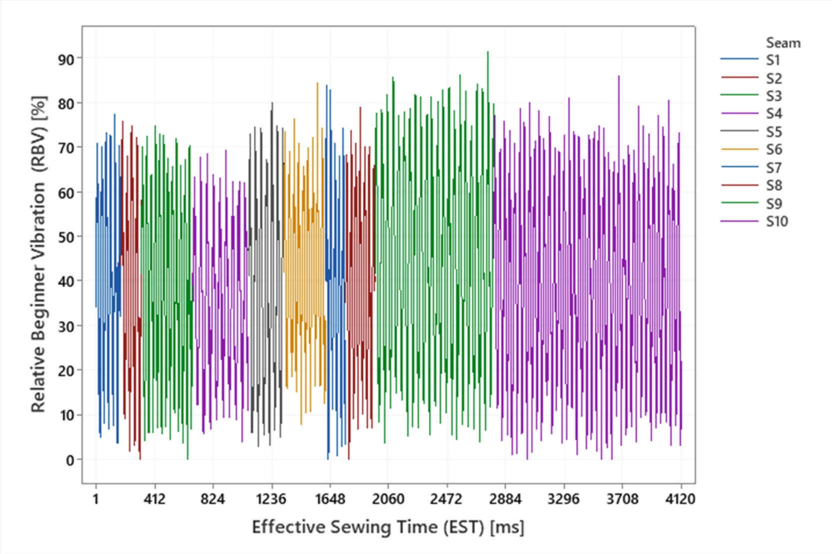

Fig. 8. Vibration measures of the needle bar during the fabrication of the children's t-shirt by a beginner. Only the effective manufacturing intervals for each seam are shown.

3.4 Foot Pedal Force Measurement

Figure 9 indicates the behavior of the expert operator when activating the pedal with his foot. The force was normalized to 0–100 scale for reading purposes. The pedal is a switch used to start the sewing function. As evidenced, the skilled operator operates the pedal very uniformly in the fabrication of each seam, which is indicative of a high speed of manufacture (and production). This uniformity is also related to the quality of the seam. Figure 10 shows the beginner's behavior when activating the pedal with his foot. In this case, the pedal actuation is quite uneven, which can produce severe vibration of the needle bar, excessive motor heating, and poor sewing quality. Thus, an imperfect pedal operation may cause considerable damage to the sewing machine, which implies high maintenance costs for repair and unnecessary equipment downtime.

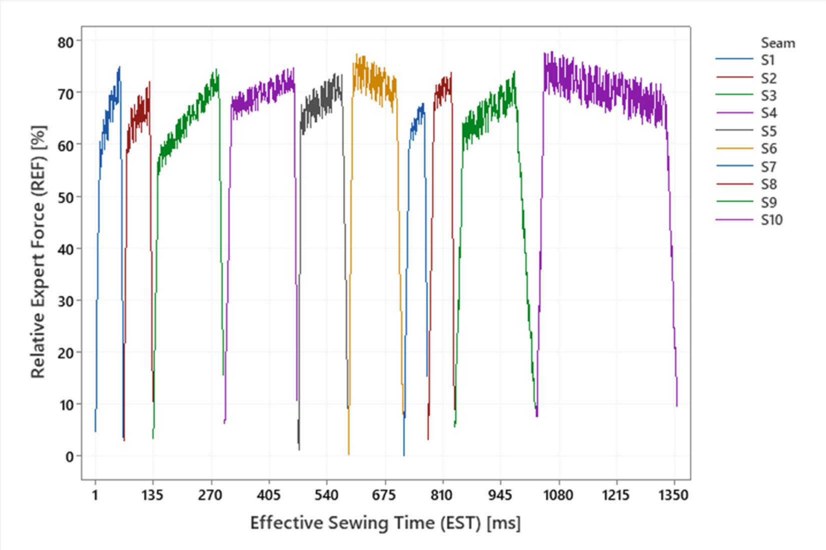

Fig. 9. Measurements of the foot pedal force during the fabrication of the children's t-shirt by an expert. Only the effective manufacturing intervals for each seam are shown.

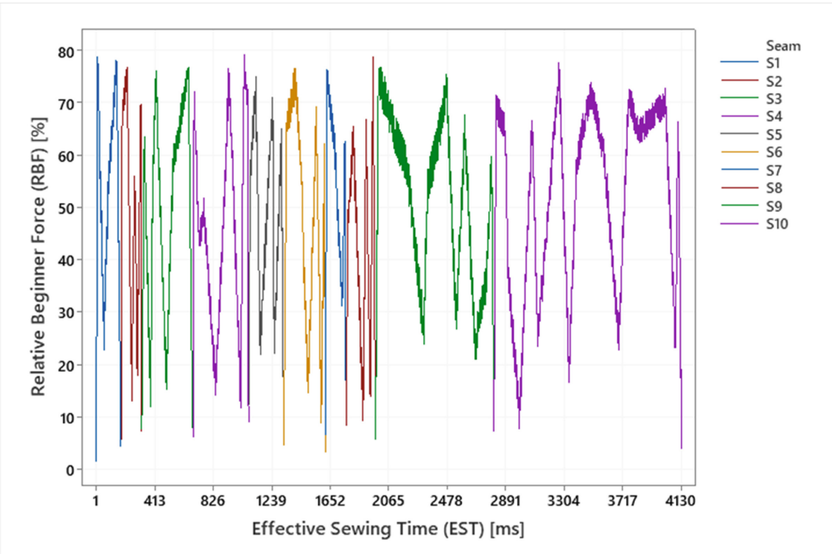

Fig. 10. Measurements of the foot pedal force during the fabrication of the children's t-shirt by a beginner. Only the effective manufacturing intervals for each seam are shown.

4 Conclusions

The apparel companies require a transformation in developing countries to achieve competitiveness. The path taken by various industries around the world is Industry 4.0. In the present study, an IoT system connected to a sewing machine was presented to monitor three variables to identify the operator's behavior when using the machine. Differences were determined between the use by experts and beginners when they manufacture the same clothing. This information helps develop strategies to improve production times and increase competitiveness. The data obtained in real-time can be used for preventive maintenance activities and facilitate operational effectiveness in the clothing industry. Future work will explore additional techniques to give more robustness to the system and connect IoT systems on several machines for a global analysis of the factory.

References

1. El sector textil, un puntal de la industria que busca levantarse—Gestión. https://www.revistagestion.ec/economia-y-finanzas-analisis/el-sector-textil-un-puntal-de-la-industria-que-busca-levantarse. Accessed 23 May 2021
2. Lakmali, E., Vidanagamachchi, K., Nanayakkara, J.: Industry 4.0 readiness assessment for apparel industry: a study in the Sri Lankan context. In: 2020 International Research Conference on Smart Computing and Systems Engineering (SCSE), Colombo, Sri Lanka, September 2020, pp. 174–181 (2020). https://doi.org/10.1109/SCSE49731.2020.9313026
3. Hassan, Q.F. (ed.): Internet of Things A to Z: Technologies and Applications. Wiley, Hoboken (2018)
4. The challenge of preparing developing countries for Industry 4.0—UNIDO. https://www.unido.org/news/challenge-preparing-developing-countries-industry-40. Accessed 31 June 2021
5. Kashyap, M., Sharma, V., Gupta, N.: Taking MQTT and NodeMcu to IOT: communication in internet of things. Procedia Comput. Sci. **132**, 1611–1618 (2018). https://doi.org/10.1016/j.procs.2018.05.126
6. Kumar Koditala, N., Shekar Pandey, P.: Water quality monitoring system using IoT and machine learning. In: 2018 International Conference on Research in Intelligent and Computing in Engineering (RICE), San Salvador, August 2018, pp. 1–5 (2018). https://doi.org/10.1109/RICE.2018.8509050
7. Ismail, M.I.M., Dziyauddin, R.A., Samad, N.A.A.: Water pipeline monitoring system using vibration sensor. In: 2014 IEEE Conference on Wireless Sensors (ICWiSE), Subang, Selangor, Malaysia, October 2014, pp. 79–84 (2014). https://doi.org/10.1109/ICWISE.2014.7042665
8. Sakashita, R., Nagamune, K., Kuroda, R.: A development of ankle joint range of motion measurement system using electromagnetic tracking device and force sensor. In: 2018 World Automation Congress (WAC), Stevenson, WA, USA, June 2018, pp. 1–5 (2018). https://doi.org/10.23919/WAC.2018.8430462

Electronic and Control

Learning Model Predictive Control in a Virtual Environment Through a Practical Case: A Continuous Stirred Tank Reactor

Diego González(✉), Oscar Gonzales, Christian Ortega, Christian Llumiquinga, and Homero Torres

Instituto Superior Tecnológico Sucre, Campus Sur Av. Teodoro Gómez de la Torre S14 - 72 y Joaquín Gutiérrez, Quito, Ecuador
{dgonzalez,ogonzales,cortega,cllumiquinga, htorres}@tecnologicosucre.edu.ec

Abstract. This article presents a virtual platform to learn Model Predictive Control (MPC) through a brief analysis of the mathematical model of a continuous stirred tank reactor (CSTR). The control algorithm was developed from a linearity process to regulate the CSTR at the operation point. The MPC optimization took the temperature in the jacket and the molar concentration as the control objectives. The final version of the virtual platform presented flexibility to change every parameter of the MPC to see their effect on the control algorithm to learn effectively the MPC regulation.

Keywords: Algorithm · CSTR · MPC · Linearity · MATLAB™

1 Introduction

The Model-based Predictive Control (MPC) has been used for several decades in industrial processes, where exceptional results have been observed in various aspects, such as efficiency and long-term performance. The above noted contrasts with the MPC computational load, in other words, the algorithm needs high-hardware characteristics to solve mathematical complexity in the generation of an optimal control law [1].

MPC success has been recognized for outstanding results in the field of industrial process control [2]. However, in recent years this regulation technique has been forwarded to the field of robotics, with several works such as [3–5], where represent a latent limitation for applying the MPC algorithm, the computational load.

The MPC accomplishment lies in predictions obtained from the mathematical model of the process to be controlled. These predictions let the MPC know how state variables of the process will change in a defined horizon of the discrete period to develop a proper control law. The prediction horizon visualizes state variables change, and the control horizon takes this information to formulate an anticipative control law. The control law is acquired by minimizing the cost function that considers the error and the control effort. One or more variables can be prioritized using their respective weight parameters that are considered in the cost function [6].

© The Author(s), under exclusive license to Springer Nature Switzerland AG 2023
M. Zambrano Vizuete et al. (Eds.): RITAM 2021, LNNS 512, pp. 29–42, 2023.
https://doi.org/10.1007/978-3-031-11295-9_3

MATLAB™ has been developing several versions of a toolbox for learning and implementing MPC [7]. This toolbox is designed as a proper structure to develop research and projects at different industrial and investigation bounds. Although the user's guide provides detailed guidelines for conducting the MPC study under basic examples of application, a fundamental understanding of the algorithm is unconceived due to the mathematical complexity in each element of the interface. When a user looks for key MPC algorithms under the mask of each block in the toolbox, the understanding is unaccomplished because of the owner's rights in the toolbox.

In [8], the authors developed an interface for learning MPC with GenOpt, which is a software from Berkeley Lab for mathematical analysis and minimization of functions. A user can perform the optimization of the cost function in the MPC to obtain optimal control values. However, the algorithm is implemented in a temperature analysis process that includes a slow dynamic and does not represent a challenge for the MPC. From the learner's view, the interface shows the performance of primary MPC parameters, such as prediction and control horizons, but applicability in fast dynamics is not performed to give users a different perspective of MPC capabilities.

On the other hand, authors in [9] developed an interface for the non-linear MPC is implemented and developed to regulate parameters at an electrical vehicle. This is a sophisticated tool that does not take linear MPC as its starting point because the interface is designed for advanced users. Therefore, tools of this type cannot be employed to undertake the learning basis of the MPC, especially for grade students who are learning one step at a time in the field of automatic control.

For all the reasons above, this work presents the implementation of a visual learning environment through software to understand the application of the MPC. This project proposes the MPC algorithm on a continuous stirred tank reactor (CSTR) to observe the regulator performance. In addition, this project teaches a basic MPC linear design in systems with non-linear dynamics. The propose is to apply fundamental concepts to achieve set-point objectives such us, establishing values of prediction and control horizons or variable weights.

This paper is presented as follows: Sect. 2 describes the dynamics of the CSTR for MPC implementation, Sect. 3 developed MPC design, Sect. 4 presents the results of the project and finally in Sect. 5 the paper emphasizes the main conclusions of this work.

2 Mathematical Model of a CSTR

The CSTR (Fig. 1) represents an industrial process that produces reactive components from reactant products and constant heat agitation. The reference model for the CSTR is taken from [1] which is taken in several works for analysis and research at process control.

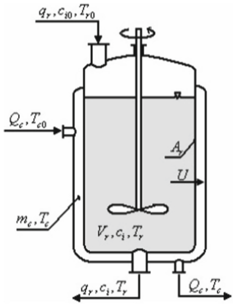

Fig. 1. CSTR variables [10].

Table 1 contains all main parameters used for modelling the CSTR.

Table 1. CSTR parameters.

Parameter	Description
ρ	Density of the material in the system
ρ_c	Density of the material in the ith inlet stream
V	Total volume of the system
F_i	Volumetric flow rate of the ith inlet stream
F_c	Volumetric flow rate of the cooling stream
F	Volumetric flow rate of the product
T_i	Temperature of flow rate of the ith inlet stream
T_{ci}	Temperature of cooling of the inlet
T_{c0}	Temperature of cooling of the outlet
T	Temperature of the product
n_A	Number of moles of component A in the system
c_A	Molar concentration of A in the system
c_{Ai}	Molar concentration of A in the ith inlet
r	Reaction rate per unit volume for component A
U	Internal energy
K	Kinetic energy
P	Potential energy
Q	Amount of heat exchanged in the process
H	Enthalpy of the system
c_ρ	Heat capacity of the reactant

The CSTR parameters at the operation point are presented in [1].
Parameters of a CSTR for the operating point are presented in Table 2.

Table 2. Parameters and units of CSTR equations.

Parameter	Value
F	1000 [L/min]
CAi	1 [mol/L]
Ti	350 [K]
V	100 [L]
p	1000 [g/L]
Cp	0.239 [J/gK]
Hr	50000 [J/mol]
E/R	8750 [K]
ku	$7.1{*}10^{10}$ [min^{-1}]
UA	50000 [J/minK]
Tc	300 [K]
CA	0.5 [mol/L]
T	350 [K]

To produce a stable mixture of two components, the jacket temperature must be considered, clarifying that it is carried out in an exothermic model, therefore, the non-linearity of the system implies making a mathematical model that manages to linearize the CSTR by taking the inputs through transducers to form a base algorithm for the possible predictions of a control [11].

This is described using Eq. (1) and Eq. (2).

$$\frac{\mathrm{dCA}}{\mathrm{dt}} = \frac{\mathrm{F}}{\mathrm{V}}(\mathrm{CAi} - \mathrm{CA}) - \mathrm{koe} - \frac{\mathrm{E}}{\mathrm{RT}}\mathrm{CA} \tag{1}$$

$$\frac{\mathrm{DT}}{dt} = \frac{F}{V}(\mathrm{T}i - \mathrm{T}) + \frac{(-\Delta\mathrm{Hr})\mathrm{koe} - \frac{E}{RT}CA}{pcCpc} - \frac{UA}{pcCpcV}(T - Tc) \tag{2}$$

The first input of the tank is the temperature, this will vary according to the cooling flow of the system, so it is called by Eq. (3):

$$\mathrm{Tc} = \frac{PcCpcFc\mathrm{Tco} + UA\mathrm{T}}{\mathrm{P}cCpc\mathrm{Fc} + \mathrm{UA}} \tag{3}$$

Taking into account these three equations, the mathematical model of the tank can be developed taking into account the following:

- Actuator model.
- Transmitter model.
- Identification system.

2.1 Actuator Model

Actuators allow modifying the process output for a specific result, thus generating a force that is generated by liquids, [12] electrical, solar energy, etc. This force is transferred to a solenoid valve and is defined by Eq. (4).

$$\mathrm{Gv(s)} = \frac{\mathrm{Kv}}{\mathrm{Tvs} + 1} \tag{4}$$

where:

Gv is the transfer function of the valve
Kv is the gain of the transfer function
Tvs is the time constant of the valve reaction

Gain of the mechanical part in Eq. (5):

$$\mathrm{G1} = \frac{(51-15)\left[\frac{\mathrm{L}}{\mathrm{min}}\right]}{(15-3)[\mathrm{psig}]} = 3\left[\frac{\mathrm{L}}{\mathrm{psig\ min}}\right] \tag{5}$$

Gain of the electrical part in Eq. (6):

$$G1 = \frac{(15-3)[psig]}{(20-4)[\mathrm{mA}]} = 0.75\left[\frac{psig}{mA}\right] \tag{6}$$

2.2 Transmitter Model

The temperature of the jacket is received by a transmitter which directs the signal to the controller to be converted and emitted towards the valve that is represented in Eq. (7) and Eq. (8) [13].

$$G\mathrm{CT}(s) = \frac{16}{0.1\mathrm{s} + 1} \tag{7}$$

$$GTT(s) = \frac{0.79}{0.1s + 1} \tag{8}$$

where:

GTT is the transfer function of the temperature transmitter.
GTC is the transfer function of the concentration transmitter.

3 Linearization

The CSTR is a non-linear system so it presents problems in obtaining results. To linearize it, an MPC is required since it has better performance and is easy to access [14] and can be simulated using MATLAB™.

It is based on the equivalent of Taylor series, which will be evaluated at the operating point.

3.1 Taylor Method

The Taylor method is frequently used to approximate results of differential equations in which it consists of approximating a function through the sum of integer powers of polynomials from the obtaining of derivatives to determine a value of the equation [15].

Therefore, the non-linear function is expressed in Eq. (9), which depends on the states of the model and the input signal to it.

$$\dot{\mathrm{X}} = \mathrm{f}(\mathrm{X}, \mu) \tag{9}$$

where its equivalent is based on Taylor series [13] where it is shown in Eq. (10):

$$\dot{\mathrm{X}} = f(X_{\mathrm{r}}, \mu_{\mathrm{r}}) + \frac{\partial \mathrm{f}(X, \mu)}{\partial \mathrm{X}}\bigg|_{\substack{\mathrm{X} = X_{\mathrm{r}} \\ \mu = \mu_r}} (\mathrm{X} - X_r) + \frac{\partial f(X, \mu)}{\partial \mu}\bigg|_{\substack{X = X_r \\ \mu = \mu_r}} (\mu - \mu_r) \tag{10}$$

The terms equal to and greater than the second order are simplified and cancelled, obtaining at the points χr, μr a linear function.

As a consequence, a small error is presented because the higher order terms do not have an impact on the operation point and function evaluation [14].

In this way, the state matrices used to represent the linearized model are obtained in Eq. (11) and Eq. (12):

$$\mathrm{A} = \frac{\partial \mathrm{f}(\mathrm{x}, \mu)}{\partial \mathrm{x}}\bigg|_{\substack{\mathrm{x} = \mathrm{x}_r \\ \mu = \mu_r}} \tag{11}$$

$$\mathrm{B} = \frac{\partial f(\mathrm{X}, \mu)}{\partial \mu}\bigg|_{\substack{\mathrm{x} = \mathrm{x}_r \\ \mu = \mu_r}} \tag{12}$$

4 Controller Design

4.1 Euler's Algorithm

It is a numerical method that allows finding the solution of a differential equation by transforming the differential equation to a finite difference equation [16].

This algorithm makes changes in the analysis of a curve and in the analysis of several lines, which is why it is called "constant slope".

4.2 Discretization of the Model

For the model to be discrete, the Euler algorithm is used, [14] for this reason, the system is expressed by Eq. (13):

$$\tilde{x}(k+1) = \bar{\mathrm{A}}\tilde{\mathrm{x}}(\mathrm{k}) + \bar{\mathrm{B}}\tilde{\mathrm{u}}(k) \tag{13}$$

Due to linearity, now the system has certain deviations with respect to the state and control variables [14] therefore, these deviations are considered with the use of Eq. (14) and Eq. (15). The sampling time considered is 0.1 s due to the CSTR is a plant with lower dynamics.

$$\tilde{x} = x_r - \mathrm{x} \tag{14}$$

$$\tilde{\mathrm{u}} = \mathrm{u}_r - \mathrm{u} \tag{15}$$

4.3 Aliasing Phenomenon

It is an effect that produces induced oscillations that have the ability to disturb the sensitivity, monitoring and prediction system of the process, so that the results of theprocess will present changes or certain errors in their obtaining due to the fact that the digital sampling will present signals that cannot distinguish.

Aliasing is constantly present in the transformation of analog to digital signals, due to the fact that these signals present an erroneous sampling [17].

Due to the aliasing effect, the MPC sampling time will present very high times and very low times that consequently will present errors in the precision of obtaining numerical results [14].

4.4 Controller Formulation

The MPC is formulated as a function of the state spaces presented in Eq. (16) and as variables in Eq. (17).

$$\mathrm{x_m}(k+1) = \mathrm{A}x_m(k) + \mathrm{B}\Delta \mathrm{u}(k) \tag{16}$$

$$x_m(k) = \left[\Delta\tilde{x}(k)^{\mathrm{T}} \;\; \tilde{\mathrm{y}}(k)\right]^{\mathrm{T}} \tag{17}$$

The deviation increments of the state variables and the deviations of the outputs to be controlled are needed. Output variables are controlled for best performance.

The changes of the state variables through the prediction horizon *Np* are predictable, therefore these are the actions that should be taken due to these changes, with the control horizon *Nc* [14].

4.5 Cost Function

To minimize Eq. (18) is used.

$$\mathrm{J} = \left(\mathrm{R_s} - \widetilde{\mathrm{Y}}\right)^{\mathrm{T}}\mathrm{Q}\left(R_s - \widetilde{Y}\right) + \Delta\mathrm{U}^{\mathrm{T}}\mathrm{R}\Delta U \tag{18}$$

The errors of the variables to be controlled and the increase in the control effort are taken into account. Furthermore, the terms mentioned above can be examined using the matrices *Q* and *R* [14].

4.6 Constraints

The constraints are implemented in the control variables, following Eq. (19):

$$\Delta \mathrm{u}^{\min} \leq \Delta u(\mathrm{k}) \leq \Delta \mathrm{u}^{max} \tag{19}$$

Said restriction is implemented in the temperature of the CSTR jacket and is represented in Eq. (20).

$$0[\mathrm{K}] \leq T_c(k) \leq 350[K] \tag{20}$$

4.7 How the System Works Using MATLAB™

MATLAB™ is a software written in C language that allows the programming, simulation and creation of user interfaces (GUI) of problems regarding automation systems, prediction, electrical circuits, among others.

To understand the operation of the CSTR system, a diagram of the reactor is required, followed by an MPC and the symbols that complement the system. By means of a flow diagram we can represent the operation of the system (Fig. 2).

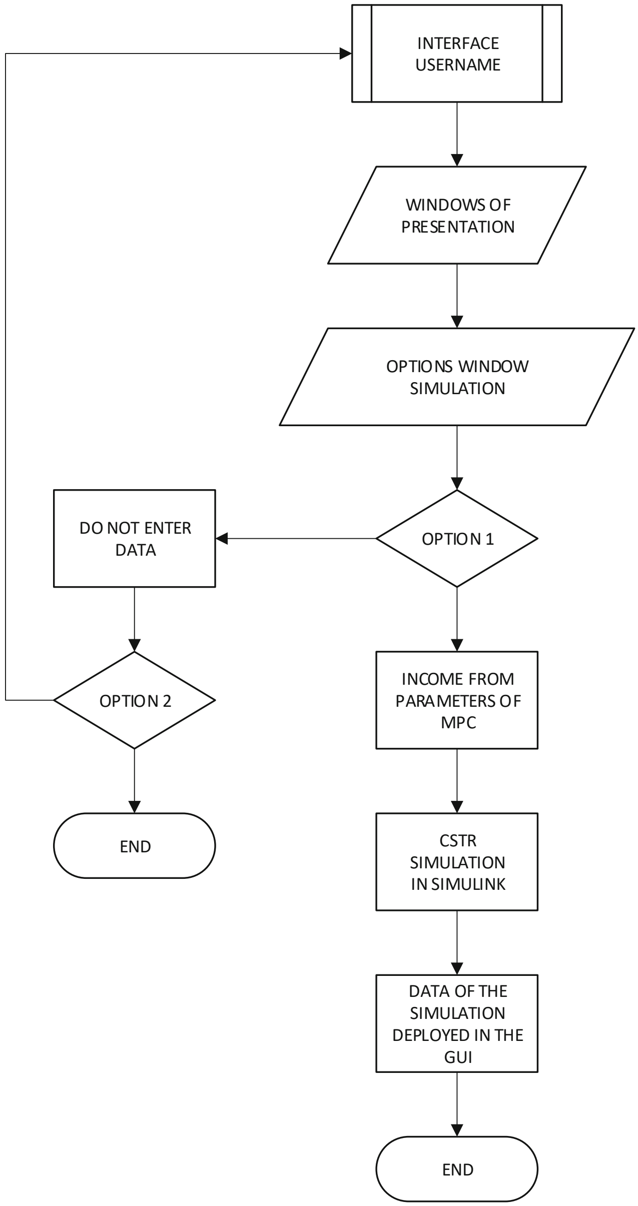

Fig. 2. Flow diagram of a CSTR to integrate an MPC.

5 Results

A simulation is performed in MATLB™ Simulink regarding the operation of the CSTR (Fig. 3).

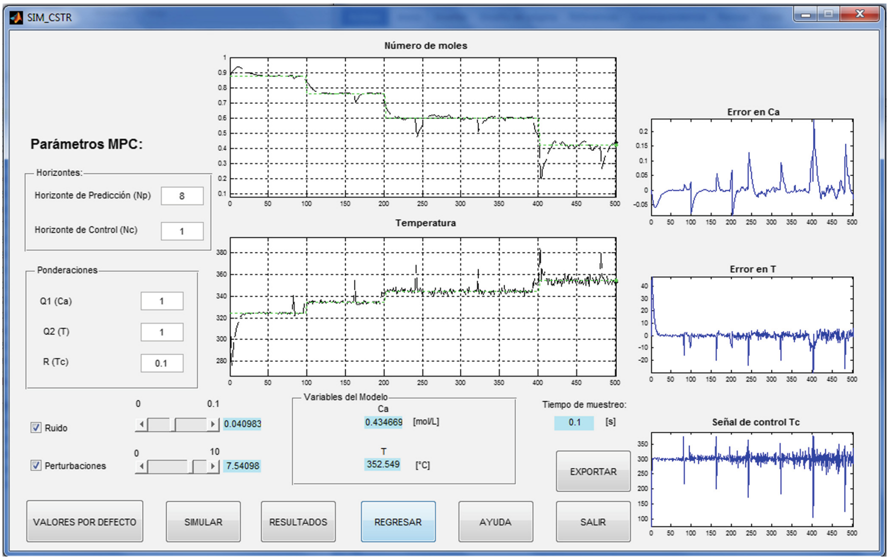

Fig. 3. Simulation of the CSTR in a GUI interface.

User can configure MPC parameters for tuning. In this case, tuning is a fundamental factor because it makes the plant robust in its operation and efficiency in the face of disturbances and noises that may occur.

MPC parameters used to achieve the operation point in the CSTR were:

- Prediction horizon (Np) = 8
- Control horizon (Nc) = 1
- Weight for control signal, R = 0.1
- Weight for CSTR's number of moles, Q1 = 1
- Weight for CSTR's temperature, Q2 = 1

The setpoint tracking is achieved as specified in the operation point. The software shows flexibility to change each value and see the effects in the performance of the CSTR. A detailed view for input and output variables are shown as follows (Fig. 4).

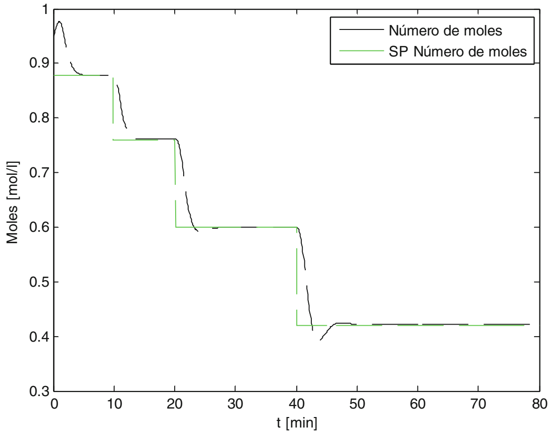

Fig. 4. Simulation of the CSTR in a GUI interface.

The maximum impulse changes its amplitude in every step of the setpoint. Despite of these changes, the number of moles shows a practical tracking in the linear zone of operation of the CSTR (Fig. 5).

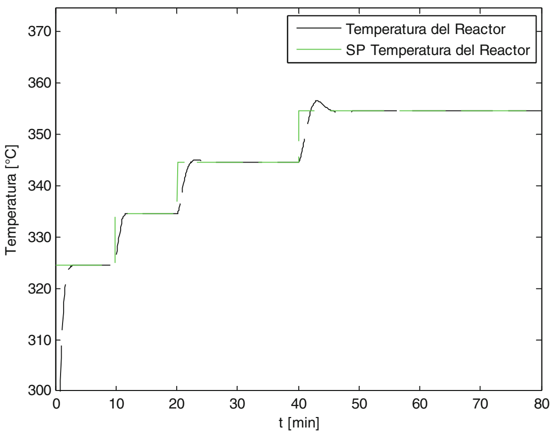

Fig. 5. Simulation of the CSTR in a GUI interface.

The temperature in the jacket reacts at the same tendency as the number of moles. These two variables are correlated, and the maximum impulse shows an increasing value in a far region of the operation point (Fig. 6).

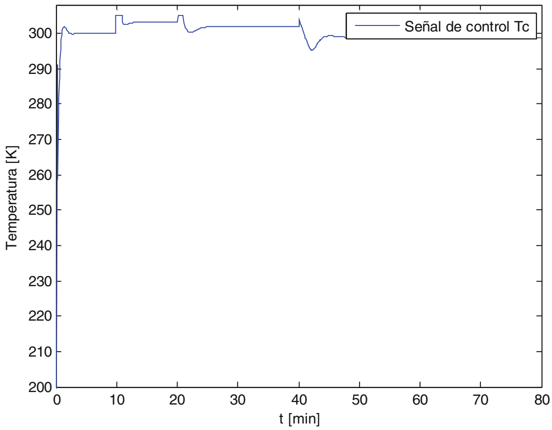

Fig. 6. Simulation of the CSTR in a GUI interface.

The control signal establishes its variations for different values steps. The control temperature varies in a region closed to the operation point. A final parameter to determine the effectivity on a MPC regulation is the algorithm time. This parameter shows the computational cost to resolver problem control and the applicability for a real-time implementation. In other words, if in each time where the MPC is solved the time is larger than the sampling time of the plant, the algorithm is not applicable because the closed-loop regulator cannot comply with the CSTR's dynamics (Fig. 7).

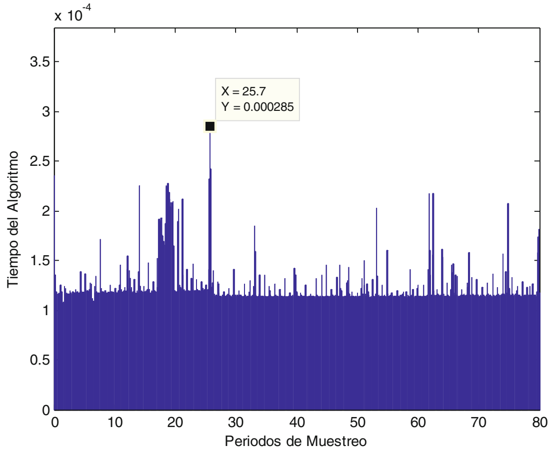

Fig. 7. Simulation of the CSTR in a GUI interface.

The time of the algorithm shows its peak at 28.5 μs. This value represents a lower quantity compared to the sampling time of 0.1 s.

The learning process for understanding MPC algorithm was performed with the observation of individual effects on MPC's parameters. The graphical interface showed the changes in control law and control variables after changing weights on control variables or prediction and control horizons. Variables with higher ponderation increased control performance but produced a control law with higher values. The individual changes on MPC parameters clearly shows a better understanding on how to tune slow-dynamic-processes such as CSTR.

6 Conclusions

The linearization of the plant becomes a valid alternative to adapt a linear control system in a non-linear one. Considering an effective region in spite of the nature of the plant produces a slight error, and the tuning parameters of the controller in the contiguous area must be changed until the set-point will be accomplished.

The algorithm of Euler represents a suitable option in schemes where the sampling time is not preponderant because some plants need very small steps to emulate the analog system. The step represents the sampling period in this project. As a numerical method alternative, the Runge-Kutta algorithm can be implemented, which is more accurate than the Euler technique.

Changing values one by one in the learning system provides the key information to understand the MPC variables and their impact on the process. The use of slow dynamic system such as the CSTR, produces the software an excellent tool to project real-life models in a simulation environment.

References

1. Gonzales, O., Rosales, A.: Robust MPC tuning by quadratic weights online estimation of the cost function through extended Kalman filter. In: 2018 International Conference on Information Systems and Computer Science (INCISCOS), pp. 49–54. IEEE (2018)
2. Khaled, N., Pattel, B.: Practical Design and Application of Model Predictive Control: MPC for MATLAB^{TM} and SIMULINK^{TM} Users. Butterworth-Heinemann (2018)
3. Khatoon, S., Chaturvedi, D.K., Hasan, N., Istiyaque, M.: Optimal controller design for two wheel mobile robot. In: 2018 3rd International Innovative Applications of Computational Intelligence on Power, Energy and Controls with their Impact on Humanity (CIPECH), pp. 1–5. IEEE (2018)
4. Saputro, J.S., Rusmin, P.H., Rochman, A.S.: Design and implementation of trajectory tracking motion in mobile robot skid steering using model predictive control. In: 2018 IEEE 8th International Conference on System Engineering and Technology (ICSET), pp. 73–78. IEEE (2018)
5. Incremona, G.P., Ferrara, A., Magni, L.: MPC for robot manipulators with integral sliding modes generation. IEEE/ASME Trans. Mechatron. **22**(3), 1299–1307 (2017)
6. Rossiter, J.A.: Model-Based Predictive Control: A Practical Approach. CRC Press (2017)
7. Dittmar, R.: Model predictive control mit matlab und simulink-model predictive control with MATLAB and SIMULINK. IntechOpen, Technical report (2019)
8. Coffey, B., Haghighat, F., Morofsky, E., Kutrowski, E.: A software framework for model predictive control with GenOpt. Energy Build. **42**(7), 1084–1092 (2010)

9. Chen, Y., Bruschetta, M., Picotti, E., Beghi, A.: MATMPC-a MATLAB based toolbox for real-time nonlinear model predictive control. In: 2019 18th European Control Conference (ECC), pp. 3365–3370. IEEE (2019)
10. Faedo, N., Olaya, S., Ringwood, J.V.: Optimal control, MPC and MPC-like algorithms for wave energy systems: an over- view. IFAC J. Syst. Control **1**, 37–56 (2017)
11. Kouvaritakis, B., Cannon, M. (eds.): Non-linear Predictive Control: Theory and Practice, no. 61 (2001)
12. Kouvaritakis, B., Cannon, M.: Model Predictive Control. Springer, Heidelberg (2016). https://doi.org/10.1007/978-3-319-24853-0
13. Gonzales Zurita, O.O.: Desarrollo de software para el aprendizaje y estudio del control predictivo en base a modelo (MPC) (Bachelor's thesis, Quito: EPN, 2014) (2014)
14. Gao, D.X., Liu, H., Cheng, J.: Optimal output tracking control for chemical process of non-isothermal CSTR. In: 2016 Chinese Control and Decision Conference (CCDC), pp. 4588–4592. IEEE, May 2016
15. Román, W., Barreno, N.: Desarrollo de un módulo didáctico en matlab para el análisis y expansión de las series de taylor y laurent development of a didactic module in matlab for the analysis and expansion of the taylor and laurent series. Revista Enegía Mecánica Innovación y Futuro (2), 15 (2016)
16. Garrao, R.B.: Estrategia EE (Excel-Euler) en la enseñanza de la Física. Latin Am. J. Phys. Educ. **1**(1), 19 (2007)
17. Ortiz Perdomo, J.L., Zapata Peña, J.: Uso del submuestreo para la detección de señales de la banda de dos metros por medio del aliasing en la aplicación de un scanner de alta velocidad. Revista Avances: Investigación en Ingeniería **12** (2015)

Implementation of a Sliding Mode Control in a Brushless DC Motor for the Emulation of a Robust Control in an Electric Bicycle

Oscar Gonzales(✉), Diego González, Christian Llumiquinga, Christian Ortega, and Mauricio Rosero

Instituto Superior Tecnológico Sucre, Campus Sur Av. Teodoro Gómez de la Torre S14 - 72 y Joaquín Gutiérrez, Quito, Ecuador
{ogonzales,dgonzalez,cllumiquinga,cortega, mrosero}@tecnologicosucre.edu.ec

Abstract. In this article a closed-loop regulation based on Slide Mode Control (SMC) is presented. The main objective is to control the speed of a brushless DC motor (BLDC) used in electric transportation such as electric bikes. The SMC algorithm represents and advanced and robust method to achieve setpoints in linear and non-linear plants. In this scenario, the SMC is an excellent alternative to control BLDC motor. This paper shows the process of designing MPC structure and reference tracking for speed values. Results are compared with a traditional control method like PID. Finally, compressions between these two control methods are performed to show the effectivity of SMC.

Keywords: BLDC · SMC · Close-loop control · IAE · ISE

1 Introduction

Currently, the use of electric transport systems has increased due to the need to reduce the production of CO_2 that deteriorates the quality of the air. According to the study carried out in [1], it is imperative to find a solution to mitigate environmental damages. There are different sources for electricity generation in Ecuador, where the most notable is diesel, which produces 261.31 tCO_2/Gwh. The importance of using brushless motors (BLDC) in transportation systems has increased in recent years due to the energy efficiency they can generate, as in the case of hybrid electric vehicles [1, 2].

The massive implementation of alternative transport methods is getting more customers in this field. These advances in technology provide benefits to human beings. Renewable energy or clean energy is a short-term objective to mitigate the deterioration of the quality of the atmosphere. An example of application is the bicycle that transforms mechanical energy into electrical energy through the universal principle of electrical machines. This energy can be used through batteries in any application coupled

© The Author(s), under exclusive license to Springer Nature Switzerland AG 2023
M. Zambrano Vizuete et al. (Eds.): RITAM 2021, LNNS 512, pp. 43–56, 2023.
https://doi.org/10.1007/978-3-031-11295-9_4

to the bicycle [3]. This application tries to replace the use of fossil fuels in transportation systems such as cars and motorcycles, which are the main origins of CO_2 for the environment. In this way, it is expected to spread the use of electric bicycles based on an innovative concept of renewable energy to alleviate the environmental damage caused by the high use of fossil fuels. These means of transport offer better efficiency in energy consumption, reduce technical problems such as less use on mechanical elements [3]. The use of a BLDC motor allows it to be adapted in applications with a varied range of speeds, its behavior is mostly linear with respect to voltage changes, for that reason it is an excellent option for transport systems such as electric bicycles [4]. On the other hand, the control of these systems has varied applications from basic controllers such as proportional-integral (PI) to advanced controllers such as fuzzy control [6]. However, in recent years more robust controllers such as Sliding Mode Control (SMC) have been implemented in electric machines regulation to control motor current and speed [7], with precise tracking for different references and robustness to reject external disturbances [8].

There are some works aimed to control BLDC motors, as in [9] where the authors carried out a fuzzy scheme to test the efficiency of the controller in the adjustable control of torque and speed. The results showed a high precision of the parameters adjusted online. In addition, the authors of [10] explained the operation of the Linear Quadratic Regulator Controller (LQR); the objective was the control on torque. The results showed an overshoot improvement in a specific rise time. According to [14], the main objective was to improve the control system on the feedback effects of the plant. The state of the hall effect sensor on the BLDC was adjusted to change the control system activity. If the sensor fails or the motor is damaged, an emergency signal stopped the motor. If the sensor is inactive, another signal seeks for establishing the optimal operation state of the BLDC system.

In [11], the authors regulated BLDC torque through a current controller. It showed a wide range of linear speed since it is very feasible to regulate BLDC motor currents, the controller converts the current, so it does not need an additional converter. In the study carried out [12] the ideal proportional derivative controller (PID) mentions characteristics that were considered as disturbances. The paper mentioned a good output response either due to fluctuations or sudden changes in the load, it will depend on the placement of poles for a better response time and frequency.

The mentioned works contemplate a wide range of applications for a better control of electrical machines. These reasons encourage to design and control a BLDC motor through a SMC controller for values of speed tracking. The SMC technique was used mainly on industrial processes but in the last years, this algorithm is improving plants with fast dynamics. These reasons represent the origin to develop the following work.

This paper is organized as follows: Sect. 2 resumes the main features of BLDC motor, Sect. 3 performs an identification process to determine the equivalent mathematical model of BLDC motor, Sect. 4 shows the mathematical design of SMC controller, Sect. 5 contemplates the results of this work, and finally conclusions are made out to emphasize the main ideas encountered in this paper.

2 BLDC Motor

To understand the main goal of this paper, it is imperative to analyze each section of the entire closed-loop system. Feedback signals form BLDC motor are recovered through an encoder located inside the motor. It allows to have speed variation and to identify these values on a control unit. To change the dynamic response of BLDC motor, a power electronic converter is needed, the control signal indicates what power switch must commute at specific time [13] (Fig. 1).

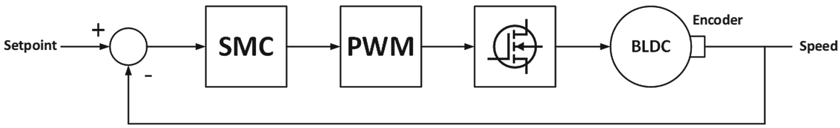

Fig. 1. System schematic of closed-loop control on BLDC

BLDC motor is characterized for having no brushes, so its weight is light, and it represents an excellent option to build an electric bicycle. The differences in weight and size are notable compared with similar motors without permanent magnets, with more power than a conventional DC motor. The BLDC motor operates on electromagnetism principles that makes a change on polarity to each coil inside it. The individual activation on the coils lets the BLDC motor change its movement and its speed as well.

2.1 Mathematical Modelling

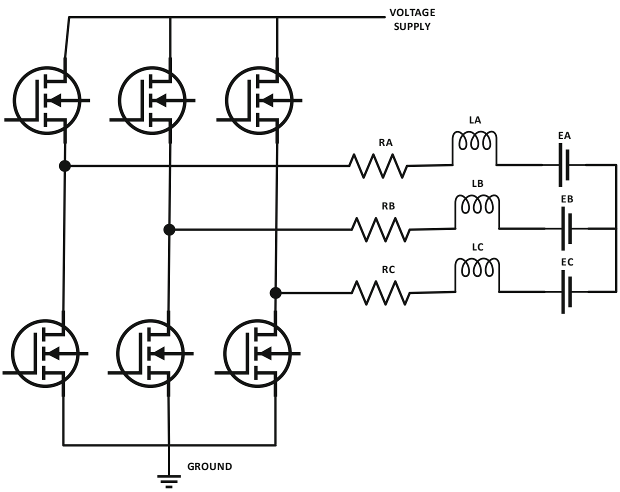

Fig. 2. Inverter bridge connected to a brushless DC motor.

In Fig. 2 the internal equivalent elements are seen in the BLDC motor. Each coil is surrounded by a resistance and electromagnetic force (EMF) source. The hall sensor is placed along the rotor to determine its positions in a determined time. In Eq. 1 is performed the Kirchhoff's Voltage Law at points A and B. The voltage $VPWM$ is supplied by the power converter adapted to the BLDC motor.

$$VPWM = (RA + RB)i + (LA + LB)L\frac{di}{dt} + (E1 + E2) \tag{1}$$

The EMF voltage is pointed out as E. In each phase of BLDC motor, the value of E is calculated from:

$$E = Ke * W(t) \tag{2}$$

Ke is the electrical constant of the motor and $W(t)$ is the motor speed. At the same time, equations for other relations between phases in the BLDC motor are performed:

$$\begin{aligned} \begin{pmatrix} VPWM1 \\ VPWM2 \\ VPWM3 \end{pmatrix} &= \begin{pmatrix} R1+R2 & 0 & 0 \\ 0 & R2+R3 & 0 \\ 0 & 0 & R1+R3 \end{pmatrix} \begin{pmatrix} i1 \\ i2 \\ i3 \end{pmatrix} \\ &+ \begin{pmatrix} L1+L2 & 0 & 0 \\ 0 & L2+L3 & 0 \\ 0 & 0 & L1+L3 \end{pmatrix} \begin{pmatrix} di1/dt \\ di2/dt \\ di3/dt \end{pmatrix} \\ &+ \begin{pmatrix} ke1+ke2 & 0 & 0 \\ 0 & ke2+ke3 & 0 \\ 0 & 0 & ke1+ke3 \end{pmatrix} w(t) \end{aligned} \tag{3}$$

The global equations for equivalent resistance, inductance and EMF in the BLDC motor are presented as follows:

$$R = 2/3\ (R1 + R2 + R3) \tag{4}$$

$$L = 2/3\ (L1 + L2 + L3) \tag{5}$$

$$ke = 2/3\ (ke1 + ke2 + ke3) \tag{6}$$

In this sense, the dynamical equation corresponding to the equivalent values or R, L and E is:

$$VPWM = R * i + \frac{diF}{dt} + ke * w \tag{7}$$

On the other hand, the equation that expresses the motor torque at the winding currents is:

$$Te = kt * i_f \tag{8}$$

Te is the electrical torque, *kt* is the mechanical constant of the motor and i_f is the current in each coil. Considering the electrical torque is equivalent to the inertia of the rotor, resulting in a friction loss, the dynamics of torque is expressed as:

$$Te = Tcte + J\frac{dw(t)}{dt} + Tloss \tag{9}$$

Tcte is the load torque, J is the inertia of the motor and $\frac{dw(t)}{dt}$ is the speed variation. The last two parameters represent the mechanical torque generated by the motor. *Tloss* is the torque lost by friction, it can be calculated as:

$$Tloss = B * W(t) + Kc * sign * W(t) \tag{10}$$

The new terms are B as the damping coefficient, Kc is a constant value and $W(t)$ is the speed. At last, the new equation with torque dynamics for BLDC motor is:

$$Kt * i_f = Tcte + J\frac{dw(t)}{dt} + B * W(t) + Kc * sign(w(t)) \tag{11}$$

3 Identification Process

3.1 Switching Sequence

Previously, it was mentioned that every coil on BLDC motor is energized to keep the motor moving at a specific speed. The switching sequence of coils is seen as follows (Table 1):

Table 1. Ignition switching of coils of a BLDC motor

Feeding		Hall effect sensor		
+	–	Ha	Hb	Hc
B	A	0	0	1
C	A	1	0	1
C	B	1	0	0
A	B	1	1	0
A	C	0	1	0
B	C	0	1	1

Depending on the polarity of feeding, the hall effect sensor located in phases A, B and C changes its value from 0 to 1 and vice-versa. The value is 1 if the rotor is under a specific phase, if not 0. This information makes the power converter triggers each power switch with the following sequence (Table 2):

Table 2. Semiconductor trigger sequences based on hall sensor states.

Hall effect sensor			Semiconductor					
Ha	Hb	Hc	Q1	Q2	Q3	Q4	Q5	Q6
0	0	1	0	0	1	1	0	0
1	0	1	0	0	0	1	1	0
1	0	0	0	0	0	0	1	1
1	1	0	1	0	0	0	0	1
0	1	0	1	1	0	0	0	0
0	1	1	0	1	1	0	0	0

Where Q1 to Q6 are the power switches commanded by the information of hall effect sensors.

In practical situations, it is recommended to extract an equivalent of first-order or second-order model of the plant from an open-loop response [15]. This equivalent model simplifies the mathematical expressions of the plant generating a feasible structure to develop the control algorithm. In this sense, the open-loop response of BLDC motor is seen as follows (Fig. 3):

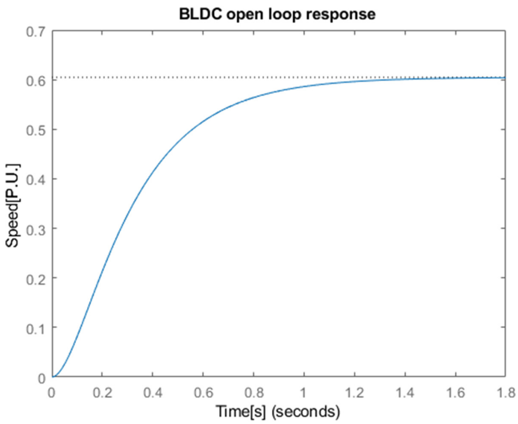

Fig. 3. Plant's open-loop response to a step input. [1]

Using MATLAB, the transfer function that indicates the BLDC response to a step input is in Eq. (12). This equivalent has 2 poles that will determine an election of a specific sliding surface for SMC design.

$$Gp(t) = \frac{f(s)}{\delta(s)} = \frac{26.22}{s^2 + 15s + 43.36} \tag{12}$$

4 Sliding Mode Controller (SMC)

The SMC consists of 2 functions: a continuous function and discontinuous one. In the first case, a sliding surface is needed to reach the objective as fast as possible. The sliding surface chosen for the BLDC control is:

$$S(t) = \left(\frac{d}{dt} + \Lambda\right)^n \int_0^t e(t)dt \tag{13}$$

where n is the degree of the characteristic polynomial of the system, e(t) is the error between the input signal and the output measurement.

The purpose of the control is to maintain the stability of a single value, so e(t) and its derivatives must be zero. When S(t) reaches a constant value, this means that e(t) will be zero throughout the execution time.

In the following equation it is possible to express the sum of the continuous part $U_c(t)$ and the discontinuous part $U_D(t)$, in order to demonstrate the sliding mode.

$$U(t) = U_c(t) + U_D(t) \tag{14}$$

The chosen sliding surface corresponds a PID-like structure:

$$S(t) = \frac{de(t)}{dt} + \Lambda_1 e(t) + \Lambda_0 \int_0^t e(t)dt \tag{15}$$

The derivative of the sliding surface equal to zero:

$$\frac{dS(t)}{dt} = \frac{d^2(t)}{dt^2} + \Lambda_1 \frac{de(t)}{dt} + \Lambda_0 e(t) = 0 \tag{16}$$

Replacing e(t) the one that gives the mean value that giving the expression:

$$\frac{d^2(t)}{dt^2} - \frac{d^2x(t)}{dt^2} + \Lambda_1 \frac{dx(t)}{dt} + \Lambda_0 e(t) = 0 \tag{17}$$

Thus, having the following expression with 2 poles:

$$Gp(S) = \frac{x_{(s)}}{U_{(s)}} = \frac{k}{(\tau_1 s + 1)(\tau_2 s + 1)} \tag{18}$$

Considering the expression of time:

$$\tau_1 \tau_2 \frac{d^2X(t)}{dt^2} + (\tau_1 + \tau_2)\frac{dX(t)}{dt} + X(t) = KU(t) \tag{19}$$

Through the Eqs. (15) and (17) it is possible to obtain the form of the continuous controller by means of the following expression:

$$U_c(t) = \left(\frac{\tau_1\tau_2}{K}\right)\left[\left(\frac{\tau_1+\tau_2}{\tau_1\tau_2} - \lambda_1\right)\frac{dX(t)}{dt} + \frac{X(t)}{\tau_1\tau_2} + \lambda_0 e(t) + \frac{d^2R(t)}{dt^2} + \lambda_1\frac{dR(t)}{dt}\right] \tag{20}$$

Since the input $R(t)$ is constant, the expression changes to:

$$U_c(t) = \left(\frac{\tau_1\tau_2}{K}\right)\left[\left(\frac{\tau_1+\tau_2}{\tau_1\tau_2} - \lambda_1\right)\frac{dX(t)}{dt} + \frac{X(t)}{\tau_1\tau_2} + \lambda_0 e(t)\right] \tag{21}$$

To have a more defined equation, consider the following values to replace in λ_1:

$$\lambda_1 = \frac{\tau_1+\tau_2}{\tau_1\tau_2} \tag{22}$$

To obtain an overdamped critical system, it is considered the following value for λ_0:

$$\lambda_0 \le \frac{\lambda_1^2}{4} \tag{23}$$

The continuous function is expressed by:

$$U_c(t) = \left(\frac{\tau_1\tau_2}{K}\right)\left[+\frac{X(t)}{\tau_1\tau_2} + \lambda_0 e(t)\right] \tag{24}$$

The discontinuous control is chosen according to [15]:

$$U_D(t) = K_D\frac{S(t)}{|S(t)| + \sigma} \tag{25}$$

Eliminating the derivative of the reference gives S(t):

$$S(t) = sign(K)[-\frac{dx(t)}{dt} + \gimel_1 e(t) + \gimel_0\int_0^t e(t)dt] \tag{26}$$

Obtaining K_D and δ values, a single equation is formed between (26) and (27).

$$K_D = \frac{0.51}{|K|}\left(\frac{\lambda_1}{\lambda_0}\right)^{0.76} \tag{27}$$

$$\delta = 0.68 + 0.12|K|KK_D\lambda_1 \tag{28}$$

When calculating the dimension of the input resistance where it is replaced in (7) having:

$$\mathrm{Gp(s)} = \frac{\mathrm{f(s)}}{\delta\mathrm{(s)}} = \frac{0.604}{(0.255\mathrm{s}+1)(0.09\mathrm{s}+1)} \tag{29}$$

where through (22) and (23) it is obtained that $\lambda_1 = 15$ and $\lambda_0 = 100$. Replacing in Eqs. (24) and (25): $K_D = 0.307$ and $\delta = 1.01$.

Considering the two equations as much as (14) and (21):

$$U_C(t) = (0.2)[0.023X(t) + 100e(t)] \tag{30}$$

The discontinuous part that ends with the equation:

$$\mathrm{U_D(t)} = 0.307\frac{\mathrm{S(t)}}{|\mathrm{S(t)}| + 1.01} \tag{31}$$

Remaining the following expression:

$$S(t) = \left[-\frac{dX(t)}{dt} + 15e(t) + 100\int_0^t e(t)dt\right] \tag{32}$$

In order to maintain a more stable control, the referential derivatives are eliminated since they are detrimental to the system in order to obtain a more robust and reliable control.

5 Results

In Fig. 4, the control scheme is presented:

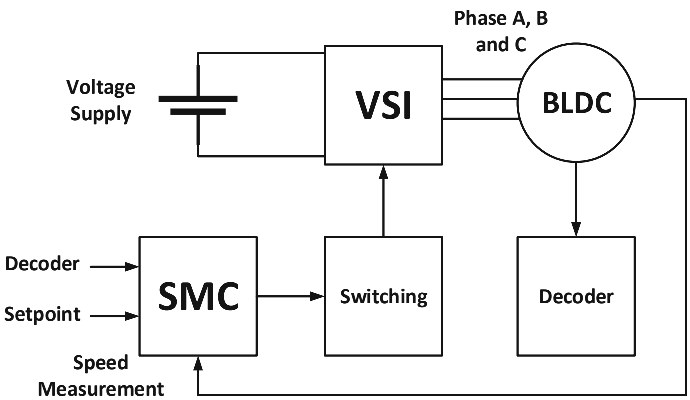

Fig. 4. Controller diagram in slider mode [2].

It is observed that the controller inputs are the setpoint and the measured value, while the output is the value of the odd semiconductor working relationships. The BLDC motor is controlled by a power converter called Voltage Source Inverter (VSI). Signals from speed and the states of the hall sensors are feedback data for the SMC controller in order to generate de control law (Fig. 5).

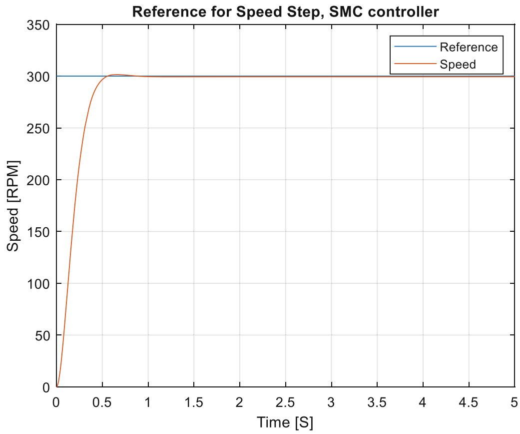

Fig. 5. SMC controller at a 300 rpm reference.

A step of 300 rpm is placed as setpoint. The SMC controller achieves its objective at a settling time of 0.48s. On the other hand, a PI controller is used to compare performance between these two algorithms. The PI controller, which was expressed as:

$$GG_{PI}(s) = 0.00039\left(1 + \frac{609.105}{s}\right) \tag{33}$$

The Fig. 6 represents a system that reaches the reference of 300 rpm like in the case of SMC:

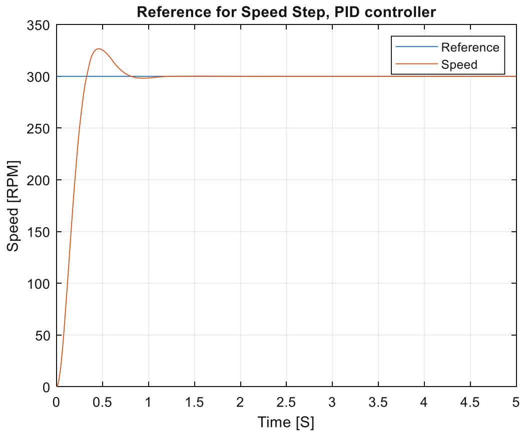

Fig. 6. System with the PI controller at a reference of 300 rpm.

The settling time is 0.68 s and has an overshoot of 8%. In this sense, other actions are takes like the setpoint tracking for different speed values. The SMC response and the PI response are observed as follows (Figs. 7 and 8):

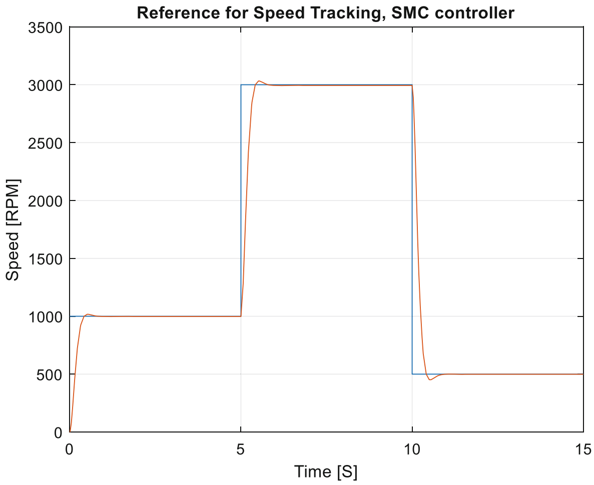

Fig. 7. SMC controller tracking to reference.

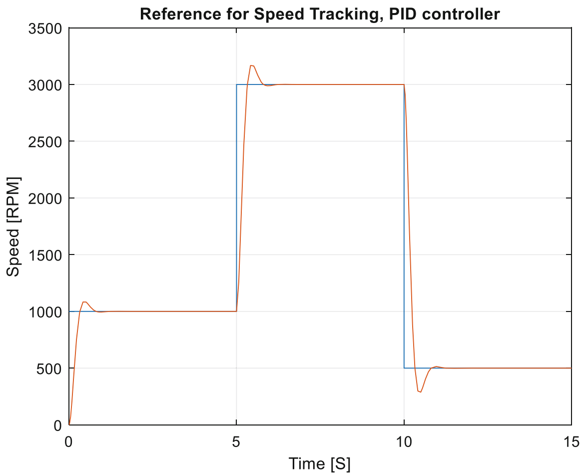

Fig. 8. PI controller tracking to reference.

The SMC presents better capabilities compared to the PI. The step values were placed to analyze an increasing and decreasing speed situation. Finally, a comparison between the SMC and the PI is placed in one graph to notice the main advantages of the SMC, especially in fast dynamics and minimum overshoot (Fig. 9).

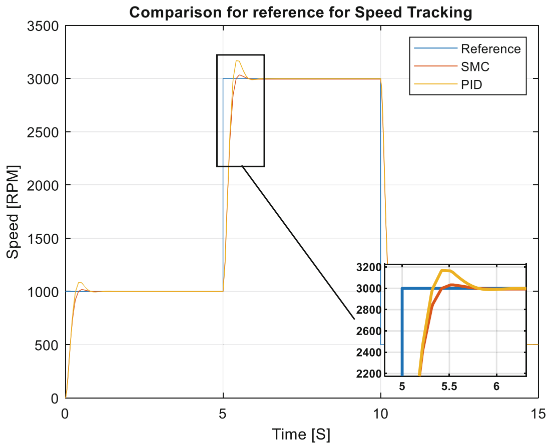

Fig. 9. System response comparison between SMC and PID controllers.

A zoom in the time of 5 s shows a massive overshoot of the PI regulator while the SMC has a soft change to reach the reference. The step changes are sudden changes that shows the clear differences on the dynamics on the SCM and PI. The SMC is faster, this is realized due to the action of the discontinuous function. The action of the continuous function keeps the tracking at almost zero error at steady state. Finally, a numerical approach to observe the efficiency of the SMC over the PI. This approach is the numerical indexes Integral of Absolute Error (IAE) and Integral of Square Error (ISE) [16].

$$IAE = \int_0^t |e(t)|dt \tag{34}$$

$$ISE = \int_0^t e(t)^2 dt \tag{35}$$

The graphical bars of these values are seen in the next graph (Fig. 10):

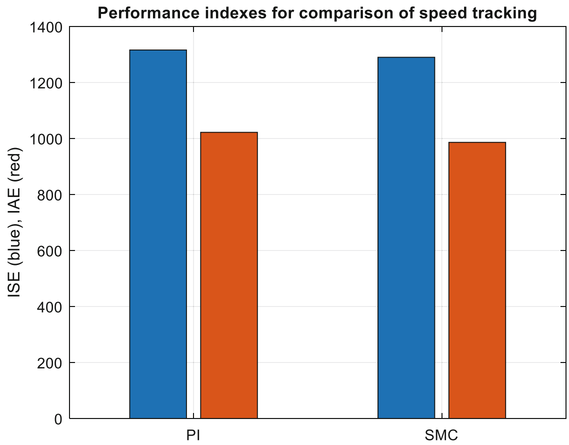

Fig. 10. Performance index of SMC and PID controllers.

The *IAE* is 1311.15 and *ISE* is 1011.7 in the SMC while the values in the PI are *IAE* is 1380.2 and *ISE* is 1019.6. Clearly, the SMC represents a better control method, specially for sudden changes of the reference of speed.

6 Conclusions

The SMC controller is versatile for control linear and non-linear plants. In the case of BLDC motor, the fast dynamics are achieved with short settling time and almost zero overshoot.

The identification method based on a step response of the plant shows a mathematical model usable for control design. The BLDC has linear dynamics where the step response corresponds to a viable method to model complex systems.

For a fast change of setpoint values, the discontinuous function shows robustness to these sudden changes. The discontinuous function based on a switch principle with softness parameters achieves high requirements of control.

References

1. Paredes, L., Pozo, M.: Movilidad Eléctrica y Eficiencia Energética en el Sistema de Transporte Público del Ecuador un Mecanismo para Reducir Emisiones de CO_2. Rev. Técnica “Energía” **16**(2), 91–99 (2020). https://doi.org/10.37116/revistaenergia.v16.n2.2020.356
2. Rakhmawati, R., Irianto, Ruwano, F.T.: Implementation of fuzzy logic control for soft-starting method brushless DC motor at electric bicycle. In: Proceedings - 2019 International Seminar on Application for Technology of Information and Communication: Industry 4.0: Retrospect, Prospect, and Challenges, iSemantic 2019, pp. 497–502 (2019). https://doi.org/10.1109/ISEMANTIC.2019.8884281
3. Cita 5 Pronóstico, vol. 4, pp. 4–6 (2017)
4. Montazerigh, M.: Suspensión Energía Regeneración en, vol. 60, no. 10, pp. 4546–4553 (2013)

5. Bou-mosleh, C., Rahme, P., Beaino, P., Mattar, R., Nassif, E.A.: Contribución a la producción de energía limpia utilizando un Nuevo convertidor de energía de onda, pp. 108–111 (2014)
6. Wu, H.C., Wen, M.Y., Wong, C.C.: Speed control of BLDC motors using hall effect sensors based on DSP. In: 2016 IEEE International Conference on System Science and Engineering, ICSSE 2016 (2016). https://doi.org/10.1109/ICSSE.2016.7551633
7. Rhyu, S.H., Khaliq, S., Eun, R., Doek, K.: Diseño y Análisis de Flujo Axial Permanente Motor de imán para bicicletas eléctricas con Núcleo de estator híbrido (2017)
8. Xintong, M., Yang, Y., Introducción, I.: Motor DC sin escobillas basado en el modo deslizante de múltiples órdenes DC SIN ESCOBILLAS, no. 2, pp. 1157–1162 (2020)
9. Zhan, Y.D., Guo, Y.G., Zhu, J.G.: Terminal sliding mode speed controller based on vector control for brushless doubly fed machine. In: 2011 International Conference on Applied Superconductivity and Electromagnetic Devices, ASEMD 2011, pp. 200–203 (2011). https://doi.org/10.1109/ASEMD.2011.6145100
10. Zarma, T.A., Mustapha, B.M., Suleiman, H.U., Galadima, A.A., Ashigweke, E.C., Thomas, S.: Torque control in brushless DC motor using intelligent linear quadratic regulator controller. In: IEEE International Conference on Adaptive Science and Technology, ICAST, vol. 2018-Augus, no. 1, pp. 1–7 (2018). https://doi.org/10.1109/ICASTECH.2018.8507030
11. Nama, T., Gogoi, A.K., Tripathy, P.: Application of a smart hall effect sensor system for 3-phase BLDC drives. In: Proceedings of the 2017 IEEE 5th International Symposium on Robotics and Intelligent Sensors, IRIS 2017, vol. 2018-Janua, pp. 208–212 (2018). https://doi.org/10.1109/IRIS.2017.8250123
12. Sarala, P., Kodad, S.F., Sarvesh, B.: Analysis of closed loop current controlled BLDC motor drive. In: International Conference on Electrical, Electronics, and Optimization Techniques, ICEEOT 2016, pp. 1464–1468 (2016). https://doi.org/10.1109/ICEEOT.2016.7754925
13. Shekhar, S., Saha, P.K., Thakura, P.R.: Optimal PID tuning of BLDC drive using LQR technique. In: Proceedings of the 2019 IEEE International Conference on Intelligent Systems and Green Technology, ICISGT 2019, vol. 2, pp. 57–61 (2019). https://doi.org/10.1109/ICISGT44072.2019.00028
14. Balseca, J.: Lazo de control de velocidad de un motor busheles por modos deslizantes
15. Gonzales, O., Rosales, A.: Sliding mode controller based on a linear quadratic integral regulator surface for power control on a dual active bridge converter. In: 2018 IEEE Third Ecuador Technical Chapters Meeting (ETCM), pp. 1–6. IEEE, October 2018
16. Gonzales, O.: Parametric and non-parametric mathematical modelling techniques: a practical approach of an electrical machine identification. Ecuadorian Sci. J. **5**(1), 30–36 (2021)

CFD Evaluation of an Adaptable Protective Cabinet for Patients with Infectious-Contagious Diseases

Bruno Vallecilla Amores[1,2], Diana Belén Peralta-Zurita[1(✉)], Jaime Vinicio Molina Osejos[1], and Edison Corrales Segovia[2]

[1] Universidad Internacional SEK del Ecuador, Quito 170302, Ecuador
{bgamores.mdin,diana.peralta,jaime.molina}@uisek.edu.ec
[2] Instituto Superior Tecnológico Cotopaxi, Tanicuchí, Ecuador
{bgamoresv,ejsegoviac}@istx.edu.ec

Abstract. Infectious diseases are those generated by microorganisms, such as viruses, bacteria, fungi and parasites, which can be transmitted through direct contact with infected patients, their blood or their secretions. In this sense, the objective of this study is to analyze the design and manufacture of a prototype of a safe cabin for patient care, in order to protect the lives of health personnel and the need to adapt to the coronavirus crisis. In this research, methods of documentary review, scientific observation, Inductive Deductive were used. As a result of the validation in computational fluid dynamics CDF on the behavior of sneezing and coughing in patients or with infectious diseases, the sizing and simulation of a safe, ergonomic and functional cabin is proposed that allows to improve protection against infectious diseases of health professionals in Ecuador. It is concluded that the visualization and understanding of the behavior of sneezing within a cabin contributes to improving the designs of protection cabinets and reducing the spread of pathogenic particles as much as possible. Getting a maximum velocity as 14.4 m/s in 0.25 s.

Keywords: Infectious contagious · CFD · Design · Spread · Coronavirus

1 Introduction

Infectious contagious diseases are those generated by microorganisms, such as viruses, bacteria, fungi, and parasites, which can be transmitted through direct contact with infected patients, their blood, or their secretions. Of the most common in certain social settings, we have: hepatitis B or C, HIV/AIDS, tuberculosis, meningitis, flu, chickenpox, measles, pediculosis, coronavirus [1] An exemplary case according to [2] cited by [3] are the coronaviruses that affect humans by zoonotic transmission, they usually cause epidemic health problems in outbreaks of greater severity and social impact. This was the case of the MERS-CoV, which from April 2012 to May 16, 2015, originated 1,373 cases of MERS with 528 deaths. All the cases had been reported in the Arabian Peninsula, whether they were indigenous people or travelers from that area, until an outbreak in

© The Author(s), under exclusive license to Springer Nature Switzerland AG 2023
M. Zambrano Vizuete et al. (Eds.): RITAM 2021, LNNS 512, pp. 57–70, 2023.
https://doi.org/10.1007/978-3-031-11295-9_5

South Korea in May 2015. Since July 4, 2015, there were no more cases of MERS-CoV, which is why the international alert regarding this outbreak was closed in September 2015. Since Ecuador was not prepared for this pandemic, the number of infections increased by tens of hundreds of people in a day. Ecuador was one of the countries hardest hit during the first weeks of the spread of the coronavirus in Latin America, this burden is transferred to doctors and nurses who did not have enough protective material [4], until May 18, the National Institute for Public Health Research (INSPI) has taken 96,536 samples of which 33,582 are positive for COVID -19 [5].

The virus that causes COVID-19 spreads very easily and continuously between people who are in close contact (up to about 6 feet away), through respiratory droplets that are produced when an infected person coughs, sneezes or speech, these droplets may end up in the up in the mouth or nose of those close by or possibly be inhaled and reach the lungs [6]. According to the manual of Prevention and Control Guidelines for Suspected or Confirmed Cases of SARS CoV-2/COVID-19 of the Public Health Mystery of Ecuador, the health professional who provides direct care to patients with COVID19 WITH procedures that generate aerosols, you must use a particulate protection respirator with a minimum protection level of N95 (certified by the National Institute for Occupational Safety and Health (NIOSH), FFP2 (European Union standard (EU) or similar, a disposable long-sleeved gown with reinforced cuffs, Eye protection (single glasses), Handling or non-sterile gloves and a hair cap [4].

The importance of generating safe cabins, which in certain cases the designs come from foreign sources and are adapted in the country, that are making protection cabins and are distributing them in Latin America, having these greater presence and acceptance. Other efforts by Universities to develop prototype cabinets to take samples of coronavirus or Covid-19. According to [7], a sneeze, approximately 40,000 microdroplets are expelled at a speed of 14 m/s (average), being able to reach a distance of 6 m, or by recent data up to 8 m. Coughing expels around 3000 microdroplets, reaches 2 m in distance and at a speed of 10 m/s. Talking for "5 min" is the same as coughing (3000 microdroplets of burden) at a speed of 1 m/s, reaching 1 m away (Fig. 1).

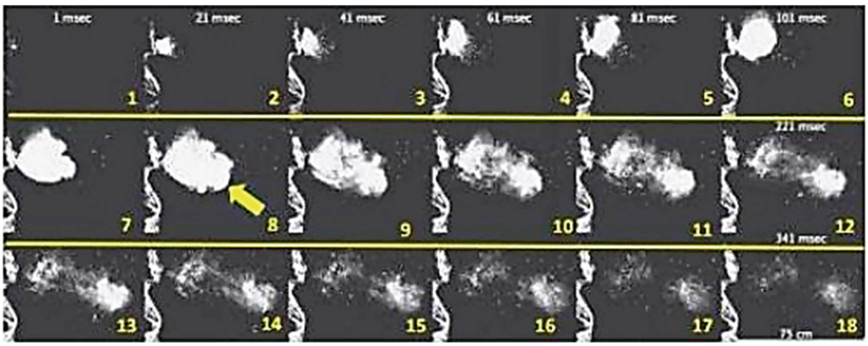

Fig. 1. Sneeze with 1000 f/s in 18 frames every 20 ms.

2 Methodology

This research was developed in three phases, the first is the elaboration of the cabin model, the second stage simulating the prototype (closed cabin) in the CFD XFLOW software, this in order to understand the behavior of sneezing. In the third stage, the simulation will be carried out with the cabin open, here the behavior of the fluid in the environment is analyzed under normal conditions.

2.1 Numerical Method

Over the last few years, schemes based on minimal kinetic models for the Boltzmann equationare becoming in creasingly popular a sareliable alternative to conventional CFD approaches. The Lattice Boltzmann method (LBM) was originally developed as an improved modification of the Lattice Gas Automata to remove statistical noise and achieve better Galilean invariance [16, 17].

2.2 Discrete Phase Modeling

The force balance for a droplet is given in a Lagrangian reference frame, which contains inertia, stokes drag and gravitational force. For x direction in Cartesian coordinates

$$\frac{du_p}{dt} = F_D\left(u - u_p\right) + F_g$$

where u_p is the droplet velocity, u is the fluid phase velocity, F_g is the gravitational force, and $F_D\left(u - u_p\right)$ is the Stokes drag force.

$$Fg = \frac{\mathrm{g}x\left(\rho_p - \rho\right)}{\rho_p}$$

$$FD = \frac{18\mu}{\rho_p d_p^2 C_c}$$

where rp and r are the density of droplet and air, respectively, m is the molecular velocity of air, dp is the droplet diameter, and Cc is the Cunningham correction to Stokes [18] (Fig. 2).

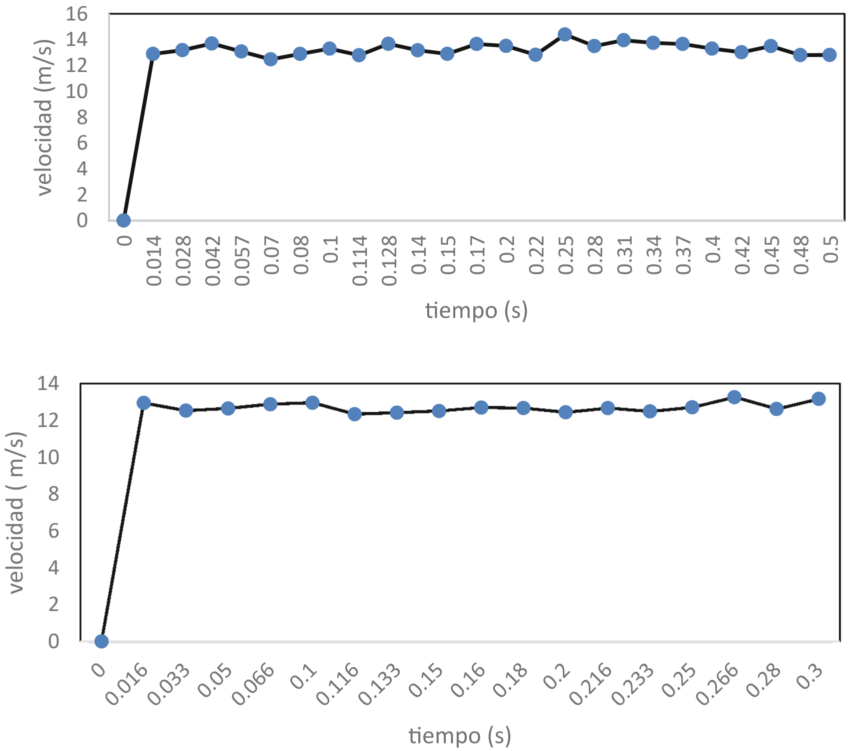

Fig. 2. Airflow velocity dependent on the time of sneeze 1 and 2

2.3 Stability Parameter

The key parameter of a simulation in order for the results to be valid is the stability parameter, XFLOW defines the mathematical convergence and stability in the simulation. The stability parameter must satisfy the Courant condition.

The Courant number is the quotient between the time interval and the re-silence time of a finite volume.

$$C = \frac{\Delta t}{\Delta X} = \frac{\mu \Delta t}{\Delta X}$$

2.4 System Mass Balance

The simulation must meet the mass balance in our study case, two substances intervene obtaining [19]:

$$m_{inH2O} + m_{in\dot{A}IRE} - m_{outH2O} - m_{outAIRE} = \frac{d(\dot{m}_{H2O} + \dot{m}_{AIRE})}{dt}$$

One of the elementary factors to generate a product based on the Design Thinking technique is to satisfy the design from the user's point of view, therefore, it is important to define the user as the main element, that is, based on the standard precautions intended to reduce the risk of transmission of transmissible pathogens that should be applied in the care of any patient regardless of their diagnosis or presumed infection status. To develop the proposal, it is necessary to have a list of attributes generated for the development, such as: identifying key characteristics based on recommendations from health professionals, for which an interview is developed (see Table 1), which establishes an indicator of importance on a scale from 0 to 10, where 10 is considered the most relevant and 0 is considered unimportant [10].

Table 1. Interview about product design specifications.

Necessity	Parameter	Importance 1–10 metric
The protection screen is made of hard material	Amount of protection	10
Contains holes in the back for aerosol work	Number of holes	10
Filters to protect against particles must be fitted	Number of filters	1
Contains holes on top and sides for handling work using globes	Number of holes	1

2.5 Safety Cabinet Modeling

The model has measures of the cabin are 692 × 590 × 578 mm, the material selected for the protection cabin was transparent polypropylene PP of 6 mm. Once the model is made, it is assembled with the 3D head modeling. The measurements of the protection cabin were based on the width and length of the stretchers that can be found in medical centers, hospitals and places of care for patients with infectious diseases. In this research, in order to understand the behavior of sneezing, a closed cabin is modeled and whose volume will be the domain for the study in X FLOW, for test 2 the following changes are made to this cabin:

- Opening the inlet holes
- 692 × 590 mm rear wall opening (Fig. 3)

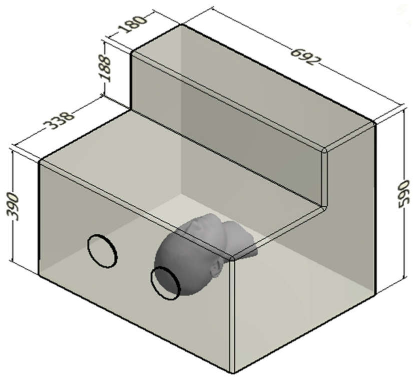

Fig. 3. 3D protective cabin modeling

2.6 3D Head Model

To take the anthropometric measurements of the head as a reference, the analysis of the mannequin and the details of the facial features used in the turbulent thermal effect CFD performed by [11] was performed. The views of the mannequin and the details of the facial features, (all lengths are in centimeters. The anthropometric measurements of the 3D head that will be used for the CFD simulation are detailed below. manikin from [11] obtaining the same measurements and validating their morphology for the CFD simulation. The image shows the anthropometric measurements of the mannequin to be simulated.

2.7 Simulation Settings

To perform the sneeze analysis in XFLOW, it will first be done in a closed cabin, to understand the sneeze and how it behaves according to the parameters to be established. The simulations will be developed in two stages (Fig. 4).

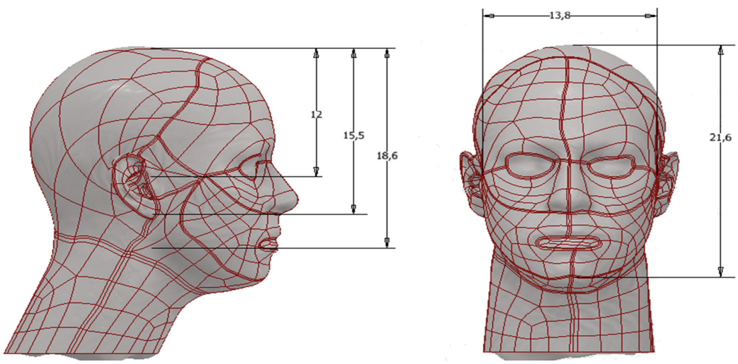

Fig. 4. Anthropometric measurements of mannequin to simulate

- First stage simulation with the cabin completely closed.
- Second stage simulation with the cabin open.

The main characteristic is that it does not require the creation of meshes since it performs a kinetic approximation based on particles. This avoids the creation of the traditional non-uniform mesh that would limit the complexity of the surfaces of geometric objects. Specifically, it uses a proprietary technology based on Lattice Boltzmann (LBM) methods. The use of LBM enables efficient execution on massively parallelized architectures. How XFlow performs the discretization frees the user to configure specific parameters of the algorithms, facilitating the learning of the simulator. It is only necessary to configure the parameters that control the arrangement and sizes of the cells of the discretization [12]. The table below describes the material parameters.

2.8 XFLOW Temporal Discretization

XFLOW automatically calculates the time step that will remain constant during the simulation. This is calculated considering the maximum initial velocity and the pressure gradient of the domain, the minimum cell size and the value of the Courant grouper given by the user. The Courant number by default is set to 1, since it is the stability limit (Table 2).

Table 2. Material parameters

Property	Value	Unit	
Operating temperature	308		K
Viscosity model	Newtonian		
Liquid	Water		
Gas	Air		
	Water	Air	
Density	998,3	1,225	kg/m^3
Dynamic viscosity	0,001	1,79E−05	$Pa \cdot s$
Molecular weight	18,015	28,996	g/mol
Surface tension	0,072		N/m
Contact angle	90	degrees	

The stability parameter must satisfy the Courant-Friedrichs-Lewy (CFL) condition and, therefore, its value must be less than 1. If it reaches 1, it means that somewhere in the CFL domain it is not being fulfilled, the stability of simulation is not assured. A stability parameter less than 1 means that the stability of the number scheme is guaranteed and therefore the solution must be consistent. If it is very close to 0, the Courant number can be increased to save calculation time. XFLOW recommends a stability parameter

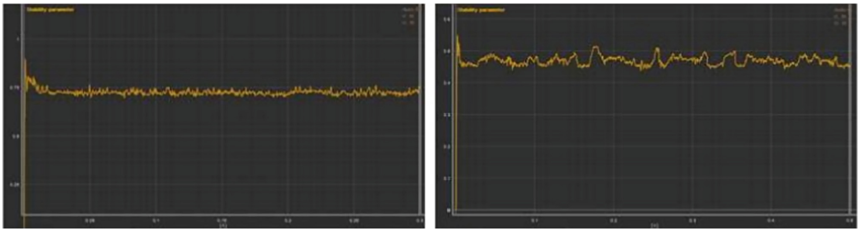

Fig. 5. Anthropometric measurements of mannequin to simulate

between 0.1 and 0.3 [14]. The following graph shows the stability parameter of the CFL simulation in stage 1 and stage 2 (Fig. 5).

The results obtained are corroborated with the Courant-Friedrichs-Lewy (CFL) number obtained in each simulation of the XFLOW program, where the stability must be less than 1. The Courant number of sneeze 1 is 0.75, while which in sneeze 2 is 0.5.

3 Results and Discussions

3.1 Outcome 1 (Sneeze 1 Fully Enclosed Protective Cabin Simulation)

To achieve the best result, this simulation was programmed with 4 cores, for 1.35 h. In total, they consumed 4 × 1.35 = 5.4 h of computing. the resolution scale is 0.008 m, from the research of [13], and his team found that the size of the droplets ranges between 160 μm and 1 mm in diameter, and they leave at a speed of about 14 m/s (about 50 km/h) Bearing: The full domain has 169404 elements, the equivalent single resolution domain has 270396, the equivalent single resolution domain size is (58 × 63 × 74). To carry out the simulation, there are two elements that will be given the boundary conditions.

3.2 Droplet Dispersion Inside the Enclosed Cabin

The sequence below shows the beginning of the sneeze and how the flow changes when a refinement algorithm (Near static wall) is used, simulation time 0.3 s, and it is represented with the letter t, resolution scale 0.008 m. In the time 0.02 s at the beginning of the sneeze, it is appreciated how the fluid begins to exit through the mouth to appreciate this behavior, visualization perspectives are determined:

- A) Side. To track particles, it is necessary to capture at different times: a) t = 0.016 s, b) t = 0.05 s, t = 0.083, c) t = 0.15 s, d) t = 0.21 s, e) t = 0.3 s, determining that the fluid collides in the protection cabin generating the dispersion of drops throughout the cabin.

3.3 Speed

Natural human exhalation streams, such as coughing, sneezing, and breathing, can be thought of as 'jet-shaped' airstreams in the sense that they are produced from a single source in a single exhalation effort. The following graphs detail the speed with which the flow interacts with the environment around the booth. The maximum speed of 13.25 m/s in 0.26 s. For this analysis, the following is taken as a reference: t = 0.016 s and t = 0.3 s. According to the results, the speed is between A) 12.9 m/s and B) 13.16 m/s (Figs. 6 and 7).

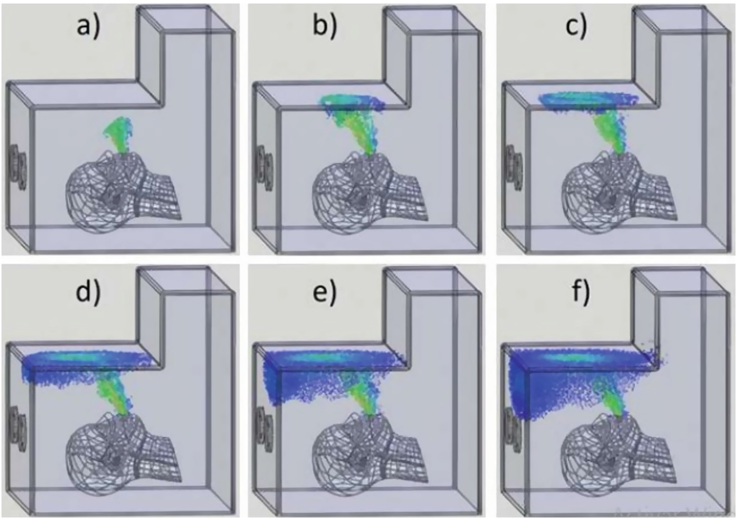

Fig. 6. Sneezing behavior 1

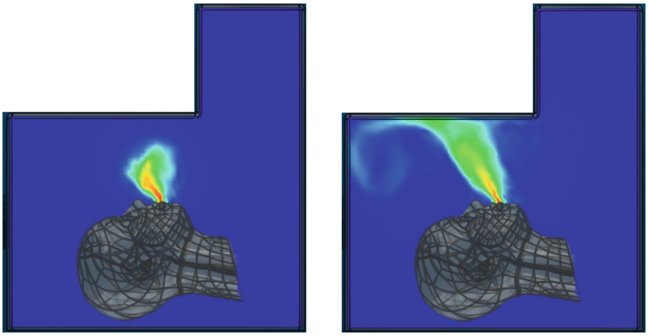

Fig. 7. Sneezing speed 1

3.4 FOV Field of View

The field of view or field of perspective, also known by its equivalent acronym FOV (Field of view) is the extent of the observable world at a given moment (Fig. 8).

In the case of 3D computer graphics, it refers to the angle that can be perceived from the virtual world generated in the display device associated with the position of

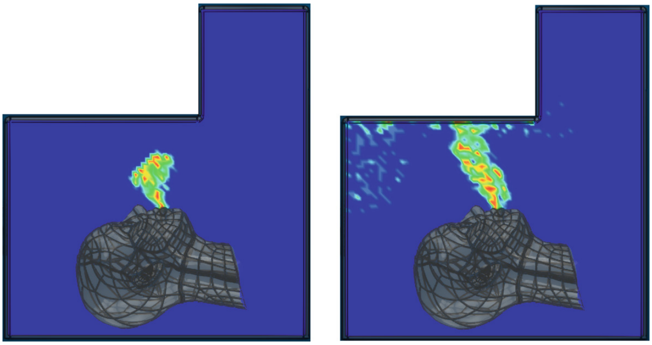

Fig. 8. Field FOV sneeze

the point of view. The VOF model can model two or more immiscible fluids by solving a single set of moment equations and tracking the volume fraction of each of the fluids throughout the domain. Typical applications include the prediction of jet rupture, the movement of large bubbles in a liquid, the movement of the liquid after a dam rupture, and the constant or transient monitoring of any liquid-gas interface [15].

3.5 Vorticity

The vorticity is one of the important parameters to analyze in the results, especially the vortices that are generated at the tip of the mouth as the sneeze begins, it can be seen that there is air resistance around it, to have a perspective from its behavior, a sequence of images is generated from t = 0.1 s to t = 1.82 s.

3.6 Analysis 2 (Sneeze 2 Fully Open Protective Cabin Simulation)

To achieve the best result, this simulation was programmed with 4 cores, for 2 h. In total they consumed $4 \times 2 = 8$ h of computing. the resolution scales 0.017 m for all with a reference speed of 14 m/s. Bearing: The full domain has 849053 elements, the equivalent single resolution domain has 270396, the equivalent single resolution domain size is (58 $\times$ 63 $\times$ 74) (Fig. 9).

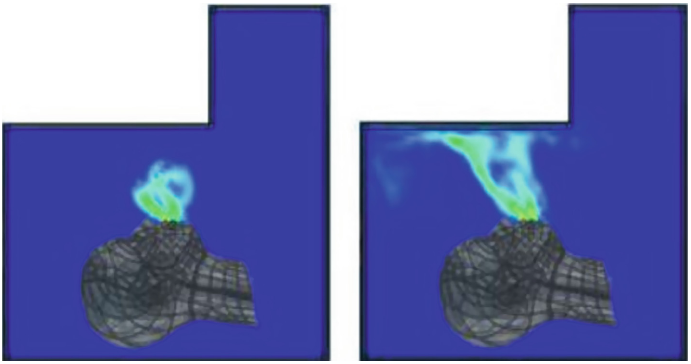

Fig. 9. Sneeze vorticity 1

3.7 Droplet Dispersion in and Out of the Open Cabin

The sequence below shows the beginning of the sneeze as the flow changes when using a refinement algorithm (Near static walls), simulation time is 0.5 s. In the time 0.014 s, it is appreciated how the fluid begins to come out of the mouth, the results are attached in a perspective:

A) Lateral

In this scan of images, it can be seen how the flow leaves the mouth and spreads in the cabin very quickly, that is to say, in 0.1 s the volume is fully occupied and leaves the cabin to the outside. The speed of the fluid in the environment can be seen through the different colors. During the entire time interval, the behavior of the droplets when sneezing can be appreciated and as the speed varies, the movement of the particles is considered in a) t = 0.014 s, b) t = 0.05 s, c) t = 0, 12, d) t = 0.242, e) t = 0.37 s, f) t = 0.5 s.

- Time t = 0.017 s the maximum speed is 13.2 m/s.

3.8 Velocity

The following graphs detail the speed with which the flow interacts with the environment around the booth, this must be included in the interaction with the environment under normal conditions, the maximum velocity obtained was 14.4 m/s in 0.25 s. For this analysis, the following is taken as a reference: Time t = 0.242 s, it is observed that the flow begins to exit from the inside of the protection cabin to the outside, the blue dots represent the flow outside the cabin (Fig. 10).

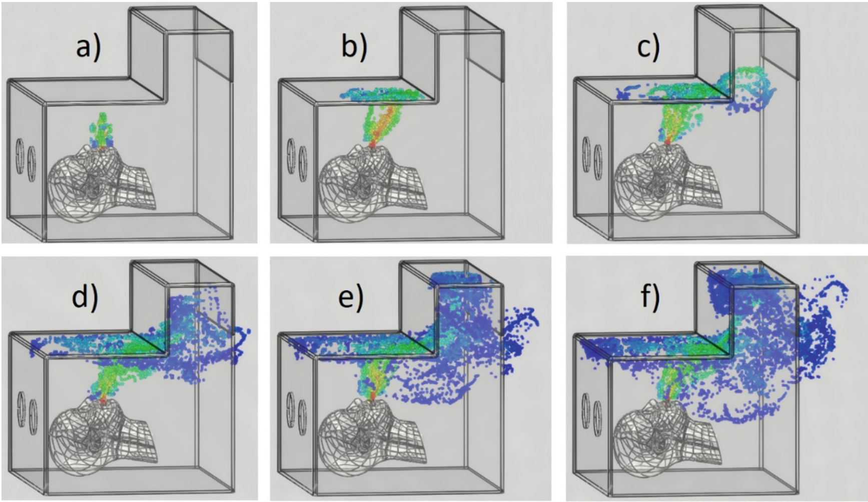

Fig. 10. Sneezing behavior 2

3.9 FOV Field of View

Effective field of view (FOV) analysis, at t = time, for analysis t = 0.014 s t = 0.22 s t = 0.5 s is considered (Fig. 11).

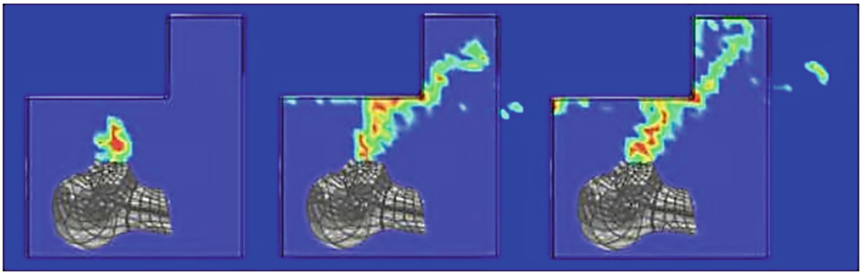

Fig. 11. Field FOV sneeze

3.10 Droplet Distance in Open Protective Booth Simulation

For the analysis of this result, sneeze 2 was taken into account since the simulation occurs in an open cabin, in a time of 0.5 s the particles travel is approximately 0.7 mt, considering the vertical position of the manikin and that the fluid hits the walls of the cabin. The following image verifies the distance traveled by the particles in side and top view. The grid scale (0.1 m) of the XFLOW program was taken into account for this measure (Fig. 12).

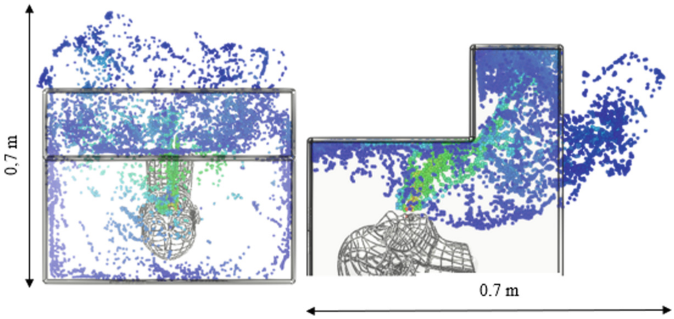

Fig. 12. Sneezing behavior 2

The data obtained was compared with a study carried out by (Busco, Yang, Seo, & Hassan, 2020) comparing the distribution of the accumulated time of the sneeze droplets. Front view (a) and top view (b). In this study at $t = 0.45$ s with a speed of 17 m/s the manikin in vertical position and without elements that interfere with the trajectory, the distance traveled was 1 m and at 2 s 4 m.

4 Conclusions

Another verification result is the flow velocity from the mouth to the part closest to the protection booth whose distance is 157 mm. In sneeze 1 the velocity is 13.15 m/s. In sneeze 2, the speed is 13.96 m/s, while in the study by (Bahl, M. de Silva, Chughtai, & MacIntyre, 2020), where it is observed that the speed ranged between 12 and 15 m/s. 50 mm distance.

The flow path of sneeze 1 and sneeze 2 is different due to booth conditions and boundary parameters. The sneeze 1, being in a completely closed environment, the particles collide with the walls of the cabin spreading at high speed, immediately the particles descend to the floor due to the action of gravity.

The results of the CFD simulation in XFLOW predicted the movement of the ejected droplets in terms of spatial distribution under initial conditions and compared them with real sneezing studies around the laboratory obtaining very similar results.

References

1. Purushothaman, S., et al.: Electroconvulsive therapy, personal protective equipment and aerosol generating procedures: a review to guide practice during Coronavirus Disease 2019 (COVID-19) pandemic. Australas. Psychiatry **28**(6), 632–635 (2020)
2. Velay, A., et al.: Tick-borne encephalitis virus: molecular determinants of neuropathogenesis of an emerging pathogen. Crit. Rev. Microbiol. **45**(4), 472–493 (2019)
3. Baker, M.G., Wilson, N., Blakely, T.: Elimination could be the optimal response strategy for Covid-19 and other emerging pandemic diseases. BMJ **371** (2020)
4. Chiquito, K., Monard, S., Zhangallimbay, D., Perez, M.: Evaluación de fac tores del comportamiento ciudadano y acceso a servicios relacionados con la vulnerabilidad de contagio del sars-cov-2 en ecuador. Compendium: Cuadernos de Economía y Administración **7**(2), 109–119 (2020)

5. Alcivar, F.V.: Modelación de Covid-19 en ecuador. Matematica **18**(2) (2020)
6. Piñera, M., de Esteban, C., Rodríguez, A., Arrieta, F., et al.: Recomendaciones para la prevención de la desnutrición en pacientes con enfermedad del coronavirus 2019 en seguimiento por atención primaria: Papel del control nutri- cional. Aten. Primaria **53**(1), 122 (2021)
7. Lombardero, M.: En un estornudo, aproximadamente 40.000 microgotas son expulsadas a una velocidad de 75 mts/seg (promedio), pudiendo alcanzar un recorrido de 6 metros, o por datos recientes hasta 8 metros
8. Saldivia, R.K.O., Ojeda, S., Ivanissevich, M.L.: Envejecimiento y enfer-medades respiratorias en las personas adultas mayores. el caso de un centro de jubilados de rio gallegos. Informes Científicos Técnicos-UNPA **12**(3), 166–193 (2020)
9. Contaminacion del aire, el medio ambiente de la superficie y el equipo de proteccion personal por el s´ındrome respiratorio agudo severo coronavirus 2 (sars-cov-2) de un paciente sintomatico, Jama
10. Flores Benitez, F.R.: Diseño y construccion de un bullbar delantero para adaptar un winche para rescate, en las camionetas dmax rt50 empleadas por el cuerpo de bomberos ibarra (2018)
11. Naseri, A., Abouali, O., Ahmadi, G.: Efecto de la pluma térmica turbulenta sobre la eficiencia de aspiracion de micropartículas. Building and Environment
12. Garcıa Villanueva, A.: Estudio cfd del flujo turbulento alrededor de álabes de turbomáquinas con modelo TRANS SST. B.S. thesis, Universitat Politècnica de Catalunya (2015)
13. Ilyas, S., Srivastava, R.R., Kim, H.: Disinfection technology and strategies for COVID-19 hospital and bio-medical waste management. Sci. Total Environ. **749**, 141652 (2020)
14. Chávez-Modena, M., Martínez, J.L., Cabello, J.A., Ferrer, E.: Simulations of aerodynamic separated flows using the lattice Boltzmann solver XFlow. Energies **13**(19), 5146 (2020)
15. Chumchan, C., Rattanadecho, P.: Experimental and numerical investigation of dam break flow propagation passed through complex obstacles using LES model based on FVM and LBM. Songklanakarin J. Sci. Technol. **42**(3) (2020)
16. Guo, Z., Xu, K.: Progress of discrete unified gas-kinetic scheme for multiscale flows. Adv. Aerodyn. **3**(1), 1–42 (2020). https://doi.org/10.1186/s42774-020-00058-3
17. Peng, Y., et al.: Application of computational fluid dynamics in subway environment without fire and smoke—literature review. Build. Environ. 108408 (2021)
18. Zhang, Y., Li, X.: Monitoring and analysis of subway tunnel thermal environment: a case study in Guangzhou China. Sustain. Cities Soc. **55**, 102057 (2020)

Electronic Device Designed for Object Recognize and Navigation Assistant by Artificial Vision for People with Visual Impairment

Lesly Cadena(✉), Xavier David Rógel, and Nelson Sotomayor

Escuela Politécnica Nacional, Quito, Ecuador
leslycadena@hotmail.com, nelson.sotomayor@epn.edu.ec

Abstract. In this project, a prototype of object recognition and mobility aid is developed for people with visual disabilities using artificial vision, stereo vision, and neural networks. This prototype has two operation modes, the first generates obstacle-free routes using mobile robotics navigation algorithms and the second recognizes the objects that are around the user and indicates what type of objects there are and where they are placed in the work environment, this information is delivered to the user through spanish audio messages. The system design was developed in the Python programming language in a single board computer Raspberry pi 4B. The prototype has two web cameras that were used to acquire the visual environment.

Keywords: Neuronal networks · Stereo vision · Artificial vision

1 Introduction

People with visual disabilities face a series of issues that complicate their personal and professional life, mobility being one of the main problems they face. Blind people tend to be hit with obstacles that are out of the reach of the white cane, mainly elevated objects or that have protruding parts, in addition, the white cane is not able to identify what type of obstacle is restricting the user way or if it represents any danger to the user.

For these problems, the electronic prototype designed allows the users to navigate in closed environments and help them to identify objects that are inside their environment. The information of the work environment is sent to the user by an audio message through a single earphone. The object of this work is to let the people with visual disabilities can to develop the ability to create mental maps of the environment in the walk, in such a way they can mobilize with their autonomy. This device has a stereo vision system to know the position of the obstacles with which the user could hit and also the system uses object recognition algorithms to identify what type of objects are inside the user's mobilization environment.

As the prototype uses a stereo vision system and objects recognition algorithms, it is necessary to mention two main topics which are neural networks and stereoscopic vision.

© The Author(s), under exclusive license to Springer Nature Switzerland AG 2023
M. Zambrano Vizuete et al. (Eds.): RITAM 2021, LNNS 512, pp. 71–86, 2023.
https://doi.org/10.1007/978-3-031-11295-9_6

1.1 Neuronal Networks

Neural networks are a set of machine learning algorithms that use already known information to generate new solutions or responses to variable environments [1]. The prototype uses a convolutional neural network named Yolo to identify 12 different objects commonly found in houses, buildings, and parking lots. This algorithm was used due to its learning capacity and its reduced response time.

1.2 Stero Vision

Stereoscopic vision is part of artificial intelligence, the stereo vision system aims is to reconstruct a three-dimensional environment using the information provided by many image sources. In this case, the prototype has two web cameras aligned on the horizontal axis that work as a stereo camera. This prototype allows the calculation the depth of the obstacles that are found using SAD matching algorithms [2].

2 State of Art

At present there are some commercial devices that help the mobility of people with visual impairment. Devices such as ultracane, allow the user to evade the obstacles using ultrasonic sensors that detect obstacles that are closer, this type of sensors are placed in a white walking stick. Many of these devices have a reduced range of obstacles detection and also they do not have the option to recognize what type of objects are in front of the user. The electronic device that is detailed in this work has the ability to detect twelve different objects while the user navigates in an specific environment [3].

3 Method

This section will address the development of the hardware and software of the designed device.

3.1 Hardware

The prototype has a single board computer Raspberry pi 4b, two webcams with 1080 pixel resolution and 78° horizontal viewing angle, a headset, a 5200 mAh Li-ion battery and, a user interface that has three connected buttons to the single board, which help the user to interact with the prototype. Figure 1 shows the hardware architecture of the prototype, the type of signals sent by each of the peripherals to the main computer is detailed and the Fig. 2 shows the prototype built.

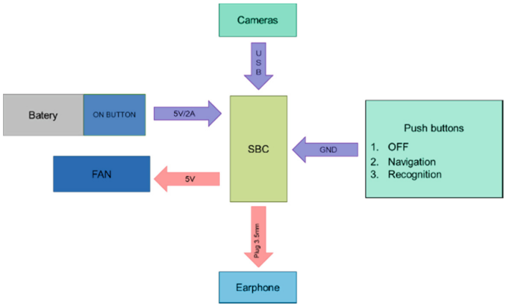

Fig. 1. Hardware architecture.

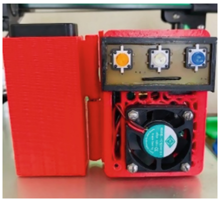

Fig. 2. Prototype built.

3.2 Software

Figure 3 shows the software architecture of the device. The execution of the different algorithms depends on the reading of the user interface. Pressing the power button releases battery power by turning on the Raspberry Pi and then running the main system program, this algorithm constantly captures images of the environment and stays running until one of the three remaining buttons is pressed. The system is divided into two operating modes, in the first is the object recognition algorithm and in the second mode, the obstacle-free route generation algorithm is developed. Each of the algorithms uses the images captured by the main program as input information.

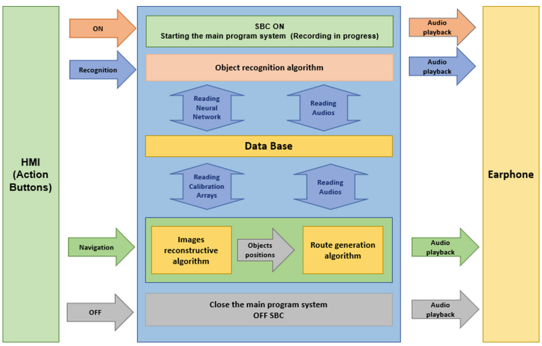

Fig. 3. Software arquitecture.

3.3 Object Recognition Algorithm

This algorithm uses a YOLO-type neural network model, made up of a convolutional neural network (CNN), and also uses one-phase deep learning techniques. The operation of this algorithm is divided into 4 stages [4].

1. The first one divides the input image into an S × S size grid.
2. In the second stage, a location algorithm is executed for each grid and a vector is obtained that stores the position, size, and reliability of the existence of a certain type of object. With this information bounding boxes grouping those squares that have detected the same object [5].
3. In stage three, a specific color is placed on each grid to classify the object detected in each one of them.
4. Finally, in stage four, the location information obtained with the bounding boxes and the classification results is used to eliminate those bounding boxes that have a low probability that an object exists, in this way the prediction is obtained correct or closest to the actual object and a final bounding box is drawn.

In Fig. 4 the four stages previously described are shown.

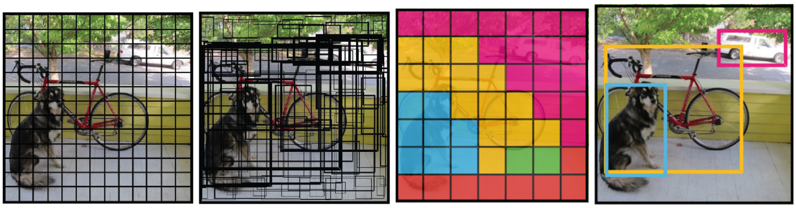

Fig. 4. Final detection result [6].

The prototype can recognize 12 different types of objects such as Bicycles, Cars, Screens (televisions or monitors), Doors, Laptops, Chairs, Couch, Apples, Bottles, Cups, Toothbrushes, and Toilets. To train the network, it is necessary to follow an orderly process. Figure 5 shows the flow chart that indicates the stages of the training and validation process of the YOLO network.

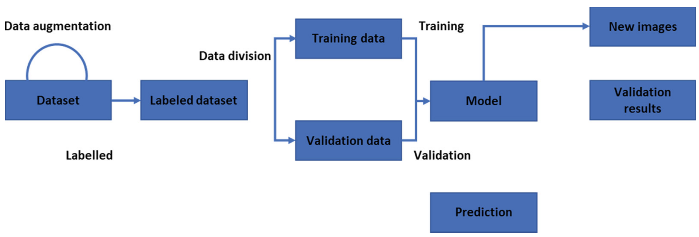

Fig. 5. Working diagram to build a detection model in YOLO [7].

Dataset: For the training of this network, around 9600 images were collected, obtained from the "Desafío Pascal VOC 2012" database, downloaded directly from the internet, and also taken directly by the developers. To avoid fit problems, it is necessary to train the neural network with at least 1000 samples per object, for this reason, the data augmentation technique was used to increase the number of images of each class of object.

Data Augmentation: With this method, it is possible to change the size, light, position, color, and intensity of the images previously collected using the Open CV and skimage libraries. At the end of this stage, around 12000 total images were obtained. In Fig. 6 an example of the image augmentation process is observed.

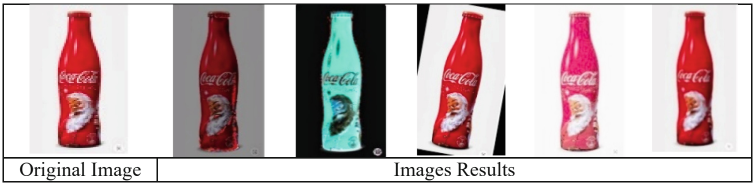

Fig. 6. Data augmentation process of the original image.

Data Labeling: Once the data augmentation stage is finished, the labeling of the images begins, in this process the object to be detected is framed and a label is placed on it. An example of a labeled bicycle is shown in Fig. 7 for this process the labelimage software was used.

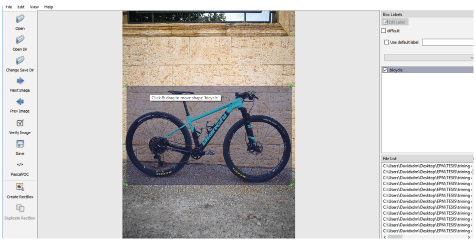

Fig. 7. Process of labeling a bicycle in the labelimage program

Dataset Split: Once all the images are labeled, the database is divided into two sets, 90% is used for training the network, and the remaining 10% for the validation process.

Net Training: The training process was carried out on a computer with Windows 10 operating system, Intel (R) Core (TM) i7-8550 processor, 1.8 Hz speed, and 12 GB RAM. Before starting the training process, a virtual environment was created with Python 3.6 and the darkflow repository was downloaded, which allows training on the YOLO network. It is necessary to establish the number of object classes that the network will identify and the number of filters that will be modified during training. In addition to these values, it is necessary to specify the following parameters.

Batch: Define the number of images that will enter the network learning process each time the network adjusts to the real model, this value is set to 32 images for each learning step.

Epoch: Number of times the network evaluates the entire set of training images. In this work, a value of 30 epochs was established.

Learning Rate: The learning speed of the network, for this process a value of 0.001 was used. With these values established, the training process took a total of 30 continuous hours, and the model was prevented from having overfitting problems.

Model Validation: After training the model, its validation begins, 10% of images from the database were used. To evaluate the performance of the network, the contingency matrix was considered for the calculation of the following validation parameters.

mAp (Mean Average Precision): Evaluates the precision of the model considering only the true positive predictions, focusing on the predicted location with the real one.

F1-Score: Evaluate how accurate the trained model is considering true-positive, false-negative, and false-positive predictions.

With the results obtained in Fig. 8(a) the precision of the model was calculated, which in this case is 60.54%. Finally, Fig. 8(b) shows the global precision of the object identification algorithm and the individual precision of each of the classes of objects that the device can identify.

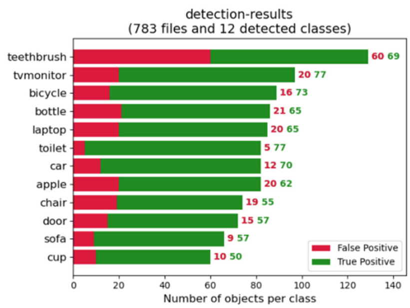

(a)

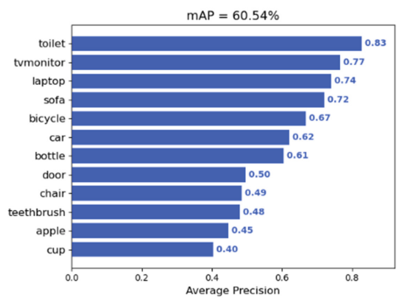

(b)

Fig. 8. Resultsof the validation process

3.4 Navigation Algorithm

The navigation algorithm has the ability to find the position of obstacles that are within the work environment, and with this information generate an obstacle-free route for the user. Figure 9 shows the stereo vision system that uses two Logitech HD cameras adapted in a 3D structure designed specifically for this application.

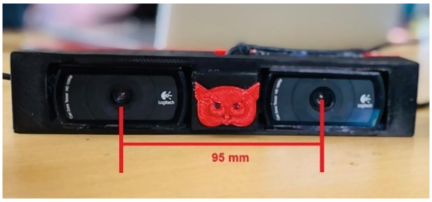

Fig. 9. Vision stereo system case

To better understand this stage, it is necessary to define two important parameters of stereoscopic vision, epipolar geometry, and disparity.

Epipolar Geometry: To obtain the distance of each point in the image, a search process of correspondence between the stereo images is carried out, once it is known which pixels correspond to each other, the disparity between them is calculated. If the cameras that make up the stereo system are perfectly aligned to the horizontal axis, it is ensured that the corresponding points between the two images have the same coordinates on the "y" axis. Due to this phenomenon, the search for corresponding pixels is no longer carried out on the entire image but only on the row that corresponds to the vertical axis of the pixel whose correspondence is sought [2].

The Disparity of a System: The disparity is the difference between the coordinates of the projection of a point on two optical planes, considering that the optical axes are parallel and there is no distortion in the camera lenses. The disparity is defined by Eq. (1) and the geometry of the stereo system is shown in Fig. 10.

$$d = X_I - X_D \tag{1}$$

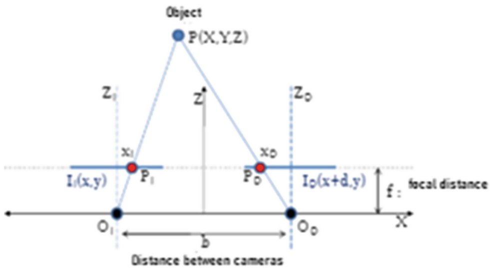

Fig. 10. Stereo vision system triangulation [8].

After performing some mathematical operations and applying the disparate equation, for each focal plane the final result is Eq. (2).

$$Z = \frac{f * b}{d} \tag{2}$$

In this way, it follows that the disparity is inversely proportional to the distance from point P. As observed in Eq. 2 to obtain the depth value it is necessary to use the focal length of the cameras, for this particular case it is used cameras with automatic focus since the focus value (f) is variable, it is necessary to make a linear approximation to know the relationship between the disparity values and the measured distance of an object towards the stereo system. Table 1 keeps the values of disparity and distance as a result of varying the position of an object captured by the stereo system. The data are captured from the distance 330 cm to 40 cm taking the stereo system as reference. Considering this information, the maximum and minimum detection distance are configured.

Table 1. Disparity and distance data.

	Distance (cm)	Disparity		Distance (cm)	Disparity
1.	330	104	**9.**	125	173
2.	300	119	**10.**	100	192
3.	275	121	**11.**	90	206
4.	250	131	**12.**	80	207
5.	225	134	**13.**	70	210
6.	200	139	**14.**	60	162
7.	175	140	**15.**	50	150
8.	150	154	**16.**	40	155

The data of Table 1 shows the disparity is inversely proportional to the distance, this information generates a curve approximately, explained with the Eq. (3). Figure 11 shows the resultant curve of the Table 2 data.

$$y = 1460, 3e^{-0,014x} \tag{3}$$

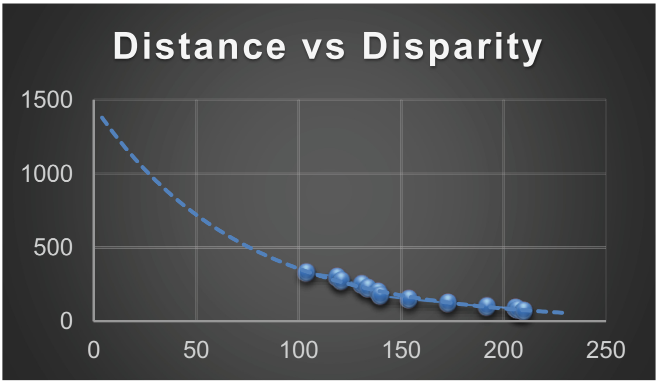

Fig. 11. Resultant of linear approximation of disparity and distance data.

Equation (3) is used to calculate the depth of the detected obstacles regarding disparity values generated by the image reconstruction algorithm.

3.5 Image Reconstruction Algorithm [2]

The image reconstruction algorithm SGBM(Semi-Global Block Matching) is based on the development of the SAD matching technique, it calculates the depth of each pixel contrasting the areas of two stereo images which are one the same epipolar line. This algorithm needs two images aligned to the horizontal axis as inputs, consequently, the cameras must be calibrated. The first step of the calibration process is setting the cameras into a previously designed case where they are perfectly aligned to the horizontal axis and also have a separation know the distance. The next step is taking 45 double images of a chessboard that has 9 × 6 inner corners, they are used to calculated rectification arrays which aligned the left with the right image of the stereo camera. The calibration process is only performed once because the rectification arrays must be saved in the database of the prototype to be used at any time. Figure 12 shows the input images for the calibration process [9].

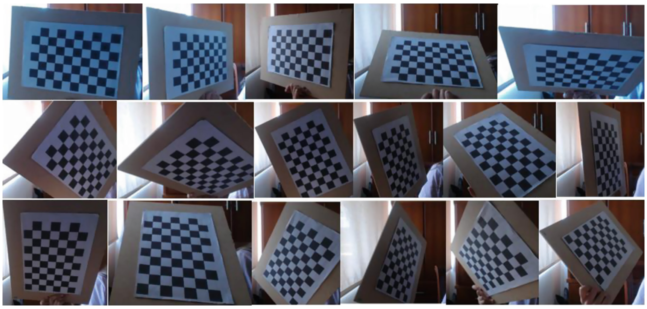

Fig.12. Input images for the calibration process.

After finishing the calibration process, the arrays mentioned are used to rectify the images captured by the stereo camera, and then they are sent to the SGBM algorithm. In Fig. 13 appear the result of the image reconstruction algorithm, where pixels that have dark tones are far from the estero system while pixels that have white tones are near it. This result has the name disparity map [9].

Fig. 13. Disparity map.

The disparity map calculates the depth of each pixel that forms the environment captured by the stereo system, to detect the nearest obstacles that approximate the user is necessary to filter the rest of the pixels which have a disparity value of more than 175 units. After the end of this process, the prototype can detect any obstacle that could be inside a distance less than 125 cm from the user. The obstacle positions are kept in the database of the prototype.

3.6 Route Planning Algorithm [10]

Potential field with fictitious force algorithm generates and attraction between the robot and the goal, it gives a repulsing force to the obstacles for avoiding the robot hits with some of them, the addition of these forces produces an only fictitious force. The robot uses this force to identify the route that it should take to avoid obstacles. In this case, the robot is considered the user.

Before starting the calculation of the fictitious force, the algorithm establishes the coordinates axis represented in Fig. 14(a) and takes obstacles position from the database. The attraction force is related to the user and remained over the positive “y” axis, the Fig. 14(b) shows the size and the position of the attracion force in this case has a constant magnitude of 1.

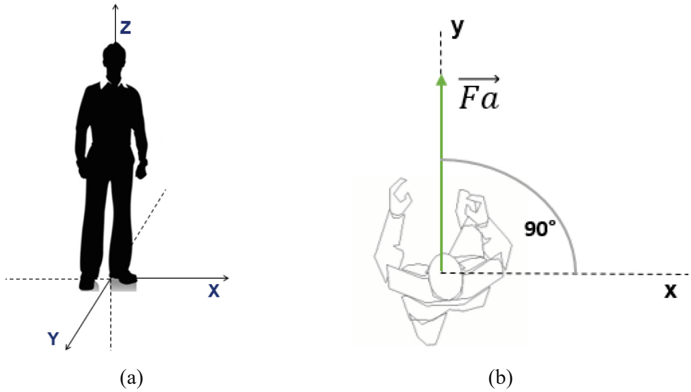

Fig. 14. Route generation algorithm parameters.

The repulsion force avoids the user hit with the obstacles, the algorithm needs to get the position of the obstacles in the coordinates axis (x, y) for calculating the direction and the magnitude of this force. The angle of it is related to the obstacles mass center and with the viewing angle of the stereo system, this value is 78°. Figure 15 shows the angle of repulsion force [10].

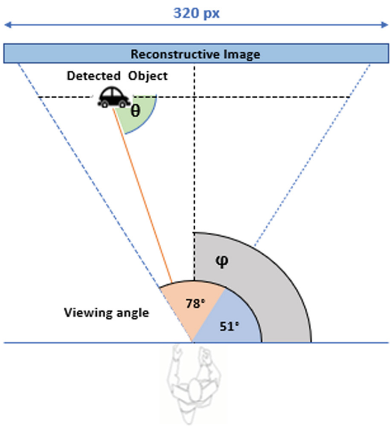

Fig. 15. Repultion force angle.

Equation (4) explains the repulsion angle of any obstacle inside the captured environment [11].

$$\varphi = (p - x)\left(\frac{\sigma}{p}\right) + 51 \tag{4}$$

$$\theta = 180 - \varphi$$

p = width of dispary map (pixels).
x = mass center of the obstacule detected.
σ = viewing angle of stereo system.

The size of repulsion force is inversely proportional to the distance between the detected obstacle and the user, therefore it increases while the obstacles approach the user. The repulsion force module is defined by Eq. (5) [11].

$$|Fr| = \left\{ \begin{array}{cc} 0 & SiPmed > Pmax \\ \frac{Pmax-Pmed}{Pmax-Pmin} & SiPmed < Pmax \end{array} \right\} \tag{5}$$

Finally, the vector of repulsion force is calculated by Eq. (6).

$$\overrightarrow{Fr} = (|Fr|\cos(\theta), |Fr|\sin(\theta)) \tag{6}$$

The next step is adding the x and y components of repulsion and attraction force respectively, the resultant force is used to select the free route. The module and the angle of this force are show in Eqs. (7) and (8).

$$\overrightarrow{Fe} = \overrightarrow{Fa} + \overrightarrow{Fr} = \left[(Fa_x + Fr_x), \left(Fa_y + Fr_y\right)\right] \tag{7}$$

$$\theta_e = \arctan\left(\frac{Fe_y}{Fe_x}\right) \tag{8}$$

The fictitious force angle is used to choose the appropriate audio which suggests the user avoid hitting with any obstacles. The Fig. 16 exhibits the different values of the fictitious force. According to the angle value, the device plays specific audio [10].

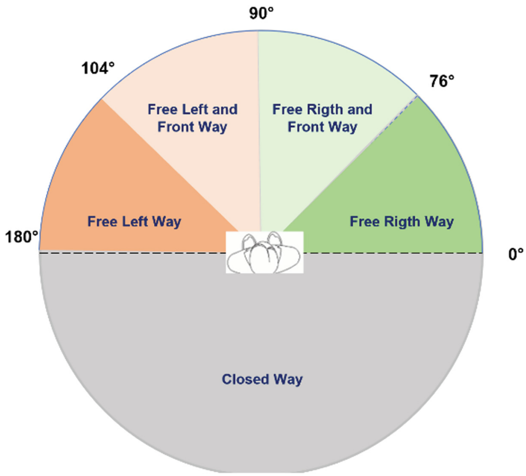

Fig. 16. Differents ranges of fictitious forces angle

3.7 Final Device

Figure 17 shows the prototype final device which has a stereo camera holds in a pair of straps that fitting easily to the user height and the prototype main computer is hanging over the user belt.

Fig. 17. Assistive device for blind people.

4 Results

This section exhibits the prototype tests with different users who have a visual disabilities.The first test shows the behavior of the object recognition algorithm and the second test exhibit the performance of the navigation algorithm. The tests were executed with younger and older blind people. Each user interacted with the two different operating modes, all the tests were done in a dynamic environment as houses and offices one of them were only lit with sun and the others were lit with artificial lights, in the case of the gardens, the light depends directly on the weather.

4.1 Object Recognition System Tests

Figure 18 shows an example of the recognition algorithm test with an older person who is 59 years old, he interacted with the system many times. During the performance of the test, the system could saw 17 different objects as apples, cups, bottles placed inside the camera visual environment.

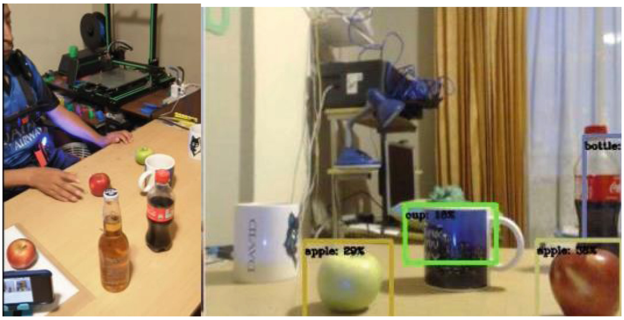

Fig. 18. Recognition system test with an older blind person.

Table 2 exhibits global results of the different tests, these results are registered after listening to the audio and watching the images generated by the prototype, this image shows the object detected framing in a colored square.

Table 2. Recognition test result with blind people.

N° Test	Age	N° Real Object	Detected Object	N° Correctly classified
1	13	22	19	17
2	14	21	17	17
3	14	17	13	12
4	15	20	18	18
5	16	15	14	14
Total		95	81	78
Percentage hit			85.26%	96.3%

The result of the recognition algorithm shows the system performance is satisfactory because the purpose of the system is assistive the user as supplementary help. In this case, the results aren't a risk for the user to take important decisions like medical applications where the results are essential to give a true diagnosis. The object detect error percentage is 14.74% and the classification error percentage is 3,7%, these values may be caused by the camera blur when the users suddenly move while they are taking the picture, causing the captured objects might not be recognized by the algorithm.

4.2 Navigation System Tests

Figure 19 shows an example of the navigation system test, in the left side is the user interacted with the system, and the white cane and the right side shows the response of the device. The first image is the reconstruction environment and the second exhibits the obstacles detected with a red contour. In this case, the system detected the right wall as an obstacle, after that the prototype play audio that suggests which direction the user should take to avoid the obstacle.

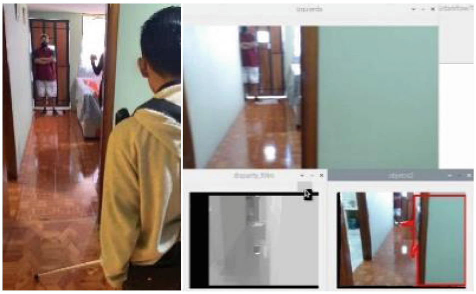

Fig. 19. Navegation system test with a younger blind person.

At the end of the test, the users explained the device is a great help, specifically younger users said that the object recognition performance is really interesting and a suggestion they advised us to increase the number of the object the system can identify. Also, they said that the navigation system is truly useful when any obstacle crosses inside the user's way specifically detecting an object that are at the height of the user's chest. Moreover, the older users said that both operating modes were convenient, and emphasizing the navigation system was more interesting and useful because some of them get visual disabilities during their life and they don't have enough ability to walk without hitting. This system helped this group of users to walk around the environment with more confidence.

5 Conclusion

- The stereo system must be held at chest height to capture the best viewing angle of the environment where the system can identify objects efficiently and detected obstacles that could be a danger for the user.
- The number of training images must show the principal features of each object to identify, if the number of training images is limited, it will recommend applying the data augmentation technique to avoid underfitting and overfitting issues.
- The distance between cameras of the stereo system must be as smallest as possible with the final purpose of detecting objects that are nearest to the user. The minimum detection distance increase as well as the distance between cameras.
- The artificial vision algorithms design and the training process of the neuronal network should be made in a computer with great computational resources, for that reason the prototype was developed in cross-platform programming language Python, which let share information between computers with the different operating system.
- The development device let the users identify objects that are in different positions inside the work environment, also it can share a free route quickly to avoid the user hit with any obstacles.

References

1. Jain, A., Jain, H., Chandan G.: Real time object detection and tracking using deep learning and OpenCV. R. V. College of Engineering, Telecommunication Engineering, Bengaluru, India (2018)
2. Saad, M., Emara, H., Bahgat, A., Farag R.M.A.: Three-dimensional localization of known objects for robot arm application based on a particle swarm optimized low end stereo vision system. Electrical Power and Machines Department, Cairo University, Giza, Egypt (2018)
3. S. F. T. Limited: Ultracane, 25 May 2018. https://www.ultracane.com/index.php?route=checkout/cart. Accessed 3 Mar 2020
4. Zhonga, Y., Wanga, X., Li, Q.: Classification of female apparel using convolutional neural network. Donghua University, Shanghai, China (2018)
5. Sun, X., Huang, Q., Li, Y., Huang, Y.: An improved vehicle detection algorithm based on YOLOV3. School of Computer and Information, Hohai University, Nanjing, China (2019)
6. Angela, C.: Biblioteca Unirioja (2018). https://biblioteca.unirioja.es/tfe_e/TFE004595.pdf. Accessed 05 Mar 2020
7. Luo, X., Yin, X.: A system for real-time detecting and recognizing object person. University of Electronic Science and Technology of China, Chengdu, China (2018)
8. Guerrero, J.M.: Técnicas de procesamiento de imágenes estereoscópicas. Dpto. de Ingenieria de Inteligencia Artificial, Universidad Complutense, Madrid (2011)
9. Pires, B., Hebert, M., Narasimhan, S., Zhi, T.: Deep material-aware cross-spectral stereo matching. Carnegie Mellon University, United States (2018)
10. Andaluz, G.: Modelación, Identificación y control de robots moviles. Escuela Politécnica Nacional, Quito (2011)
11. Chavez, D., Camacho, O., Taramuel, V., Sarzosa, M., Sotomayor, N.: An approach for helping the mobility of people with visual impairment: Design and implementation. RISTI – Rev. Iberica Sist. Tecnol. Inf. **2019**(E23), 194–205 (2019)

Optimization of a Mobile Audio and Video System Powered by a Bicycle Dynamo

Abraham Loja(✉), Alan Cuenca, Elizabeth Armas, and Jerson Colcha

Escuela Politécnica Nacional, Escuela de Formación de Tecnólogos, Ladrón de Guevara E11-253, Quito, Ecuador
{abraham.loja,alan.cuenca,elizabeth.armas, jerson.colcha}@epn.edu.ec

Abstract. Cynecycle tries to promote sport, electricity generation through a dynamo and learning through the projection of educational and cultural videos. The mobile audio and video system is made up of a dynamo, a voltage collection box or "Power Box", an amplifier box, a projector and two speakers. The system does not have a base to hold the dynamo while the cyclist pedals it, in addition, the "Power Box" of the system is damaged and the components for its repair are not available in the country. Other parameters to consider are the weight and the operating time, this due to the capacitor bank available in the system, which makes the transportation very difficult and the long projection of videos. To solve those problems, a metal base has been built, which allows the dynamo to be held against the bicycle wheel when the cyclist generates energy to charge the battery bank through the new "Power Box" designed. The charging and discharging time of the battery was considerably improved by replacing the capacitor bank with a lithium battery bank, in this way the duration of the video projection was increased and the total weight of the new "Power Box" was reduced. The loudspeaker material was modified to improve the sound quality. Therefore, the work comprises the results of the optimization of an audio and video system powered by a dynamo to generate power by moving the rim anchored to the stem of the dynamo.

Keywords: Dynamo · Bicycle · Optimization

1 Introduction

The mobile audio and video system comes from France. This aspect makes the repairing and maintenance difficult because the components are not available on the local market. In the case where the modules are affected by any anomaly, the parts or elements must be imported from the country of origin, which increases the cost and repair time. The "Power Box" of the system does not work and the parts for repair are not available in the country. Also, the operating time of the audio and video system is limited to 2 min, because the battery is based on capacitor banks.

On the other hand, the material from which the speakers are constructed contributes to distortion. Likewise, the weight is another parameter to improve, since the capacitors

© The Author(s), under exclusive license to Springer Nature Switzerland AG 2023
M. Zambrano Vizuete et al. (Eds.): RITAM 2021, LNNS 512, pp. 87–103, 2023.
https://doi.org/10.1007/978-3-031-11295-9_7

to store the required voltage are heavier than the batteries. Also, the system does not have a base to hold the dynamo while the rider is pedaling. Due to the problems, the mobile audio and video system cannot be used. To solve these problems, a new “Power Box” was designed and built. It meets the voltage and current requirements that the system requires, using elements that are available in the local market in case of any future repair. In addition, to optimize the battery lifetime, the capacitor bank is replaced by a lithium battery bank. In this way, the operating time is prolonged; and the total weight of the new “Power Box” is reduced. The new loudspeakers were constructed of wood to improve sound quality, as it is an acoustic wave absorbing material. On the other hand, a base was built that allows the dynamo to be anchored to the bicycle, both for use in presentations and for transporting the system from one place to another. The project has been running for 3 months on Cinecyclo, making 2 to 3 weekly presentations.

2 Methodology

2.1 Description of the Methodology

In the initial stage of the project, a visual and technical inspection of the old “Power Box” was carried out. Since it was designed and built in France, in the review, the elements that make up the system were observed (capacitor banks, acoustic box, controller and electronic devices). It was also found that some electronic devices are not available in the country, so it was necessary to design and build a new “Power Box”.

Research about the damage that batteries cause to the environment and the long duration of their charge concluded that Lithium batteries are the best option to store direct voltage and current (DC), since they are recyclable and allow the system to work for long periods due to its capacity. To control the state of charge and therefore charge the lithium batteries, a charge regulator is needed. To select the controller, the maximum and minimum voltages, and currents with which the system will work, were established. Additionally, the input voltage and direct current supplied by the dynamo were considered; With all these data, it was determined that the charge regulator controller must meet the following specifications: Input 50 (Vmax), 10 (A) and Output 12 (V), 5 (A).

It should be noted that the output voltage will depend on the charging time of the batteries and the parameters programmed in the controller. For this system the batteries must work with a DC voltage of 12 (V) and 5 (A). To achieve these parameters, a lithium battery bank was built, which has 6 batteries with a maximum voltage of 4.2 (V), a working voltage of 3.7 (V) and a current of 3 (A). Batteries connected in series generate a voltage of 12.6 (V) and adding the current in parallel provides 6 (A), which is enough for the system to work. To improve sound quality, various types of materials were investigated that meet the parameters of Airtightness and sound absorption; It was determined that the ideal material for making the boxes is wood, since it is an acoustic material that absorbs sound, and due to its porous composition, it absorbs waves and transforms them. The structure of the boxes must be uniform and homogeneous, in this way it does not affect the sound quality.

3 Results and Discussion

3.1 Description

Cinecyclo is an organization whose unique concept combines adventure, cultural diffusion, environmental awareness, and development. Cinecyclo makes presentations in various places in Ecuador and its main tool is the bicycle. For this reason, the mobile audio and video system powered by a dynamo has been improved and is structured in 4 stages: generation, control, amplification, and audio (see Fig. 1).

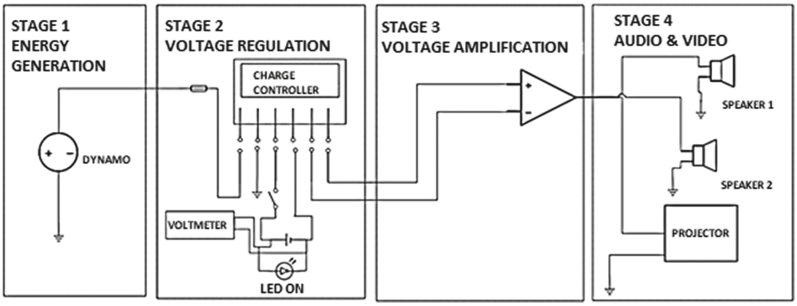

Fig. 1. Stages of the audio and video system.

3.2 Fabrication of the Dynamo Base

The dimensions of the base of the dynamo were obtained from the rim 26 of the bicycle and the available support points were found on the rear axle of the bicycle wheel.

The maximum weight that the bicycle supports by default is 101 (kg), which includes all the audio and video equipment necessary for the presentations including the cyclist (see Fig. 2).

Fig. 2. Loading weight.

Therefore, the maximum force supported by the base and the support points is 989.8 (N) according to Eq. (1):

$$w = m * g \tag{1}$$

where:

g: 9.8 (m/s^2) gravity
m: 101 (kg) mass
w: (N) weight.

Using Eq. (1) it is obtained:

$$w = 989.8\ (\mathrm{N})$$

With the calculated value and following the dimensions shown in Fig. 3, the metal base was built to support the dynamo and transport the system.

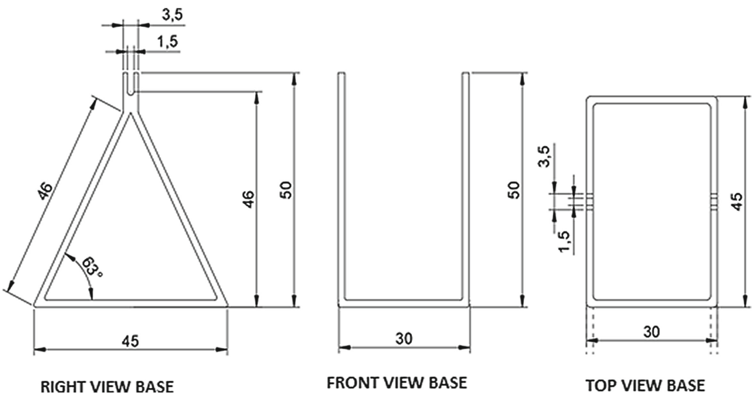

Fig. 3. Structure of the metal base.

Axes for the Base. The axes of the base are the rear support points that allow attaching the base of the system to the bicycle, they also allow 180° rotation of the base. The measurements for the construction of the shafts are specified in Fig. 4:

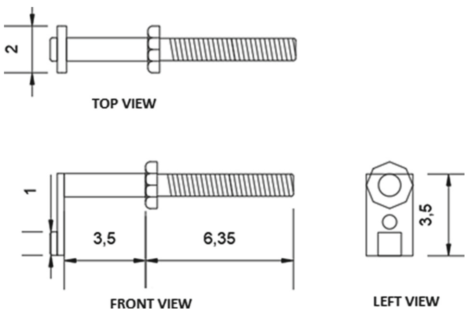

Fig. 4. Axes for the base.

Fig. 5. Base of the dynamo.

Figure 5 shows the results, the base and the support axes built and integrated to the bicycle.

3.3 Power Required by the System

To determine the power of the system, maximum voltage and current values were taken at the input and output of the voltage regulation stage. Based on these dimensions, the voltage, and current values necessary to size the new "Power Box" were established.

Later, the Eq. (2) was used to obtain the maximum power.

$$P = V * I \tag{2}$$

where:

V: 12 (V) supply voltage
I: 5 (A) nominal voltage
P: (W) power consumption.

Using Eq. (2) it is obtained:

$$P = 60\,(W)$$

The calculated power value allows the following components to be selected.

Solar Charge Controller. A solar charge controller was selected that allows to regulate, limit, and control the charging parameters of the battery bank and the power supply of the audio and video system (see Fig. 6).

The controller was programmed with the levels of maximum, minimum voltages and power cut to limit those voltages. In addition, the controller complies with the technical characteristics of robustness since it supports an input voltage of up to 50 (V) and a maximum current of 10 (A) [2].

Battery Bank. Based on the power required by the system and the maximum voltage level programmed in the charge controller, a battery bank was designed with series and parallel configurations.

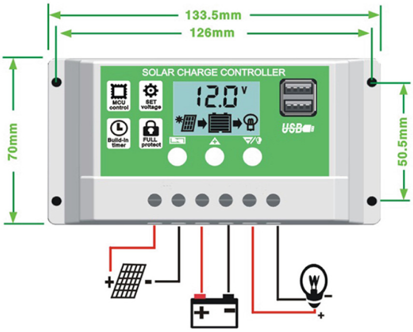

Fig. 6. Selected solar charge controller [3].

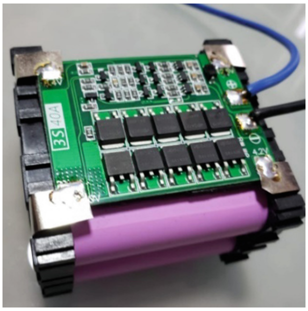

Fig. 7. Battery bank.

Batteries with voltage and current of 4.2 (V) and 3 (A) respectively were used, being necessary the use of 6 batteries to build the bank that stores 12.6 (V) and 6 (A) (see Fig. 7).

BMS Charge Regulator Card. It is necessary to connect a BMS charging card, since it measures the charging voltage individually in each of the batteries and interrupts the power when the charge is complete.

The BMS charging card has operating parameters: a voltage of 12 to 13.6 (V) and a current of 40 (A), for which it is robust to regulate the charge level of the battery bank [4]. The battery bank and BMS card connections are shown in Fig. 8.

Connection Cable. To size the cable that conducts the current from the generation stage to the voltage regulation stage, the dynamo datasheet was taken as indicated in Table 1.

From the dynamo parameters, it is obtained:

$$I = 13.5\,(A)$$

Therefore, the cable used for the connection of stages 1 and 2 of the system is the flexible cable # 14-AWG that withstands a current of up to 15 (A) under the American Wire Gauge standard.

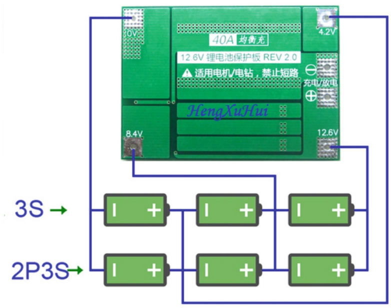

Fig. 8. BMS card connection [4].

Table 1. Dynamo datasheet.

Voltage	Current	Output
24 (Vdc)	13,5 (A)	250 (W)

Assembly of "Power Box". The manuals and diagrams related to the assembly of each of the electrical elements were used. In addition, appropriate techniques and operations were investigated for the correct assembly of the components under conditions of safety and quality of the system [6].

The established dimensions of the "Power Box" were considered to make a diagram of the distribution of the components (see Fig. 9).

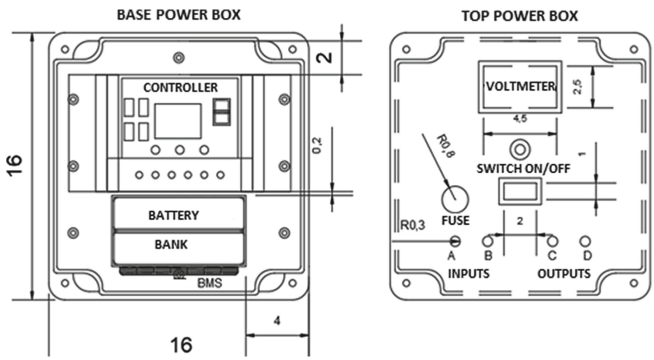

Fig. 9. Distribution of the "Power Box" components.

The Fig. 10 shows the connection diagram for the "Power Box" elements. The most important connection is the charging controller connection because the load must be connected first, later the battery bank and finally the dynamo. Only in this order, the controller will not be damaged.

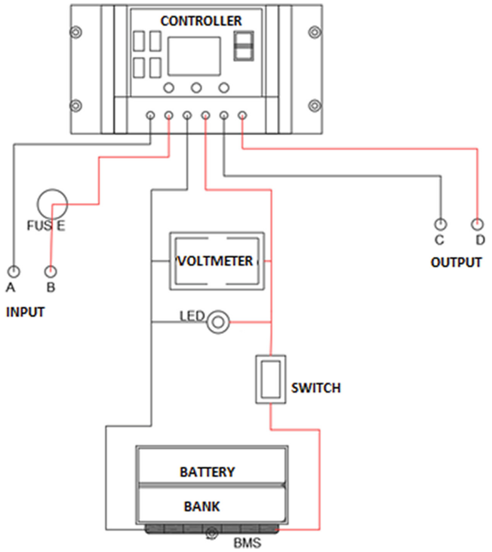

Fig. 10. Elements Connection.

The battery bank is made up of batteries and the BMS charging card. Battery bases, aluminum sheets, tin solder and spot solder were used for the union of the batteries. Double-sided tape, hot silicone, was used to hold the battery bank. And, to locate the battery bank, the "Power Box" distribution designs were used.

The splices of the connections between all the components were coated with tin and with heat-shrinkable material to ensure a robust fixation when transporting the components on a bicycle.

As a result of the selection of all the components, the new "Power Box" shown in Fig. 11 is obtained.

Fig. 11. "Power Box" in operation.

Acoustic Boxes Building. The transport and use requirements of the equipment in remote communities require that the sealed box model be adequate for the manufacture of the loudspeakers. The material chosen for the construction is wood. It was due to its high acoustic resonance capacity and lightweight.

The "Winisd" program allowed to analyze the characteristic curve of decibels (dB) concerning the frequency (Hz), that is, the cut-off frequency response of the boxes. The analysis of this curve (Fig. 12) allows obtaining the dimensions of the loudspeakers for their construction.

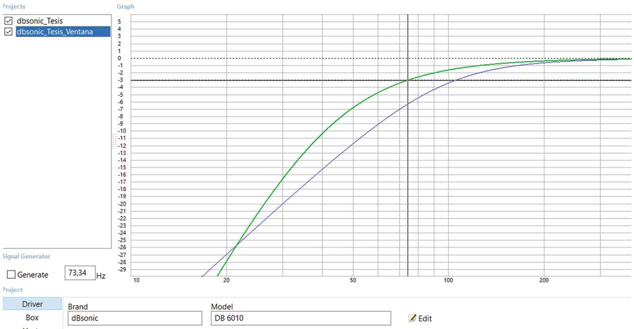

Fig. 12. Characteristic curve of the ventilated speaker.

The dimensions of the acoustic boxes obtained are shown in Fig. 13.

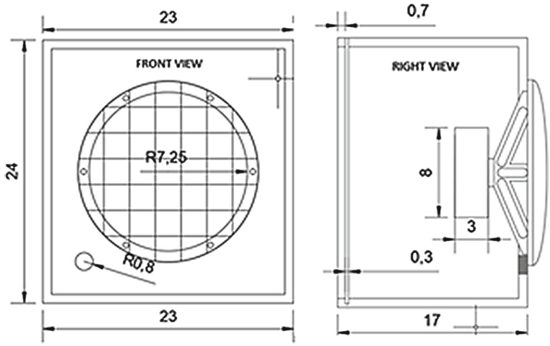

Fig. 13. Dimensions of the box.

Next, speakers are located one with respect to the other, forming a Port for the superposition of lower frequencies; a better frequency response curve is obtained.

Testing and Analysis of Results. The connection of all the components allowed the performance tests to be carried out, where the analysis of the transmission ratio of the bicycle chain and its impact on the Power Box charge was carried out, as well as the effect of discharge due to consumption of the audio and video components. The tests performed are detailed below.

Transmission Ratio for Charging and Discharging. The test was carried out to define the optimal transmission ratio between the front sprocket and the rear sprocket of the bicycle, for the process of charging the "Power Box".

The system was connected, and the voltage value was taken from the "Power Box", then the charge was started with the speed ratio. The bicycle has two gears (P1 and P2) for the front sprocket, while for the rear sprocket it has 8 gears. The possible combinations between the bicycle sprockets were made to find the best charging ratio.

Table 2 shows the data obtained for the transmission ratio between the rear sprockets and the front sprocket of gear 1, the variation between the minimum and maximum voltage in a unit of time of 3 min, the initial and final charging voltage variation, and the level of difficulty of each gear ratio.

Table 2. Results obtained from forward gear 1.

Rear sprocket	Voltage in 3 min.		Δ min. & max. voltage (V)	Δ Load voltage (V)	Difficulty level
	V min. (V)	V max. (V)			
1	9	10	1	0,03	1
2	9,5	10,4	0,9	0,04	1
3	10	11,3	1,3	0,06	1
4	10	11,6	1,6	0,08	1
5	11,9	12,5	0,6	0,12	2
6	12	13	1	0,15	2
7	11,5	16	4,5	0,15	3
8	11	17	6	0,14	3

The data obtained allows to identify that the least damaging voltage variation for the charge controller is found in the change of sprockets from 5 to 6, as shown in Fig. 14.

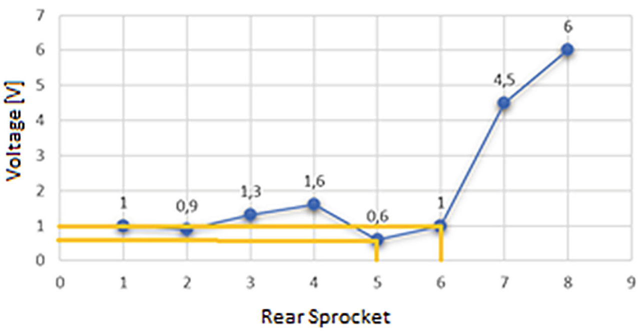

Fig. 14. Minimum and maximum voltage variation in gear 1.

Focusing on the gear ratio of the change of pinions 5 to 6, it is observed that the charging voltage is satisfactory, with a positive rate of change as observed in Fig. 15.

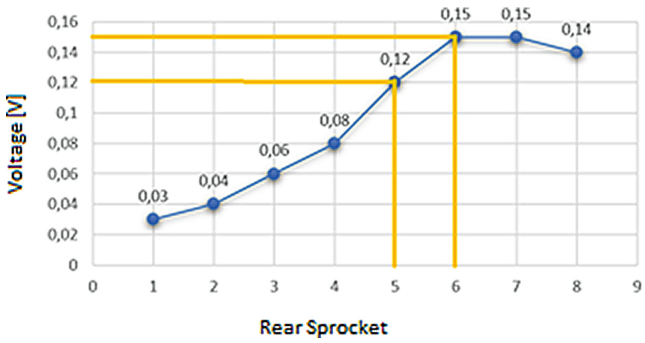

Fig. 15. Charging voltage variation in gear 1.

The level of difficulty perceived by the users who collaborated with the performance of these tests allows to locate the gear change from 5 to 6 as a medium difficulty value; noting that for low difficulty, it is assigned as 1 and with 3 as the maximum difficulty. This result can be seen in Fig. 16.

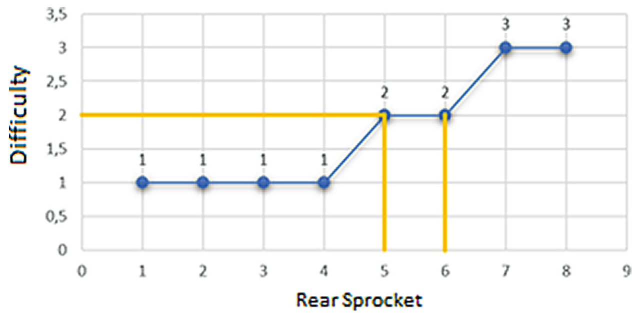

Fig. 16. Pedaling difficulty level.

Once the test in gear 1 of the front sprocket was completed, the test in gear 2 on said sprocket was proceeded in a similar way, and the respective combinations were applied with the 8 gears of the rear sprocket. The result is the data shown in Table 3.

For the transmission ratio with gear 2 of the front sprocket it is observed that the rear sprocket changes from 3 to 4 provides a non-harmful variation of voltage for the charge controller, as it can be seen in Fig. 17.

The analysis is carried out again to identify the rate of change of the battery bank charging voltage, resulting in a favorable situation as shown in Fig. 18.

Finally, the level of difficulty detected corresponds to a mean value (Fig. 19), which is acceptable for the usefulness of exercise, clean energy generation and use of equipment for children and adults in remote communities.

Table 3. Results obtained from forward gear 2.

Rear sprocket	Voltage in 3 min.		Δ min. & max. voltage (V)	Δ Load voltage (V)	Difficulty level
	V min. (V)	V max. (V)			
1	9	11,5	2,5	0,01	1
2	11	12,5	1,5	0,06	1
3	12	13,5	1,5	0,11	2
4	12	14	2	0,14	2
5	12	16	4	0,16	2
6	11,5	16	4,5	0,16	3
7	11,5	16	4,5	0,15	3
8	11	16	5	0,13	3

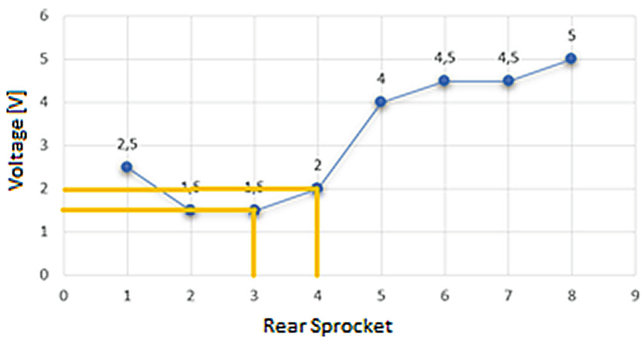

Fig. 17. Minimum and maximum voltage variation in gear 2.

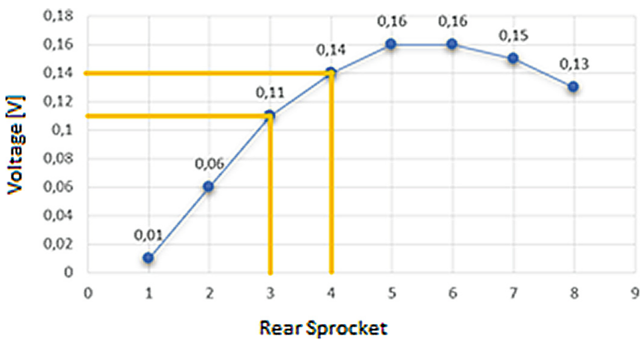

Fig. 18. Charging voltage variation in gear

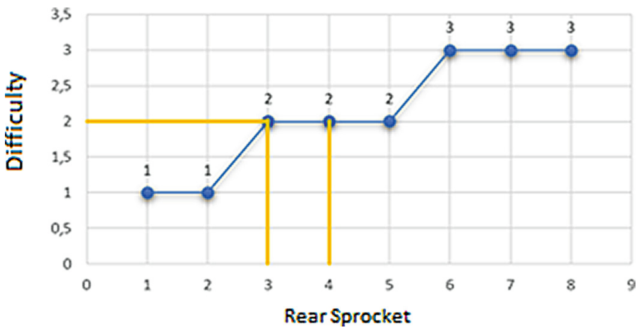

Fig. 19. Difficulty level pedaling in gear 2.

Through the tests carried out, the best transmission ratios were determined to charge the "Power Box", the charge level must be taken every certain interval of time with each of the gears of the bicycle. The measurements are made with a high-resolution multimeter, since the voltage increase with some gears reaches the level of hundredths of voltage.

The transmission ratios analyzed based on the voltage and difficulty parameters are in the following recommended order of use as shown in Table 4.

Table 4. Recommended gear ratios for charging the battery bank

Rear sprocket	Front sprocket	V min (V)	V max. (V)	Δ Voltage (V)	Difficulty
6	1	12	13	0,15	2
4	2	12	14	0,14	2
5	1	11,9	12,5	0,12	2
3	2	12	13,5	0,11	2

The next test to be carried out is the Power Box charging and discharging time by combining the rear sprocket at 6 and the front sprocket in gear 1 for charging, and the connection to maximum consumption by all the audio and video components.

Charging and Discharging Time of "Power Box". The objective of the test is to determine the time required to charge and discharge the "Power Box" employing the transmission ratio determined in the previous test. Also, the time in which the "Power Box" is discharged when the entire system is operating at full speed. 100% capacity, to later compare between the data of the old system and the new system.

Using a stopwatch, the time it takes to charge battery 1 (V) was measured, and then how long it takes to discharge that volt was measured. In Fig. 20 after taking the measurements there is a total charge time of 1 (V) in 21 (min).

Subsequently, the discharge test is carried out when the system works at 100%; obtaining as a result a time of 35 (s) to discharge in 1 (V), as observed in Fig. 21.

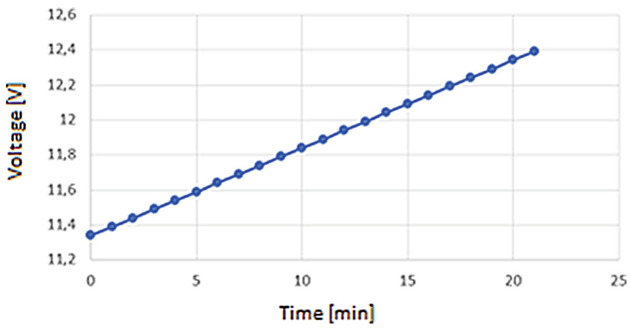

Fig. 20. Charging the battery bank.

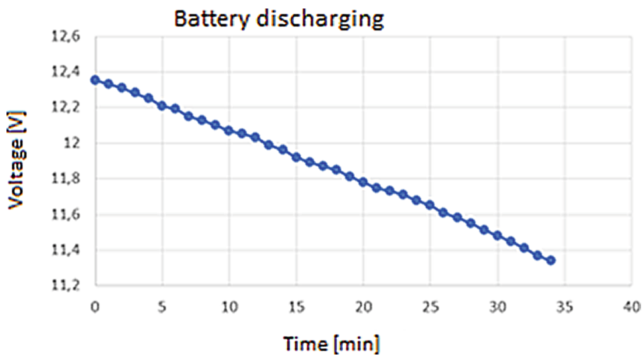

Fig. 21. Battery bank discharge.

The charging and discharging voltage parameters are based on the voltages programmed into the controller, the charging time depends on the constant speed with which the cyclist is pedaling; on the other hand, the discharging time depends on the capacity at which the audio and video system is operating.

Charging and Discharging Test of the Old System. The old system based on a bank of capacitors to store energy was charged, an operating voltage of 12.6 (V) was reached

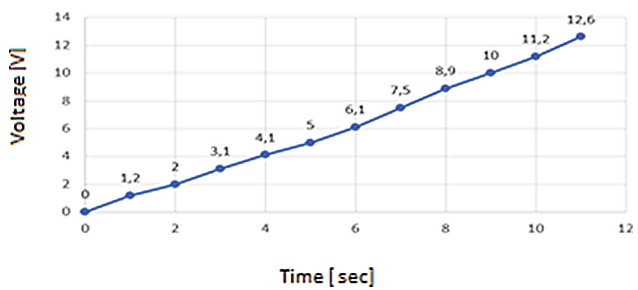

Fig. 22. Charging time of the old system.

and the time it takes to do it 11 (min) was taken, the data obtained can be viewed in Fig. 22.

For the measurement and discharge analysis, a limit of 70% of the voltage of the capacitor bank was determined, resulting in a discharge time of up to 9 (V) in just 2.7 (s). The measurements made can be viewed in Fig. 23.

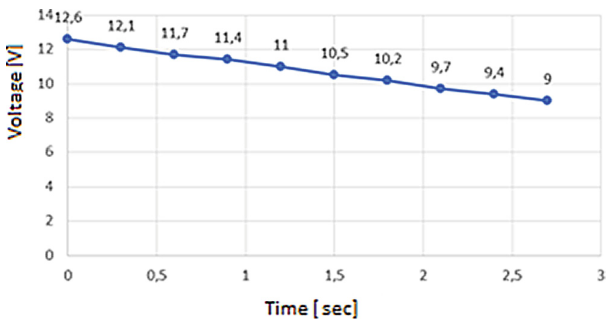

Fig. 23. Discharging time of the old system.

The measured data of the new system were compared with the old one. The discharge time is notably shorter because the capacitors cannot store energy for a long period of time. The tests and measurements carried out clearly showed the advantages of the new implemented system, and whose comparison can be seen in Table 5.

Table 5. Comparison of parameters of the old and the new system.

Parameters	Old Kit	New Kit
Charging time	50 (S)	21 (min)
Discharging time	1.5 (min)	35 (min)
Charging voltage per minute	1.2 (V)	47.62 (mV)
Discharging voltage per minute	0.66 (V)	28.57 (mV)
Weight	156.8 (N)	117.6 (N)
Mass	16 (Kg)	12 (Kg)

4 Conclusions

- The built-in dynamo base guarantees both the balance in the transport of the complete kit of the system, as well as the necessary power generation (wheel rotates freely) during the operation of the kit.

- The maximum and minimum operating voltages of the "Power Box" are equal to 12.6 (V) and 10.4 (V), respectively.
- The elements that make up the new system are a solar charge controller, a battery bank, a charge regulator card, a switch, and the external frame. The mentioned elements are easily acquired in the local market and cheap.
- The solar charge controller was specified from 12 (V) and 5 (A), electrical characteristics that the system requires for its operation. In addition, the controller regulates, limits, and controls the maximum and minimum voltage levels that are injected into the battery bank.
- The battery bank is made up of six batteries connected in series and parallel. This bank stores 12.6 (V) and 6 (A). The bank's charging control is done through the BMS.
- The external frame made of wood (acoustic boxes) meets the parameters of tightness, resistance, and sound absorption. The loudspeaker built is closed, the back of the loudspeaker is joined with another to become a window type loudspeaker, improving the cutoff frequency.
- The operating time of the "Power Box" depends on the operating capacity of the system; that is, if the system is operating at 100% capacity, the batteries are discharged in 35 min; on the other hand, if the system is operating at 70% capacity, the batteries are discharged in 44 min.
- The operating time of the old system was 15 min with the new system it has been possible to double that time.
- A user and maintenance manual were prepared complying with all the characteristics, specifications, and indications so that the people who use the audio and video system can make it work correctly, as well as the basic maintenance activities and the elements in the case replacement is required.

References

1. Ruz, L.J.R., Castro, D.A.C.: Ondas electromagnéticas. In: Teoría electromagnética para estudiantes de ingeniería Notas de clase, pp. 77–100 (2018)
2. Carreras, M.B.: Instalaciones solares fotovoltaicas (2019). https://books.google.com.ec/books?id=bKyZDwAAQBAJ&pg=PA113&dq=controlador+de+carga+solar+2019&hl=es&sa=X&ved=2ahUKEwiArIjHlf3vAhXBVDUKHYycBxkQ6AEwAHoECAIQAg#v=onepage&q=controladordecargasolar2019&f=false. Accessed 14 Apr 2021
3. d271b58b-c7d2-4fc1-9e90-bec3cf5b22db.jpg (800×800). https://imgaz.staticbg.com/images/oaupload/ser1/banggood/images/92/E2/d271b58b-c7d2-4fc1-9e90-bec3cf5b22db.jpg. Accessed 22 Mar 2021
4. Trashorras Montecelos, J.: Vehículos eléctricos - Ed.2018 (2018). https://books.google.com.ec/books?id=FMqwDwAAQBAJ&pg=PA58&dq=tarjeta+de+carga+bms+para+baterias&hl=es&sa=X&ved=2ahUKEwip7-Se4_7vAhWnnuAKHbERBTwQ6AEwAHoECAEQAg#v=onepage&q=tarjetadecargabmsparabaterias&f=false. Accessed 14 Apr 2021
5. Alberto, M.L.: Cable eléctrico - tabla de calibres electricidad, Cableado eléctrico, April 2021. https://br.pinterest.com/pin/828732768922590136/. Accessed 23 Mar 2021
6. Garcia Rodrigo, J.: Técnicas y procesos en instalaciones eléctricas, 2nd edn. (2019). https://books.google.com.ec/books?id=tdSuDwAAQBAJ&pg=PA327&dq=montaje+de+elementos+electricos+2019&hl=es&sa=X&ved=2ahUKEwirpcmUlv_vAhVIc98KHavTAK

8Q6AEwAXoECAMQAg#v=onepage&q=montajedeelementoselectricos2019&f=false. Accessed 14 Apr 2021
7. Dimi Avram, M.S.E., Lacho Pop, M.S.E.: Los 40 Errores Más Caros Que Cometen los Novatos en Energía Solar: Tu Guía Inteligente para Tener Energía Solar en el Hogar y Negocio. Booksinprint.Bg (2021)
8. Enríquez, G.: Tecnologías de generación de energía eléctrica. Camion Escolar (2009)
9. de Kuyper, J.C.V.: Principios y aplicaciones de la energía fotovoltaica y de las baterías. Ediciones UC (2018)

Evaluation of Data Acquisition System for PES Membranes Permeability Analysis in Water Treatment

David Trajano Basantes Montero[1](✉), Bryan Rafael Rosero Ortiz[2], Daniel Isaías Barzallo Núñez[1], Luis Miguel Quishpe Quishpe[2], Néstor Xavier Maya Izurieta[1], and Miguel Herrera Robledo[2]

[1] Instituto Superior Universitario Central Técnico, Quito, Ecuador
dtbasantesm@gmail.com

[2] Geosciences Laboratory, Universidad Regional Amazónica Ikiam, Tena, Ecuador
luis.quishpe@ikiam.edu.ec

Abstract. Wastewater treatment has become a momentous field today. Membrane ultrafiltration processes are booming due to their versatility of use. However, there are limited studies related to the technology of automatic data acquisition systems (DAQ) for the analysis of pore fouling based on the permeability of the membranes. Thus, the objective of this research was to evaluate a DAQ system through its implementation in permeability tests of polyethersulfone (PES) membranes. For this, through the ANOVA-non-replicable method, the repeatability and reproducibility (r & R) of the data obtained from manual measurements (MA) and DAQ system measurements were analyzed. The tests were carried out through scenarios of filtering distilled water (W) and filtering water contaminated with standard foulant (BSA). The results show a percentage of the r & R relationship between 10% and 30%, concluding that the measurement system through the DAQ system is acceptable according to its use.

Keywords: DAQ · ANOVA · Repetibilidad · Reproducibilidad · Ultrafiltración · Membranas PES

1 Introduction

1.1 Data Acquisition in Membrane Filtration Processes

Pressure-driven filtration membranes have emerged as an indispensable operating unit for large-scale industrial applications. These processes include reverse osmosis (RO), nanofiltration (NF), ultrafiltration (UF), and microfiltration (MF) [1]. Ultrafiltration is mainly used in the food [2], pharmaceutical [3], and wastewater treatment [4] industries due to the high degree of purification, retention, and fractionation of colloids, proteins, and microorganisms. Its use has spread in such diverse fields due to its versatility, selectivity, effectiveness, and low operating costs.

The increasing use of membranes described by Benito and others [5] suggests the need for new data acquisition systems for laboratory tests focused on the study of filtration

© The Author(s), under exclusive license to Springer Nature Switzerland AG 2023
M. Zambrano Vizuete et al. (Eds.): RITAM 2021, LNNS 512, pp. 104–117, 2023.
https://doi.org/10.1007/978-3-031-11295-9_8

processes. The precision, accuracy, and repeatability of the data acquired will allow a breakthrough in the commercialization of membrane technology [6]. Likewise, JC Salcedo and others carry out studies with a membrane technology to determine the recovery of water and minimize consumption in the paper industry by analyzing the influence of operational variables such as tangential velocity and pressure through the acquisition of manual data through analog instrumentation [7]. Maxim Shurygin and others studied the effective treatment of wastewater from the ceramic industry using membranes using in their procedure manual data acquisition from analog instrumentation such as pressure gauges and flow meters during preset time range to determine the type of membrane that gave the best results in the process [8]. Meerholz et al. Noted the use of analog instrumentation, as well as the existence of previous automation studies for experimental setups of membrane-based solvent extraction units [6]. Data acquisition methods through the use of programmable logic controllers and LabViewTM software have recently been used by Nilusha and others to study the effects of solid retention time on membrane anaerobic bioreactors [9]. B Guo et al. Used for their study an analog data acquisition process using a balance that measured the mass of the permeate from the filtration that was used to calculate the proportion of concentrates for the quantification of cultivable viruses [10]. J. Starr et al. Used an automatic data acquisition procedure using an electronic balance that transmits the acquired permeability data to a computer, and through this process, the data are obtained to comparatively evaluate two methods for coating a microporous surface of a support layer. membrane with a photocatalyst [11].

On the other hand, studies such as those carried out by A. Deratani and others remain with the use of manual data acquisition protocols through analog instrumentation which, through experiments with various wastewater and using different types of membrane, determine the feasibility of using membranes to improve wastewater quality [12]. Considering the above, it is possible to suppose that automated processes in laboratory membrane tests have been developed while maintaining the manual acquisition of data through analog instruments. Therefore, a validation study of the results obtained through automatic data acquisition processes is necessary. The objective of this research was to evaluate a data acquisition system (DAQ) through its implementation in permeability assays of polyethersulfone (PES) membranes.

1.2 Ultrafiltration, Polyethersulfone (PES) Membranes, BSA, and Permeability

At a commercial level, ultrafiltration membranes are characterized by working at pressures between 1 and 10 bar, retaining solids between 1 and 10 nm or molecules between 500 and 100,000 Da [13]. According to their application, they can be found in different materials: hydrophilic polymers (eg, Polysulfone (PSF) [14], Polyethersulfone (PES) [15], Cellulose acetate [16]), and hydrophobic polymers (eg, Polyethylene (PE), Polypropylene (PP), Polyvinylidene fluoride (PVDF). The implementation of membranes based on Polyethersulfone (PES) has been used in recent years for the separation of contaminants in ultrafiltration processes due to their physical and chemical properties [17] Excellent chemical reluctance, thermal stability, and mechanical resistance make this type of membranes the favorite candidates for ultrafiltration processes [18–20]. However, there are still limitations in this class of technologies, related to the clogging of pores, adsorption of solutes, formation of coatings that limit the passage of fluids and exacerbate the flow reduction [21].

Fouling mechanisms are usually studied through the interaction between macromolecules with the surface of polymeric membranes. A model macromolecule widely used to evaluate these interactions is bovine serum albumin (BSA), the most abundant protein in blood plasma, which has been used mainly for tests in the fields of biochemistry, biophysics, and physicochemistry in recent years [22]. However, its use has been extended to the field of filtration processes as a standard fouling substance to evaluate permeabilities in membranes that serve as health indicators in the ultrafiltration process [23, 24].

Among the main investigations that have used BSA as a white fouling agent to evaluate permeability. There is the case of Razi et al. (2019), where the retention of BSA was determined in a PES membrane modified with Tetronic 304. In this investigation they reached permeabilities of 5.6 L/m^2.h.bar after 120 min of filtration, leaving as a conclusion a better retention thanks to the coating on the membrane [25]. Additional research, such as that of Kuz-menko et al. (2005), evaluate the chemical cleaning of PES membranes fouled with BSA, the permeabilities obtained vary around the pH of the solutions, and the effects of fouling caused a reduction in permeability by 10% with a pH of 10.1 at a pressure of 0.5 bar in 20kDa polyethersulfone membranes [21]. The studies mentioned must necessarily carry out permeability tests on their experimental block to describe their results. It can be seen that these investigations do not have standard parameters (fouling concentration, working pressure, sample volume, etc.) to carry out these tests. That is, they do not apply similar experimental designs despite using the same foulant, making the performance of the membrane difficult to compare.

Permeability tests describe the passage of water flow over the surface of the membrane at a given pressure and are based on the hydraulic resistance model mentioned by Hira et al. (2015) [26].

$$\mathrm{J} = \frac{\Delta \mathrm{P}}{\mathrm{R_t}\mu} \tag{1}$$

where J is obtained experimentally from Eq. 2.

$$J = \frac{\Delta V}{\Delta t \cdot A \cdot \Delta P} \tag{2}$$

where V is the volume of water in liters, A is equivalent to the area of the membrane (m^2), P is the pressure of the system in bar which is constant and t is the variation of time in hours.

To evaluate the performance of a membrane it is essential to acquire its permeability value (K). Wang et al. (2010) summarizes several studies where the performance of membranes infiltration processes is evaluated [27]. Most of these do not use similar conditions, generating scattered and not very comparable results. For this reason, it is necessary to establish standard conditions that allow evaluating the different permeability characteristics of the membranes.

The evaluation of permeability in polymeric membranes has been described in several studies, most of these focus on improving the passage of water over its surface

[28–30]. For example, the study by Louisiana et al. (2020), increases the permeability of PES membranes by coating them with an anionic polymer [30]. In other studies, zirconium oxide particles are immobilized to evaluate the performance of PES membranes, resulting in a polymeric membrane with higher transmembrane pressure [29]. The studies described need permeability tests to describe the performance of the membranes, but they are imprecise in describing their methodology. Therefore, it is necessary to establish a design that guarantees the repeatability of tests to reduce adverse errors and approach a real value.

2 Materials and Methods

2.1 Reagents and Materials

BSA (66 Kda, 583 amino acids residues, CAS number 9048-46-8, catalog no. 5470, Sigma-Aldrich, USA) was used as standard foulant, commercial polyethersulfone membrane (PBGC06210, Millipore) with a 10 kDa molecular weight cut-off and effective area of 31.67 cm^2. The membrane was flushed with 50 mL of deionized distilled water before use.

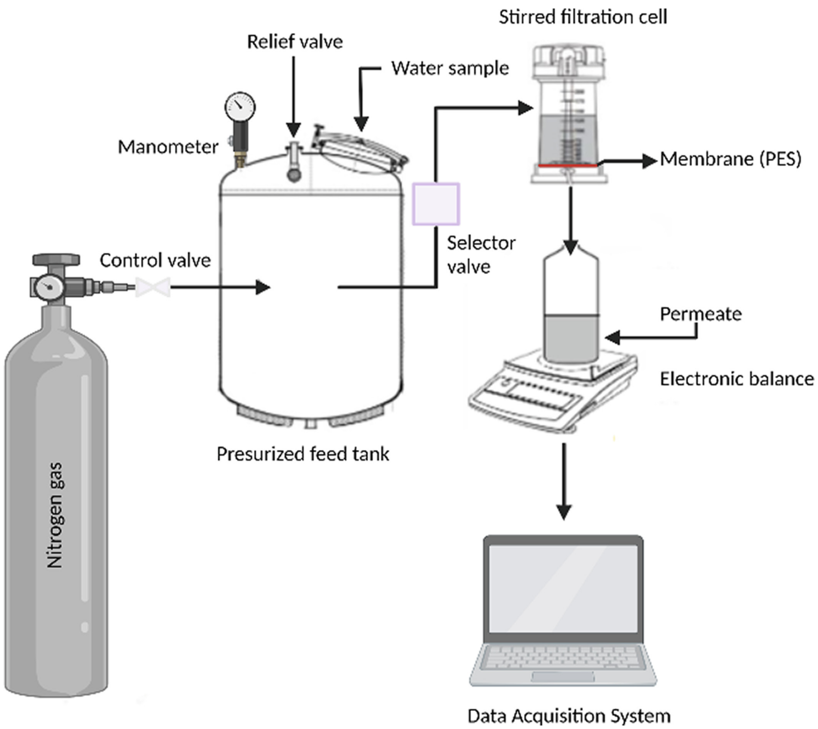

Fig. 1. Diagram of the experimental apparatus

2.2 Experimental Apparatus and Ultrafiltration Protocol for Permeability Analyses

All membrane experiments were conducted at room temperature using an Amicon®-StirredCells system (Catalog No. UFSC 20001, EMD Millipore Corporation, USA) connected by a selector valve (Amicon 6003, Milli-pore) with a 10-L stainless-steel storage tanks (Model XX6700P1, Millipore, USA) at 2 bars under nitrogen gas pressure under 20 °C.

The ultrafiltration's experiments were development in 2 ways, first with 500 mL of deionized water as a control essay and the second one with a standard foulant. BSA was dissolved in deionized water to be 0.03 wt% (3g/L), and was stirred for 2 h at room temperature. Subsequently, 200 mL of the BSA solution was used in ultrafiltration experiments. Stirring was applied to avoid concentration polarization speed for the experiments was set at 400 rpm.

To calculate the permeability, the permeate mass was measured with a precision balance (RADWAG, WTC600), and the data was collected manually and with a data acquisition development in LabVIEW as a function of time. The general diagram of the system is shown in Fig. 1.

2.3 Data Acquisition System

Through the RS-232 interface provided in the RADWAG, WTC600 precision balance, and the Radwag Balances & Scales controller installed in the LabVIEW environment, communication and data acquisition were established allowing the determination of the mass and permeability values in real-time. The designed interface shown in Fig. 2 can generate a configurable maximum value alarm in the range of 0 to 700 g of permeate mass allowed, as well as define the acquisition interval in seconds and export autonomously .ma the data to files .xlcx. For the permeability calculation, the editing of constant data such as the membrane area in square meters and the pressure applied in the test in bars are allowed. The table and resulting graphs show the permeate mass and permeability values.

2.4 Nested ANOVA for Non-replicable Tests

M, Botero and others mention that the ANOVA method is the most accurate method when you want to calculate the variability that occurs due to the interaction between operators and the parts of a process, so the study of repeatability and reproducibility (r & R) helps to detect when it is working under abnormal conditions, in this way, corrective strategies can be sought [31]. Understanding that the membranes despite having the same molecular cut size, there are differences when evaluating the permeability of each one, due to the random aggregation of the fouling agent on the surface of the membrane, as well as the difficult recovery of initial conditions used in each of the trials [21]. This makes it impossible to generate an analysis of data from replicable tests, therefore, the method that obeys the analysis whose data varies in time due to the change of the sample is defined as nested ANOVA for non-replicable tests.

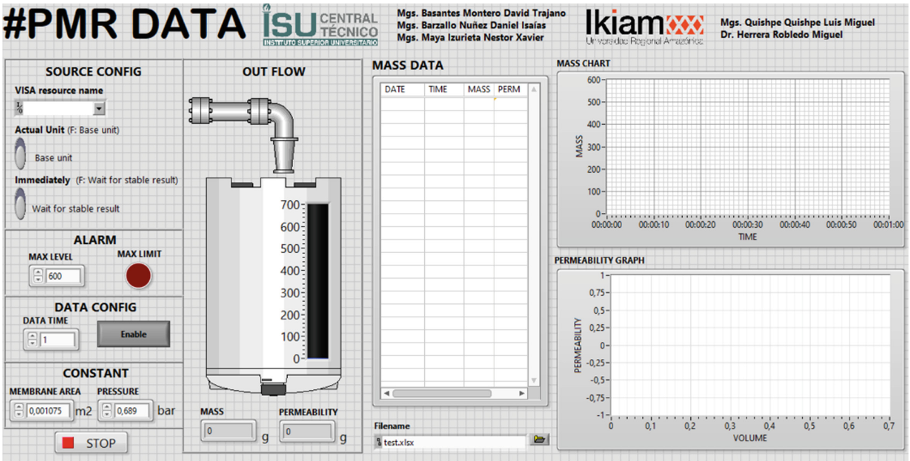

Fig. 2. DAQ system interface

The DAQ is validated by evaluating the measurement system through an (r & R) study, for which three sources of variation are included: variation within a sample, between operators or reproducibility and repeatability or inherent errors in the instrument.

The nested ANOVA method described in Table 3 simultaneously analyzes the effects of two sources of variation: operators (MA and DAQ) and filtering scenarios (W and BSA). The data were taken by the operators every ten seconds which are summarized in Table 1 and 2.

Column GL describes the degrees of freedom where k is the number of operators, n is the number of parts and r is the number of replicas. The column SS determines the sum of squares and MS the mean square between SS and GL of the operator, parts, and error. F represents the significant factor for the operator and the parts.

Table 4 describes the equations used for the non-replicable R&R study based on the analysis of variance values in Table 3.

3 Results and Disssions

Each permeability test was accompanied by manual measurements (MA) and measurements with the data acquisition system (DAQ). For both the water tests (W) and the tests with BSA (BSA), two experiments were carried out. The permeability results with deionized water can be seen in Fig. 3. The flow through the membrane stabilized at 450 ml and the permeability values were 149.26, and 138.02/m^2.h.bar for the DAQ-MEMBRANE1-W, and DAQ-MEMBRANE2-W measurements. On the other hand, the MA-MEMBRANE1-W and MA-MEMBRANE2-W obtained values of 156.32 and 138.02 m^2.h.bar respectively. The slight reduction in flux presented in Fig. 3a may be caused by slow hydration at the membrane surface [11]. The permeability values obtained are similar to those described in the study by Sumisha et al. (2015) where the same commercial membrane is used for ultrafiltration processes [32]. The permeability results with DAQ yielded a deviation of 20.4 and with MA it was 23.8. These variations

Table 1. Statistical summary membrane 1

DAQ: MEMBRANE 1 - W		*DAQ: MEMBRANE 1 - BSA*		*MA: MEMBRANE 1 - W*		*MA: MEMBRANE 1 - BSA*	
Mean	134,06	Mean	56,44	Mean	138,65	Mean	56,67
Standard error	1,43	Standard Error	0,50	Standard Error	0,95	Standard Error	0,47
Median	138,23	Median	56,52	Median	140,24	Median	56,64
Mode	139,53	Mode	62,16	Mode	138,58	Mode	58,37
Standard deviation	18,47	Standard deviation	6,44	Standard deviation	12,30	Standard deviation	6,02
Sample variance	341,15	Sample variance	41,48	Sample variance	151,33	Sample variance	36,29
Kurtosis	35,76	Kurtosis	47,17	Kurtosis	99,91	Kurtosis	53,02
Skewness	−5,71	Skewness	−6,09	Skewness	−9,26	Skewness	−6,26
Range	140,00	Range	62,20	Range	144,43	Range	62,54
Minimum	0,00	Minimum	0,00	Minimum	0,00	Minimum	0,00
Maximum	140,00	Maximum	62,20	Maximum	144,43	Maximum	62,54
Sum	22254,10	Sum	9369,55	Sum	23015,62	Sum	9406,85
Count	166,00	Count	166,00	Count	166,00	Count	166,00

Table 2. Statistical summary membrane 2

DAQ: MEMBRANA 2 - W		*DAQ: MEMBRANA 2 - BSA*		*MA: MEMBRANA 2 - W*		*MA: MEMBRANA 2 - BSA*	
Mean	155,91	Mean	51,26	Mean	163,77	Mean	53,32
Standard error	1,25	Standard Error	0,49	Standard Error	1,26	Standard Error	0,49
Median	155,89	Median	51,23	Median	163,51	Median	53,16
Mode	149,82	Mode	57,08	Mode	176,55	Mode	58,66
Standard deviation	16,08	Standard deviation	6,26	Standard deviation	16,29	Standard deviation	6,28
Sample variance	258,53	Sample variance	39,13	Sample variance	265,52	Sample variance	39,49
Kurtosis	59,31	Kurtosis	39,49	Kurtosis	64,58	Kurtosis	39,69
Skewness	−6,68	Skewness	−5,39	Skewness	−6,84	Skewness	−5,24
Range	170,25	Range	57,98	Range	178,99	Range	60,85
Minimum	0,00	Minimum	0,00	Minimum	0,00	Minimum	0,00
Maximum	170,25	Maximum	57,98	Maximum	178,99	Maximum	60,85
Sum	25880,46	Sum	8509,28	Sum	27185,41	Sum	8851,15
Count	166,00	Count	166,00	Count	166,00	Count	166,00

Table 3. Nested ANOVA

Source	GL	SS	MS	F
Operator	$k-1$	SS_A	$\frac{SS_A}{k-1}$	$\frac{\frac{SS_A}{k-1}}{\frac{SS_{P(A)}}{k(n-1)}}$
Parts (op)	$k(n-1)$	$SS_{P(A)}$	$\frac{SS_{P(A)}}{k(n-1)}$	$\frac{\frac{SS_{P(A)}}{k(n-1)}}{\frac{SS_{Error}}{nk(r-1)}}$
Error	$nk(r-1)$	SS_{Error}	$\frac{SS_{Error}}{nk(r-1)}$	
Total	$nkr-1$	SS_{Total}		

Table 4. R&R study - not replicable

Non-replicable model analysis	% TOTAL variation
Repeatability - Equipment Error (EV): $\boldsymbol{EV = \sqrt{MS_{Error}}}$	*% Repeatability - Equipment Error (EV):* $\%VE = \frac{EV}{TV} \times 100$
Reproducibility - Operator Variation (AV) $\boldsymbol{AV = \sqrt{\frac{MS_A - MS_{P(A)}}{nr}}}$	*% Reproducibility - Operator Variation (AV)* $\%AV = \frac{AV}{TV} \times 100$
Repeatability and Reproducibility (GR&R) $\boldsymbol{GR\&R = \sqrt{(EV)^2 + (AV)^2}}$	*% Repeatability and Reproducibility (GR&R)* $\%GR\&R = \frac{GR\&R}{TV} \times 100$
Variation between parts (PV) $\boldsymbol{PV = \sqrt{\frac{MS_{P(A)} - MS_{Error}}{r}}}$	*% Variation between parts (PV)* $\%PV = \frac{PV}{TV} \times 100$
Total Variation (TV) $\boldsymbol{TV = \sqrt{(GR\&R)^2 + (PV)^2}}$	*Number of distinctive categories- ndc* $ndc = 1.41\frac{PV}{GR\&R}$

are consistent with those previously reported (e.g. [29, 32, 33]). It is not necessary to rule out errors in handling the membranes, which can also affect the measurement of permeability as mentioned by Cath et al. (2013) [33].

Permeability with BSA is found in Fig. 4. DAQ-MEMBRANE-BSA and DAQ-MEMBRANE2-BSA values of 52.19, and 52.69. While the data from manual measurements were 51.11, and 52.9for MA-MEMBRANE1-BSA, and MA-MEMBRANE2-BSA2. Previous investigations reach similar permeabilities considering the use of the same fouling agent [21]. It can be seen that the permeability data with BSA are less dispersed between each experiment because the protein is standard and has a defined molecular weight cutoff (66 KDa).

The results of the nested ANOVA method applied to membrane 1 are shown in Table 5.

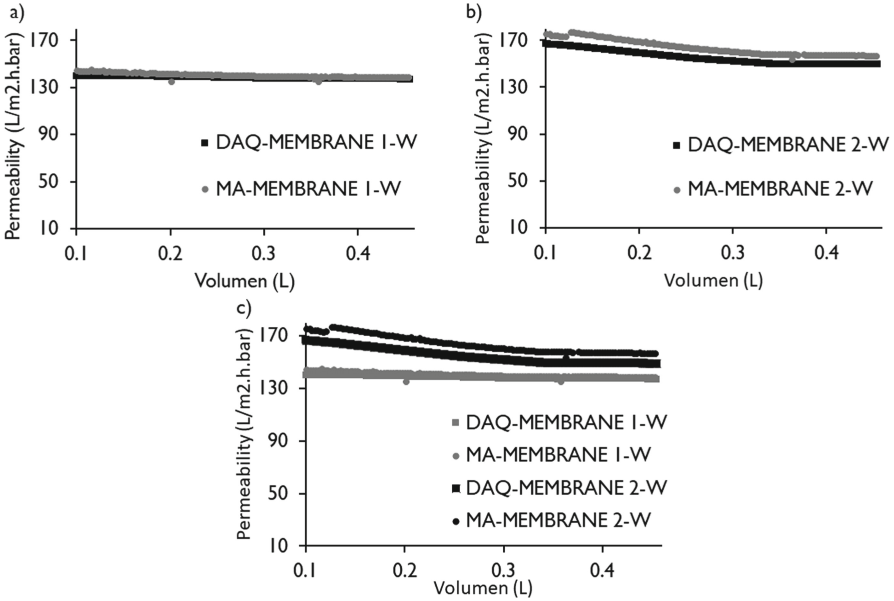

Fig. 3. Permeability with water

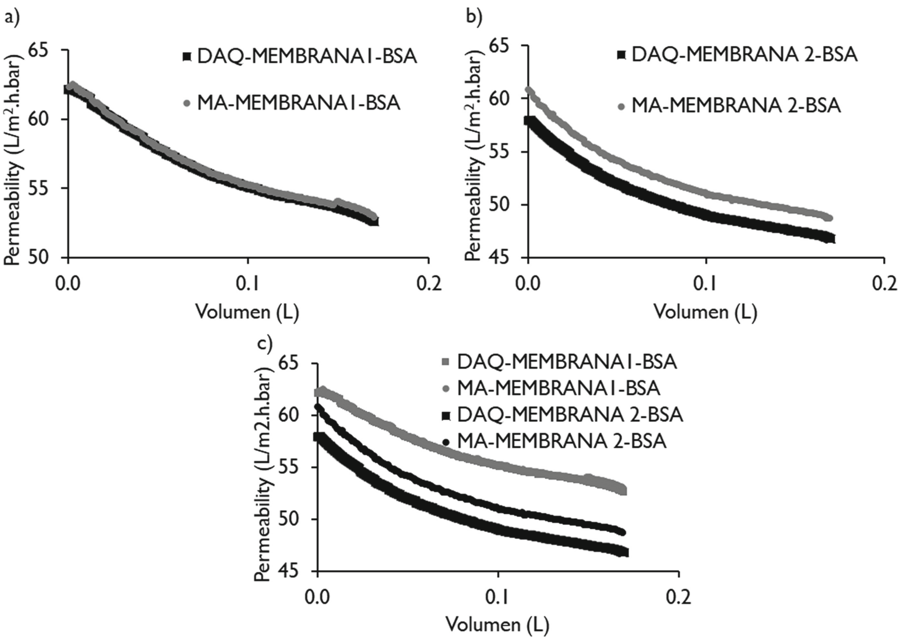

Fig. 4. Permeability with BSA

Table 5. Nested ANOVA – membrane 1

Source	GL	SS	MS	F
Operator	1	961,03	961,03	0,001816926
Parts (op)	2	1057861,97	528930,98	3710,176814
Error	660	94091,05	142,56	
Total	663			

The first analysis is done on the DAQ and MA operators, the comparison between the FOPERADOR and FA data allows to determine if there is a reproducibility error, this means that the variations between the averages of the operators are not significant. The significant critical value (FA) is calculated with the inverse of the probability distribution of the relationship of the degrees of freedom of the operator and error, then: FA = 3.855586816. As F < FA it can be concluded that there is no significantly large reproducibility error.

The second analysis is carried out on the permeability of the membranes, this allows to determine if the variation that exists between the tests of the W and BSA membranes is significantly large, for them the value of F PARTS is compared with the FP (A) value which is calculated with the inverse of the probability distribution of the relationship of the degrees of freedom of the parts and the error, then: FP (A) = 3.009371107. As F > FP (A) it can be concluded that the variation of the two scenarios is significantly large.

This same analysis is performed for the second membrane, obtaining the results shown in Table 6:

Table 6. Nested ANOVA – Membrane 2

Source	GL	SS	MS	F
Operator	1	4084,34	4084,34	0,00425143
Parts (op)	2	1921394,23	960697,11	6376,27931
Error	660	99440,45	150,67	
Total	663			

Where: FA = 3.855586816 and FP (A) = 3.009371107, therefore, F < FA and F > FP (A) it can be concluded that the results are the same as for membrane 1.

Finally, the criteria to interpret the R&R results are If% GR & R < 10% the measurement system is acceptable if 10% < % GR&R < 30% the measurement system can be acceptable according to its use, if% GR & R > 30% the measurement system is considered unacceptable and requires improvements regarding the operator, equipment, method, conditions, etc. Taking these criteria into account, the results shown in Table 7 and 8 are obtained.

Table 7. R&R study - not replicable membrane 1

Non-replicable model analysis	% TOTAL variation
Repeatability - Equipment Error (EV): $\boldsymbol{EV = \sqrt{MS_{Error}} = 11.94}$	*% Repeatability - Equipment Error (EV):* $\%VE = \frac{EV}{TV} \times 100 = 20.7\%$
Reproducibility - Operator Variation (AV) $\boldsymbol{AV = \sqrt{\frac{MS_A - MS_{P(A)}}{nr}} = 0}$	*% Reproducibility - Operator Variation (AV)* $\%AV = \frac{AV}{TV} \times 100 = 0\%$
Repeatability and Reproducibility (GR&R) $\boldsymbol{GR\&R = \sqrt{(EV)^2 + (AV)^2} = 11.94}$	*% Repeatability and Reproducibility (GR&R)* $\%GR\&R = \frac{GR\&R}{TV} \times 100 = 20.7\%$
Variation between parts (PV) $\boldsymbol{PV = \sqrt{\frac{MS_{P(A)} - MS_{Error}}{r}} = 56.44}$	*% Variation between parts (PV)* $\%PV = \frac{PV}{TV} \times 100 = 97.8\%$
Total Variation (TV) $\boldsymbol{TV = \sqrt{(GR\&R)^2 + (PV)^2} = 57.69}$	*Number of distinctive categories- ndc* $ndc = 1.41\frac{PV}{GR\&R} = 6$

Table 8. R&R study - not replicable membrane 2

Non-replicable model analysis	% TOTAL variation
Repeatability - Equipment Error (EV): $\boldsymbol{EV = \sqrt{MS_{Error}} = 12.27}$	*% Repeatability - Equipment Error (EV):* $\%VE = \frac{EV}{TV} \times 100 = 15.9\%$
Reproducibility - Operator Variation (AV) $\boldsymbol{AV = \sqrt{\frac{MS_A - MS_{P(A)}}{nr}} = 0}$	*% Reproducibility - Operator Variation (AV)* $\%AV = \frac{AV}{TV} \times 100 = 0\%$
Repeatability and Reproducibility (GR&R) $\boldsymbol{GR\&R = \sqrt{(EV)^2 + (AV)^2} = 12.27}$	*% Repeatability and Reproducibility (GR&R)* $\%GR\&R = \frac{GR\&R}{TV} \times 100 = 15.9\%$
Variation between parts (PV) $\boldsymbol{PV = \sqrt{\frac{MS_{P(A)} - MS_{Error}}{r}} = 76.07}$	*% Variation between parts (PV)* $\%PV = \frac{PV}{TV} \times 100 = 98.7\%$
Total Variation (TV) $\boldsymbol{TV = \sqrt{(GR\&R)^2 + (PV)^2} = 77.05}$	*Number of distinctive categories- ndc* $ndc = 1.41\frac{PV}{GR\&R} = 8$

When interpreting the results using the acceptance criteria described above, it was observed that the percentage of the relationship between repeatability and reproducibility was between 10% and 30%, this means that the measurement system is acceptable according to its use.

4 Conclusions

The measurement system via DAQ is acceptable based on non-replicable R&R results.

The low percentage of reproducibility error between the data acquisition of the operators and the significantly large variation expected between the permeability of W and BSA validates the correct operation of the DAQ system.

The data acquisition system developed can adapt to the use of different membranes, as well as provide accurate information in real-time to the operator based on the acquired mass values and autonomously executing the necessary operations to determine the resulting permeability values.

The permeability values for W and BSA are within the ranges reported in studies with the same commercial membrane for ultrafiltration processes, confirming the acceptability of the results.

The deviations obtained from the permeability results with DAQ are consistent with those previously reported and confirmed by the use of nested ANOVA that allows the analysis of data acquired from non-replicable assays.

References

1. Huang, Y., Feng, X.: Polymer-enhanced ultrafiltration: fundamentals, applications and recent developments. J. Mem. Sci. **586**, 53–83 (2019). https://doi.org/10.1016/j.memsci.2019.05.037
2. Mohammad, A.W., Ng, C.Y., Lim, Y.P., Ng, G.H.: Ultrafiltration in food processing industry: review on application, membrane fouling, and fouling control. Food Bioprocess Technol. **5**(4), 1143–1156 (2012). https://doi.org/10.1007/s11947-012-0806-9
3. Javier Benitez, F., Acero, J.L., Real, F.J., Roldán, G., Rodriguez, E.: Ultrafiltration and nanofiltration membranes applied to the removal of the pharmaceuticals amoxicillin, naproxen, metoprolol and phenacetin from water. J. Chem. Technol. Biotechnol. **86**, 858–866 (2011). https://doi.org/10.1002/jctb.2600
4. Peter-Varbanets, M., Zurbrügg, C., Swartz, C., Pronk, W.: Decentralized systems for potable water and the potential of membrane technology. Water Res. **43**, 245–265 (2009). https://doi.org/10.1016/j.watres.2008.10.030
5. Benito, J.M., Conesa, A., Rodríguez, M.A.: Membranas cerámicas. Tipos, métodos de obtención y caracterización. Bol. Soc. Espanola Ceramica Vidrio. **43**, 829–842 (2004). https://doi.org/10.3989/cyv.2004.v43.i5.410
6. Meerholz, K., van der Westhuizen, D.J., Krieg, H.M.: Automation of membrane based solvent extraction unit for Zr and Hf separation. Sep. Purif. Technol. **179**, 204–214 (2017). https://doi.org/10.1016/j.seppur.2017.01.064
7. Salcedo, J.C., Rojas, R., Bullón, J., Cárdenas, A.: Utilizando membranas cerámicas de microfiltración. Uso de policloruro de aluminio como agente para mejorar la filtración
8. Shurygin, M., Guenther, C., Fuchs, S., Prehn, V.: Effective treatment of the wastewater from ceramic industry using ceramic membranes. Water Sci. Technol. **83**, 1055–1071 (2021). https://doi.org/10.2166/wst.2021.039
9. Nilusha, R.T., Yu, D., Zhang, J., Wei, Y.: Effects of solids retention time on the anaerobic membrane bioreactor with Yttria-based ceramic membrane treating domestic wastewater at ambient temperature. Membranes (Basel) **10**(9), 1–18 (2020). https://doi.org/10.3390/membranes10090196

10. Guo, B., Snow, S.D., Starr, B.J., Xagoraraki, I., Tarabara, V.V.: Photocatalytic inactivation of human adenovirus 40: effect of dissolved organic matter and prefiltration. Sep. Purif. Technol. **193**(November), 193–201 (2018). https://doi.org/10.1016/j.seppur.2017.11.012
11. Starr, B.J., Tarabara, V.V., Herrera-Robledo, M., Zhou, M., Roualdes, S., Ayral, A.: Erratum: corrigendum to 'coating porous membranes with a photocatalyst: comparison of LbL self-assembly and plasma-enhanced CVD techniques'. J. Membr. Sci. **514**, 340–349 (2016). https://doi.org/10.1016/j.memsci.2016.08.063
12. Deratani, A., Palmeri, J., Theorique, L.D.P.: Uso de la tecnología de nanofiltración a través de membranas para el tratamiento de las aguas residuales de la industria cerámica, pp. 1–13 (2015)
13. Cui, Z.F., Jiang, Y., Field, R.W.: Fundamentals of pressure-driven membrane separation processes. In: Membrane Technology (2010)
14. Mamah, S.C., et al.: Recent development in modification of polysulfone membrane for water treatment application. J. Water Process Eng. **40**, 101835 (2021). https://doi.org/10.1016/j.jwpe.2020.101835
15. Basri, H., Ismail, A.F., Aziz, M.: Polyethersulfone (PES) ultrafiltration (UF) membranes loaded with silver nitrate for bacteria removal. Membr. Water Treat. **2**, 25–37 (2011). https://doi.org/10.12989/mwt.2011.2.1.025
16. Gebru, K.A., Das, C.: Removal of bovine serum albumin from wastewater using fouling resistant ultrafiltration membranes based on the blends of cellulose acetate, and PVP-TiO2 nanoparticles. J. Environ. Manage. **200**, 283–294 (2017). https://doi.org/10.1016/j.jenvman.2017.05.086
17. Ouyang, G., Hussain, A., Li, J., Li, D.: Remarkable permeability enhancement of polyethersulfone (PES) ultrafiltration membrane by blending cobalt oxide/graphene oxide nanocomposites. RSC Adv. **5**, 70448–70460 (2015). https://doi.org/10.1039/c5ra11349k
18. Jin, F., et al.: High-performance ultrafiltration membranes based on polyethersulfone-graphene oxide composites. RSC Adv. **3**, 21394–21397 (2013). https://doi.org/10.1039/c3ra42908c
19. Shin, S.J., Kim, J.P., Kim, H.J., Jeon, J.H., Min, B.R.: Preparation and characterization of polyethersulfone microfiltration membranes by a 2-methoxyethanol additive. Desalination **186**, 1–10 (2005). https://doi.org/10.1016/j.desal.2005.03.092
20. Sun, M., Su, Y., Mu, C., Jiang, Z.: Improved antifouling property of PES ultrafiltration membranes using additive of silica-PVP nanocomposite. Ind. Eng. Chem. Res. **49**, 790–796 (2010). https://doi.org/10.1021/ie900560e
21. Kuzmenko, D., Arkhangelsky, E., Belfer, S., Freger, V., Gitis, V.: Chemical cleaning of UF membranes fouled by BSA. Desalination **179**, 323–333 (2005). https://doi.org/10.1016/j.desal.2004.11.078
22. Gelamo, E.L., Silva, C.H.T.P., Imasato, H., Tabak, M.: Interaction of bovine (BSA) and human (HSA) serum albumins with ionic surfactants: Spectroscopy and modelling. Biochim. Biophys. Acta - Protein Struct. Mol. Enzymol. **1594**, 84-99 (2002). https://doi.org/10.1016/S0167-4838(01)00287-4
23. Liu, Y., Huang, H., Huo, P., Gu, J.: Exploration of zwitterionic cellulose acetate antifouling ultrafiltration membrane for bovine serum albumin (BSA) separation. Carbohydr. Polym. **165**, 266–275 (2017). https://doi.org/10.1016/j.carbpol.2017.02.052
24. Kiani, S., Mousavi, S.M., Saljoughi, E., Shahtahmassebi, N.: Preparation and characterization of modified polyphenylsulfone membranes with hydrophilic property for filtration of aqueous media. Polym. Adv. Technol. **29**, 1632–1648 (2018). https://doi.org/10.1002/pat.4268
25. Razi, F., Mulyati, S., Arahman, N.: The performance of bovine serum albumin filtration by using polyethersulfone-tetronic 304 blend ultrafiltration membrane. F1000Research **8**, 953 (2019). https://doi.org/10.12688/f1000research.18740.2

26. Amjad, H., Khan, Z., Tarabara, V.V.: Fractal structure and permeability of membrane cake layers: effect of coagulation-flocculation and settling as pretreatment steps. Sep. Purif. Technol. **143**, 40–51 (2015). https://doi.org/10.1016/j.seppur.2015.01.020
27. Wang, K.Y., Ong, R.C., Chung, T.S.: Double-skinned forward osmosis membranes for reducing internal concentration polarization within the porous sublayer. Ind. Eng. Chem. Res. **49**, 4824–4831 (2010). https://doi.org/10.1021/ie901592d
28. Cheng, C., et al.: The hydrodynamic permeability and surface property of polyethersulfone ultrafiltration membranes with mussel-inspired polydopamine coatings. J. Memb. Sci. **417–418**, 228–236 (2012). https://doi.org/10.1016/j.memsci.2012.06.045
29. Maximous, N., Nakhla, G., Wan, W., Wong, K.: Performance of a novel ZrO2/PES membrane for wastewater filtration. J. Memb. Sci. **352**, 222–230 (2010). https://doi.org/10.1016/j.memsci.2010.02.021
30. Lusiana, R.A., et al.: Permeability improvement of polyethersulfone-polietylene glycol (PEG-PES) flat sheet type membranes by tripolyphosphate-crosslinked chitosan (TPP-CS) coating. Int. J. Biol. Macromol. **152**, 633–644 (2020). https://doi.org/10.1016/j.ijbiomac.2020.02.290
31. Botero Arbelaez, M., Mendoza Vargas, J., Arbeláez Salazar, O.: Método ANOVA utilizado para realizar el estudio de repetibilidad y reproducibilidad dentro del control de calidad de un sistema de medición. Sci. Tech. **5**(37), 533–537 (2007). https://doi.org/10.22517/23447214.4181
32. Sumisha, A., Arthanareeswaran, G., Lukka Thuyavan, Y., Ismail, A.F., Chakraborty, S.: Treatment of laundry wastewater using polyethersulfone/polyvinylpyrollidone ultrafiltration membranes. Ecotoxicol. Environ. Saf. **121**, 174–179 (2015). https://doi.org/10.1016/j.ecoenv.2015.04.004
33. Cath, T.Y., et al.: Standard methodology for evaluating membrane performance in osmotically driven membrane processes. Desalination **312**, 31–38 (2013). https://doi.org/10.1016/j.desal.2012.07.005

Energy and Material

Design and Implementation of a Three-Phase Analyzer in a Free Software Platform for Power Quality Measurement at Industrial Activities

Ricardo Rosero(✉), Oscar Gonzales, Christian Llumiquinga, Anabel Portero, and Gabriel Vásquez

Instituto Superior Tecnológico Sucre, Campus Sur Av. Teodoro Gómez de la Torre S14 - 72 y Joaquín Gutiérrez, Quito, Ecuador
{rrosero,ogonzales,cllumiquinga,aportero,gvasquez}@tecnologicosucre.edu.ec

Abstract. Power quality analyzers are instruments that have various residential and commercial applications. These electrical devices measure various variables from basic quantities such as voltage, current or power to complex parameters such as harmonic content or power factor. Energy analyzers are too expensive instruments due to the high technological development involved in their manufacture. For this reason, this article shows an alternative in which a three-phase energy analyzer was designed and built with basic characteristics for measuring energy parameters. The energy analyzer was built with a RASPBERRY PI 4 platform in which voltage and current sensors were implemented to measure energy at different loads. The final prototype was validated with the use of standardized laboratory instruments and the utilization of different electrical loads to be able to size the scope to which the analyzer can be used.

Keywords: PyQt5 · Coding · Python · Rasberry Pi4 · Electrical magnitudes · THD

1 Introduction

Nowadays, there are different measurement equipment for the quality of electrical energy as well as for the different measurement magnitudes. Examples of this equipment are voltmeters, ammeters, wattmeters, harmonic analyzers, power quality analyzers, among others. These teams are built with the purpose of satisfying the needs of users on a professional and educational level. The functionality of the different modules offered by the market on this subject varies according to their construction; for example, some of them allow data to be stored, sent, and viewed in real time in a computer screen [1].

One of the equipment that is most in demand in the industrial field is the energy analyzer that allows establishing the quality of the electricity supplied by the consumer grid. End users benefit from proper monitoring of the level of energy quality resulting from efficient use of energy.

© The Author(s), under exclusive license to Springer Nature Switzerland AG 2023
M. Zambrano Vizuete et al. (Eds.): RITAM 2021, LNNS 512, pp. 121–137, 2023.
https://doi.org/10.1007/978-3-031-11295-9_9

There are different models of energy analyzers, due to the type of supply they can be found as single-phase or three-phase. The acquisition of any of these devices depends on the purpose for which they are designed. The benefits of energy analyzers make these kits quite expensive. This characteristic implies that certain higher-level educational institutions that are training their students in power quality analysis may not be able to accomplish this end because of the high investment immersed in buying power quality analyzers [2].

There are works that have promoted the creation of these devices in order to put into practice knowledge in advanced electronic systems. In the case of the work developed by [3], a three-phase analyzer was built for a laboratory at the Polytechnic University of Valencia by means of an ARDUINO microcontroller. Although the mentioned microcontroller is useful for many electronic applications, it should be noted that there are other advanced platforms that have advantages over the ARDUINO in the resolution of the analog variables or in the memory capacity.

Another development of a three-phase analyzer carried out by [4], shows a functional unit with the necessary implements to measure voltage, current, power and the revision of the quality of the energy by means of the quantification of harmonics. However, the final prototype shows dimensions of $40 \times 26 \times 29$ cm which represents an obstacle in terms of portability.

On the other hand, [5] developed a three-phase energy analyzer for low voltage installations. The analyzer showed good performance especially in data processing. However, the maximum power value is limited to 1 kW where residential loads that exceed this value could not be measured as is the case with a washing machine that exceeds 1.5 kW.

The reasons previously analyzed led the authors of this work to design and build a three-phase energy analyzer with an open platform processor with performances superior to those of ARDUINO, with dimensions that ensure the portability of the instrument and with measurements of powers greater than 1 kW. The present work shows the construction process of a three-phase energy analyzer starting from low-cost elements. In the construction of this equipment, a RASPBERY PI4 platform was used, which allowed the extraction of data from the measurements carried out in the different test equipment. In the same way, a 7″ HDMI screen was used as a data display where the magnitudes of voltage, current, power, power factor and harmonic content THD were observed.

The article is divided into the following sections: the methodology describes the parameters observed for the design and construction of the equipment. The Tests and Results section shows the tests that allowed the equipment to be validated. Finally, the conclusions section presents the representative ideas obtained from the project.

2 Method

This section describes the materials and steps that were necessary for the design and implementation of the three-phase energy analyzer.

2.1 Schematic of the Energy Analyzer

The stages of electronic development and the elements related to them are shown in Fig. 1. The signals captured by the voltage and current sensors are conditioned to have values that will later be processed. The use of filters improves signals that are affected by noise or magnetic interference phenomena. The power supplies allow the use of different electronic elements that operate at different voltages, such as the RAPBERRY PI 4 platform or voltage and current sensors.

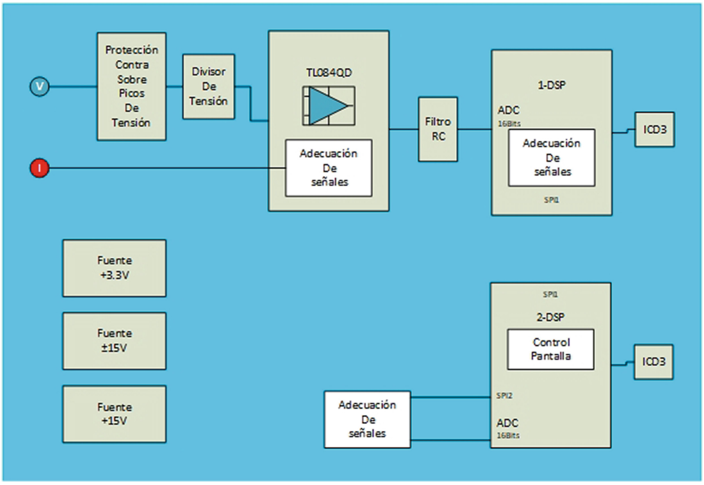

Fig. 1. Design stages of the three-phase analyzer [6].

The voltage and current data are processed in the electronic platform to be able to display active and reactive power values, power factor and THD.

2.2 Elements Considered for the Construction of the Energy Analyzer

RAPBERRY PI 4: It is a computer the size of a credit card, it has a lot of versatility to be able to adapt to a television and a keyboard. This electronic platform has several components the same as a common computer CPU. For these reasons, the electronic card can be used as a desktop PC. The RASPBERRY 4 platform is characterized because it is capable of performing different tasks such as: the implementation of spreadsheets, word processors, programming and video game interfaces. Other activities such as playing videos and sounds in high definition are also mentioned [7]. The electronic platform can be seen in Fig. 2 and its characteristics in Table 1.

Non-invasive Current Sensor SCT-013: It is a non-invasive current sensor that measures current up to 30 amps. These sensors have advantages over similar devices in the aspect of making measurements without the need to cut the conductors.

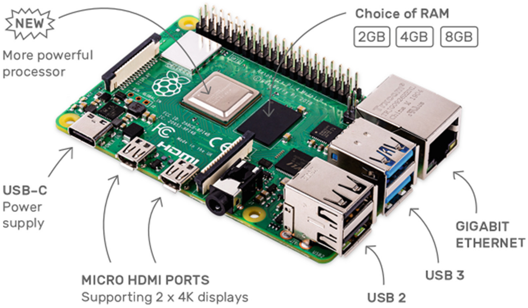

Fig. 2. RASPBERRY PI 4 [7].

Table 1. RASPBERRY PI 4 features [7].

Characteristic	Description
Number of cores	4
Processor	ARM Cortex-A72
CPU	1.5 GHz 64-bit quad-core Cortex-A72
GPU	Broadcom Video Core VI, OpenGL ES 3.0, 1080p30 H.264/MPEG-4 AVC, 4kp60 H.265
Memory	1 GB, 2 GB, 4 GB or 8 GB (shared with the GPU)
USB stations	USB 2.0 X 2 USB 3.0 X 2
Video input	MIPI CSI connector that allows installing a camera module developed by the RASPBERRY PI Foundation
Video outputs	RCA connector (PAL and NTSC), HDMI (rev1.3 and 1.4), DSI interface for LCD panel
Network connectivity	10/100/1000 Mbps RJ-45 port via USB 3.0 hub Wi-Fi 802.11ac dual band Bluetooth 5.0 BLE
Supported operating systems	GNU/Linux: Raspbian
Power supply	5 V via USB-C or GPIO port
Dimensions	85 mm × 53 mm

These non-invasive AC sensors are a good way to measure actual consumption without altering the electrical composition of the loads. They work by magnetic induction, in other words, the field generated in the wire that is used to power the device produces a current induction in the transformer built into the sensor. In this way, the current calculation is not limited only to loads with a low current value but also to loads with higher consumption as long as they do not exceed the maximum value of the sensor measurement [8].

In these sensors, the number of turns represents the relationship between the current flowing through the cable and the amount of current delivered by the sensor. This relationship is the difference between various sensor models that allow them to operate at different maximum current measurement values. Additionally, some models have a load resistor at the output terminals that allow them to obtain a voltage output. Voltage values are easier to process in instrumentation in measurement circuits compared to current values. The diagram of the current sensor can be seen in Fig. 3 and the characteristics of this device are shown in Table 2.

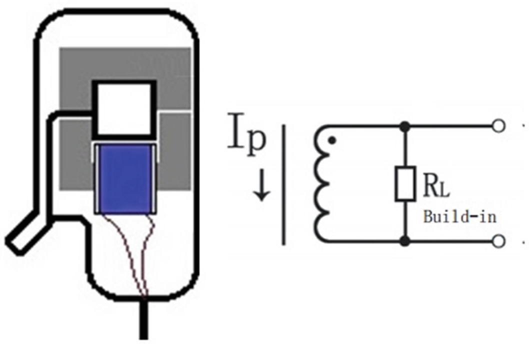

Fig. 3. Non-invasive current sensor [8].

Table 2. Characteristics of the non-invasive current sensor SCT-013 [8].

Characteristic	Description
Output mode	0–1 V
Input current	0–30 Amp AC
Dielectric Strength	1000 V AC/1 min 5 mAmp
Work temperature	−25 °C/70 °C
Core material	Ferrite
Sensor output connector	3.5 mm
Output current	0–50 mAmp
Cable length	1 m

ZMTP 101b Voltage Sensor: Voltage measurement (AC) was performed with the ZMTP 101b alternating voltage transformer module. This device represents one of the most feasible solutions for adaptability to microcontrollers because its output voltage values are in the range of 3 V–5 VDC.

The main function of this sensor is to reduce the voltage to measure and monitor signal data in real time. For voltage measurement, this sensor delivers values that are instrumented to be able to view the results through an HMDI screen that will be connected to the RASPBERRY PI4. You can see in Fig. 4 the image of the voltage sensor and in Table 3 the characteristics of this device.

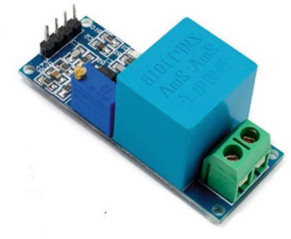

Fig. 4. ZMTP 101b voltage sensor [9].

Table 3. ZMTP 101b voltage sensor features [9].

Characteristics	Description
Supply voltage	3.3 V–5 VDC
Alternating input voltage	250 VAC max
Exit sign	Sine analog
Input electrical isolation	Up to 3000 V
Rated input and output current	2 mA
Linearity	1%
Precision	0.2%

2.3 Calculation of Electrical Parameters

The calculations of the electrical parameters are made from the measurements of the voltage and current sensors [10]. For the case of active power, the formula that allows the calculation of active power is shown below:

$$\mathrm{P} = \mathrm{U} * \mathrm{I} * \cos\varphi \quad (1)$$

The angle of the cosine function represents the phase shift that exists between the voltage wave and the current wave. Theoretically, the phase angle is understood to be the value generated by relating the reactive and resistive part of a load:

$$\varphi = \mathrm{arctg}\frac{\mathrm{X}}{\mathrm{R}} \quad (2)$$

However, the meter must be able to measure this angle without first knowing the load at which it is being measured. Where X is the reactance and R is the resistance of the connected load being the impedance.

$$Z = R + jX \tag{3}$$

An alternative is the use of a counter that measures the lag time between the amplitudes of the voltage and current waves. These values can be obtained through the maximum values of each signal. In this way, the lag value measured in time will be transformed to its equivalent in angle, taking into account that the complete cycle of an alternating current wave is generated at 16.6 mS. Finally, with all the values already mentioned, the calculation of the active power is achieved, and the same procedure is carried out for the calculation of the reactive power.

$$Q = U * I * \mathrm{sen}\varphi \tag{4}$$

On the other hand, the apparent power value is obtained by multiplying the effective voltage and current values of each of the sensors.

$$S = Vrms * Irms \tag{5}$$

The values delivered by the sensors as a function of time are processed inside the microcontroller to obtain their effective values.

$$FP = \cos\varphi = \frac{P[KW]}{S[KVA]} \tag{6}$$

The previously found values of active and apparent power allow the calculation of the power factor. To finish the section of calculations that the energy analyzer performs, the harmonic content THD is taken into account. This parameter is obtained through the expansion of the Fourier series:

$$X(jw) = \sum_{n=0}^{L-1} x(n) * e^{-jwn} \tag{7}$$

The operation between these functions is developed in terms of the periodic functions like sine and cosine:

$$X(jw) = \sum_{n=0}^{L-1} x(n)\left[\cos(wn) - j\mathrm{sen}(wn)\right] \tag{8}$$

The calculation ends with obtaining the magnitude of the previous expression that allows evaluating the voltage or current signal to determine its harmonic content.

$$|X(jw)| = \sqrt{\left[\sum_{n=0}^{L-1} x(n)\cos(wn)\right]^2 + \left[\sum_{n=0}^{L-1} x(n)\mathrm{sen}(wn)\right]^2} \tag{9}$$

2.4 Electronic Scheme

In the electronic design of the three-phase analyzer, elements that have been mentioned in the different sections of this work have been taken into account. In Fig. 5, it is shown how the different sensors and their coupling circuits are connected.

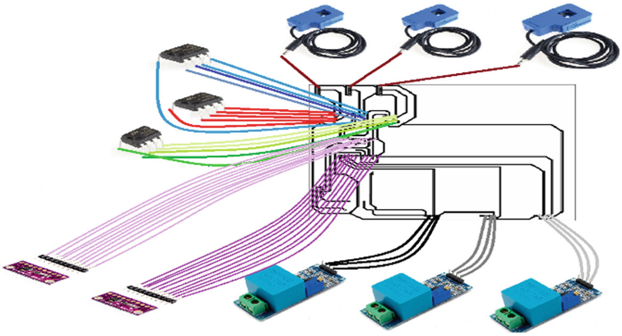

Fig. 5. Sensor connection on the PCB.

In Fig. 6, the connection diagram of the control card and a digital signal adapter is shown.

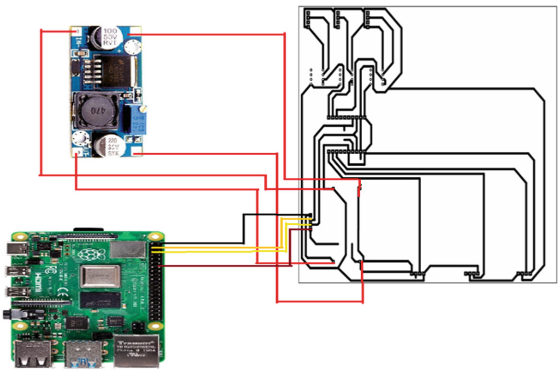

Fig. 6. Connecting the Raspberry Pi 4 and the LM2596.

The data reading obtained with these sensors will be processed by the ADS 115, which takes the analog input of the sensor and converts it into a digital output connected to the pins of the RASPBERRY PI 4, which are digital inputs, such as the SDA and SDL.

2.5 Programming

After measuring the voltage and current variables, it should be taken into account that on some occasions the data must be distorted. This phenomenon is generated by the influence of electromagnetic interference that the environment where the measurement is made may have. One of the alternatives to overcome this inconvenience is the use of filters. Filters can be analog or digital. In this case, digital filters are used that are programmed by means of the corresponding libraries of the control platform that allow setting cut-off frequencies and thus obtain more actionable data. ADAFRUIT's filter libraries were used, which allows the sensor to be better encoded and to obtain voltage signals without very significant distortions (Fig. 7).

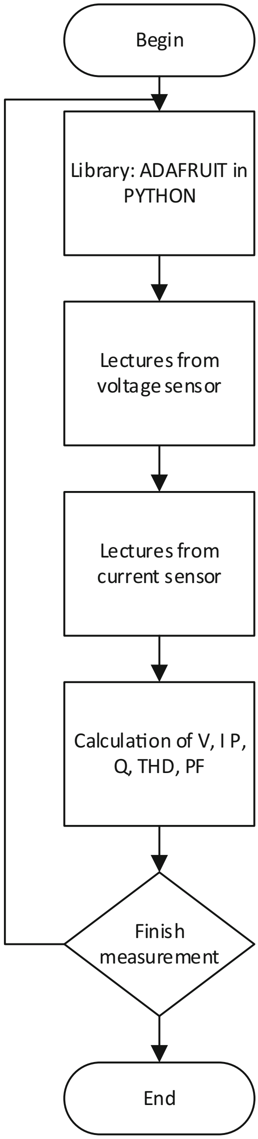

Fig. 7. ZMPT 101B AND ADS1115 voltage measurement reading flow chart.

After obtaining, filtering and processing the data, the calculations of the voltage, current, powers, power factor and THD parameters are performed.

3 Results

In this section the report of the performance tests and analysis of the results obtained is carried out. The different tests carried out to which the prototype has been subjected will be detailed. Different electrical devices were considered that will be measured both by the prototype and by calibrated electrical measuring elements. The tests were carried out on different equipments which include: a washing machine, a miter saw, a welding machine and an industrial motor. Due to the extension that must be fulfilled with the elaboration of this article, only the data produced by the washing machine has been taken into account.

In the case of the washing machine, different current values were taken from its different operating modes. In the case of voltage, this value was always constant because its minister did not change in the operation of the washing machine. Although there are certain variations that correspond to small units in the voltage, these variations are admissible because they depend on the electrical supply and the loads that are connected in the electrical installation.

Table 4. Measurement of voltages and currents in different devices, in the premises (Metal mechanics the locksmith)

Equi. measured	Low three phase analyzer	Commercial multimeter	Percentage relative error (%)
Voltage values (v)			
Washing machine	113.92 V	114.05 V	0.11%
	113.89 V	114.0 V	0.096%
	114.02 V	113.98 V	−0.035%
	113.96 V	114.03 V	0.061%
Current values (A)			
Washing machine	9.951A	9.29 A	0.71%
	9.729 A	9.20A	0.57%
	9.706 A	9.33 A	0.40%
	9.651 A	9.26 A	0.42%

Table 4 shows different measurements taken by both the commercial multimeter and the network analyzer prototype, and it has been observed that; The range of error in percentage shows that the equipment built gives between 0 and 2% of error, which is satisfactory, and an adequate result is obtained for the project carried out.

Next, an image is shown showing the process carried out for the validation with calibrated instruments (Fig. 8).

Fig. 8. Measurement obtained by the commercial multimeter, of the voltage supplied in the premises (Metal mechanics the locksmith).

The graphical interface of the prototype is shown below, where the different quantities that have been measured are provided. Additionally, two panels are presented in which voltage or current waves can be observed depending on the needs of the end user. This prototype has a display system through a 7-in. screen which helps a lot to the graphic interpretation and the values obtained in the measurement processes (Fig. 9).

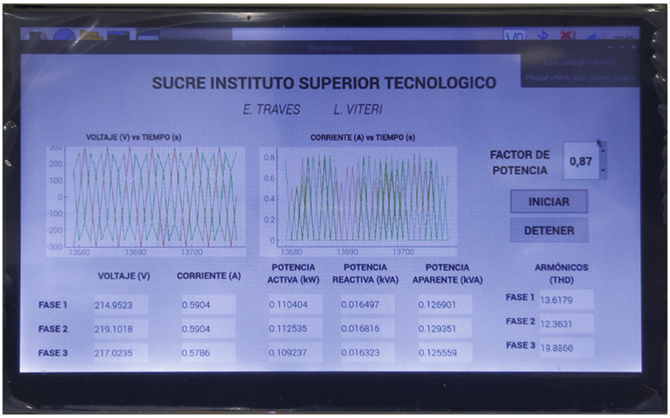

Fig. 9. Measurement obtained by the built-in analyzer, of the vertical compressor, with a failure rate of 0.55%.

On the other hand, for a quantitative validation of the values obtained by the prototype, a numerical and graphic analysis was chosen. The analyzed data of the different measurements are shown below (Figs. 10 and 11).

By means of the number of measurements, the different magnitudes of voltage and current measured by the prototype and by the industrial instruments were established. In voltage measurements, the most distant values between the aforementioned instruments have a difference of around 1 V, which is quite a small value compared to the magnitude

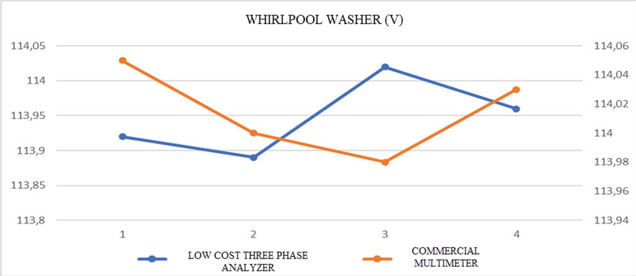

Fig. 10. Low cost three-phase analyzer vs commercial multimeter, measured in voltage of a washing machine.

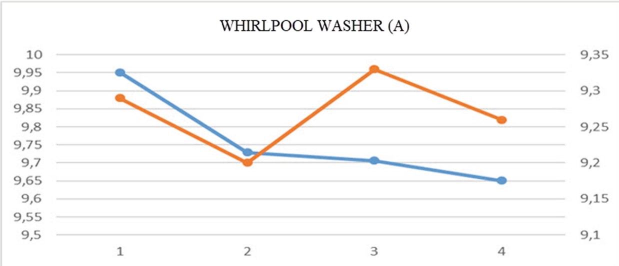

Fig. 11. Low cost three-phase analyzer vs commercial multimeter, measured in current (A) of a washing machine.

offered by the signal from the 110 V electrical network effective. With regard to current values, the most distant values have a difference of about a little more than a tenth of an ampere. This means that for the requirements requested by the end user, the current values are extremely precise and in this way there is a direct impact on the calculation of other values such as power with the harmonic content THD.

These values have a very pronounced closeness between the commercial instruments and the developed prototype. In terms of power, you should always be very careful with the precision because due to this it is possible to estimate subsequent actions; for example, the power factor correction that a company needs to meet the standards that exist from who supplies the electricity locally. In this way, the company is favored by strictly complying with electricity quality regulations and by avoiding financial penalties for unnecessary production and excess reactive power (Table 5).

Finally, Table 6 shows a comparative analysis between a developed device and a commercial one. For the comparison of these devices, the search for a device with similar characteristics represents a challenge that was completed with the choice of the Fluke 1732 device with characteristics and low cost.

Currently, there are some alternatives for choosing this type of electrical equipment. However, the equipment of the brand has stood out over the years for its quality for energy measurement. In the analysis, it is observed that for the basic needs that a company has

Table 5. Measurement comparison table

Washing machine				
	Active power (kw)	Reactive power (KVAR)	Apparent power (KVA)	Relative error (%)
Low cost three-phase analyzer	0.908398	0.227099	1.135497	0.39%
Commercial multimeter	0.841	0.114	1.051	

in the measurement of electrical parameters, the prototype meets the expectations generated, there are characteristics that can give a plus to the project and that are recommended for future development. These characteristics have to do with communication capacity, data storage, remote operability, among others. Although there are certain characteristics of the commercial device that show it as a better alternative with respect to devices of similar brands, it is observed in Table 6 that the project has a very promising achievability if it is taken into account that the budget allocated for the implementation of this is much less than what a basic industrial instrument can cost.

After having finished with all the tests to which the analyzer has been subjected, the construction of the analyzer is concluded. It should be noted that in the software part, the different calibrations of the sensors were carried out, the complete review of the code, the visualization of the graphical interface which is user-friendly to make the prototype comply with the operating conditions you need an electrician or a student of this branch.

Meanwhile on the hardware, the design was done on different boxes to decide on a viable alternative for the purposes of the project. Other important factors were taken into account such as presentation and safety that must be met with the components that are inside and outside and with the user to avoid injuries to the user. The test was carried out in a metal box measuring 15 cm × 20 cm × 10 cm, in which the results were not favorable since the space was very small for all the components that the analyzer has. A 25 cm * 25 cm * 13 cm metal box was purchased. With this box there were no problems in space, but there were problems in isolating it because some elements were damaged when placing them in the box, and the isolation was not enough because there were parasitic currents that ran through this box in obtaining signals (Figs. 12 and 13).

Table 6. Three phase analyzer comparison (low cost three phase analyzer-commercial three phase analyzer) [11]

Characteristics	Low cost three-phase analyzer	Commercial analyzer (Fluke 1732)
Voltage and Current Measurement	*	*
Power triangle measurement	*	*
Measurement of THD with respect to current	*	No
Measurement of different harmonics in the network	No	No
Viewing the voltage and current graphs	*	*
Power factor desired by the user	*	*
Power factor measurement	No	*
Wi-Fi/Bluetooth	*	Optional
Expansion of functions	*	No
Web browsing	*	No
Connection via Wi-Fi router	*	Requires license
Measuring range	0 to 400 V 0 to 40 Amp	600/1000 V Up to 300 Amp
Measurement failure range	1%	0.5%
Memory expansion	*	No
Data storage	*	No
Touch screen	*	*
Rechargeable battery	No	*
Equipment cost	$ 1,050.20	$ 2,869.00

Fig. 12. Finished analyzer.

Fig. 13. Internal connection of the analyzer.

The placement of the elements inside the control box allows an adequate operation of future maintenance. The maintenance has to do with the calibration of sensors or their replacement if the maximum operating values for the analyzer's current voltage are not respected, such as 400 V and 40 A.

4 Conclusions

After the completion of the construction of this measurement equipment, the following conclusions have been reached:

By implementing each of the elements that were used in the design and construction of the three-phase energy analyzer starting from low-cost elements, the use of current sensors was established, as well as voltage sensors, and a more optimal way was found to couple these elements to the RASPBERRY PI4 board, the different communication methods, as well as the programming languages that can be used for RASBPERRY PI 4, where the use of the PYTHON programming language was established, the same that was used for the construction of the equipment. Adequate operation was observed where it could be noted that there was no greater variation and loss of measurements with respect to commercial measurement equipment, as far as the visualization can be observed on an HDMI screen, the different mentioned electrical parameters throughout the development of the degree work.

The equipment designed (coded) in the PYTHON programming language shows great performance since it was used in a RASPBERRY PI 4 board, which is a small computer, which at the time of the presentation of the electrical parameters on the screen HDMI are almost immediately viewable, in the same way for voltage readings.

Regarding the development of the graphical interface, modules of the same PYTHON called PyQt5 were used, which is generally used for applications with graphical interface where the text boxes were designed to read the different parameters to be measured.

In the construction of the three-phase energy analyzer modeling, a compact and robust system was used where a casing was made designed so that all the elements implemented in the construction of the equipment fit in it, in order to have a protection from environmental factors such as dust, humidity among others, an electronic plate was manufactured from it that was designed in the PROTEUS software and its printing was done in a traditional way, where the electronic elements that this equipment uses to its correct operation.

The tests carried out on different machines and equipment show that the equipment presents an error of 3.3%, where it was determined that the built equipment is optimal for industrial use, taking into account that the equipment used at the industrial level presents an error between 1–3%, with all these specifications and characteristics indicated, the conclusion can be reached; than the three-phase energy analyzer using low-cost elements, because at the time of measurement as well as its sampling, it causes a minimum delay of 1 s in the presentation of the results on the HDMI screen.

References

1. Tokheim, R.L.: Electrónica digital. Reverté (2021)
2. Tejeda, R.A., González, L.C.M., Monarrez, F.L.: Sistema de monitoreo de consumo eléctrico inalámbrico y analizador de la calidad de la energía. Cult. Científica Tecnol. (63) (2018)
3. Maícas Muñoz, R.: Diseño y montaje de un analizador de redes trifásico mediante un microcontrolador Arduino, programación de una HMI y comunicación del sistema a través de Modbus. Aplicación a una microrred basada en Energías Renovables (2017)
4. Enriquez Quintana, A.L.: Diseño y construcción de un analizador de redes para implementar el laboratorio de metrología en la Facultad de Ingeniería Eléctrica y Electrónica (2020)
5. Ramirez, D., Vanegas, J., Santamaria, F., Trujillo, C.: Diseño de un Prototipo para el Monitoreo de Armónicos y Parámetros de Estado Estable en Redes de Tensión menor a 1 kV Design of a prototype for monitoring of harmonics and steady state parameters in networks of voltage less than 1 kV
6. Revelo Aguilar, F.R.: Analizador de calidad de energía eléctrica con supervisión en tiempo real. Bachelor's thesis, Universidad Técnica de Ambato. Facultad de Ingeniería en Sistemas, Electrónica e Industrial. Carrera de Ingeniería en Electrónica y Comunicaciones (2018)

7. Atiqur, R., Li, Y.: Automated smart car parking system using raspberry Pi 4 and iOS application. Int. J. Reconfig. Embed. Syst. (IJRES) **9**(3), 229–234 (2020)
8. Hajar, I., Hafizd, M., Dani, A.W., Miharno, S.: Monitoring of electrical system using internet of things with smart current electric sensors. Sinergi **22**(3), 211–218 (2018)
9. Haglan, H.M., Ali, H.J.: An automatic system for detecting voltage leaks in houses to save people's lives. Indon. J. Electr. Eng. Comput. Sci. **21**(3), 1485–1492 (2021)
10. Castillo, J.C.M.: Electrónica de potencia (Electrónica). Editex (2017)
11. Rancilio, G., et al.: Modeling a large-scale battery energy storage system for power grid application analysis. Energies **12**(17), 3312 (2019)

Electrical Consumption Optimization Based on Clustering of Consumers' Data Applying K-Means Algorithm

Oscar Gonzales[1(✉)], Alexandra Jácome[2], Christian Ortega[1], and Diego González[1]

[1] Instituto Superior Tecnológico Sucre, Campus Sur Av. Teodoro Gómez de la Torre S14 - 72 y Joaquín Gutiérrez, Quito, Ecuador
{ogonzales,cortega,dgonzalez}@tecnologicosucre.edu.ec
[2] Universidad Técnica del Norte, Av. 17 de Julio 5-21, Ibarra, Ecuador
ajacome@utn.edu.ec

Abstract. This new era demands the use of electricity in an efficient way. The growth of population and the increasing percentage of urban zones shows several needs for preparing the actual electrical infrastructure to reach higher demands. In this paper, the optimization of consumer's data is performed through metaheuristic methods. The first step was to determine the higher electricity consumers from K-means algorithm. After identifying the data to be optimized, the Particle Swarm Optimization (PSO) minimized the cost function related to the energy consumption. Finally, conclusions were analyzed from the results of the experiment.

Keywords: K-means · PSO · Cost function · Optimization · Energy saving

1 Introduction

Energy consumption is the subject of primary importance. Today research proposals seek to optimize the use of electricity in an efficient way. In this sense, it is desired to acquire various benefits, such as: reduction of the payment of the electricity bill, adaptation of renewable energies, improving the reliability of the electrical system, among others. The importance of the efficient use of electrical energy is high because it faces a global problem such as climate change. Nowadays, it is an undeniable reality that greenhouse gases cause damage to the planet's environment, causing various problems that deteriorate the quality of life on Earth. An example of these environmental disasters represents the increase of Earth's temperature from 0.4 to 0.8 °C in the last 100 years; it is expected that by the year 2100 the increase will reach a maximum value of 5.8 °C. This reality, unfortunately, would mean the melting of the polar caps and an extremely severe increase in the level of water in the seas and oceans [1].

© The Author(s), under exclusive license to Springer Nature Switzerland AG 2023
M. Zambrano Vizuete et al. (Eds.): RITAM 2021, LNNS 512, pp. 138–150, 2023.
https://doi.org/10.1007/978-3-031-11295-9_10

In Ecuador, a new productivity matrix is trying to change the constant dependency of fossil fuels for utilization of renewable energies. This alternative might mitigate the undesirable climate change's problems presented around the world. The installed capacity increased since 2007 from 4478 MW to 6005 MW at the end of 2015. The hydro power constitutes a strong power source, since 2017 new hydroelectrical projects started development like Sopladora of 487 MW and Coca Codo Sinclair of 1500 MW [2]. On the other hand, energy waste represents a latent problem. Many consumers who possess electrical or electronic equipment turned on and are not necessarily employing it. Residential consumption is characterized by this problem because there is no culture of proper use of electricity. This problem can generate significant consequences such as the decrease in the reliability of the electrical service when consumption is in peak hours. If it is considered that apart from residential consumption there is also industrial consumption, the consumer must be prudent with electricity consumption to continue with a constant and uninterrupted electricity service. In [3], a study was carried out on the constant losses that are generated in Ecuador through the public lighting system and how this problem is reflected in residential consumers. Many homes in the country still have fluorescent lamps where their ballasts generate losses due to the Joule effect, which is produced by the circulation of current through the conductor that makes up the ballast coil. Since the ballast must deliver a high discharge to the fluorescent lamp, its coil must be large enough in size to meet this objective.

The previously mentioned problems have generated different research that seek to optimize electricity consumption. There are several alternatives suggested to diminish energy losses at residential consumption suggest. From control algorithms to hardware structures, the alternatives seek to optimize the control algorithms for closed-loop regulation, and the use of semiconductors for stable fewer consuming appliances [4]. Also, sellers of electricity give consumers some suggestions to pay less money for electricity bill. For example, turning off equipment that is unused or using equipment in non-peak hours where it will not represent a problem for the electrical system. In this sense, there are proposals that use computer processing to generate intelligent solutions; these techniques are identified as metaheuristic algorithms. These processes seek a solution from a problem that the algorithm designer chooses. In [5], authors developed a work where they incorporate different metaheuristic techniques with artificial neural networks (ANN) to model energy consumption in Thailand. The paper showed different alternatives such as the ant colony algorithm, the harmonic search algorithm, or the teaching learning method optimization algorithm. This work showed several alternatives for the analysis of consumption, however the identification of the largest consumers of electricity is not clearly determined. Authors in [6] studied other alternatives for metaheuristic algorithms such as particle swarm optimization (PSO), cuckoo optimization or gray wolf optimization (GWO). The results showed an accurate prediction about consumers demanding a specific level of electrical energy. However, it was necessary to use data from smart devices to identify all these consumptions, leaving aside possible consumers who do not possess these elements. Also [7] developed an algorithm for search economics home appliance scheduling to address the home appliance consumption to minimize electricity bill. The metaheuristics were placed as consumption simulations to find research results but other capabilities of these algorithms such us cost optimization were unused [7].

The earlier mentioned investigations adequately use metaheuristics algorithms, but other options such as clustering or classification algorithms can be explored. These algorithms perform an intelligent classification of data according to objectives such as: levels, intensities, hierarchies, among others. For this reason, this work looks for to offer an energy optimization method with the previous classification of consumers through a clustering algorithm. This algorithm will take the consumption data samples to divide them into three groups: high, medium, and low. The essential goal is to reduce high consumption by optimizing the time your non-essential loads are on. This paper is divided as follow, Sect. 1 shows the introduction of this research, Sect. 2 briefly describes the metaheuristics algorithms needed in this work, Sect. 3 shows experiments and assessments, and lastly, Sect. 4 determines the main conclusions obtained after completing this research.

2 Metaheuristics Algorithms

2.1 K-means Clustering

The K-means algorithm is a clustering technique designed for partitioning a set of raw data. K-means. This method finds K groups of clusters depending on similarities placed by the algorithm's designer. The algorithm places one centroid on each iteration to find K groups where the closest neighbors to each centroid are identified. Finally, each data belongs to one exclusive cluster, that is why this method is known as hard clustering [8].

As previous mentioned, each point on the data set is grouped to the closest centroid where the distance is obtained by Euclidean distance as follows:

$$d = \sqrt{\sum_{i=1}^{d} (x_i - y_i)^2} \tag{1}$$

where d is the Euclidean distance, x_i and y_i are the point for a 2-dimentional Euclidean space. At first place, the algorithm selects randomly K centroids, also known as seeds. Each data point is assigned to the closest centroid and the position of the point is updated in each iteration where the centroid is redistributed according to the optimization of a cost function. The main objective is to minimize the Sum of Square Error (SSE) of the Euclidean distance of each point to its closest centroid by:

$$SSE = \sum_{i=1}^{d} \sum_{x_i \in C_k} (x_i - c_k)^2 \tag{2}$$

where c_k is the centroid and it is defined as:

$$c_k = \frac{\sum_{x_i \in C_k} x_i}{c_k} \tag{3}$$

The iterative steps of K-means are described as follows (Table 1):

Table 1. K-means pseudocode [9].

```
Generate k random centroids;

For each step:
        Assign the instance to cluster with closest centroid;
Repeat;
        Update the centroid;
        Reassign the instances to clusters;
Until end process;
```

An example of data classification is presented in Fig. 1, where raw data is classified into 3 groups according to the closest centroid for each point in the data set.

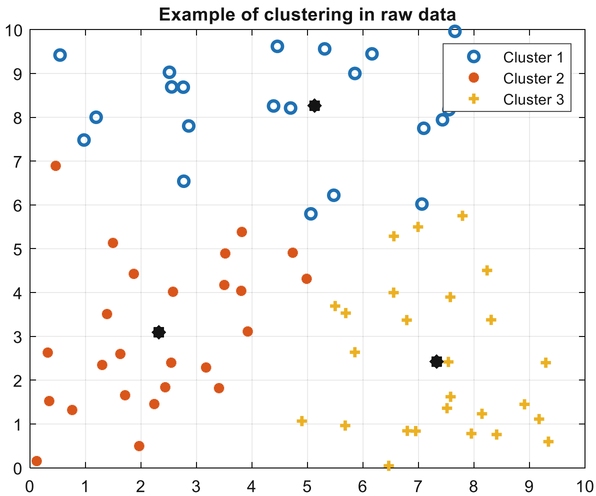

Fig. 1. K-means clustering in random data to determine 3 groups.

2.2 Particle Swarm Optimization (PSO)

PSO algorithm is a metaheuristics process developed by Kennedy and Eberhart [10] to simulate the behavior of biological systems. In a detailed way, the algorithm is compared with a search process performed by a group of birds or a group of fishes. Everyone in the group collaborates with its neighbors to find a specific objective.

The PSO algorithm is simple, and it is described as follows: The objective is in a space of D solutions. At first, N particles are distributed in the solution space as random points. Each particle represents a point with coordinates:

$$X_i = (x_{i1}, x_{i2}, \cdots, x_{iD}) \tag{4}$$

Each element moves with a velocity:

$$V_i = (v_{i1}, v_{i2}, \cdots, v_{iD}) \tag{5}$$

When the search process begins, each particle updates its velocity and position on each iteration:

$$V_i = \omega V_i + c_1 r_1 \left(p_{besti-x_i}\right) + c_2 r_2 (g_{best} - X_i) \tag{6}$$

$$X_i = X_i + V_i \tag{7}$$

where p_{besti} is the best position of each particle, g_{best} is the best global position of the swarm, c_1 and c_2 represent learning factors, r_1 and r_2 random numbers between 0 to 1, and ω the inertial weight commonly represented by values between 0.1 to 0.9.

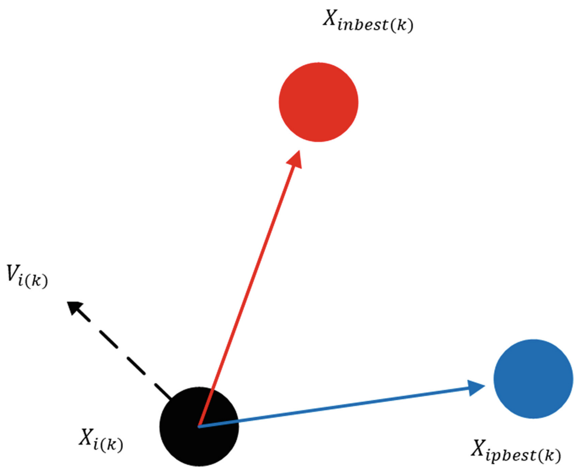

Fig. 2. Position transition of each particle.

Figure 2 shows a graphical representation of the movement and position of each particle from the previous best solution (blue) to the current solution (black) related to the global best solution (red). In the following Table, the PSO process is resumed (Table 2):

Table 2. PSO pseudocode [11].

Setting of N-particles population;
Initialization of position and velocity of each particle;
For each iteration:
Fitness value calculation;
Update personal and global best.
Until meeting stopping criterion;
Optimal output value;

PSO is a very versatile algorithm that can be combined with other optimization techniques [12–14] to acquire better results. These alternatives solve the local optimum problem, where particles in PSO tend to be moving around a specific point and finds a solution that it is not necessary the global optimum [15].

3 Experiments and Assessments

3.1 Clustering of Consumer's Data

The experiment data comes from a collection of electricity bills of 80 consumers from southern part of Quito city. The consumer's bill shows the cost of energy and the KWh consumed in a month. An average of the last 3 months was used to determine the use of energy and cost for each consumer. The classification of data with K-means algorithm is presented as follows:

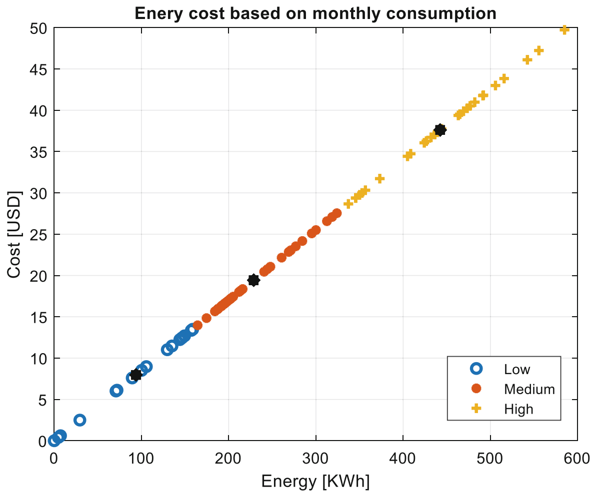

Fig. 3. Energy cost and consumption of experiment's data.

The number of clusters founded were 3 for low, medium, and high consumption of electricity. The consumption is proportional to the cost of energy as seen in Fig. 3. From the data set, the main points are determined for consumption and cost are (Table 3):

Table 3. Limits from dataset.

Cluster	Lower consumption [KWh]	Higher consumption [KWh]	Lower cost [USD]	Higher cost [USD]
Low	0	163.8	0	13.92
Medium	173.4	318	14.74	27.03
High	327	584.4	27.79	49.67

After clustering, the centroids for each group as placed as follows:

Table 4. Differences from centroid and average points from dataset.

Cluster	Centroid consumption [KWh]	Average consumption [KWh]	Centroid cost [USD]	Average cost [USD]
Low	96.7	81.9	8.22	6.96
Medium	241.2	245.7	20.50	20.89
High	439.5	455.7	37.35	38.78

Table 4 shows the differences between positions of centroid and average from minimum and maximum points. K-means takes properly the centroids because its values are closest to the average points and the 3 groups are clearly determined.

3.2 Optimization of Consumption by PSO

The optimization process takes the data from clustering at the last step. The main objective is to minimize a cost function represented by the quadratic difference between the electrical energy consumed monthly and the maximum value of the medium consumption. The energy consumed by each user is represented as follows:

$$E/day = \sum_{k=1}^{n} P_i t_i \tag{8}$$

where E/day is the energy consumed in a day in Kwh, P_i is the power of each appliance in W and t_i is the time of the use of each appliance in hours. The values are calculated by a period of 30 days to meet the data set from each consumer's bill.

Before applying PSO method to minimize this problem its mandatory to analyze what appliances can be adopted for this task. In other words, some appliances are important to do daily tasks and are not susceptible for reducing the time of use. Moreover, there are other electrical and electronical devices that can reduce the time of use because are not primordial. A priority matrix [16] is developed to analyze in general, the most important devices for electricity consumers. This matrix compares all home appliances between them and gives a grade of importance. The matrix was developed with a common group of appliances existing in each consumer and a criterion for a hierarchical classification. In the process of comparing each element, values are dismissed when comparing an appliance with itself. Values of 1 are assigned to the most important element and 0 to the less important. The important elements mean appliances that can not be reduced its use. The assignation values are performed from row-row analysis.

Results show the components with higher value of priority can be taken as part of the objective function to find a solution by minimizing the cost function. A priority of lower values means the appliance is very important at home and a higher value means the opposite. The criterion is the same as previously explained with the difference of the number of appliances taken to calculate the electrical energy consumed monthly. Values highlighted will be used for this new optimization process (Table 5).

Table 5. Priority matrix for domestic appliances.

	TV	Com-puter	Fridge	Micro wave	Washing Machine	Drying Machine	Induction Cooktop	Lamp	Shower	Water Heater	Charger	Stereo	Iron	Total	Priority
TV		0	0	0.5	0.5	1	0	0.5	0.5	0.5	0	0.5	0.5	4.5	7
Computer	1		0.5	1	1	1	0.5	0.5	1	1	0.5	1	1	10	1
Fridge	1	0.5		1	1	1	0.5	0.5	0.5	1	0.5	1	1	9.5	3
Micro wave	0.5	0	0		0	0.5	0	0	0.5	0	0	0.5	0.5	2.5	12
Washing Machine	0.5	0	0	1		1	0.5	0	0.5	0.5	0	1	1	6	6
Drying Machine	0	0	0	0.5	0		0	0	0	0.5	0	0.5	0.5	2	13
Induction Cooktop	1	0.5	0.5	1	0.5	1		0.5	1	1	0.5	1	1	9.5	3
Lamp	0.5	0.5	0.5	1	1	1	0.5		1	1	0.5	1	1	9.5	3
Shower	0.5	0	0.5	0.5	0.5	1	0	0		0.5	0	0.5	0.5	4.5	7
Water Heater	0.5	0	0	1	0.5	0.5	0	0	0.5		0	0.5	0.5	4	9
Charger	1	0.5	0.5	1	1	1	0.5	0.5	1	1		1	1	10	1
Stereo	0.5	0	0	0.5	0	0.5	0	0	0.5	0.5	0		0.5	3	10
Iron	0.5	0	0	0.5	0	0.5	0	0	0.5	0.5	0	0.5		3	10

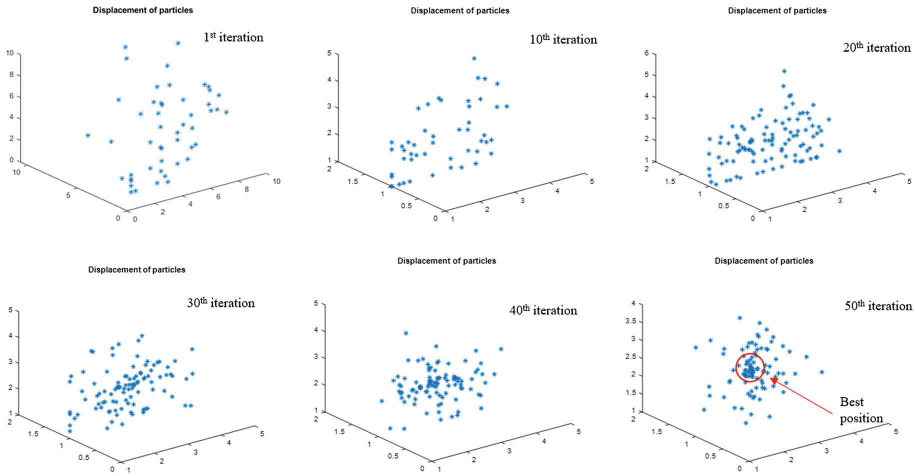

Fig. 4. Displacement of particles in PSO for optimum search.

Figure 4 presents the displacement of particles on each iteration until getting closer to the optimum point. In this case, the energy of 3 appliances were used to determine a const function. The number of particles utilized were 50 and the iteration number was changed to observe the improvement of the best cost.

Table 6. Results of PSO for different number of iterations.

Iterations	Drying machine's time [h]	Washing machine's time [h]	Iron's time [h]	Best cost	Saving [%]
10	1.8526	3.3	5.29	10.64	37.36
20	3.761	3.34	1	0.4169	27.64
30	1.6313	1.223	3.6576	0.059	22.04
40	2.661	1	2.641	0.0052	19.06
50	2.0981	1	2.1379	0.00056594	18.65

This analysis was performed in one user; it means the optimization on the rest of higher electricity consumers followed the same procedure. The evolution of best cost is presented in the next figure as follows (Fig. 5):

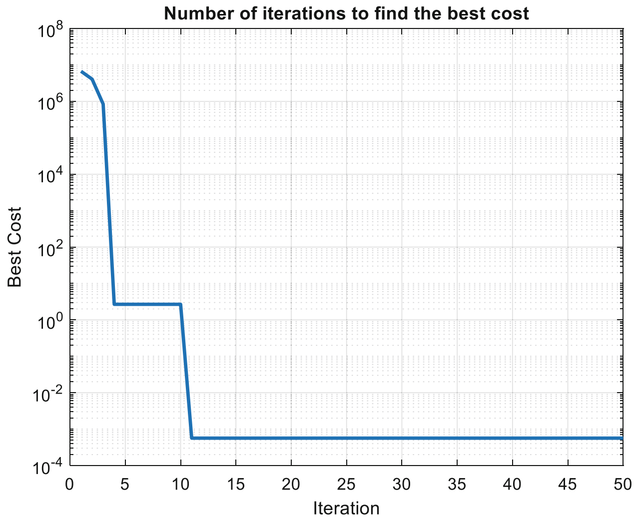

Fig. 5. Number of iterations vs best cost.

The algorithm reaches a value of 0.00056594 as expressed in Table 6, the PSO response is better after adding more iterations. To reach this objective, various tests need to be performed.

Finally, the perspectives for energy savings are presented (Fig. 6):

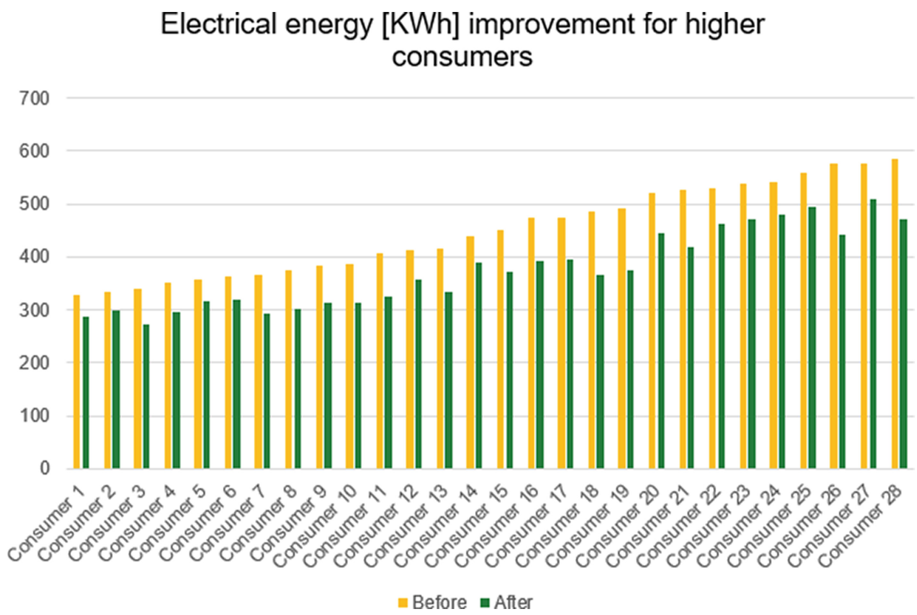

Fig. 6. Electrical energy improvement for higher consumers.

The consumers for high energy demand will receive benefits from paying less cost of electricity bill between 5 to 20%.

4 Conclusions

PSO algorithm has a precise response to minimize the objective function. Less time of using appliances was put under the tests extracting new times of use for non-essential loads. The analysis performed better results with a larger horizon of iterations.

K-means method divided in 3 well-known groups the data set for consumers of electricity. The groups could take a perspective of more than 3 groups, but the first data point of high consumption was almost $28 which means a good start point of optimization for a conventional family of more than 3 members.

Savings reaches maximum values of almost 20% monthly, which represents an annual improvement in energy consumption proportional to the saving value. The perspectives projected after this experiment emphasizes an increasing in the reliability of the interconnected electrical system.

References

1. Arroyo, F., Miguel, L.J.: Analysis of energy demand scenarios in Ecuador: national government policy perspectives and global trend to reduce CO_2 emissions. Int. J. Energy Econ. Policy **9**(2), 364 (2019)
2. Rivera-González, L., Bolonio, D., Mazadiego, L.F., Valencia-Chapi, R.: Long-term electricity supply and demand forecast (2018–2040): a LEAP model application towards a sustainable power generation system in Ecuador. Sustainability **11**(19), 5316 (2019). https://doi.org/10.3390/su11195316
3. Otero, P., Ayala, R., Calle, V.: Metodología de cálculo de pérdidas de potencia y energía en el sistema de alumbrado público del Ecuador. Rev. Técn. Energía **17**(1), 43–51 (2020)
4. Gonzales, O., Rosales, A.: Sliding mode controller based on a linear quadratic integral regulator surface for power control on a dual active bridge converter. In: 2018 IEEE Third Ecuador Technical Chapters Meeting (ETCM), pp. 1–6. IEEE, October 2018
5. Phatai, G., Chiewchanwattana, S., Sunat, K.: A comparative of neural network with metaheuristics for electricity consumption forecast modelling. In: 2018 22nd International Computer Science and Engineering Conference (ICSEC), pp. 1–4 (2018). https://doi.org/10.1109/ICSEC.2018.8712736
6. Tilwalia, R., Jain, A., Gupta, D.: Optimization of electricity consumption using grey wolf algorithm. In: 2020 IEEE 5th International Conference on Computing Communication and Automation (ICCCA), pp. 401–407 (2020). https://doi.org/10.1109/ICCCA49541.2020.9250899
7. Fan, C., Chen, H., Tsai, C.: SEHAS: a novel metaheuristic algorithm for home appliances scheduling in smart grid. In: 2019 IEEE International Conference on Systems, Man and Cybernetics (SMC), pp. 786–791 (2019). https://doi.org/10.1109/SMC.2019.8914018
8. Hot, E., Popovic-Bugarin, V.: [IEEE 2015 23rd Telecommunications Forum Telfor (TELFOR) - Belgrade, Serbia (24–26 November 2015)]. 2015 23rd Telecommunications Forum Telfor (TELFOR) - Soil data clustering by using K-means and fuzzy K-means algorithm, pp. 890–893 (2015). https://doi.org/10.1109/telfor.2015.7377608

9. Banerjee, S., Choudhary, A., Pal, S.: Empirical evaluation of K-Means, bisecting K-means, fuzzy C-means and genetic K-means clustering algorithms. In: 2015 IEEE International WIE Conference on Electrical and Computer Engineering (WIECON-ECE), pp. 168–172 (2015). https://doi.org/10.1109/WIECON-ECE.2015.7443889
10. Peng, W., Yang, Z., Liu, C., Xiu, J., Zhang, Z.: [IEEE 2018 5th IEEE International Conference on Cloud Computing and Intelligence Systems (CCIS) - Nanjing, China (23–25 November 2018)] 2018 5th IEEE International Conference on Cloud Computing and Intelligence Systems (CCIS) - An Improved PSO Algorithm for Battery Parameters Identification Optimization Based on Thevenin Battery Model, pp. 295–298 (2018). https://doi.org/10.1109/CCIS.2018.8691341
11. Lodhi, V., Chakravarty, D., Mitra, P.: [IEEE 2018 Fourth International Conference on Research in Computational Intelligence and Communication Networks (ICRCICN) - Kolkata, India (22–23 November 2018)] 2018 Fourth International Conference on Research in Computational Intelligence and Communication Networks (ICRCICN) - A Study of PSO and its Variants for Fractional Abundance Estimation in Hyperspectral Data, pp. 197–201 (2018). https://doi.org/10.1109/ICRCICN.2018.8718733
12. Yan, C., Lu, G., Liu, Y., Deng, X.: A modified PSO algorithm with exponential decay weight. In: 2017 13th International Conference on Natural Computation, Fuzzy Systems and Knowledge Discovery (ICNC-FSKD), pp. 239–242 (2017). https://doi.org/10.1109/FSKD.2017.8393146
13. Mohamad Ali Tousi, S., Mostafanasab, A., Teshnehlab, M.: Design of self tuning PID controller based on competitional PSO. In: 2020 4th Conference on Swarm Intelligence and Evolutionary Computation (CSIEC), pp. 022–026 (2020). https://doi.org/10.1109/CSIEC49655.2020.9237318
14. Qiu, G., Zhao, W., Xiong, G.: Estimation of power battery SOC based on PSO-Elman neural network. In: 2018 Chinese Automation Congress (CAC), pp. 91–96 (2018). https://doi.org/10.1109/CAC.2018.8623184
15. Cai, J., Wei, H., Yang, H., Zhao, X.: A novel clustering algorithm based on DPC and PSO. IEEE Access **8**, 88200–88214 (2020). https://doi.org/10.1109/ACCESS.2020.2992903
16. Khatib, M., Al Khudir, K., De Luca, A.: Task priority matrix under hard joint constraints (2020)

Reliability of Wind and Solar Energy in the Electric Generation System Using Computational Methods

Alan Cuenca[1](✉), Henry Miniguano[2], Santiago Illescas[2], Livio Miniguano[2], and Darwin Cuasapaz[2]

[1] Escuela Politécnica Nacional, Quito, Ecuador
alan.cuenca@epn.edu.ec
[2] Instituto Superior Tecnológico Sucre, Quito, Ecuador

Abstract. This research includes the results of the integration of wind and solar energy in the electricity generation system by substituting conventional energy. The renewable resource data used correspond to the province of Loja in Ecuador, where the Villonaco Wind Farm is currently operating and thermosolar and photovoltaic energy projects are being developed, where the peak demand data of 30.27 MW was used. To verify the reliability of renewable energies, four case studies have been established, and reliability indexes and capacity credit have been calculated, using the Matlab tool, through the Monte Carlo method which is a numerical statistical method. The use of computational tools made it possible to verify the possibility of reducing conventional power generation plants while maintaining the reliability of the system. Therefore, the work carried out establishes a reliable tool for the integration of non-conventional renewable energies into the electric system. It concludes that wind, solar thermoelectric, and photovoltaic technologies not only improve the reliability of the system but also provide power that can be used to meet the demand of other sectors.

Keywords: Non-conventional · Renewable energies · Reliability · Capacity credit · Monte Carlo method · Matlab

1 Introduction

Non-conventional renewable energies correspond to all those sources of energy generation in which the consumption, expense, or depletion of its generating source is not incurred [1]. Renewable energy source technologies have reached a high level of development at a global level, which has allowed them to become competitive with traditional energy generation alternatives. According to the International Renewable Energy Agency (IRENA), the use of renewable energies worldwide should more than double by 2030 to advance the global energy transformation (“10 Years: Progress to Action”, 2020). In addition, it should be noted that the link between energy and climate change is very strong since it is the high consumption of fossil fuels that has caused the variations in global temperatures. For this reason, the use of renewable energies as sources

© The Author(s), under exclusive license to Springer Nature Switzerland AG 2023
M. Zambrano Vizuete et al. (Eds.): RITAM 2021, LNNS 512, pp. 151–165, 2023.
https://doi.org/10.1007/978-3-031-11295-9_11

of energy generation has developed in recent years. Technologies such as wind and solar concentrated in 2019 almost three-quarters of the new energy installations commissioned worldwide. Latin America and the Caribbean are rich in renewable natural resources, so the increase of projects based on non-conventional renewable technology allows a significant reduction of greenhouse gas emissions and a positive contribution to international agreements on climate change.

Ecuador through its Plan Maestro de Electricidad (EMP) 2018–2027 [2] has established objectives in which it points out that the participation of renewable energies should be increased in the national production, following the objectives of improving the productive matrix. To meet this objective, projects are currently being developed for the use of renewable energies: hydro, wind and solar. However, reliability should be pointed out as a very important factor in the planning, design, operation and maintenance of the electric power system. Within this, generation is a fundamental part since it has to be able to meet the demand at all times.

The integration of renewable energies in the electric power system poses new challenges in its operation. Some of these are related to the inherent characteristics of the system itself: reliability, quality and efficiency [3]. This paper studies the reliability of the electric power system as wind and solar power are used in the province of Loja, Ecuador because several projects with renewable technologies are currently being developed in this part of the Ecuadorian national territory. Due to the complexity of the electrical system, it can be divided into hierarchical levels such as generation, transmission and distribution, which can be analyzed correspondingly [4]. In this way, the present work addresses the generation level. The reliability of a generation system is related to the existence of enough generators within it to satisfy the consumers' electricity demand; considering static conditions of the system and without taking into account dynamic and transient system disturbances [5]. To evaluate how reliable a generation system is, the following reliability indices are used: expected loss of load (LOLE), expected loss of energy (LOEE), loss of load probability (LOLP) and expected demand not supplied (EDNS) [6]. In addition, the capacity credit (ECCP) is established to determine the possibility of increasing the penetration of renewable energy, decreasing the conventional power without modifying the reliability of the system. It should be noted that deterministic and probabilistic methods are used to calculate these indexes, for which reason stochastic Monte Carlo simulation is used in this study, which imitates the operation of the systems considering their random characteristics using computational methods [7].

To perform the reliability analysis of the electric generation system by integrating non-conventional renewable technologies such as wind, solar thermal and photovoltaic, data from the area of Loja located in the south of Ecuadorian territory are used. The importance of this work lies in the application of a computational method for the evaluation of renewable energies in the generation system by providing clean and sustainable energy. Finally, the present study intends to contribute to the research on the integration of renewable energies in the Ecuadorian electrical system, to take all the necessary measures and apply them in the change of the energy matrix of the country.

2 Methodology

The study carried out through the present work is structured as follows: selection of the research area, obtaining wind and solar resource data, simulation of renewable generation, processing of conventional generation data, the study of electricity demand, application of the Monte Carlo method, calculation of reliability indices and capacity credit and finally the analysis of results.

2.1 Location of the Study Zone

The area chosen for this research is the province of Loja in Ecuador. This area has a high presence of renewable solar and wind resources suitable for electricity generation. The province of Loja, as shown in Fig. 1, is located in the southern part of the Ecuadorian Sierra and has an area of 11,026 km^2. It is part of the Southern Region, which also includes the provinces of El Oro and Zamora Chinchipe, with some 450,000 inhabitants at the provincial level.

Fig. 1. Location of the province of Loja in Ecuador.

The Ministerio de Electricidad y Energía Renovable (MEER) and the Escuela Politécnica Nacional (EPN) have developed the Wind Atlas and Solar Map of Ecuador respectively, which establish that the area of Loja has a very high potential in terms of renewable resources that can be used for electricity generation due to the presence of the Andes Mountains [8, 9]. Some of the country's emblematic projects are currently operating in Loja, including the Villonaco wind farm, as well as solar technology projects such as Sabiango Solar, Surenergy, Lojaenergy, among others [10]. In addition, it is worth noting that within the 2018–2027 generation expansion plan that promotes the use of renewable energy resources, the construction of new projects in the Loja area is established due to its high penetration of wind and solar resources [2].

2.2 Renewable Resources Data

According to the availability of wind and solar resources in the area of Loja, the appropriate sites for the location of renewable electricity generation plants are established. For this reason, the search and compilation of information corresponding to the variables of renewable resources and electricity demand in the area of Loja was carried out, such data were requested to national organizations involved in the electric-renewable field.

Wind Resource. The pressure, relative humidity, temperature, wind speed and direction data obtained correspond to the Villonaco wind farm area (latitude: 4°00′01.5″ S, longitude: 79°15′33.4″ W, elevation: 2720 msnm) in the province of Loja-Ecuador and were provided by Corporación Eléctrica del Ecuador (CELEC EP) [11] and the Instituto Nacional de Meteorología e Hidrología (INAMHI) [12].

Solar Resource. The direct radiation data correspond to the area of La Ceiba (latitude: 4°18′07.9″ S, latitude: 80°13′10.9″ W, elevation: 200 msnm) and the global radiation and temperature data correspond to the area of Saucillo (latitude: 4°15′59.9″ S, longitude: 80°12′11.8″ W, elevation: 200 msnm) both locations are located in the Zapotillo canton, in the province of Loja-Ecuador. Solar resource data were provided by the Corporación para la Investigación Energética (CIE).

The wind and solar resource data used are hourly and cover the period from January 1 to December 31, 2018, i.e. a full year. The simultaneous data collection has the purpose of knowing the production of three types of renewable technology: wind, solar thermoelectric and solar photovoltaic hour by hour to know how much they can cover a given demand without producing any type of interruption. Figure 2 shows the location of the renewable generation plants.

Fig. 2. Location of renewable generation plants.

Due to the increasing presence of power generation plants based on renewable resources throughout the Ecuadorian territory to achieve the energy transition and meet the objectives established in the Plan Maestro de Electricidad, it is of vital importance the existence of tools that can provide flexibility to the operation of the system, which is essential to maximize the use of renewable primary resources. For this reason, it is convenient to study the integration of wind and solar renewable energies while maintaining the reliability of the electrical system.

2.3 Renewable Generation

Once the renewable resource data is available, the simulation of renewable generation is carried out using computer tools to obtain the necessary information for the calculation of the reliability indexes and the capacity credit.

Wind-Photovoltaic Production. The Hybrid Optimization Model for Electric Renewables HOMER software [13] is used to simulate wind and photovoltaic production. This information can be seen in Fig. 3.

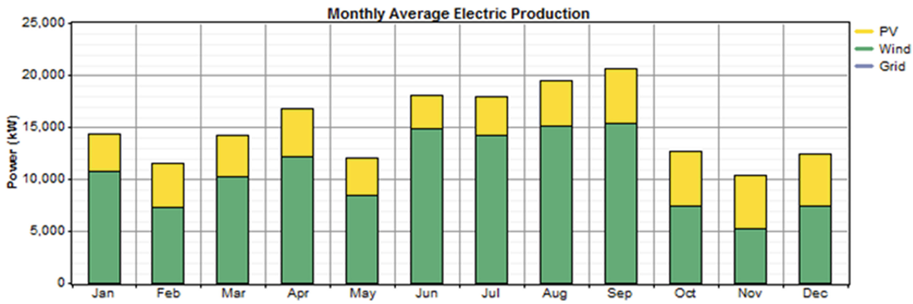

Fig. 3. Simulated wind-photovoltaic production at HOMER.

Solar Thermoelectric Production. The Solar Advisor Model SAM software [14] is used to simulate solar thermoelectric production, which can be seen in Fig. 4.

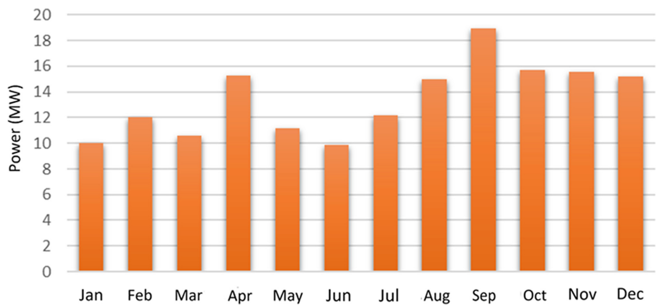

Fig. 4. Simulated solar-thermoelectric production at SAM.

2.4 Conventional Generation

For a conventional generation, the data provided by Empresa Eléctrica Regional del Sur S.A. (EERSSA) and the parameters of mean time between failures MTTF and mean time to repair MTTR [15]. The distribution system of the province of Loja receives contributions from the Catamayo MCI (Internal Combustion Engine) Thermal Power Plant and the main contribution from the Sistema Nacional Interconectado in Table 1.

Table 1. Conventional generation units in Loja.

Central	Unit	Type	Nominal power (MW)
Catamayo	U1	Thermic MCI	1.8
Catamayo	U2	Thermic MCI	1.28
Catamayo	U3	Thermic MCI	1.575
Catamayo	U4	Thermic MCI	1.575
Catamayo	U5	Thermic MCI	1.575
Catamayo	U6	Thermic MCI	2.88
Catamayo	U7	Thermic MCI	2.88
Catamayo	U8	Thermic MCI	2.5
Catamayo	U9	Thermic MCI	2.5
Catamayo	U10	Thermic MCI	2.5
Cuenca-Loja	SNI	Interconnection	25.2

2.5 Demand Curve

The reliability of renewable generation requires hourly power demand data, for this reason, Empresa Eléctrica Regional del Sur S.A.-EERSSA provided the respective consumption data for the province of Loja. Figure 5 shows the historical behavior of demand throughout 2018, with the maximum peak demand, is 30.27 MW.

2.6 Monte Carlo Method

Monte Carlo methods are computational algorithms that rely on repetitive random sampling to compute their results. These methods are often used in computational simulations of physical and mathematical systems [16].

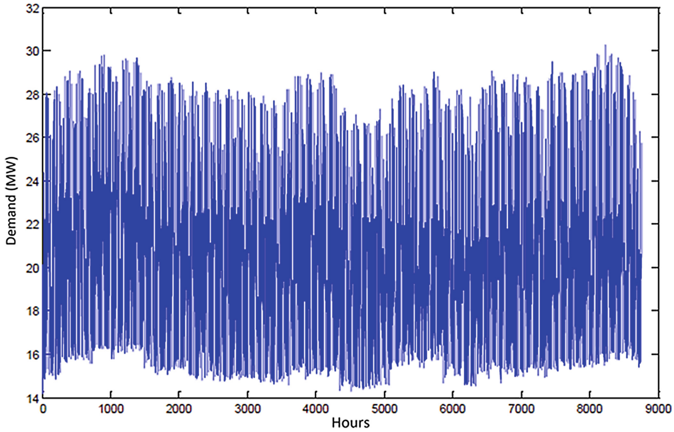

Fig. 5. The demand of the province of Loja.

The Monte Carlo method performs a sampling simulation using sequences of uniform random numbers, generating a random state of the system, this state is composed of: random generation, operating states and random time points. The generation operating states will have a corresponding generation power, while the time points will have a corresponding generation power and demand [4].

In the present study, the following Monte Carlo methods are applied to perform a comparison between them and observe the variations of the reliability indices.

Non-sequential Method. To calculate the reliability indices in the non-sequential method, the monotonic curve of the scheduled demand is used. The reason for using this curve is to try to avoid the sequential effect of using the cumulative frequency distribution (CDF) of wind, solar PV and solar thermal generation.

In addition, for this method, the probability of unavailability of conventional generation plants and interconnections is calculated and different renewable production curves are introduced based on the data obtained with the simulation software.

Sequential-Non-sequential Hybrid Method. This method comprises a combination of the sequential method and the non-sequential method.

It consists of obtaining at a given time the thermal demand, i.e. the resulting demand to be satisfied by the conventional thermal units after the intervention of the renewable power plants.

Once the thermal demand is available, the non-sequential method is applied, i.e. the load monotonic of the thermal demand is obtained and the respective draw is made only for the conventional power plants to obtain the demand not supplied (DNS) and from here the different reliability indexes of the system.

Total Sequential Method. This method comprises a variation of Sequential Monte Carlo, in which the input variables are used sequentially, thus working with scheduled demand data and production data from renewable and conventional power plants. For each sample, an hour-by-hour draw is made for each conventional plant, which allows knowing the moments in which the plant has failed and its respective repair time until it starts operating again. In the end, the power of all the power plants is added up and, in this way, the available conventional power is obtained for each sample.

For the renewable power plants, the simulated production data are used and the generation is compared with the scheduled electricity demand to obtain the unsupplied demand, from which the respective reliability indexes can be calculated.

2.7 Reliability Indexes

To reach the values of the reliability indexes of the system, it is necessary to perform a simulation during a certain time interval, since the Monte Carlo method does not ensure the convergence of the process due to its oscillating nature, the greater the number of repetitions, the greater the confidence interval will be [7]. However, to avoid an excessive number of repetitions, a convergence criterion is established which consists of quantifying the error as repetitions are added, and establishing a maximum value for this error [6].

The software used to apply the Monte Carlo algorithm is in Matlab, due to its very useful characteristics when processing large amounts of data. The main characteristics taken into account for the calculation of the reliability indices are:

- Convergence process: number of repetitions adequate for the results to be reliable and the error to remain within established margins.
- Unavailability index (FU): random status of the generating unit generated: 0 (unavailable) and 1 (available at rated power).
- Mean Time To Failure (MTTF): mean time between failures.
- Mean Time To Repair (MTTR): mean time to repair.
- Average number of failures in a year (λ): number of failures of a plant in a year.
- Average number of repairs in a year (β): number of repairs of a power plant in a year.

Taking into account these parameters and the characteristics of both renewable and conventional generation plants, the following reliability indexes can be calculated: LOLE, LOEE, LOLP and EDNS.

LOLE, "Loss of load expectation" is measured in hours/year. The general expression is:

$$LOLE = \sum\nolimits_{i \in s} piT \tag{1}$$

pi: the probability of state *i* of the system; *s:* set of all the times when the demand is greater than the available generation; *T*: a period in which it remains in that state.

LOEE, "Loss of energy expectation", is measured in MWh/year. The general expression is:

$$LOEE = \sum\nolimits_{i \in s} 8760Cipi \tag{2}$$

Ci: the difference between demand and available generation in state *i*.

LOLP, “Loss of load probability”, being a probability is dimensionless.

$$LOLP = \text{LOLE}/8760 \tag{3}$$

EDNS, “Demand not supplied” is measured MW/year:

This index indicates the amount of power not supplied over a year.

In the present study, a margin of error has been established with a maximum value of 5% and a maximum number of samples equal to 3000, since this number of iterations ensures a reliable convergence of the indexes and an error value that is within the established margin.

2.8 Capacity Credit

There are several definitions for capacity credit, the two most commonly used are equivalent load-carrying capacity (ELCC) and equivalent conventional power capacity (ECPP). For the present study, the ECPP is calculated and is defined as the amount of installed conventional power Y (MW) that can be substituted with X (MW) of a power of another technology without modifying the reliability of the system [17].

$$ECPP = Y/X \tag{4}$$

For the calculation of the capacity credit, four case studies of renewable power penetration in the system have been carried out using the Monte Carlo method to check and highlight the reduction of conventional power without modifying the reliability of the system [18].

3 Performance and Results

The study carried out through the present work is structured as follows: selection of the research area, obtaining wind and solar resource data, simulation of renewable generation, processing of conventional generation data, the study of electricity demand, application of the Monte Carlo method are considered because only one year’s data is available, calculation of reliability indices and capacity credit and finally the analysis of results.

Based on the current conditions of the electric generation system, four case studies were carried out, which have eleven states of penetration of conventional and renewable power to meet the electric demand. The case studies are described below:

– Case 1: non-sequential simulation without variation in the simulated production data of renewable power plants (base case).
– Case 2: non-sequential simulation with a variation of the renewable production data by a normal distribution concerning the base case.
– Case 3: hybrid sequential-non-sequential simulation using simulated renewable production data from the base case.

– Case 4: full sequential simulation using the simulated renewable production data from the base case sequentially.

Table 2 and Table 3 show the values of the reliability indices calculated for case 1 and case 2 respectively.

Table 2. Results of simulated scenarios Case 1.

State	Power (%)	LOLE (hour/year)	LOEE (MWh/year)	EDNS (MW/year)	LOLP
0	100% PC	8.066	295.043	35.163	0.00093
1	90% PC-10% PR	6.140	164.413	24.781	0.00071
2	80% PC-20% PR	5.237	127.944	22.048	0.00060
3	70% PC-30% PR	4.904	119.135	21.690	0.00056
4	60% PC-40% PR	4.740	119.740	22.079	0.00054
5	50% PC-50% PR	4.564	120.039	22.960	0.00052
6	40% PC-60% PR	4.396	121.700	24.162	0.00050
7	30% PC-70% PR	4.246	125.539	25.584	0.00048
8	20% PC-80% PR	4.120	130.116	27.165	0.00047
9	10% PC-90% PR	4.083	137.704	28.888	0.00046
10	100% PR	4.832	172.614	31.290	0.00055

Table 3. Results of simulated scenarios Case 2.

State	Power (%)	LOLE (hour/year)	LOEE (MWh/year)	EDNS (MW/year)	LOLP
0	100% PC	8.051	295.770	34.943	0.00092
1	90% PC-10% PR	6.867	207.294	28.381	0.00078
2	80% PC-20% PR	6.300	181.333	26.914	0.00072
3	70% PC-30% PR	6.126	177.205	26.169	0.00070
4	60% PC-40% PR	5.984	178.727	28.084	0.00068
5	50% PC-50% PR	5.825	182.306	29.420	0.00066
6	40% PC-60% PR	5.634	186.707	31.049	0.00064
7	30% PC-70% PR	5.435	192.281	32.905	0.00062
8	20% PC-80% PR	5.243	198.306	34.948	0.00060
9	10% PC-90% PR	5.098	206.764	37.149	0.00058
10	100% PR	5.362	232.071	39.708	0.00061

Table 4 and Table 5 show the values of the reliability indices calculated for case 3 and case 4 respectively.

Table 4. Results of simulated scenarios Case 3.

State	Power (%)	LOLE (hour/year)	LOEE (MWh/year)	EDNS (MW/year)	LOLP
0	100% PC	8.046	292.585	34.806	0.00092
1	90% PC-10% PR	6.112	180.039	27.077	0.00070
2	80% PC-20% PR	5.515	160.869	26.107	0.00063
3	70% PC-30% PR	5.362	159.354	26.067	0.00061
4	60% PC-40% PR	5.320	164.759	27.564	0.00060
5	50% PC-50% PR	5.211	171.517	29.173	0.00059
6	40% PC-60% PR	5.119	179.854	31.041	0.00058
7	30% PC-70% PR	5.029	188.390	33.061	0.00057
8	20% PC-80% PR	4.943	197. 277	35.195	0.00056
9	10% PC-90% PR	4.888	208.593	37.421	0.00055
10	100% PR	6,792	307,823	41,058	0,00078

Table 5. Results of simulated scenarios Case 4.

State	Power (%)	LOLE (hour/year)	LOEE (MWh/year)	EDNS (MW/year)	LOLP
0	100% PC	8.222	296.368	35.023	0.00093
1	90% PC-10% PR	6.149	177.688	27.118	0.00070
2	80% PC-20% PR	5.679	162.120	26.408	0.00064
3	70% PC-30% PR	5.507	161.513	26.290	0.00062
4	60% PC-40% PR	5.474	168.119	28.122	0.00061
5	50% PC-50% PR	5.368	175.215	29.796	0.00060
6	40% PC-60% PR	5.237	183.123	31.691	0.00059
7	30% PC-70% PR	5.109	191.843	33.732	0.00058
8	20% PC-80% PR	4.994	200.286	35.877	0.00057
9	10% PC-90% PR	4.910	210.210	38.105	0.00056
10	100% PR	6.833	310.050	41.709	0.00078

Figures 6, 7, 8 and 9 show the convergence process of the LOLE index for the four case studies respectively for the 100% Conventional Power and 100% Renewable Power scenarios.

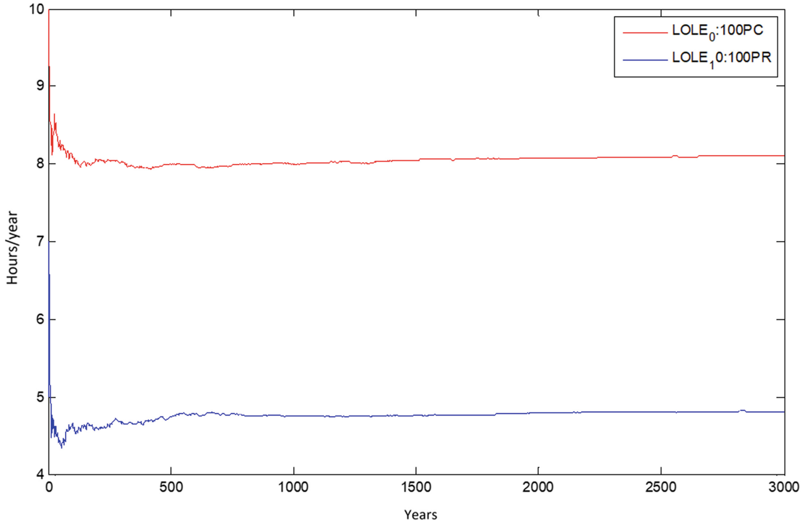

Fig. 6. Non-sequential method: LOLE convergence (state 0 and state 10) Base case 1.

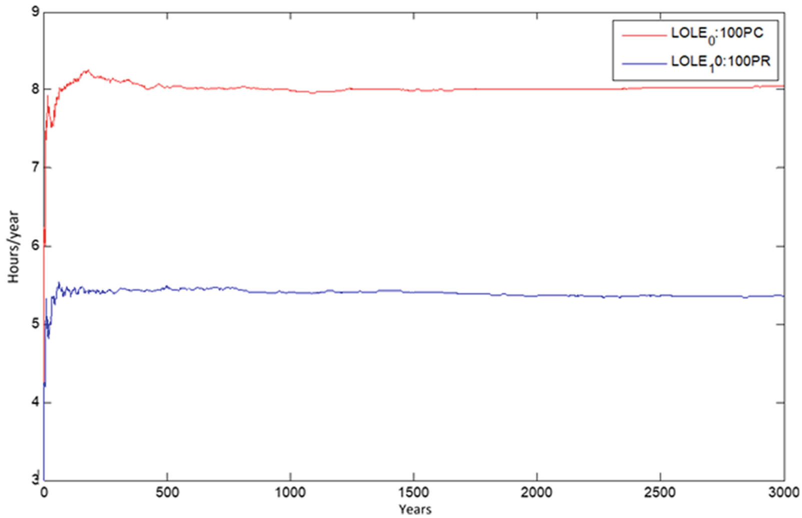

Fig. 7. Non-sequential method: LOLE convergence (state 0 and state 10) Base case 2.

By comparing the results in the four case studies it can be observed that either by the Sequential or Non-Sequential Monte Carlo method as renewable energy is integrated into the system the LOLE index starts to decrease which establishes the reliability of the electrical generation from wind and solar energy. In addition, from the values of the reliability indices, the capacity credit of the case studies was calculated. Figure 10 shows the evolution of the capacity credit (ECPP) of the four case studies, as renewable energy increases in the system the capacity credit, ECPP decreases. Finally, the results

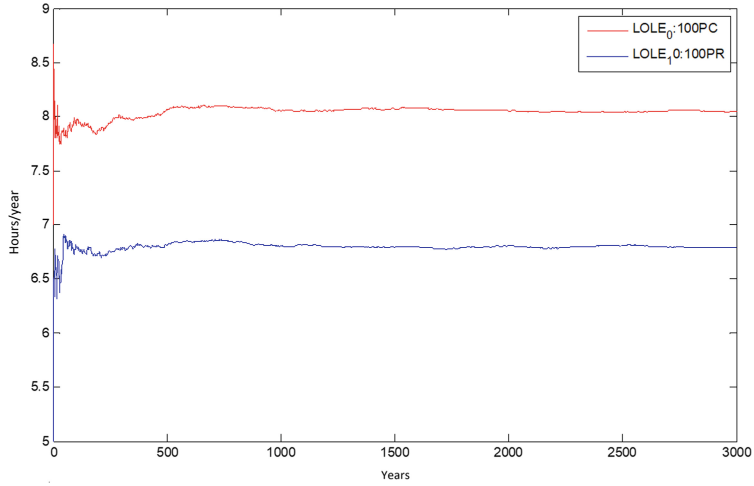

Fig. 8. Hybrid method: LOLE convergence (state 0 and state 10) Base case 3.

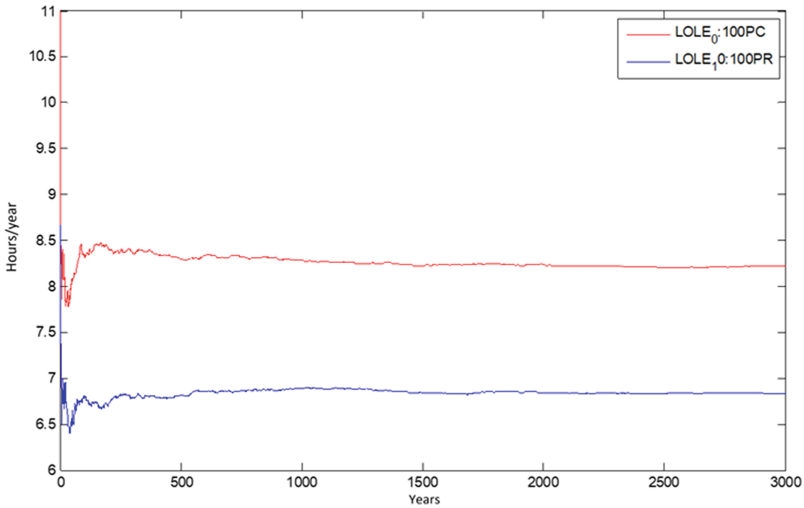

Fig. 9. Total sequential method: LOLE convergence (state 0 and state 10) Base case 4.

obtained show that it is possible to increase the penetration of renewable power in the system and reduce conventional power plants while maintaining system reliability.

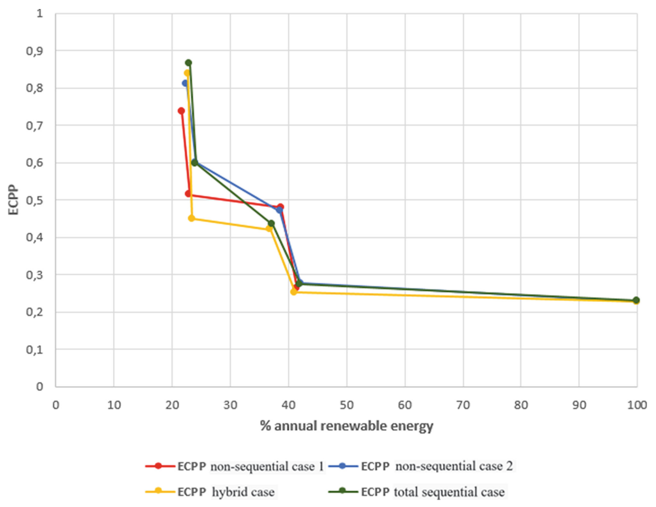

Fig. 10. Capacity credit evolution, ECPP.

4 Conclusions

- As the integration of renewable power in the system increases while maintaining the contribution of the Loja-Cuenca interconnection in all the cases considered, the LOLE index (expected loss of load) is reduced from approximately 8 h/year to 4 h/year, i.e. the system becomes more reliable (change from state 0 to state 9). However, despite this increase in LOLE the reliability of the system is maintained.
- The LOEE (expected energy loss) index obtained in all the cases considered is reduced with low penetration of renewable technologies (change from state 0 to state 3) while as this penetration becomes noticeable and conventional plants are reduced, the LOEE increases, which means that the severity of the expected failure is higher (change from state 3 to state 10).
- The probability of loss of load, or LOLP, observed decreases as the penetration of renewable energies in the system increases and conventional power plants are reduced, which means that the integration of renewable technology into the system allows for a greater possibility of keeping demand covered in a given period. The observed increase in LOLP is higher in the case of a fully renewable system (state 10 of all case studies).
- The expected demand is not supplied or EDNS follows the same process as the LOEE index, i.e. it decreases with low penetration of renewable technologies (change from state 0 to state 3) while as this penetration becomes noticeable and conventional plants are reduced, the EDNS starts to increase.
- Through the results obtained from this study, it is concluded that the integration of renewable energies in the electrical system is feasible and that it maintains the reliability of the electrical generation, which allows reducing the presence of conventional power plants, contributing to the diversification of the energy matrix of Ecuador.

References

1. Energías Renovables No Convencionales (ERNC): Revista Energía. https://www.revistaenergia.com/1135/. Accessed 04 Aug 2020
2. Plan Maestro de Electricidad (PME) 2018–2027: Agencia de Regulación y Control de Electricidad ARCONEL. https://www.centrosur.gob.ec/wp-content/uploads/2020/01/Plan-Maestro-de-Electricidad.pdf. Accessed 16 Feb 2021
3. Carbajo, A.: La integración de las energías renovables en el sistema eléctrico. Fundación Alternativas, Madrid (2012)
4. Cárdenas, V.: Análisis de confiabilidad de la generación considerando el ingreso de energías renovables no convencionales en el Sistema Nacional Interconectado del Ecuador. Universidad de las Fuerzas Armadas ESPE. http://repositorio.espe.edu.ec/handle/21000/12947. Accessed 16 Dec 2018
5. Billinton, R.: Reliability considerations in the utilization of wind energy, solar energy and energy storage in electric power systems. In: 2006 International Conference on Probabilistic Methods Applied to Power Systems, pp. 1–6. Stockholm, Sweden. IEEE (2006). https://doi.org/10.1109/PMAPS.2006.360204
6. Billinton, R., Li, W.: Reliability Assessment of Electrical Power Systems Using Monte Carlo Methods. New York (1994)
7. Imbarack, F.: Elaboración de una Herramienta Computacional para la Evaluación de la Confiabilidad de Sistemas de Transmisión Eléctricos. Pontificia Universidad Catolica de Chile, Santiago de Chile (2006)
8. Atlas Eólico del Ecuador: Ministerio de Electricidad y Energía Renovable MEER. http://historico.energia.gob.ec/ministerio-de-electricidad-y-energia-renovable-presento-el-primer-atlas-eolico-del-ecuador/ (2013)
9. Atlas Solar del Ecuador 2019 (2020). Escuela Politécnica Nacional EPN. https://www.ingenieriaverde.org/2020/01/28/atlas-solar-del-ecuador-2019/. Accessed 12 Mar 2021
10. Las renovables son el futuro energético de Ecuador. Revista Eólica y del Vehículo Eléctrico REVE (2020). https://www.evwind.com/2020/01/25/las-renovables-son-el-futuro-energetico-de-ecuador/. Accessed 11 May 2021
11. CELEC Homepage: https://www.celec.gob.ec/gensur/index.php/cev/central-eolica-villonaco-en-cifras. Accessed 15 Nov 2020
12. INAMHI Homepage: http://186.42.174.236/InamhiEmas/. Accessed 22 May 2021
13. HOMER - Hybrid Renewable and Distributed Generation System Design Software: Homer Energy. https://www.homerenergy.com/
14. SAM System Advisor Model: SAM. https://sam.nrel.gov/
15. Barrows, C., Bloom, A., et al.: The IEEE Reliability Test System: A Proposed 2019 Update. IEEE, pp. 1–9 (2019)
16. Cepeda, J.: Evaluación de la Vulneravilidad del Sistema Eléctrico de Potencia en Tiempo Real usando Tecnología de Medición Sincrofasorial. Universidad Nacional de San Juan, Argentina (2013)
17. Casado, A., Usaola, J.: Fiabilidad de un sistema eléctrico con energía eólica. Crédito de capacidad. Madrid: Universidad Carlos III (2012)
18. Akhtar, I., Kirmani, S., et al.: Reliability Assessment of Power System Considering the Impact of Renewable Energy Sources Integration Into Grid With Advanced Intelligent Strategies. IEEE Acces, pp. 1–13 (2021)

Optimal Capacitor Placement and Sizing in Radial Distribution Networks, Using Modified IGHS

Santiago Marcial M.(✉), Alexander Aguila T., and Darwin Cuasapaz

Universidad Politécnica Salesiana, Quito, Ecuador
rsmarcialm@gmail.com, rmarcial@eersa.com.ec

Abstract. This research focuses on the optimization of electrical distribution networks by the means of locating and sizing capacitors, for reducing system losses. In the iterative and combinational process of finding the most optimal results, an Improved Global Harmonic Search (IGHS) algorithm has been used, in combination with the Matpower tool in order to solve radial power fluxes. For the purpose of locating the buses where the best results are obtained, and to reduce the search space, a Loss Sensitivity Factor (LSF) was used. In the minimization model, voltage restrictions, power factor, and reactive overcompensation were considered; the time considered for the study was fifteen years. To test the method used, two model radial systems (IEEE 33 and 69 buses) have been optimized. The technical and economic analysis of the results, allows us to conclude that the investment in reactive compensation equipment for the two model systems is recommended, and brings improvements corcerning not using them, the implementation will allow solving problems concerning losses, better use of the networks, the longer useful life of the equipment connected to it, power factor correction, and voltage improvement. The study with capacitors with automatic steps is presented, since compared to better technology equipment they are more economical and practical for their application in radial distribution networks, whose characteristic is that they reach many kilometers in length. For more polluted networks where capacitors cannot be used, this study can serve as a starting point for the location and sizing of other compensation devices.

Keywords: Optimization · Radial distribution system · Reactive power compensation · Loss sensitivity factor · LSF · Improved global harmony search · IGHS · Matpower

1 Introduction

The optimization of electrical distribution networks focuses on maintaining service quality parameters within tolerable ranges [1]. The optimization of a distribution network starts from the current analysis of the system and its projection some years ahead, to plan the changes to keep both all components and [2, 3] parameters operative. The result of this analysis implies the best system solution at the lowest possible cost. For finding

© The Author(s), under exclusive license to Springer Nature Switzerland AG 2023
M. Zambrano Vizuete et al. (Eds.): RITAM 2021, LNNS 512, pp. 166–179, 2023.
https://doi.org/10.1007/978-3-031-11295-9_12

the least amount of devices, adequate distribution of the circuit components, and their sizing, the designed systems must foresee the necessary considerations to provide the power supply that satisfies the users' needs both for the year of implementation and in the long term. Finding the solution of all of these parameters for an efficient distribution system requires a long iterative process, therefore computational solving methods are used.

Research on the optimization of capacitor sizing and capacitor location has proposed several system solution methods, such as voltage stability index (VSI) [4], improved harmonic methods [5], genetic algorithms [2], bacterial search algorithms [6], plant growth simulation algorithms [7], clustering based on search (CBO) [8], accelerated particle swarm [9], search Cuckoo (CSA) [10], differential evolution (DE) [11], heuristics with multiobjective functions [12], linear mixed-integer problem resolution [13], in addition to mixed-integer nonlinear programming [14]. To find the global minimum in this case, we used the approximation algorithm IGHS, which will be solved by programming in Matlab together with the Matpower program [15].

As suggested in [16], for the sizing of the components of the primary distribution network, a demand projection period of fifteen years is considered. The issue of demand projection was not studied in-depth as it is a criterion that depends on several factors such as the place where the study is developed, expansion plans, the designer's criteria, and more of 3.9%, [17], from annual growth in demand.

2 Method

To solve the problem of losses in the radial systems IEEE 33 and IEEE 69, we propose the location and sizing of the capacitors, with the aims of finding an optimal answer we minimized an objective function using the IGHS algorithm. In order to reduce the search space we used an LSF factor; the model considers technical and economic constraints, for the iterative search we used the results of the radial power flows of Matpower.

A timeframe of fifteen years was established for the present study [18], on the basis of the useful life of the devices, as well as the growth in demand due to the increased use of devices by users [19, 20]; the expected trend growth rate of 3.9% per year was used [21], which are entered in the PD and QD columns for each case, for the execution of the power flows, where PD and QD are nomenclature used in Matpower for active power and reactive power.

2.1 Radial Power Flows

The power summation method in Matpower (PQSUM) was performed. Concerning the simulation of the shunt-connected capacitors, they were placed in the mpc matrix in the column corresponding to MVAR susceptance values or Column 6 (BS). The results obtained from the software were used throughout the iterative process of the search, for the minimization of the objective function.

2.2 The Objective Function

The objective function to be minimized has to do with the monetary cost since the focus of the research is based on finding an efficient alternative in terms of technical performance, as well as the one with the lowest implementation cost. Therefore, the function includes power and energy loss cost of the system, capacitor capacity investment and installation cost.

$$FO = \mathrm{LossP} \times \mathrm{Fper} \times \mathrm{kloss} \times \mathrm{t} + \mathrm{LossP} \times KP + \mathrm{Frc} \times \left(\mathrm{kcap} \times \sum_{i}^{Cb} \mathrm{vectQci} + \mathrm{Cb} \times \mathrm{kinst}\right) \quad (1)$$

where:

$$Fper = 0.3 * Fc + 0.7 * Fc^2 \quad (2)$$

$$Frc = (int \times (1 + int)^{years}) \div (((1 + int)^{years}) - 1) \quad (3)$$

$LossP = Active\ power\ losses$
$Kloss = Cost\ of\ active\ power\ losses\left(\frac{90\ USD}{MWh}\right)$
$t = 8760\ hours\ for\ one\ year$
$kp = Cost\ of\ power\ osses,\ \left(\frac{57{,}500.00\ USD}{MW}\right)$
$kcap = Cost\ per\ installed\ MVAR,\ \left(\frac{25{,}000.00\ USD}{\mathrm{MVAR}}\right)$
$vectQci = Vector\ with\ the\ values\ of\ the\ capacitors\ found$
$Qc = Discrete\ vector\ with\ commercial\ capacitor\ values\ including\ 0$
$Frc = Capital\ recovery\ factor$
$Cb = Number\ of\ resulting\ capacitors$
$LossP = Active\ power\ losses$
$Kinst = Constant\ installation\ cost\ of\ each\ capacitor(1,000.00\ USD)$

The loss factor (Fper) is calculated based on the load factor (Fc), it is necessary to consider that the loads are not constant for all days of the year [18], for this study, a load factor of 0.8 was used.

In the case of the total cost of the capacitors, this value was divided for various periods during the projection time of the study; the cost of the capacitors was multiplied by Frc, where int is the interest rate at which the investment will be paid with a value of 9.03% taken from the Central Bank in August 2020 [17]; another variable taken into account in Eq. 3 is the number of years of financing, which in this case is 15 years.

To solve the objective function, we took into account the voltage restrictions at each busbar as in the Eq. (4), the power factor at the feeder's head as in Eq. (5), the reactive compensation that must not exceed the reactive power of all loads, and the power factor at the feeder's head as in Eq. (6) [20].

In expression number (4) Vi corresponds to the voltage modulus at each node or busbar of the distribution network system [5, 19]. On the other hand, the voltage was regulated to ±10% concerning the nominal voltage.

In Eq. (5); the power factor was calculated with the reactive and active power provided in Matpower from the previous calculations, employing [results.gen].

$$0.9 \leq Vi \leq 1.1 \tag{4}$$

$$0.9 \leq fpsys \leq 1.0 \tag{5}$$

$$\sum_{i=1}^{Cb} vectQc \leq \sum_{i=2}^{bars} QD \tag{6}$$

Loss Sensitivity Factor (LSF)

The distribution of the capacitors in each system is another essential parameter of the optimization study; the use of LSF allowed obtaining a reduced sample of the location where the capacitors can be placed, LSF helps to identify the bars where the reactive compensation should be installed to achieve a greater reduction of losses [20, 22]. LSF is defined by the Eqs. (7) and (8) [22].

$$\frac{\partial PLdlossj}{\partial QDj} = \frac{2 \times QDj \times R(i-j)}{Vj^2} \tag{7}$$

where:

$$PLdloss(j) = \frac{\left(PD^2(j) + QD^2(j)\right)}{V^2(j)} \times R(i-j) \tag{8}$$

$Vj = Modulus\ of\ voltage\ at\ bars\ j\ at\ receiving\ end$
$R(i-j) = Resistance\ of\ the\ line\ between\ the\ bars\ i\ and\ j$
$PLdloss(j) = Distribution\ line\ losses\ reaching\ the\ busbar\ j$
$QDj = Reactive\ power\ at\ busbar\ j$
$PDj = Active\ power\ at\ the\ busbar\ j$

Busbars with normalized voltage values greater than 1.01 were removed from the search, (9) [20].

$$Vnorm(i) = \frac{V(i)}{0.95} \tag{9}$$

where:

$Vnorm(i) = corresponds\ to\ the\ normalized\ voltage\ for\ each\ busbar\ in\ the\ system$

2.3 IGHS Considering LSF

The GHS global harmonic search and IGHS enhanced global harmonic search are inspired by the swarm intelligence upon which the PSO heuristic is based [23, 24]. Under this principle, the harmonic search reaches to find better global optimums.

$$PAR(i) = PAR_{min} + \frac{PAR_{max} - PAR_{min}}{NI} * i \tag{10}$$

The PAR and BW variables according to [24], can be fixed or dynamic; for the purposes of the present study they were calculated dynamically according to the progress of the iterations. According to [23] PAR and BW have a profound effect on harmonic search performance.

The study variables have the following conditions:

$HMS = 500$

$HMCR = 0.95$

$PARmax = 0.99$

$PARmin = 0.01$

$dQc = vector\ dimension\ with\ commercial\ capacitor\ values$

$n = 5000\ iterations$

With fixed capacitor values, the BW parameter was not used, as in GHS, thus eliminating the difficulty of selecting the BW parameter [24], in its place is rnd1, which will allow or not to change in one position the value of the capacitors of the vector Qc.

The IGHS algorithm used is described below [24]:

Algorithm 1: Pseudocode for IGHS algorithm

```
for(i=1:n)
  for(j=1:busbars)
   if(r1≤=HMCR)
      if(r2≤=PAR);    where       r1,r2∈(0,1);
      Xnew_j = Xbest_(j) + rnd1; where       rnd1∈(-1,0,1);
      else
      Xnew_j = X(rnd2_(j)); where       rnd2 ∈ (1,2,…,HMS);
      end if
   else
      Xnew_j = Qc_rnd(j) ; where       rnd ∈ (1,2,…,dQc);
   end if
  end for
end for
```

where:

$[L] = vector\ with\ the\ order\ of\ the\ bars,\ from\ highest\ to\ lowest\ LSF\ value$

$U = randi[1\ busbars];\ random\ value,\ from\ 1\ to\ the\ number\ of\ busbars\ in\ the\ system$

$X = variable\ for\ sizing$

The algorithm described above was applied considering the bars selected by LSF for the optimization in year 15. For previous years, the same algorithm was applied without the application of LSF because the location remains fixed for each capacitor in the location defined for the last year. In these new iterations, the capacitors must obtain results less or equal to those of year 15, as shown in the following expression (11).

$$vectQc(j, t) \leq vectQc(j, t + 1) \tag{11}$$

where:

$j = busbar\ number$

$t = years\ of\ the\ design\ period\ that\ varies\ from\ 14\ to\ 1$

$t + 1 = years\ of\ the\ design\ period,\ which\ varies\ from\ 15\ to\ 2$

3 Results and Discussions

3.1 IEEE 33 Bus System

The values of P and Q of the loads, R and X of the conductors, nominal voltage, and other parameters of the IEEE 33-bus system can be found in the article 'Network reconfiguration in distribution systems and load balancing to reduce losses.' [25]. The starting conditions for the system are obtained after the 15-year evaluation period, with the proposed demand growth conditions of 3.9%; with this data, the projection of voltage values for all the busbars of this system is obtained. In Fig. 2, the red line show for the last year there will be a voltage drop of more than 10% tolerance, this is considered outside the proposed design limits.

Figure 1 shows the results of applying the LSF equation to the system, the bars with high sensitivity values are: 8, 13, 14, 20, 24, 24, 25, 29, 30, 31.

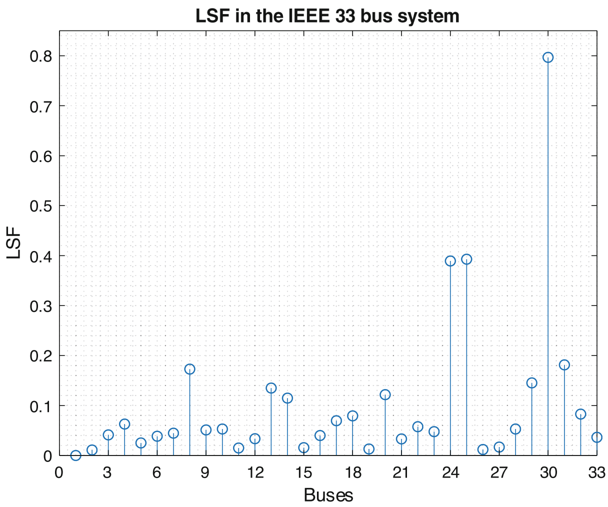

Fig. 1. The sensitivity level is given by LSF in the IEEE 33-bus system

Optimization Results with Capacitors for Year 15

A total of 5000 iterations of the algorithm proposed were run, the results are presented in Table 1.

Table 1. Results for the last year

Description	Base case	IGHS with LSF
Losses MW	0.5630	0.3483
Position (busbars)	–	8;13;14;24;25;29;30;31
Capacity (MVAR)	–	0.6;0.5;0.1;0.15;0.5;0.25;1.2;0.3
V. min	0.8544	0.9002
fp in ahead	0.8486	0.9925
F.O. (USD)	337,769.163	221,107.431
Iterations		5000

Through the use of LSF, an optimization of 116,661.732 USD was projected for year 15, since the initial objective function (OF) resulted in 337,769.163 USD and the optimized OF resulted in a value of 221,107.431USD. Also, losses were of 0.563 MW, later with the application of the algorithm and LSF, the losses decreased to 0.348 MW.

Optimization Results for Previous Years

The results found for years 1 to 15 are described in Table 2, the same that allows having an idea of the steps of the capacitors. Additionally, it is possible to know the installation period, with which it will be possible to elaborate a plan of implementation of the devices. It has been established that the capacitors implemented are automatic to vary their configuration as the daily demand changes as well as the annual demand, thus ensuring that there are no violations to the restrictions [26].

Table 2. Results of capacitor placement in MVARs

	Year 1	**Year 2**	**Year 3**	**Year 4**	**Year 5**
Location	8;13;25;30	8;13;25;30	8;13;25;30	8;13;25;30;31	8;13;25;30;31
Sizing	0.25;0.3;0.3;1.2	0.25;0.3;0.3;1.2	0.25;0.3;0.3;1.2	0.25;0.3;0.3;1.2;0.1	0.25;0.5;0.3;1.2;0.1
	Year 6	**Year 7**	**Year 8**	**Year 9**	**Year 10**
Location	8;13;25;30;31	8;13;25;30;31	8;13;25;30;31	8;13;25;30;31	8;13;25;30;31
Sizing	0.25;0.5;0.5;1.2;0.15	0.3;0.5;0.5;1.2;0.15	0.3;0.5;0.5;1.2;0.25	0.3;0.5;0.5;1.2;0.3	0.5;0.5;0.5;1.2;0.3
	Year 11	**Year 12**	**Year 13**	**Year 14**	**Year 15**
Location	8;13;25;30;31	8;13;25;29;30;31	8;13;25;29;30;31	8;13;24;25;29;30;31	8;13;14;24;25;29;30;31
Sizing	0.5;0.5;0.5;1.2;0.3	0.5;0.5;0.5;0.15;1.2;0.3	0.5;0.5;0.5;0.25;1.2;0.3	0.6;0.5;0.15;0.5;0.25;1.2;0.3	0.6;0.5;0.1;0.15;0.5;0.25;1.2;0.3

Figure 2 shows a comparison of the voltage profiles in year 15, before and after the installation of capacitors, showing that the solution found complies with the voltage restriction.

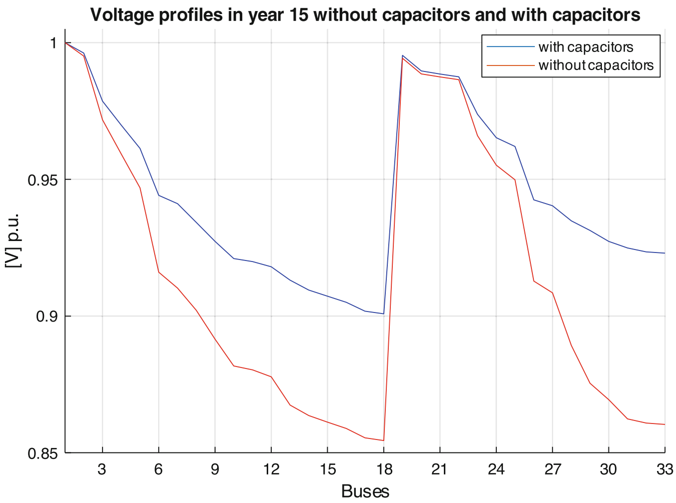

Fig. 2. Comparison of voltage profiles as of year 15.

Figure 3 shows in blue the results of the objective function for each year of study without capacitors, and in red the objective function for each year with capacitors installed. Subtracting the cost of the initial objective function from the final objective function gives the annual savings or benefit of the implementation. For calculating the NPV it is necessary to bring to the present value the benefits obtained for each of the 15 years.

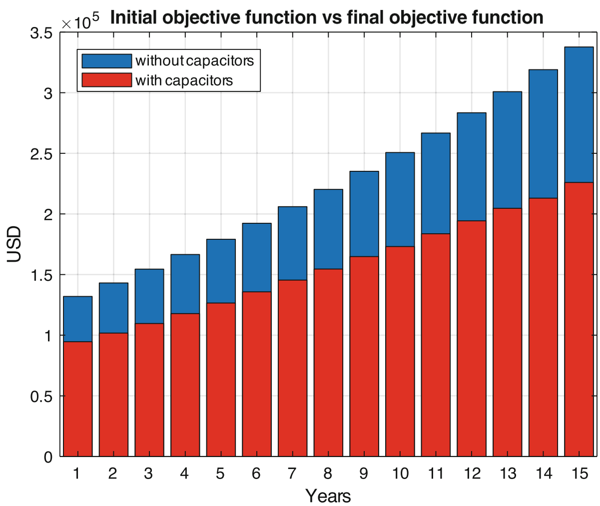

Fig. 3. Comparison of the objective function.

Table 3. Calculation of benefits at present value

Results present value					
Years	1	2	3	4	5
Cn/(1 + int)^n	36,229.64	36,517.97	36,536.14	36,471.24	36,380.7
Years	6	7	8	9	10
Cn/(1 + int)^n	36,250.18	36,041.74	35,760.44	35,364.12	34,933.08
Years	11	12	13	14	15
Cn/(1 + int)^n	34,410.03	33,849.7	33,237.61	32,609.42	31,896.15
				ΣTotal	526,488.16

$$Co = \frac{Cn}{(1 + int)^n} \tag{12}$$

where:

$Co = current\ cost$

$Cn = future\ cost$

$Int = interest$

$n = year\ of\ calculation$

Applying Eq. 12 to each of the values of the profit obtained per year, we obtained:

The calculation of the disbursement to be made for the 8 capacitors obtained from the search is 98,000.00 USD, considering the installed capacity and the installation cost. To obtain the NPV, the disbursement was subtracted from the sum of the benefits of all the years brought to present value, which gave an NPV of 428,488.16 USD.

$$B/C = \frac{VAN + disbursement}{disbursement} \tag{13}$$

Equation 13 was used to calculate the cost-benefit ratio, from which a value of 5.37 was obtained, and since it is greater than 1, it can be concluded that the investment is viable.

3.2 IEEE 69 Bus System

The parameters of the IEEE 69 bus system can be found in the article Optimal capacitor location in radial distribution systems [27]. In Fig. 5, the red line show for the last year there will be a voltage drop of more than 10% tolerance, considering the 3.9% growth in demand.

In Fig. 4, it can be seen that the bars with high sensitivity values are: 12, 21, 34, 49, 50, 59, 61, 64, 65.

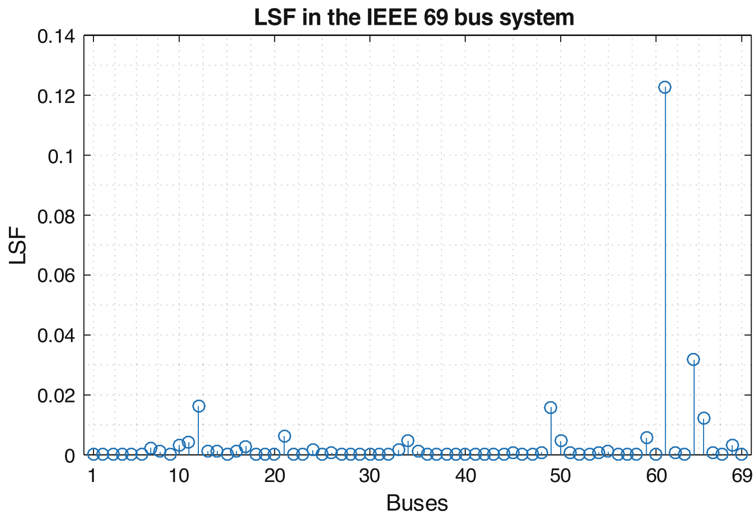

Fig. 4. The sensitivity level is given by LSF in the 69-bus system

Optimization Results with Capacitors for the Year 15

For the 69-bus system, 5000 iterations were applied with the proposed objective function; the results are presented in Table 4.

Table 4. Results for the last year

Description	Base case	IGHS with LSF
Losses MW	0.6381	0.4210
Location (busbars)	–	12; 21;59;61;64;65
Capacity (MVAR)	–	0.5; 0.3;0.25;2.5;0.1;0.6
V. min	0.8462	0.9
fp in ahead	0.8254	0.99
F.O. (USD)	382,816.31	266,488.39
Iterations	–	5000

A reduction in losses was achieved because there is a savings of 116,327.92 USD; the initial objective function resulted in 382,816.31USD and at finalization in 266,488.39 USD. In the first scenario, the losses resulted in 0.6381 MW and after optimization, they were reduced to 0.4210 MW.

Optimization Results for Previous Years

Table 5 presents the capacitances found for the capacitors and their distribution in the system for all years.

Table 5. Results of capacitor placement in MVARs

Year 1	Year 2	Year 3	Year 4	Year 5
12;21;61	12;21;61	12;21;61;65	12;21;61;65	12;21;61;65
0.25;0.25;1.5	0.25;0.25;1.5	0.3;0.25;1.5;0.1	0.3;0.25;1.5;0.1	0.3;0.25;1.6;0.1
Year 6	Year 7	Year 8	Year 9	Year 10
12;21;61;65	12;21;61;65	12;21;61;65	12;21;61;65	12;21;61;65
0.3;0.25;1.75;0.1	0.3;0.25;1.75;0.1	0.5;0.25;1.75;0.1	0.5;0.25;1.9;0.1	0.5;0.3;1.9;0.1
Year 11	Year 12	Year 13	Year 14	Year 15
12;21;61;65	12;21;61;65	12;21;61;65	12;21;61;64;65	12;21;59;61;64;65
0.5;0.3;2.2;0.1	0.5;0.3;2.3;0.25	0.5;0.3;2.3;0.5	0.5;0.3;2.5;0.1;0.5	0.5;0.3;0.25;2.5;0.1;0.6

Figure 5 shows the comparison of the voltage profiles in year 15, before and after optimization, where the correction of the voltage values is observed.

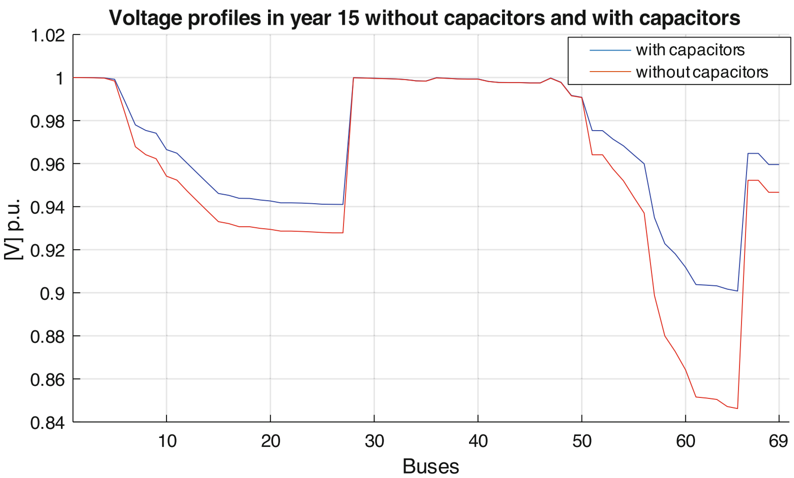

Fig. 5. Voltage profile comparison in year 15

Figure 6 shows a comparison of the costs of the objective function before and after optimization, for fifteen years. By subtracting the costs of the initial objective function minus the final objective function, the annual savings or benefit of the optimization was obtained. To calculate the NPV it is necessary to bring to the present value the benefits obtained for each of the 15 years, with Eq. 12, where the following Table 6 was obtained.

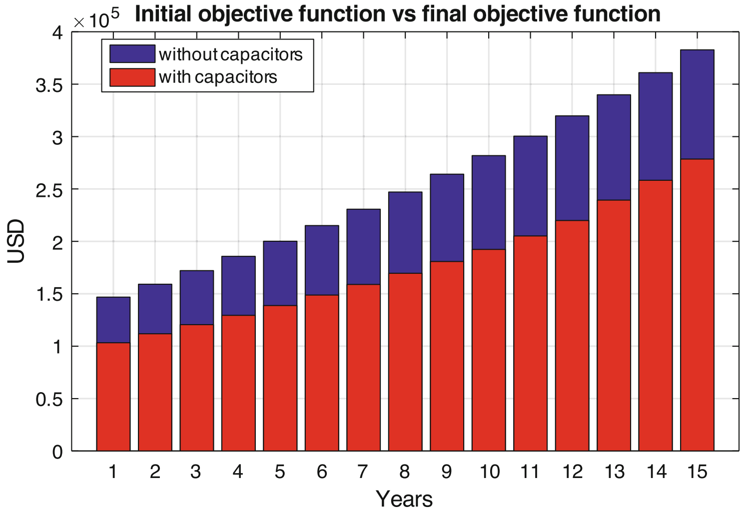

Fig. 6. Comparison of the objective function

Table 6. Calculation of benefits at present value

Results present value					
Years	1	2	3	4	5
Cn/(1 + int)^n	41,732.68	42,006.18	42,087.96	42,034.68	41,899.25
Years	6	7	8	9	10
Cn/(1 + int)^n	41,607.93	41,287.92	40,864.92	40,445.12	39,888.73
Years	11	12	13	14	15
Cn/(1 + int)^n	39,182.14	38,068.00	36,432.91	34,325.91	31,804.88
				ΣTotal	593,669.21

The calculation of the disbursement to be made for the 6 capacitors obtained from the search is 112,250.00 USD, considering the installed capacity and the installation cost. To obtain the NPV, the disbursement was subtracted from the sum of the benefits of all the years brought to present value, which gave an NPV of 481,419.21 USD. For the calculation of the cost-benefit Eq. 13 was used, from which the value of 5.29 was obtained, being greater than 1, it can be said that the investment is viable.

4 Conclusions

In the 33-bus system during the fifteen years, losses of 5,650 MW were obtained in the simulation executed without capacitors; in the simulation proposed with capacitors, losses were 3,572 MW. On the other hand, the objective function for this same period reached a very significant optimization since it went from 3,050,439.93 USD to the value of 2,279,147.43 USD bringing a saving of 771,292.50 USD.

In the proposed IEEE 69-bus system during the fifteen years, losses of 6.3457 MW were obtained in the simulation run without capacitors; in the proposed simulation with capacitors, losses were 4.0564 MW. On the other hand, the objective function for this same period reached a very significant optimization since it went from 3,806,898.30 USD to the value of 2,570,665.97 USD; this function takes into consideration several parameters such as the cost of energy and power losses, installation of capacitors and savings of up to 1,236,232.34 USD.

The LSF parameter was used to search for the loss sensitivity through which capacitors can be distributed in an optimal location within the distribution circuit, with this value order can be established at the busbars for the location and distribution of capacitors in the system.

It should be noted that the optimization of the location and sizing of capacitors has taken into account the cost of using these devices, so it was found that the cost of acquisition and financial expenses are covered at the end of the design period; another advantage in the implementation of reactive compensation is that the devices have a long-life span, and can continue to operate even after the time considered for the design has elapsed.

References

1. ARCONEL: Regulación 005-18, Calidad del servicio de distribución y comercialización de energía eléctrica. Ecuador, p. 38 (2018)
2. Antunes, C.H., Pires, D.F., Barrico, C., Gomes, A., Martins, A.G.: A multi-objective evolutionary algorithm for reactive power compensation in distribution networks. Appl. Energy **86**(7–8), 977–984 (2009)
3. Castillo Munoz, F.A., Aguila Tellez, A., Gonzalez Sanchez, J.W.: Analysis of stability of tension and losses of electric power in distribution networks with distributed generation. IEEE Lat. Am. Trans. **14**(11), 4491–4498 (2016)
4. Krishnamurthy, S., Mohlwini, E.X.: Voltage stability index method for optimal placement of capacitor banks in a radial network using real-time digital simulator. In: Proceedings of the 24th Conference on the Domestic Use of Energy (DUE) (2016)
5. Ali, E.S., Abd Elazim, S.M., Abdelaziz, A.Y.: Improved harmony algorithm for optimal locations and sizing of capacitors in radial distribution systems. Int. J. Electr. Power Energy Syst. **79**, 275–284 (2016)
6. Devabalaji, K.R., Ravi, K., Kothari, D.P.: Optimal location and sizing of capacitor placement in radial distribution system using bacterial foraging optimization algorithm. Int. J. Electr. Power Energy Syst. **71**, 383–390 (2015)
7. Rao, R.S., Narasimham, S.V.L., Ramalingaraju, M.: Optimal capacitor placement in a radial distribution system using plant growth simulation algorithm. Int. J. Electr. Power Energy Syst. **33**(5), 1133–1139 (2011)
8. Vuletić, J., Todorovski, M.: Optimal capacitor placement in radial distribution systems using clustering based optimization. Int. J. Electr. Power Energy Syst. **62**, 229–236 (2014)
9. Basyarach, N.A., Penangsang, O., Soeprijanto, A.: Optimal capacitor placement and sizing in radial distribution system using accelerated particle swarm optimization. In: 2017 International Seminar on Intelligent Technology and Its Applications (ISITIA), pp. 93–97. IEEE (2017)

10. Mohamed, A.A., Kamel, S., Aly, M.M.: A simple analytical technique for optimal capacitor placement in radial distribution systems. In: 2017 Nineteenth International Middle East Power Systems Conference (MEPCON), pp. 928–933. IEEE (2017)
11. Neelima, S., Subramanyam, P.S.: Optimal capacitor placement in distribution networks for loss reduction using differential evolution incorporating dimension reducing load flow for different load levels. In: 2012 IEEE Energytech, pp. 1–7 (2012)
12. Gupta, N., Swarnkar, A., Niazi, K.R.: An efficient greedy approach for reactive compensation on large-scale distribution systems. In: 2011 IEEE Power and Energy Society General Meeting, pp. 1–7 (2011)
13. Khodr, H.M., Olsina, F.G., De Oliveira-De Jesus, P.M., Yusta, J.M.: Maximum savings approach for location and sizing of capacitors in distribution systems. Electr. Power Syst. Res. **78**(7), 1192–1203 (2008)
14. Nojavan, S., Jalali, M., Zare, K.: Optimal allocation of capacitors in radial/mesh distribution systems using mixed integer nonlinear programming approach. Electr. Power Syst. Res. **107**, 119–124 (2014)
15. Zimmerman, R.D., Murillo-Sánchez, C.E., Thomas, R.J.: MATPOWER: steady-state operations, planning, and analysis tools for power systems research and education. IEEE Trans. Power Syst. **26**(1), 12–19 (2011)
16. Empresa Eléctrica Quito, "NORMAS PARA SISTEMAS DE DISTRIBUCIÓN - PARTE A – GUÍA PARA DISEÑO DE REDES DE DISTRIBUCIÓN.," in Guia para diseño de redes de distribución, 2015th ed., R. E. Sosa Marco, Muñoz Christian, Ed. Quito, p. 166 (2015)
17. Banco Central del Ecuador: Tasas de Interés Agosto 2020 (2020). https://contenido.bce.fin.ec/documentos/Estadisticas/SectorMonFin/TasasInteres/Indice.htm. Accessed 23 Aug 2020
18. Yebra, J.A.: Sistemas eléctricos de distribución, Primera ed. México (2009)
19. Muthukumar, K., Jayalalitha, S.: Multiobjective hybrid evolutionary approach for optimal planning of shunt capacitors in radial distribution systems with load models. Ain Shams Eng. J. **9**(4), 1975–1988 (2018)
20. Dixit, M., Kundu, P., Jariwala, H.R.: Optimal allocation and sizing of shunt capacitor in distribution system for power loss minimization. In: 2016 IEEE Students' Conference on Electrical, Electronics and Computer Science (SCEECS), pp. 1–6. IEEE (2016)
21. Consejo Nacional de Electricidad: Estudio y gestión de la demanda eléctrica. Plan Maest. Electrif. 2013–2022 **2**(206), 2013–2022 (2013)
22. Babu, P.V., Singh, S.P.: Capacitor allocation in radial distribution system for maximal energy savings. In: 2016 National Power Systems Conference (NPSC), pp. 1–6 (2017)
23. Omran, M.G.H., Mahdavi, M.: Global-best harmony search. Appl. Math. Comput. **198**(2), 643–656 (2008)
24. Lin, Y., Xing, C.M.: A new improved harmony search algorithm for continuous optimization problems. In: Proceedings of 2011 International Conference on Computer Science and Network Technology, vol. 2, pp. 686–689 (2011)
25. Mesut, F.W.: Network reconfiguration in distribution systems for loss reduction and load balancing. Justice Syst. J. **13**(3), 79–385 (1988)
26. Marcial, S., Águila, A.: Optimal compensation of reactive power in radial distribution networks considering design period. In: 2019 International Conference on Information Systems and Computer Science (INCISCOS), pp. 108–115. IEEE (2019)
27. Das, D.: Optimal placement of capacitors in radial distribution system using a Fuzzy-GA method. Int. J. Electr. Power Energy Syst. **30**(6–7), 361–367 (2008)

Check for updates

Photovoltaic Generation Potential for Vehicles with Solar Panels

Robert-Javier Machuca-Ordoñez[1], Carlos Flores-Vázquez[1,2,3](✉), Juan-Carlos Cobos-Torres[1,2], and Daniel Icaza Álvarez[1,2]

[1] Catholic University of Cuenca, Av. Américas y G. Torrres, 010101 Cuenca, Ecuador
cfloresv@ucacue.edu.ec

[2] GIRVyP Visible Radiation and Prototyping Research Group, Cuenca, Ecuador

[3] CIITT Lighting Laboratory, Av. Ricaurte Bibín, Ricaurte, Ecuador
https://www.ucacue.edu.ec/,
https://investigacion.ucacue.edu.ec/ciittinvestigacion/

Abstract. Ecuador, due to its geographical location, has a high amount of direct energy from the sun. This makes it a country with high potential for the use of renewable and clean energies. Here is exposed as a case study the city of Cuenca that receives constant solar radiation and without significant variations throughout the year. This research consists of the development of a measurement system to obtain the average radiation, through the installation of photovoltaic solar panels on a mobile unit (vehicle) for the analysis of radiation in transport trajectories in the city of Cuenca - Ecuador. The system is capable of performing radiation profiling in a database. This will allow to record accurate information to design mobile solar installations taking into account the incidence of solar radiation on a photovoltaic panel installed on vehicles. This study allows to have a real conception of the opportunities of the implementation of photovoltaic panels on vehicles. Existing studies consider only fixed panels on buildings, but as evidenced in this study, having panels moving on the streets of the city, the situation is different from the above mentioned. Electric mobility is accompanied by new challenges for sustainable energy, this article proposes a new methodology to address photovoltaic systems in vehicles.

Keywords: Electric mobility · Solar radiation · Renewable energy · Solar panels movement

1 Introduction

Renewable energies in the world are the main sources of clean and planet-friendly energy production [22]. The generation of solar energy with solar panels is lim-

Supported by organization GIRVyP Visible Radiation and Prototyping Research Group, CIITT Lighting Laboratory, Energy Optimization Project for the Collection System in Urban Transportation Units.

© The Author(s), under exclusive license to Springer Nature Switzerland AG 2023
M. Zambrano Vizuete et al. (Eds.): RITAM 2021, LNNS 512, pp. 180–194, 2023.
https://doi.org/10.1007/978-3-031-11295-9_13

ited by the unavailability of the main variable which is sunlight, causing the production of electricity to vary with respect to the weather.

This integration by electrical systems is currently reflected in the goal of being environmentally friendly, as current concerns about climate change and fossil fuel energy security. Renewable energy sources will become key components in combating the threat of the climate factor. The global trend will have a near evolutionary mission towards renewable energy sources [18].

Nowadays the electrical system has been implemented by independent systems but with the vision related to energy, these energetic changes look for a sectorial integration towards electricity and transportation, with the purpose of obtaining a unique and efficient system [18,20]. It is called Smart Urban Energy Network or Smart Cities, this idea will offer us a highly flexible and integrated service with energy efficiency [28].

Electric vehicles have fixed charging systems, which limit the time and location for recharging. This considerably reduces the desired autonomy for the use of electric vehicles.

To improve the availability of charging systems for electric vehicles and other complementary systems in combustion vehicles, this research focuses on the analysis and development of a mobile charging system [11]. It is intended to measure the solar radiation considering urban transport routes in the city of Cuenca. The analysis of solar radiation data in the city of Cuenca was generated considering the different inferences of collection (buildings, shadows and climatic factors) in the city [26].

Due to the growing energy consumption nowadays, the energy demand presents higher demand rates, recent research works have shown that fossil fuels have certain limitations such as limited resources and economic problems which will lead to an energy crisis, [34]. to overcome the problems coming from fuels it is required a renewable energy exploitation [12], solar energy for example is an effective alternative because it presents availability, profitability and environmentally friendly.

Recent research has established that approximately 1 kW of photo voltaic energy is capable of avoiding the combustion of 77 kg of coal, thus reducing carbon emissions by approximately 136 kg per year [13,33]. The benefits can be achieved even at low levels of photo voltaic efficiency (12 and 20%) [1], so photo voltaic energy is an energy alternative capable of supplying the world's energy demand if solar collection systems were more accessible.

There are several parameters established as critical for a solar system to present the highest possible efficiency [2,10,17], showing as a main point the technological improvements of the systems to minimize the cost and environmental impact of solar systems. One of the most significant parameters studied is the amount of irradiation received by a photo voltaic system [7,25], which determines the efficiency and feasibility of use of a system, whether it is a mobile or static system [29,35].

Previous research has shown the monitoring of photo voltaic panels to determine the efficiency and irradiation of the panels through the use of spectrometers, weather and radiation sensors [32] used to measure the incidence of irradiation on static photo voltaic systems [29]. Due to the increasing demand for electric mobility, a way has been sought to implement back-powered charging systems for this type of vehicles [23].

Studies on electric mobility present vehicles with solar power systems [4,8,19] show prototypes of electric vehicles powered by solar energy, there are even studies that show improvements to electric vehicles that have similar systems [30], most of the studies presented seek the implementation of a secondary charging system using solar energy [6,14].

2 Material and Method

For the analysis of radiation in the city of Cuenca, a system was developed to collect all the radiation data during the respective measurements [27]. The tests carried out cover specific routes of high traffic bus lines [37], the data collection has a duration of one week, to obtain variant data with respect to the behavior of the climate. The collection of radiation data was carried out in the month of July, being this statistically the most unfavorable month of the whole year with respect to the average solar radiation according to [39].

This section describes in detail the whole process developed to obtain the required radiation data, from formulations, simulations, first prototypes, routes to the interpretation of the data obtained during the respective measurements. All the equipment and methods used in each of the processes are presented and described.

2.1 Operating Principle

The electromagnetic spectrum coming from the sun, captured by the surface of the planet encompasses different wavelengths, such as ultraviolet (UV), infrared (IR), x-rays, gamma rays, etc. [13]. A photovoltaic cell is capable of capturing only a part of the electromagnetic spectrum known as the visible light spectrum. This spectrum covers a wavelength from 400 nm to 700 nm [9].

For the development of the proposed system, a monocrystalline photovoltaic cell is used. The monocrystalline silicon panels are characterized by higher efficiency than their counterparts, efficiency of 15% to 22%, and also are not affected by high temperatures as polycrystalline [36] in Fig. 1 is observed the technical data of the panel used.

The main objective of the proposed system is to measure solar radiation in watts per square meter (w/m^2) [3,32]. To obtain this data the system uses ACS712 DC current sensors. The SCC (Short Circuit Current) of the panel used, SCC = 1.19. For wider ranges of SCC the sensor module can be replaced by one with a wider current range (15 A–30 A).

Figure 1 (b) shows the initial diagram for the operation of the system [21], the current sensor module requires that the photovoltaic panel is connected in

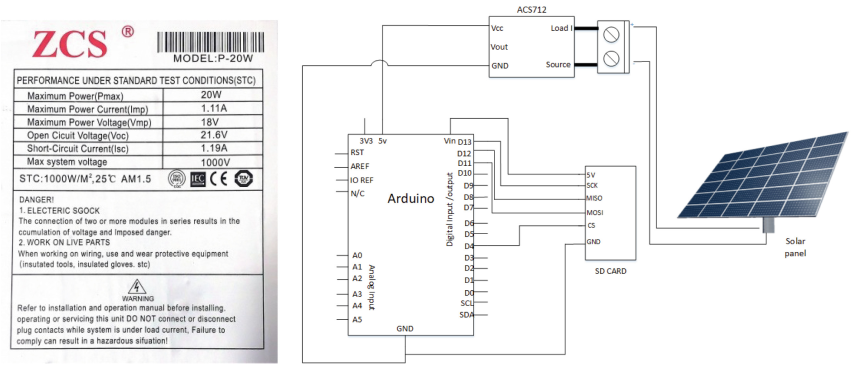

(a) (b)

Fig. 1. (a) Technical data and (b) General structure.

short circuit, since the base measurement value to obtain the irritation is the short circuit current (SCC), process detailed in Sect. 2.2.

The current values are interpreted by the current sensor module as voltage values in mV. This is necessary since the microcontroller used for data interpretation can only receive voltage values from 0 to 5 V and interpret them as integer values between 0 and 1024 at a resolution of 4.9 mV per unit [5].

2.2 Formulation

For the calculation of radiation and irradiation, the main variable is the short-circuit current, considered with SCC. It should be noted that this value may vary depending on the climatic factor, however, it is possible to use the values established in the technical sheet of the panel.

$$SCC \approx 1.19A \tag{1}$$

The voltages received by the current sensor must also be considered. For accuracy of reading and interpretation of the data, two constants are required for the respective calculations. The first constant is the mean module voltage value (mMv) which represents the mean supply voltage of the sensor. For a 5 V supply it is 2500 mV and for a 3 V supply 1650 mV.

As a second constant the sensor supply voltage value (mSv) for this variable the value of 5000 mV for the power supply is considered.

$$mMv = 2500\,\mathrm{mV}. \tag{2}$$

$$mSv = 5000\,\mathrm{mV}. \tag{3}$$

As mentioned above, the current sensor module is only capable of measuring voltage values in mV. So in order to obtain the current values from the voltage values a ratio constant is required to interpret the values. This variable is set as millivolts per amperage value (mVpA), this value depends on the module used, for a 5 A current sensor will have a value of 185 mv, i.e. 1 A is equivalent to 185 mv.

$$mVpA = 185\,\mathrm{mV} \tag{4}$$

Then the formulation procedure will be as follows:

$$CSR = CAI - \left(\frac{mMv}{mSv} * 1024\right) \tag{5}$$

Where:

CSR = Current sample read.

CAI = Current analog input.

The current readings will be stored and an overall average of the samples taken is obtained, one sample per millisecond to obtain the final current. You will then have the following formulations:

$$I_{final} = \frac{\frac{I_{average}}{1024} * mSv}{mVpA} \tag{6}$$

$$Irradiation = \frac{I_{final}}{SCC * 1000} \tag{7}$$

Finally we obtain the accumulated irradiation per day:

$$Irradiation\ Accumulated = \frac{I_{final}}{3600 * Irradiation\ period/1000} \tag{8}$$

The radiation period refers to the time during which the measurements are made. These formulas have been implemented in the program [40].

2.3 Programming

As this is a prototype equipment, it uses the Arduino platform for its development. The main program focuses on the analysis of solar radiation measurement [16,31]. The programming was done with a task and decision approach as shown in the Fig. 2.

2.4 Calibration

Prior to the implementation of the system in the mobile unit, a test run was carried out to verify that the system has the correct measurements. The sensor used for the developed prototype is the ACS712.

For the SCC current, a digital multimeter was used to measure the actual short-circuit current provided by the panel under conditions of high solar incidence [15,38]. The measurements obtained were SCC = 1.51 A (See Fig. 3), the

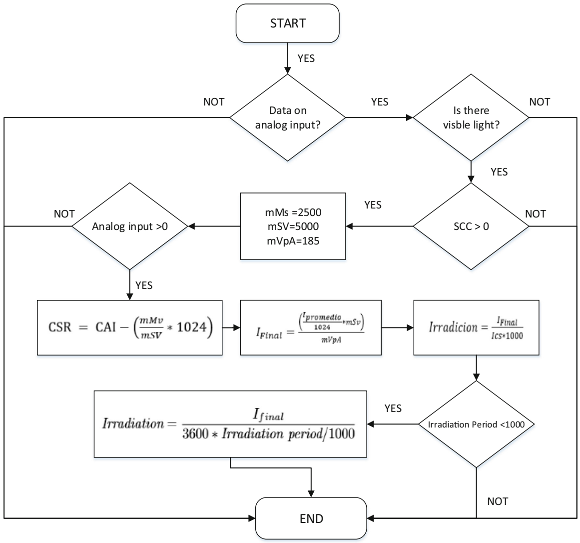

Fig. 2. Program flow diagram

measurements presented oscillating values between 1.10 and 1.53 A, the technical data of the panel indicate a SCC = 1.19 A (See Fig. 1).

The actual current required by the system was checked by measuring the irradiance with a pyranometer. By using the pyranometer it is possible to verify the irradiance values measured with the standard instrument (Apogee MP-200) [24] versus those of our system. In this verification, a short-circuit current of Ics = 1.32 A has been used for data acquisition.

(a) (b)

Fig. 3. (a) Pyranometer Apogee MP-200, (c) Measurements with multimeter fluke 115.

2.5 Data Collection

For the measurements we selected an urban bus route through the city of Cuenca. Specifically the route Trigales - San Joaquín. This route presents several characteristics that allow to typify shading obstacles that directly influence the solar panel. In detail the historical center of the city (narrow and dark streets) and the modern area with optimal conditions for the use of solar energy (wide avenues and clear in height). View Fig. 4.

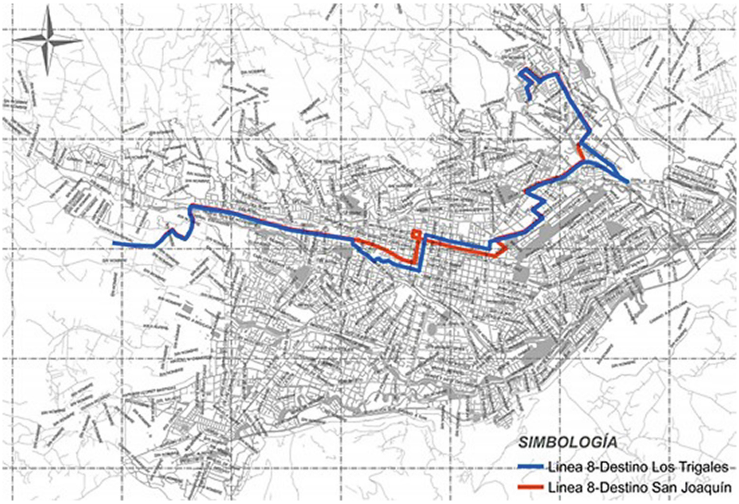

Fig. 4. Proposed data collection path Trigales - San Joaquín. Source: GAD Cuenca 2016

The data collection process took place over the course of one week, from July 5th to July 11th, 2021. Once the system has been calibrated, it is implanted in a mobile unit to perform the routes established previously. The assembly of the system in the mobile unit can be seen below (See Fig. 5).

With the system set up, the data collection was carried out, the data were collected during a schedule from 8:00 to 16:00. During this time, the system was able to run the established route a total of 4 times. The system stores irradiation data every second, thus presenting a very large database.

(a) (b)

Fig. 5. (a) Vehicle mounted solar panels, (b) Prototype measurement system developed

3 Result and Discussions

The data obtained in the measurements were extracted and plotted for their respective analysis, the graphs presented in this section show the radiation in w/m^2 with respect to the hours of the day. In general, the graphs are presented with the highest and lowest incidence of the study days, all measurements and graphs are available at: https://www.dropbox.com/s/r3x6ffg36tsxgt7/DATOS%20DE%20IRRADIACION.xlsx?dl=0

So that they can be used and analyzed in further research.

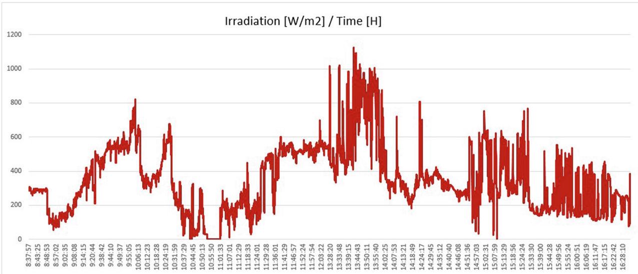

Fig. 6. Radiation sunny day

3.1 Database Analysis over Time

The Fig. 6 shows the radiation/time graph obtained for July 6, 2021, from which the following general criteria can be obtained:

- In the morning hours there is a radiation of 300 to 600 W/m^2 between 8am and 9:50am.
- First radiation peaks occur between 10:04am and 10:25am with an approximate of 700 to 800 W/m^2.
- The highest radiation levels occur during the middle of the day from 12pm to 2pm with peaks of more than 1000 W W/m^2.
- Radiation remained at values of 600 W/m^2 from 2:40pm to 4:00pm and then began to decrease progressively.
- Radiation decreased to levels of up to 200 W/m^2 in the afternoon hours 16:23.

The values obtained in Fig. 6 were obtained in a climate with normal solar radiation conditions. Radiation increases in the morning until midday, then the graph show decreasing values as time progresses in the evening hours. The decreasing values of radiation in Fig. 6 represent also obstacles that cause shadows on the path taken. This analysis is presented in more detail in the next section.

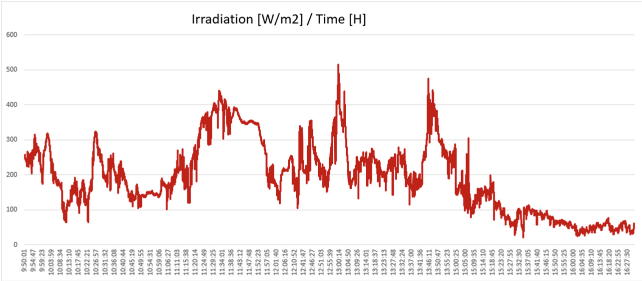

Fig. 7. Radiation partially sunny day

Figure 7 shows the data obtained on July 9, 2021, the data were taken on a day with partly cloudy weather conditions, by analyzing the figure you can extract the highest and lowest peaks of radiation depending on the time in which the values are shown:

- In the first hours of the path from 9:40 to 10.29 there are radiation peaks of 300 W/m^2.
- In the hours from 11:20 to 12:00 p.m. radiation values of 350 W/m^2 with peaks of 400 W/m^2.
- In the critical hours of the day, from 12:00 to 14:00 pm the radiation is maintained at approximately 300 W/m^2 with peaks of 500W/m^2 at 13:00 pm.
- After 14:00 there is a considerable decrease in radiation reaching levels below 100 W/m^2.

As it can be seen, these data present a radiation with median low values with respect to other days, this is mainly due to the type of weather that was had on the day of the measurements. Although the values present low radiation peaks, they still present radiation levels that can be exploited.

Finally, we present an analysis of a completely cloudy day in which the radiation does not present a considerable intensity. Figure 8 shows the radiation/time graph for July 10, 2021.

According to the radiation data obtained, the following general criteria can be obtained:

- Radiation in the morning hours, 8:50 am to 10:00 am, shows radiation data ranging from 400 to 600 W/m^2.
- Due to the climatic conditions the measured radiation has a very high decrease from 10:00 am to 15:20 pm with radiation values varying between 200 and 300 W/m^2.
- There is a slight increase in radiation from 15:30 with values of up to 600 W/m^2.

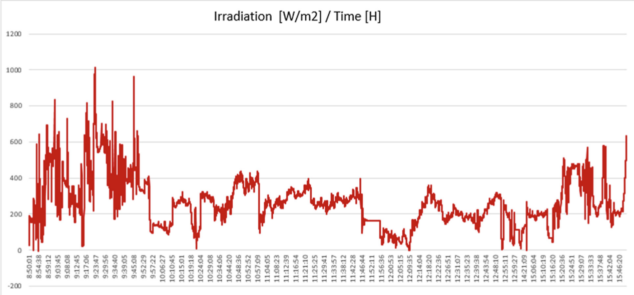

Fig. 8. Radiation cloudy day

As could be seen in unfavorable weather conditions the radiation presents very low levels of radiation, however there is still a margin of use for the photovoltaic systems.

3.2 Analysis of the Database with Respect to Urban Structure

With the implementation of GPS systems to measure position (latitude and longitude) in real time, the irradiation zones explained below Fig. 9 were obtained. The measurements were carried out during the seven days mentioned above in different weather conditions:

– Propitious conditions (Sunny)
– Prevailing conditions (Partially sunny)
– Adverse conditions (Cloudy)

In the information about the trajectories, the presence of obstacles (shadow) can be seen, which causes the performance of the solar panel to be affected. Places where the roads are wide generate as expected total incidence of solar radiation.

– Ordóñez Lasso Avenue: has a wide section with buildings away from the avenue, this allows better collection of solar radiation to the photovoltaic panels Fig. 10.
– Gil Ramírez Dávalos Avenue: it has a 4-lane road with obstacles that are not so repetitive but are present along the route, such as decorative trees placed in the middle of the road, which produce shadows and interfere with solar radiation Fig. 10.
– Pío Bravo Street: presents a narrow road with a variety of obstacles that directly generate shadows and solar radiation collection losses vary with respect to the number of existing houses and the angle of solar incidence Fig. 11.
– Sangurima Street: presents the entrance to the historical center of the city of Cuenca. The geo-referential analysis shows how the performance of the solar panels decreases and varies due to the presence of obstacles such as the buildings constructed in the center of the city Fig. 11.


(a)


(b)


(c)


(d)


(e)

Fig. 9. (a) Ordóñez Lasso Avenue (b) Gil Ramírez Dávalos Avenue (c) Pío Bravo Street (d) Sangurima Street (e) Americas Avenue.

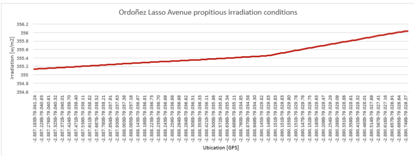

(a)

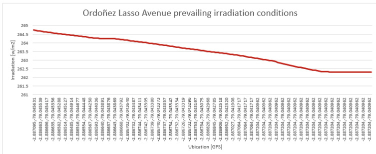

(b)

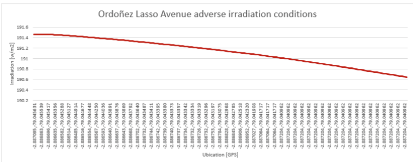

(c)

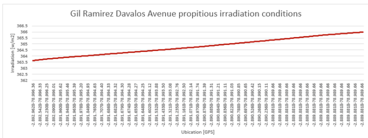

(d)

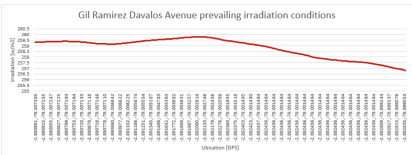

(e)

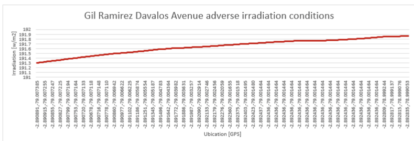

(f)

Fig. 10. Ordóñez Lasso Avenue: (a) Propitious conditions (b) Prevailing conditions (c) Adverse conditions. Gil Ramírez Dávalos Avenue: (d) Propitious conditions (e) Prevailing conditions (f) Adverse conditions.

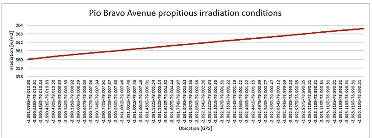

(a)

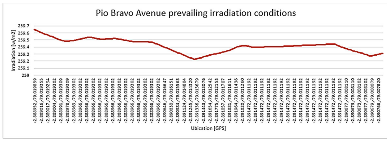

(b)

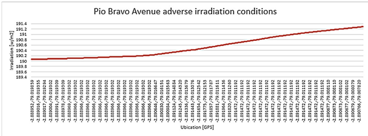

(c)

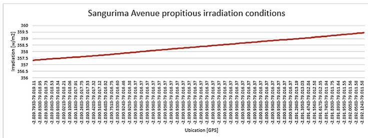

(d)

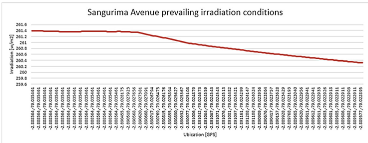

(e)

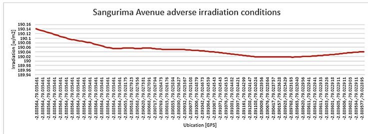

(f)

Fig. 11. Pío Bravo Street: (a) Propitious conditions (b) Prevailing conditions (c) Adverse conditions.Sangurima Street: (d) Propitious conditions (e) Prevailing conditions (f) Adverse conditions.

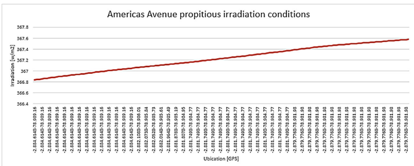

(a)

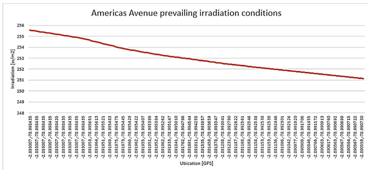

(b)

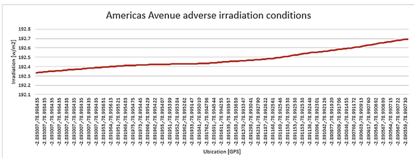

(c)

Fig. 12. Americas avenue: (a) Propitious conditions (b) Prevailing conditions (c) Adverse conditions.

– Americas Avenue: it presents an extended road, avoiding the presence of shadows obstacles, allowing an optimal generation. It is defined as an optimal avenue to produce clean energy in motion Fig. 12.

4 Conclusions

In this article a prototype for portable and geo-referenced solar radiation measurement was developed. This allowed to obtain solar radiation measurements and relate them to trajectories and the environment in a vehicle. This is a different approach to the usual approach to solar generation potential with static panels and on buildings.

The results obtained in Sect. 3.1 show that radiation has a high dependence on weather conditions such as a cloudy sky and despite being in hours with a direct angle of solar incidence (12:00 to 14:00 h) could decrease the values of captured radiation.

One of the most relevant data in this research is the plots of radiation versus location in the trajectory of a vehicle (streets and avenues) Sect. 3.2. This shows the incidence of obstacles such as trees and hight buildings in the shadows that affect the solar panels. However, in the worst conditions with shadows and cloudy weather it is evident that we can obtain useful radiation values for power generation. The applications for this generated energy could be to contribute to the charging of batteries in electric vehicles or the operation of auxiliary systems among others.

In Sect. 3 we attach a link to the database obtained in this case study so that it can be used in other investigations.

References

1. Aashoor, F., Robinson, F.: A variable step size perturb and observe algorithm for photovoltaic maximum power point tracking. In: 2012 47th International Universities Power Engineering Conference (UPEC), pp. 1–6. IEEE (2012)
2. Alsema, E., de Wild-Scholten, M., Fthenakis, V.: Environmental impacts of PV electricity generation-a critical comparison of energy supply options. In: 21st European Photovoltaic Solar Energy Conference, pp. 3201–3207 (2006)
3. Ansari, S., Ayob, A., Lipu, M.S.H., Saad, M.H.M., Hussain, A.: A review of monitoring technologies for solar PV systems using data processing modules and transmission protocols: progress, challenges and prospects. Sustainability **13**(15), 8120 (2021)
4. Arévalo Molina, J.P., Ortiz Jiménez, R.D., Gama, E.N., Ramos, O.L., Duque, J.: Diseño e implementación de un prototipo de vehículo solar con almacenamiento de energía. Revista científica **1**(18), 160–166 (2013)
5. Badamasi, Y.A.: The working principle of an arduino. In: 2014 11th International Conference on Electronics, Computer and Computation (ICECCO), pp. 1–4. IEEE (2014)
6. Bedir, A., Ozpineci, B., Christian, J.E.: The impact of plug-in hybrid electric vehicle interaction with energy storage and solar panels on the grid for a zero energy house. In: IEEE PES T&D 2010, pp. 1–6. IEEE (2010)

7. Blanc, I., Beloin-Saint-Pierre, D., Payet, J., Jacquin, P., Adra, N., Mayer, D.: Espace-PV: key sensitive parameters for environmental impacts of grid-connected PV systems with LCA. In: 23rd European Photovoltaic Energy Conference (2008)
8. Carreño Aguillon, E.D.P., Vacca Melo, E.A., Lugo Ariza, I.: Diseño y fabricación de un vehículo autónomo impulsado por energía solar. Tecnura **16**(32), 92–107 (2012)
9. CCEEA: Electromagnetic spectrum and the pickup of the photo voltaic module. Electrical Training and Alternative Energies Center (2021)
10. Chow, L.S., Abiera, M.: Optimization of solar panel with solar tracking and data logging. In: 2013 IEEE Student Conference on Research and Developement, pp. 15–19. IEEE (2013)
11. Cortez, O.O.F., Rosa, G.A.: Internet de las cosas: aplicación en monitoreo de un sistema de generación fotovoltaico. Entorno **1**(61), 40–46 (2016)
12. Dincer, I.: Renewable energy and sustainable development: a crucial review. Renew. Sustain. Energy Rev. **4**(2), 157–175 (2000)
13. Gottschalg, R., Infield, D., Kearney, M.: Experimental study of variations of the solar spectrum of relevance to thin film solar cells. Sol. Energy Mater. Sol. Cells **79**(4), 527–537 (2003)
14. Granda-Gutiérrez, E., Orta, O., Díaz-Guillén, J., Jimenez, M., Osorio, M., González, M.: Modelado y simulación de celdas y paneles solares. In: Congreso Internacional de Ingeniería Electrónica, vol. 35, pp. 17–22 (2013)
15. Grzeczka, G., Klebba, M.: Automated calibration system for digital multimeters not equipped with a communication interface. Sensors **20**(13), 3650 (2020)
16. Jumaat, S.A., Othman, M.H.: Solar energy measurement using arduino. In: MATEC Web of Conferences, vol. 150, p. 01007. EDP Sciences (2018)
17. Kannan, R., Leong, K., Osman, R., Ho, H., Tso, C.: Life cycle assessment study of solar PV systems: an example of a 2.7 kWp distributed solar PV system in Singapore. Sol. Energy **80**(5), 555–563 (2006)
18. Khalid, F., Dincer, I., Rosen, M.A.: Analysis and assessment of an integrated hydrogen energy system. Int. J. Hydrog. Energy **41**(19), 7960–7967 (2016)
19. Lee, W., Choi, D., Sunwoo, M.: Modelling and simulation of vehicle electric power system. J. Power Sources **109**(1), 58–66 (2002)
20. Marique, A.F., Reiter, S.: A simplified framework to assess the feasibility of zero-energy at the neighbourhood/community scale. Energy Build. **82**, 114–122 (2014)
21. Mendoza, E.N.A., Suarez, W.F.B.: Prototipo para la orientación automática de paneles solares. Publicaciones e Investigación **11**(1), 103–111 (2017)
22. Mueller, S., Frankl, P., Sadamori, K.: Next generation wind and solar power from cost to value. International Energy Agency: Paris, France (2016)
23. Oh, M., Kim, S.M., Park, H.D.: Estimation of photovoltaic potential of solar bus in an urban area: case study in Gwanak, Seoul, Korea. Renew. Energy **160**, 1335–1348 (2020)
24. Olano, X., Sallaberry, F., de Jalón, A.G., Gastón, M.: The influence of sky conditions on the standardized calibration of pyranometers and on the measurement of global solar irradiation. Sol. Energy **121**, 116–122 (2015)
25. Pacca, S., Sivaraman, D., Keoleian, G.A.: Parameters affecting the life cycle performance of PV technologies and systems. Energy Policy **35**(6), 3316–3326 (2007)
26. Peláez-Samaniego, M., Garcia-Perez, M., Cortez, L., Oscullo, J., Olmedo, G.: Energy sector in Ecuador: current status. Energy Policy **35**(8), 4177–4189 (2007)
27. Pierantonelli, M., Medina, J.C., Quintilla, T.: Generación distribuida fotovoltaica asociada a vehículos eléctricos. Avances en Energías Renovables y Medio Ambiente **22** (2018)

28. Poponi, D., et al.: Energy technology perspectives 2016: towards sustainable urban energy systems. International Energy Agency (2016)
29. Puentes, E.P., Medina, A.L., Sánchez, F.A.: Diseño de instrumentación para el monitoreo de instalaciones solares fotovoltaicas. Ingeniería y Región **1**(9), 115–124 (2012)
30. Reinoso, L., Ortega, J.: Incremento de la autonomía de un vehículo eléctrico dayang chok-s mediante paneles solares. Revista Digital Novasinergia **3**(2), 40–46 (2020)
31. Rohkamper, H., Ritschel, W.: Energy optimization for electric vehicles using dynamic programming. Res. Educ. Mechatronics REM 2017 **1**(80), 40–46 (2017)
32. Romero, F., et al.: Desarrollo de un sistema de monitoreo de radiación solar basado en un espectrómetro de amplio espectro. Revista Investigación & Desarrollo **1**(11) (2011)
33. Roper, L.D.: World photovoltaic energy. World Photovoltaic Energy (2011)
34. Sasikumar, G., Sivasangari, A.: Design and development of solar charging system for electric vehicles: an initiative to achieve green campus. Nat. Environ. Pollut. Technol. **20**(2), 801–804 (2021)
35. Sepúlveda, S.: Radiación solar: factor clave para el diseño de sistemas fotovoltaicos. Mundo FESC **4**(8), 60–65 (2014)
36. Taşçıoğlu, A., Taşkın, O., Vardar, A.: A power case study for monocrystalline and polycrystalline solar panels in bursa City, Turkey. Int. J. Photoenergy **2016** (2016)
37. Teshima, Y., Hirakoso, N., Shigematsu, Y., Hirama, Y., Kawabata, H.: Optimal driving strategy for solar electric vehicle. IEEJ J. Ind. Appl. **10**(3), 303–309 (2021)
38. Tingting, K., Yan, L., Lei, Z., Yan, H.: Development of multi-channel automatic digital multimeter calibration device. In: 2019 14th IEEE International Conference on Electronic Measurement & Instruments (ICEMI), pp. 108–113. IEEE (2019)
39. Vargas, J., Medina, J., Pozo, M., Ávila, E., Pozo, N., Salazar, G.: Análisis del uso de micro convertidores dc/dc enfocados en la extracción máxima de energía en una granja fotovoltaica. Enfoque UTE **10**(1), 205–217 (2019)
40. Vera-Dávila, A.G., Delgado-Ariza, J.C., Sepúlveda-Mora, S.B.: Validación del modelo matemático de un panel solar empleando la herramienta simulink de matlab. Revista de Investigación, Desarrollo e Innovación **8**(2), 343–356 (2018)

Evaluation of Capacity Curves in Generators, Transformers, and Transmission Lines for the Analysis of Permanent Stability in Electric Power Systems

Freddy Tamayo(✉), Ricardo Rosero, Mauricio Rosero, Christian Llumiquinga, and Cristina Chamorro

Instituto Superior Tecnológico Sucre, Campus Sur Av. Teodoro Gómez de La Torre S14 - 72 y Joaquín Gutiérrez, Quito, Ecuador

{ftamayo,rrosero,mrosero,cllumiquinga, cchamorro}@tecnologicosucre.edu.ec

Abstract. The purpose of the research is to present an application for the analysis of electrical power systems (EPS), by comparing their capacity curves. Generators, transformers, and transmission lines have their operating limits based on geometric locations that are defined according to the mathematical models that determine their mode of operation in each case. The advantage of using the proposed tool is that it has a direct visual information that indicates whether the equipment is working normally or is overloaded. The application was made for the analysis of operation data from any EPS with the help of Matlab and DIgSILENT Powefactory software.

Because EPSs are dynamic systems in which multiple operations are performed such as: connection and disconnection of loads, integration of generators in case of increased demand, disconnection of lines, transformers, or generators when some type of disturbance appears, all these operations presented by the EPS have to be studied in a timely manner by an analysis of permanent stability or safety of operation of the system for its correct operation. The proposed tool, for its evaluation, was carried out in the IEEE 39-bus system, carrying out an analysis in a normal state and in an overload of the elements of the system state, by means of the variation of the input or configuration parameters of EPS.

Keywords: Matlab · DIgSILENT · Capacity curve · Synchronous generator · Transmission lines · Stability

1 Introduction

Capacity curves have been used for the design and operation of synchronous generators of electricity generating plants [1]. The capacity curves of the transmission lines are based on the St Clair curves published in 1953, which have been of great importance for the planning of transmission systems in electrical power systems [2]. The life of transformers

© The Author(s), under exclusive license to Springer Nature Switzerland AG 2023
M. Zambrano Vizuete et al. (Eds.): RITAM 2021, LNNS 512, pp. 195–210, 2023.
https://doi.org/10.1007/978-3-031-11295-9_14

depends to a high degree on the duration of some events such as: overvoltage, short circuits in the systems to which they are connected, in such a way that their capacity curve depends to a great extent on the active power values of the load and its power factor. In this aspect, the capacity curve of a transformer indicates the limits of active and reactive power in which it can work [3].

The continuous growth of electrical power systems (EPS), with changes in their electrical variables and the evolution of new technologies has caused a new way of approaching the study and analysis of the operation of EPS equipment [1]. EPSs continuously suffer a great variety of serious or minor disturbances, which can appear as small disturbances [2], (load changes) or more serious as a short circuit in a line or output of a large power generator, to which the system must be able to adapt and function favorably. When a disturbance occurs there are two possible subsequent resulting states; that the system maintains its stability or that the system enters a process of instability that causes a ripple effect after the disconnection of some elements and finally a possible voltage collapse [3].

Determination of electrical energy transfer limits is a fundamental task to guarantee the safety of electrical energy systems [4], where these systems are highly non-linear and are constantly exposed to load variations. In transmission lines from the electrical point of view, the maximum energy transfer by the conductors is obtained by estimating the operating limits among which the thermal limit, the voltage drop limit and the stability margin limit are considered [5]. A similar situation occurs in power transformers, in which electrical, thermal and mechanical failures can occur, it is considered that 61% of the failures are associated with external conditions, that is, with the system to which it is connected, a 7% due to overcurrent, 4% due to bus bar system failures and 13% due to undetected factors [6].

In synchronous generators, in addition to the thermal type limits, there are mechanical limitations of the turbines and operational restrictions imposed by the power system. The restrictions of the electrical components consider the heating limits of the stator and rotor windings, while the mechanical type restrictions are imposed by the equipment that transforms the primary source of energy into mechanical energy. When a synchronous generator works in under-excitation condition, criteria of stability margins must be defined, this will allow delivering using low field currents the necessary power to the system [7].

Being a system in continuous operation, instabilities could appear in it due to disturbances of different origins, which could cause a blackout; Therefore, it is important to permanently analyze the capacity curves, to guarantee the optimal functioning of the equipment that makes EPS up [1]. Understanding these limits as the maximum possible power flow that can circulate through a particular point of the power system [8]. Maintaining stability in a system is of vital importance because a deficiency in this behavior makes the system inoperable [9], even representing economic losses due to energy not supplied at the load points. Aspects such as the impedance of transmission systems and transformers play an important role in the stability of a system.

The analysis of the stability of power systems is inevitably related to studies of voltage stability. Among the classic methods of analysis are simulation in the time domain, sensitivity analysis through Jacobian matrix, nodal analysis of eigenvalues, estimation of maximum operating values through PV and QV curves. In recent years, the use of voltage stability indices has been chosen with the implementation of PMUs (Phasor Measurement Unit), which provide real-time information that allows monitoring the status of the system continuously. Communications network applications such as WAMS networks [10] (wide area monitoring system) together with PMUs and a global positioning satellite link system (GPS) has made it possible to have control over the stability of an EPS by timely identification of oscillation modes. This allows to operate the system in real time from dynamic data [11].

In this research, a method was developed to monitor the status of the main equipment of an EPS such as: generators, transformers, and transmission lines when they work at the limit of their operating capacity in such a way as to forecast the continuity of system services from the data obtained.

Different equations have been developed that allow to obtain the graphs of the curves of the operating limits of each equipment that makes up an EPS and from this, the algorithms for entering the data in Matlab environment are defined, in which it will be graphed the capacity curves of generators, transformers and transmission lines. The IEEE 39-bus system has been selected as a case study [12]. To represent the scenarios in which the proposed problem will be analyzed, PowerFactory software is used, where the different power flows will be obtained, which will be exported to Matlab software for the graphical representation of each of the equipment of an EPS. The application allows to simulate contingency conditions in which the loss of a generator, a transformer or a transmission line has occurred.

2 Theoretical Framework

Generators, transmission lines and transformers have operating limits that must be observed to verify the permanent stability of a power system. Permanent stability is verified if the operating point of an element is within the allowed limits, despite having existed a contingency, whose transitory stage has been successfully overcome [13].

2.1 Transformers

The lifetime of a transformer is closely linked to its chargeability, based on the fact that its useful life can be deduced by studying the duration of its solid insulation [14]. A transformer that operates in very high load regimes with operating temperatures above 140 °C [15] is reduced the duration of its insulation at a much higher rate than a transformer that works in lower load. Estimating the constant state of power transformers due to the damage of their insulation is a decisive element to prevent risks associated with the stability and reliability of the transmission lines and also to maintain a quality electrical service [16].

The transformer capacity curve is modeled as a radius circle equal to the nominal apparent power of the transformer and its coordinate axes represent true power in x and reactive power in y. The resulting curve is indicated in Fig. 1. The locus that describes the apparent power in the PQ plane is given by the following expression:

$$S^2 = P^2 + Q^2 \tag{1}$$

$$P = Vx.Ix.cos\,\theta \tag{2}$$

$$Q = Vx.Ix.sin\,\theta \tag{3}$$

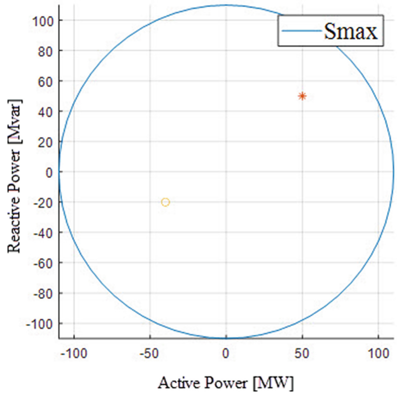

Fig. 1. Transformer capacity curve.

The curve represented in Fig. 1 indicates that the radius of the circumference constitutes the module of the apparent power and a coordinate point formed by the true (x-axis) and reactive (y-axis) power indicates the point of transformer operation. In this way it is possible to know if the equipment is working in terms of its nominal values or with a light, medium or high overload.

2.2 Synchronous Generator

The synchronous generator is an important part of a power system, as it provides the electrical power that is required by the loads [17]. These rotating machines have their limits defined by the reactive power curves of the generator provided by the manufacturers [18]. The way to model the capacity curve of synchronous generators is based on the phasor diagram [19] of the equivalent see Fig. 2 and 3. Salient pole generators use the two-axis theory to explain the behavior of the synchronous machine in generator mode. Using this theory, the operating limits of the generator can be graphically modeled [20].

The capacity curve of a salient pole generator is indicated in Fig. 4, where its safe operating area is delimited by the mechanical and electrical operating limits [21, 22].

The factors that intervene in the equations that allow to draw the synchronous generator curve and the model that describes the loci of each limit is indicated below:

Mechanical power: it values imposed by the turbine that moves the generator rotor. The minimum limit depends on the type of generator control unit, an acceptable value can be 15%.

$$Pm_{max} = S\ x\,fp \tag{4}$$

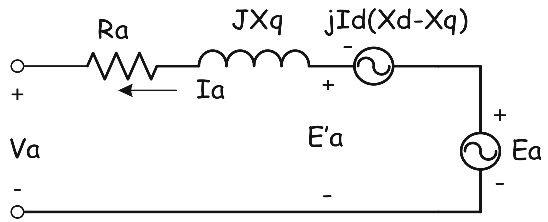

Fig. 2. Equivalent circuit of a salient-pole synchronous generator.

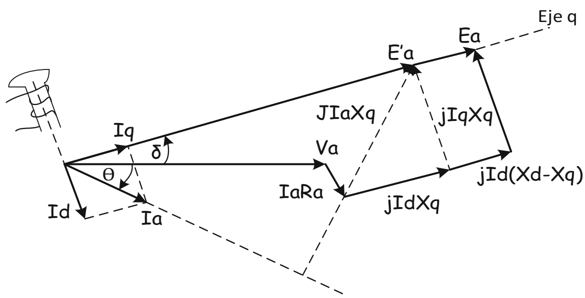

Fig. 3. Phasor diagram of a salient pole synchronous generator.

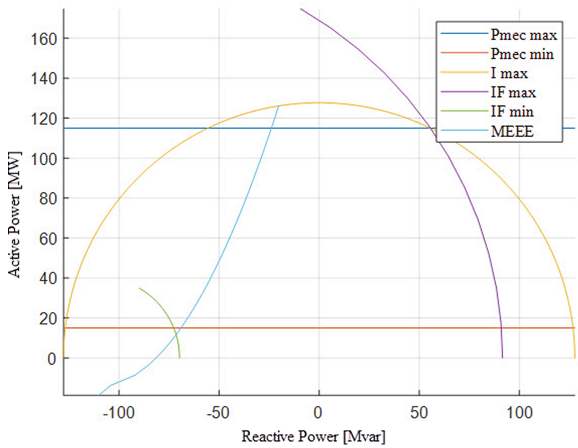

Fig. 4. Synchronous generators capacity curve.

$$Pm_{min} = 15\% \; x \; Pm_{max} \tag{5}$$

$$P_{ar} = \sqrt{S^2 - Q^2} \tag{6}$$

Armature current: it relates to the rated armature current of the generator.

Field current: it is defined as the maximum and minimum currents that can flow through the rotor winding. In the case of the maximum current, it is related to the nominal current of the winding. Regarding the minimum current, it has to do with the operation in reactive power consumption mode of the generator [23]. The equations that model the locus of these two limits are listed below.

$$P_{E_{\max}} = \frac{V_t \times E_{\max}}{X_d} \operatorname{sen}\delta + \frac{V_t^2}{2}\left(\frac{1}{X_q} - \frac{1}{X_d}\right) sen\, 2\delta \tag{7}$$

$$Q_{E_{\max}} = \frac{V_t \times E_{\max}}{X_d} \cos\delta + \frac{V_t^2}{2}\left(\frac{1}{X_q} - \frac{1}{X_d}\right)\cos 2\delta - \frac{V_t^2}{2}\left(\frac{1}{X_q} + \frac{1}{X_d}\right) \tag{8}$$

$$P_{E_{\min}} = \frac{V_t \times E_{\min}}{X_d} \operatorname{sen}\delta + \frac{V_t^2}{2}\left(\frac{1}{X_q} - \frac{1}{X_d}\right) sen\, 2\delta \tag{9}$$

$$Q_{E_{\min}} = \frac{V_t \times E_{\min}}{X_d} \cos\delta + \frac{V_t^2}{2}\left(\frac{1}{X_q} - \frac{1}{X_d}\right)\cos 2\delta - \frac{V_t^2}{2}\left(\frac{1}{X_q} + \frac{1}{X_d}\right) \tag{10}$$

Steady state stability margin: this limit refers to the minimum reactive power that a synchronous generator can absorb, a typical stability margin can range from 15% to 25% [24].

$$P_0 = P_1 - S \times fp \times \frac{MEEE}{100} \tag{11}$$

In the generator, the factors that define the safe operating zone are determined by the mechanical power, the armature current, the field current and the steady state stability margin. By means of the graph of these factors its stable state of operation is determined.

2.3 Transmission Lines

The useful life of a transmission line depends on the maximum permissible levels under which it operates. The chargeability of a line can be assessed from the ratio of true power flow versus reactive power (PQ) through itself or from a curve of the length of the line as a function of the true power referred to the line of SIL (Surge Impedance Loading) [25].

The operating limits of transmission lines are known as Saint Clair curves [12]. The chargeability of a transmission line indicates the power capacity that can flow through the line under acceptable operating conditions; and this is a function of the gauge and the length of the line [26]. The capacity limits on the Saint Clair curves are:

Thermal limit.

Voltage drop limit.

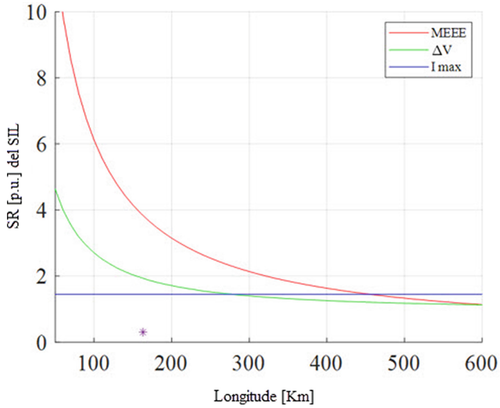

Fig. 5. Saint Clair curve

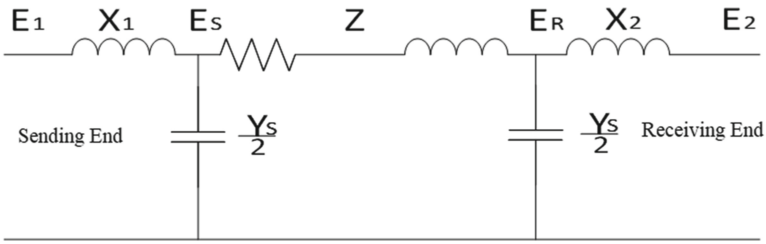

Fig. 6. Diagram of the proposed transmission line

Steady state stability margin limit.

The line model used to form the capacity curve is indicated in Fig. 5, which uses the pi model of a transmission line with concentrated parameters Fig. 6 [27].

The modeling of these curves is based on defining the loci of the sending and receiving powers at the ends of a line.

Power at the sending terminal:

$$SE = E_1 \times (cos\ \theta_1 + jsen\theta_1) \times I_1 \tag{12}$$

Power at the receiving terminal:

$$SR = E_2 \times I_2 \tag{13}$$

Characteristic impedance:

$$Z_0 = \sqrt{\frac{z}{y}} \tag{14}$$

True power at reception as a function of SIL:

$$PR_{SIL} = \frac{Re(SR)}{SIL} \tag{15}$$

In transmission lines, three limits can be considered to take into account: the thermal limit, voltage drop limit and stability limit. The graphs of these limits are determined by the coordinates in terms of SIL units and their length defines the point of operation of the line. The following graphs show three operating conditions, when there is a voltage drop limit, a thermal limit, and a stability limit.

3 Materials and Methods

3.1 Materials

Generators, transformers, and transmission lines have operating limits that must be observed to verify the permanent stability of a power system. Permanent stability is verified if the operating point of an element is within the limits despite having existed a contingency, whose transitory stage has been successfully overcome.

For the analysis of the permanent stability or operational safety of the EPS, the IEEE 39-bus system represented in Fig. 10 is used as a test model.

The system consists of 39 buses, 10 generators, 12 three-phase transformers and 46 transmission lines. This system has a base of 100 MVA. DIgSILENT PowerFactory software was used to obtain the power flows of the applied system, the generated data is exported to Matlab software in which, through programming, it forms ordered pair data for the graphical representation of the capacity curves of the system equipment. With these graphs it is possible to analyze whether the EPS equipment is working in a safe zone, or it is outside its normal operation.

The application development steps to obtain the capacity curves in the generators, transformers and transmission lines of the EPS are indicated in Fig. 7.

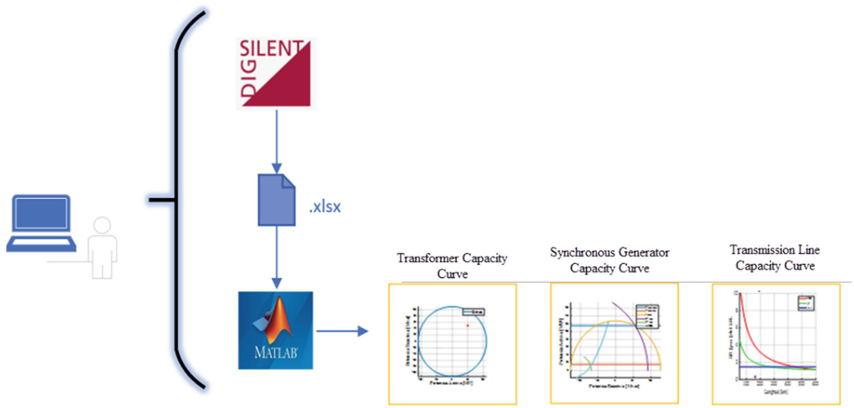

Fig. 7. Diagram of stages to obtain the capacity curves

3.2 Methods

Applied research aims to generate knowledge with direct application in the productive environment; this method helped to generate knowledge in the creation of the application for the graphs of capacity curves of the equipment of an EPS, allowing to go from the theoretical to the practical or applied; the tools used to develop this research are based on previous knowledge and previous experiences acquired in the classroom and that constitute the pillar of any investigation in which it is intended to develop an application that helps to understand a phenomenon.

In this article, it has also been tried to deepen the knowledge of the operational limits of the main components of the EPS with a descriptive degree of the phenomena that intervene and their possible causes, constituting the bases of an application of explanatory research.

Because the EPSs are composed of a great variety and quantity of generators, transformers and transmission lines which together contribute to the system working optimally, are continuously exposed to instabilities that must be controlled to avoid possible system collapses. In this context, the application allows verifying the operating status of the EPS equipment, in a graphical way with the interpretation of their capacity curves, it is established that the equipment is within the operating limits, thus making it possible to know in advance possible failures of generators, transformers or transmission lines.

For the case study, the IEEE 39-bus system was used, with the help of DIgSILENT PowerFactory software, it allowed to establish the EPS model and simulate power flows, short circuits, and other contingencies within the system. The data base of the power flows is exported to Matlab software, where by means of programming the capacity curves for all EPS equipment are graphically established as indicated in Fig. 8.

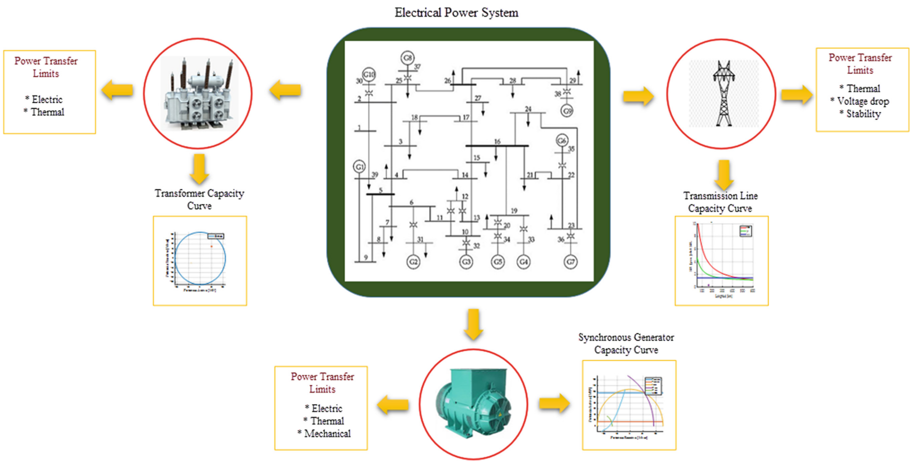

Fig. 8. Capacity curves of EPS elements

3.3 Test System

To test the developed tool, the IEEE 39-bus system known in the literature as New England is used [12]. This power system has all the features to serve as a testing rig; and so, it has been used over the years. From this system the results of the generators, transformers and transmission lines that could be generated from a contingency will be obtained. The one-line diagram of the selected test network is presented in Fig. 9 (Table 1).

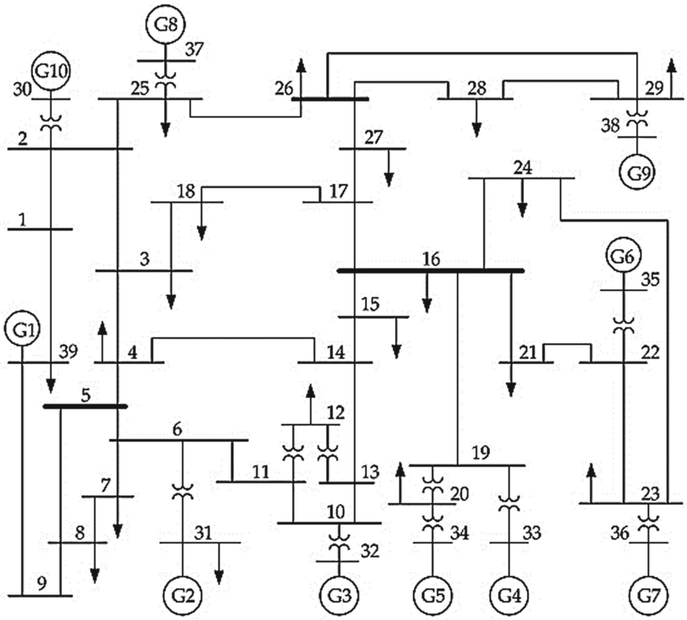

Fig. 9. IEEE39-bus New England test system

4 Results

Some generators, transformers and transmission lines have been chosen for the analysis, which have been disconnected assuming that they have suffered some type of contingency forcing them to leave the system. In the capacity curves of each element its operating condition is evidenced, the visible point on the graph (ordered pair) will be located within its normal operating zone or outside it, indicating an overload in the selected equipment. In this manner, the developed model can be scalable to any power system and any contingency n − 1, n − 2 or the disconnection of the equipment that is chosen, in order to establish its operating limits and strategies that prevent the elements of the EPS in the event of contingencies with a high probability of occurrence from remaining in unsafe areas of operation and shortly after resulting in a disconnection.

Table 1. IEEE 39-bus system general data

Loads				Generator			
Bus N°	Voltage	P [MW]	Q [Mvar]	P [MW]	Q [Mvar]	Type	N°
1	0.0000	0.0000	0.0000	0.0000	0.0000	PQ	
2	0.0000	0.0000	0.0000	0.0000	0.0000	PQ	
3	0.0000	322.00	2.4000	0.0000	0.0000	PQ	
4	0.0000	500.00	184.00	0.0000	0.0000	PQ	
5	0.0000	0.0000	0.0000	0.0000	0.0000	PQ	
6	0.0000	0.0000	0.0000	0.0000	0.0000	PQ	
7	0.0000	233.80	84.000	0.0000	0.0000	PQ	
8	0.0000	522.00	176.00	0.0000	0.0000	PQ	
9	0.0000	0.0000	0.0000	0.0000	0.0000	PQ	
10	0.0000	0.0000	0.0000	0.0000	0.0000	PQ	
11	0.0000	0.0000	0.0000	0.0000	0.0000	PQ	
12	0.0000	7.5000	88.000	0.0000	0.0000	PQ	
13	0.0000	0.0000	0.0000	0.0000	0.0000	PQ	
14	0.0000	0.0000	0.0000	0.0000	0.0000	PQ	
15	0.0000	320.00	153.00	0.0000	0.0000	PQ	
16	0.0000	329.00	32.300	0.0000	0.0000	PQ	
17	0.0000	0.0000	0.0000	0.0000	0.0000	PQ	
18	0.0000	158.00	30.000	0.0000	0.0000	PQ	
19	0.0000	0.0000	0.0000	0.0000	0.0000	PQ	
20	0.0000	628.00	103.00	0.0000	0.0000	PQ	
21	0.0000	274.00	115.00	0.0000	0.0000	PQ	
22	0.0000	0.0000	0.0000	0.0000	0.0000	PQ	
23	0.0000	247.50	84.600	0.0000	0.0000	PQ	
24	0.0000	308.60	−92.00	0.0000	0.0000	PQ	
25	0.0000	224.00	47.200	0.0000	0.0000	PQ	
26	0.0000	139.00	17.000	0.0000	0.0000	PQ	
27	0.0000	281.00	75.500	0.0000	0.0000	PQ	
28	0.0000	206.00	27.600	0.0000	0.0000	PQ	
29	0.0000	283.50	26.900	0.0000	0.0000	PQ	
30	1.0475	0.0000	0.0000	250.00	0.0000	PV	Gen10
31	0.9820	9.2000	4.6000	0.0000	0.0000	PV	Gen2

(*continued*)

Table 1. (*continued*)

Loads				Generator			
Bus N°	Voltage	P [MW]	Q [Mvar]	P [MW]	Q [Mvar]	Type	N°
32	0.9831	0.0000	0.0000	650.00	0.0000	PV	Gen3
33	0.9972	0.0000	0.0000	632.00	0.0000	PV	Gen4
34	1.0123	0.0000	0.0000	508.00	0.0000	PV	Gen5
35	1.0493	0.0000	0.0000	650.00	0.0000	PV	Gen6
36	1.0635	0.0000	0.0000	560.00	0.0000	PV	Gen7
37	1.0278	0.0000	0.0000	540.00	0.0000	PV	Gen8
38	1.0265	0.0000	0.0000	830.00	0.0000	PV	Gen9
39	1.0300	1104.0	250.00	1000.0	0.0000	PV	Gen1

Table 2. Executed contingencies, results, and analysis.

Contingency	Results			Analysis of results
G-03 out of order	G02 generator operating limits outside the safe zone. Dispatch greater than their nominal values	06-31 transformer overloaded in a 182,2%. Operating limits outside its capacity curve	05-06 transmission line within its thermal operating limit, line overloaded in a 101,3%	G02 generator overloaded by more than 150%. 06-031 transformer overload at almost at 200%. Line 5-6 suffers a slight overload is at its thermal limit
G-06 out of order	G08 generator operating limits outside the safe zone on the capacity curve. Generator with overload	06-31 transformer overloaded in a 117,4%. Operating limits outside its capacity curve	05-06 transmission line within its thermal operating limit, line overloaded in a 100,2%	In this contingency, the generator, transformer, and transmission line suffer slight overloads, which do not exceed 20%

(*continued*)

Table 2. (*continued*)

Contingency	Results			Analysis of results
04-14 line out of order	–	–	(05-06) transmission line with an overload ofl 103,9%, it has exceeded its thermal limit	In this contingency line 04-14 produces a slight overload on line 05-06
23-24 and 26-29 line out of order	G02 generator with overload 168%	06-31 transformer overload of 185,3%	05-06 line slight overload of 103,1%. It works in its zone of the thermal limit 21-22 line with overload of 159,1%. It has exceeded its thermal limit and works in the voltage drop limit zone	In this case, when two pieces of equipment leave the system, the lines that link generators that share their dispatches to common loads produce an effect of overloads in transformer generators and transmission lines

Table 2 and Fig. 10 show that when an output occurs from any of the equipment in the system; when verifying that it affects some other generator, the data show the status or condition of its operating limits. For example, when simulating the output of the G03 generator and checking the effect on the G02 generator, it is possible to observe its capacity curve shows it is very overloaded, of its coordinates in x and y it is verified that it has an overload of 182.2%, the same happens with the 06-31 transformer, which is overloaded by 200%.

Also, it follows that the consequences produced in a EPS are fundamentally a function of the type of contingency and equipment in which such event occurred. Thus, for example, it can be seen that from the curves obtained there is more repercussion when a generator or transformer leaves the grid than when a transmission line leaves (contingency $n - 1$).

The more equipment goes out simultaneously the system will be closer to collapse as it proves by producing a failure in two transmission lines simultaneously.

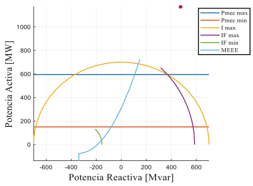

02 generator
03 generator out of order

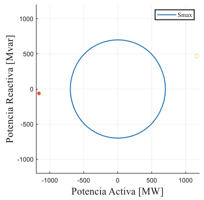

06-31 transformer
03 generator out of order

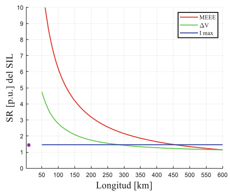

05-06 line
03 generator out of order

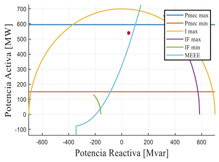

08 generator
06 generator out of order

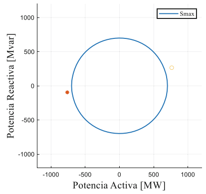

06-31 transformer
06 generator out of order

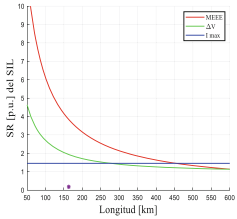

03-04 line
06 generator out of order

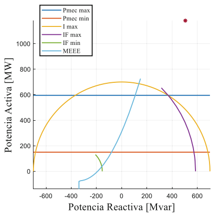

02 generator
23-24 and 26 line
out of order

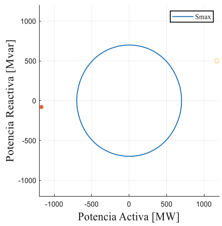

06-31 transformer
23-24 and 26-29 line
out of order

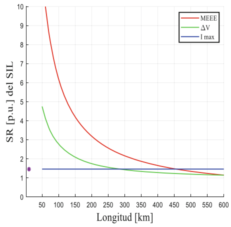

05-06 line
23-24 and 26-29 line
out of order

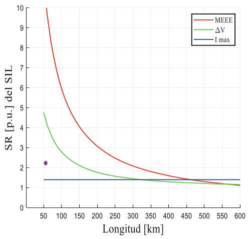

21-22 line
23-24 and 26-29 line
out of order

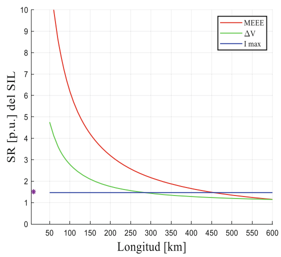

05-06 line
04-14 line out of order

Fig. 10. Curves obtained as a result of the executed contingencies.

5 Conclusions

The supervision of the power systems is a preventive action that can avoid major failures that can cause the loss of service in the users. New real-time measurement technologies where PMUs are used can be a viable alternative to feed the information of the tool developed by transforming it into an online analysis.

The mathematical models that allow evaluating whether an element of the SEP operates within its limits are the loci, which describe the maximum power values that a line, a transformer or a generator can cross.

The developed tool allows to carry out an analysis of the power flows through the graphs of the capacity curves and to know if they are working normally or under overload. Moreover, it allows to establish operating strategies that prevent the elements of the EPS in the event of contingencies with a high probability of occurrence from remaining in unsafe areas of operation and that in a short time they result in a disconnection.

Through applied and explanatory research, the tool was developed for the analysis of permanent stability or operational safety in electrical power systems, based on the loci that are defined according to the mathematical models that determine their mode of operation for generators, transformers, and transmission lines.

References

1. Kundur, P., et al.: Definition and classification of power system stability IEEE/CIGRE joint task force on stability terms and definitions. IEEE Trans. Power Syst. **19**(2), 1387–1400 (2004)
2. Ortiz, A.: Análisis de Estabilidad de Voltaje en Estado Estable del Sistema de Subtransmisión. Statew. Agric. L. Use Baseline **1**(Xc) (2015)
3. Zheng, L., Hu, W., Min, Y., Ma, J.: A novel method to monitor and predict voltage collapse: the critical transitions approach. IEEE Trans. Power Syst. **33**(2), 1184–1194 (2018). https://doi.org/10.1109/TPWRS.2017.2737465
4. Grisby, L.L.: Electrical Power Engineering Handbook: Power System Stability and Control, vol. 53, no. 9 (2012)
5. Lauria, D., Mazzanti, G., Quaia, S.: The loadability of overhead transmission lines - Part II: Analysis of double-circuits and overall comparison. IEEE Trans. Power Deliv. **29**(2), 518–524 (2014). https://doi.org/10.1109/TPWRD.2013.2280963
6. Rexhepi, V.: An analysis of power transformer outages and reliability monitoring. Energy Procedia **141**, 418–422 (2017). https://doi.org/10.1016/j.egypro.2017.11.053
7. Thakar, S., Vijay, A.S., Doolla, S.: Effect of P-Q limits on microgrid reconfiguration: a capability curve perspective. IEEE Trans. Sustain. Energy **11**(3), 2040–2048 (2020). https://doi.org/10.1109/TSTE.2019.2952043
8. Murty, P.S.R.: Power System Stability, 2nd edn. BS Publicatios, India (2017)
9. Evans, R.D., Wagner, C.F.: Studies of transmission stability. Trans. Am. Inst. Electr. Eng. **45**, 51–94 (1926). https://doi.org/10.1109/T-AIEE.1926.5061208
10. Fallis, A.: Analisis de estabilidad de tension considerando sistemas de monitoreo de area amplia y caracterısticas de carga mixtas. J. Chem. Inf. Model. **53**(9), 1689–1699 (2013)
11. Qiu, M., Gao, W., Chen, M., Niu, J.W., Zhang, L.: Energy efficient security algorithm for power grid wide area monitoring system. IEEE Trans. Smart Grid **2**(4), 715–723 (2011). https://doi.org/10.1109/TSG.2011.2160298

12. Athay, T., Podmore, R., Virmani, S.: A practical method for the direct analysis of transient stability. IEEE Trans. Power Appar. Syst. **PAS-98**(2), 573–584 (1979). https://doi.org/10.1109/TPAS.1979.319407
13. McCalley, J.D., et al.: A risk-based security index for determining operating limits in stability-limited electric power systems. IEEE Trans. Power Syst. **12**(3), 1210–1219 (1997). https://doi.org/10.1109/59.630463
14. Pérez, R., Torrez, H., Fernández, E., Fernández, S.: Sistema de Monitoreo en Tiempo Real para el Diagnóstico de Transformadores de Potencia en una Empresa de Energía. Lat. Am. Caribb. Conf. **2**, 11 (2012)
15. Rodríguez, J., Orejuela, V.: Modelo computacional para determinar el nivel óptimo de cargabilidad de los transformadores de potencia del sistema nacional interconectado. Ingenius (9), 36–41 (2013). https://doi.org/10.17163/ings.n9.2013.05
16. Lai, W., Li, W., Meng, H., Ding, R., Wang, Y., Fang, S.: Research on the relation between load coefficient and hot spot temperature of oil-immersed power transformer. In: 2019 IEEE International Conference on Power, Intelligent Computing and Systems ICPICS 2019, pp. 393–396 (2019). https://doi.org/10.1109/ICPICS47731.2019.8942454
17. Guru, B.S.: Hiziroglu, 242659502-Maquinas-Electricas-y-Transformadores-GURU-B_pdf.pdf. Oxford University Press, Oxford
18. Moghadam, D.E., Shiri, A., Sadr, S., Khaburi, D.A.: A practical method for calculation of over-excited region in the synchronous generator capability curves. In: 2014 IEEE 23rd International Symposium on Industrial Electronics (ISIE), pp. 727–732 (2014). https://doi.org/10.1109/ISIE.2014.6864702
19. Carmichael, I.F., Gove, R.M.: Geometric construction of the stability limits of synchronous machines. Proc. Inst. Electr. Eng. **113**(3), 506 (1966). https://doi.org/10.1049/piee.1966.0081
20. Adibi, M.M., Milanicz, D.P.: Reactive capability limitation of synchronous machines. Power Syst. Restor. Methodol. Implement. Strateg. **9**(1), 130–141 (2000). https://doi.org/10.1109/9780470545607.ch18
21. Aronés, M.F.B.: CURVA DE CAPABILIDAD D. Zocimo Ñaupari Huatuco. vol. 1 Lima, Pe, p. 14 (2011
22. Berizzi, A., Silvestri, A., Zaninelli, D., Marconato, R.: The capability of alternators in voltage collapse analysis. Electr. Mach. Power Syst. **25**(2), 169–180 (1997). https://doi.org/10.1080/07313569708955731
23. Maljković, Z., Gašparać, I.: Operating limits of underexcited synchronous generator. In: 4th International Conference on Power Engineering, Energy and Electrical Drives, pp. 1374–1377 (2013). https://doi.org/10.1109/PowerEng.2013.6635814
24. Da Costa, P., de Souza, A.N., Da Silva, P.S., do Cogo Castanho, J.E.: A visual tool for building synchronous generator capability curves. In: 2012 Proceedings of IEEE Southeastcon (2013). https://doi.org/10.1109/SECON.2013.6567431
25. Gutman, R., Marchenko, P.P., Dunlop, R.D.: Analytical development of loadability characteristics for EHV and UHV transmission lines. IEEE Trans. Power Appar. Syst. **PAS-98**(2), 606–617 (1979)
26. D.G. Camilo Narvaez Pérez. Ciindet 2008, p. 10
27. Jesús Játiva, N.N.: Estudio_de_las_caracteristicas_de_cargabilidad L-T (jornadas)(26).pdf. Jortnadas de Ingeniería Eléctrica y Electrónica, Quito_ecuador, p. 15 (1985)

Technology Trends

Changes of Land Use and Land Cover in Hotspots Within the Western Amazon: The Case of the Yasuní Biosphere Reserve

Jhenny Cayambe[1], Bolier Torres[2,3], Francisco Cabrera[4,5], Carlos G. H. Díaz-Ambrona[6], Theofilos Toulkeridis[7,8,9], and Marco Heredia-R[3,6,7](✉)

[1] Facultad de Ciencias Agropecuarias y Ambientales, Pontificia Universidad Católica del Ecuador Sede Ibarra (PUCESI), Imbabura 100112, Ecuador
[2] Departamento de Ciencias de la Vida, Universidad Estatal Amazónica, UEA, Puyo, Pastaza 160101, Ecuador
[3] Corporación para el Desarrollo Sostenible, Conservación y Cambio Climático (DSC), 150150 Tena, Ecuador
mherediar@uteq.edu.ec
[4] School of Surveying, Geodesy and Cartography Engineering, Universidad Politécnica de Madrid (UPM), 28040 Madrid, Spain
[5] Instituto Geográfico Militar, 170413 Quito, Ecuador
[6] AgSystems, Ceigram, itdUPM, Centro de Innovación en Tecnología para el Desarrollo, Universidad Politécnica de Madrid (UPM), 28040 Madrid, Spain
[7] Universidad de las Fuerzas Armadas ESPE, Sangolquí, Ecuador
[8] Universidad de Especialidades Turísticas, Quito, Ecuador
[9] Facultad de Ciencias Agropecuarias, Universidad Técnica Estatal de Quevedo (UTEQ), Av. Quito km. 1 1/2 vía a Santo Domingo de los Tsáchilas. Los Ríos, Quevedo 120550, Ecuador

Abstract. The predominant aim of the current research has been to quantify and map the pattern of changes in land use coverage (LULC), using a variety of tools of geographic information systems. The study area comprises the southern zone of the Diversity and Life Zone (DLZ), located in the Yasuní Biosphere Reserve, within the western Amazonian lowland. The processes for conducting the LULC in the DLZ included 1) data collection and analysis, 2) remote sensing data processing, 3) thematic land cover and 4) transformation from raster to vector. The analysis period was of about ten years (2009–2018), with the use of Landsat 7−8 satellite images. The classified classes were forest, traditional productive system, herbaceous vegetation, infrastructure and water. It was determined that the herbaceous vegetation increased by 0.81%, as well as the surface of traditional productive systems by some 0.73%, while the forest decreased by 0.93% . Therefore, we may state that the LUCL allows different local and international actors to contribute in agri-environmental and conservation decisions in order to minimize deforestation within the study area.

Keywords: GIS · LULC · Yasuni · Amazon · Ecuador

© The Author(s), under exclusive license to Springer Nature Switzerland AG 2023
M. Zambrano Vizuete et al. (Eds.): RITAM 2021, LNNS 512, pp. 213–223, 2023.
https://doi.org/10.1007/978-3-031-11295-9_15

1 Introduction

Data on land use and land cover (LULC) are fundamental inputs for countries to monitor how their soil and land use are changing over time [1]. It is also possible to identify the impacts of the increase in urban environments on different ecosystems [2], the monitoring of protected areas, and the expansion of deforested areas in tropical forests [3], as well as to monitor emissions reduced by deforestation and forest degradation (REDD +) [4] and also for modeling and valuing ecosystem services (ES) [5].

Remote sensing techniques have been recognized as a powerful means of obtaining information about the characteristics of the Earth's surface [6] at different spatial and temporal scales [7–9]. Since the early 1970s, scientists have used various types of remote sensing data, acquired by the Landsat series of satellites, in identifying LULC changes [10]. More recently, several researchers have focused on assessing the potential of satellite data on land use classification, monitoring land use, or quantifying and analyzing changes in land use [11].

The western Amazon is the biologically richest part of the Amazon Basin, being the home to migrant settlers and a wide variety of indigenous ethnic groups including some of the last groups in the world living in voluntary isolation [12]. In this territory, occur large oil and gas reserves, many of which are still unexploited and the growing demand for hydrocarbons worldwide is leading this region to unprecedented exploration and exploitation [13]. In addition, the dynamics of land occupation and livelihoods are related to the opening of roads, the scarce sustainability of traditional productive systems, poverty, high fertility rates, among other developments [14, 15]. Based on the aforementioned antecedents, the objective of this research has been to quantify and map the pattern of changes in land use coverage within a delicate study area.

2 Materials and Methods

2.1 Geographical Setting

The study has been performed in the southern zone of the Diversity and Life Zone (DLZ), which overlaps in the parish of Ines Arango (17,354 ha), of the Francisco de Orellana canton in the province of Orellana (Fig. 1). The geographical limits of the south of DLZ are to the north the Dayuma parish, to the east the limits of the Yasuní National Park (PNY) (980,000 ha) and to the southeast the Waorani Ancestral Territory (809,339 ha). The study area belongs to the Yasuní Biosphere Reserve (RBY), comprising an area of 2,700,000 ha, which were established as a biosphere reserve by the UNESCO Man and Biosphere program in 1989 [16]. In the RBY, 99.73% is represented by original natural vegetation. Its central conservation area is the PNY [17], which is a biodiversity hotspot [18], extending between the provinces of Orellana (50.51%), Pastaza (39.40%), Napo (8.64%) and Sucumbíos (1.45%).

2.2 Methodology

Within the conducted methodology, we included particularly all the processes applied in the LULC on the DLZ, being data collection and analysis, remote sensing data processing, thematic land cover and transformation from raster to vector (Fig. 3).

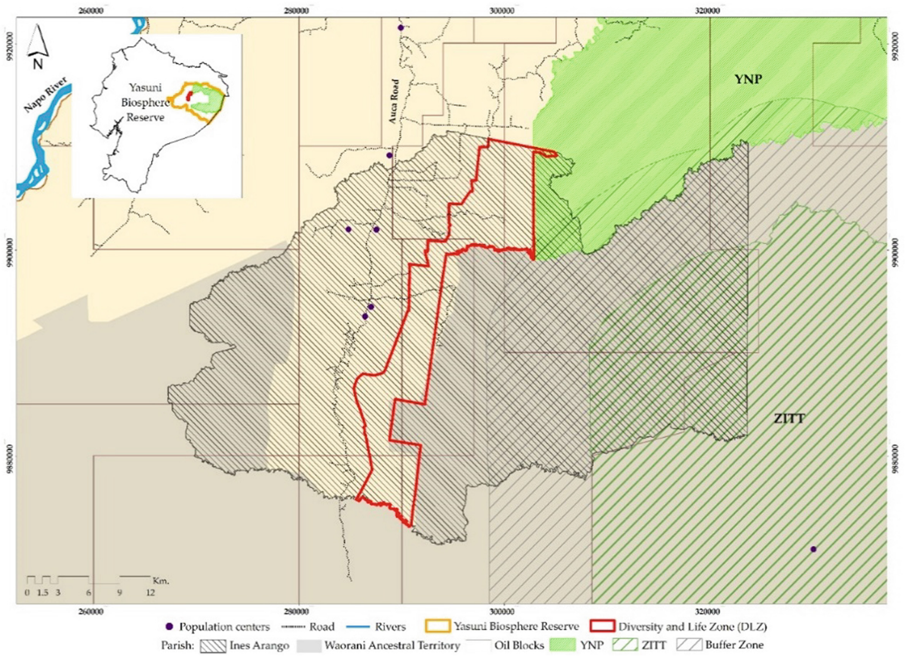

Fig. 1. Diversity and life zone in the yasuni biosphere reserve, ecuadorian amazon.

Data Collection and Analysis. Landsat satellite images were obtained, which have a high technological development [19], which were taken at an altitude of 705 km and an inclination of 98º, with a periodicity of 16 days. The LULC spatial dynamics was analyzed for a time interval of approximately 10 years (2009–2018) and have been downloaded from the site of the United States Geological Survey (USGS) based on the Earth Explorer (https://earthexplorer.usgs.gov/), with a spatial resolution of 30 m (Table 1). The selection of the images was performed while trying to avoid the presence of clouds as much as possible, considering that the Ecuadorian Amazon Region (EAR) is located in the intertropical convergence zone, which represents the highest cloud cover of the planet [20].

Table 1. Satellite images used in spatial analysis LU-LC

Mission	Sensor	Strip	Path/Row	Date
Landsat 7	ETM +	1, 2, 3, 4, 5, 7	9/60 y 61	05/26/2009
Landsat 8	OLI	2, 3, 4, 5, 6, 7	9/60 y 61	10/18/2018

Remote Sensing Data Processing. The images were standardized, below the same coordinate system (SIRGAS, UTM Zone 18 S/EPSG: 31993), and corrected, eliminating the presence of anomalies, thus allowing data to be available as closely as possible to an ideal acquisition [21]. The first step has been to conduct a radiometric correction, which allows the passage from digital counts to physical magnitudes, specifically with values of radiances (Wm-2 sr-1 µm-1), and then, through the use of radioactive transfer models, mitigate the atmospheric effect, allowing to obtain surface reflectivity values. Only for the Landsat 7 image, due to the banding it presents, a simple interpolation was applied, which replaces the empty pixels with their neighbors, calling this technique the Neighborhood Similar Pixel Interpolator (NSPI) [22].

Thematic Land Cover. Prior to the extraction of information per se, the thematic legend was structured in a scale of 1:100,000, with the classes forest, traditional production system, herbaceous vegetation, infrastructure and water. This has been similar to level II of the legend elaborated by public institutions such as the former Ministry of Agriculture, Livestock, Aquaculture and Fisheries (MAGAP) being currently the Ministry of Agriculture and Livestock (MAG), the Ministry of Environment, Water and Ecological Transition and the former Ecuadorian Space Institute (IEE) being the current Military Geographical Institute (IGM) [23, 24].

Subsequently, the selection of training samples was conducted using as secondary information, the map of use and coverage prepared by SIGTIERRAS (http://ide.sigtierras.gob.ec/geoportal/), on a scale of 1: 25,000. In addition, object-based segmentation was applied to the input images, prior to the application of the classification algorithm, and, on the other hand, spectral signatures were obtained (Fig. 2), mitigating to the maximum in this way the error that may occur when selecting the samples.

The training samples collected are spatially distributed throughout each of the images, and in terms of quantity. Hereby, it was considered between 10th and 100th pixels [25], with "a" being the number of stripes. Therefore, the number of pixels should fluctuate between at least 60 and 600 for each class. These samples were evaluated with the Jeffries Matusita index [26].

Once the key information had been collected, we proceeded with the supervised classification called neural networks, and through test samples (different from training samples), the precision of the results obtained was evaluated, through the parameters global precision (OA) and kappa index (K) [27, 28].

Raster to Vector Transformation. Finally, a smoothing filter was applied to the classified images in order to obtain greater homogenization and eliminate possible noise, and the product obtained was converted to vector format. For scales 1: 100,000, the minimum mappable unit is 5 ha. However, in order to avoid any loss of the information extracted, 1 ha has been taken as the minimum unit [29].

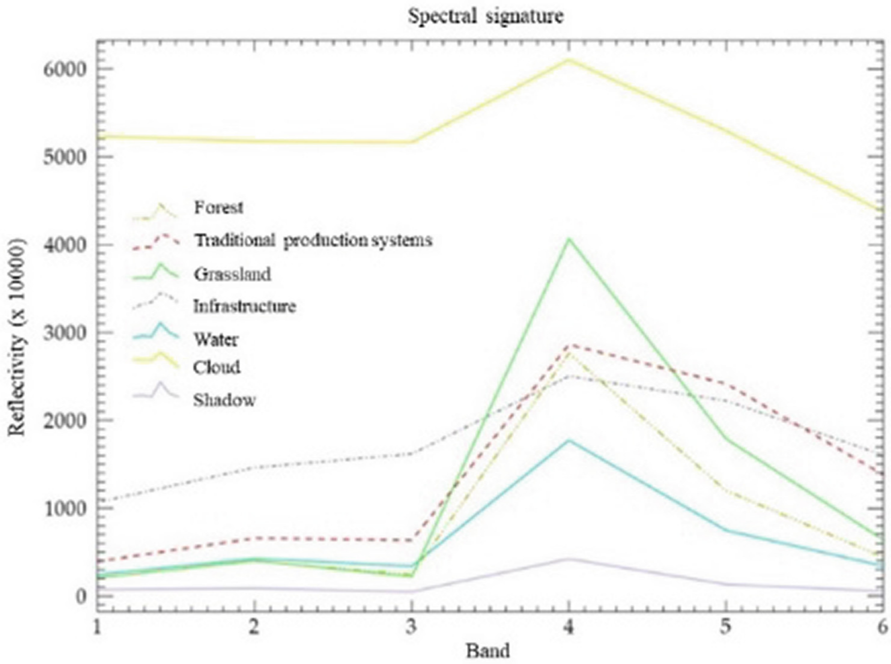

Fig. 2. Typical spectral signature resampled to landsat of the DLZ.

3 Results and Discussion

3.1 Classification Validation

The LULC classification levels for dates range from 98.0% to 99.6%, with Kappa concordance rates between 0.97 and 0.99. Accuracies by individual LULC class, that is, User Accuracy (UA) and Producer Accuracy (PA) are listed in Table 2. These Kappa values are satisfactory for the study area as they comply the minimum accuracy of 85%, as stipulated by the Anderson classification scheme [30]. These results provide a fundamental platform for subsequent analysis of LULC changes. The spectral separability index applied to the training samples, Jeffries Matusita, indicated distances above 1.8 between classes, which means that, when executing the classification algorithm, the confusion is minimal.

The precision values might be overestimated for the year 2018. However, a comparison was performed with the map of use and coverage of SIGTIERRAS, prepared in 2015, obtaining a degree of similarity of 88.7% (34,472.19 ha of 38,857.5 ha of DLZ). It should be noted that SIGTIERRAS operated with orthophotos and used the visual interpretation methodology.

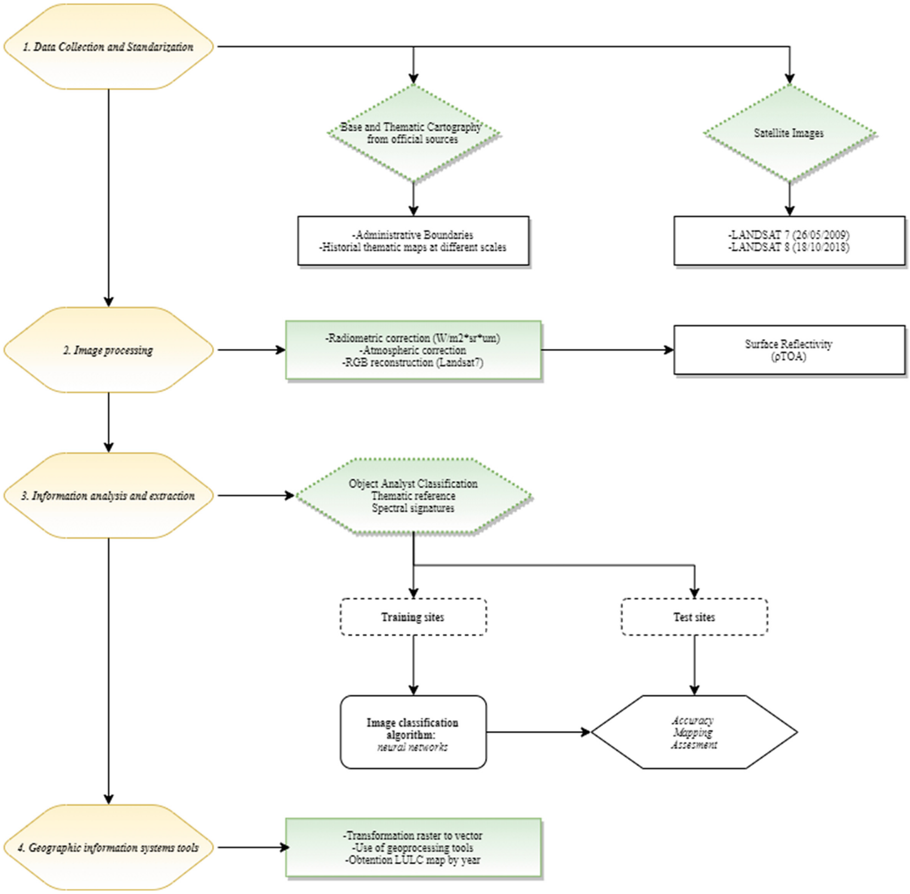

Fig. 3. Workflow for the LULC methodology, in the period 2009–2018

Table 2. Evaluation of the accuracy of the LULC classification in the DLZ.

Classes	2009		2018	
	PA (%)	UA (%)	PA (%)	UA (%)
Forest	100.00	97.94	100.00	100.00
Traditional productive system	97.40	99.47	100.00	97.78
Herbaceous vegetation	96.02	100.00	100.00	100.00
Infrastructure	96.06	92.42	96.91	100.00
Water	93.85	88.41	100.00	100.00
OA (%)	98.0		99.6	
K	0.97		0.99	

3.2 Changes in Land Use and Cover (LULC)

In Table 3 and Table 4, together with Fig. 4, the dynamics of change of LULC from 2009 to 2018 are synthesized, based on the five classes extracted from the South Zone of the FDV (Inés Arango Parish). Furthermore, the spatial representation of the LULC types from 2009 to 2018 is illustrated in Fig. 5. From a study surface (17,872.17 ha), the LULC pattern in 2009 was dominated by the forest, covering 92.66%, followed by herbaceous vegetation (4.89%), traditional production systems (1.20%), water (0.85%) and infrastructure (0.35%). While in 2018 the forest predominated with 91.57%, herbaceous vegetation (5.85%), traditional productive systems (2.06%), water (0.33%) and infrastructure (0.20%). The dynamics studied agree with the global report by FAO and UNEP in 2020, that agricultural expansion continues to be the main cause of deforestation and fragmentation of the forest and the associated loss of forest biodiversity [31]. Additionally, it should be considered that indigenous peoples inhabit the FDV (Waorani, Shuar and Kichwa) and their livelihoods are traditional productive systems and often unsustainable hunting, which is one of the main causes of biodiversity loss, just behind agriculture [32].

In addition, the results coincide with scenarios such as the Sumaco Biosphere Reserve, where there is evidence of increased deforestation in the Ecuadorian Amazon [3, 33]. However, the opposite is certain, with scenarios such as Santa Cruz Island where there is a spontaneous recovery of the plant cover [7].

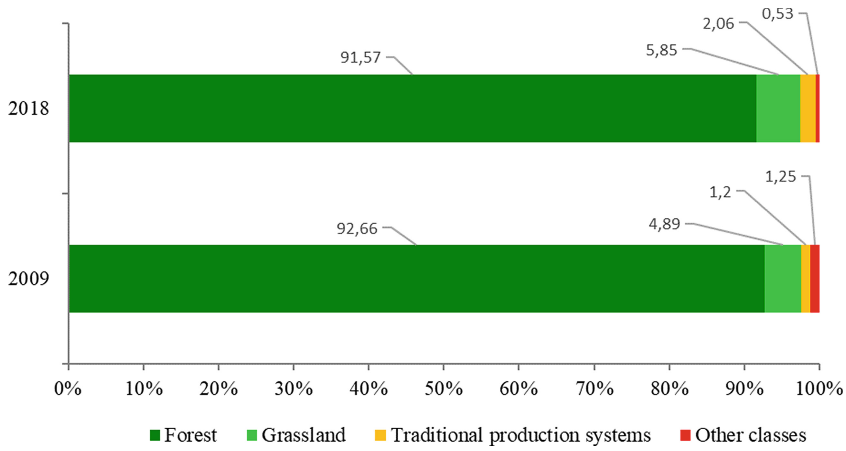

Fig. 4. Graph of the LULC change for 2009, as well as for 2018 at the south zone of the DLZ

The traditional production systems in the period 2009–2018 increased by 0.73% (Table 4). This might be attributed to the existing distance to the populated centers (between 60 and 125 km to the city of Coca). The traditional systems promote food sovereignty and security as they are high in biodiversity [34]. They is also a strategy to mitigate the effects of climate change [35] and to promote diversified diets in a scenario such as the DLZ, which is superimposed by oil block, where there is a precariousness of the livelihoods of migrant and indigenous colonist populations [36]. It has been determined that due to gas flaring activities within the oil industry, indigenous communities, population centers, schools and traditional production systems may be affected [13].

Table 3. LULC classification results for 2009 and 2018 images illustrating each class area and percentages by class at south zone of the DLZ

Classes	Area 2009		Area 2018	
	ha	%	ha	%
Forest	16560,08	92,66	16364,74	91,57
Traditional production system	214,83	1,20	368,25	2,06
Herbaceous vegetation	874,55	4,89	1045,51	5,85
Infrastructure	62,21	0,35	35,16	0,20
Water	151,23	0,85	58,51	0,33
Cloud	6,84	0,04	0,00	0,00
Cloud shadow	2,43	0,01	0,00	0,00
TOTAL	17872,17	100,00	17872,17	100,00

Along the same lines (Table 4), similar alterations in the landscape are evidenced, based on the LULC study in oil block No. 47, located in the province of Orellana (RAE). There it was identified that, over time, the areas of forest cover were displaced mainly by agricultural lands and urban areas, which fragmented the few segments of tropical forest present in the oil block [13].

Table 4. Results of the LULC classification for 2009 and 2018 images showing the area changed and percentage at South Zone of the DLZ

Classes	2009–2018 (Area)	
	ha	%
Forest	−195,35	−0,93
Traditional production system	153,43	0,73
Herbaceous vegetation	170,96	0,81
Infrastructure	−27,05	−0,13
Water	−92,72	−0,44

The geospatial dynamics between classes presents a variability between the years 2009 and 2018 of 8.56%, and of 11.27% throughout the entire studied period.

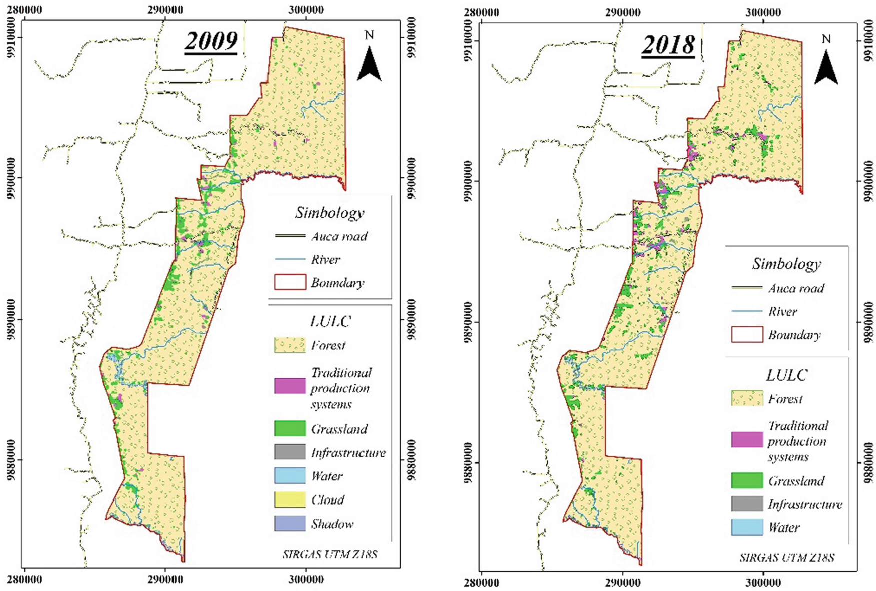

Fig. 5. LULC Maps for 2009 and 2018 in the south zone of the FDV

4 Conclusions

LULC maps play an important and primary role in planning, managing and monitoring programs at the local, regional and national levels. This type of information, on the one hand, provides a better understanding of land use aspects and, on the other hand, plays a fundamental role in shaping the policies and programs necessary for development planning in multi-ethnic and multi-ethnic areas. multicultural such as the western Amazon.

The analysis of satellite images with remote sensing methodologies allowed to quantify and map the pattern of change in LULC to the south of the Diversity and Life Zone of the Yasuní Biosphere Reserve, providing a baseline of understanding about the dynamics of LULC in colonist territories, migrants, indigenous populations, governmental and international actors.

References

1. Zhang, Y., Wang, Y., Wang, Y., Xi, H.: Investigating the impacts of Landuse-landcover (LULC) change in the pearl river delta region on water quality in the pearl river estuary and Hong Kong's coast. Remote Sens. **1**, 1055–1064 (2009). https://doi.org/10.3390/rs1041055
2. Shalaby, A., Tateishi, R.: Remote sensing and GIS for mapping and monitoring land cover and land-use changes in the Northwestern coastal zone of Egypt. Appl. Geogr. **27**(1), 28–41 (2007)
3. Torres, B., Andrade, L., Navarrete, A.T., Vasco, C., Robles, M.: Cambio de uso del suelo en paisajes agrícolas-forestales: análisis espacial en cinco comunidades Kichwas de la Región Amazónica Ecuatoriana. Revista Amazónica Ciencia y Tecnología **7**(2), 105–118 (2018)

4. Redowan, M., Phinn, S.R., Roelfsema, C.M., Aziz, A.A.: REDD+ project design study for quantifying activity data for historic forest degradation in a Bangladesh forest using landsat data. J. Appl. Remote Sens. **13**(4), 046518 (2019)
5. Szostak, M., Knapik, K., Wężyk, P., Likus-Cieślik, J., Pietrzykowski, M.: Fusing sentinel-2 imagery and ALS point clouds for defining LULC changes on reclaimed areas by afforestation. Sostenibilidad **11**, 1251 (2019). https://doi.org/10.3390/su11051251
6. Satyanarayana, B.; Thierry, B.; Seen, D.L.; Raman, A.V., Muthusankar, G.: Remote sensing in mangrove research-relationship between vegetation indices and dendrometric parameters: a case for Coringa, east coast of India. In: proceeding of the 22nd Asian Conference on Remote Sensing, Singapore, vol. 5, p. 9 (2001)
7. Barreto-Álvarez, D.E., Heredia-Rengifo, M.G., Padilla-Almeida, O., Toulkeridis, T.: Multi-temporal evaluation of the recent land use change in santa cruz island, galapagos, Ecuador. In: Rodriguez Morales, G., Fonseca C., E.R., Salgado, J.P., Pérez-Gosende, P., Orellana Cordero, M., Berrezueta, S. (eds.) TICEC 2020. CCIS, vol. 1307, pp. 519–534. Springer, Cham (2020). https://doi.org/10.1007/978-3-030-62833-8_38
8. Liang, D., Zuo, Y., Huang, L., Zhao, J., Teng, L., Yang, F.: Evaluation of the consistency of MODIS land cover product (MCD12Q1) based on Chinese 30 m globeland 30 datasets: A case study in Anhui Province China. ISPRS Int. J. Geo-Inf. **4**, 2519–2541 (2015)
9. Viera-Torres, M., Sinde-González, I., Gil-Docampo, M., Bravo-Yandún, V., Toulkeridis, T.: Generating the baseline in the early detection of bud rot and red ring disease in oil palms by geospatial technologies. Remote Sens. **12**(19), 3229 (2020)
10. Townshend, J.R.G., Gayler, J.R., Hardy, J.R., Jackson, M.J., Baker, J.R.: Preliminary analysis of LANDSAT-4 thematic mapper. Int. J. Remote Sens. **4**, 817–828 (1983)
11. Baumann, M., Ozdogan, M., Wolter, P.T., Krylov, A., Vladimirova, N., Radeloff, V.C.: Landsat remote sensing of forest windfall disturbance. Remote Sens. Environ. **143**, 171–179 (2014)
12. Rengifo, M.G.H., Díaz-Ambrona, C.G.H.: Comportamiento demográfico: dinámico-Probabilístico de los pueblos indígenas en aislamiento de la amazonía ecuatoriana. Revista Científica Axioma **20**, 25–34 (2019)
13. Facchinelli, F., et al.: Unburnable and unleakable carbon in western amazon: using VIIRS nightfire data to map gas flaring and policy compliance in the yasuní biosphere reserve. Sostenibilidad **12**, 58 (2020). https://doi.org/10.3390/su12010058
14. Heredia-R, M., Torres, B., Cayambe, J., Ramos, N., Luna, M., Diaz-Ambrona, C.G.H.: Sustainability assessment of smallholder agroforestry indigenous farming in the amazon: a case study of ecuadorian kichwas. Agronomía **10**, 1973 (2020). https://doi.org/10.3390/agronomy10121973
15. Lang, M.A.: ¿ Erradicar la pobreza o empobrecer las alternativas? Universidad Andina Simón Bolívar Ecuador. Ediciones Abya-Yala, Quito (2017)
16. UNESCO. Yasuni Biosphere Reserve: Biosphere reserves in Latin America and the Caribbean. https://en.unesco.org/biosphere/lac/yasuni. Accessed 15 June 2021
17. Taco, M.P.E.: Parque nacional yasuní. In: Jorgenson, J.P., Rodríguez, M.C. (eds.) Conservación y desarrollo sostenible del Parque Nacional Yasuní y su área de influencia, pp. 48–51. Ministerio del Ambiente/UNESCO/Wildlife Conservation Society, Quito, Ecuador (2001)
18. Finer, M., Vijay, V., Ponce, F., Jenkins, C.N., Kahn, T.R.: Ecuador's yasuni biosphere reserve: a brief modern history and conservation challenges. Environ. Res. Lett. **4**(3), 034005 (2009)
19. Sobrino, J., et al.: Teledetección, 467 pp. Servicio de Publicaciones Universidad de Valencia. Valencia, España (2000)
20. Vargas, G.: La tropicalidad y el análisis geográfico. Reflexiones, vol. 81. Costa Rica (2002)
21. Chuvieco, E.: Teledetección ambiental, 591 pp. Editorial Planeta. Barcelona, España (2010)
22. Saldarriaga, L.: Reconstrucción de base de datos Landsat7 ETM+ SLC-off para cuantificar, detectar cambios y cartografiar la cobertura vegetal del valle bajo del río Chira – Perú, durante

el período 2005–2014, 68 pp. TFM, Máster en Teledetección, Universidad de Valencia. Valencia, España (2014)

23. MAE. Línea base de deforestación del Ecuador Continental, 32 pp. Disponible en (2012). http://sociobosque.ambiente.gob.ec
24. IPCC. Guidelines for national greenhouse gas inventories - volume 4: agriculture, land use and forestry (AFOLU) (2006). http://www.ipcc-nggip.iges.or.jp
25. Jensen, J.: Introductory Digital Image Processing: A Remote Sensing Perspective, 316 pp. Editorial Prentice Hall. Michigan, Estados Unidos (1996)
26. Richards, J.A.: Remote Sensing Digital Image Analysis: An Introduction, p. 250. Springer-Verlag, New York (1993). https://doi.org/10.1007/978-3-642-30062-2
27. Congalton, G.R.: A comparison of sampling schemes used in generating error matrices for assessing the accuracy of maps generated from remotely sensed data. Photogramm. Eng. Rem. S. **54**, 593–600 (1988)
28. Hubert, L.: Kappa revisited. Psychol. Bull. **84**(2), 289 (1977)
29. Lencinas, J., Siebert, A.: Relevamiento de bosques con información satelital: resolución espacial y escala. Quebracho **17**, 101–105 (2009)
30. Anderson, J.R.: A Land Use and Land Cover Classification System for Use with Remote Sensor Data; Geological Survey Professional Paper 964. US Government Printing Office: Washington DC, USA (1976)
31. FAO y PNUMA. El estado de los bosques del mundo 2020. Los bosques, la biodiversidad y las personas. Roma (2020). https://doi.org/10.4060/ca8642es
32. Maxwell, S.L., Fuller, R.A., Brooks, T.M., Watson, J.E.: Biodiversity: the ravages of guns, nets and bulldozers. Nature News **536**(7615), 143 (2016)
33. Heredia-R, M., Villegas Rugel, G.M., Torres, B., Alemán, R., Barreto, D., Bravo, C., et al.: Towards the sustainability of traditional agroforestry systems kichwa: sumaco biosphere reserve case, amazonia. In: 1st International Electronic Conference on Agronomy, vol. 3, p. 17. (2021)
34. Torres, B., Vasco, C., Günter, S., Knoke, T.: Determinants of agricultural diversification in a hotspot area: evidence from colonist and indigenous communities in the Sumaco biosphere reserve ecuadorian amazon. Sustainability **10**(5), 1432 (2018)
35. Torres, B., Maza, O.J., Aguirre, P., Hinojosa, L., Günter, S.: The contribution of traditional agroforestry to climate change adaptation in the Ecuadorian Amazon: the chakra system. In: Filho, W.L. (ed.) Handbook of climate change adaptation, pp. 1973–1994. Springer, Heidelberg (2015). https://doi.org/10.1007/978-3-642-38670-1_102
36. Arsel, M., Pellegrini, L., Mena, C.: Maria's paradox: oil extraction and the misery of missing development alternatives in the Ecuadorian Amazon (2019)
37. Llerena-Montoya, S., Velastegui-Montoya, A., Zhirzhan-Azanza, B., et al.: Multitemporal analysis of land use and land cover within an oil block in the ecuadorian amazon. ISPRS Int. J. Geo Inf. **10**(3), 191 (2021)

Virtual Learning Object Based on a Virtual Laboratory for Microcontroller Practices

Fabricio Tipantocta(✉), Ricardo Rosero, Oscar Gómez, Flavio López, and Alex Merino

Instituto Superior Tecnológico Sucre, Campus Sur Av. Teodoro Gómez de la Torre S14 - 72 y Joaquín Gutiérrez, Quito, Ecuador
{ftipantocta,rrosero,ogomez,flopez, amerino}@tecnologicosucre.edu.ec

Abstract. The Virtual Learning Objects (OVA) have generated positive changes in teaching, availability and accessibility to knowledge, with the purpose of offering more flexible and multiple consultation mechanisms to consolidate a broader content of knowledge. The OVAs are digital tools that are used in virtual education, but they do not exist for specific subjects in the area of electronics, so it has been seen the need to create a virtual laboratory for teaching of microcontrollers, through a web service and the use of Google's Fire-base database.

The virtual laboratory will run on as a tool for teacher and as information and access mechanisms for the development of practices for students. Through the web application, the students will have access to the information of the practices and when connecting an Arduino card remotely, it will be linked to the database, thus achieving two-way communication, with the virtual laboratory the teacher will be able to demonstrate the operation of microcontroller practices, in real time. For the development of the virtual laboratory, a mixed methodology based on AODDEI (Analysis, Obtaining, Design, Development, Evaluation, Implementation) and component-based software engineering was used. As a result of the evidence of the operation of the virtual laboratory, a practice with 28 students connected at the same time was carried out.

Keywords: Virtual lab · Microcontrollers · Simulation · Firebase

1 Introduction

Virtual education introduced new ways of understanding and treating the educational process to face new challenges. The use of information and communication technologies in the educational field is increasingly broad and diverse, the roles in the teaching-learning process in virtual mode have evolved, the teacher is presented as pedagogical support and the student has reinforced learning autonomously [1].

Web-based learning environments have become very popular in higher education; One of the most important pedagogical resources is the virtual laboratory, which allows the student to easily access a wide variety of tools through an interactive interface.

© The Author(s), under exclusive license to Springer Nature Switzerland AG 2023
M. Zambrano Vizuete et al. (Eds.): RITAM 2021, LNNS 512, pp. 224–238, 2023.
https://doi.org/10.1007/978-3-031-11295-9_16

The teaching processes, supported by computer tools, grant the interactive participation of students and teachers in cyberspace, with access to multiple didactic resources and information sources, in addition to the use of different scenarios or simulations of the traditional classroom, experimenting with new activities and roles in the educational process [2]. Laboratory practices are a powerful pedagogical strategy for the construction of procedural competencies and for this reason it is used in a great variety of academic programs, usually synchronized with its corresponding theoretical subject.

Nowadays the teaching-learning process poses new academic challenges, especially with regard to methodologies capable of building competencies aimed at achieving greater student autonomy, since learning will be more effective if at some stage of the learning process. experience the student can participate actively through experimentation, analysis and decision making. To that effect, virtual laboratories are very useful, which can be used as a reinforcement and support tool for students to enhance their knowledge on their own or can be implemented as a didactic element in lectures to promote a participatory and constructivist environment. In addition, its use also enhances the acquisition of skills in the management of information and communication technologies (ICT) [3].

Virtual Learning Objects (OVA) are fundamental in the online teaching process. [4] They define OVA as “a set of digital resources that can be used in various contexts, with an educational purpose and made up of at least three internal components: content, learning activities and contextualization elements”. They have to be aligned with the curricular contents of the subject. The main features of OVA [4] are:

- Reusable: the resource must be modular to serve as a base or component of another resource.
- Accessible: they can be indexed for more efficient localization and retrieval, using schemas, metadata standards.
- Interoperable: they can operate between different hardware and software platforms.
- Portables: they can be moved and housed on different platforms, transparently without any change in structure and content.
- Durable: they must remain intact after software and hardware upgrades.

To optimize the creation of the OVAs, several methodologies have been designed that support the process, among which are Medhime 2.0, a methodology for the development of Virtual Learning Objects in free platforms such as Moodle, based on the SCORM standard, this methodology It has 4 stages which are: domain analysis, conceptual design, navigational design and communicational design [5].

On the other hand, AODDEI is a methodology to develop OVAs and integrate them into a learning management system, taking into account the analysis, obtaining, design, development, evaluation and implementation phases. This methodology had its first application in an intensive course of the teacher training unit at the Autonomous University of Aguascalientes, with outstanding performance in its application [6].

The declaration of COVID-19, as a global pandemic in mid-March 2020, with the consequent restriction of quarantine and forced isolation, resulted in the impossibility of continuing to maintain the traditional model of the face-to-face class, and have forced both students and teachers to use alternative educational work models such as online classes and e-learning [7]. Thus, according to [8], 29 countries in Latin America and the Caribbean continued with their educational processes through different modalities, such as virtual at all levels of training.

The virtualization of education has long been the protagonist in this period of pandemic and has allowed education to reach different geographical points, in the form of digital content that contributes to the learning process of students [7], among which are remote or virtual laboratories. [9] These could be defined as sets of hardware and software technologies that with the use of the Internet can carry out an experiment in the same way as in person, and also have the instrumentation, control and access to real equipment and become laboratories not conventional [10].

In the field of Electronics and Automation, different remote laboratories have been developed and implemented, whose field of action ranges from didactic applications to the use of complex industrial environments [7]. Within this theme, the cloud-based approach, which provides monitoring and control in real time, is beginning to gain ground [11].

It is important to mention that humanity is going through its fourth industrial revolution, which is based on the development of systems; internet of things, also known by its acronym in English, IoT; internet of people and services; artificial intelligence; additive manufacturing; reverse engineering; 3d printing; big data and data analytics, among others [12].

IoT allows the integration of different technologies such as microcontrollers, PLC's, Raspberry Pi, sensors, among others and thus bring information to the cloud and have applications such as smart homes, smart buildings, smart agriculture, smart factories and smart cities [13].

In the midst of the crisis derived from the pandemic and given the need for students to develop the necessary skills and abilities in terms of handling electronic devices and thanks to the use of web tools available today, it has been possible to create a virtual laboratory, as a support tool for the teacher, which allows him to visualize, monitor and evaluate the laboratory practices of micro-controllers without the need for a face-to-face meeting.

2 Material and Method

Due to technological advances in education and with the advent of the Internet, a new concept related to telecommunications arises such as tele-education, web-based learning and as a final point a scheme that formalized the previous ones called E-Learning, which makes use of multimedia tools, internet and web technologies in order to support the teaching-learning process.

Otherwise, the rise of mobile technology has given rise to Mobile Learning or M-Learning, which is defined as the dissemination of training content through mobile devices [14]. According to [15], M-Learning seeks to strengthen the capacities for interaction and support in the teaching-learning process, and the communication capacities in the different processes of the educational model.

In order to establish a methodology capable of developing the virtual laboratory OVA, a mixed methodology based on AODDEI was used for the development of OVA and component-based software engineering (ISBC) for the selection of the technical characteristics of the system. In Table 1, the way in which both methodologies were intertwined is explicitly found.

Table 1. AODDEI phases, ISBC phases and the final proposed mixed methodology

AODDEI		ISBC	Mixed (Proposal)
Phases	Steps		
1.- Analysis and obtaining	Analysis obtaining the material	Communication with the customer	Requirements analysis
2.- Design	Generation of the OVA structure	Planning risk analysis	Design and identification of tools
3.- Development	Construction	Construction and adaptation of engineering components	Construction and adaptation of components
4.- Evaluation 5.- Implantation	OVA evaluation Integration of the OVA into a learning management system	Customer evaluation	Evaluation and implementation

2.1 Phase 1. Requirements Analysis

In this phase, the analysis of the following aspects was carried out for the creation of the virtual laboratory.

Analysis

- The problem to be solved with the development of the OVA.
- The target audience for the project.
- The proposed solution to the problem and the theme to be addressed.
- The basic characteristics of the OVA to be developed.

Obtaining

The functional and non-functional requirements of the OVA based on the way in which the problem will be addressed. The inventory of the topics or contents that are going to go in the virtual laboratory (practices) is obtained.

Digitalizar el material

Multimedia materials and circuits are generated by means of some electronic application simulation or editing software.

The construction of the virtual laboratory is carried out, due to the lack of technological aids for the teaching of the Microcontroller subject in the development of practices in virtual mode, for students of the electronics career of the Sucre Superior Technological Institute. It is proposed to carry out an OVA through a virtual laboratory, in which they will find theoretical content, guides for the development of different practices and the possibility of interacting in real time with the applications of the virtual laboratory environment.

2.2 Phase 2. Design and Identification of Tools

In this phase, the design of the informative content, circuits, activities and the evaluation were carried out, as part of the design in the structure of the OVA, the tools to be used for the creation of the virtual laboratory were also identified.

Design
The organization of the contents immersed in the OVA of the virtual laboratory for microcontroller practices was carried out. Taking as a starting point that the OVAs seek to support the appropriation of knowledge on a specific topic.

These contents are organized as follows:

- *Informative content:* Indicate how the information will be presented, navigability and its organization.
- *Activities:* Indicate the activities that will be carried out in the OVA in order to support the appropriation of the concepts presented.
- *Evaluation:* It is carried out in order to measure the level of appropriation of the concepts exposed in the OVA.

The different environments were designed for the presentation of the contents in the web platform, the information, activities, evaluation and guides for the practices of microcontrollers.

Tool identification
In this section, an exhaustive investigation was carried out on the tools and components of virtual laboratories that best adapt to the characteristics of the project.

Tool analysis
To choose the best tool for the design of the virtual laboratory OVA, priorities were established within the characteristics of the different programs or tools that allow the development of the virtual laboratory (Fig. 1).

2.3 Construction and Adaptation of Components

In this phase, the development of the application corresponding to the implementation of the OVA for the virtual laboratory of the subject of Microcontrollers was carried out.

Parts of the Virtual Lab

- **Web Application**
  One of the functions of the virtual laboratory is the handling of data and its visualization through a browser. According to [16], a web application is software that is hosted on a server. In the case of the project, a web server is used.

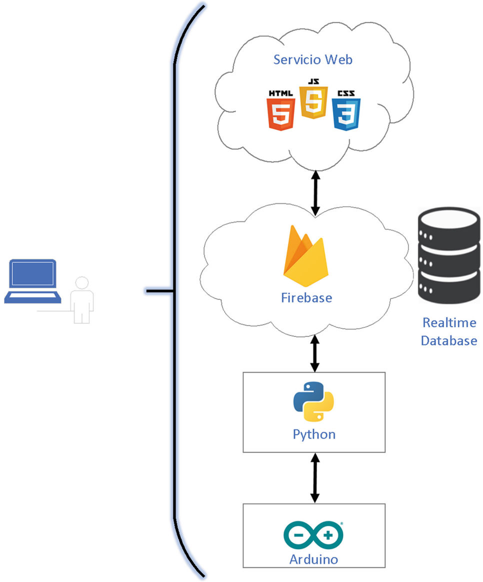

Fig. 1. Virtual lab setup

A web application allows tasks and processes to be carried out that, without the need to physically install other software, can be accessed through an electronic device connected to the internet. For the front-end of the web application, which serves as the development interface of the virtual laboratory, the bases of HTML5 were used, which consists of the composition of three fundamental elements such as HTML, CSS and JavaScript. Figure 2 shows the menu within the user interface for the different microcontroller virtual laboratory practices.

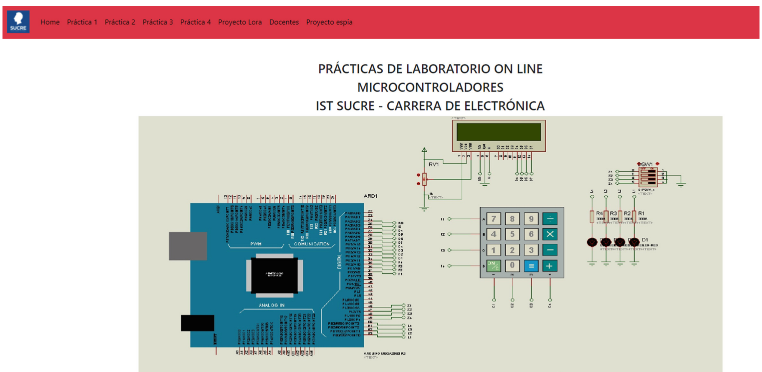

Fig. 2. Microcontroller practice menu interface

For the design of the menu, the requirements for four development practices of the microcontroller material were taken into account, which are:

- Digital inputs and outputs;
- Peripheral handling;
- HMI, and;
- Engine handling.

Figure 3, the virtual environment to carry out the practice within the web application is presented, for the link with the student's Arduino board, the creation of a user account, position request and execution time of the practice.

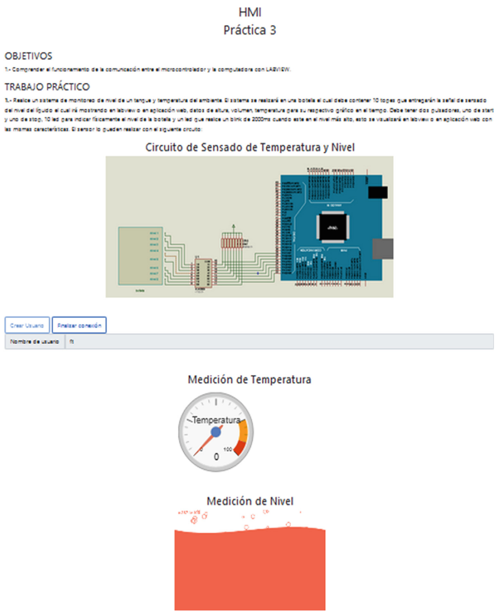

Fig. 3. Practice model

- **User account**
  In order for a student to carry out a practice within the virtual laboratory, first, it is necessary to create a user account, after which, several resources are deployed such as the connection node to be able to establish communication with the database, Fig. 4.
- **Request for location and execution time**
  In order to know the place of access of the execution of the practice, at the moment of the beginning of the execution, a confirmation menu is displayed for the registration of the location in the Firebase database. For the evaluation of the practice, an execution time is established, which begins at the moment of acceptance of the location registration, which is shown in Fig. 5.

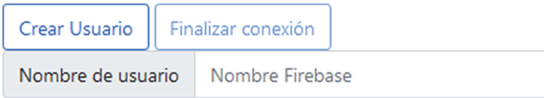

Fig. 4. Login interface

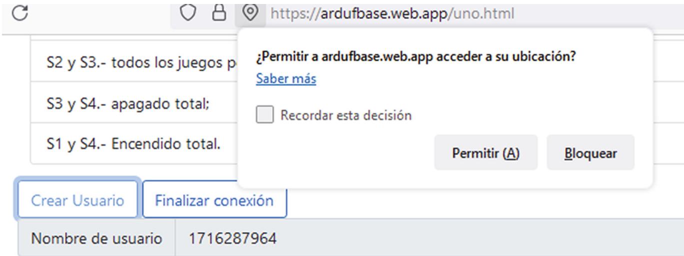

Fig. 5. Login, record of location and time used in practice.

- **Using Firebase, open database in real time**

 Firebase, from Google is a web and mobile application development platform located in the cloud, it is available for different platforms such as Android, IOS and Web. This service is used in the project as a back-end, with a database source in real time and easy to connect with the web application that is implemented as a virtual laboratory [17].

 For the connection of the web application with the Fire-base real-time database, it was necessary to include in the JavaScript of the web application, the configuration and access string, which is presented in Fig. 6.

```
var firebaseConfig = {
    apiKey: "AIzaSyB-ISHaTgQi-GZuQssejZthbpm9P1xqfyo",
    authDomain: "fir-arduino-1f94a.firebaseapp.com",
    databaseURL: "https://fir-arduino-1f94a.firebaseio.com",
    projectId: "fir-arduino-1f94a",
    storageBucket: "fir-arduino-1f94a.appspot.com",
    messagingSenderId: "345212173874",
    appId: "1:345212173874:web:2084ffd6ad937a3667062b",
    measurementId: "G-6JG0P8QCK2"
  };
firebase.initializeApp(firebaseConfig);
```

Fig. 6. Access string for firebase from web application

The information of the web application, which is used for user accounts, location information and execution time are stored in the Firebase real-time database and are hosted in the Google cloud, the data is NoSQL and the information is stored in JSON format. In Fig. 7, the cloud storage structure for the first lab is shown.

Fig. 7. Structure of practice 1 storage in the cloud and activity registered by user

The information of the accounts logged in the system, which are stored, for each student is the identification number, and in each record or node the activity carried out within the practice can be displayed.

- **User interface in Python**

Each student of the Microcontrollers course of the Electronics career of the Sucre Higher Technological Institute, at the time of the presentation of the practice, performs it remotely from their homes, by means of the connection of the Arduino to the computer and the link of the communication interface to the virtual laboratory.

The communication interface has been made by means of a window coded in the Python programming language, which allows the Arduino to connect with the web application, thus allowing students to demonstrate the development and operation of their programming practices. remotely, Fig. 8.

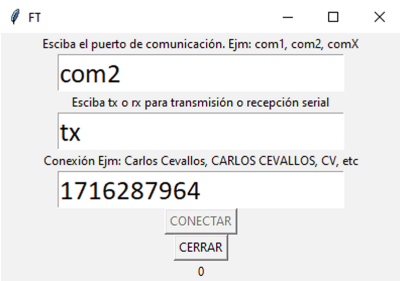

Fig. 8. Interface between the virtual lab and Arduino

It is requested to place in the dialog boxes the physical communication port of the Arduino (comX), if it transmits or receives RX or TX data, and the student's identification number so that the program connects with the database. The Firebase database allows an access of 200,000 simultaneous connections, for this reason all students of the Microcontrollers course can connect without having problems or loss of information. To activate the connection with Python and the Firebase real-time database, it was necessary to also connect with the connection keys provided by the platform, as shown in Fig. 9.

```
import firebase_admin
from firebase_admin import credentials
from firebase_admin import db
cred = credentials.Certificate({
  "type": "service_account",
  "project_id": "fir-arduino-1f94a",
  "private_key_id": "51f58c5747bdc9ef3d73b48ddab4c8dbcce51fa7",
  "private_key": "-----BEGIN PRIVATE KEY-----\nMIIEvAIBADANBgkqhkiG9w0BAQEFAASCBKYwggSiAgEAA
  "client_email": "firebase-adminsdk-orhij@fir-arduino-1f94a.iam.gserviceaccount.com",
  "client_id": "108220206074595758152",
  "auth_uri": "https://accounts.google.com/o/oauth2/auth",
  "token_uri": "https://oauth2.googleapis.com/token",
  "auth_provider_x509_cert_url": "https://www.googleapis.com/oauth2/v1/certs",
  "client_x509_cert_url": "https://www.googleapis.com/robot/v1/metadata/x509/firebase-admins
})
firebase_admin.initialize_app(cred,{'databaseURL':'https://fir-arduino-1f94a.firebaseio.com'
dato1=""
dato2=""
```

Fig. 9. Firebase-Arduino connection string

As already mentioned in the virtual laboratory web application, the student must create a session which becomes his identification number as well as the computer application will connect with the same number, as shown in Fig. 10.

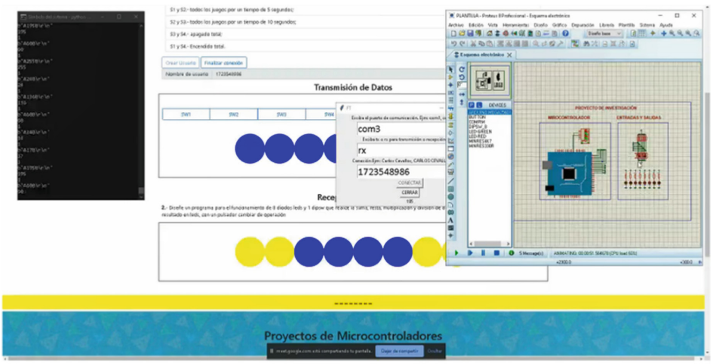

Fig. 10. Interface of a practical presented to the student

2.4 Evaluation and Implementation

In this phase, the OVA evaluation process was carried out. First under the supervision of qualified personnel, then by the public to whom the OVA of the virtual laboratory is directed.

Evaluation by qualified personnel
In this instance, the OVA is presented to the expert personnel on the subject of the project, to verify that they meet the desired characteristics. Compliance with functional and non-functional requirements is taken into account. In case of presenting corrections, they must be addressed before proceeding to the next instance.

Student assessments
In this step, it is important that the OVA is already endorsed by qualified personnel, to be later evaluated by the students, making use of the virtual laboratory, verifying its usefulness in the learning process and indicating possible improvements according to the need.

The students of the Microcontrollers subject made the use of the virtual laboratory, with the application of different microcontroller practices and through a survey it was concluded that the virtual laboratory is a tool that supports the teaching-learning process of the Microcontrollers subject, through virtual teaching. Access to the virtual laboratory for microcontroller practices is done by entering the virtual laboratory link: https://ardufbase.web.app/

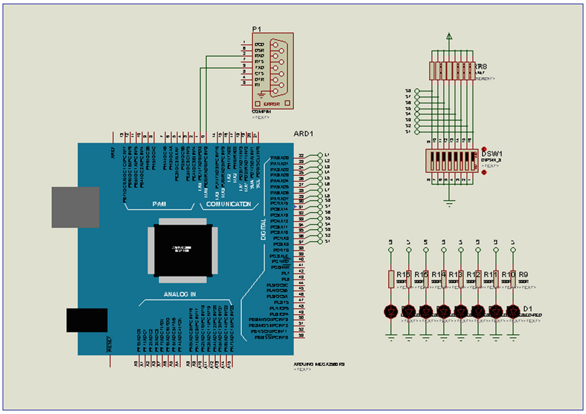

Fig. 11. Armed circuit example developed with Arduino

3 Results and Discussions

The subject of microcontrollers in the Electronics Career of the IST Sucre, is oriented so that the student develops the necessary skills in working with digital/analog electronics, programming tools and is able to control different processes at the industrial and domestic level.

Students must present the laboratory practices of the subject, with the AT Mega2560 microcontroller, which is included in the Arduino Mega board and is programmable in C++. In face-to-face practices, for this purpose, a guide sheet is given to the student, in which the objectives and details for the development of the practice were indicated. Due to the effects of the pandemic, the student must assemble the requested circuits of the practices with the help of simulation or electronic design tools such as Proteus, Tinkercad, among others; test the operation of the hardware of the practice and transfer the program from the Arduino software to the microcontroller to verify the operation of the circuit, as shown in Fig. 11.

After assembling the circuit, the student presents it through a videoconference using the Zoom or Google Meet platforms, showing the armed circuit via web camera, activating and deactivating the requested elements, among which are digital/analog inputs, digital/analog outputs, 7-segment display, LCD, matrix keyboard, among others; as presented in Fig. 12.

As can be seen in Fig. 12, the student presents his practice, but in some cases, and depending on the webcam, it is not correctly appreciated what is being presented. With the help of the virtual laboratory, the student accesses the information necessary for the development of the practice and the presentation remotely, allowing to visualize in a digital way what the student is presenting in a physical way.

First, the student must start the application on their computer, which allows transferring the data from Arduino to the database in Firebase, the program opens a communication port which allows receiving the data from Arduino and passing it to the base of data in reception mode, but it is also possible to pass the information from the database to the Arduino in transmission mode, and both in real time.

As the student presents his practice using the web application with Arduino, each action that takes place in the physical system is digitally presented in the virtual laboratory as shown in Fig. 13.

The final result for the evaluation serves both the teacher and the student. The teacher digitally compares the performance that the student presents remotely, in real time and ensures that the objectives set in practice are met.

In the first experimental tests in a class of 28 students, around 24 computers worked since they had a 64-bit operating system and the application for the computer allowed them to work without any problem. The remaining 4 students could not work because

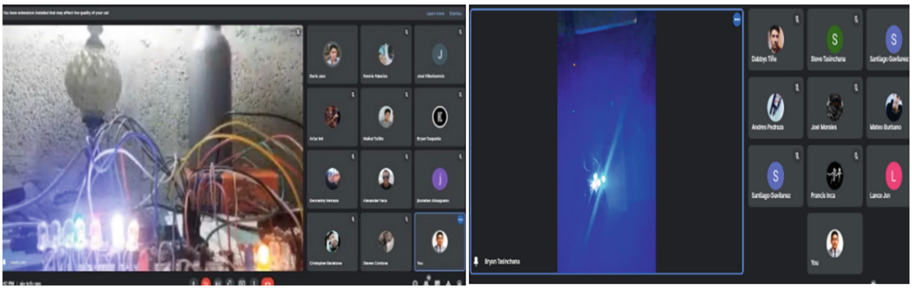

Fig. 12. Example of support of practices

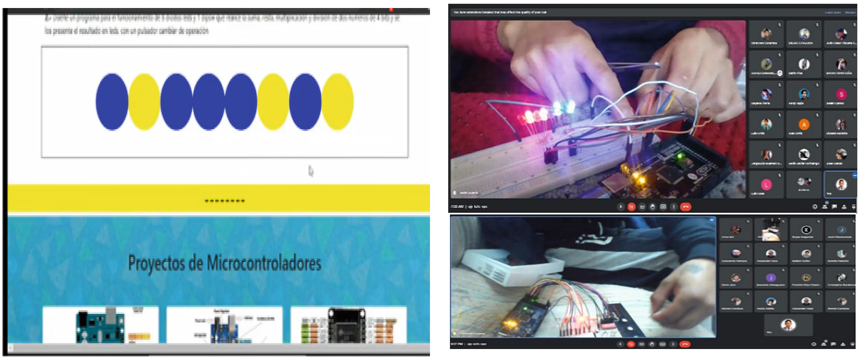

Fig. 13. Arduino-web application Interaction

they had a computer with a 32-bit operating system. This problem was solved by lowering the version of the application to 32-bit.

As mentioned above, when executing the virtual laboratory web application and starting the session with the identification number, access to the location where the practice is being carried out is requested, recording the lati-tud and length information in the database, with which the graph presented in Fig. 14 can be generated.

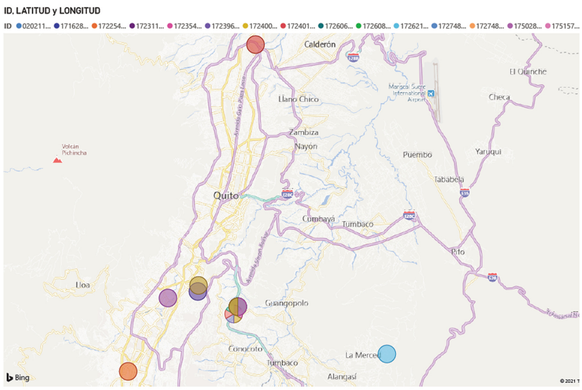

Fig. 14. Locations from which the pilot virtual practice was accessed.

According to what is presented in Fig. 14, all the students are in the city of Quito, geographically distributed both to the north, to the south of the city and in the valleys.

A counter was also placed, in order to count the times that a student has needed to enter the virtual laboratory to carry out the practice: for example, in the practice of digital outputs, it was reported that the majority of students did them with few interventions, as indicated in Fig. 15. With this information, a reinforcement can be given to subjects in which the students have entered a great number of times.

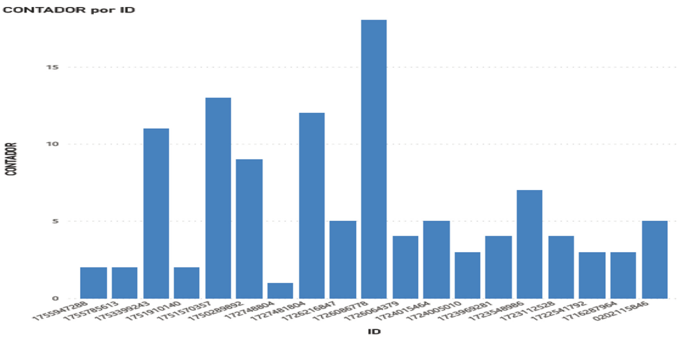

Fig. 15. Concurrency of users to the same virtual laboratory practice

4 Conclusion

The health emergency caused by COVID-19 accelerated the change from face-to-face learning scenarios to virtual learning scenarios, this abrupt change in most higher education institutions was carried out in the best way with the adaptation of virtual learning environments, but with the limitation of not being able to be applied in the best way in professional subjects, as is the case of the Microcontrollers subject, as it is a subject in which its practical component is significant, it was necessary to carry out an OVA for means of a virtual laboratory for the development of microcontroller practices.

The designed virtual laboratory fulfills the function of facilitating a virtual working environment through which, on the one hand, students carry out their laboratory practices on the subject of Microcontrollers from their homes, or workplace; and on the other, it allows the teacher to monitor, provide feedback and evaluate in real time, thus ensuring compliance with the objectives set for the practices.

Firebase is in a robust, open source and easily accessible database in the cloud that allows you to connect to the virtual laboratory web application with any mobile device or computer, and through the latter, with Arduino cards.

For development of the virtual laboratory, a mixed methodology was used that helped to achieve the silver objectives, with the ISBC complementing AODDEI, making it more versatile, because it is not only functional to be applied in OVA type web pages and software desktop, but it can also be used to create OVAs that use emerging technologies such as augmented reality on mobile devices.

The virtual laboratory is a valuable digital tool that helps teachers and students develop microcontroller practices, with the advantage of being available and accessible all the time.

References

1. Aguilar Gordón, F.D.R.: From face-to-face learning to virtual learning in pandemic times. Estud. Pedagog. **46**(3), 213–223 (2020). https://doi.org/10.4067/S0718-07052020000300213
2. Margarita, N., Molero, C., Maigualida, L., Castro, H., González, R., De Ojeda, U.A.: La educación virtual como apoyo instruccional durante el proceso de aprendizaje en la educación superior de Venezuela

3. Miguel, J., Jordá, M.: Herramientas virtuales: laboratorios virtuales para ciencias experimentales-una experiencia con la herramienta VCL (2012)
4. Tovar, I.C.: VIRTuAl lEARNINg obJECTs ANd THEIR ImpACT oN THE quAlITy of TEACHINg IN VIRTuAl EduCATIoN (2014). http://servicio.bc.uc.edu.ve/educacion/eduweb/v8n1/art08.pdf. Accessed 04 Sep 2021
5. Américo Sirviente. MeDHiME 2.0. Metodología para diseñar objetos de aprendizaje, migrando rápidamente a los docentes no informáticos | Portal Educativo de las Américas (2011). https://recursos.educoas.org/publicaciones/medhime-20-metodolog-para-dise-ar-objetos-de-aprendizaje-migrando-r-pidamente-los. Accessed 04 Sep 2021
6. Beatriz, O.U., Jaime, M.A., Mercado, Á.R.F.C.A.: Metodología para elaborar Objetos de Aprendizaje e integrarlos a un Sistema de Gestión de Aprendizaje. Univ. Auton. no. 8, pp. 1–8 (2003). http://www.colombiaaprende.edu.co/html/mediateca/1607/articles-172721_archivo.pdf
7. Vargas, J., Cuero, J., Torres, C.: Laboratorios Remotos e IOT una oportunidad para la formación en ciencias e ingeniería en tiempos del COVID-19: Caso de Estudio en Ingeniería de Control. Espacios **41**(42), 188–198 (2020). https://doi.org/10.48082/espacios-a20v41n42p16
8. CEPAL-UNESCO. La educacion en tiempos de la pandemia COVID-19. Com. Económica para América Lat. y el Caribe, Santiago Of. Reg. Educ. para América Lat. y el Caribe la Organ. las Nac. Unidas para la Educ. la Cienc. y la Cult. vol. 11, pp. 11–13 (2020)
9. Sains, G., Jose, G.: Evaluación del uso de laboratorios remotos en el aprendizaje de microcontorladores. Congr. TAEE 2010 Tecnol. Apl. a la Enseñanza la Electrónica, no. November 2014 (2010)
10. Zamora-musa, R.: Laboratorios remotos Análisis características y su desarrollo como alternativa a la práctica en la Facultad de Ingeniería. Inge-Cuc **6**(1), 267–280 (2010)
11. Pujari, U., Patil, D., Bahadure, D., Asnodkar, M.: Internet of Things based integrated smart home automation system. SSRN Electron. J. (2020).https://doi.org/10.2139/ssrn.3645458
12. Becerra, L.: Tecnologías de la información y las Comunicaciones en la era de la cuarta revolución industrial: Tendencias Tecnológicas y desafío en la educación en Ingeniería.pdf. Entre Cienc. e Ing. **14**(19098367), 76–81 (2020)
13. Le, G.T., Tran, N.M., Tran, T.V.: IoT system for monitoring a large-area environment sensors and control actuators using real-time firebase database. In: Singh, M., Kang, D.-K., Lee, J.-H., Tiwary, U.S., Singh, D., Chung, W.-Y. (eds.) IHCI 2020. LNCS, vol. 12616, pp. 3–20. Springer, Cham (2021). https://doi.org/10.1007/978-3-030-68452-5_1
14. Bocanegra, F., Alejandro, L., González, M., Ignacio, Á.: Modelo de desarrollo de servicios m learning , una propuesta desde la concepción del servicio hacia l a pedagogía M Learning Services Development Model, a Proposal from the Perspective of a Service Focused on Pedagogy (2007)
15. Montoya, M.S.R.: Dispositivos de mobile learning para ambientes virtuales: implicaciones en el diseño y la enseñanza. Rev. Innovación Educ. **8**(9), 82–97 (2008)
16. Castellano, Á., Valencia, M.: Desarrollo de un prototipo de sistema para adquisición y monitoreo de datos de la captación de radiación solar para la Escuela Politécnica *Nacional*. Quito: EPN (2019)
17. Duque, O.: Aplicación Web para el seguimiento y creación y manejo de contenidos, requeridos empresa del sector de seguro*s* Autor Oscar Giovanny Duque Perdomo Universidad de Antioquia Facultad de Ingeniería, Departamento de Ingeniería Electrónica y Telecomunicacione (2021)

Diagnostic Value of Knee Osteoarthritis Through Self-learning

Darwin Castillo[1,2,4,5](✉), Joseph Cueva[1,5](✉), Patricia Díaz[3,5], and Vasudevan Lakshminarayanan[3,4,5]

[1] Facultad de Ciencias Exactas y Naturales, Departamento de Química, Universidad Técnica Particular de Loja, 11-01-608, Loja, Ecuador
{dpcastillo,jhcueva1}@utpl.edu.ec

[2] Instituto de Instrumentación para Imagen Molecular (i3M), Universitat Politècnica de València – Consejo Superior de Investigaciones Científicas (CSIC), Valencia, Spain

[3] Facultad de Ciencias de la Salud, Universidad Técnica Particular de Loja, 11-01-608, Loja, Ecuador
pvdiaz@utpl.edu.ec

[4] Theoretical and Experimental Epistemology Lab, School of Optometry and Vision Science, University of Waterloo, Waterloo, ON, Canada
vengulak@uwaterloo.ca

[5] Departments of Physics, Electrical and Computer Engineering and Systems Design Engineering, University of Waterloo, Waterloo, ON, Canada

Abstract. Osteoarthritis (OA) is the most common chronic and progressive musculoskeletal disorder. These chronic disorders are not diagnosed early nor is the treatment adequate, resulting in challenges for health care systems. Radiography is the most widely used imaging method for OA diagnosis since it allows a two-dimensional evaluation, whose main advantages its low cost and wide availability. We present a computer-assisted diagnostic (CAD) system for OA based on the analysis of X-ray images of the knee using deep learning to automatically score the Knee OA. The scoring is based on the Kellgren-Lawrance (KL) scale. The model was implemented in PyTorch and was based on Deep Siamese convolutional neural networks and fine-tuned ResNet-34 through transfer learning for the classification task. A public dataset was used for training and validating, and a private dataset for testing. The results indicate a multiple-class accuracy of the test set of 61%. The highest accuracy was obtained with KL-3 at 89%. It is expected that this software will be useful for training of medical students and can be used as a second opinion for the correct prediction of OA knee diagnosis. Early diagnosis is necessary to alleviate symptoms, delay the evolution of the disease and improve the functional capacity and quality of life of the patient.

Keywords: Knee Osteoarthritis · Deep learning · CAD · CNN · X-ray images · KL grades

1 Introduction

Osteoarthritis (OA) is the most frequent progressive musculoskeletal pathology in older adults. It has a significant economic burden on the health system of the countries. The

© The Author(s), under exclusive license to Springer Nature Switzerland AG 2023
M. Zambrano Vizuete et al. (Eds.): RITAM 2021, LNNS 512, pp. 239–249, 2023.
https://doi.org/10.1007/978-3-031-11295-9_17

mechanical and biological factors such as age, female gender, obesity, sedentary lifestyle, absence or minimal activity, genetic predisposition, joint mechanics, and joint trauma increase the OA prevalence. OA affects nearly 240 million people worldwide, and its prevalence increases with age and obesity.

Knee and hip OA are the most common forms of arthritis [2, 3]. The knee is the largest joint in the human body and has a highly complex structure. The knee is prone to injury and degenerative changes (osteoarthritis) due to the massive loads endured during standing and walking [4]. Joint pain, stiffness, and limited function are common symptoms of OA, resulting in reduced quality of life and disability that contributes to a substantial financial burden for individuals [5]. When symptoms appear, they are usually ignored for many years and medical attention is usually sought in the late stages of the disease or when it interferes with daily activities.

The progressive nature of OA and its multifactorial etiology characterize the changes that include cartilage, synovial inflammation, and subchondral sclerosis with osteophyte formation. Osteophytes have been described as outgrowths of bone and cartilage that occur in the joint area. The direction of growth of osteophytes is sensitive to the size and local narrowing of the cartilage, except in the lateral compartment and medial patella [6].

For the diagnosis of OA, radiography has become the basic tool because of its cost and easy access. The commonly used projections, anteroposterior with load, lateral with 90° flexion and axial at 30° and 60°, are used and the loss of cartilage is evaluated. Loss of cartilage leads to a narrowing of the joint space and bone changes that result in subchondral sclerosis, cysts and osteophyte formation. By the time these changes are visible in the radiographs the condition has significantly deteriorated. [7]. The radiographic pattern to consider the severity of OA is through the Kellgren and Lawrence (KL) scale. This scale consists of five grades with Grade 0 indicating no evidence of OA and grade 4 indicating severe OA condition [8].

Chronic OA pathology results in an increase in patient comorbidities, limitation of the patient to carry out their daily or work activities, and has a negative effect on mood, producing depression in many cases. These can lead to significant societal costs. This study was designed to expedite the diagnosis of OA in primary health care settings and consists of a predictive model with easily interpretable image characteristics. It uses artificial intelligence to extract patterns or characteristics of lesion detection, progression, and prediction of musculoskeletal diseases from radiographs.

Currently there is extensive research in the processing, segmentation and classification of medical images resulting in a computer-assisted diagnostic, (CADx) tool that can be used as a second diagnosis [9].

The computer-assisted diagnostic CADx system based on deep learning algorithms can help in the diagnosis of different pathologies and brain disorders from medical images [10–12]. However, a major limitation is the lack of large datasets or image collections of the pathology. These datasets are necessary in order to train and the resultant decision of deep learning models.

In the case of knee OA, there are two important initiatives dedicated to collecting images, namely the Multicenter Osteoarthritis Study (MOST) and the Osteoarthritis Initiative (OAI) [2]. These are the standard datasets that are commonly used in designing deep learning models for automated knee OA diagnosis [13].

A deep learning and machine learning model for the automated quantification of severity of OA is one proposed by Antony et al. [13]. This convolutional neural network model was trained and optimized a weighted ratio of two-loss functions: categorical cross-entropy and mean-squared loss. The authors concluded that the method proposed had more classification accuracy with KL grade 3 and 4 than grades 0, 1 and 2 which have small variations in the image(s).

Tiulpin et al. [2] proposed a method based on the Deep Siamese Convolutional Neural Network. Their results show an average multiclass KL accuracy of 66.71%. Thomson et al. [14] proposed a methodology which employed shape and texture analysis of the radiograph knee, and a random forest classifier was employed resulting in a classification performance with an AUC of 0.849.

Chen et al. [3] proposed a method that combined two deep convolutional neural networks (YOLOv2 and ResNet) to detect and classify knee joint as per the KL scale with a classification accuracy of 69.7%.

The principal aim of this project was to develop a computer-assisted diagnostic (CAD) system based on the analysis of X-ray images of the knee. This model utilizes deep learning to automatically score the Knee OA using the Kellgren-Lawrance (KL) scale. The model architecture was implemented in PyTorch and was based on Deep Siamese convolutional neural networks and a fine-tuned ResNet-34 employing transfer learning for the classification task. It used a public dataset for training and validating, and a private dataset for testing. The results indicate a multiple-class accuracy of the test set of 61%. The largest classification accuracy for the KL-3 at 89%.

This software will be useful for training of medical students and can be used as a second opinion for the correct prediction of OA knee diagnosis. Early detection and treatment can alleviate symptoms, delay the evolution of the disease and improve the functional capacity and quality of life of the patient.

2 Materials and Methods

2.1 Data

This work used a public dataset from Chen et al. [3] for training and validating the model. For testing, a dataset composed of 376 knee X-ray images from a private hospital in Ecuador was used. The dataset employed by Chen et al. [3] consisted of 9182 knee X-ray graded according to the Kellgren-Lawrance scale [8].

The dataset was preprocessed and all images that cannot be clearly seen were discarded. This dataset [3] did not have balanced classes with 35% of the images belonging to the grade KL-0, while 3% of the dataset were graded a KL-4.

In order to balance the dataset, the images were preprocessed. Image and data augmentation (contrast, brightness, gamma, rotation) was applied to all classes which had fewer images. All images were scaled to 224×224 pixels because the pre-trained model ResNet-34 was used as a baseline (Table 1).

Table 1. Description of the datasets used in this project. The numbers provided in the tables indicate the number of knee images used in each group.

Group	Dataset	Images	KL-0	KL-1	KL-2	KL-3	KL-4
Train	Chen et al. 2019	20,022	4,422	4,395	4,262	4,648	2,295
Validation	Chen et al. 2019	1,359	270	270	270	270	270
Test	Private hospital	376	58	65	95	113	45

2.2 Network Architecture

The neural network used in this work is a fine-tuned ResNet-34, which was pre-trained on the ImageNet dataset [15] using the transfer learning approach [16]. For the classification task, the architecture was modified and the fully connected (*fc*) layers of the original model were increased by adding two more fc layers (see Fig. 1).

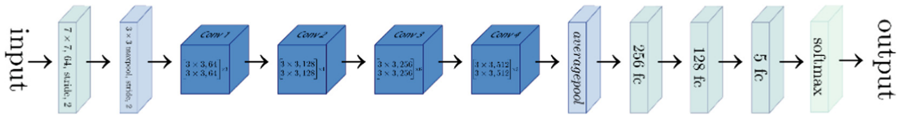

Fig. 1. Representation of the modified ResNet-34 architecture

This architecture was based on the Deep Siamese CNN networks architecture. This configuration is used to learn a similarity metric between pairs of images. This was applied to a face verification task [17].

Using this approach [2] the symmetry of a pair of knee X-ray images, was investigated. The images were cropped on the lateral and medial sides. For the medial side, the number of images were increased by horizontally flipping. Thus, increasing the dataset size.

The proposed network consists of two branches, each one having convolutional blocks, max pooling, rectified linear unit, batch normalization, global average pooling concatenated to a fully connected layer (see Fig. 2). The lateral side images of the knee joint were fed to one branch of the Deep Siamese CNN network and the medial side images were fed to the other branch.

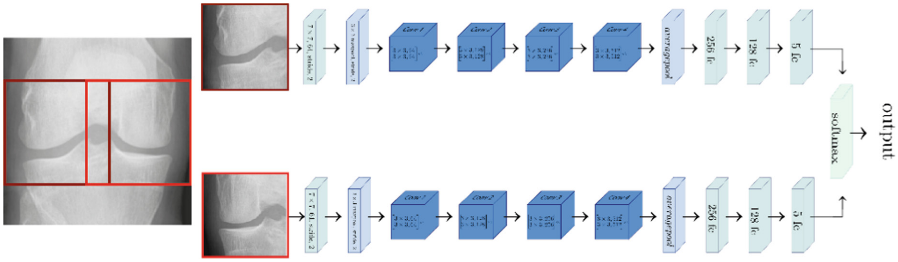

Fig. 2. Representation of the proposed Siamese network architecture. First, image patches from the lateral and medial sides of the knee joint were assembled. The medial side images were horizontally flipped. The cropped images feed the branches of the model which consisted of the following blocks having the shared weights (parameters). The first block denotes a convolution (Conv), the next block denotes a max pooling. The blue blocks denote convolution, batch normalization (BN), and a rectifier linear unit (ReLU). The next blocks denote average pooling, and the subsequent blocks denote fully connected layers connected to the SoftMax layer. The numbers inside the Conv-BN-ReLU blocks indicate the parameters $K \times K$, S where K is the filter size and S the output channels.

2.3 Model Training

Transfer learning is a common and effective strategy to train a network on a small dataset. Here a network is pre-trained on an extremely large dataset, such as ImageNet [16]. The fine-tunning method was used to not only to replace the fully connected layers of the pre-trained model ResNet-34, but also to fine-tune parts of the kernels in the pre-trained convolutional network.

To train the fine-tuned ResNet-34, Pytorch was employed and was run on a Nvidia TESLA P100 with 16 GB of memory and a fixed random seed of 42. In experiments with the architecture, a batch size of 64, Adam optimizer, and a cross-entropy loss function giving it a learning rate of $1e-4$, to reduce and avoid the overfitting was used. In addition, the L2-norm regularization (weight decay) with the coefficient $1e-4$ and a dropout of 0.5 was used. The regularization parameters were optimized based on the validation set loss.

2.4 Software Interface

For the implementation and development of the software, Python was used since it is open source and has a large number of libraries and packages for graphical interfaces, computer vision, deep learning, and medical images. The interaction between the different libraries and packages used in the software is illustrated in Fig. 3.

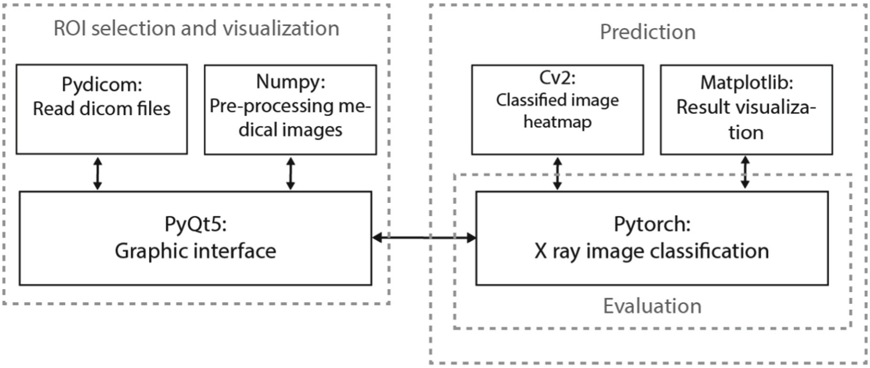

Fig. 3. Software architecture.

The software was divided into three principal parts: 1. visualization of the X-ray images, 2. region of interest (ROI) selection and, 3. neural network classification of the ROI according to the Kellgren-Lawrance grading scale (see Fig. 4).

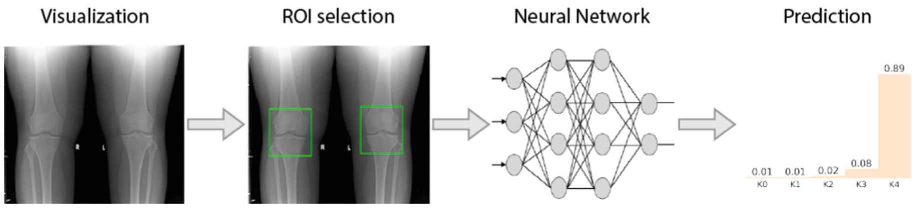

Fig. 4. Software pipeline.

3 Results and Discussion

3.1 User Interface

The graphic user interface of the software has different elements (see Fig. 5). These elements are: upper bar, navigation panel, patient information panel, toolbar, X-ray image panel, and results panel.

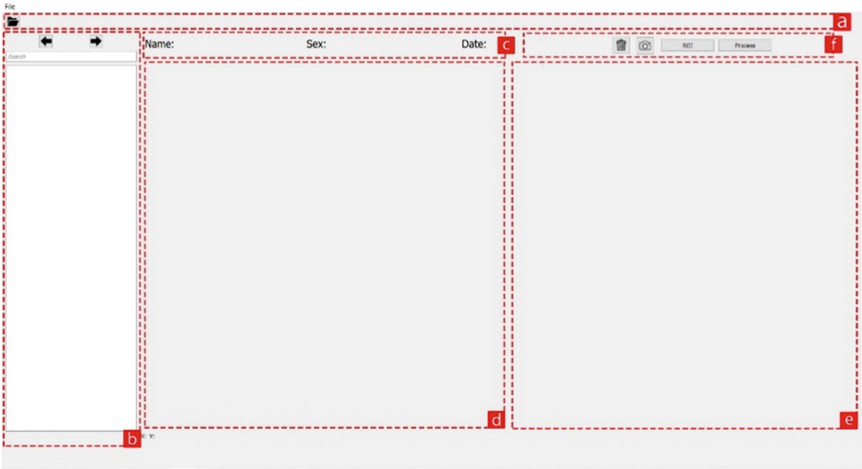

Fig. 5. Distribution of the elements of the graphical interface: a) top bar, b) navigation panel, c) patient information panel, d) X-ray images panel, e) results in the panel, f) toolbar.

The user selects the directory with the files to analyze in the upper navigation bar. The files in *.dcm format will be listed in the navigation panel. The file selected in the navigator panel will be visualized in the X-ray images panel. By clicking the ROI button in the toolbar, the ROI selector will appear in the X-ray image panel. The user can delineate the region that is to be analyzed. Once the ROI is selected by clicking on the process button in the toolbar, the ROI will be analyzed by the model (see Fig. 6).

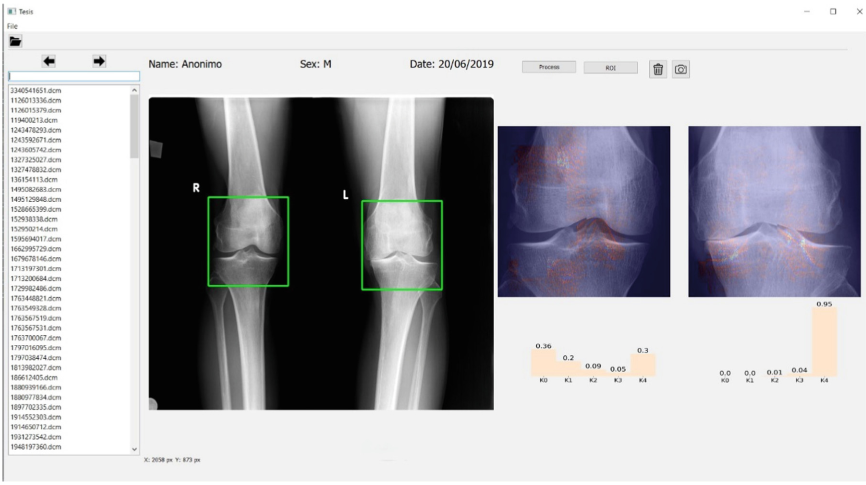

Fig. 6. Graphical interface

The results will appear in the "results panel" as a distribution of probabilities, the class with the higher probability is the class predicted by the model as described in Fig. 7.

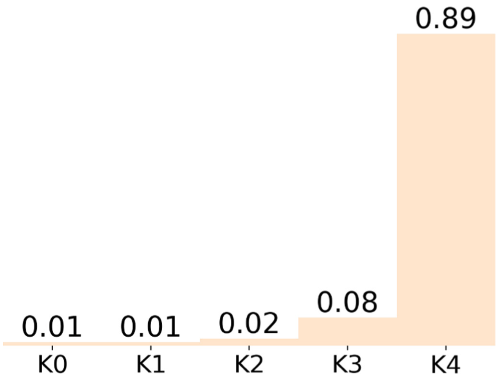

Fig. 7. Model prediction presented as a distribution of probabilities

3.2 KL Grade Classification

The model was tested and evaluated using a private clinic dataset. The metrics considered for the analysis of the results were confusion matrix, accuracy, precision, and recall.

The private dataset consisted of 225 images with 45 images for each class. These images were classified by two trained clinic radiologists.

The results of classification for this dataset were:

- KL-0 the model correctly predicted 32 images out of 45 images,
- KL-1 the model correctly predicted 20 images out of 45 images,
- KL-2 the model correctly predicted 27 images out of 45 images,
- KL-3 the model correctly predicted 40 images out of 45 images, and
- KL-1 the model correctly predicted 20 images out of 45 images.

The confusion matrix evaluates the accuracy of a classification. It is a visual representation of the true positive, false positive, true negative, and false negative values of the predictions.

The confusion matrix of the KL grading of our model is presented in Fig. 8. Table 2 summarizes the number of the true positive (TP), false positive (FP), and false negative (FN) values for each KL class.

Table 2. Summary of TP, FP and FN values foe each KL class

Kellgren-Lawrance scale	TP	FP	FN
KL-0	32	14	13
KL-1	20	17	25
KL-2	27	17	18
KL-3	40	36	5
KL-4	20	2	25

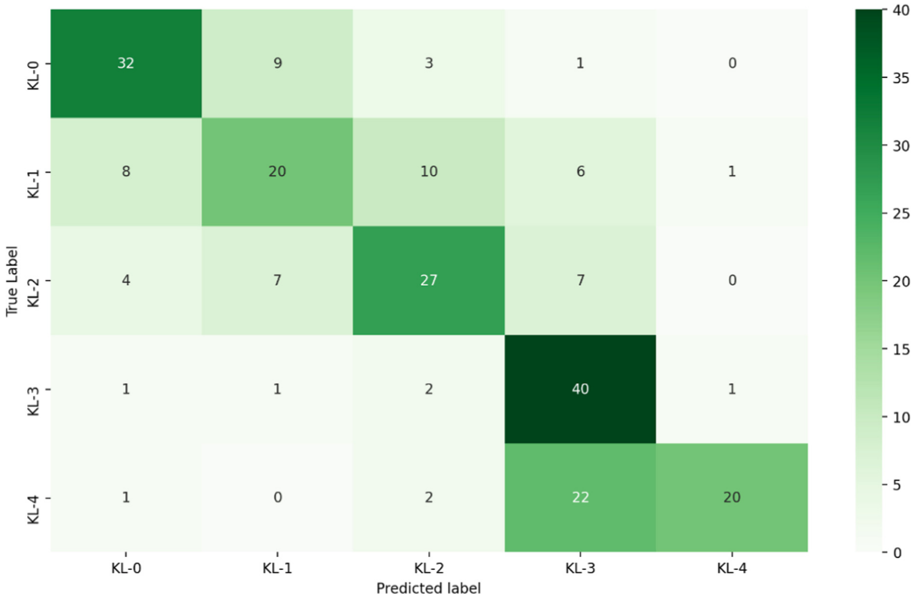

Fig. 8. Confusion matrix of KL grading.

The precision and recall sensitivity of the predictions for each class classification is shown in Table 3. The class with the highest precision was KL-4 with 91% and the class with the major recall was KL-3 with 89%.

The average test set multi-class accuracy achieved by the model was 61%, which is in agreement with the accuracy of 69.7 and 66, 71% reported by Chen et al. [3] and Tiulpin et al. [2], respectively.

The results on precisions agreed with the models proposed by [2, 3, 13, 14]. These studies also reported that the best accuracy in the multiclass classification were classes KL 3 and KL 4. The reason for the difficulty in detection and classification of the lower classes are complex due to the small variations that are present in the OA of the knee images [13].

Table 3. Precision and recall sensitivity for each class

Kellgren-Lawrance scale	Precision	Recall
KL-0	70%	71%
KL-1	54%	44%
KL-2	61%	60%
KL-3	53%	89%
KL-4	91%	44%

4 Conclusions

The proposed and trained model achieved good performance in the multi-class accuracy. It was highly effective (89%) in detecting osteoarthritis KL-3 and a precision of 91% (91%) for KL-4 class. For the other three classes, KL0, KL1, and KL2, the confusion matrix and metrics show a less accurate predictions. These results are in agreement with the literature, and is principally due to the complexity in the detection and differentiation of the small variation in the space joint of the knee OA images.

In addition, this work used transfer learning fine-tuning in order to take the advantage of a pre-trained model trained by a large dataset such as ImageNet.

Overall, the results show that the trained model can learn features from training and validation datasets and apply them to a different dataset. The construction and results of these prediction models will improve decision-making in diagnosis and optimal treatments in the nearest future, e.g., use and complement with other techniques such as generative adversarial networks (GANs) network architectures. The source code developed in this work is open-source and can be found at https://github.com/jhcueva/OA-Analyzer.

Although this model does not have very high prediction it is expected that the software developed for this study will be useful to train medical students and can be useful to new specialists and help them achieve optimal diagnostic prediction.

Acknowledgment. The authors acknowledges the research support to Universidad Técnica Particular de Loja through the project PROY_INV_QUI_2020_2784.

References

1. Nelson, A.E.: Osteoarthritis year in review 2017: clinical. Osteoarthritis Cartilage **26**, 319–325 (2018). https://doi.org/10.1016/J.JOCA.2017.11.014
2. Tiulpin, A., Thevenot, J., Rahtu, E., Lehenkari, P., Saarakkala, S.: Automatic knee osteoarthritis diagnosis from plain radiographs: a deep learning-based approach. Sci. Rep. **8**(1), 1–10 (2018). https://doi.org/10.1038/s41598-018-20132-7
3. Chen, P., Gao, L., Shi, X., Allen, K., Yang, L.: Fully automatic knee osteoarthritis severity grading using deep neural networks with a novel ordinal loss. Comput. Med. Imaging Graph. **75**, 84–92 (2019). https://doi.org/10.1016/J.COMPMEDIMAG.2019.06.002
4. Debi, R., et al.: Knee osteoarthritis, degenerative meniscal lesion and osteonecrosis of the knee: can a simple gait test direct us to a better clinical diagnosis. Orthop. Traumatol. Surg. Res. **103**, 603–608 (2017). https://doi.org/10.1016/J.OTSR.2017.02.006
5. Cross, M., Smith, E., Hoy, D., et al.: The global burden of hip and knee osteoarthritis: estimates from the global burden of disease 2010 study. Ann. Rheum. Dis. **73**, 1323–1330 (2014). https://doi.org/10.1136/ANNRHEUMDIS-2013-204763
6. Nagaosa, Y., Lanyon, P.: Characterisation of size and direction of osteophyte in knee osteoarthritis: a radiographic study. Ann. Rheum. Dis. **61**(4), 319–324 (2002). https://doi.org/10.1136/ard.61.4.319
7. Loeser, R.F., Goldring, S.R., Scanzello, C.R., Goldring, M.B.: Osteoarthritis: a disease of the joint as an organ. Arthritis Rheum. **64**, 1697–1707 (2012). https://doi.org/10.1002/ART.34453

8. Kellgren, J.H., Lawrence, J.S.: Radiological assessment of osteo-arthrosis. Ann. Rheum. Dis. **16**, 494–502 (1957). https://doi.org/10.1136/ARD.16.4.494
9. Shen, D., Wu, G., Suk, H.-I.: Deep learning in medical image analysis. Annu. Rev. Biomed. Eng. **19**, 221–248 (2017). https://doi.org/10.1146/annurev-bioeng-071516-044442
10. Castillo, D., Lakshminarayanan, V., Rodríguez-Álvarez, M.J.: MR images, brain lesions, and deep learning. Appl. Sci. **11**, 1675 (2021). https://doi.org/10.3390/APP11041675
11. Litjens, G., et al.: A survey on deep learning in medical image analysis. Med. Image Anal. **42**, 60–88 (2017). https://doi.org/10.1016/J.MEDIA.2017.07.005
12. Jiménez-Gaona, Y., Rodríguez-Álvarez, M.J., Lakshminarayanan, V.: Deep-learning-based computer-aided systems for breast cancer imaging: a critical review. Appl. Sci. **10**, 8298 (2020). https://doi.org/10.3390/APP10228298
13. Antony, J., McGuinness, K., Moran, K., O'Connor, N.E.: Automatic detection of knee joints and quantification of knee osteoarthritis severity using convolutional neural networks. In: Perner, P. (ed.) MLDM 2017. LNCS (LNAI), vol. 10358, pp. 376–390. Springer, Cham (2017). https://doi.org/10.1007/978-3-319-62416-7_27
14. Thomson, J., O'Neill, T., Felson, D., Cootes, T.: Automated shape and texture analysis for detection of osteoarthritis from radiographs of the knee. In: Navab, N., Hornegger, J., Wells, W.M., Frangi, A.F. (eds.) MICCAI 2015. LNCS, vol. 9350, pp. 127–134. Springer, Cham (2015). https://doi.org/10.1007/978-3-319-24571-3_16
15. Russakovsky, O., et al.: ImageNet large scale visual recognition challenge. Int. J. Comput. Vision **115**(3), 211–252 (2015). https://doi.org/10.1007/s11263-015-0816-y
16. Yamashita, R., Nishio, M., Do, R.K.G., Togashi, K.: Convolutional neural networks: an overview and application in radiology. Insights Imaging **9**(4), 611–629 (2018). https://doi.org/10.1007/s13244-018-0639-9
17. Chopra, S., Hadsell, R., LeCun, Y.: Learning a similarity metric discriminatively, with application to face verification. In: Proceedings - 2005 IEEE Computer Society Conference on Computer Vision and Pattern Recognition, CVPR 2005. I, pp. 539–546 (2005). https://doi.org/10.1109/CVPR.2005.202

Interactive Software for the Learning of Mathematics in Elementary School Students in the Province of Tungurahua

Paulina Sánchez[1](✉), Ligia Jácome[2], Cinthya Sancho[3], and Richard Sánchez[4]

[1] Universidad Tecnológica Indoamérica, Av. Manuelita Sáenz y Agramonte, 180103 Ambato, Ecuador
paulinasanchez@uti.edu.ec
[2] Píllaro 180207, Ecuador
[3] Ideanautas Lam, La Península, 180104 Ambato, Ecuador
[4] Universidad Tecnológica Israel, Quito 170516, Ecuador

Abstract. This article shows a study on the impact of the development of a video game for the teaching of mathematics in elementary school students, developed mainly to strengthen knowledge as a new educational resource for teachers to give interactive classes changing the usual way in which they teach, which would cause the student's interest in learning. The methodology used was based on three phases: first, exploratory research was carried out in the Gabriela Mistral institution in San Pedro de Pelileo (Ecuador), second, the video game was developed with an agile methodology, applying an adaptive algorithm in its architecture that helps the children's knowledge to be modified through the game, expanding the knowledge information they have. Finally, a determined group of students was evaluated to know whether or not the game contributed to their education and it was found that an increase of 27.78% was achieved in their knowledge, in relation to the levels they had with the conventional learning method.

Keywords: Learning · Mathematics · Interactive program · Video games

1 Introduction

Education is extremely important in Ecuador, which is why there are articles in the Constitution that prioritize this issue: Art. 26.- Education is a right of people throughout their lives and an inescapable and inexcusable duty of the State. It constitutes a priority area of public policy and state investment, a guarantee of equality and social inclusion, and an indispensable condition for a good life. Individuals, families and society have the right and the responsibility to participate in the educational process [1].

Education is the formation of individuals in the evolution of intelligence, knowledge, thought and conscience that provide significant advances for their survival, i.e., education in human beings is the process by which they acquire knowledge and this allows them to integrate into society in a given professional environment [2].

© The Author(s), under exclusive license to Springer Nature Switzerland AG 2023
M. Zambrano Vizuete et al. (Eds.): RITAM 2021, LNNS 512, pp. 250–263, 2023.
https://doi.org/10.1007/978-3-031-11295-9_18

Nowadays new teaching methods have been increasing for education that humans did not have before, since technology had not advanced so much, but today technology and learning go hand in hand, since we live in a network society, in which education is essential to have knowledge and for the future development of individuals both in the economic and social sphere and the systems that most attribute to this knowledge is the information found by browsing the network as: interactive applications that allow the student to learn in a broader and less monotonous way [3].

Interactive applications are multimedia systems that can be accessed through a computer. These systems present and combine text, graphics, audio and video, allowing direct contact with the user, since they can navigate, interact, create and communicate through these platforms, which are currently very necessary to capture the attention of students [4].

Applications are video games, which are programs designed to amuse and entertain. They can be found in various media such as computers, cell phones and consoles that provide users with playful experiences through the audiovisual languages they transmit [5].

The creator must offer the user applications that are easy to manipulate, for the target group to which this proposal is being dedicated and must have two key concepts in its undertaking: usability and accessibility, which will result in the student's interest in the educational content and contextualize their lectures on their own, facilitating their own learning [6].

These can play an important role in children's learning, since nowadays the perception of a video game is no longer the same. Now they can be a pastime with pedagogical values that serve to motivate and stimulate learning, resulting in the concentration of students [7].

Mathematical learning for elementary school students through video games allows the development of content where, while having fun, the child acquires substantial information, which facilitates the way in which he/she captures and retains information. These are characterized by awakening the students' interest in learning, facilitating the teacher's work [8].

In these games, students learn by trial and error, the error does not cause any frustration in them, but rather motivates them to reach the goal with the rules of the game, but without the pressure of winning or losing [9]. The methodology was developed through exploratory research that evidences the contribution of an interactive video game in education, the development of the video game was through a planning process and finally a determined group of students was evaluated to know if the game contributed or not in education. The results show that with the use of the video game the levels of knowledge in mathematics increased in relation to the levels of achievement with the conventional method.

2 Related Projects and Articles

Here are some applications that used this type of technology and have contributed significantly to the learning of mathematics. Hearthstone is a game for children that teaches them mental arithmetic operations using cards during the game [10].

The Number Race is a videogame which was created with the purpose of teaching kindergarten children about topics such as numerical comparison of numbers and words [11].

Video games such as Pokemon Go, Angry Birds and Tetris occupy a fundamental place in the leisure time of children, they learn without realizing mathematical and physical concepts that are given to them only in school environments [10].

These investigations have contributed in some way to cognitive development in the area of mathematics in children in regular education in different countries. However, in Ecuador, few studies have been conducted in this area. And those that have been analyzed by the research team are limited, boring and unchallenging. Many have game possibilities; others do not show degrees of complexity or different levels of difficulty. There are few tools that provide a dynamic adaptation in the games and an adaptive workflow, which makes these tools unsustainable. This fact has provided the opportunity to create a video game, evaluating its usefulness in a quasi-experimental study in a real context.

3 Method

The method used was based on the following phases: first, exploratory research was conducted to find out how an interactive video game would contribute to education, which was applied to students, teachers who teach classes and parents who have direct contact with the target group; second, the video game was developed through a planning process; and finally, a specific group of students was evaluated to find out whether or not the game contributed to education. The phases are detailed below.

3.1 Exploratory Research

The analysis was carried out with thirty-eight people, including parents, boys and girls of 8 and 9 years of age, plus interviews with 7 teachers of the Gabriela Mistral school in San Pedro de Pelileo (Ecuador), which is the staff of this school in the area of teaching at the basic levels. First, an observation sheet of a class was given to sixth grade students to visualize the strengths and weaknesses that exist in that classroom and it was noted that the teacher shows mastery in the topics he teaches in class, but does not use any technology to make the class more dynamic and interactive. On the other hand, in the interviews conducted with the teachers, it was found that the classes they teach are still the same as years ago, due to the limited technological resources to teach their classes. However, when the possibility of creating a technological solution to support their work in the classroom was mentioned to them, they were very interested and agreed with the implementation of interactive teaching, since it would help them to reinforce the topics developed in class. The surveys concluded that children in their homes do have access to electronic devices for entertainment, but parents did not know that they can also use these elements as teaching tools, which seemed to them a very interesting and positive idea for the education of their children. For all these reasons, it was timely and relevant to create a video game for teaching.

3.2 Development of the Video Game

The methodology applied in the development of the video game is shown in Fig. 1 below.

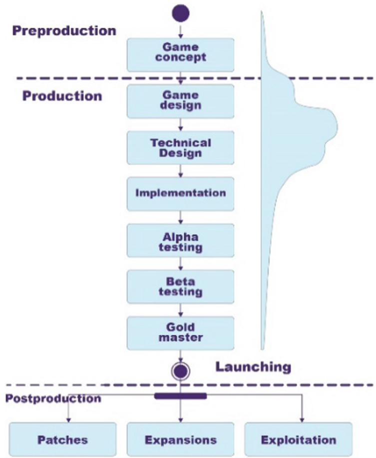

Fig. 1. Production process of an adapted video game: the production process of a video game: production phases.

Pre-production Phase. The pre-production phase consisted of the planning process that served to define the game and the aspects that would have to be carried out for its materialization. The genre of the video game is educational action with a 2d realistic aesthetics for the teaching of mathematics in elementary school students, the plot that will be discussed is that children as they grow up are learning with the guidance of a teacher who will help them in their evolution. In its architecture it will be characterized for being a realistic game with a linear story, that is to say, as the student evolves in his knowledge, the character with whom he will play will also evolve, so there will be levels with certain degrees of difficulty. This is why it is a game with an adaptive mechanism and will always be entertaining, provocative and sustainable for the student [12].

The script includes some parts such as: the type of game, the idea and the premise. The type of game is a video game in which there are two characters Ana and Pepe who must go through three different levels of difficulty, with certain enemies and a teacher who will ask them questions so they can continue playing, the idea is that while they go through difficulties with their enemies they solve the questions to reach the goal and finally the premise has the purpose that the video game serves as audiovisual material to increase knowledge on the subject of the multiplication tables.

The plot covers some topics such as: the implication, which is based on the fact that any of the two characters chosen by the user must fulfill the mission to reach the goal and move to the next level through the questions that the teacher asks, if they are incorrect the question will be different preventing the player from reaching the goal, the events are about the help that the teacher gives to the children to see the interest they have to learn and the series of levels to pass, The surprise is that in each level the difficulty of the game is increasing and has different scenarios that helps to not be something routine, in the denouement to reach the final goal of the three levels there will be a scene in which you can see the children go home after meeting their goal and finally the gameplay in which the person-je's mission is to collect numbers to go adding and the teacher can make him the questions that must be answered correctly.

The sketches were made by hand in order to visualize the features, clothing and characteristics that the characters of the game have before making them digitally (Fig. 2).

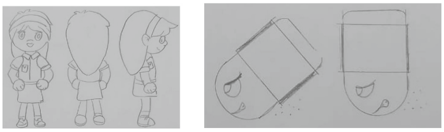

Fig. 2. Sketches.

It was also observed that the game is dramatic, since the character must interact with the objects in his environment through certain actions that will lead him to a clear objective, which are the questions he must answer. As the player goes through levels, the scenery, objects and some characters will change in order to make the game complex and interesting for the user. The Game Design Document is the part that allows to synthesize in depth everything related to the game, which includes the following parts: the genre, as previously mentioned is purely educational action with a multiplatform, players will have a single player mode, the story is based on two children who while going through the game learn to multiply, the look and feel refers to the characters formed in 2d with chibi-realistic style, In the user interface the game was made for the student to play using the up, down, right and left keys, the space key to jump and the mouse to interact with the objects in the game, in the objectives we talk about each level. Level 1, 2 and 3 consisted of the character having to collect number balls and correctly answer the questions asked by the teacher in order to pass to the next level, but in level 3 what will change is that the character will reach a sign that will say exit and the game will end.

The rules of the game were based on that the characters must collect all the balls so they can answer the teacher's questions, the characteristics in the children is that they jump, run and answer questions, the chalk dust walks and the balls are distributed on the game map, in the design of levels, the first one is based on the implementation of platforms made of chalk, in the level design, the first one is based on the implementation of platforms made of chalk, blackboard erasers and rulers, in which the character cannot be touched by the enemy that is a chalk dust and if he touches him he cannot reach the goal, in level two the platforms are made of tables, books and rulers and has an eraser as enemy and finally in level three the platforms are made of blocks and backpacks with an enemy of pa-pel ball.

Production Phase. In this phase the game was elaborated digitally. Here you can find the artistic design of the game or also known as the art bible of the game, which has to do with the appearance and physique that will have this interactive platform, here are four elements such as: the story, sound, interface and graphics, these artistic aspects made it different from other games that exist in the market [13].

The story of the game 9K multiplication tables is about two cousins (Ana and Pepe) who studied in downtown, they have to deal with is multiplication tables in a math class, the teacher is good and teaches in a fun way.

Ana is a 7-year-old Ecuadorian girl who was born on October 29, 2012, with cinnamon skin, long brown hair and a round face. She is cheerful and sporty, she is dressed in a white short-sleeved shirt with blue parts, a blue skirt, black shoes with white, white socks and a headband (Fig. 3).

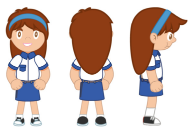

Fig. 3. Girl-Ana.

Pepe is a 7-year-old Ecuadorian boy who was born on September 1, 2012, with cinnamon skin, short brown hair and a round face. He is a cheerful and sporty person; he is dressed in a white short-sleeved shirt with blue parts, blue pants and black shoes with white (Fig. 4).

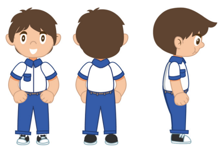

Fig. 4. Boy-Pepe.

Professor Yoli is 33 years old, Ecuadorian born on July 25, 1986, her physical appearance is cinnamon skin, has short brown hair and an oval face. Her special characteristics are that she is a happy and confident person; she is dressed in a gray uniform with blue parts, a white shirt and black shoes.

The sound is the sound elements that the game will have. The music that was used in the start menu, controls scene, scene to choose the characters and the description scene of each level is called Rock Me- Jan Boyle, the music of level 1,2 and 3 is by Kevin MacLeod- B-Roll Ska version, the music of the failed level scene is under a starry sky- Axess and the final sound of the victory scene is a happy children's scream (Fig. 5).

Fig. 5. Teacher.

The interface refers to how the GUI (Graphical User Inter-face) and HUD (Head-Up Display) elements will be visualized, which in the game are in charge of informing the player the amount of balls he has collected and how many lives he has, being an important element of the game (Fig. 6).

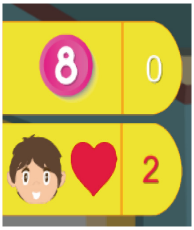

Fig. 6. Interface.

The graphics of the game were designed in 2D, which was made using sprites (bitmap) and tiles (backgrounds or scenarios) elaborated with Adobe Illustrator CS6.

Likewise, the mechanical design contextualized the interaction guidelines with the game, the internal rules and the type of communication that the game will have. The student could interact with the game through his computer, using the keys to perform the actions of the character and would use the mouse to answer the questions, the rules that this platform has is that you must collect all the balls without touching the enemies, but if you do so you would be deducted a life and have to start the level again, to prevent this from happening you should jump over the enemies to reach the goal and the teacher will ask the question (Fig. 7).

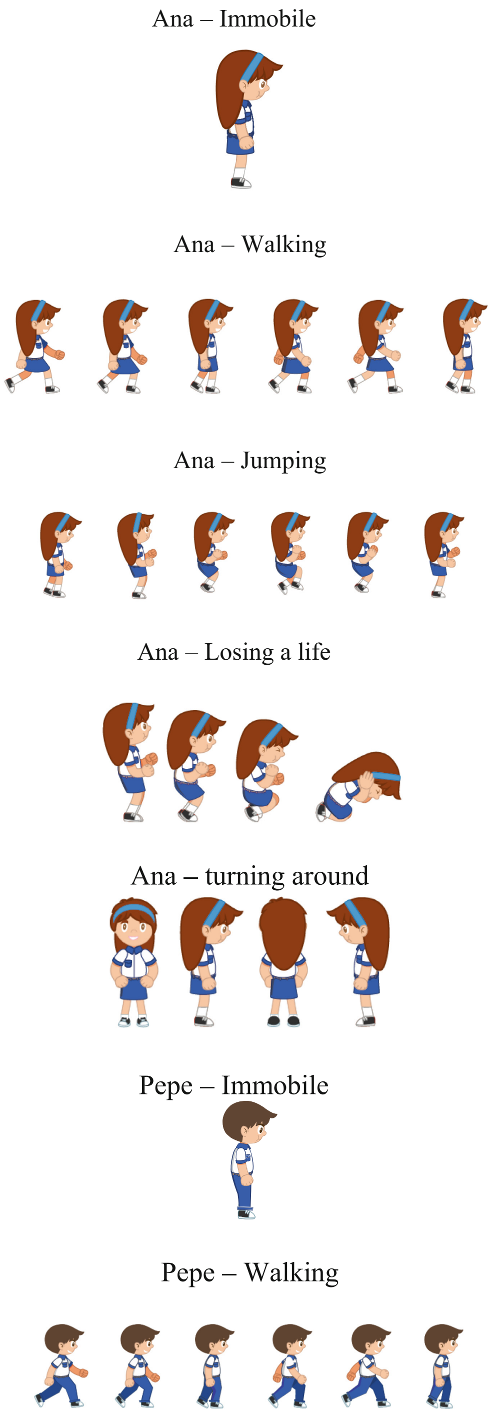

Fig. 7. Character animation (Sprites).

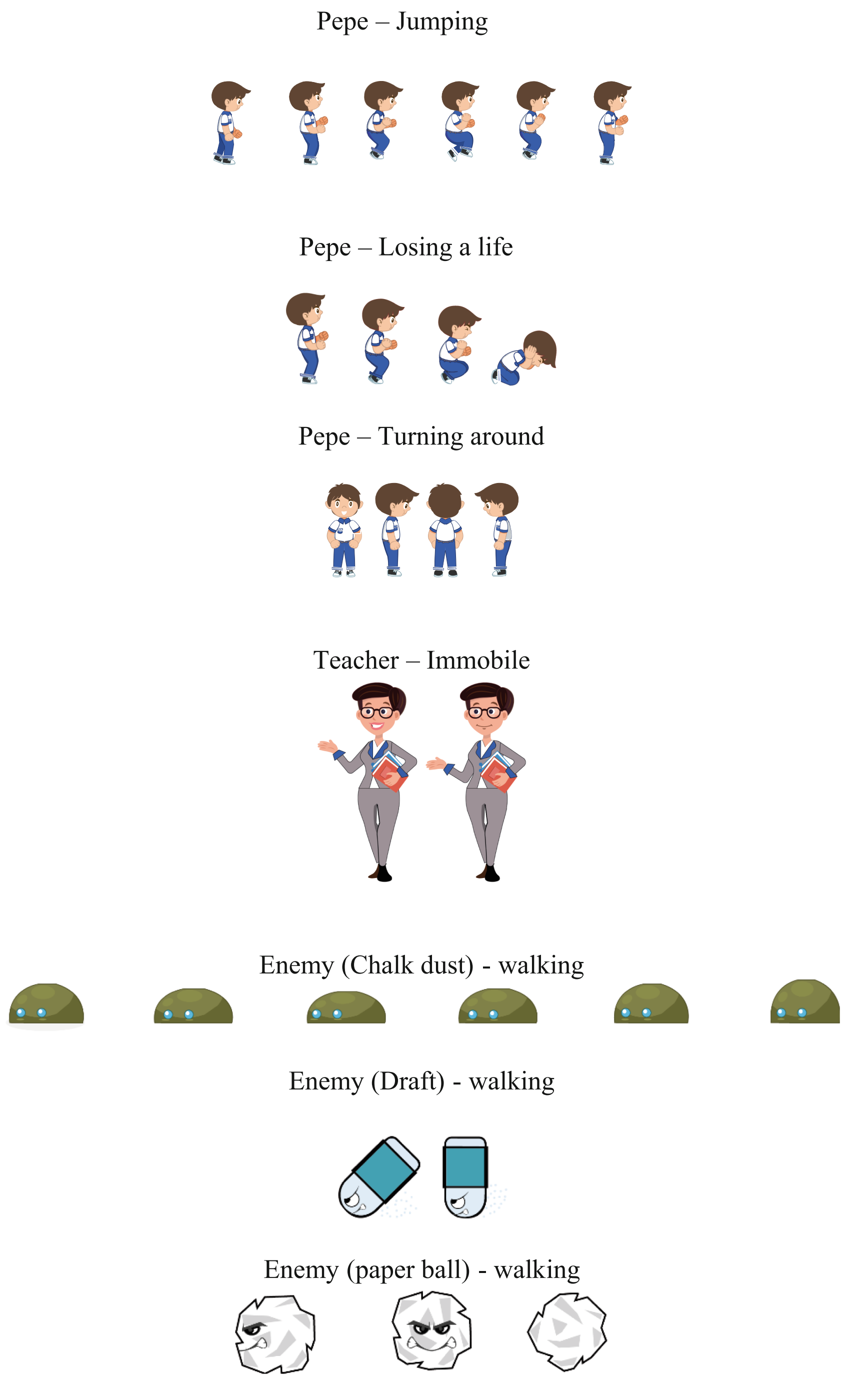

Fig. 7. continued

The game was distributed for its use by means of a cd that had the application to be installed in the computer. Finally, the engine with which the game was made is called Unity, which is a tool that allows making video games through an editor and a scripting that are easy to use, supported by Visual Basic, which is responsible for the programming language. Unity as mentioned above is an engine that is used for the creation of interactive games with architectural designs in real time, as its main feature is that their results are of the highest quality and are made with minimal effort, as it is a very easy to use system.

The video game architecture is shown in Fig. 8 below.

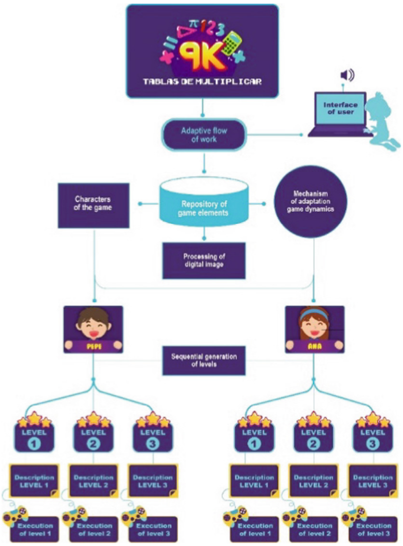

Fig. 8. Architecture of 9K multiplicative tables

In its architecture, the videogame had a dynamic game difficulty adaptation algorithm and adaptive workflow, which allowed the tool to be always challenging and sustainable for the child. The first, which is based on the child's performance in the game, causes the game to change difficulty without the child noticing it; and consisted of increasing or decreasing the degree of difficulty between two related levels according to the mastery achieved in the current level. If at the end of a level, his performance has not been completely achieved, the next challenge would be easier to overcome; but, on the contrary, if at the end of a certain level, he has completely overcome the challenge, the next level would be a little more difficult to achieve, all this accompanied by the flexibility in the child's work flow, as he makes his own decisions through the game, since he can decide on which challenge, he wants to face. Figure 9 shows the development and coding block.

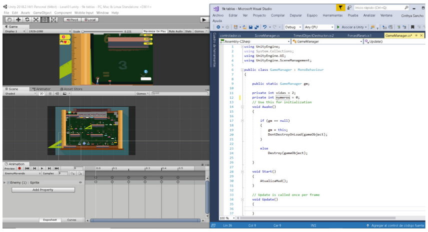

Fig. 9. Unity and visual basic - game engines.

The unified model is a language that allows to describe the game map, in which you can see the interaction that will take place in each scene. In the alpha-ha tests of the video game, first it was tested with a small group and thanks to this it was possible to know some errors such as: the player or avatar that when walking did not flow correctly, some balls with numbering were not valid to be counted with the counter and some interactions with the teacher did not allow the player to follow his path because she obstructed the passage. The beta tests were carried out after having corrected the previous faults of the game; these tests were performed on 12 children of basic education who were in the fourth grade. Finally, the gold master could not be executed since this process is for more commercial video games and the purpose for which this project was developed was experimental in the area of education.

Post-production Phase. The objective of this phase was to commercialize the product, but the purpose of the project was as an experimental program for the area of education.

After the development of the game, a test was carried out with the participation of students from the Gabriela Mistral Institution in San Pedro de Pelileo, in which the prototype of the game was evaluated, seeing positive processes in the children, since it kept them motivated and very focused on the action they were performing, the following evaluation will be described below.

Experimentation in a Real Context

Participants. A total of 12 elementary school children in the fourth grade participated in this study (Table 1).

Table 1. Participants' demographic data

Type	Boys and girls	Chronological age	Level of education
Regular	12	8 y 9	Fourth grade
Total	12		

Experimental Instrument. A laptop and the school's computer room were used as experimental instruments, and the program was installed on the desktop computers using a flash memory (Fig. 10).

Fig. 10. Children using the video game 9K multiplication tables.

Note. Adapted from Aplicaciones interactivas para el aprendizaje de contenidos educativos a nivel básico medio en el cantón Ambato (p.90), Sancho Cinthya, 2019, Universidad Tecnológica Indoamérica.

Procedure. With the authorization of the authorities and parents, we approached the children to validate the function of the video game. First of all, tests were carried out to see if the equipment worked in order to evaluate the tool. Then, with the equipment turned on and the game installed in each machine, the children were told how to play, the purpose of this proposal and some questions were asked to the students to find out their degree of mathematical knowledge. Finally, they were told that they could start playing the game activities and high levels of motivation and concentration could be noticed in them.

Statistic Analysis. For the quantitative statistical analysis, the achievement level data obtained by the students in this new learning strategy were calculated; a quantitative analysis of the data was applied, and it was verified, in the first instance, that the achievement level data, with the two moments of the study (T1/T2), behaved normally; for this purpose and due to the size of the sample, the Shapiro Wilks test was applied ($p > 0.05$). Subsequently, the parametric Student's t-test ($p < 0.05$) with a confidence level of 95% was applied to determine whether or not there were significant statistical differences between the levels of achievement at these two moments.

4 Results

The means, standard deviation and statistics of the achievement levels obtained by the group of students at these two points in time T1 and T2 are shown in the following table (Table 2 and Fig. 11).

Table 2. Means, standard deviations and percentages of achievement level results according to students' knowledge before and after the video game.

Moment	N	M	SD	Achievement level
Before the videogame (T1)	6	8.33	3.771236	69.44
After the videogame (T2)	6	11.67	0.745356	97.22

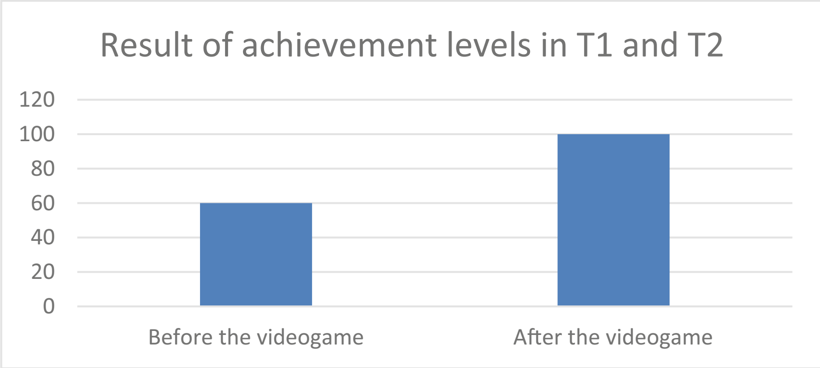

Fig. 11. Statistics of average achievement levels for the methods used.

These results show that with the use of the video game, the levels of knowledge in mathematics increased by 27.78%, in relation to the levels of achievement with the conventional method. However, to determine if there were significant statistical differences between the achievement levels using the video game and the achievement levels using the traditional method, first, the Shapiro-Wilks test was applied, showing the following results: The data of the achievement levels, with the conventional method ($p = 0.500$), and using the video game ($p = 0.172$); which indicates that the data of the achievement levels with the two methods did come from normalized samples. Subsequently, with the results of normality of the data; the parametric Student's t-test was applied to analyze the statistical differences when comparing the achievement levels of the experimentation; showing as a result: ($t = -6.75$, $gl = 12$, $p = 0.000$).

Therefore, it could be concluded that, with the use of the 9K in the classroom, the performance measured by the levels of achievement in the children were superior, compared to the use of the conventional method, since there were significant statistical differences, with a 95% confidence level and a significance level of 0.

5 Conclusions

This research, carried out jointly with teachers, parents and students, was fundamental for the execution of this study. The first interviews gave indications of the importance of creating an interactive software to strengthen the teaching of mathematics in elementary school children. For the realization of the video game, agile methodological principles were applied, resulting in an interface that meets the needs of the target group to which the proposal is being offered, which, when realized, provided the students with all the expected characteristics such as: interest in the subject, concentration, motivation and entertainment at the time of learning. When the game was shown to the fourth grade students of the Gabriela Mistral school in San Pedro de Pelileo, through an analysis of statistical data, it was noted that the game was positive, since an increase of 27.78% was achieved in their knowledge, in relation to the levels they had with the conventional method of learning. The statistical model applied showed that in this study there were significant statistical differences in learning with the use of the video game versus the traditional method; with a significance level of ($p = 0.000$).

6 Future Work

In this study an intervention was made in the area of mathematics learning through the evaluation of a video game in third grade children. As a future work, it would be interesting to evaluate the tool with children with some type of disability, since in the province of Tungurahua there is a great need for technological tools to help in special education centers. It would also be advisable to address other areas such as learning a second language by implementing tools of this type.

References

1. Constitución de la República del Ecuador (2008)
2. Rodríguez, J.M.: Temas relevantes en teoría de la educación, Ediciones Universidad Salamanca (2011)
3. Mominó, J., Sigalés, C., Meneses, J.: La escuela en la sociedad red, UOC (2007)
4. Melero, M.A., et al.: Aplicaciones de las nuevas Tecnologías en el aprendizaje de la lengua castellana, Sociedad Anónima de Fotocomposición (2002)
5. Juárez, A., Mombiela, T.: Los videojuegos, UOC (2007)
6. Granollers, T., et al.: Diseño de sistemas interactivos centrados en el usuario, UOC (2005)
7. Gutiérrez, G.C., Zambrano, P.R.: Sistemas Educativos, UCP, Ed. (2014)
8. Guerrero, A.: Las habilidades sociales en el aula (2009)
9. Bruner, J.: El proceso de educación, Ediciones Uteha (1972)
10. Masip, N.C., Fernández, T.T., Bosco, A.: Los videojuegos como medio de aprendizaje: un estudio de caso en matemáticas en Educación Primaria, **5**(2), 133–150 (2017)
11. Wilson, A., Dehaene, S., Dubois, O., Fayol, M.: Effects of an adaptive game intervention on accessing number sense in low-socioeconomic-status kindergarten children. Mind Brain Educ. Soc. **5**(3), 224–234 (2009)
12. Manrubia, M.: El proceso productivo del videojuego: fases de producción, Historia y comunicación social, 19 (2014)
13. Ouazzani, I.: Ingeniería en Informática, Universidad Carlos III de Madrid. Departamento de Informática (2012)

ICT and Interactive Multimedia in Teaching 3D Sculpting Design

Richard Patricio Sánchez Sánchez[1](✉), Diana Gabriela Flores Carrillo[2], María Cristina Paredes Morales[3], and Paulina Elizabeth Sánchez Sánchez[4]

[1] Universidad Tecnológica Israel, Quito 170516, Ecuador
rsanchez@uisrael.edu.ec
[2] Pontificia Universidad Católica del Ecuador Sede Ambato, Ambato 180207, Ecuador
[3] Instituto Superior Tecnológico Pelileo, MFG6+CW, Pelileo, Ecuador
[4] Universidad Tecnológica Indoamérica, Av. Manuelita Sáenz y Agramonte, 180103 Ambato, Ecuador

Abstract. This research has focused on how information and communication technologies and interactive multimedia have transformed the field of education through the application of interactive multimedia resources oriented to learning three-dimensional design and sculpting through the use of Z Brush. The methodology is based on three phases: Analytical, Creative, and Executive. A quantitative and qualitative approach is presented with the use of surveys and interviews as research techniques. The surveyed group were the students of the Graphic Design School at the Technological University Israel in Quito, Ecuador. The survey's main goal was to determine the student's knowledge of handling Z Brush to create an interactive educational product that could help students learn this software. Experts in 3D design and sculpting were interviewed in order to know the feasibility of this project. In addition, with the prototype of the product, a focus group was held with the students.

Finally, it is concluded that student learning involves improving their learning pace by incorporating ICTs in the classroom, thereby developing new skills and competencies in the construction of knowledge, managing high results, educational quality and opening new possibilities in 3D sculpting learning and teaching.

Keywords: ICT · Interactive multimedia · 3d sculpting · Z brush

1 Introduction

The Israel Technological University (Quito, Ecuador) has always been up-to-date as regards the incorporation of technological resources, in order to be faithful to the fulfillment of its objectives as a university institution. That is why, under the fact of continuing to contribute to the construction of knowledge of the students of the School of Design, this project consists of carrying out the development of a didactic tool to contribute to the learning and teaching of the student body.

© The Author(s), under exclusive license to Springer Nature Switzerland AG 2023
M. Zambrano Vizuete et al. (Eds.): RITAM 2021, LNNS 512, pp. 264–276, 2023.
https://doi.org/10.1007/978-3-031-11295-9_19

To achieve and reinforce the construction of knowledge, one of the highly efficient resources is the creation of an interactive multimedia product that will facilitate the teacher's task in terms of teaching Z Brush since the interactive content will include video tutorials that will facilitate the student learning the software in question. The design student will have the possibility to review the product in the university library. Also, you will find didactic videos recorded by the teacher who will gradually explain the management of the software from its basic mode to a medium level of learning.

The key to the universe of information is now available to any individual or entity due to the innovation and evolution of information and communication technologies (ICT), which have allowed the transformation of access to the most precious and treasured in the digital era: Information and communication. "By new technologies, we mean the set of support tools and channels for the treatment and access to information. ICTs are systems or products capable of taking information, storing it, processing it, and transmitting it. Facilitating decision-making and making the senses intelligible" [1].

ICTs have transformed and revolutionized the daily lives of individuals around the world, as well as different fields, including education inside and outside the classroom. Thus, ICTs play a relevant role in current education, since, by taking advantage of them, it can contribute to academic institutions developing ways of integration and academic training processes in students, thus enabling the introduction of new forms of collaborative teaching and learning. "ICTs can enhance the quality of education in several ways: by increasing learner motivation and engagement, by facilitating the acquisition of basic skills and by enhancing teacher training" [2].

A new panorama in the pedagogical model may arise when the teacher makes use of educational technology as a support alternative that contributes to learning and teaching, as well as to better construction of knowledge from an emotional and sensory perspective. "Educational technology is a dynamic, progressive and important mechanism in the field of education which modifies teaching and learning process" [3]. Integrating ICT by the teacher within their chair contributes to the pedagogical model used by the teacher, increasing student learning effectively. Likewise, the teacher, at the time of imparting knowledge of a certain topic, optimizes time, since, with the implementation of a virtual educational tool, he will not see the need to repeat topics already covered.

To the extent that knowledge regarding 3D Design is built and formed, remembering and/or reinforcing topics already covered in class through the creation of a hypermedia learning system can be of great help to the teacher as well as the student. This also implies that the teacher does not find himself in the task of repeating fundamental topics already covered in the classroom.

"Within the framework of the increasingly demanding use of ICT, organizational and management forms must be provided for teaching practices in virtuality" [4].

Daily tasks - be they simple or complex - have been adapted to new working methods, reconfiguring and modifying organizations in any field. That said, since the appearance of the computer and its evolution by leaps and bounds, it has allowed the birth of a society immersed in the ever-changing and innovative universe of technology, as well as information. Because the internet has become the primary means of accessing information and communication, a sequence of events has occurred that have enabled the processing of data to be deployed, whether sent or stored.

The ICT are immersed in several areas of a social sphere, as a human fact, "The use of technology marks transformative practices that have consequences not only in our ways of doing and in the fields of the social, economic or political, but in our interactions, in the way of understanding the collective or community" [5]. From a sociological point of view, ICT are the nucleus of the information society and are agents of socialization that promote a specific culture. Also, they are cognitive mediators in human activity. They are part of a political and economic project. And, from didactics, they are part of teaching resources.

2 Background

2.1 Multimedia

The term multimedia is not new, since it has gradually been incorporated into the language of the public, making it a familiar term. It emerged in parallel with ICT, which offer the user the experience of obtaining, processing and storing information.

Its etymological definition comes from the Latin Multi (many, multiple) and Medium (medium). So, it involves the combination of multiple media.

Piñeira defines multimedia as "all that integrated narration, devoid of fissures, of different types of data –text, images, sound, audiovisual– in a single digital information environment" [6].

2.2 ICT and Multimedia in the Classroom

Teachers have taken on a new challenge by incorporating ICT, developing skills and competencies to provide relevant learning as a necessary complement and a much more effective method than traditional teaching, and improving learning styles and rhythms by using ICT to manage educational results or quality in a context that operates the information and communication society. "Multimedia learning, as a media and digital technology-based learning experience, enables the learner to engage with instructional content and solve problems by means of self-exploration, collaboration and active participation" [7].

ICTs are a support for the teacher as a complementary parallel activity oriented to their chair, respecting the pedagogical discourse in the training process, where the teacher embraces various technological resources with the purpose that students can self-control their tasks, as well as having greater access to various alternatives and learning resources, thus complementing the construction of knowledge with the use of educational tools that recall, clarify and deepen a specific topic covered by the teacher, doing activities through the online application/offline of ICT, thus contributing to the teaching process and taking advantage of the instantaneous nature of ICT, which facilitates rapid access and exchange of information.

The role of the teacher is not only limited to following the guidelines of a text and transferring their knowledge to students but currently, it is the teacher who recognizes the need to develop in students a digital culture that contributes to the learning process and teaching through the application of multimedia resources which have virtual environments and spaces related to the subject in their content, so the student can interact and associate topics taught in class using an easy-to-understand, intuitive and friendly graphical interface.

ICTs do not have the absolute capacity to comply with the student's educational process, the role of the teacher in the educational process is not limited to informing or communicating through ICT, but the teacher, in addition to teaching the class, relies on multimedia products to direct students to carry out specific activities related to the class.

2.3 Advantages of the Use of ICTs in Education

According to the current constitution of Ecuador in the third section of Information and Communication Article 16 it is established that: All people, individually or collectively, have the right to universal access to information and communication technologies. [8].

The use of ICT by the teacher in the training and process of higher education leads to produce important transformations within the field of education, providing multiple advantages in the teaching of the chair such as:

"The application of Technologies to Education has become a new feature of professional teaching. This forces the teacher to understand the pedagogical potential of this tool, to be trained and to be able to integrate it efficiently into the teaching-learning process" [5].

The space-time barriers to which teaching-learning has been conditioned are eliminated, thereby achieving the construction of a non-real physical space (cyberspace), in which communicative media interactions tend to develop at any place and time.

Although the teacher is addressing a group of students, ICTs act as a personal teacher for each student, thus achieving personalized, objective and effective teaching.

It gives the student as well as the instructor the ease and easy access to information, obtaining current and not obsolete information, and not only textual but also tone, visual and dynamic information.

Using ICT in the classroom means having a subject that is difficult for the student to assimilate into a subject that can be easily understood through a digital program that helps in the student develop awareness.

ICTs visually bring the user to the environments he knows, because they must be identical in the actual and physical settings in which the user lives so that the user feels satisfied with the interface interaction.

ICTs have an impact on the student to catch their attention and interest, inspiring them to dig further into a subject covered by courses, and therefore to learn more.

With greater training and instructional performance, ICT will help to enhance the production of new teaching technologies.

ICTs serve as encouragement to the teacher inside and outside the classroom, so that he can organize and spend his time in other tasks directed at his chair.

3 Method

This research work is built on the basis of 3 phases established by Bruce Archer's systematic model: Analytical, Creative and Executive.

3.1 Analytical Phase

The research approach of this work is compound of a hybrid type since it is qualitative and quantitative. The field research was carried out with the technique of a structured survey, the same one that was oriented to the students of the School of Design of the Israel Technological University in Quito, Ecuador. The sample was 123 senior and sophomore students at senior students at the Technological University Israel, indistinct gender, from 23 to 25 years of age. Through the survey, it was identified that the student's level of knowledge of Z Brush is zero due to this software does not appear within the curriculum of the School of Design of the university in question. That is why the survey determined the interest of the students in learning this software. Thus, the results of the survey were that 90% of the students did not know about the use of Z Brush. Only 11% can differentiate between 3D modeling and sculpting. 86% only use Cinema 4D. 10% have ever heard of Z Brush. 100% of the students would be willing to learn how to use the Z Brush through a multimedia product.

Also, two structured interviews were conducted with Santiago Campaña (Professor at the Israel University in charge of the Chair of Multimedia Design III) and Esteban Durán, Art Director of Norlop Thompson in the city of Quito, Ecuador. Campaña, stated that "The creation of interactive multimedia whose content is the incorporation of video tutorials, it seems to me that it is a very useful tool can be used to reinforce what is explained to them in class, so we do not explain class again to class. Such a project would be quite feasible for students to have a reference and a memory of classes because sometimes writing in a notebook does not make things easier" technologies.

Durán, referring to the use of 3D design and sculpting in his advertising agency, claims that: "There are several factors in which the budget and execution time turn out to be highly determining factors. There are situations where the only solution that can be given to a graphic product is through 3D design. Here, the creative team can have the most spectacular ideas, which could not materialize without the use of this technology".

3.2 Creative Phase

To propose a product name that is easy to associate for the target group, the creative Brainstorming technique was used, in such a way that ideas relevant to 3D sculpting were emitted. This can be seen in Table 1.

The ideas thrown up by the brainstorming were outlined using the Tony Buzan's Mind Maps technique to find a name for the interactive product. In the mind map, 5 different optics were established (language, Z Brush, Design, Target and Visual), the same ones that are considered as the mother roots. Above each root there is a word related to the problem as shown in Fig. 1.

Table 1. Product name brainstorming

Ideas regarding 3D sculpting	Ideas regarding to 3D education
Clay	Beginners
Pixels	New software
Brushes	Video classes
Chiselling	Video tutorials
Chisel	3D sculpted
Z Brushing	Teaching and learning

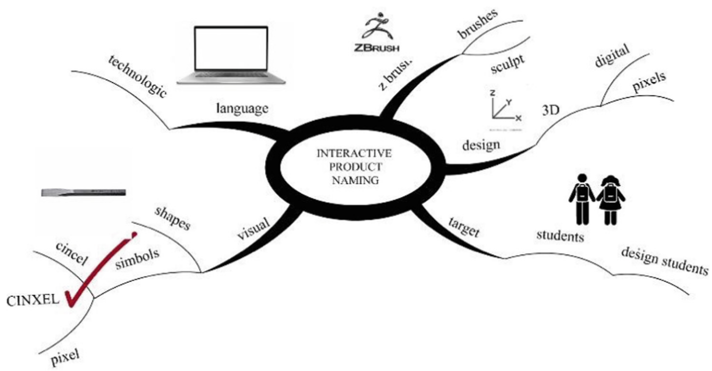

Fig. 1. Mind map naming

An analogy to a sculpting tool was established: the chisel. This tool turns out to be the protagonist of the product identifier. With the guiding idea of taking a chisel into account, the first identifier sketches were made as shown in Fig. 2.

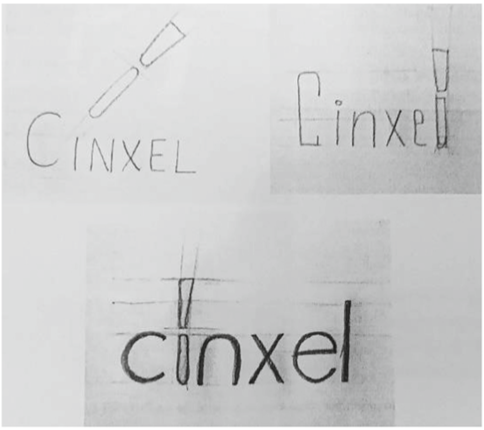

Fig. 2. Logo sketches (Cinxel)

To turn the thought towards the evolutionary and technological, it was taken into account that the pixel is the smallest unit within the digital design, as well as the interface, the aforementioned being the basis for combining the term chisel (cincel in spanish) with a pixel, in such a way that its amalgamation resulted in the product name: CINXEL. Figure 3.

cinxel

INTERACTIVO DE ZBRUSH

Fig. 3. Logo

The character's sketch to be sculpted in 3D in Zbrush is shown in Fig. 4.

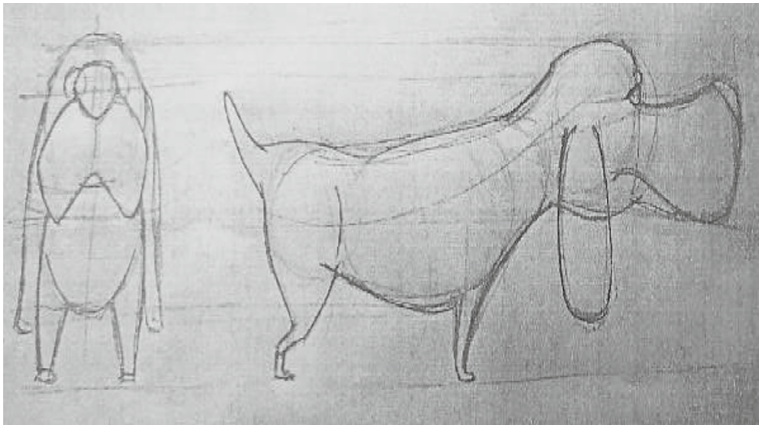

Fig. 4. Character's Sketch

User Interface Design. The constitution of the virtual environment of the product was built based on the affective and cognitive of the principle of multiple entries of Guillem Bou Bouza, hence the graphic and interactive concept is faithfully represented by the content offered to the user: Learning Z Brush as shown in Fig. 5.

Fig. 5. Cinxel graphic user interface

Buttons Design. The buttons on the interface are distributed and organized according to the degree of hierarchy they have and are classified in the following order: Main content buttons, incidental buttons, and recurring buttons Table 2.

Table 2. Buttons classification.

Main content Buttons	Incidental Buttons	Recurring Buttons
NAVEGACION ESCULPIDO APLICACIÓN	shortcuts créditos	atrás home

Interactivity Design. Three-dimensional objects remain static in their UP state, unleashing an animation and sound in their OVER state at the moment the user hovers the mouse over said buttons. Once the user clicks an animation is displayed. Similarly, if the user decides to remove the mouse from the button, a regressive animation or ROLLOUT state of the button occurs Table 3.

Table 3. States of three-dimensional main content buttons

Inactive State (UP)	Actiive State (RollOver)	Animation	Sound
 The letters x and z refer to the 3 three-dimensional axes.	 Movement in the x axis.	The letters x and z are positioned one after the other when the mouse is positioned over them. Color change from red to black.	Letters friction with the ground
 Three-dimensional sphere	 Symmetrical sculpting on the x axis	Animated Deflate indentation sound reminiscent of ZBrush sculpting a 3D object. Color change from red to black.	
 Character to sculpt	 Character reacts to mouse	Character turns his head and wags his tail. Color change from red to black.	Sound of movement

The design of the interaction was oriented to reinforce the message that was wanted to emit, thus achieving an active participation on the part of the user, that is, we wanted to give security to the user to interact with the interface, mainly with the main content buttons (Navigation, sculpting and application). These buttons have a hierarchical location and scale in relation to the other graphic elements of the composition. “Multimedia content, associated with human perception, including acoustic and visual effects, such as animation and graphics, as well as feedback forces, have become very attractive to learners because of the human computer interactions” [12]. Regarding the content of the multimedia product, the video tutorials are grouped hierarchically and numerically, in such a way that the student makes use of the information in a systematic and organized way. The main content sections of the product offer 5 video tutorials as follows:

Navigation: 1) Moving the Interface, 2) Using the Tool and LightBox tool, 3) Applying Color and Material, 4) Symmetry Mode, 5) Handling Brushes.

Sculpting: 6) Types of Brushes, 7) Creation of Masks, 8) Handling Stroke, 9) Alpha, 10) Z-Spheres.

Application: 11) Creation of the Body Part I, 12) Creation of the Body Part II, 13) Creation of the Body Part III, 14) Sculpting of the Body I, 15) Sculpting of the Body II, 16) Preparation for Retopology, 17) Retopology I, 18) Retopology II, 19) Retopology III, 20) Reconstruction, 21) 3D export.

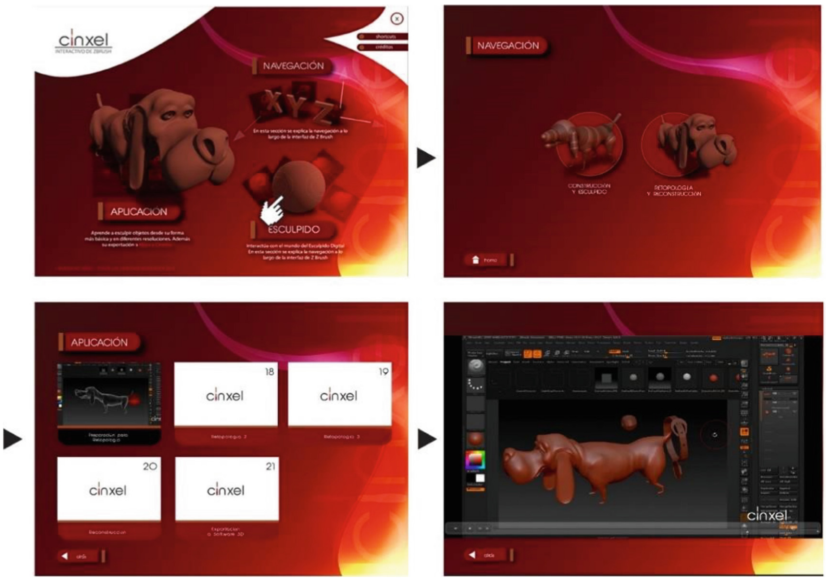

Fig. 6. UI navigation path

Each button of the main content of the interface leads to subsections where explanatory video tutorials are found at different levels. Thus, the most basic level of Z Brush learning corresponds to the "Navigation" section, the intermediate level to "Sculpted" and the advanced level to "Application". In Fig. 6 the UI (User Interface) path to navigate from the Home section to the Aplication series of video tutorials.

3.3 Executive Phase

Experimentation in a Real Context. 12 students participated in a focus group which was held with fourth-year students from the Israel Technological University School of Graphic Design in order to execute a heuristic test of the product interface.

Statistic Analysis. First, the level of understanding data obtained by the students when using the multimedia product was calculated. In this way, a quantitative analysis of the data was applied and it was verified that the data of the levels pointed to the two moments of the study (T1/T2). Second, due to the size of the sample, the Shapiro Wilks test ($p > 0.05$) was applied. Finally, the parametric Student's t test ($p < 0.05$) was applied with a confidence level of 95%, to determine whether or not there were significant statistical differences between the levels of achievement, at these two moments.

During this evaluation, it was observed that the accessibility and language used was understandable, the coherence between the navigation elements allowed familiarization with the student, thus offering a pleasant interactive experience and showed interest in doing the Z Brush video tutorials from its most basic to advance level Fig. 7.

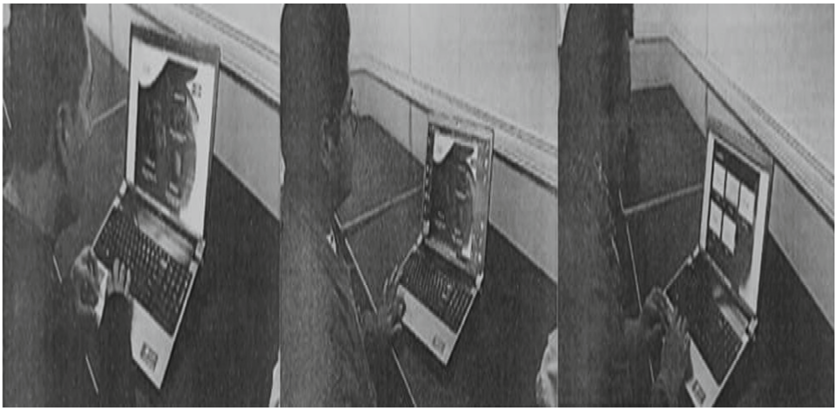

Fig. 7. School of graphic design students focus group

4 Results

Table 4 shows the average, standard deviation, and statistics of the levels of achievement achieved by the group of students in these two moments T1 and T2.

After conducting the Focus Group, it was identified that: 85% of the students rated the Cinxel interface as user-friendly to navigate due to its understandable and direct content. 100% to the distribution of the interface elements as excellent. 75% said that interactivity lent itself to correct navigation. 100% indicated that they would be interested in learning Z Brush with the help of the featured product.

Table 4. Percentages of the results of achievement levels according to the knowledge that the students had before and after the use of the multimedia product

Interaction	N	M	SD	Achievement level
Before using the multimedia product (T1)	6	8.33	3.771236	69.44
After using the multimedia product (T2)	6	11.67	0.745356	97.22

Finally, video tutorials regularly are recorded in English or Spanish with an accent from Mexico or Spain, the students' empathy with the product was to take into account the Ecuadorian Spanish accent in the instructor's voice.

4.1 Critical Appraisal

Changes were made to improve usability, navigation and functionality detected in the Focus Group. It was observed that the background of the audio that the interface had was uncomfortable for users, in such a way that it was removed.

The duration time of the button arming and disarming animation has been improved. Intro animation time for video tutorials has been reduced. Following Bouza's feedback principle, a closing section was implemented where the user has an active participation until the moment, he decides to leave the virtual environment, that is why said section was added where the user is asked if you really want to exit Cinxel, having 2 options to choose from: YES (to leave the interactive), and NO (to return to Home) Fig. 8.

Fig. 8. Asking the user to return to the home section

5 Conclusions

After completing and researching this project, the following conclusions were reached:

The inclusion of ICT and Multimedia within the classroom supposes to be a pedagogical tool of great use for both the student and the teacher in the context of the educational process.

This multimedia product for the learning and application of Z Brush implies applying the knowledge obtained in the professional and work environment in advertising agencies and creative studios.

The interactive product is valid since the students corresponding to the graphic design faculty of the Israel Technological University have little knowledge of digital sculpting in 3 dimensions.

Also, the great demand for professionals with knowledge of three-dimensional sculpting makes this project viable in its development and interest on the part of the student.

The teacher in charge of the three-dimensional design subject will have at their disposal a didactic multimedia material that allows the student to combine the three-dimensional modeling with the digital sculpting.

Finally, it is concluded that the multimedia product presented to the Technological University Israel is unique in its own right and its content corresponds to the first version of several that can be further developed.

References

1. Simon, J.: Experiències multimèdia en la docència de la Facultat de Farmàcia (UB). I Jornades Multimèdia Educatiu, Barcelona (1999)
2. Sharmila, V.: ICT in Education. 1st (edn.). Lulu, USA (2019)
3. Tripathi, H.: Educational Technology and ICT in Education. Redshine, USA (2019)
4. Tenaglia, P.R.: Las TICs en el aula: narrativas de práctica docente y gestión directiva. Córdoba: Editorial Brujas (2016)
5. Caballero, F.S., y Benítez-Eyzaguirre, L.: TIC y comunicación para el desarrollo. Barcelona: Editorial UOC (2020)
6. Piñeiro, T., Otero, C., Sánchez, C.: Multimedia communication strategies. Barcelona: Editorial UOC (2014)
7. Jenlik, P.: Multimedia Learning Theory. Rowman & Littlefield, London (2019)
8. Ministerio de Educación: Constitución del Ecuador. Retrieved on 18 August 2021. https://educacion.gob.ec/wp-content/uploads/downloads/2012/08/Constitucion.pdf

Management Tools for Process Mapping and Modeling in Assembly Industry

Rodrigo Arcentales-Carrion[1](✉), Eliezer Colina Morles[2], Dolores Sucozhanay[3], Regina Duran[4], and Lorena Siguenza-Guzman[5]

[1] Faculty of Economic and Administrative Sciences, University of Cuenca, Cuenca, Ecuador
rodrigo.arcentales@ucuenca.edu.ec
[2] Research Direction, University of Cuenca, Cuenca, Ecuador
[3] Interdisciplinary Department of Space and Population, University of Cuenca, Cuenca, Ecuador
[4] Southwestern Provincial University, Bahía Blanca, Argentina
[5] Department of Computer Sciences, Faculty of Engineering, University of Cuenca, Cuenca, Ecuador

Abstract. In a highly globalized world affected by economic policies and a latent COVID-19 pandemic, companies need to organize or reorganize to achieve efficient operations. The correct management of organizations has led their administrators to adopt resourceful management models that guide their activities towards fulfilling their objectives. Thus, management tools have been presented as an effective alternative to control processes and activities. According to a previous study, the main tools that allow process mapping and modeling are Business Process Management (BPM), Business Process Reengineering (BPR), and Event Process Chain (EPC). This article analyzes their characteristics based on compatibility and affinity with four case studies dedicated to the assembly industry using this previous study. In addition, the advantages and disadvantages of the three tools related to the possible adaptability in the four companies are studied. This work uses qualitative qualification matrices, which answer specific questions, determine the potential improvement of organizational management, and create a methodology for mapping and modeling processes.

Keywords: Business process management (BPM) · Business Process Reengineering (BPR) · Event Process Chain (EPC) · Management tools · Process

1 Introduction

Today, assembly industries face increasingly complex challenges generated, on the one hand, by external factors such as globalization, the development of new technologies, regulations, and government policies, and, on the other hand, by internal factors such as the limitation of resources, slow response to change and low productivity. These factors have altered the management of companies, directly impacting their operating costs and, therefore, their results. Consequently, achieving its objectives is undoubtedly affected and can directly affect the fulfillment of activities and processes.

© The Author(s), under exclusive license to Springer Nature Switzerland AG 2023
M. Zambrano Vizuete et al. (Eds.): RITAM 2021, LNNS 512, pp. 277–290, 2023.
https://doi.org/10.1007/978-3-031-11295-9_20

In the Ecuadorian economy, the assembly sector has become one of the fundamental pillars of its development and growth. However, this sector has been dramatically affected by government decisions such as the opening of borders to imported products, increased tariffs, new tax burdens in addition to the global pandemic generated by COVID-19. Thus, among the most affected companies are those dedicated to the assembly of motorized vehicles and televisions [1]. In 2020, around 700,000 televisions were marketed, with a reduction in sales of about 10% compared to 2019. Of these, 86% were assembled in the country, which marks a direct relationship with companies that manufacture electronic components to produce these devices.

Furthermore, according to the data presented by [2], the motorcycle assembly sector sold around 130,000 motorcycles in 2020, showing a drop of approximately 10% compared to the previous year. Finally, unlike the earlier sectors, the bicycle assembly sector, which assembled around 350,000 units in recent years, increased its production by 30% and its sales by approximately 300% in 2020. However, as described above, significant losses have been recorded. They have even forced its temporary or permanent closure [3, 4]. Therefore, adopting management models and tools would allow companies to face the complications and economic losses described in the search for efficiency in their management.

In [5], three tools immersed in the management tools were prioritized, Business Process Management (BPM), Business Process Reengineering (BPR), and Event Process Chain (EPC). Based on its characteristics, advantages, and disadvantages, the study analyzed the connection between the international standard ISO 9001 and Time-Driven Activity-Based Costing (TDABC). Using this preliminary analysis, the purpose of the present study is twofold. First, perform a compatibility analysis of the main characteristics of the tools prioritized by four case studies that assemble televisions, printed circuit boards (PCBs), motorcycles, and bicycles). Second, perform an affinity analysis of the strengths and weaknesses of these tools in the same companies. These two objectives intend to establish a methodology for mapping and modeling processes that improve organizational management and optimize processes, times, and costs. The structure of the remainder of this paper is as follows. Section 2 presents a theoretical background that addresses management, processes, and those tools that enable the mapping and modeling process. Section 3 builds the methodology through which this study was carried out. Section 4 covers the results obtained along with their analysis and discussion. Finally, Sect. 5 determines the main findings, conclusions, and future research.

2 Theoretical Background

According to [6], the verb to manage comes from the Italian maggiore, which derives from the Latin manus (hand). The French word “mesnagement” influenced the English word “management” in the 17th and 18th centuries. The evolution of this concept over time from the earliest civilizations denotes the ability to organize large-scale activities that were efficient and effective. Nowadays, the modern use of management stems from the rapid development of North American industries in business and entrepreneurial skills

[7]. For its part, [8] indicates that management must clearly understand that business processes are a fundamental part of business success and defines how things are done. Thus, the different processes depending on the people who execute them, their contribution to management, and their degree of contribution to achieving the proposed objectives. Consequently, these procedures are classified into macro-processes, sub-processes, and sub-process activities. Macro-processes contribute to the fulfillment of the mission; the sub-processes are the disaggregation of processes, facilitating their management; and the activities are tasks that help generate products or services [9]. The classification of the types of processes depends, among other factors, on the function they fulfill, the people operating them, and their impact on the company's performance. Thus, the processes are classified into strategic, support, and operational processes. Strategic processes, carried out by senior management, are often long-term. In general, operational processes are related to the production of goods and directly impact customer satisfaction. Finally, the support processes aim to help operational processes [10].

Authors such as [8] indicate that process management should be a fundamental part of the business, where executive commitment is essential. However, many companies use standards or different reference models to establish documents and maintain management systems, which allows them to promote and control their organizations. Therefore, defining process mapping stages is essential for companies to function regardless of the model used. According to [5], process mapping is a manner of representing processes, sub-processes, and activities as accurately as possible in search of achieving a particular result or product.

According to [11–13], there is a series of tools for the mapping and modeling process; being the most common in the literature, BPM, EPC, BPR, Definition of Integration for Modeling Functions (IDEF), Unified Modeling Language (UML), Data Flow Diagram (DFD), Structured Analysis and Flow Model of Design Techniques (SADT), and Business Activity Monitoring (BAM). However, [5] prioritize the first three by analyzing their characteristics, advantages, and disadvantages. In addition, the authors indicate that the tools have a high degree of compatibility with the ISO 9001 standard [14] and their affinity with the TDABC costing system [15].

BPM seeks to develop a process-oriented organization, eliminating activities that do not add value and improving its flow within the organization's limits [16]. According to [12], BPM is implemented in many organizations through a series of steps and activities called the BPM life cycle. Authors such as [17–19] present this tool as a form of organizational change characterized by the strategic transformation of interrelated organizational subsystems that produce different levels of impact. BPR is recognized as an organizational change characterized by strategic shifts and interrelated organizational subsystems with other effects levels [19]. This tool is process-oriented; simultaneously, it pursues breakthrough improvements in quality, speed, and cost. BPR is holistic, leverages technology, empowers people, and begins with a willingness to abandon current practices [20]. Finally, EPC is one of the best-known Business Process Modeling Languages (BPML) [21]. This tool is commonly chosen because it was developed using the concepts of stochastic networks and Petri nets within the framework of the Architecture of Integrated Information System (ARlS) [22]. In the EPC model, a process consists of sequences of events that trigger business functions, resulting from other parts, and the initial events that initiate the entire process [23]. EPC modeling originates from the idea of an event transaction diagram, a graphical formalism to model the dynamic part of the global informal schema of an organization. It is compatible with BPR in the identification and redesign of critical business processes [24].

3 Materials and Methods

The present work arises from work [5], through which a theoretical analysis of management models and tools for the mapping and modeling process was carried out. The authors analyzed their features, advantages, and disadvantages based on prioritized devices and ISO and TDABC compatibility. Based on this, the current article validates the prioritized tools in four case studies. The first case is related to a company dedicated to assembling televisions, which partially automates its processes. The second is an organization devoted to PCB assembly, which features automation in its operations. The third, a company dedicated to motorcycles, carries out its manual processes in work cells. Finally, the fourth case corresponds to an entity devoted to the assembly of bicycles, which also executes its strategies manually.

For the corresponding analysis, this work first performed a study related to the characteristics of each prioritized tool, in contrast to each case study. The following questions were raised: 1) Is the function compatible to be considered in the company? 2) Is the characteristic suitable to be considered in the company? Based on this, Table 1 presents the analysis of the BPM, BPR, and EPC tools, the main characteristics, and the degree of compatibility with the television case study. In Table A2, the same process is presented for the case study of PCBs, Table A3 for the analysis of the case study of motorcycles, and Table A4, for the analysis of the case study of bicycles. It should be clarified that in each table, the symbol (o) refers to characteristics that comply with the answer to the questions based on the organization's compatibility and/or convenience analysis. At the same time, (x) symbolizes not being fulfilled. (Complete Table 1 and summary of the list of features examined based on each case study can be found online at: https://imagineresearch.org/pmm_appxa/).

Table 1. Main features analysis based on the case study of televisions

Features	BPM – x/o	BPR – x/o	EPC – x/o
Use new or existing processes	o	x	o
Risk	o	x	o
Change	o	x	o
Time required for implementation	o	o	o
Collaboration	o	o	o
Separately work/Simultaneously work	x	x	x
Financial impact	o	x	o
Cultural impact	o	x	o
Cost of implementation	o	x	o

A second analysis was carried out based on the main advantages and disadvantages of the BPM, BPR, and EPC. For this, each tool was verified according to its affinity with each case study. In conducting the review, the following question was asked: 1) Is the one described as an advantage/disadvantage for the company? Table 2 compares the advantages and disadvantages of BPM, BPR, and EPC, with the case study of TVs. In turn, Table B2 presents an analysis for the PCBs case study. Finally, Tables B3 and B4 also perform a similar review with the motorcycle and bicycle case studies, respectively. As in the previous analysis, the symbol (o) refers to whether the advantage or disadvantage is presented, complying with the affinity analysis of the organization, while (x) symbolizes not fulfilled. Finally, it is worth mentioning that, to guarantee the quality of the research, an expert on the subject verified the findings and compatibility of each feature of the tools and their affinity analysis of advantages and disadvantages of BPM, BPR, and EPC with each company. (Complete Table 2 and summary of advantages and disadvantages analyzed based on each case study can be found online at: https://imagineresearch.org/pmm_appxb/).

Table 2. Analysis of advantages and disadvantages based on the case study of televisions

	Advantages	x/o	Disadvantages	x/o
BPM	- Applicable to any project - Design and modeling of the process are prioritized	o o	- Starts without being prepared - Does not contemplate an initial analysis phase	x x
	- Follow up can be performed by any user, not only technical	o	- Thinking is based only on functions	x

(*continued*)

Table 2. (*continued*)

	Advantages	x/o	Disadvantages	x/o
	- Processes are modeled through BPMN	o	- Does not consider the end-users	o
	- Techniques applied are commonly used	o	- Approach is based on the short term	x
	- Improves understanding and visualization of processes	o	- Decision making becomes empirical	o
	- Allows improvements in time and costs	o	- Sometimes, it applies techniques or steps	o
	- Provides a continuous process improvement approach	o	- Must be complemented with other methods	o
	- Provides robust tools to increase the development and automation of processes	x	- Requires a multidisciplinary team for its implementation	o
			- Requires time to verify results obtained	o
BPR	- Effort concentrated in areas of the organization and specific procedures	x	- Resistant to change	o
	- Get improvements in a short time	o	- Implies a high risk since changes that arise are radical	o
	- Generates a reduction of defective products	o	- Initially, it only took into account the operational section and neglected the redesign of the Administration	x
	- Increases productivity and directs the organization towards competitiveness	o	- Reengineering has served as a perfect excuse for the dismissal of staff and elimination of jobs	x
	- Contributes to the adaptation of the processes to the constant technological advances	o		
	- Allows eliminating repetitive processes	o		
EPC	- Powerful and easy to understand for end-users - Used to capture and discuss business processes	o o	- Presents an unclear link between activities and objects	o
	- Models can be refined and used for the definition of requirements of an information system - Connections to traditional modeling methods have been very useful	o o	- Occasionally, far from being complemented, EPC has been gradually replaced by BPMN	x

4 Results and Discussion

In this section, the results and the discussion of the compatibility and affinity analysis of the BPM, BPR, and EPC management tools are detailed in the four case studies of companies that assemble televisions, PCBs, bicycles, and motorcycles.

4.1 Compatibility Analysis

The characteristics present in each tool prioritized by [5] were fundamental for developing this work since it allowed knowing the degree of affinity of each tool in terms of the ISO 9001 standard and the TDABC system. The questions described above were applied to determine the compatibility of these characteristics with each case study analyzed. Therefore, the responses decided whether their compatibility would allow proposing a possible mapping and process modeling methodology.

TV Assembly Case Study. Based on the results presented in Table 1, corresponding to the televisions case study, it has been determined that this organization is dedicated to the assembly of its products through the semi-automation of production lines. Therefore, the answers to the questions based on the BPM characteristics included that the automation or reuse of existing processes is crucial. It is agreed that the implicit risk in its application is low and that the change processes are continuous since it will always migrate to new television models that come with new technologies. Furthermore, the time of BPM implementation is indifferent since, in this organization, it has partially worked based on a process management system. In addition, the collaboration of people and information technologies is essential for its adoption. It is also positively associated that its implementation leads to the optimization of assets, that it does not affect the organizational culture and that the cost of its performance is not high. When working by processes, it already has specific inputs that would minimize the time required. However, it is also found incompatibility when referring to the fact that one or more processes can be taken and work simultaneously because assembling the products is contemplated step by step, later for the conception of the final product.

Subsequently, the television assembly company was subjected to questions based on the characteristics presented by BPR. The answers determined the compatibility with only two characteristics; in the first place, considering the time it takes to implement it and the optional collaboration of information technologies indifferent because it already has partially adopted processes. In addition, it could not work with processes simultaneously, since as previously indicated, the entity works sequentially step by step. The characteristics with which it disagrees are those in which the organization does not consider an applicable characteristic to reuse existing processes and even less start operations from scratch. This would lead to delays in production. Similarly, as the impact risk of its implementation is high, this organization may not be able to use this alternative. Also, it will consider leaving the most significant changes until the end, when the practice of its walk is already marked in its assembly processes. Finally, unlike BPM, the possible implementation of BPR has high economic impacts; since recreating processes can cause massive layoffs of personnel, the cultural influence can be substantial. Consequently, the cost of starting from scratch in many cases is very high, depending on the time it takes to implement it. For these reasons, these characteristics would not be supported by the organization.

A third analysis corresponds to the same case study based on the characteristics of the EPC tool. In this sense, the responses show that EPC is dedicated to processing modeling. It can become a primary or complementary tool to other similar tools that allow compatibility. Therefore, the organization supports most of the functions, and it is accepted to work with the process map of another tool to develop flowcharts. The administrative risk of being implemented is low, which is accepted by the company. When mentioning that the change is continuous, it is agreed that it favors the adaptability of new models (very common in this entity). In addition, the implementation time is not representative, and the collaboration of information technologies is attractive because, being a technological tool, it is essential for its implementation. Also, it is not culturally impactful and inexpensive since it is only dedicated to developing flowcharts. Finally, the only character it disagrees with is that it is considered to work simultaneously with several processes since, as indicated, this entity develops a sequential assembly (step by step).

PCBs Assembly Case Study. A similar analysis, in which the exact characteristics of the BPM, BPR, and EPC tools were considered, is presented in Table A2 through the PCBs assembly case study. According to what has been described, to achieve its final products, this entity performs an automated assembly due to the technical degree it must have. Thus, the analyses carried out from the three tools were similar in compatibility and incompatibility characteristics to assembling televisions, presenting practically the same responses related to the shift of their activity and assembly modality.

Motorcycle Assembly Case Study. The following analysis is presented in Table A3 for the case study of motorcycle assembly. This organization is dedicated to the manual assembly through work cells of its products; therefore, labor is considered a critical factor in its processes. The review agrees that the administrative risk in case of implementation is low, which would be beneficial since it would not involve problems in its adoption. In addition, the entity considers the time it takes to be able to adopt it with indifference. Besides, there must be collaboration since it is a crucial issue to be done. Considering that, regarding the characteristic that it is possible to work with different processes simultaneously, it is deemed to be compatible with this company due to its manual operation. The assembly is carried out even in parts. Continuing with the review, like any organization, it agrees on the importance that there can be an optimization of assets and that it is not culturally and monetarily affected. However, it finds incompatibility in two characteristics: the automation or reuse of existing processes, since it has not considered for the moment to change its manner of operating and, the fact that the change process is continuous due to its manual form to perform.

The analysis of the characteristics related to the BPR determines the compatibility with the creation of processes from scratch because its assembly is manual. This organization does not previously have a management system that has previously managed the mapping of its operations. In the same manner, it is considered indifferent that significant changes and the implementation time are left until last since, as there is currently no system, this would be viewed as an improvement. In addition, despite being optional, it appreciates the collaboration for its adoption. Moreover, it could work with different processes simultaneously; in fact, the assembly of these products is carried out in parts from start to finish. Therefore, it is appropriate as indifferent and compatible to opt for the technification or the change in its assembly form since it would take a considerable time to continue maintaining their jobs in the medium term. It would also support that the company could be technologized or switched to production on a semi-automated or automated line, despite the high cost of implementation. Therefore, the compatibility analysis is almost complete, except for the characteristic related to the administrative risk in a possible implementation that could be managed with a good project analysis if considered.

Finally, in the case of EPC, the compatibility is almost total, only showing incompatibility in the fact that the change process is continuous due to the manner it operates (for now, the company does not plan to change it but sees with good eyes that half term may happen). Although the compatibility with the rest of the characteristics is explained in that, as EPC is a tool dedicated to processing modeling, it could become a primary or complementary tool to other similar that allow compatibility. Thus, it is feasible to carry out the process maps based on the elaboration of flowcharts. Therefore, the administrative risk of a possible implementation is considered low, and that the time is practically insignificant. However, it deems fundamental the point of the participation of information technologies (because it is a technological modeling tool), as well as, it could work with several processes at the same time and, considering that it does not affect the cultural impact and that make only flowcharts, the cost of adoption is not considered high.

Bicycles Assembly Case Study. Regarding the characteristics presented in Table A4, the final analysis corresponds to the case study of the bicycle assembly company. Thus, an analysis similar to those described above was carried out. However, it is worth mentioning that this company also operates similarly to the motorcycle assembly case study dedicated to manual assembly. Therefore, the analyses carried out using the three tools were practically identical in terms of compatibility characteristics with the motorcycle case study, related to the shift of their activity and assembly method. At the same time, it considers incompatibility concerning the same as in the case of motorcycles, for the same reasons already described.

4.2 Analysis of Advantages and Disadvantages of BPM, BPR, and EPC

This analysis arises from the advantages and disadvantages found at the literature level of each of the prioritized tools in terms of integration with the ISO 9001 standard and the TDABC system [5]. Thus, the question posed for the analysis was: is the referenced advantage/disadvantage an advantage/disadvantage for the company? For example, when describing that BPM applies to any project, regardless of the Business Process Management Suite (BPMS), the answers consider an advantage marked with the sign "o" for the case study. Those who believe that it is not advantageous were represented by the symbol "x". A similar analysis occurred with the disadvantages of each tool.

TV and PCBs Assembly Case Studies. Table 2 and B2 present the main advantages and disadvantages of the prioritized tools for their analysis with the assembly of TVs and

PCBs case study. These organizations carry out their assembly activities semi-automated in the case of televisions and automated in electronic components. In this sense, when completing the question, it can be mentioned that the answers to the advantages and disadvantages of each tool respond similarly. Depending on the analysis, all those described by the BPM tool were recognized as advantages, among other things, since the two entities had partially adopted ISO process certification [14] some time ago. Thus, they agree benefits such as that BPM applies to any project involved in these organizations. Likewise, prioritization in the design and modeling processes is essential because the entities had already recognized adopting a process management system based on the ISO standard. Next, the fact that anyone can implement it is crucial, although it is considered that it should be guided by someone who knows the subject. In addition, working with BPMN (Business Process Model and Notation) for modeling is a great advantage since it is an easy language to understand through commonly applied techniques. Likewise, collaborating in the visualization and understanding of processes and allowing improvements in time and costs is crucial for any company, permanently improving processes. However, the only advantage they disagree with is how their tools increase method development and automation. As mentioned, these organizations already assemble through automation and/or semi-automation process.

Although, regarding the disadvantages of BPM, it is indifferent not to start without being prepared, nor to contemplate an initial analysis phase, since, as mentioned, they already have a partial management system, adopted previously; therefore, it is not considered a real disadvantage. Likewise, not considering the end-users is a disadvantage for these entities since the feedback will be constant in all the company's controls. But, on the contrary, they agree that the rest of the characteristics, such as thinking is based solely on functions, are a real disadvantage since they expect integral work by processes. In addition, the fact that decision-making becomes empirical without using fundamental reasoning and without adopting specific steps could delay its implementation, being real disadvantages. Furthermore, as it is not a comprehensive system, it would be necessary to integrate it with other methods (to cover time, costs, among others). Likewise, anyone could implement it without requiring someone specialized to guide the team. Finally, verifying the results obtained can take a significant time; thus, it is effectively considered a disadvantage.

In terms of advantages, the analysis of the BPR tool suggests coinciding with all those mentioned, mainly achieving visible improvements in a short time and a significant reduction in products with defects. In addition, it increases productivity, keeping up with the technological advances that may exist. However, it disagrees with concentrating efforts only on specific areas since it is considered in these companies that the analysis must be comprehensive. Furthermore, in studying the BPR disadvantages, organizations agree on resistance to change. If required, they should tend towards it, assuming that it would be expected to imply an immediate improvement despite the risk it would entail. At the same time, they do not consider it a disadvantage because it is applied only to redesign the operative section since this work is fundamentally based on that section. Finally, the possible application of this tool does not see the elimination of jobs as a disadvantage, since, being semi-automated in televisions and automated in PCBs, the people who work are few, and their jobs would be guaranteed.

A final analysis considers the contrast of the advantages and disadvantages of EPC in comparison with the two assembly companies. This tool is considered for process diagramming. Its application benefits are many, that is why the two companies are under the advantages it presents in terms of its ease of application and uses, that no previous knowledge is needed for its application, and its ability to be combined with other tools to improve the results. For its part, a disadvantage is that it is not very clear and specific in the link between activities and objects, but that it is replaced or, failing that, combined with BPMN.

Motorcycles and Bicycles Assembly Case Studies. The analyses corresponding to the advantages and disadvantages of the prioritized tools in the motorcycle and bicycle case studies are presented in Tables B3 and B4. The quality that identifies and familiarizes these two organizations is that their form of assembly is manual. For this reason, in analyzing the advantages and disadvantages of each tool, the answers of agreement or not, both advantages and disadvantages, are practically the same. In this sense, in the analysis of the benefits of the BPM tool, the two case studies show agreement with all those described. For this reason, they consider it essential that the tool be applied to any project and applied in any case study. For their part, these companies do not currently have the adoption of a process management system. Therefore, they consider it essential to move towards it and be certified through the ISO 9001: 2015 standard (in the medium term). Those advantages such as prioritization in the design and modeling of processes, the use of diagramming through BPMN, and the establishment of visualization and understanding improvements from the mapping of processes are considered of utmost importance. Therefore, they would collaborate in a possible adoption of the tool. Likewise, improving the time of completion of the processes would mean a considerable advance in product assembly efficiency. They coincide in pointing out that it is not essential to provide tools for process automation since they are assembled manually. As for the disadvantages, begin without prior preparation, or an initial analysis phase is indifferent or fails. Furthermore, it does not consider the end-users since it is assumed that all collaborators would be reached, which would allow feedback to all interested parties. However, they agree that it is based on features only and is seen as real downsides, that its focus is short-term only. This decision-making reaches a point where it becomes empirical because if these organizations decide to make a radical change in their manner of assembly, it must be established in the long term and promote informed decision-making and not only based on empiricism.

For its part, the advantages presented by the BPR tool coincide with the structure and administration conditions offered by the case studies. For example, its improvements are reflected in the short term as a consequence of its application. It collaborates in reducing the production of defective products. It increases productivity and competitiveness, is open to the insertion of technological advances, and allows restructuring and eliminating those repetitive processes that do not contribute to the organization's growth. At the same time, they only do not coincide in their appreciation with the case studies. This advantage indicates that efforts are concentrated only in certain areas since it has been determined that these organizations require application in their entire infrastructure by themselves. Internal organization with which they operate. In terms of disadvantages, they agree to resist change since they hope to maintain their manner of performing at least in the medium term; since these changes can be radical, affect their operation, and involve significant risks. Likewise, they disagree that working in operational areas is a disadvantage since, in these organizations, the administrative section is correctly delimited. It does not determine the issue of reengineering as a risk in the medium term. Therefore, its workers would have their jobs secured and contemplate massive layoffs in the face of significant structural changes.

Finally, regarding the EPC tool, its advantages and disadvantages are presented, of which, when considered, it is known as a valuable tool for process diagramming. The two companies coincide in their application benefits and the advantages presented, such as ease of application and use. Furthermore, no prior knowledge is required for its application and its ability to be combined with other tools to improve results. Regarding its disadvantages, they agree that the link between activities and objects is not very clear and specific, but shows their dissatisfaction with what has been expressed as to whether it is complemented or replaced by BPMN since it would be considered that this would enrich its application and use.

From the results presented in Tables 1, A2, A3, and A4, it can be determined that there is high compatibility between the characteristics of the tools and the case studies when answering the questions posed. Thus, companies assembling televisions and PCBs have greater compatibility with BPM and EPC than with BPR because the latter suggests more remarkable and more profound changes in internal processes. Although the case studies of motorcycles and bicycles also show compatibility with all three tools, profound changes should be adopted internally due to the lack of automated or semi-automated processes. The results presented in Tables 2, B2, B3, and B4 indicate a strong affinity between the advantages of the tools and the case studies. Therefore, the benefits determined in the four case studies are strongly related. At the same time, the disadvantages almost go unnoticed, regardless of the products or their manner of production and in the search for an improvement in management.

5 Conclusions and Future Research

Management is a subject in continuous evolution that provides industries with precise control of their operations and the resources consumed in their execution. Thus, management has become a fundamental piece in the daily work of organizations. Immersed in it, some tools collaborate in the mapping and modeling of processes. In this study, three have been specifically considered: BPM, BPR, and EPC, based on their characteristics, advantages, and disadvantages, which connect with the ISO 9001 and TDABC standards. To do this, first, the characteristics of each tool were analyzed according to their compatibility in four assembly companies: televisions, PCBs, motorcycles, and bicycles. The answers to the two questions posed about the tool's compatibility with the case studies allowed, through the qualitative tables, Table 1, A1, A2, and A3, to determine those characteristics that presented compatibility in adopting the analyzed characteristics. Thus, most of them have a very high degree of receptivity to each tool and, at the same time, a lower degree of incompatibility. Therefore, it would be acceptable due to the characteristics of a possible application of the tools in the organizations studied.

Next, a second analysis was carried out through the advantages and disadvantages of each tool and its affinity with the case studies. The answers obtained allowed determining the degree of association or not of each benefit and/or burden based on BPM, BPR, and EPC and the entities dedicated to assembling televisions, PCBs, motorcycles, and bicycles. The final tables have made it possible to determine that most of the benefits are well received by organizations. In turn, few disadvantages would lead to a decline in its application. Therefore, it would be interesting to think about the possible compatibility of tools, which allow the mapping and modeling of processes in assembly companies as essential inputs to adopt an ISO 9001 standard and a TDABC costing system that improves their management and results.

Future research is underway to design a new methodology that integrates the tools analyzed for process mapping and modeling and a more in-depth analysis to define the phases, stages, and steps required in its implementation.

Acknowledgments. This study is part of the research project "Modelo de gestión para la optimización de procesos y costos en la Industria de Ensamblaje," supported by the Research Department of the University of Cuenca (DIUC). The authors gratefully acknowledge the contributions and feedback provided by the IMAGINE Project team.

References

1. Ministerio de Producción Comercio Exterior Inversiones y Pesca – Ecuador. https://www.produccion.gob.ec/
2. Banco Central del Ecuador. https://www.bce.fin.ec/
3. Servicio de Rentas Internas. https://www.sri.gob.ec/web/intersri/home
4. Superintendencia de Compañías. https://www.supercias.gob.ec/portalscvs/
5. Arcentales-Carrion, R., Morles, E.C., Sucozhanay, D., Duran, R., Siguenza-Guzman, L.: Process mapping and modeling: a theoretical tool analysis. TEST Eng. Manag. **83**, 25914–25925–25914–25925 (2020)
6. Saxena, P.K.: Principles of Management: A Modern Approach. Global India Publications (2009)
7. Easterby-Smith, M., Thorpe, R., Jackson, P.R.: Management Research. SAGE (2012)
8. Jeston, J., Nelis, J.: Business Process Management. Routledge (2014).https://doi.org/10.1007/b98280
9. Barros, O., Julio, C.: Enterprise and process architecture patterns. Bus. Process Manag. J. **17**, 598–618 (2011). https://doi.org/10.1108/14637151111149447
10. Holweg, M., Davies, J., Meyer, A.D., Schmenner, R.: Process Theory: The Principles of Operations Management. Oxford University Press, Oxford (2018)
11. Chen, C.C., Jones, K.T.: Management tools. CPA J. **77**, 50 (2007)
12. Dumas, M., La Rosa, M., Mendling, J., Reijers, H.A.: Fundamentals of business process management. Springer, Heidelberg (2013).https://doi.org/10.1007/978-3-662-56509-4_10
13. Ten Have, S., Ten Have, W., Stevens, F., Van der Elst, M., Pol-Coyne, F.: Key management models: the management tools and practices that will improve your business. Pearson Education (2003)
14. ISO, S.: 9001: 2015. Sist. Gest. Calid.-Requisitos. (2015)
15. Kaplan, R.S., Anderson, S.R.: Time-Driven Activity-Based Costing. Social Science Research Network, Rochester (2003)

16. Kujansivu, P., Lönnqvist, A.: Business process management as a tool for intellectual capital management. Knowl. Process Manag. **15**, 159–169 (2008). https://doi.org/10.1002/kpm.307
17. Davenport, T.H., Short, J.E.: The new industrial engineering information technology and business process redesign. Sloan Manage. Rev. 11–27 (1990)
18. Hammer, M., Champy, J.: Reengineering the Corporation: Manifesto for Business Revolution, Zondervan, A. (2009)
19. Kettinger, W.J., Teng, J.T.C., Guha, S.: Business process change: a study of methodologies, techniques, and tools. MIS Q. **21**, 55 (1997). https://doi.org/10.2307/249742
20. Klein, M.M.: Reengineering methodologies and tools. a prescription for enhancing success. Inf. Syst. Manag. **11**, 30–35 (1994). https://doi.org/10.1080/10580539408964633
21. Amjad, A., Azam, F., Anwar, M.W., Butt, W.H., Rashid, M.: Event-driven process chain for modeling and verification of business requirements–a systematic literature review. IEEE Access. **6**, 9027–9048 (2018)
22. Dehnert, J.: A methodology for workflow modeling. Bus. Process Model. Sound Work. Specif. Diss. Univ. Berl. Ger. (2003)
23. Nüttgens, M., Feld, T., Zimmermann, V.: Business process modeling with EPC and UML: transformation or integration? En: Schader, M., y Korthaus, A. (eds.) The Unified Modeling Language, pp. 250–261. Physica-Verlag HD, Heidelberg (1998)
24. Kim, Y.-G.: Process modeling for BPR: event-process chain approach. En: Proceedings of The Korea Society of Management Information Systems, pp. 41–47. The Korea Society of Management Information Systems (1996)

Check for updates

Motivation and Job Performance: Human Capital as a Key Factor for Organizational Success

Emanuel Bohórquez(✉), William Caiche, Verónica Benavides, and Arturo Benavides

University Península of Santa Elena – UPSE, La Libertad, Ecuador
ebohorquez@upse.edu.ec

Abstract. In today's world, organizations must prioritize keeping the human talent motivated, considered to be the most important capital due to its invaluable contribution in providing development and productivity; In this way, the main problem in this research is to analyze the motivation and its influence on the work performance of the employees of the Government of the province of Santa Elena.

For the study, a qualitative and quantitative approach was used with a descriptive research scope, supported by a bibliographic research method, which involved both managers and collaborators, whose main results obtained show that 80% of collaborators have a high level of satisfaction with the remuneration received with which they manage to cover their physiological needs; 60% satisfied that they have the power to direct, influence and control their own activities and/or a certain group within the institution; on the other hand, it can be seen that 42% are dissatisfied with organizational equity. Finally, establish as a recommendation the implementation of a plan of motivational strategies as a factor in the construction of human capital and that will improve work performance in the institution.

Keywords: Motivation · Job performance · Human capital

1 Introduction

At the global level, organizations are adopting changes according to market trends, however, few are those that implement new systems exclusively for human talent that make them feel motivated to carry out the assigned activities, because their work is not valued or compensated adequately, creating a job dissatisfaction that minimizes the productivity of the organization.

In order for employees to feel motivated, there must also be an adequate work environment that generates confidence when carrying out their work, that is, it has the appropriate conditions to do a good job, for this it must be focused on the well-being and safety of the same.

A large part of the organizations choose to implement strategies in the product or service, leaving aside the human talent that plays a fundamental role for it to achieve

© The Author(s), under exclusive license to Springer Nature Switzerland AG 2023
M. Zambrano Vizuete et al. (Eds.): RITAM 2021, LNNS 512, pp. 291–302, 2023.
https://doi.org/10.1007/978-3-031-11295-9_21

success, because they express that it causes them expenses when carrying out performance evaluations, training, even that the worker has the necessary resources to achieve their job.

Thus, motivation becomes a relevant factor in the performance of organizations' collaborators [1] in 2015 conducted a study by Global Engagement Index (GEI) worldwide to measure the level of motivation, took as a reference 13 countries: United States, China, India, Brazil, Italy, Australia, Great Britain, Germany, France, Canada, Mexico, Argentina, Spain; by means of an evaluation reaching the conclusion that very few employees are really committed to the company and their position. The countries with the highest percentage of fully motivated people are: The United States and China with 19%.

[2] mentions that companies or organizations that suffer from low labor productivity is because they do not give the necessary importance to the causes that produce it, although it is easily observed from outside the organization that there is no other reason greater than the motivation of the workers. collaborators.

Worldwide, all organizations need to maintain a good relationship between bosses and subordinates to achieve the goals of this, because human capital is considered the most valuable asset of the same, since with a satisfied staff we can maintain or improve the productivity, due to behavior, commitment that the employee has with the organization, therefore it is essential that the boss assumes the role of leader, maintaining certain guidelines with his collaborators that strengthen motivational aspects such as: respect among themselves, adequate communication, recognizing the work of the employees, this will help them to assume their work with responsibility, approaching the mission and vision of the organization, on the other hand, if we have an unsatisfied staff it will lower their performance and quality of work will suffer.

This research is structured as follows: the second section presents the principles and theories regarding motivation and job performance; the third section describes the methodology used and the results obtained from the study. Finally, in the fourth section, the discussion with the conclusions and recommendations is presented.

2 Motivation and Job Performance

2.1 Motivation

To begin with, the study of [3] is valued where they indicate that human motives consist of needs, conscious and unconscious, some are primary, such as the physiological ones of water, food, sleep and shelter, others can be called secondary, such as self-esteem, status, such as affiliation with other affections, achievement, and self-assertion. Motivation is a factor used to satisfy needs and desires.

On the other hand, [4] defines motivation as an internal impulse that activates the predisposition of an individual to carry out any activity or behavior oriented towards a goal, in the direction of achieving a specific objective. People's motivations can be identified within the framework of any area of action. In the work environment, the reason for the actions of the collaborators who perform specific functions can promote or slow down the performance that each one may have in their work. This implies that it is necessary to know what each subordinate needs and try to satisfy his demands to obtain better results of productivity, quality and service.

In conclusion, the motivation must be considered in the institutions and companies to obtain positive results in their subordinates so that all the activities that are carried out are carried out through the objects of this, that is, in relation with work. Motivation is often linked to incentives due to the enthusiasm that is noticeable in the workers, positively influencing the behavior of the individual, thus having intrinsic and extrinsic motivations, both constituting as impulses to achieve their objectives in the workplace. organization, in addition to achieving their personal goals because it improves the level of satisfaction in the activities carried out.

Motivation Theories

The findings of [5] indicate that it is essential to describe the approaches of each of the motivation theories established, which are mentioned below.

Need: within the organization, individuals have different needs, the leaders are in charge of motivating the workers, satisfying those desires. For this approach, the following theories are specified:

- Maslow's theory of needs
- Alderfer's ERG theory

Individual Difference: individuals can be differentiated by various aspects are these: personal traits, key values and the work they perform. Likewise, this approach contains the following theories:

- McClelland's theory
- Herzberg theory

Cognitive: people feel motivated when they have the objectives set, because they feel capable of achieving them taking into account that with their effort they will receive rewards and incentives. It is necessary to detail the following theories:

- Goal setting theory
- Expectations theory
- Equity theory

Maslow's Theory of Needs

The contributions of [6] on this theory show that Maslow's pyramid of motivation is based on the so-called pyramid of needs, that is, needs can be ranked or classified in order of importance and influence on behavior human. Abraham Maslow stated the following needs:

- Physiological needs
- Security needs

- Social needs
- Esteem needs
- Self-realisation needs

Alderfer's ERG Theory

In the research work carried out by [7], it is stated that the ERC theory is established considering Maslow's pyramid, where it is summarized in three needs that are summarized below:

- Existence needs
- Relationship needs
- Growth needs

McClelland's Theory

In their article [8] they included the contribution of (McClelland & Burnham 1976) pointing out that achievement, power and affiliation are the three important needs that help to explain the motivation of people like this:

- Achievement needs
- Power needs
- Membership needs

Herzberg Theory

Regarding this theory [9] he added the contributions of (Herzberg, 1968) that summarizes his theory as follows: "The components that contribute to job satisfaction (and motivation) are different and independent of the factors that tend to incite dissatisfaction", and which are described below:

- Motivational factors (satisfaction)
- Hygienic factors (dissatisfaction)

Goal Setting Theory

In the report carried out by [10] he details that the goal setting theory put forward by Locke determines:

> "The motivation of the worker arises from his actions and that the level of his performance is directed at the level of difficulty that it has to achieve an established goal. In which objectives are established that are granted to workers and convince them to concentrate their efforts"

In the same way [11] he emphasizes this theory, where he emphasizes that it is of great importance that organizations and institutions establish goals, since they help to have a better direction in the employees.

Equity Theory
[2] states "The role that equity plays in motivation; employees compare what they contribute to their jobs with what they get from them in relation to those of other people. We perceive what we get from a job in relation to what we contribute, then we compare our input-output ratio with that of others that don't even matter".

We can summarize that there is a variety of motivation theories that play an important role in collaborators within the organization, because different types of intrinsic and extrinsic incentives are applied considering their personal and professional needs.

2.2 Job Performance

To begin with, [12] sustains that "Job performance is a tool that measures the perception that both suppliers and internal customers have of a collaborator. This tool proposes information on their performance and their individual competencies in order to identify areas for continuous improvement that increase their collaboration in achieving the organization's objectives".

In addition, [13] indicates that "Work performance measures the performance exhibited by workers to the organization, the same that allows identifying areas with positive and negative effects, the intention of measuring performance is to improve them to achieve compliance with the proposed objectives".

Work performance refers to the performance that each worker has at the time of carrying out the assigned activities, the development with which he acts, that is why a large part of the organizations evaluate performance to measure the degree of effectiveness and efficiency with which carry out their activities.

Competences
For [14] in their article they add the definition of (Urbina, 2007) who conceptualizes competences as the integration of knowledge, skills, behaviors, attitudes, aptitudes, and motivations leading to adequate and timely performance in various contexts.

In addition, [15] include the contribution of (Tobón, 2010) which indicates that the competencies are integral actions in the face of activities and context problems with suitability and ethical commitment.

Knowledge: [16] mentions that "the knowledge possessed by individuals is considered an asset of the company, it is also emphasized that the knowledge of the areas and levels allows them to have a greater commitment and obtain a better result from according to their level of performance shown in the work area".

Skills: [17] considering the contributions made by Vicente Caballo, the skills comprise a set of behaviors that the individual expresses within a context where they relate to other people, showing attitudes, feelings and opinions to provide alternatives that contribute to problem solving.

The competences are immersed in each individual and they are developed through the attitudes, capacities, abilities with which they develop in the different situations that arise and that allow them to achieve an appropriate performance.

Behavior

We highlight what was stated by [18] that defines behavior as the attitude of the employee that has a fundamental contribution to job performance. Indeed, [6] establishes that behavior in an organization is classified into three groups:

Individual Behavior: within the organization, it is due to the preparation, values, desires and desires, indicating that each person has different characteristics, for them the individual must be directed to the interests of the institution [19].

Group Behavior: the authors [20] consider it as acts and the capacity that individuals present in the work team, promoting the participation of all those involved and focusing personal interests to achieve the objectives of the organization.

Organizational Behavior: understands the attitudes of employees since success rests with them. Behavior is immersed in different changes, but nevertheless adequate behavior is a tool that benefits the institution and reflects the extent to which motivation and productivity are promoted [21].

In conclusion, through good organizational management, an adequate organizational behavior can be achieved and therefore take advantage of the effort of human talent to achieve the strategic goals.

Performance Evaluation

Regarding this issue [12] defines performance evaluation as "a systematic and periodic process that serves to quantitatively and qualitatively estimate the degree of effectiveness and efficiency of people. Its main objective is to determine if employees are doing their job correctly. This can provide information on the need to improve the collaborator in terms of knowledge and skills".

For [3] the performance evaluation is a system that allows defining the objectives of the company with all its subordinates so that progress can be verified until reaching the goal. But this control and measurement scheme is not the fundamental component to efficiently manage the development of the institution's human talent.

Performance evaluation is an instrument used to verify the degree of fulfillment of the objectives proposed at the individual level. This system allows a systematic, objective, and comprehensive measurement of professional conduct and performance or achievement of results.

3 Methodology

The main objective of this research is to analyze the motivation and work performance of the personnel in the Government of the province of Santa Elena, being a non-experimental study of a non-probabilistic nature carried out between 2018 and 2019.

Thus, for the present research a qualitative and quantitative approach was used with a descriptive research scope, relying on a bibliographic research method related to motivation and job performance, as well as field research that in the present project was applied to collect primary information in situ provided by the appointing authority, departmental heads, administrative personnel and workers belonging to the Government of the province of Santa Elena, applying information collection tools such as interviews and surveys that allowed identifying the qualities and characteristics of the problem posed, as well as for its analysis, understanding and measurement of results.

For the development of this project, 11 people made up of the appointing authority and departmental heads were considered as the population for the interview. While for the survey there was a population of 66 people made up of departmental heads, administrative staff and workers; in this case, the sample corresponds to the total population as it is finite and achievable, which will contribute with their opinion about the degree of motivation and job performance in the Government of the province of Santa Elena.

The main research instrument were the surveys, which were applied to the 66 collaborators; It is made up of 17 closed questions, structured in three parts: the first with sociodemographic data, a second section with questions related to motivation and a third section with questions oriented to job performance, the last two sections with options for scale of evaluation. Likert.

4 Results and Discussion

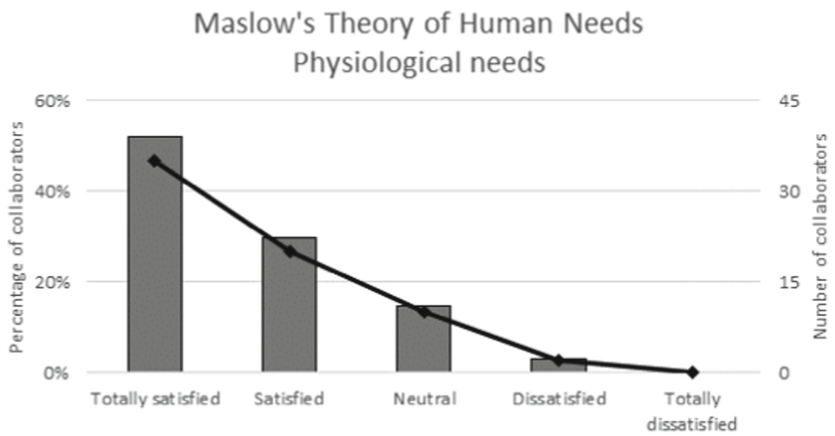

Fig. 1. Satisfaction of physiological needs (Maslow's theory of human needs)

In Fig. 1, referring to the satisfaction of physiological needs, it can be highlighted that 52% of the collaborators are totally satisfied, 30% satisfied and only 3% dissatisfied. Concluding that most of the collaborators feel satisfied with the remuneration received, which allows them to meet their own physiological needs and those of their family environment, constituting a motivating factor for the development of tasks.

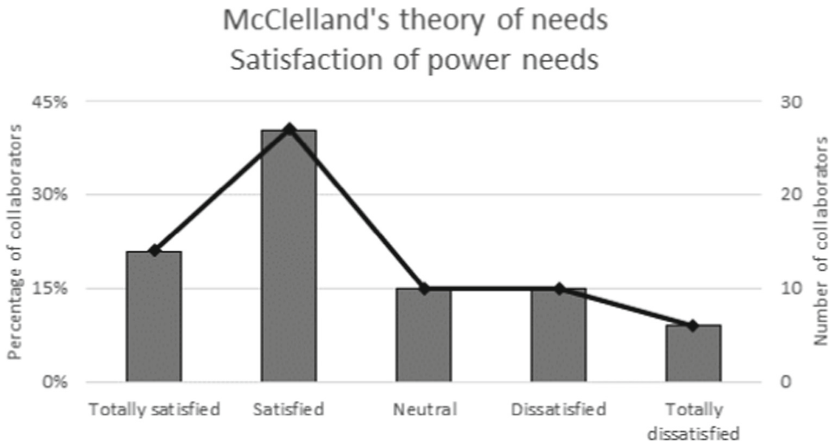

Fig. 2. Satisfaction of power needs (McClelland's theory of needs)

Figure 2, related to the satisfaction of power needs, shows that 40% of employees are satisfied, 21% are fully satisfied and 9% are completely dissatisfied. Therefore, it can be concluded that for 60% of collaborators they have the power to direct, influence and control their own activities and/or a certain group within the institution; being a way of intrinsic satisfaction for them.

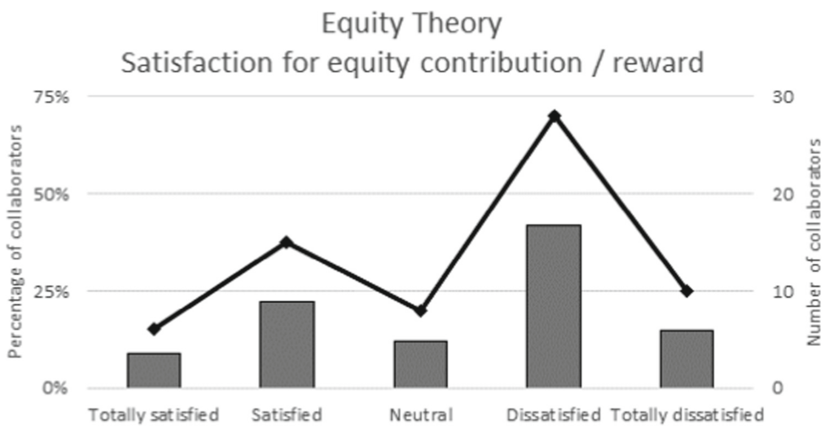

Fig. 3. Satisfaction for equity between contribution/reward (Equity theory)

In Fig. 3, concerning the level of satisfaction with the equity between contribution/reward, it can be seen that 42% are dissatisfied, 22% satisfied and 9% totally satisfied. With this, it can be deduced that the relationship of equal result achieved equal recognition in comparison with other co-workers is not emphasized, recommending that the work be recognized equitably, to motivate staff and strengthen performance work and thus be more productive.

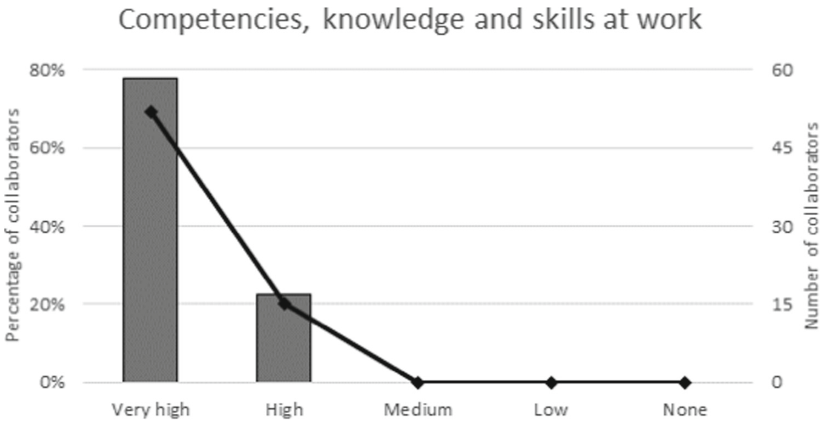

Fig. 4. Work competencies

In Fig. 4, referring to the degree of contribution of the competences, knowledge and skills for the job, it shows that 78% of the collaborators consider that their labor competences do need a lot for their work and 22% sufficient. The aforementioned characteristics are a very important role in them, ensuring that the activities are achieved in the best way, positively favoring the work performance of each one.

Fig. 5. Work efficiency

In Fig. 5, regarding the level of work efficiency, it can be seen that the majority with 66% always indicates and 27% almost always. Being able to argue that more than 90% of employees carry out their activities within the scheduled time, which benefits good individual performance.

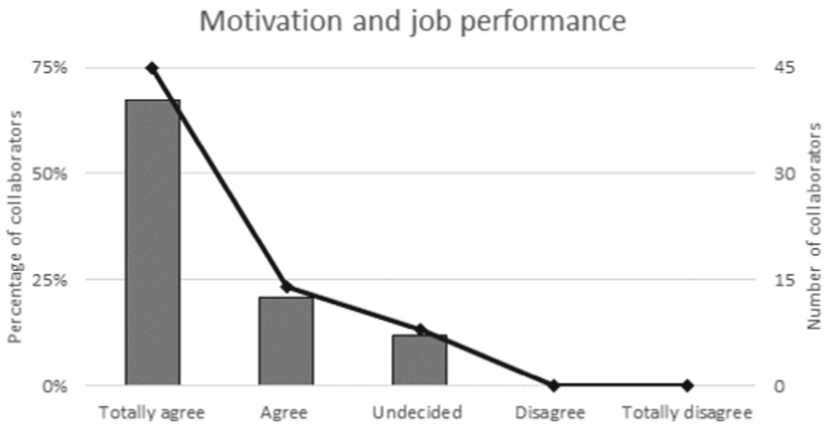

Fig. 6. Motivation and job performance

In Fig. 6, about the implementation of motivational strategies to improve job performance, 67% of employees indicate that they fully agree, also 21% agree and 12% are neutral. Consequently, the proposal of motivation strategies would allow collaborators to feel valued, identify with the institution, feel part of a good work environment and as a result an effective work performance.

5 Conclusions and Recommendations

In today's world, staff motivation has become a key element for adequate work performance to exist, allowing organizations to fulfill that mission and vision outlined for the benefit of society.

In this research, the motivation and work performance of the personnel in the Government of the province of Santa Elena has been analyzed.

Being able to conclude regarding the motivation of the staff at work, on the one hand, that more than 80% of the collaborators have a high level of satisfaction with the remuneration received with which they manage to cover their own physiological needs and that of his family nucleus; very closely with 60% of collaborators they would be satisfied of being able to have the power to direct, influence and control their own activities and/or a certain group within the institution. On the other hand, 42% are dissatisfied in the relationship of the same result achieved the same recognition compared to other co-workers.

Consequently, concluding about job performance that 100% of employees consider that their skills, knowledge, and abilities do contribute significantly to their daily work; Furthermore, 90% of employees always mention carrying out their activities within the scheduled time. In this way, 88% of employees mention that they fully agree that the implementation of a plan of motivational strategies would allow improving job performance.

Finally, it is possible to establish that in a general way that there is an adequate level of work motivation in most of the collaborators in relation to remuneration and the need for power, however, it would be necessary to look for alternatives that allow to reduce the perception of lack of equity between contributions and rewards obtained for work performed compared to other co-workers. And that in relation to job performance in general, employees would be fulfilling their obligations efficiently and effectively. In short, there is an adequate degree of motivation, which would positively influence the work performance of the employees of the Government of the province of Santa Elena.

It can be recommended according to the results obtained that the authorities of the Government of the province of Santa Elena, through their human resources department, can implement a plan of motivational strategies that allows maintaining job satisfaction in some and improving job satisfaction in others, emphasizing that it becomes a key factor in the construction of human capital, all with the purpose of positively influencing the commitment and work performance of all members of the institution.

The present investigation was limited in some cases by the limited availability of time on the part of the collaborators of the Government of the province of Santa Elena. Future research could compare and contribute to the discussion of results in different contexts regarding the level of motivation and its influence on job performance. In addition, the recommendations are expected to make viable and improve work motivation in all members of the institution.

References

1. Expok. https://www.expoknews.com, [En línea]. https://www.expoknews.com/que-motiva-a-los-trabajadores-en-cada-pais/. Último acceso 10 June 2019
2. Ochoa, K.: Motivación y productividad laboral, Universidad Rafael Landívar, Quetzaltenango (2014)
3. Harold, K., Weirich, H., Canicce, M.: Administración una perspectiva global, empresarial y de innovación. McGraw Hill, México (2017)
4. Rubió, T.: Recursos Humanos, Dirección y gestión de personas en las organizaciones. Octaedro, Barcelona (2016)
5. Hughes, R., Ginnett, R., Curphy, G.: Liderazgo: Cómo aprovechas las lecciones de la experiencia. McGrawHill, México (2007)
6. Chiavenato, I.: Comportamiento Organizacional. McGraw Hillç, México (2017)
7. León, G.: La motivación y el desempeño laboral de los trabajadores en la municipalidad distrital de Cajay - Huari, año 2017, Universidad Nacional José Faustino Sánchez Carrión, Huacho (2017)
8. Lozano, D., Barragán, J.: La necesidad de apreciar historias dentro de las teorias sobre las necesidades humanas. Innovaciones de Negocios **12**(24), 295–326 (2015)
9. Palomo, T.: Liderazgo y motivación en equipos de trabajo. ESIC, Colombia (2017)
10. Lagos, V.: La motivación laboral y su incidencia en el desempeño organizacional en empresas copelec, Universidad del Blo-Blo, Chillán (2015)
11. Santacruz, J.: La influencia de la motivación en el desempeño laboral de los funcionarios del Municipio del Distrito Metropolitano de Quito, Administración Zonal Eloy Alfaro en el año 2016, Universidad Central del Ecuador Sede Sur, Quito (2017)
12. Asch, J: La evaluación de desempeño en las empresas y la resilencia Fidélitas, 5, 4–14 (2015)
13. Mejillón, A.: Análisis del clima organizacional y su influencia en el desempeño del talento humano del Instituto de Seguridad Social, Universidad Península de Santa Elena, La Libertad (2017)

14. Véliz, P., Jorna, A., Berra, E.: Consideraciones sobre los enfoques, definiciones y tendencias de las competencias profesionales, Educación Médica Super. 30(2) (2016)
15. Ortiz, M., Caicedo, A., González, S., Recino, U.: Las múltiples definiciones del término competencia y la aplicabilidad de su enfoque en ciencias médicas. Edumecentro **7**(3), 20–31 (2015)
16. Villar, M.: Movilizando a las personas y sus recursos humanos para el logro de los resultados empresariales. Universidad Santos Tomás, Chile (2018)
17. Ontoria, M.: Habilidades Sociales. Eeditex, España (2018)
18. Ríos, I.: Equipos motivados, equipos productivos: Manual práctico para directivos. Tébar Flores, Madrid (2018)
19. Juárez, G.: La administración y el comportamiento organizacional, Rev. Caribeña de Cien. Sociales, 9–12 (2016)
20. Hidrugo, J., Pucce, D.: El rendimiento y su relación con el desempeño laboral del talento humano en la clínica San Juan de Dios-Pimentel, Universidad Señor de Sipán, Pinimentel (2016)
21. Molina, L., Briones, Í., Arteaga, H.: El comportamiento organizacional y su importancia para la administración de empresas. Rev. Científica Dominio de las Cienc. **2**(4), 13 (2016)

Assessing the Needs of an Innovation Resource to Promote the Touristic Sector of a Small Andean City. Riobamba, Ecuador

Luis Quevedo(✉), Silvia Aldaz, Héctor Pacheco, and Danilo Quintana

Universidad Nacional de Chimborazo UNACH, Riobamba 060150, Ecuador
luis.quevedo@unach.edu.ec

Abstract. To address the challenge of sustainable development, the use of technology and innovation tools is imperative for tourism stakeholders.

This paper examines the needs of an innovation resource to promote the touristic sector of Riobamba (Ecuador), through an approach to the global trends of technologic innovation globally used in tourism, the identification of the perception about the needs of an innovation resource to promote the touristic sector, and based in those results, describes the profile and preferences of touristic cycling users, the main natural sites of tourist interest near to Riobamba as well as the offer of MTB (mountain bike) routes provided by the Tourism Ministry of Ecuador.

Our findings support the statement that cooperation between touristic destinations is a key factor to implement innovation resources in touristic regions, evidencing that in Riobamba is pertinent the implementation of a resource of innovation to promote tourism based on a sustainability paradigm.

Keywords: Technology · Tourism · Riobamba · Ecuador · Innovation

1 Introduction

The integration between information and communication technologies (ICTs) and tourism is known as smart tourism. I that sense, organizations, and people involved in touristic activities use to work together to build social ecosystems that allow information exchange via internet [1].

Nowadays, the increasing development of emerging ICTs is contributing to restructuring processes and systems, altering the way in which products and services are offering and operating in the touristic market [2–4]. Thus, technology has become a main aspect of the touristic industry, and it is integrated into daily operations related with the provision of services and products of organizations that pursue to satisfy customer expectations. In this context, destinations are implementing actions to consolidate a smart tourism system which is associated to the use of technologies to collect data and to provide support to the stakeholders [1, 5, 6].

There are several technologic trends associated with tourism like robots, artificial intelligence, chat-bots, internet of things, recognition technology, virtual reality

© The Author(s), under exclusive license to Springer Nature Switzerland AG 2023
M. Zambrano Vizuete et al. (Eds.): RITAM 2021, LNNS 512, pp. 303–314, 2023.
https://doi.org/10.1007/978-3-031-11295-9_22

(VR), and augmented reality (AR) [7], being mobile technologies, specially the use of smartphones one of the most relevant for the development of smart tourism [5].

Globally, it is evident that to face the challenge that implies a development based on a sustainability paradigm, the use of technology and innovation is a key factor, and the touristic sector is no exception. Therefore, dynamic changes are being implemented by businesses and localities that aim to satisfy the needs of tourists.

This study aims to assess the needs of an innovation resource to promote the touristic sector of Riobamba, through an approach to the global trends of technologic innovation used in tourism, the identification of the perception about the needs of an innovation resource to promote the touristic sector, the description of the user's profile, the identification of sites of interest and presenting the offer provided by the tourism official agency of Ecuador.

2 Methodology

2.1 Study Area

Riobamba is an inter-Andean small city of Ecuador located in the center of the country (Fig. 1); its coordinates are 1°40′00″S–78°39′00″O. There are several large mountains and volcanoes (Chimborazo, Carihuayrazo, Altar, Igualata, Tungurahua, Sangay) surrounding Riobamba. Administratively, Riobamba has 5 urban parishes (Velasco, Veloz, Maldonado, Lizarzaburu, and Yaruquíes) and 11 rural parishes (Licto, San Juan Cubijíes, Punín, Cacha, Licán, Calpi, Flores, Pungalá, Químiag, and San Luis).

Fig. 1. Location of the study area

Riobamba has an altitudinal average of 2750 m.a.s.l. and an annual temperature average of 12 °C. The main natural touristic attraction around Riobamba is the Chimborazo volcano, which is the highest mountain in Ecuador with 6.263 m.a.s.l.

2.2 Methods

To assess the needs of an innovation resource to promote the touristic sector of Riobamba, we structured our work in three sections: the first part comprises an approach to the global trends of technologic innovation used in tourism; a second section that identifies the perception about the needs of an innovation resource to promote the touristic sector of Riobamba and, a third part that based on the previous results obtained, describes the profile and preferences of touristic cycling users, the main natural sites of tourist interest near to Riobamba as well as the offer of MTB (mountain bike) routes provided by the Tourism Ministry of Ecuador.

The data were collected between July and December 2020, throughout structured questionnaires, that provided elements that contributed to understanding the topics under study. The process entailed sending the questions and receiving the responses by mail, to respect the healthy protocols applied during the Covid-19 pandemic.

The research was based on two questionaries: The first questionary was directed to non-governmental organizations (NGOs), regional and local governmental organizations, and universities located in the region to identify their perception about the needs of an innovation resource to promote the touristic sector of Riobamba. A total of 85 questionnaires were applied. While the second questionary was directed to touristic cycling users to identify their profile and preferences. A total of 143 questionaries were applied.

3 Results

3.1 Global Trends of Technologic Innovation Used in Tourism

The first part of the study is an approach to the global trends of technologic innovation used in tourism and are listed in Table 1, which includes the resource, a brief description, and its uses in the tourism industry. The main resources identified include: voice search & voice control, robots, contactless payments, virtual reality, chatbots, internet of things, recognition technology, augmented reality, artificial intelligence, and mobile apps.

Table 1. Trends of technologic innovation associated with tourism.

Resource	Description	Uses in tourism
Voice search & voice control	Application used in smart speakers, smartphones, and AI assistants to pay actions or duties based on voice commands	Booking airline tickets Obtaining tourist information Controlling hotel devices

(*continued*)

Table 1. (*continued*)

Resource	Description	Uses in tourism
Robots	Automatically operated machines that re place human effort	Providing information Cleaning Luggage handling Food preparation Booking systems
Contactless payments	Technology associated to process that includes the reduction or elimination of con tact during payments	Payment process
Virtual Reality (VR)	Devices that allow experimenting situations similar or completely different from the real world	Experiencing far away locations VR tours 360 tours
Chatbots	Software application used to conduct an online chat conversation instead of providing direct contact with a live human agent	Swift answers to questions on a 24/7 basis, regardless of staff availability
Internet of Things (IoT)	Network of objects embedded with software, sensors, and other technologies to connect and exchange data with other systems and devices	Connecting several devices in touristic locations Data analytic platforms
Recognition technology	Technology employed to authenticate users through ID verification services (includes fingerprint recognition, retina scanning, facial recognition, and other bio-metric identifiers)	Safety and easy purchasing Accessing defined spaces by tourists Automatic payment systems Providing quick and complete information of tourist and passengers
Augmented Reality (AR)	Interactive experience where the objects are enhanced by computer-generated perceptual information	Enhancing the customer experience, providing valuable information of touristic locations
Artificial Intelligence (AI)	Machines programmed to simulate the human intelligence	Accurately and continuously sorting and processing data to decisions making in aspects that include business trends and customer satisfaction
Mobile app	Applications with software designed to mobile devices	Integrating several utilities to assist and satisfy the needs of tourists

Voice search and voice control are based on technology with spoken conversational systems allowing users to obtain the information they request with a spoken query [8], and for tourism sector, voice search is becoming a useful tool with a growing impact on tourist experience through several options like simplify the booking process and providing a quick response to tourist request of information [9]. Studies reporting their application in the tourism sector e.g. [7, 9] demonstrate that voice search has now a days a significant role in tourism.

Robots play an increasing role in tourism and hospitality services, and their participation includes the use of robots in reception assistants, security robots, and robots that serve food and drinks to visitors. Their use is well documented in cases as the Hennna Hotel located in Nagasaki (Japan), which has been recognized as the first hotel with robots in the world and uses robots at reception [10, 11]; Hilton, which have implemented a robot called Connie [12, 13]; and HMSHost, which have launched a robot that welcomes tourists to restaurants, providing menu details, and even is able to offer recommendations [7].

Contactless Payments includes technology that contributes to touristic services through the reduction of transaction costs and adapting process that increase the confidence of the parties involved. Contactless technology enables travel without physical documents, making a mobile phone all that a visitor needs at a touristic destination [14]. In fact, studies like the presented by Basily et al. [15] describe a wide range of services integrated into an app, demonstrating a wide range of opportunities in the future for mobile technology associated with contactless payment.

Virtual Reality (VR) includes technology offering several opportunities to the tourism business. VR allows to tourists have experiences associated with extreme activities as kayak, rafting, or snowboard [7]. It also makes it possible to visit virtually inaccessible destinations like caves, waterfalls, or archeological sites. Advances in this technology will generate new opportunities and several possibilities of application for the tourism industry [3].

Chatbots make it possible to obtain quick responses to customer inquiries being available 24/7 (24 h/7 days of the week), regardless of human staff availability. Chatbots have gained importance with several applications including Amazon's Alexa or Apple's Siri [16]. Nowadays many tourists make their bookings through internet chatbots, and trends point out that the potential of chatbots in diverse areas of the tour ism industry is vast [17].

Internet of Things (IoT) aims to maintain a connectivity system that allows them to be controlled by interned [18], and devices equipped with IoT are able to share their information online making it possible that any physical object can have a virtual reflection in the service space. This provides a huge space for developing and applying new business models and will have a major impact on the development of e-Tourism services [19]. Nowadays is common to find users integrating sensors for heating and cooling systems, devices for room service, and car rental.

Recognition Technology has already begun to be implemented in an experimental way in some hotel companies (e.g. Bluebay Group) and, in Spain, the Campanile hotel chain use sensors that allow to recognize facial expressions of emotions to evaluate and improve the protocols used in customer services [20].

Augmented Reality (AR) could be explained as the technology that augments the real world with virtual components. Instead of replace the reality, this technology superimposes virtual objects onto the physical world though the integration of object recognition technology with computer programs [21]. AR is a technology that provides useful information to visitors about the destinations they selected. Museums, galleries, and touristic attractions are using it to view historical exhibitions in their original form through the use of virtual overlaying and maps.

Artificial Intelligence (AI) is a growing trend in touristic business and can be used to design a personalized and adapted proposal for customers and to help in the analysis of business data. The potential of artificial intelligence (AI) technologies in the tourism sector is huge and some travel business are already using elements of artificial intelligence to analyze large volumes of data learning from their own and from the experience of other people to fulfilling customer needs [22].

Mobile Apps are able to integrate several of the resources mentioned above and have been designed for a wide gamma of touristic services as accommodation (Airbnb, Homeaway, 9Flat), transport (Uber, Grab), dining (VizEat, EatWith), and travel experiences (ToursByLocal, Contexttravel). The use of internet is increasing and there are uncountable possibilities to enable online platforms day by day. Therefore, the popularity of mobile technologies and applications is growing day by day and undoubtedly changing the behavior of consumers and providers [5].

Even when the use of technology and innovation resources is highly recommended and valuated, some voices consider it as a risk for the maintenance of employees. So, there are authors e.g. [23] that conclude that is better to implement these technologies in activities that will make easier the work of employees instead of replacing them completely.

3.2 Perception About the Needs of an Innovation Resource to Promote the Touristic Sector of Riobamba

In the second part of our study, we identified the perception about the needs of an innovation resource to promote the touristic sector of Riobamba. The statements with the highest percentages obtained when we applied the questionaries are available in Table 2.

Table 2. Perception about the needs of an innovation resource to promote the touristic sector of Riobamba.

ID	Question	Statement with the highest percentage
Q 1	At which level the tourism sector has been affected by the COVID-19 pandemic?	Tourism has been highly affected by COVID-19 (82%)
Q 2	How important do you consider the implementation of an innovation resource in Riobamba for the reactivation of tourism?	The implementation of an innovation re source is very important for the reactivation of tourism (56%)
Q 3	Would an innovation resource benefit the tourism in Riobamba?	An innovation resource would highly benefit tourism in Riobamba (79%)
Q 4	In which tourism category do you consider priority the implementation of an innovation resource?	It is a priority the implementation of an innovation resource in tourism of nature (52%)
Q 5	Which innovation resource, you consider appropriate for its application in Riobamba?	Smartphone App is a resource appropriate for its application in Riobamba (48%)
Q 6	Do you consider that the use of the in novation resource should be free or paid?	The use of the innovation resource should be free (83%)
Q 7	Which organization should manage the innovation resource?	The innovation resource should be managed by the University Nacional de Chimborazo (46%)
Q 8	In which activities could be an innovation resource applicable?	An innovation resource could be applicable in cycling routes (37%)

An 82% of interviewed consider that the tourism industry has been highly affected by COVID-19; 56% consider very important the implementation of an innovation resource to reactivate tourism, and 79% point out that an innovation resource would highly benefit tourism in Riobamba. When we ask about the category that is considered a priority for the implementation of an innovation resource, most of the interviewed (52%) select tourism of nature, and considering that a mobile application (48%) will be the resource appropriate to its implementation in Riobamba. Additionally, the inter-viewed mentioned that the use of the resource should be free of pay (83%), managed by the Universidad Nacional de Chimborazo (46%), and applied to cycling routes (37%).

3.3 Profile and Preferences of Touristic Cycling Users, Natural Sites of Interest and, the Official Offer of Bike Routes

Based on the results obtained in the analysis of the perception about the needs of an innovation resource to promote the touristic sector of Riobamba, we identified: the profile and preferences of touristic cycling users (Table 3), the main natural sites of tourist interest near to Riobamba (Table 4) and the offer of MTB routes provided by the Tourism Ministry of Ecuador (Table 5).

Table 3. Profile and preferences of users of touristic activities (cycling).

ID	Feature	Statement with the highest percentage
Q 1	Age	21–40 years old (40%)
Q 2	Preferred schedule	Morning (68%)
Q 3	Days of the week preferred to practice	Weekends (79%)
Q 4	Time spending on cycling or trekking activities	2–3 h (74%)
Q 5	Preferred routes	Second-order pathways (54%)
Q 6	Preferred places	Natural areas (47%)
Q 7	Preferred surface of the road	Paved road (42%)
Q 8	Key elements in a Mobile App	Altitude, distance, and difficulty level (87%)
Q 9	Preferred characteristics of the App	Touristic information, hydration points, type of route, informative audio and image (91%)
Q 10	Relevant element to choose the routes	Type of road (34%)
Q 11	Preferred operative system for an App	Both IOS and Android (81%)
Q 12	Availability to use an App in a demo phase	Yes (89%)

The highest range of age in users is 21–40 years old, presenting a preference to develop biking activities in the morning (68%) during the weekends (79%) for a period ranging between 2 and 3 h (74%). The preferred routes are second-order pathways (54%), located in natural areas (47%) with a paved road (42%). The elements considered key in a mobile application were: altitude, distance, and difficulty level (87%); while as preferred characteristics of the applications were mentioned: touristic information, hydration points, type of route, informative audio, and image (91%). The main element when users select a route was the type of road (34%), and use both operative systems (IOS and Android). Finally, most of the users (89%), mention to be able to use the application in a demo phase.

There are two main natural sites classified as protected areas that influencing the tourism activities around Riobamba: The Chimborazo Fauna Production Reserve which was created in 1986, has a length of 58560 hectares and, an altitudinal range from 3200 to 6268 m.a.s.l., this reserve is home to a large population of vicuñas, llamas, and alpacas; and the Sangay National Park which was created in 1975, has a length of 517765 hectares and, an altitudinal range from 1000 to 5230 m.a.s.l., in 1983 UNESCO declared it a World Heritage Site due to this unique geography and extraordinary biodiversity. Both sites have several interest points and the main have been identified in Table 4.

Table 4. Natural sites of tourist interest near to Riobamba.

Chimborazo fauna production reserve	
Interest point	Short description
Chimborazo volcano	The highest volcano in Ecuador (6268 m.a.s.l.)
Carihuairazo volcano	Three peaked volcanic boiler (5018 m.a.s.l.)
Last ice merchant route	Millenary route where the Ice Merchant extract ice from the old glaciers
Whymper's needles	A rock formation named in honor of Edward Whym-per
Machay temple	Sacred cave of volcanic material, used by indigenous people as a ceremonial center
Solitary tree	Large bush (5m high and 6m in diameter) located in the middle of the moor, surrounded by dunes
Polylepis forest	Remnant of Polylepis forest
Chorrera canyon	Rocky formation with a waterfall of approximately 25 m high
Inca fortress	Archeological site considered a ceremonial center
Cunuyaku	Thermal water spring: considered as a healing center
Sangay national park	
Interest point	Short description
Sangay volcano	One of the highest active volcanoes in the world (5230 m.a.s.l.). It has a cone shape and the top is covered by glacier
Altar volcano	An extinct stratovolcano (5321 m.a.s.l.). It was active about 2 million years ago and contains a caldera open to the west, where there is a lake
Tungurahua volcano	An active volcano (5023 m.a.s.l.) its activity has been characterized by frequent powerful explosions and ash emanation
Ozogoche	Complex of 45 lakes that are deep, cold, and have a striking dark blue color

Finally, it is presented a list of MTB routes in the province of Chimborazo (Table 1), which were considered by the Tourism Ministry of Ecuador in a published document [24] with the aim of increase competitiveness, attractiveness, profitability, and benefits for the stakeholders involved in touristic activities related with cycle routes.

Table 5. MTB routes of Chimborazo

N	Route	Distance (km)	Average time (hours)	Height (m)		Level (high-medium-low)	
				Max	Min	Physical	Technical
1	Urbina - Guano - Riobamba	37,8	4	3.618	2.750	Medium	Medium
2	Riobamba - Tunshi - Riobamba	36,7	3	2.839	2.657	Medium	Medium
3	Riobamba - Licto - Chambo - Riobamba	50	3,5	3.214	2.657	Medium	Low
4	Riobamba - Chambo - Quimiag - Riobamba	36	2,5	2.904	2.545	Medium	Low
5	Laguna de Colta	37	4,5	3.574	2.763	Medium High	Low
6	Riobamba - Guano - Riobamba	21,2	2	2.862	2.650	Low	Low
7	Riobamba - Batzacón - Guano	26,2	2,5	3.071	2.748	Low	Low
8	Penipe - Palitahua	28,6	2	2.503	2.401	Low	Low
9	Tzalaron - Laguna de Colta	27,7	2	3.591	2.948	Low	Low
10	Guamote - Riobamba	38,6	35	3.228	2.702	Medium	Low
11	Chimborazo - San Juan	32	1,5	4.800	3.200	Low	Low
12	Chimborazo Tambohua-sha	36,8	3	4.840	3.290	Medium	Low
13	Chimborazo - Urbina	40	3,5	4.800	3.335	Medium	Medium

4 Conclusions

New technologies have been developed and it has led to transformations in the tourism industry and it is imperative to face global challenges and opportunities. Moreover, in the global context of the COVID-19 pandemic, technological innovation associated with tourism has become highly appreciated for the potential to reduce human-human contact and for the possibility to reactivate and dynamize the economic sector. This study supports the statement that tourism destinations should cooperate between them to implement innovative resources in touristic regions.

When we analyze the perception about the needs of an innovation resource to promote the touristic sector of Riobamba, it was evidenced that the stakeholders consider that the implementation of a free use mobile application that allows the integration of nature tourism and cycle routes could benefit and dynamize the touristic activities in Riobamba. Then, we identified the profile of the cycle routes users and found a clear tendency pointing to well-informed young people that enjoy developing this activity in natural places and willing to integrate a mobile application that should have included data like altitude, distance and, difficulty level to support their performance. Therefore, 14 points of interest that belong to the two main natural sites influencing tourism activities in Riobamba were briefly detailed and were consistent with the structure of MTB (mountain bike) routes provided by the Tourism Ministry of Ecuador.

The information presented in this study evidence that in Riobamba it is pertinent the implementation of a resource of innovation to promote tourism based on a sustainability paradigm. Therefore, our work plans include as the next step, the technical design of a mobile application including the parameters here identified.

References

1. Asia Hunter, W.C., Chung, N., Gretzel, U., Koo, C.: Constructivist research in smart tourism. Pac. J. Inf. Syst. **25**, 103–118 (2015)
2. Antti Pesonen, J.: Information and communications technology and market segmentation in tourism: a review. Tourism Rev. **68**, 14–30 (2013). https://doi.org/10.1108/TR-02-2013-0006
3. Beck, J., Rainoldi, M., Egger, R.: Virtual reality in tourism: a state-of-the-art review. Tourism Rev. **74**, 586–612 (2019). https://doi.org/10.1108/TR-03-2017-0049
4. Rincon, F.O., Tommasini, E., Rainoldi, M., Egger, R.: The Future of Wearable Devices On-Site: A Scenario Technique Approach. In: Schegg, R., Stangl, B. (eds.) Information and Communication Technologies in Tourism 2017, pp. 285–299. Springer, Cham (2017). https://doi.org/10.1007/978-3-319-51168-9_21
5. Dorcic, J., Komsic, J., Markovic, S.: Mobile technologies and applications towards smart tourism – state of the art. Tourism Rev. **74**, 82–103 (2019). https://doi.org/10.1108/TR-07-2017-0121
6. Gretzel, U., Werthner, H., Koo, C., Lamsfus, C.: Conceptual foundations for understanding smart tourism ecosystems. Comput. Hum. Behav. **50**, 558–563 (2015). https://doi.org/10.1016/j.chb.2015.03.043
7. Konstantinova, S.: Digital transformation in tourism. Knowl. Int. J. **1**(35), 188–193 (2019)
8. Wang, Y.-Y., Yu, D., Ju, Y.-C., Acero, A.: An introduction to voice search. IEEE Sign. Proces. Mag. **25**, 28–38 (2008). https://doi.org/10.1109/MSP.2008.918411

9. Rozumowski, A., Kotowski, W., Klaas, M.: Resistance to customer-driven business model innovations: an explorative customer experience study on voice assistant services of a swiss tourism destination. AJT **7**(4), 191–208 (2020)
10. Lawlor, J.: Are you being served? The rise of robots in the services sector. Contrib. TU Dublin (2019). https://doi.org/10.21427/168n-c530
11. Osawa, H., et al.: Analysis of robot hotel: reconstruction of works with robots. In: 2017 26th IEEE International Symposium on Robot and Human Interactive Communication (RO-MAN), pp. 219– 223 (2017). https://doi.org/10.1109/ROMAN.2017.8172305
12. Bowen, J., Whalen, E.: Trends that are changing travel and tourism. Worldwide Hospitality Tourism Themes **9**, 592–602 (2017). https://doi.org/10.1108/WHATT-09-2017-0045
13. Ivkov, M., Blešić, I., Dudić, B., Pajtinková Bartáková, G., Dudić, Z.: Are future professionals willing to implement service robots? Attitudes of hospitality and tourism students towards service robotization. Electronics **9**, 1442 (2020). https://doi.org/10.3390/electron-ics9091442
14. Dragović, N., Stankov, U., Vasiljević, Đ: Contactless technology as a factor of tourism industry development - a review of current practices and future directions. Econ. Themes. **56**, 179–202 (2018). https://doi.org/10.2478/ethemes-2018-0011
15. Basili, A., Liguori, W., Palumbo, F.: NFC smart tourist card: combining mobile and contactless technologies towards a smart tourist experience. In: 2014 IEEE 23rd International WETICE Conference, pp. 249–254 (2014). https://doi.org/10.1109/WETICE.2014.61
16. Nica, I., Tazl, O.A., Wotawa, F.: Chatbot-based tourist recommendations using model-based reasoning. In: ConfWS, pp. 25–30 (2018)
17. Ukpabi, D., Aslam, B., Karjaluoto, H.: Chatbot adoption in tourism services: a conceptual exploration. In: Ivanov, S., Webster, C. (eds.) Robots, Artificial Intelligence, and Service Automation in Travel, Tourism and Hospitality, pp. 105–121. Emerald Publishing Limited (2019). https://doi.org/10.1108/978-1-78756-687-320191006
18. Wise, N., Heidari, H.: Developing smart tourism destinations with the Internet of Things. In: Sigala, M., Rahimi, R., Thelwall, M. (eds.) Big Data and Innovation in Tourism, Travel, and Hospitality, pp. 21–29. Springer, Singapore (2019). https://doi.org/10.1007/978-981-13-6339-9_2
19. Balandina, E., Balandin, S., Koucheryavy, Y., Mouromtsev, D.: IoT use cases in healthcare and tourism. In: 2015 IEEE 17th Conference on Business Informatics, pp. 37–44 (2015). https://doi.org/10.1109/CBI.2015.16
20. Rosario González-Rodríguez, M., Carmen Díaz-Fernández, M., Gómez, C.: Facial-expression recognition: an emergent approach to the measurement of tourist satisfaction through emotions. Telematics Inf. **51**, 101404 (2020). https://doi.org/10.1016/j.tele.2020.101404
21. Chiu, C.-C., Wei, W.-J., Lee, L.-C., Lu, J.-C.: Augmented reality system for tourism using image-based recognition. Microsyst Technol. (2019). https://doi.org/10.1007/s00542-019-04600-2
22. Kazak, A.N., Chetyrbok, P.V., Oleinikov, N.N.: Artificial intelligence in the tourism sphere. In: IOP Conference Series: Earth and Environmental Science, vol. 421, p. 042020 (2020). https://doi.org/10.1088/1755-1315/421/4/042020
23. Ivanova, L.: Cutting-edge technologies and innovations in the tourism. Presented at the Youth forum Science, Technology, innovation, business (2018)
24. Ministerio de Turismo del Ecuador: Guía de Rutas MTB Chimborazo. MINTUR, Quito (2012)

Intruder Detection System Based Artificial Neural Network for Software Defined Network

Hernán Domínguez-Limaico(✉), Willams Nicolalde Quilca, Marcelo Zambrano, Fabián Cuzme-Rodríguez, and Edgar Maya-Olalla

Universidad Técnica del Norte, Av. 17 de Julio, Ibarra, Ecuador
hmdominguez@utn.edu.ec

Abstract. This paper shows the implementation of an Intruder Detection System (IDS) integrated into an Artificial Neural Network (ANN), called (Snort + RNA); as an option to mitigate the risks of active computer attacks towards a Software Defined Network (SDN). Which leverages the network hyperconverged of the data center of the Faculty of Engineering of Applied Science (FICA) at the Technical University of the North. This proposal is tested under the PDCA model offered by the ISO/IEC 27001 standard and the processes provided by the hacker circle. The results show that Snort + RNA detects the anomalies that cause active-type attacks against the SDN, this is visible both in the alerts generated and in the record of the captured traffic, however, it is not possible to analyze all the packets it receives from attacks from DoS since some packages remain on hold or rejected. This shows that, although the system does not evaluate all the packets that circulate on the network, that it takes care of the protection of the SDN, providing alerts when its third parties tried to violate it with attacks that caused an increase in network traffic.

Keywords: Intrusion Detection System · Artificial Neural Network · Software Defined Network SDN · Active type attacks · PDCA model · Hacker circle

1 Introduction

The Software Defined Network (SDN) has emerged in recent years to solve network management problems since the term refers to the fact that this architecture allows the control plane to be separated from the data plane, to achieve more programmable networks, automatable and flexible [1].

Every type of network, no matter how current it is, has vulnerabilities, of which hackers can take advantage of to obtain information, however, to avoid this there are several solutions and one of them is the Intrusion Detection Systems (IDS) [2], its operation consists of detecting or monitoring events within a computer or a network in search of unauthorized access. [3] and [4] propose proposals in which this security tool is used to protect the SDN controller against DDoS attacks.

© The Author(s), under exclusive license to Springer Nature Switzerland AG 2023
M. Zambrano Vizuete et al. (Eds.): RITAM 2021, LNNS 512, pp. 315–328, 2023.
https://doi.org/10.1007/978-3-031-11295-9_23

However, the disadvantage of these protection systems is that for them to detect whatever anomaly, they need a network behavior profile for comparison, which must be programmed manually and must change each time the network does so. The reason why [5] presents an analysis of the design of an SDN with a focus on security, in which they evaluate Deep Learning techniques for the development of an IDS, concluding that the design of this type of IDS has not been tested in infrastructures with high speed since that is the future that is taking these systems with machine learning.

2 Experimental Design

This section presents the design of this proposal step by step and how it is governed by the PDCA model guide, which is made up of four stages; Plan (P), Do (D), Check (C), and Act (A). This model is mentioned by the ISO/IEC 27001 standard and indicates that it offers continuous improvement (constant cycle) in the security management of a network [6].

2.1 SDN Design

For the design of the SDN, a platform that serves as the base hardware infrastructure is necessary and in this way to leverage the layers that compose it (Application Layer, Control Layer, Infrastructure Layer), in this work the hyperconverged infrastructure is used proposed in the research of [7] since it allows the virtualization of other telecommunication networks such as SDN, said infrastructure is implemented in the proxmox servers (PV1, PV2, and PV3) of the data center FICA [7] since it allows the virtualization of other telecommunication networks such as SDN, said infrastructure is implemented in the proxmox servers (PV1, PV2, and PV3) of the FICA data center.

Figure 1 shows the proposed design, specifying its implementation in the physical server PV2 of the aforementioned hyperconverged infrastructure, besides, it indicates the virtual machines created and connections between virtual interfaces from the control layer to the infrastructure layer and all of these to their time with PV2; Within the virtual machines, the software used in each layer stands out, such as the application layer with the web interface and REST API, the control layer with the Opendaylight (ODL) controller and the infrastructure layer with Open Virtual Switch (OVS) in addition to the services that you want to implement in the SDN.

2.2 Snort + RNA Design

The proposed Snort + RNA design does not have a specific requirement regarding hardware and software allocation, which is why it is based on the recommendations of [8] with the following characteristics: Centos 7 minimum, 2 GB RAM, Hard Drive 100 GB, Two network interfaces.

Regarding its operation, it uses the preprocessor offered [9], which is integrated into a Multiple Layer Perceptron (MLP) network. This preprocessor enables Snort + RNA to perform real-time analysis and anomaly detection in the telecommunication infrastructure traffic without the need to establish rules. Each detected anomaly is notified through an alert that is observed in the system console, and this can be classified as real (99%) or false (less than 99%) depending on the percentage of certainty.

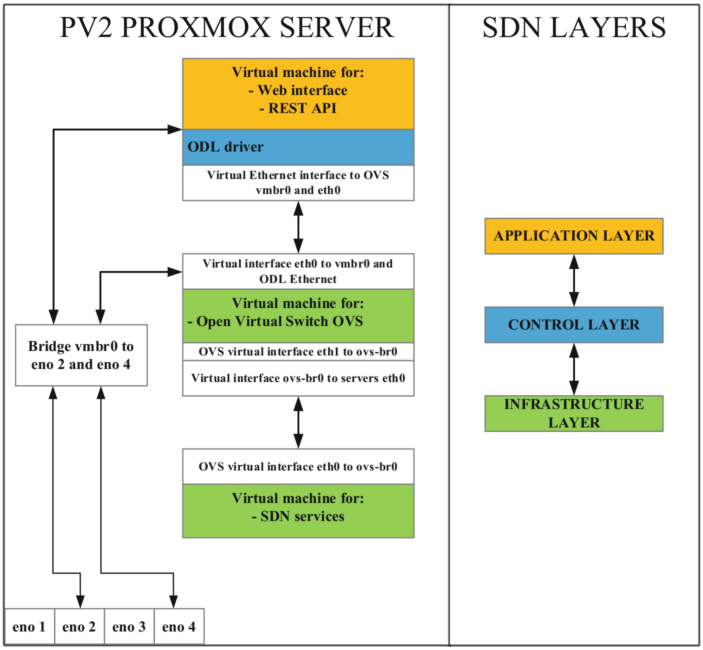

Fig. 1. SDN design on PV2 server

Another quality of Snort + RNA is the web interface that contains a record of the analyzed traffic, which is created automatically at the end of each system process, in which the veracity of the alerts generated during the analysis can be verified. Table 1 indicates the values that the system evaluates and that are presented in the traffic log.

Table 1. Variables analyzed by SNORT + RNA

Variable	Definition
hits_as_dst	(hits as destination): Number of connection initiation packets (flows) in which this IP address was listed as the destination. That is, the number of connection attempts that the IP received. A value higher than 10^3 in this parameter may mean that the IP is being the victim of a scan
hits_as_src	(hits as source): Number of connection initiation packets (flows) in which this IP address was listed as the source. That is the number of connection attempts sent by the IP. A value higher than 10^3 of this parameter may mean that the host with that IP is performing a scan
av_rcv_time	(average receive time): average time (seconds) between connection requests received by this IP. This measure tells how often connection requests are coming to a computer. A value less than10^{-3} for this parameter may mean that this host is being scanned
av_snd_time	(average send time): average time (seconds) between connection requests made by this IP. This measurement tells me how often a computer is sending connection requests. A value less than 10^{-3} may indicate that the host is performing a scan
win_count	(window counter): This value indicates how many times the measurements start; each measurement consists of 1599 connections in which an IP is marked as a destination
rel_hits	(relation hits): Number of connection initiation requests that are made between two given hosts. This parameter would be greater than 10^3 in the case of a one-to-one scan

Source: Adapted from [9]

2.3 Snort + RNA Integration to SDN

Figure 2 presents a complete design of this proposal, which consists of connecting a physical host to the physical server PV2 through its ethernet and eno2 network interfaces; the physical host contains Kali Linux and Snort + RNA in two different virtual machines, while the physical proxmox server (PV2) hosts part of the hyperconverged infrastructure that serves as a platform for SDN.

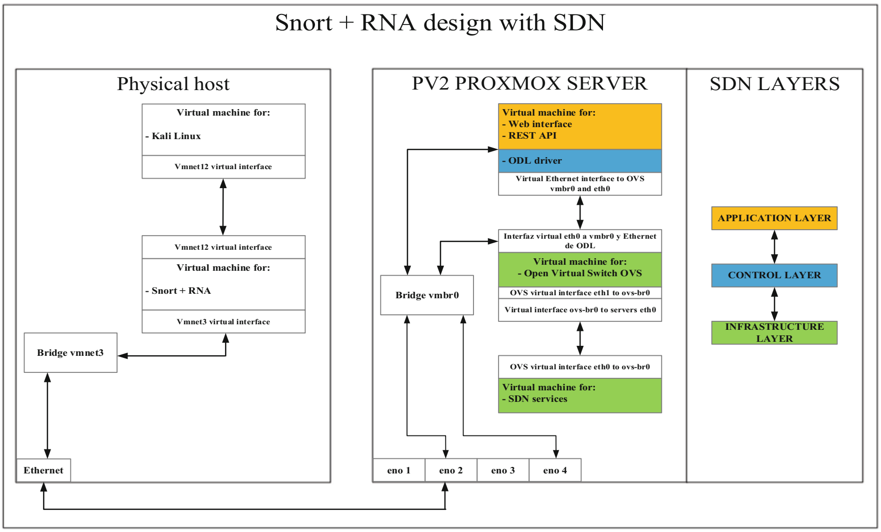

Fig. 2. Snort + RNA design with SDN

2.4 Functionality Test

The performance tests are guided by the PDCA model. Starting with the Plan stage, which shows that since SDN is a centralized network model, it makes the ODL controller a weak point against computer attacks, which is why it needs a tool like Snort + RNA to protect this area of the network.

Figure 3 is a flow diagram of what is intended to be achieved with this work, in other words, it indicates the process that is followed from the beginning of an attack and the results that this causes in case the attack is or not detected by protection tool.

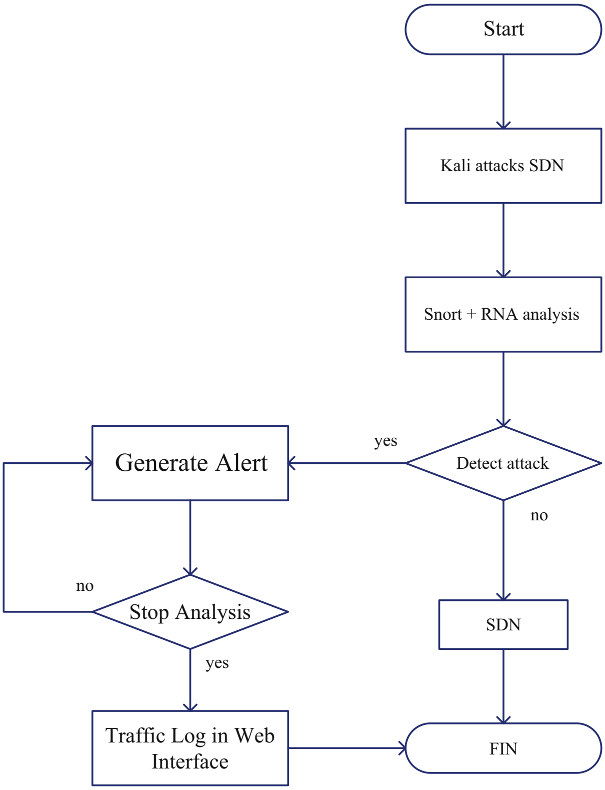

Fig. 3. Attack process flow diagram

The Do stage executes everything that is planned; For this proposal, it is the integration of Snort + RNA in SDN, which is indicated in literal C. While the Verify stage, the operation of the proposal is tested and for this, the hacker circle is used due to its Five-phase process (Inspection, Scan, Get access, Maintain access and Delete traces) to carry out computer attacks on the ODL controller and thus observe the behavior of the security system.

Inspection. It consists of obtaining all the possible information of the victim (ODL), in this case, it is intended to know his IP address, for this, the Nslookup tool is used to query a local domain (www.controlador.odl.com). The execution of this tool indicates that the IP address 192.168.100.111 corresponds to the victim.

Exploration. The purpose is to determine possible vulnerabilities that the victim has; Thus, once the IP (192.168.100.111) is known, two tools are used to scan the victim and obtain information about their ports, these tools are: Sparta and Nmap, the attack of these are found in Fig. 4.

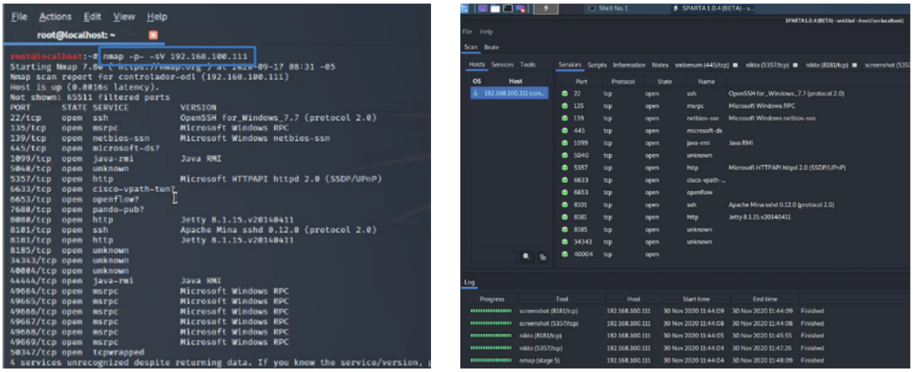

(a) (b)

Fig. 4. (a) Nmap results, (b) Sparta results.

Get access. This phase exploits the vulnerabilities obtained from the victim scan for different purposes. For this reason, as soon as the vulnerabilities are known, they begin to be exploited, and in this work, four tools are used: Metasploit, Crunch, Hydra, and Hping3.

To know if it is possible to use Metasploit on the victim, use the searchsploit command "Windows" in the attacker's terminal. If the result is similar to that shown in Fig. 5 choose one of the Metasploit functions. use (reverse_tcp).

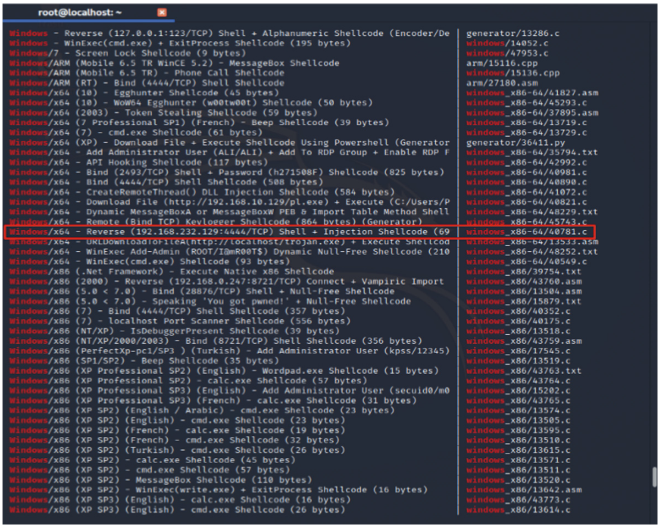

Fig. 5. Searchsploit results

This function is responsible for establishing a connection between the attacker and the victim through a payload file which must be opened from the host to be violated (ODL). The purpose of this attack is to get the administrator username in the ODL, as shown in Fig. 6, the detected user has the name, Willams.

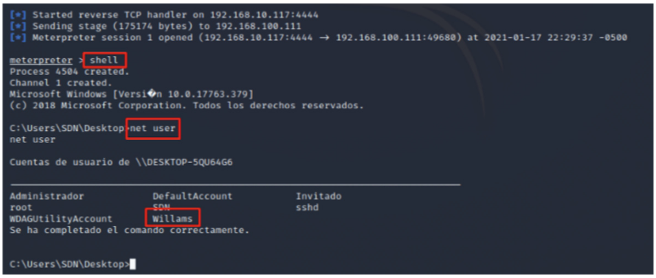

Fig. 6. Metasploit results

On the other hand, the Crunch and Hydra tools seek to obtain the password of the Willams user, the first (crunch) creates a dictionary that hydra uses to carry out a brute force attack on port 22 (ssh service) and thus achieve its mission. Figure 7 indicates that after the hydra attack the password obtained for this user is admin.

Finally, the Hping3 tool performs a DoS attack on the ODL with the purpose of truncate the web service, which allows the host control panel to be displayed. This attack is shown in Fig. 8 indicating that the IP address 10.10.10.10 floods Sync-type packets to port 8181 of the ODL IP address (192.168.100.111).

However, the ODL server does not present Denial of Service (DoS) since it continues to work normally allowing access to it and without presenting delay or slowness in accessing its web interface.

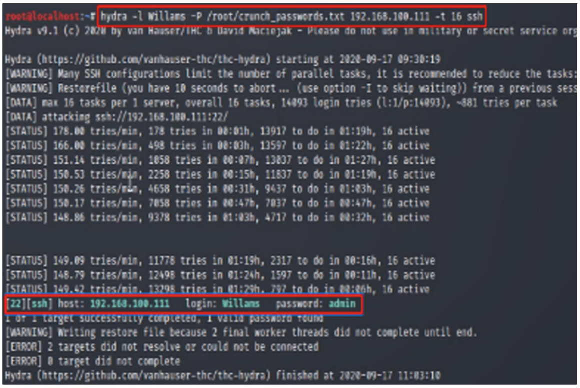

Fig. 7. Hydra results

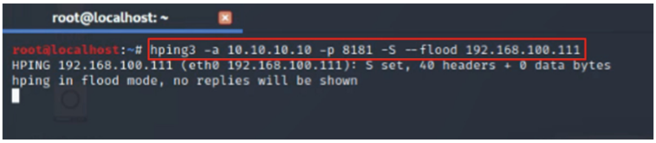

Fig. 8. Hping3 process

Maintain Access. Allows the attacker to have fully available access to the victim, without the need to go through the previous phases again. In these tests, a text file is used to store the credentials obtained that allow remote access through the ssh service to the ODL, this is how Fig. 9 shows how the credentials are transcribed in the text file.

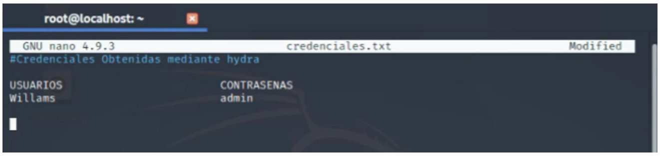

Fig. 9. Credential storage

Erase Traces. Eliminate traces that the attacker could leave throughout the process carried out by the hacker circle; in this case respective Kali Linux commands are used, which are described in Table 2.

Table 2. Commands to delete tracks

Command	Function
rm ~/.bash_history -rf	Clear history of used commands
history -c	Clear current session record
kill -9 $$	Close current sessions

3 Results

It is verified that the implemented SDN is operating because the OVS and the services integrated with it (web, FTP, and moodle) are observed in its web interface, as indicated in Fig. 10.

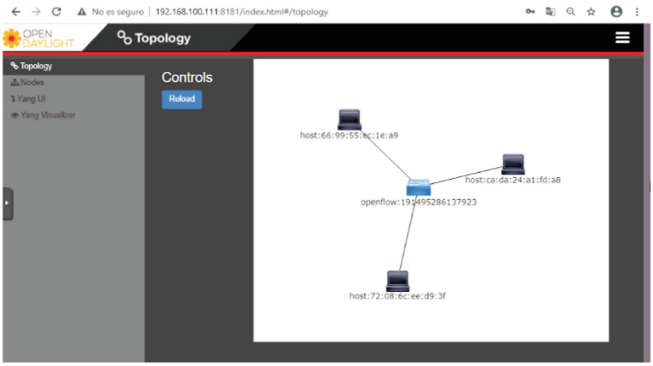

Fig. 10. ODL controller topology

It is also possible to connect a sniffer to the SDN to verify that Openflow packets are found in your network flow, as shown in Fig. 11. Openflow packets indicate that the network is working with the protocol of the same name.

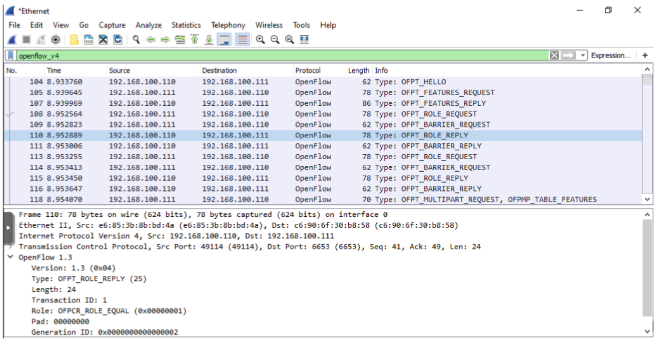

Fig. 11. Openflow packets captured by Wireshark.

During the hacker circle attacks, Snort + RNA executes an independent analysis to obtain a better interpretation of the behavior of the security system before each one of the tools used. Table 3 shows the results obtained from the packets circulating through the Snort + RNA during the different attacks.

Table 3. SNORT + RNA results

	Nslookup	Nmap	Sparta	Metasploit	Hydra	Hping3
Packages received	8	267994	713540	185	95791	4671833
Packages analyzed	4	267973	560663	185	95791	825335
Rejected packages	0	0	152877	0	0	3846498
Waiting packages	4	21	0	0	0	0
Alerts	0	166	307	0	57	516

Based on the results presented above, it is possible to conclude that the attacks by the nslookup and Metasploit tools did not generate alerts since they did not present alterations in the network. On the other hand, the nmap, Sparta, hydra, and hping3 attacks did generate alerts as these tools cause an unusual increase in network traffic. Another way to verify it is through the alerts generated by the Snort + RNA, these are classified as real because they indicate 99% certainty, Fig. 12 is taken as an example of the notifications that are generated during the attack from the Nmap tool.

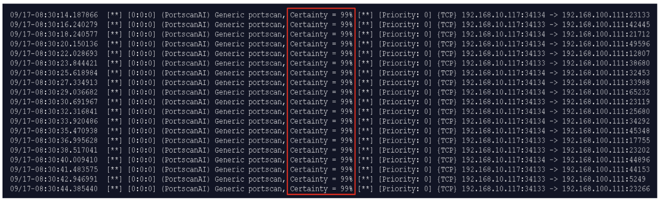

Fig. 12. Snort + RNA alerts for nmap.

It should be added what the literal B mentions, Snort + RNA has a web interface to observe the record of the traffic captured during the attacks carried out with the mentioned tools, in which it is verified if the alerts generated are real or false attacks positive, having as a point of reference the information provided in Table 1.

The registry for nslookup and Metasploit are the same in terms of ranges of normal values, however, the registry for nslookup (see Fig. 13) s taken as an example, it is observed that the numbers of packets in hits_as_src and hits_as_dst are lower to 10^3, likewise, the times in av_rcv_time and av_snd_time are higher than10^{-3}, clarifying the reasons why the Snort + RNA does not generate alerts with this attack.

Log_method: File	Logs generated: 09/17-08:28:02

IPs Hash table

IP	hits_as_src	hits_as_dst	av_rcv_time	av_snd_time	win_count
192.168.10.117	2	0	0.000000	0.000105	0
192.168.10.129	0	2	0.000105	0.000000	0

Direct Relation Hash table

IP src	IP dst	rel_hits
192.168.10.117	192.168.10.129	2

Registered IPs in IPs Hash table: 2
Registered Direct Relations: 1

Fig. 13. Nslookup attack logs

On the other hand, the registers for nmap, sparta, hydra, and hping3 show values outside the established ranges, in this way the hydra register (see Fig. 14) is used as an example, which exposes hits_as_src and hits_as_dst with numbers of packets greater than 10^3, it is necessary to clarify that for the victim IP (192.168.100.111) win_count is taken into account because it indicates that the measurements were made 31 times and in each measurement, there were 1599 hits_as_dst (number of packets as destination), likewise, av_rcv_time and av_snd_time contain times less than 10^{-3}, and in this way, it is verified that the alerts generated by the Snort + RNA are from real attacks.

Log_method: File	Logs generated: 09/17-11:03:26

IPs Hash table

IP	hits_as_src	hits_as_dst	av_rcv_time	av_snd_time	win_count
192.168.10.117	1838	755	0.018466	0.001663	0
192.168.100.111	307	341	0.001497	0.016636	31

Direct Relation Hash table

IP src	IP dst	rel_hits
192.168.100.111	192.168.10.117	755
192.168.10.117	192.168.100.111	49910

Registered IPs in IPs Hash table: 2
Registered Direct Relations: 2

Fig. 14. Hydra attack logs

Finally, in the PDCA model, the Act stage provides feedback on the efficiency of the proposal presented in the planning stage, in this case, the Snort + RNA in SDN; For this, the results obtained are analyzed and it is possible to determine that the system is not capable of examining all the packets it receives when they begin to be transmitted in large quantities, taking as an example the results of the Hping3 tool and Hydra.

In the first case with Hping3, Snort + RNA captures a total of 4′671,833 packets during its execution, however, due to the hardware resources assigned to the virtual host in which the system is implemented (section B) it randomly evaluates only 825,335 packets (equivalent to 17.67%) since the Snort + RNA processing does not allow to analyze more packets since it is limited by the hardware; For this reason, 3′846.498 packets (82.33%) are rejected, showing that to offer a complete analysis of DoS attacks, greater processing capacity is needed. On the other hand, there are the results of Hydra, in this scenario 95791 packets are generated, of which Snort + RNA manages to analyze 100% of the generated packets; which indicates that before this type of brute force attacks the system is efficient.

Thus, to obtain different results it is possible to execute three alternatives; The first alternative is to carry out the same design with another training set, which will allow the system to improve efficiency against DoS attacks, the second alternative is to make a change in the type of RNA and in this way observe the changes that the IDS presents, while the third alternative is to change the IDS and adapt it to the ANN that is proposed in this work.

4 Conclusions

The PDCA model of ISO/IEC 27001 proposed in this work was a flexible option when offering information security because it was perfectly coupled with the protection of Snort + RNA in ODL. In the same way, the process of the hacker circle was adjusted to the different tools that were proposed, since it was possible to fulfill the purpose of each phase (recognition, exploration, obtaining access, maintaining access, erasing traces) that makes it up.

In this sense, it is necessary to make clear that, although the Snort + RNA cannot analyze all the traffic that goes towards the SDN; if it generates alerts when active attacks occur, which are characterized by causing an unusual increase in traffic.

As future work, it is planned to deploy an IPS with RNA, which in addition to alerting the attacks that are carried out against the network, it executes action to mitigate the damage that these attacks may cause, among these actions may be: blocking of ports or IPs, port forwarding, IP reassignment. Additionally, it is intended to perform an analysis of performance metrics such as False-Positive, False-Negative, True-Negative, and True-Positive in the Snort + RNA system developed in the present work since the volume of packets that pass through and are processed by this security system.

References

1. Sandoval, C.: Implementación de un cluster-controlador de SDN basado en un framework de software libre para la infraestructura cloud de la facultad de Ingeniería en ciencias aplicadas, Universidad Técnica del Norte (2018)
2. Luna, J.: Sistema detector de intrusiones ocupando una red neuronal artificial (2015)
3. Manso, P., Moura, J., Serrão, C.: SDN-based intrusion detection system for early detection and mitigation of DDoS attacks. Inf. **10**(3), 106 (2019). https://doi.org/10.3390/info10030106
4. Reddy, T.N., Annapurani Panaiyappan, K.: Intrusion detection on software defined networking. Int. J. Eng. Technol. **7**(3), 330–332 (2018). https://doi.org/10.14419/ijet.v7i3.12.16052. 12 Special Issue
5. Sultana, N., Chilamkurti, N., Peng, W., Alhadad, R.: Survey on SDN based network intrusion detection system using machine learning approaches. Peer-to-Peer Netw. Appl. **12**(2), 493–501 (2018). https://doi.org/10.1007/s12083-017-0630-0
6. ESAN: La norma ISO 27001 y la mejora continua en la gestión de seguridad de la información | Tecnología | Apuntes empresariales | ESAN (2016)

7. Maya-Olalla, E., et al.: Design and tests to implement hyperconvergence into a datacenter: preliminary results. In: Botto-Tobar, M., León-Acurio, J., Díaz Cadena, A., Montiel Díaz, P. (eds.) ICAETT 2019. AISC, vol. 1066, pp. 54–66. Springer, Cham (2020). https://doi.org/10.1007/978-3-030-32022-5_6
8. CentOS: CentOS Wiki, CentOS Product Specifications, 12 December 2020. https://wiki.centos.org/About/Product. Accessed 16 Apr 2021
9. Bedon Cortazar, C. E.: Snort-AI - Browse/Documentation at SourceForge.net, Snort-AI, 14 January 2009. https://sourceforge.net/projects/snort-ai/files/Documentation/. Accessed 16 Apr 2021

Irrigation Control System Using Machine Learning Techniques Applied to Precision Agriculture (Internet of Farm Things IoFT)

Edgar Maya Olalla(✉), Héctor D. Cadena-Lema, Hernán M. Domínguez Limaico, José C. Nogales-Romero, Marcelo Zambrano, and Carlos Vásquez Ayala

Universidad Técnica del Norte, Ibarra 100105, Ecuador
{eamaya,hdcadenal,hmdominguez,jcnogalesr,omzambrano, cavasquez}@utn.edu.ec

Abstract. Many technologies are currently assisting in the remote monitoring and analysis of various sensor networks which are intended for inhospitable or difficult to access locations. Therefore, it is necessary to develop several investigations which help to deepen and facilitate such analysis and monitoring.

The objective of this research is the development of an electronic system to automate the irrigation process in crops based on artificial neural networks through remote monitoring using low power wide area networks (LPWAN). To this end, the research question is as follows: How does a technology such as LPWANs help the remote monitoring and control of crop irrigation processes (precision agriculture) and how feasible is the application of machine learning by neural networks of a system, for the automatic control of such process?

In this context, the analysis of each of the proposed scenarios will allow us to generate an answer to the question posed.

The research question is answered through a study in the farm "La Pradera" of the Technical University of the North where field analyses will be carried out in order to develop several scenarios in which the neural networks and LPWAN technologies are implemented for their analysis.

Keywords: Internet of Farm Things (IoFT) · Wireless sensors network · LPWAN · Neural networks · Irrigation

1 Introduction

In the crops, with the analysis of each of the parameters that influence the development of the plants such as: environmental temperature, floor humidity,

© The Author(s), under exclusive license to Springer Nature Switzerland AG 2023
M. Zambrano Vizuete et al. (Eds.): RITAM 2021, LNNS 512, pp. 329–342, 2023.
https://doi.org/10.1007/978-3-031-11295-9_24

relative humidity, illumination levels and CO2 levels, the aim is to analyze the behavior of these and to be able to determine how they affect the development of the crops. Making use of the analysis of the parameters previously mentioned, specifically the values of humidity of the floor, an automatic control system of the irrigation in the cultivations will be made, for which an investigation on the algorithm of artificial neuronal networks will be made which is used in the area Automatic Learning, to be able to make the predictions of when the culture requires of irrigation. To implement the algorithm, we will use Python programming software, through which we will receive data collected from a network of sensors to be analyzed by the system and it can determine whether the crop requires water irrigation or not and thus ensure that the plant receives an adequate dose for its proper development. Once the data has been received and analyzed by the software and if it determines that irrigation is needed in the field, the order will be sent wirelessly so that the electrovalve allows the flow of water to the field, until the system considers that the dose of water supplied is sufficient and thus avoid unnecessary watering of the crops thus helping the plant to have an optimal development, there will also be a considerable reduction in water consumption and also the work of irrigation that is currently used will no longer be manual and craft to become an automated system [5].

The use of Artificial Intelligence for the analysis of agricultural process data is a topic that is currently being developed. At present, many of the data in the agricultural area are taken manually, and there is no way of storing this information in an orderly manner, nor is it given the respective analysis process, in order to obtain improvements in the development of the crops. A very good alternative to overcome these problems is the implementation of precision agriculture, which, with the use of a scientific, documentary and technological base, makes it possible to make the most of the resources available [6] (Fig. 1).

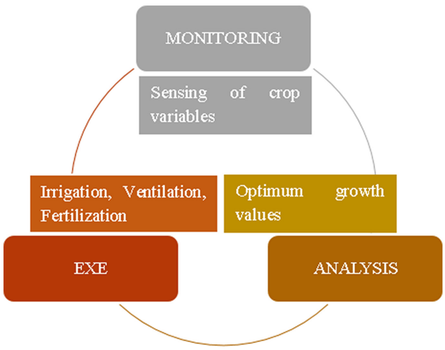

Fig. 1. Precision agriculture scheme.

Low Power Wide Area Networks (LPWAN) are wireless communication technologies used within the IoT (Intenet of Things) area. LPWAN technologies are ideal for connecting devices that require sending small amounts of data over long distances and maximizing battery life. The main features of LPWAN are: long range communication (up to 15 km with line of sight), low transmission speed (less than 5000 bits of data per second are sent) and low power consumption (a battery can last up to 10 years) [3].

Precision agriculture is a set of techniques aimed at optimizing the use of agricultural inputs and improving results in the production of quality food under the concept of crop management, based on the presence of variability in the field [1].

By using current technologies such as GPS, sensors, satellites and aerial images, information can be collected which allows us to analyze many of the factors that directly affect crop results. The decisions made from the collected information allow us to optimize the results taking into account different points of view, such as:

- The agronomic vision which allows to make arrangements according to the need of the plants, which affects in a positive way on the results in the production.
- From the point of view of the environment, it is possible to reduce the harmful impacts that the techniques applied in the cultivation could have.
- Finally, from the economic point of view, it is possible to improve the use of resources in such a way as to obtain a considerable reduction in costs, which will allow the farmer to earn much more and be more competitive in the market with better quality products.

Among the advantages of using these techniques are Reduction of costs in the use of inputs, higher yields in the crops with the same amount of materials and higher quality of the products in the crops [4].

The work analyzes how feasible is the study of neural networks and machine learning in embedded systems that can be applied to IoFT, and how a sensor network acts together with the neural network system, thus thinking the best way that these two systems coexist to carry out a precision agriculture that meets the requirements of the proposed study

2 Methodology

According to [5], the variables that influence the good development of alfalfa cultivation are Soil humidity, relative humidity, environmental temperature and luminosity, which are very important to determine when it is possible or not to activate the irrigation process.

For the development of this project it is necessary to use system design methodologies that include prototyping, for this reason the V model is chosen, which guides the integration of the system allowing feedback during the development process. Additionally, the IEEE-29148 standard is used as a complement to the V-model to make the selection of both hardware and software components involved in this titling work (Fig. 2).

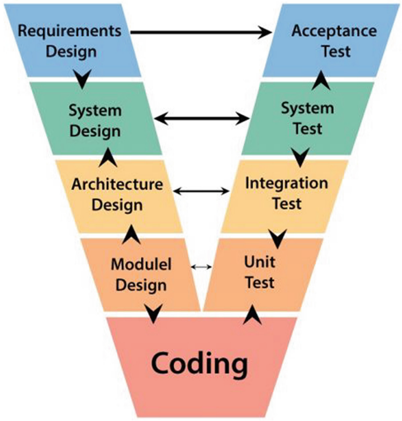

Fig. 2. V model for project development

In the first level of Fig. 19, the requirements and specifications that the present project should have should be specified and documented, collecting data and information that will allow us to know the factors that influence the implementation of the project.

Likewise, in the second level, the system requirements are determined; this level comprises one of the most important phases for the project to be successful, since they define the functionality of the proposed system. In the system integration phase, tests are performed to verify the functionality of each module that is part of the project. The third level defines all the states that will be developed in each part of the system in order to obtain a design and general vision of the project. In the unit test phase, independent verification of each part of the project is carried out, checking the correct implementation, coherence and compliance with the respective specifications. Finally, in the last level is the implementation phase with which the project design is materialized and the programming for each part of the project system to be carried out is carried out.

To determine the factors involved in the development of the proposed irrigation system, an analysis of the environment in which the present project will be implemented is needed. In this case, it has to do with the spatial aspect as far as the dimensions of implementation in the field and the studies that are made on the crop, in addition the necessary information is obtained to look for strategic places and to determine the location and model of the hardware to be used, for all this it is necessary a visit to the site of implementation of the irrigation system.

System requirements and architecture requirements are defined, to finally have a functional prototype in order to meet user needs, the scope of the system and thus ensure that this research benefits those involved in the cultivation of alfalfa (Table 1).

Table 1. Details of parameters of system

Acronym	Description
StSR	Stakeholder requirements
SySR	Functional system requirements
SRSH	Architecture requirements

3 Results

3.1 Pre-requisites Parameters

With the purpose of defining the requirements of the stakeholders in the development of the system, a common set of requirements is analyzed that express the interaction that the system will have with its environment and with the users involved in this project. Table 2 contains the operational and user requirements considered in the Stakeholder Requirements (StSR).

It refers to a list of requirements with respect to each of the functions, behavior and form of use of the system. Table 3 details the functional requirements that allow the design of the prototype.

Refers to the components that make up the system, both software and hardware, the correct analysis of these requirements allows a correct choice of materials needed, which are listed in Table 4.

The selection of both hardware and software is done through Table 4 which contains the hardware and software requirements for the proper development of the project, for this a comparison table is made between the embedded systems that can cover all or most requirements and proceeds to assign a rating (1: meets and 0: does not meet) to each of the embedded systems depending on the characteristics of each of these embedded boards and choose the one that gets the highest weighting.

Table 2. System requirements

					StSR
SySR					
System beginning requirements					
#	Requirements	Priority			Relation
		High	Med	Low	
UI requirements					
SySR1	I/O Pin	X			
SySR2	Serial communication	X			
SySR3	Electronic system should act between them	X			
Performance requirements					
SySR4	Work with a data base to administrate the info	X			
SySR5	Low power consumption	X			
SySR6					
SySR7	Low data adquisition error	X			
SySR8	Ground analysis	X			
SySR9	Begin NNA analysis	X			
State requirements					
SySR10	Irrigation actived	X			
SySR11	Estado de funcionamiento y carga con batería independiente			X	
Physical requirements					
SySR12	Ambiental resistance	X			
SySR13	Reduce height			X	

This stage is the determination of the general components of the system; in order to reduce the complexity of the system design and to optimize the distribution of the hardware resources, the best way to achieve this is to establish a division in zones over the area where the research is developed,. The following result is derived from Table 5: the component that meets the highest number of requirements for the system is an Arduino UNO microcontroller, since it is the device that best fits the needs of the project due to its reduced size (68.5 mm × 5. 8 mm) and low power consumption (46 mA), besides that its information processing capacity is sufficient for this area, compared to the Arduino Mega which is larger (101.6 mm × 53.34 mm) and also has a higher power consumption (93 mA) as well as the raspberry Pi3 with a size of 56 mm × 85 mm and a power consumption of 350 mA. The characteristics of the selected microcontroller can be seen in Sect. 3.8.2.

Between the two zones, data is constantly being sent and received. In addition to this, the geographical location of the zones makes it essential to have a wireless means of communication between them. Table 6 presents some of the wireless technologies that are related to system requirements.

The following result is derived from Table 6: The technology that meets the highest number of requirements needed by the irrigation control system based on artificial neural networks is LoRaWAN, therefore, by using this technology

Table 3. System requirements

SRSH					
Architecture requirements					
#	Requirements	Priority			Relationship
		High	Med	Low	
Hardware requirements					
SRSH1	Wireless communication stable	X			
SRSH2	Embbebed system analysis	X			
SRSH3	I/O SE	X			
SRSH4	Low power consumption	X			
SRSH5	Rx and Tx wireless transmission	X			
SRSH6	Wireless Scop around 520 m	X			
Software requirements					
SRSH7	Open source	X			
SRSH8	Compatibility with NNA	X			
SRSH9	NNA software executable analysis		X		
SRSH10	Microcontroller library compatibility	X			
SRSH11	Phyton IDE compatibility	X			
SRSH12	Electrical compatibility	X			
SRSH13	Overload	X			
SRSH14	Moodle compatibility				
SRSH15	Easy connection				
SRSH16	Less RAM usage				
Electrical requirements					
SRSH17	VCC	X			
SRSH18	VDC to charge batteries	X			

the wireless communication system is implemented between zone 1 and zone 2, because it allows a greater coverage compared to the other technologies listed in Table 6. One of the devices that works under this wireless communication technology is the RN2483 chip, which also has a reduced size, has a low power consumption which helps to extend the life of the battery and is available in the national market.

The physical structure of this system is formed by a wireless sensor network taken from previous works and the control node of the electrovalve that will be controlled by the neural network implemented in this research work, located in zone 1 referring to the location of the alfalfa crop and zone 2 or command zone where the ANN is implemented for the irrigation control part. Zone 1 is composed of the following elements: Power supply, sensors needed to measure

Table 4. System requirements

Hardware	Requirements					Total value
	SRSH3	SRSH5	SRSH7	SySR5	SRSH13	
Arduino UNO	1	1	1	1	1	5
Arduino Mega	1	1	1	0	0	3
Raspberry Pi3	1	1	1	0	1	4

1 - Comply
0 - Not cumply

Table 5. System requirements

Hardware	Requirements				Total value
	SRSH1	SRSH4	SRSH6	SRSH11	
Bluetooth	0	1	0	1	2
WIFI 802.11	1	1	0	1	2
ZigBee - IEEE 802.15.4	1	1	0	1	3
LoRaWAN	1	1	1	1	4

1 - Comply
0 - Not comply

each of the meteorological variables, relay module, solenoid valve, the Arduino UNO microcontroller and a communication module with LoRaWAN technology (RN2483). Zone 2 consists of the Raspberry Pi 3 embedded system, a LoRaWAN communication module and its respective power supply.

3.2 Results

Once the analysis and information collection for the selection of the components that will integrate the system is done, the design proceeds with the purpose of presenting a general vision of the system's operation in a structured way; in order to define the system design guidelines, the criteria and limitations taken into account during the analysis and the system requirements that will allow the development and implementation of the present project must be considered. As part of the system design, the following is a block diagram, circuit diagram and flow chart that will guide the physical and logical operation of the system, as well as the processes to adequately develop the scripts and the automatic learning algorithm, to subsequently carry out the unit testing phase to independently verify each module that is part of the irrigation system based on Artificial Intelligence, in order to guarantee its correct operation [13].

The functional process of the system is presented by means of a block diagram, which allows to have a clear perspective of the functionality of the proposed system. The figure below shows the general block diagram, which is subsequently divided into two stages; the first stage is formed by the collection of environmental data, storage of such information and the construction of the automatic learning algorithm (ANN); and, the second stage presents a feedback of the environmental data acquisition block because these are necessary for the functioning of the neural network in real time, since they are input data from the neural network which will be processed by the algorithm and thus determine whether or not it is necessary to start the irrigation process in the decision block (Fig. 3).

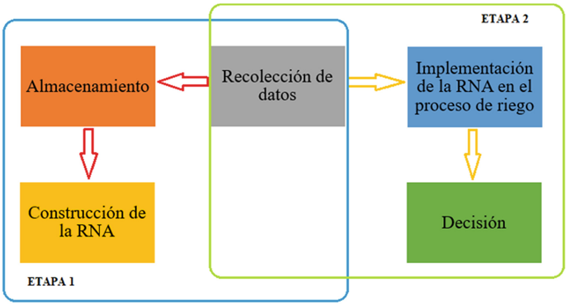

Fig. 3. Block diagram

The block diagram shown below represents the first stage, developed for the implementation of the automatic learning algorithm for irrigation automation, the first stage consists of 3 blocks which in turn contain sub-processes; the blocks have been drawn depending on the functions that each must perform. The figure shows the block diagram for this stage (Figs. 4 and 5).

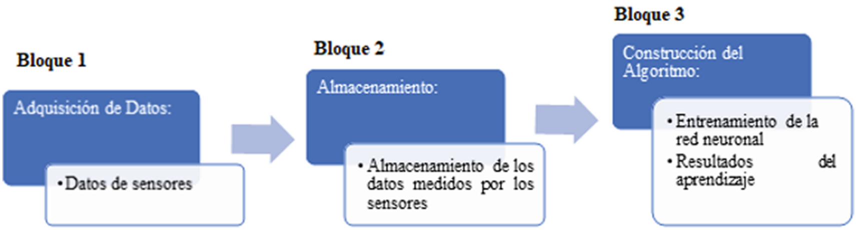

Fig. 4. Block diagram

The block diagram of the second stage of the system shown in figure, is presented for the purpose of publicizing the operation of the irrigation automation system, is composed of three blocks with a small description of the functions that each performs. The intelligent irrigation system based on artificial neural

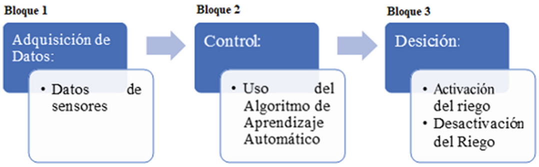

Fig. 5. Block diagram

networks is formed by a WSN network taken from previous works. The topology that allows the implementation of this system is the star topology formed by two zones, which are Zone 1 is made up of the WSN from which data on environmental temperature, relative humidity, luminosity and soil moisture are obtained; and the actuator node which is made up of the electrovalve; and zone 2 as a terminal station where data sent from zone 1 is received and stored. It is also where the neural network for automatic irrigation control will be implemented, which is the purpose of this research (Fig. 6).

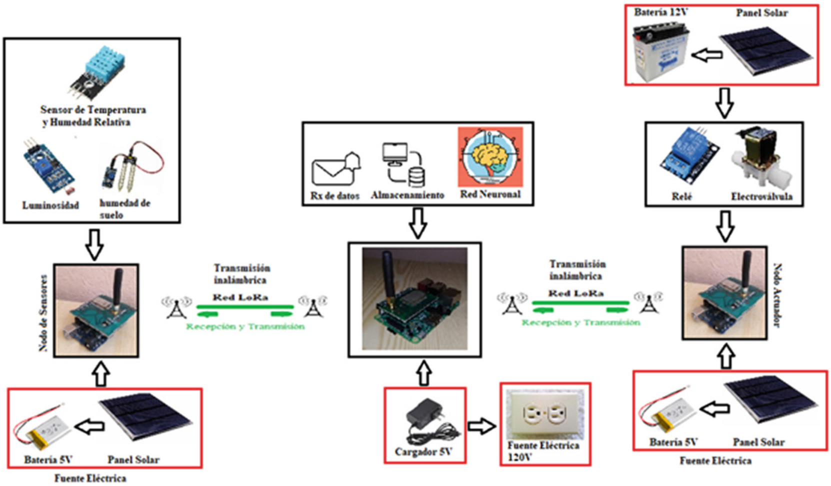

Fig. 6. Block diagram

For the collection of data to train the neural network should be taken into account the characteristics of the plant, in this case of alfalfa, for that advice was requested to an Agricultural Engineer, who knew how to say that the alfalfa is a plant that does not consume much water, also recommended to perform the watering process during the night because when performing this process during the day the water tends to evaporate much faster which takes time to hydrate the plant, which is why it does not develop in the best way and have much smaller plants, instead when watering during the night you have more time to hydrate and the alfalfa develops in a better way reaching greater size. Based on this information the sampling is done, this cycle had a duration of 20 days with a sampling period of 5 min. For the neural network output labels, the value of 1 is taken as activation and the value of 0 as non-activation of the irrigation system. The data collection and the assignment of the labels is done taking into consideration that the irrigation is going to be done during the night because the plant has more time to hydrate itself adequately, since during a sunny day the evaporation of the water is much faster which means that the water resource is wasted and the plant has less time to hydrate itself.

The design of the neural network is mainly developed from three elements: the first one is the input data that corresponds to the data collected and sent by the node of sensors of the crop, sensors of soil humidity, relative humidity, ambient temperature and luminosity, of all these sensors only the values of luminosity and humidity of the soil are taken into consideration, since it is desired to carry out the irrigation during the night; the second element corresponds to the algorithm of the neuronal network that will be the one in charge to process the information of its inputs and the third element corresponds to the output data in this case a value that represents the activation (1) or not activation (0) of the irrigation system (Fig. 7).

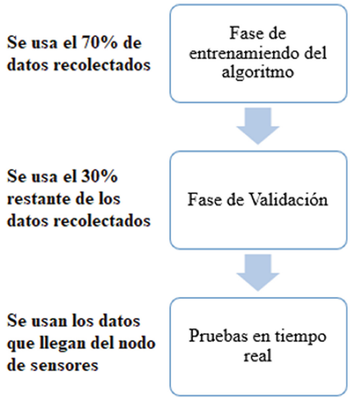

Fig. 7. Block diagram

Once the number of layers of the neural network and the number of neurons in each of the layers is known, we proceed to model the neural network which can be seen in figure, in which we have four neurons in the input layer which correspond to each of the environmental variables measured (environmental temperature, relative humidity, soil humidity, luminosity), in the hidden layer we have two neurons and in the output layer a single neuron that corresponds to the irrigation variable (on or off) (Fig. 8).

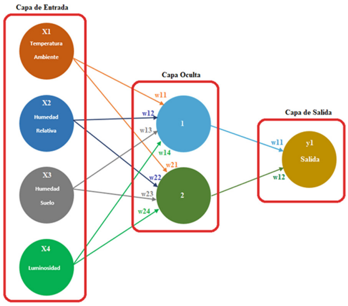

Fig. 8. Block diagram

The training of the neuronal network is based on the readjustment of the weights in each of the neuron inputs, the weights are numerical values that require the strength of synaptic link between two neurons. For this research, the backpropagation algorithm is used, which consists of a procedure for propagating the error from back to front, that is, it starts by calculating the error in the output layer and then readjusts the weights attached to this last layer to achieve a reduction of this calculated error. Then the error is calculated in the intermediate layer and in the same way that in the output layer are readjusted the weights of this layer in order to reduce the error, thus, have a better accuracy in the results.

After training the neuronal network, we proceed to verify in software the percentage of effectiveness of ANN, one of the ways in which this is done is through the use of a confusion matrix, in which we have the number of false positives, false negatives, true positives and true negatives (Table 7) .

Table 6. NNA confusion matrix

Confusion Matrix		Predicted	
		Negative	Affirmative
Real Value	Negative	a	b
	Affirmative	c	d

Table 7. System requirements

Confusion Matrix		Predicted	
		Negative	Affirmative
Real Value	Negative	570	31
	Affirmative	28	485

After replacing the values in each of the corresponding equations we have a percentage of 95.3% for the sensitivity and 93.9% for the specificity of the artificial neural network.

4 Discussion and Conclusions

Through the research conducted, it was established which parameters influence the development of alfalfa, and which have a direct impact on the process of irrigation of the crop. With the information collected from the bibliographic review, the parameters for the collection of environmental data for the training dataset of the neuronal network were established, that is why with the research carried out on the operation of the artificial neuronal networks it was possible to establish the number of capable of the neuronal network, the amount of neurons in each one of them, that is to say, it was possible to establish an ideal model for the development of the irrigation system.

During the testing period of the irrigation system based on artificial neuronal networks, it was necessary to implement two types of test scenarios, in order to make a comparison at the end of the tests and thus visualize the changes presented in the cultivation of alfalfa using traditional irrigation techniques in comparison with the irrigation system proposed in this research. It was also demonstrated that using artificial neuronal networks with supervised learning in intelligent irrigation applications is a very valid and viable option as a binary control system, even when there is a low density of data for training the neuronal network since with the implementation of the irrigation system based on artificial neuronal networks, great positive changes were achieved in terms of crop development, since it was observed that the plants reached a larger size, the amount of leaves was more abundant and a much more attractive green color than the plants with the manual irrigation system.

At the same time, each of the objectives established at the beginning of this research was met. There is an automated irrigation system that properly classifies the data patterns that come from a network of wireless sensors that indicate whether or not it is necessary to irrigate the crop.

References

1. Bongiovanni, R., Mantovani, E., Best, Á., Rogel, S.: Agricultura de Precision: Integrando conocimientos para una agricultura moderna y sustentable, Montevideo: Procisur/IICA (2006)
2. Rojas, F., Lezcano, M., Medina, F.: Agricultura de precision con sensores inalambricos, Santa Cruz de la Sierra (2016)
3. Paredes-Páliz, D.F., Maya-Olalla, E., Nogales-Romero, J.C., Padilla-Calderón, C.A.: Low power wide area network: technical review for wireless sensor networks and its utilization in smart cities deployment through internet of things (IoT) system. In: Botto-Tobar, M., Zambrano Vizuete, M., Torres-Carrión, P., Montes León, S., Pizarro Vásquez, G., Durakovic, B. (eds.) ICAT 2019. CCIS, vol. 1195, pp. 113–126. Springer, Cham (2020). https://doi.org/10.1007/978-3-030-42531-9_10

4. Garcia, E., Flego, F.: Agricultura de Precision, Buenos Aires (2015)
5. InfoAgro, El cultivo de la Alfalfa (2010). [En línea]. https://www.infoagro.com/herbaceos/forrajes/alfalfa.htm
6. Ibañez, J.: Madrid Blogs, 26 June 2006. [En línea]. http://www.madrimasd.org/blogs/universo/2006/06/26/33002
7. Leon, R.: Producción y manejo de pastos y forrajes, Editorial Universitaria, pp. 130–136 (2002)
8. Huertas, L.: Horticom, March 2008. [En línea]. http://www.horticom.com/pd/imagenes/69/757/69757.pdf
9. Peery, J.: PROMIX, 12 September 2017. [En línea]. https://www.pthorticulture.com/es/centro-de-formacion/como-influye-la-humedad-en-la-calidad-de-los-cultivos/
10. Pacheco, A.: ACEA: Invernaderos para el mundo, 7 June 2010. [En línea]. http://acea.com.mx/articulos-tecnicos/alex-j-pacheco/60-los-factores-ambientales-y-su-influencia-en-invernaderos-313-la-luz-dentro-del-invernadero
11. Iglesias, N.: INTA (2009). [En línea]. http://inta.gob.ar/sites/default/files/script-tmp
12. Martínez, A.: twenergy, 3 August 2017. [En línea]. https://twenergy.com/a/sistemas-de-riegos-para-momentos-de-necesidad-de-ahorro-de-agua-2709
13. Lara, F.: Fundamentos de Redes Neuronales Artificiales (2014). [En línea]. http://conceptos.sociales.unam.mx/conceptos_final/598trabajo.pdf

ARTANDIC: A Solution to Encourage the Purchase of Handicrafts in Ecuador

Angela Díaz Cadena[1(✉)] and Crismary Ospina Gallego[2]

[1] Universidad de Guayaquil, Guayaquil, Ecuador
angela.diazca@ug.edu.ec, criosgal@doctor.upv.es
[2] Universidad Politécnica de Valencia, Valencia, Spain

Abstract. Ecuador has great artisan potential that is not valued entirely within its own territory. Hence, the need to be resolved is based on the low level of commercialization that does not allow the Ecuadorians to foment in their desire to acquire artisanal production, thereby obtaining, consequently, low economic income for these people, in addition to the frustration of not feeling valued for their work. This work presents ARTANDIC, which is a business idea and arises as a solution in the low commercialization of handicrafts in Ecuador. This causes a cultural and economic problem for the people dedicated to this activity and for the country itself.

Keywords: Artisans · Crafts · Commercialization · Ecuador

1 Introduction

Crafts are any product that is made in small workshops, fundamentally with the hands, complemented with tools and machines for commercial, artistic, or creative purposes. In Ecuador, crafts are manifested by the conjugation of ancestral knowledge with raw materials, which has given rise to hundreds of objects that reflect, in an extraordinary way, the cultural diversity in each province.

The problem that arises in this work is the low commercialization of handicrafts in Ecuador. This produces a problem both culturally and economically for the people dedicated to this activity and for the country, since the Ecuadorian economy depends on various sectors for its progress, one of the most important being crafts, which are linked to the development of society, arts, and crafts.

Ecuador has great artisan potential that is not fully valued within its own territory, so, according to this problem, the need to solve it is based on the low commercialization that does not allow Ecuadorians to encourage the desire to acquire artisan production, resulting in low economic income for these people, in addition to the frustration of not feeling valued for their work (Cadena et al. 2018).

According to Diaz Cadena et al. there are SMEs that are dedicated to marketing this type of product. Many of them keep their hangers full, except for tourist places where most of the clients are foreigners at the time of the holiday (Díaz Cadena 2017).

© The Author(s), under exclusive license to Springer Nature Switzerland AG 2023
M. Zambrano Vizuete et al. (Eds.): RITAM 2021, LNNS 512, pp. 343–351, 2023.
https://doi.org/10.1007/978-3-031-11295-9_25

Therefore, this work presents ARTANDIC, which is a business idea and arises as part of a solution to the problem of the low commercialization of handicrafts in Ecuador as a problem. This produces a problem both culturally and economically for the people dedicated to this activity and for the country. Due to the Ecuadorian economy depends on various sectors for its progress, one of the most important being crafts, which is linked to the development of society, arts, and crafts.

ARTANDIC aims to provide a service that helps artisans have a better marketing option and, therefore, an income. On the other hand, it expects to make people dedicated to crafts feel that their work is appreciated. ARTANDIC would be a company that offers a monthly, semi-annual, or annual subscription service to Ecuadorian artisans through a website, with the purpose of offering an option that improves the marketing of their products and encourages the habit of buying handicrafts (Díaz Cadena 2017).

2 Methodology

In this study, we used different tools to determine how good the information was. Therefore, we started by stating some terminologies that help us to have an understanding related to SMEs.

2.1 Terminology

Pestel. The methodology used to review the general environment is the Pestel analysis. It consists of examining the impact of those external factors beyond the company's control, which can affect its future development. Due to this, the different environmental factors that could affect the company are analyzed below (Pedros and Gutiérrez 2012).

Porter's 5 Forces. The five forces that intervene in an industrial sector are based on the main elements of the market (Baena 2003).

- **Direct Competitors:** A group of businesses that provide the same service or product.
- **Customers:** A group of buyers and sellers of goods and services.
- **Providers:** Group of companies that supply the production companies in the sector with everything necessary for them to produce or offer their services.
- **Substitute Products:** They can appear and cover the same needs that satisfy the products that currently exist in the market (Ana et al. 2017).
- **Potential Competitors:** Companies with the capacity to compete with those belonging to a specific subsector are those with the capacity to enter a subsector determined (Enrique Burbano Salazar 2016).

SWOT Analysis. It consists of carrying out an evaluation of the strong and weak factors that together diagnose the internal situation of an organization as well as its external evaluation, that is, the opportunities and threats (Ponce Talancón 2007).

- **Strengths:** Specialized skills and resources available to the company (Acosta et al. 2017).

- **Opportunities:** Factors that have a positive and negative impact on the business environment.
- **Weaknesses:** Factors that contribute to an unfavorable competitive position (Osorio 2009).
- **Threats:** Situations that come from the environment attack the stability of the organization (Moncho Agud 2016).

Comparative Competitive Analysis. Collection and analysis of information consists of the comparison of two or more processes, documents, data sets, or other objects. (Tono 2011)

2.1.1 PEST

For the analysis of the macro environment, the Pestel tool was used, thus verifying the impact and future evolution of the political, economic, social, technological, ecological, and legal environment would have on ARTANDIC. Therefore, according to Pestel's analysis, the environment presents favorable factors since the trend of buying and selling online is gaining momentum in the country. On the other hand, ARTANDIC promotes craft activity, and this is supported by the Artisan Law in article 3. (Junta Nacional de Defensa del Artesano 2015).

Due to the activity to which ARTANDIC will be dedicated and with the novelty of exposing a story for each seller, it makes the inclination for the collaborative economy work in favor of the company, since the final customer will feel pleased when buying and has time to help a cause. Finally, environmental awareness is in fashion all over the world and considering that this project does not pose environmental problems, it is one more element in favor of the company.

2.1.2 Competitive Environment: Porter's Five Forces.

For the competitive analysis, it was necessary to implement the model of the 5 forces of Porter, since thanks to this it is possible to carry out an external analysis (see Fig. 1).

2.1.3 Strategic Elements: SWOT Analysis

Table 2 presents information for a reliable diagnosis of the internal characteristics (weaknesses and strengths) and external situation (threats and opportunities) of ARTANDIC.

2.1.4 Comparative Analysis

In the following table, you can see the things that were taken into account when making comparisons and competing analyses (Table 3).

3 Results and Discussions

Table 1 presents the future evolution and the impact of the factors in a time range of 1 to 3 years. The factors that are marked with an X are those that apply according to the

Table 1. PEST analysis.

FACTOR	FUTURE EVOLUTION					
Economic:	**12 months**	**IMPACT***	**1-3 years**	**IMPACT***	**3-5 year**	**IMPACT***
Safeguards documentation.	X	-1				
Increase in the unified basic salary	X	2	X	2	X	2
Political-Legal						
Organic Law for the Defense of Artisans	X	2	X	2	X	2
Convocatoria para acceder a financiamiento de innovadores productivos proyectos	X	2				
Sociocultural						
Collaborative economy.	X	2	X	2		
La inclinación por las compras en línea está tomando fuerza en Ecuador.	X	2	X	2	X	2
Crecimiento de la población	X	2	X	2		
Technological						
Use of the TIC'S	X	2				
Environmental						
Environmental awareness	X	2	X	2	X	2

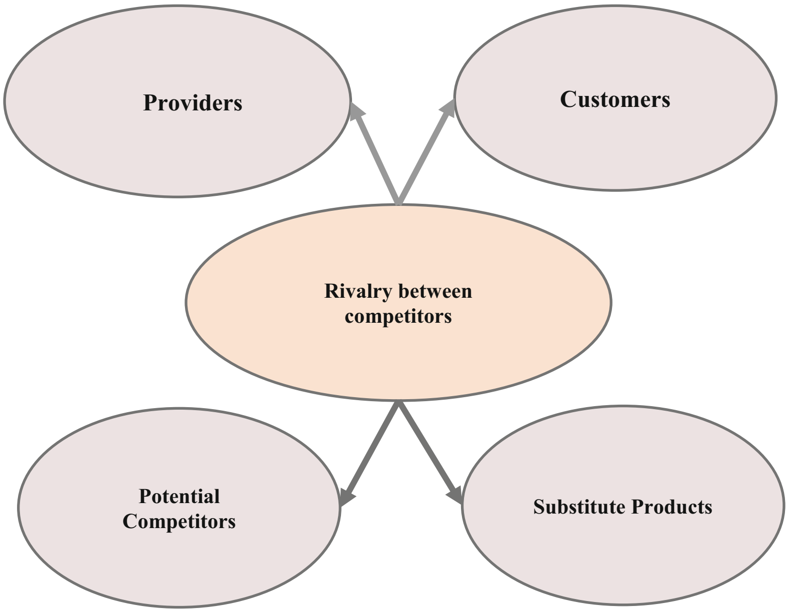

Fig. 1. Competitive forces.

Table 2. SWOT analysis

Strengths	• ARTANDIC is a source of additional revenue for any seller who joins ARTANDIC • Knowledge of the business world • Influential friends help spread the word about the new company and get at least one supplier • ARTANDIC allows small artisans to exhibit their art on a national level, making them feel important • Because of the power and influence of networks, it is simple to reach the customer • Appealing products • The fact that it is a website makes it simple to capture the audience's attention • Customers are found through social media • The cost of entering the business is low
Weaknesses	• A low level of market positioning, as it is new and has no trajectory or recognition • Distrust on the part of the artisans, who believed that by selling through ARTANDIC, they were allowing someone else to exhibit and market their work • Distrust on the part of the end customer when he believes that what he has purchased will not be delivered to him • Low sales due to skepticism about purchasing from a new company on the market • Scarce financial resources • Lack of recognition in the market • Lack of market experience
Opportunities	• Thanks to the trend of buying online, nowadays, everyone does it • This will increase demand for crafts in Ecuador • In the future, integrate craft vendors as well • Integrate other types of merchants • The competition buys handicrafts to sell, which means that the costs are a little higher. ARTANDIC will not need this procedure from the second year on • The use of electronic devices is increasing • State promotion of craft work • Constant use of social networks
Threats	• There aren't many artisan vendors • Lack of end customers because of competition substitute • Failure to succeed as a newcomer to the market because there are companies with more years of experience • It is possible that customers will misinterpret the company's goal and minimize it • Prices may be exaggerated by sellers • Technological advancements

Table 3. Analysis of the industry-competition.

Important Variables	Ecuadorian Hands	Andes Artesanía	Ecuador Mall.com	Simirika	Artesanías Folcklor	Artandic
Activity	Sell natural artisan products from Ecuador to the rest of the world on a wholesale basis. (Minimum 24 units)	They create jewelry, handmade for women. They sell wholesale.	worldwide internet sales.	Dedicated to the sale of handcrafted items with unique illustrations.	Handcrafts in wood and tagua are for sale.	A Website that provides a service aimed at small artisans offers the opportunity to display their products in a more dynamic way, improving their marketing.
Target marke	National but more international.	National and international	International.	National but more international.	National	National
Antiquity	3 years (sincen 2014)	13 years (sincen 2.004)	18 years (sincen 1.999)	unknown	unknown	0
What products does it offer?	Shampoo, pipes (a smoking utensil) and craft beer.	Hair jewelry and hair accessories	Handicrafts, books, business gifts, Christmas products, DVDs, flowers and gifts, paintings, Panama hats, silver and tagua handicrafts, souvenirs, tourism, typical costumes and sports	Cushions, bags, key rings, purses, pencil holders.	Room decoration objects, oil paintings, tagua necklaces	Depends on craftsman
Location	Manta	Quito	unknown	Quito	Quito	Guayaquil
Price range	From $1.75 and up, it depends on the amount the customer requires.	$0.71 and up, depending on the amount the customer requests.	$5 to $8,000 approximately	$6 to $50 approximately	$15 to $50 approximately	Depends on the seller
Delivery time	Within Ecuador's one day. Other countries have vacations ranging from 10 to 15 days.	Normal mail takes 30 days anywhere in the world. Express service from 3 to 7 days.	From 17 to 19 days. Express system from 6 to 8 days.	unknown	unknown	From 1 to 3 das
Publicity	Facebook, Instagram, YouTube, web, hosting	Site web, hosting	Site web, hosting	Facebook, Instagram, Twitter.	Facebook, Instagram, Twitter.	Site web, facebook, instagran, twitter, youtube, hosting
Customer service	They offer customer service calls if any issues arise in the delivery process.	unknown	Email service for claims, quotes, and providers.	service via email, fixed and mobile numbers.	Email service, forum	Customer service is via email, calls, and an after-sales call service.

Table 4. Qualitative rating scale.[1]

Success Factor	Ponderación	Ecuadorian Hands		Andes Artesanía		Ecuador Mall.com		Simirika		Artesania Folcklor		Artandic	
		Calificación	Puntuación	Calificación	Puntuación	Calificación	Puntuación	Calificación	Puntuación	Calificación	Puntuación	Calificación	Puntuación
Activity	0,10	2	0,20	1	0,1	3	0,30	1	0,10	3	0,3	3	0,30
Target marke	0,10	3	0,30	3	0,3	2	0,20	2	0,20	2	0,2	2	0,20
Antiquity	0,10	2	0,20	3	0,3	4	0,40	0	0,00	0	0	2	0,20
What products does it offer?	0,09	4	0,36	4	0,36	4	0,36	2	0,18	2	0,18	3	0,27
Location	0,06	2	0,12	3	0,18	1	0,06	1	0,06	2	0,12	3	0,18
Price range	0,10	3	0,30	3	0,3	4	0,40	4	0,40	4	0,4	3	0,30
Delivery time	0,09	2	0,18	3	0,27	2	0,18	0	0,00	0	0	3	0,27
Publicity	0,20	3	0,60	2	0,4	2	0,40	3	0,60	3	0,6	3	0,60
Customer service	0,10	3	0,30	2	0,2	3	0,30	2	0,20	2	0,2	3	0,30
Product line	0,06	4	0,24	2	0,12	2	0,12	1	0,06	2	0,12	3	0,18
	1,00		**2,80**		**2,53**		**2,72**		**1,80**		**2,12**		**2,80**

period, and the score that has been given to each of them has depended on the impact of these factors for each year.

Due to the activity to which ARTANDIC will be dedicated and the novelty of presenting a story for each seller, it makes the inclination for the collaborative economy work in favor of the company. Finally, the final client will feel pleased at the moment of buying and at the same time help a cause, environmental awareness is fashionable all over the world, and taking into account that this project does not pose problems for the environment, it is one more element in favor of the company.

Current Competitors. There are a lot of SMEs that do the same thing, but not the same, which is a good thing for ARTANDIC.

[1] *On a scale of 1 to 4,
1 Greatest weakness Representing, 2 Minor weakness, 3Less strength, 4Greater strength.

Potential Competitors. The entry of new competitors is very high, since it is not difficult to identify the business opportunity that is presented in this work. In addition, the low financial, technological, and legal entry barriers benefit these competitors. Having said this, it can even be argued that the sellers (artisans) are the potential competitors. This refers to the fact that the small artisans could dedicate themselves to marketing their products on their own website, which means that they are potential competition for the company's business.

Substitute Product. Several companies with substitute products were identified. However, their activity is not aimed at the artisan sector.

Bargaining Power of Artisan Suppliers. ARTANDIC is a company that acts as an intermediary and doesn't make the product itself. There are many artisans, so it can be said that the bargaining power of suppliers is low because there are so many people who can help you do your job.

Bargaining Power with Customers. Artisan vendors and the final customer is identified as clients. In the case of artisans, the bargaining power with the client is low because they are offered the opportunity to exhibit their art to the whole country, jointly making them earn income from it. According to the market study carried out, there is many artisans willing to market their products in another way. Due to this, ARTANDIC differs from other companies by the segment to which they are directed, and thanks to this, it can be pointed out that the power of negotiation with the client is positive. As for the final client, they also have low bargaining power since they can only accept or reject the conditions of sale. They do not have major complications or work with them. Based on the information obtained from the SWOT analysis, it can be concluded that ARTANDIC has the necessary tools to overcome weaknesses despite being a new company in the market. Regarding the distrust of the artisans and the final client, it is not something permanent due to the actions that are specified later to gain their trust. On the one hand, thanks to a bank credit, the resources will not be limited, and the lack of recognition has a solution thanks to the fact that ARTANDIC will make itself known through social networks and the experience will be given over time. Considering the threats is very important, for which a contingency plan must be in place. At this point, the most relevant threat is the technological change that could occur later, for which the company must be updated on the subject. In addition, ARTANDIC has a professional in-house, so it can be said that it can be adapted to future changes.

The company's strengths are beneficial in terms of the environment since offering a benefit to artisans stimulates their capture. In addition, knowing the area of commerce is a competitive advantage. On the other hand, the absence of social networks plays a significant role for the company since it is currently a trend that can be used to reach both artisans and the final customer. The products offered on the web are very attractive due to their shape, material, and elaboration.

The opportunities that are presented in Table 2 will be fully exploited, taking advantage of the trend of buying online that is increasing more and more. In the future, integrating vendors who are not dedicated to craft activity is a benefit for many people, which is important for everyone because economic aid is generated through the marketing of their products through the web. It would also recognize the company and give it an optimal business image. Furthermore, state promotion is very relevant since the national government promotes the productive development of the artisan sector.

The factors presented in Table 4 have been taken into account considering the importance that each of them has in comparison with the competition, for which a score has been assigned to each of them. According to the data obtained, it can be deduced that Ecuadorian Hands is one of the most direct competitions that ARTANDIC has, since the activity it develops is similar and offers handicrafts. In addition, it has a very interesting website, and is very inclined towards marketing on social networks; The advantage is that this company sells wholesale, and the idea of this project is for artisans to sell their own creations through the Artandic website.

Andes Artesanía despite the fact that it sells other articles, is its main activity. It is a product of feminine handmade jewelry, and it has a great advantage in terms of cost. 13 years on the market.

Ecuador Mall.com is a platform for handicrafts worldwide and has been in the market for many years, which gives it a great advantage, although for Artandic it is not a direct competition since it is aimed at trade outside of Ecuador.

Simirika is a company that sells handicrafts made of textile materials at an affordable price range. In addition, the differentiation of this company is due to the illustrations of each product. Artesanías Folcklor is a company dedicated to the sale of handmade items and stands out precisely in the products it sells.

4 Conclusions

- The business idea will be welcomed by artisans due to the need to better market their products.
- According to the Pestel analysis, the environmental factors are favorable to ARTANDIC. It will help for new projects in the country is also being encouraged, which means that the project can be paid for through this method.
- The segment to which this idea is directed is a differentiating factor, which is why it can be predicted that this project will be well received.
- The business idea addresses the needs of artisans, who, as previously stated, do not have the habit of purchasing this type of product due to the low commercialization of crafts, resulting in low sales for the artisans.
- It is important to note that ARTANDIC reaches out to the craftsman as a solution to his problem, as the company provides him with the opportunity to sell his products in a unique and dynamic manner.
- To sum up, the project is new because it's for a new group of people and because it's going to be done in a new country.
- To conclude, the solution to the problem posed is good.

References

Acosta, G., Aviles, B., Torres, J.P.: Gestión emocional: factor crítico de la competitividad emocional en el profesorado universitario. INNOVA Res. J. **2**(10), 132–146 (2017)

Ana, M., Luz, C., Hilda, E.: Proyecto de emprendimiento para la venta de artesanía textil mexicana (2017). https://rei.iteso.mx/bitstream/handle/11117/4949/MODELODENEGOCIOPARALACOMERCIALIZACIÓNDEARTESANÍASTEXTILESMEXICANAS.pdf?sequence=3

Cadena, A.D., Herrera, A.T., Maya, C.A: Los modelos de gestión en el cumplimiento de los objetivos empresariales. Caso de Estudio: Cia. de Transportes 27 de Mayo S.A. J. Sci. Res.: Rev. Cienc. Invest. **3**(9), 32–40 (2018). https://doi.org/10.26910/issn.2528-8083vol3iss9.2018pp32-40p

Díaz Cadena, A.: Plan de negocio Artandic 1–60 (2017). https://doi.org/10.13140/RG.2.1.1713.9600

Enrique Burbano Salazar, J.: Universitat politècnica de valència departamento de economía y ciencias sociales (2016). https://riunet.upv.es/bitstream/handle/10251/74412/BURBANO-Situaciónactualdelemprendimientoenelsectoragroalimentariode Ecuadoryplanteami.pdf?sequence=1

Baena, E.: El entorno empresarial y la teoría de las cinco fuerzas competitivas. Scientia et Technica. UTP. ISSN 0122-1701, 23(ISSN 0122-1701), 62 (2003). file:///C:/Users/Univ.de Guayaquil/Downloads/Dialnet-ELENTORNOEMPRESARIALYLATEORIADELASCINCOFUERZASCOMP-4845158.pdf

Junta Nacional de Defensa del Artesano. Pichicnha en cifras, 26 (2015). http://www.pichincha.gob.ec/phocadownload/pgd/4_pichinchacifras.pdf

Moncho Agud, R.A.: Plan de empresa para la producción y distribución de Cerveza Artesanal en la Comunidad Valenciana (2016). https://riunet.upv.es/handle/10251/72343

Osorio, A.: Diseño innovador como apoyo a la artesanía en guadua. Rev. Grafías **8**, 23–31 (2009). http://biblioteca.ucp.edu.co/OJS/index.php/grafias/article/view/305

Pedros, D.M., Gutiérrez, A.M.: An{á}lisis del entorno. Ediciones Diaz de Santos (2012). books.google.nl/books?id=LDStM0GQPkgC&printsec=frontcover&dq=Pedro,+Daniel+Martinez+Gutiérrez,+Artemio+Milla+análisis+del+entorno+2012&hl=es&sa=X&redir_esc=y#v=onepage&q&f=true

Ponce Talancón, H.: Matrix SWOT : An alternative for diagnosing and determining intervention strategies in organizations. Enseñanza e Inv. En Psicología **12**(1), 113–130 (2007). http://www.redalyc.org/articulo.oa?id=29212108

Tono, G.: La utilizacion del metodo comparativo en estudios cualitativos en ciencia politica y ciencias sociales : diseño y desarrollo de una tesis doctoral. Kairos: Rev. de Temas Sociales **27**, 1–12 (2011). https://dialnet.unirioja.es/descarga/articulo/3702607.pdf

MOOCs for Teaching in Times of COVID-19

Irma Naranjo Peña(✉), David Benavides López, and Héctor Lara Gavilanez

University of Guayaquil, Guayaquil, Ecuador
{irma.naranjop,david.benavidesl,hector.larag}@ug.edu.ec

Abstract. The COVID-19 disease, caused by the SARS-CoV-2 virus, strengthened professional training and certification processes and integrated industrial processes for professionals. As a viable solution for fortifying education in the COVID-19 era, it comprises the integration of Open Adult Learning Courses on the Internet and their integration with information stored on digital educational platforms. This work aims to establish, through the integration of Open Online Courses and digital platforms, a set of steps for improving the quality of online courses in the teaching-learning process. The Delphi with expert criterion method assesses the effectiveness of integrating open online courses and digital platforms for quality assurance. The time factor is critical for laying the groundwork for integrating Open Online Intensive Courses and digital learning platforms. It is concluded that without measuring results, the success of integrating open online courses and digital platforms for quality education cannot be measured.

Keywords: Learning · Massive Open Online Courses · Digital platforms

1 Introduction

Today, COVID-19, a disease caused by the SARS-CoV-2 virus, has resulted in unprecedented levels of human suffering, social agitation, and economic harm, putting various social activities, such as active participation in schools, on hold. Many elements have had to be changed due to this situation, and they are still evolving at a vertigo-inducing rate. Many social and economic factors have been able to continue to evaluate the difficulties that have arisen in the workplace and in daily life because of the transformation caused by the Internet and new technologies, to alleviate the world's current crisis. The adaptation to insurmountable changes caused by the presence of the COVID-19 has also been for universities, particularly for professors, who have had to adapt to relinquishing the presence of the educational and pedagogical process to assume these processes online.

Working online is a challenge for educational innovation, which has resulted in the strengthening of professional training and certification processes with a focus on the use of information and communication technology (ICT). In the current crisis, people have been using the ICT to help people get better at their jobs and use the information stored on digital educational platforms more efficiently. This is done through the integration of Massive Open Online Courses (MOOCs), which help people get better at their jobs and use the information stored on digital educational platforms more efficiently, according to their needs and interests [2].

© The Author(s), under exclusive license to Springer Nature Switzerland AG 2023
M. Zambrano Vizuete et al. (Eds.): RITAM 2021, LNNS 512, pp. 352–361, 2023.
https://doi.org/10.1007/978-3-031-11295-9_26

MOOCs have established themselves as one of the major trends in e-learning after being positively received by students and various higher education institutions (HEIs). The literature review demonstrated that MOOCs can be applied in different courses, the number of users is increasing, and they can deliver benefits to both students and companies. However, not all MOOCs performed well, and there is much debate about ways in which to attract more students. Using MOOCs, it is possible to decentralize the process of teaching and learning, which means that it will be more visible around the world, and in the current context, it has been done in a significant way in online education because it is organized academically. As a result, the process of teaching and learning will be structured by units of study, where the access to information for this organization will be done from the platforms. MOOC platforms provide clarity on the content and facilitate the interconnection of knowledge among students and teachers.

The process of integrating MOOCs with digital platforms requires continuous learning, preparation, and supervision by a professional on a permanent basis to manage with quality the information required to be used for imparting online education. This will lead to the integration of massive means of tools, platforms, and technology into education. The information contained in digital platforms and manipulated via the web constitute well-defined models of information-handling on the internet. These platforms have been solidified through mechanisms for their integration with the goal of establishing themselves as a technological tool that contributes to knowledge management in educational activities. In this sense, the importance of platforms should not be underestimated [2].

According to the cited authors, integrating web services like semantic web with MOOC is advantageous because both have plausible technological mechanisms for integrating and constituting an appropriate technological platform for education in HEIs. It is possible to work in a coordinated manner thanks to the integration of the semantic web and MOOCs, as this integration aims to facilitate resource localization through semantic metadata, which describe data content, meaning, and relationships, which leads to communication between systems and programs, which conforms to the use and reutilization of resources.

The entire process related to MOOCs has meant a revolution in access to self-improvement, on the one hand, MOOCs allow training to be extended and complemented throughout a person's life, offering opportunities for continuous recycling of their knowledge and an improvement in their job prospects. On the other hand, MOOCs have been gradually incorporated into the digital strategy of many HEIs, as a form of visibility, or as a complement to the traditional programs of study [1].

The adoption of MOOCs across the world and in different countries has been very different. According to [14], the incorporation of IES with MOOCs in Latin America began late in 2016, and the rate of MOOC production was between 4 and 5 times slower than in Europe at the time [14]. However, with the presence of the COVID-19 in 2020, the MOOCs will have to be used by nearly everyone in the world for one or more actions.

MOOCs were already well-established in the educational context, and specifically in Latin American countries such as Ecuador, Chile, Peru, Salvador, Bolivia, Guatemala, and Colombia, they helped to strengthen the professional development and training processes of professionals who take on the challenge of online learning and education, mediated by digital platforms such as Semantic Web to manage the information required in time.

MOOCs are a medium that requires different technological, didactic, and tutorial skills from teachers to successfully face the process of teaching – online learning in the COVID-19 era. In this context, there are a variety of issues to consider when registering for a MOOC, as evidenced by McAuley, Stewart, Siemens, and Cormier, such as logistical, technological, educational, and financial challenges that educators must overcome [15].

According to Kiers and Jorge, one of the main differences is the large number of students that can fill a MOOC; this, at first glance, is a disadvantage that must be overcome by integrating various resources that promote higher levels of commitment, motivation, and learning, thereby avoiding course abandonment through MOOCs [12]. For this reason, MOOCs aren't used to interact with students at the Peninsula de Santa Elena State University, Ecuador. Instead, the platform Moodle is used to guide and prepare a small group of people, who are the professors who face the challenge of online teaching and learning. It also helps manage the information needed for the strengthening of knowledge.

Developing the necessary skills in teachers to face the potential of new technologies and their application in education is a task that requires effort and practice [9]. It is important to make clear what you are going to learn in the course at the Peninsula de Santa Elena State University, Ecuador. This is because the process of learning will be done online through Moodle, and this must be done in the teacher's preparation that is done through MOOCs, which must be designed and approved.

The instructors who are being trained must choose the content of the courses as well as compile all available materials from MOOCs and their integration with digital platforms, such as the university's Semantic Web in the case of a study, before distributing them in accordance with the topics proposed in the courses. In a process divided by the constraints that one and another platform possesses, which are used as a university case study strategy to achieve different goals in terms of ensuring educational quality and controlling pedagogical management to contribute to the learning of teachers and students.

The study by Sammour and his coworkers says that one way to try to solve the problem of choosing the content of the courses and putting together the material from a MOOC is to integrate them with different types of technology and trends. This means that the information from the MOOC should be integrated with information found in portals, repositories, and especially with the information found in a MOOC [18]. These platforms and semantic web can improve content discovery, accessibility, visibility, and repurposing, and thus contribute to the quality of MOOCs.

The use of the web for information retrieval on the internet is widely used in communication, commerce, entertainment, and business, among other things [2]. Web services have been established as an essential technology for Internet collaboration, and their use is advantageous for addressing topical issues in MOOC courses, as demanded by training professionals.

It is possible to work in a coordinated manner based on the information requirements for an instructional process involving high-quality learning required for professional development by integrating Semantic Web and MOOC, which describe the content, meaning, and relationship of the data, which leads to the communication between systems and programs and enables the use and reutilization of resources that are available on the web.

According to Sammour et al., using a Web semantic based on ontologies facilitates personalization of MOOC learning because, through the ontologies, a semantic web presents a focus based on the semantic representation of knowledge of the disciplinary area that is required for a continuous process of learning [10]. The proposal is based on the use of ontologies, which is part of the fact that the professors who are involved in the online learning–advancement process have varying levels of education based on their needs or preferences, which is advantageous for a high-quality learning–advancement process.

The MOOC are monolithic and closed in data management, which means that interchanging, reusing, and recovering learning materials from different courses is difficult. In this context, they propose a change in relation to the MOOC, that is, that these Open Online Courses be connected to form a LOOC (LOOC, Little Open Online Course) [23]. This refers to a new generation of MOOCs that is supported by formal semantic interoperability using semantic web and online social networks [21].

The new MOOC generation vision is important because users and, more specifically, the professors who form the online learning process can access different MOOC courses that are relevant to what they are looking for and their educational interests, which is necessary to avoid content duplication. LOOC, as a new generation of MOOCs, is easily integrated into the Semantic Web, given that only groups of a hundred students can participate in LOOC courses, which means that the massiveness decreases and, in this way, the preparation of the courses is better controlled. From the didactic and pedagogical point of view, given the interoperability that arises between teachers, which is useful to produce educational materials, so that they are adapted to the objectives set and that they are not repetitive [3].

In MOOCs and LOOCs, the level of learning acquired by those who access the courses supported in this modality should be considered, which makes it feasible to evaluate the level of professional competencies acquired. In this regard, it is considered that the learning sequences should not only be based on the existing content in MOOCs, which provides knowledge, but also on the learning development of teachers who are trained for the online teaching-learning process that takes place during the current pandemic [11, 13, 19, 20].

For all these reasons, it is essential to approach MOOC research from different perspectives given the need for integration between MOOCs and digital platforms for a quality teaching process as required by current educational contexts, to enable the massive online learning of professionals who are trained to undertake the learning of online students in a meaningful way. To this end, an analysis of the pedagogical and technological design is conducted through the learning expectations of professionals in training.

The rationale for the integration between MOOCs and digital platforms, specifically with the Semantic Web in the teacher training process, requires changes in the learning paradigm, which is now based on the use of ICT, which leads to transformations in educational schemes, transformations based on the necessary standards that contribute to pedagogical quality evaluations [7]. Previous studies have shown that the evaluation of the pedagogical quality of MOOCs requires indicators related to pedagogical, functional, technological, and technological factors [7, 8, 17, 22].

In the previous studies, it is highlighted that another of the indicators to be considered is the time factor, since this factor is the most critical and has a direct impact on the pedagogical quality and training through MOOCs. For this reason, it is appropriate to analyze the time factor to know the importance it has in the process of integration of MOOCs and digital platforms as required by current educational contexts, to enable massive and online learning of professionals who are trained to undertake the learning of online students in a significant way in COVID-19.

2 Methodology

For the analysis of the rationale for the integration between MOOCs and digital platforms for the achievement of quality teaching, as required by current educational contexts, of teachers who are trained to undertake online student learning in a meaningful way in the times of COVID-19, it was conducted through the double-round Delphi method. For this purpose, a set of indicators was selected based on the studies of [7]. Once the set of indicators has been selected, they are evaluated and validated by selected experts from the Peninsula State University of Santa Elena, Ecuador, who are involved around educational technology and who are responsible for providing learning opportunities to teachers through the information contained in the semantic web and in the MOOC built for this purpose. The indicators are analyzed using the Delphi method with expert criteria, which consists of selecting a group of experts who are asked for their opinion on issues related to the future and carrying out successive anonymous rounds that guarantee the autonomy of the participants. The predictive capacity of this method is based on the systematic use of an intuitive judgment made by all the experts [4].

2.1 Instruments and Procedure

For the analysis, the design of the syllabuses of the professors who were prepared through MOOC courses to face online teaching and learning during the current pandemic was taken into consideration, which was analyzed by the selected group of experts. The analysis considered the use of the information hosted on the semantic web of the referred university with the objective of promoting interaction between the courses and the participants, thus favoring the use of social networks by the teachers in training. Based on the set of indicators selected, a quality questionnaire was designed, which consisted of closed questions that assessed five indicators on a 4-point Likert scale. For the analysis, the indicators were classified into 20 subcategories related to pedagogical, functional, technological, and time factors.

2.2 Participants

Thirty teachers who were experts in e-Learning and ICT at the Peninsula de Santa Elena State University, Ecuador. They were asked about the types of MOOCs, types of educational resources, types of storage and use of information, types of learning, tasks and forms of evaluation, and the functions and roles of teachers, in the instrument applied.

The questionnaire designed was addressed to teachers who will be prepared through MOOC courses to face online teaching and learning during the current pandemic. It was composed of 15 questions, which collected verbal data, teacher updating, expectations, and opinions about MOOC courses and their integration with the Semantic Web. To obtain the evaluation of indicators related to pedagogical quality, another questionnaire applied to the same experts was designed to find out the importance of MOOCs integrated with the Semantic Web in terms of teacher preparation, professional development, and educational management, based on the use of technology as a strategy for updating teachers in the teaching-learning process.

2.3 Instrument Validation

Both instruments were validated for reliability and internal consistency using Cronbach's Alpha. The basis for the application of Cronbach's Alpha was consulted in published case studies by [5] Eq. 1 was used to apply Cronbach's Alpha Coefficient.

$$\alpha = \frac{K}{K-1}\left[1 - \frac{\sum S_{i^2}}{S_{T^2}}\right] \tag{1}$$

where:

K: is the number of items.

S_{i^2}: Sum of variances of the items.

S_{T^2}: Variance of the sum of items.

α: Cronbach's Alpha coefficient.

3 Results

The results obtained when applying Cronbach's Alpha technique to the instruments designed were 0.78 and 0.76, respectively, which shows a high level of confidence in the instruments. When applying the Delphi method, the results obtained indicate that the quality of the MOOC integrated into the Semantic Web in the training and professional improvement processes, and especially the integration between industrial processes for professionals, should consider pedagogical, technological, and functional factors. The experts significantly value the indicators related to the time factor because this factor is strategic in the online training process and through MOOCs integrated with the Semantic Web.

The time factor needs to be addressed by ICT specialists and, in particular, by designers, due to the direct impact that MOOCs and the integration of digital platforms such as the semantic Web have on the adequate preparation of professionals who are trained to face the online teaching-learning process, a process that requires quality in order to assess the educational problem in the face of the current pandemic that is sweeping the world (see Fig. 1).

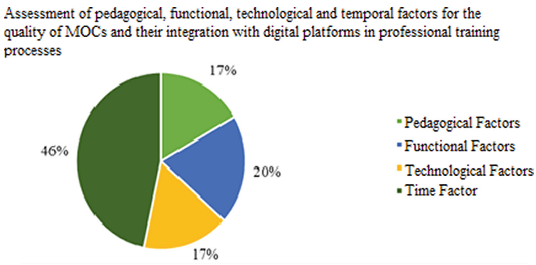

Fig. 1. Analysis of pedagogical, functional, technological, and time factors for the quality of MOOCs and their integration with digital platforms in professional training processes.

The evaluation of indicators related to pedagogical quality and the importance of MOOCs integrated with the Semantic Web in terms of teacher preparation, professional development, and educational management, based on the use of technologies as a strategy for updating teachers in the teaching-learning process, showed that for professionals in training, the time factor in learning is fundamental. This factor has a significant impact on the development of professional competencies since time-related management competencies contribute to the self-regulation of both professionals in training and members of a group of professionals in training (see Fig. 2).

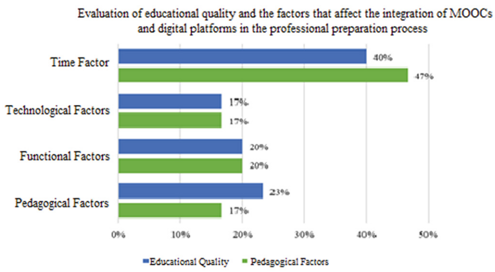

Fig. 2. Analysis of educational quality and factors affecting the integration of MOOCs and digital platforms in the professional preparation process.

Education through MOOCs, e-Learning, b-learning, and other platforms has autonomy that develops from the interest and insight of professionals in training who decide to delve into adequate learning to provide quality education and not to err between the face-to-face and online modality. According to the results obtained, it is based on the integration between MOOCs and digital platforms, the set of steps for strengthening the quality of online courses in the teaching-learning process.

The rationale for the set of steps for strengthening the quality of online courses in the teaching-learning process is based on the criteria suggested by [6], where pedagogical and technological fundamentals to be considered in the online training process, through any digital platform, are contemplated. The steps to be contemplated are:

1. Set goals
2. Set course content
3. Select the material
4. Set the course format
5. Define activities
6. Define the evaluation
7. Sequencing learning

4 Conclusions and Discussion

In this work, theoretical foundations related to the use of information and communication technologies were addressed, which are premises for the adequate achievement of the teaching process during the crisis caused by COVID-19, a disease caused by the SARS-CoV-2 virus, where MOOCs and their integration with the various digital platforms existing in HEIs were analyzed for the training and professional development processes of teachers who faced the online teaching-learning process. Specifically, the integration of MOOCs with the Semantic Web as an information support of the Peninsula de Santa Elena State University, Ecuador, was analyzed for this research.

It was evidenced that for the strengthening of teaching in times of COVID-19, the integration of Massive Open Online Courses and their integration with the information stored in the educational digital platforms is a viable solution. The integration of MOOCs and digital platforms for a quality teaching process, as demanded by current educational contexts, was based on the integration of MOOCs and digital platforms to enable the massive and online learning of professionals who are trained to undertake the learning of online students in a meaningful way.

The rationale for the integration between MOOCs and digital platforms for a quality teaching process, as required by current educational contexts, included the development that exists in terms of ICT, in the learning process of professionals who are trained, and aspects of pedagogy and technology were considered.

The analysis of the indicators related to the pedagogical and technological foundations that enable massive and online learning of professional training through MOOCs was carried out because of 20 subcategories related to pedagogical, functional, technological, and time factors. It was found that the time factor was the one with the highest score, which is an important factor that contributes to the design of adequate strategies for a quality teaching-learning process.

Without measuring the results obtained, it is not possible to evaluate the success of the integration of MOOCs and digital platforms for a quality teaching process. The set of steps established to strengthen the quality of MOOCs integrated with the Semantic Web favors the massive and online learning of the professionals being trained.

According to Montes, Aguilar-Rosales [16], ICTs in support of distance education models in higher education, and specifically MOOCs, represent a new educational modality that has made its way into international knowledge communities, seeking to provide educational opportunities through an accessible technological option to increase the professional development of any type of participant. These courses have had a massive impact on the professional development of thousands of people by providing a distance education option that offers learning and knowledge facilities that could not be obtained in the same way in a classroom.

The use of MOOCs in the professional training of teachers facing the online teaching-learning process in the time of COVID-19 opens a door to the opportunity for continuous improvement, giving teachers a space for the construction, improvement, and reaffirmation of knowledge to increase their professional skills to achieve full development in their daily work. The use of digital platforms and MOOCs in the professional training of teachers facing the online teaching-learning process seeks to supply the spaces that the curriculum has left free to reinforce the knowledge of both students and teachers in training, making this technological tool an opportunity for growth and innovation that provides a wider field of action for a profession increasingly in demand for professionalization.

5 Limitations and Prospective

This study, from the analysis carried out, offers convenient results and conclusions that contribute to the knowledge and formation of professional competencies in the use of digital platforms for the online teaching-learning process in times of COVID-19, which should be strengthened, not only for the times of pandemic, but also to promote distance learning as a development practice with appropriate technological infrastructure to transfer useful knowledge to society. It also invites us to continue deepening this line of research.

The very concepts of MOOCs, the semantic web, digital repositories, and educational platforms that have been mentioned in this research, and their relevance to the competencies to be acquired, are in a phase of delimitation both from a technological perspective and from the perspective of applied research and training.

There continues to be a digital divide and a lack of opportunities to enjoy these study modalities, specifically to acquire useful knowledge for the development of society. There is a lack of solidity and reflection in the diagnoses on the use of these resources, from the benefits and arguments that they present, to help manuals and the availability of competencies to apply in their use.

Therefore, we suggest analyzing the rationale behind the integration between MOOCs and digital platforms and the set of steps for strengthening the quality of online courses in the teaching-learning process.

References

1. Alario-Hoyos, C., et al.: MOOC-Maker: Tres anõs construyendo capacidades de gestión de moocs en latinoamérica. In: CEUR Workshop Proceedings, pp. 5–14 (2018)
2. Altamirano Di Luca, M.A., González Benítez, N.: Comparative study of RDF and OWL ontology languages as support for the semantic web. In: Botto-Tobar, M., Zambrano Vizuete, M., Torres-Carrión, P., Montes León, S., Pizarro Vásquez, G., Durakovic, B. (eds.) ICAT 2019. CCIS, vol. 1193, pp. 3–12. Springer, Cham (2020). https://doi.org/10.1007/978-3-030-42517-3_1
3. Álvarez, Y.B.: La Calidad de la Educación a Distancia. El caso de los MOOC (2015)

4. Astigarraga, E.: El método Delphi. San Sebastián: Universidad Deusto; 2008 (2008). Accessed 22 Aug 2012
5. Cabanach, R.G., et al.: Las creencias motivacionales como factor protector del estrés en estudiantes universitarios. Eur. J. Educ. Psychol. **3**(1), 75 (2010). https://doi.org/10.30552/ejep.v3i1.49
6. Cabero-Almenara, J., Llorente Cejudo, M.: Los MOOC: encontrando su camino. @Tic. Rev. D'Innovació Educ. **18**, 24–30 (2017)
7. Domingo, M., Marquès, P.: Classroom 2.0 experiences and building on the use of ICT in teaching. Comunicar. **19**(37), 169–174 (2011). https://doi.org/10.3916/C37-2011-03-09
8. Gómez-Zermeño, M.: Bibliotecas digitales : recursos bibliográficos electrónicos en educación básica = Digital Libraries : Electronic Bibliographic Resources on Basic Education (2012)
9. Gráinne, C.: Los MOOCs como tecnologías disruptivas: estrategias para mejorar la experiencia de aprendizaje y la calidad de los MOOCs. Rev. Científica Tecnol. Educ. **2**(2), 16–28 (2013)
10. Hover, K.M., Muhlhauser, M.: LOOCs - linked open online courses: a vision. In: Proceedings - IEEE 14th International Conference on Advanced Learning Technologies, ICALT 2014, pp. 546–547 (2014). https://doi.org/10.1109/ICALT.2014.160
11. Juca Maldonado, F., Burgo Bencomo, O.B.: Blended learning as a model for universities use moodle. Investig. Tecnol. e Innovación. **8**, EE SE-Article, 27–34 (2016). https://doi.org/10.53591/iti.v8iEE.140
12. Kiers, J., Jorge, N.: Experiences from 18 DelftX MOOCs. In: Proceedings Paper EMOOCs, pp. 65–70 (2015)
13. Laborde, J., et al.: Teaching process for learning probability analysis based on its application in real life cases with the programming language R and RStudio. Ecuad. Sci. J. **3**, 1 SE-Research Paper (2019). https://doi.org/10.46480/esj.3.1.22
14. Maldonado, J.J., et al.: Construction of management capacities of MOOCs in higher education Estado del arte de adopción de MOOCs en la Educación Superior en América Latina y Europa. Recuper (2016). http://www.mooc-maker.org/wp-content/files/WPD1.6_INGLES.pdf
15. Mcauley, A.A., et al.: THE MOOC model for digital practice : executive summary. Narrative introductions: massive open online courses: digital ways of knowing and learning (2010)
16. Montes, R., Aguilar- Rosales, B.: La digitalización de la educación: los MOOC como recurso educativo en la formación de docentes (2020)
17. Roig-Vila, R., et al.: Características de los ambientes de aprendizaje online para una práctica docente de calidad. Indicadores de evaluación. In: XI Jornadas de Redes de Investigación en Docencia Universitaria [Recurso electrónico]: Retos de futuro en la enseñanza superior: docencia e investigación para alcanzar la excelencia académica, pp. 2405–2419. Universidad de Alicante, Alicante, Spain (2013)
18. Sammour, G., et al.: Semantic web and ontologies for personalisation of learning in MOOCs. In: 2015 IEEE 7th International Conference on Intelligent Computing and Information Systems, ICICIS 2015, pp. 183–186 (2016). https://doi.org/10.1109/IntelCIS.2015.7397219
19. Tusa, F., et al.: The construction of an education of the good living from the study of the technologies of the communication and the information. Investig. Tecnol. e Innovación. **8**, 8 SE-Article, 97–106 (2016). https://doi.org/10.53591/iti.v8i8.141
20. Yépez, S.T., et al.: An approach to teacher training and ICT as a teaching and learning process. Ecuad. Sci. J. **4**, 1 SE-Research Paper (2020). https://doi.org/10.46480/esj.4.1.55
21. Zapata-Ros, M.: El diseño instruccional de los MOOC y el de los nuevos cursos online abiertos personalizados. Rev. Educ. a Distancia. **45** (2015). https://doi.org/10.6018/red/45/zapata
22. Zermeño, M.G.G., et al.: Estudio exploratorio-descriptivo "Curso híbrido: contabilidad V." Rev. Investig. Educ. del Tecnológico Monterrey **4**(7), 70–79 (2013)
23. Zhuhadar, L., et al.: Semantically enriched massive open online courses (MOOCs) platform. Comput. Hum. Behav. **51**, 578–593 (2015). https://doi.org/10.1016/j.chb.2015.02.067

Semantic Web Based on Ontology to Measure the Control of Promotion Indicators of Ecuadorian Universities

David Benavides López(✉), Irma Naranjo Peña, Elvis Arteaga Yaguar, and Víctor Pazmiño Morán

University of Guayaquil, Guayaquil, Ecuador
{david.benavidesl,irma.naranjop,elvis.arteagay, victor.pazminom}@ug.edu.ec

Abstract. Traditionally, the control actions of promotion indicators in Ecuadorian universities have been reduced to those that year coordinators carry out to revert the results, essentially centered on the information that the attendance and promotion cuts offer. The control of vertical efficiency, associated with a student cohort, is also limited in terms of diagnostic, prognostic, and intervention facilities. For this reason, the objective of this research is to measure the control of promotion indicators by making use of the information contained in the semantic web, based on ontology, implemented in Ecuadorian universities.

Keywords: Promotion indicators · Academic efficiency · Vertical efficiency · Student cohort · Semantic web

1 Introduction

The incorporation of Information and Communication Technologies (ICT) has created new ways to measure the control of promotion indicators in Ecuadorian universities, specifically those implemented on repositories and semantic web digital portals [4]. The semantic web is a thriving area at the confluence of artificial intelligence (AI) and web technologies that proposes to introduce explicit descriptions of the meaning of resources to allow the machines themselves to have a level of understanding of the web sufficient to take over a part of the costliest, routine, or physically unmanageable, of the work currently performed manually by users who browse and interact with the web [7].

As a result of the web's current state and limitations, there is interest from the business world, the public sector, and academia in transforming the web into a useful instrument capable of measuring any process [2]. The semantic web is widely regarded as a critical instrument for advancing the information society. Nowadays, practically everything is represented in some manner on the web, which makes it easy to locate information about almost anything using a competent search engine. On the other hand, the web enables us to carry out our everyday tasks with remarkable ease, economy, and efficiency.

The semantic web, as referred to [5], proposes to overcome the limitations of the current web by introducing explicit descriptions of the meaning, internal structure, and

© The Author(s), under exclusive license to Springer Nature Switzerland AG 2023
M. Zambrano Vizuete et al. (Eds.): RITAM 2021, LNNS 512, pp. 362–368, 2023.
https://doi.org/10.1007/978-3-031-11295-9_27

global structure of the contents and services available on the web. In response to the current web's implicit semantics, chaotic growth of resources, and lack of a clear organization, the semantic web advocates classifying, structuring, and annotating resources with explicit machine-processable semantics.

The semantic web maintains the principles that have made the current web a success, such as the principles of decentralization, sharing, compatibility, maximum ease of access and contribution, and openness to growth and use not foreseen beforehand. In this context, a key problem is reaching an understanding between the parties involved in the construction and exploitation of the web: users, developers, and programs of very different profiles. The semantic web rescues the notion of ontology from the field of artificial intelligence as a vehicle to meet this objective, not only providing access to content, but also offering interaction and services [10].

Due to the implementation of the semantic web in Ecuadorian universities, it is now possible to quantify the impact on promotion indicators, particularly those relating to academic and vertical efficiency, to ascertain the primary causes of poor teaching results and intervene in the training process via periodic sampling [4].

The formative process is characterized by the holistic and systemic integration of teaching and learning of all its components, together with the qualities of assimilation, depth, and structural levels in its three dimensions: educational, instructive, and developmental. It starts in an educational institution and is projected into society, with the task of educating man for life from social commitments, being able to face new situations and problems that arise and solve them to transform society [3].

The control of student cohort promotion indicators will support the control and evaluation of learning in the management of educational processes [4]. By semantic web, it is possible to measure the control of promotion indicators of Ecuadorian universities as a selective process, since it is not necessary to act on all parameters, but only on those that essentially determine the need that is required, monitoring the searches for the contents made by students through the web and with efficient search engines [1].

Adequate control contributes to decision making to influence the object (subject-object) directed, oriented, and guide the rectification of the detected deviations. However, it should not be lost sight of the fact that it is also possible to detect results through the different controls carried out, which, due to their positive relevance, deserve to be disseminated and generalized [6]. Regarding the management of the educational teaching process (PDE), in its control dimension, in Ecuadorian higher education institutions, this has been characterized by the application of budgetary controls due to governmental requirements for monitoring educational expenditures and to the financial control norms assumed by these institutions in different areas [13, 14, 19].

Therefore, control must be a tool that is always applied, exercising a regulatory function, since, through the control function, successes and failures will be detected at the precise moment they occur [16, 17].

1.1 Semantic Web Based on Ontologies for the Control of Promotion Indicators of Ecuadorian Universities

The simplest and best-known definition of ontology applied to the computing environment by Gruber [11], where an ontology is defined as an explicit specification of conceptualization. For AI, what exists is what can be represented. The ontology serves, in essence, to communicate. This utility applies at all levels: humans, machines, and computer systems and their design.

Ontologies are a step to try to reduce or eliminate terminological confusion and to achieve a shared understanding. Understanding or comprehension can function as a framework to unify different points of view and serve as a basis for a common language, as is the case when they serve to establish communication between people, with interoperability that is reusable and has consistency [8]. The construction of ontologies for the control of promotion indicators of Ecuadorian universities is based on universally applicable techniques, according to scholars of knowledge representation [9].

Ontologies reduce terminological and conceptual confusion by providing a unified framework within an organization. For this reason, an ontology-based semantic web for the control of promotion indicators of Ecuadorian universities facilitates understanding and communication between people with different needs and points of view originating in their own contexts [1]. This can be applied to two very specific utilities: to the different vocabulary used in different parts of an organization for the same concepts, on the one hand, and to the representation of the software system used in the organization, which will reflect that terminology.

An ontology for the control of promotion indicators of Ecuadorian universities facilitates the analysis of the contents that students use in their study schedules. So, this is part of the advantages of the use of ontologies in general (not only in the Semantic Web) because they facilitate the simultaneous interrogation of very different databases, allowing the free and independent development of these [1]. The ontology provides terminology to describe contents and axioms, specifying what the hierarchy, association, and general relationship relationships (following the terminology of the standard on monolingual thesaurus construction) of a given term are. In web portals, there is information that is usually indexed by the portal managers, who group them into large classes with subclasses. Other content is organized by tagging it for proper retrieval, or simply by metatags that identify the subject of the content [15].

The interest in using semantic web-based on ontologies for the control of promotion indicators of Ecuadorian universities lies in the possibility of reproducing or predicting a phenomenon [15]. For this reason, the semantic web based on ontologies has been used to predict the behavior of promotion indicators in Ecuadorian universities and, in particular, in the Peninsula State University of Santa Elena, in order to control the phenomenon of academic failure in the formation of professionals in higher education and, at the same time, this process is monitored, to intervene early with the causes that most affect the problem and thus raise the rigor and effectiveness of the teaching-educational process to increase the efficiency of the school cycle [12][12].

The use of an ontology-based semantic web is a crucial aspect from both a scientific and an applied point of view [15]. To the extent that it can be determined what it produces using semantic web based on ontologies for promotion indicator control, it will be easier to adapt to all Ecuadorian universities. In terms of application, understanding how to use a semantic web based on ontologies can be extremely beneficial in diagnostic and problem-solving processes [4].

Measuring the control of promotion indicators of Ecuadorian universities aims to bring together a varied set of knowledge disciplines with the objective of making clearer the nature of the processes based on the use of the semantic web. The semantic web for the control of promotion indicators will be performed on the basis of the use of AI tools, in particular, making use of ontologies, with the purpose of making changes in the ways of doing and allowing decision-making to be carried out when including actions to be carried out in the control of promotion indicators in the teaching-educational process, whose actions are mediated or achieved through the use of technologies that have specific learning objectives.

2 Materials and Methods

Different methods were used for the development of the tasks, foreseeing, as a result of their application, the fulfillment of the tasks and, consequently, the objective of this research.

The historical-logical method was used in the analysis of the bibliography and in the determination of the main manifestations, particularities, tendencies, and regularities of the measurement process of the indicators of promotion of the Educational Teaching Process (PDE) in student cohorts of higher education in Ecuador. Establishing a historical sequence of the process from its study allowed us to establish the conceptual and categorical framework of the same.

As a procedure of the theoretical methods, analysis-synthesis and induction-deduction were used in the interpretation of the documentary information to obtain the tendencies that characterize the behavior of the control of promotion indicators of the PDE in student cohorts of higher education in Ecuador. The empirical methods used were as follows:

- **Document review.** Its objective was to analyze the documentary information regarding the control of the indicators of the teaching-educational process, to allow the diagnosis of the same in student cohorts, of higher education in Ecuador.
- **Survey.** It was carried out among the teachers at the School of Systems and Telecommunications of the Peninsula de Santa Elena State University in Ecuador, whose objective was to learn about the problematic situation and make them participants in the solution thereof. It was applied to a total of 65 teachers.
- **Focus session.** It was used with the objective of pointing out elements heard orally, related to the control of the indicators of the teaching-educational process to diagnose and predict the behavior of such control in student cohorts of higher education in Ecuadorian universities. This instrument is applied in the School of Systems and Telecommunications of the Peninsula de Santa Elena State University in Ecuador, involving a total of 10 teachers.

3 Results and Discussions

The triangulation of the information collected resulted in the following conclusions:

1. The physical infrastructure available in Ecuadorian higher education, particularly at the Peninsula Santa Elena State University, demonstrates that it is possible to use a semantic web based on ontology to measure and contribute to the control of promotion indicators in student cohorts of the Educational Teaching Process (PDE).
2. Teachers from the referred university's Faculty of Systems and Telecommunications demonstrate favorable training and attitudes toward the use of semantic web-based ontology for the control of promotion indicators in PDE student cohorts.
3. There is a favorable environment to achieve innovation in the control of promotion indicators in student cohorts of the PDE. This could be verified through the instruments applied in the diagnosis carried out for this research in the Faculty of Systems and Telecommunications belonging to the Peninsula State University of Santa Elena.

The verification of the variables of the object made it possible to know:

1. The existence of an adequate technical endowment that exists in Ecuadorian higher education, to be able to use a semantic web based on ontologies as a technological tool for the control of the promotion indicators in the formation of professionals.
2. Actors of the teaching-educational process can intervene in a timely manner to reach the correct decision-making that contributes to making the correct control based on the promotion indicators that are measured in the student cohorts.
3. The application point of view in the production and use indicators were considered with the objective of obtaining satisfactory results to carry out the control of the promotion indicators.
4. The introduction of technological products that allow diagnosing, predicting, and intervening in the student cohorts of higher education in Ecuador will produce favorable changes in the Ecuadorian educational system, which will constitute a process of technological innovation in the training of professionals in the teaching-educational process from the perspective of optimization of time, resources, and scientific.

The analysis carried out through the instruments applied at the Peninsula de Santa Elena State University allows analyzing the behavior of the current state of the reality that needs to be transformed. The use of a semantic web based on ontology for the management of the control of the indicators of promotion of the Educational Teaching Process (PDE) in student cohorts of higher education in Ecuador will be carried out with the goal of mediating managers' interaction with information via means and/or technological tools. The purpose of this project is to mediate the interaction of managers with information, through technological means and/or tools, that allows opening communication channels and creates a relationship in which they learn how to diagnose, predict, and intervene in the formative process, specifically by analyzing the promotion indicators in different periods and with the purpose of seeking the good development of the educational process in society.

4 Conclusions

The evaluation of academic performance in student cohorts does not explain by itself its true dimension since it is influenced by different factors, there are diverse causal relationships, and different types of implications are produced, hence its complexity. However, the analysis of the quantitative dimension of these manifestations can be an initial and approximate point of reference, which provides valuable primary information to know the academic behavior of the students and of their transit through the system, evaluating-from one of the edges-what is happening in the formative process and its results, as well as the capacity of the system itself to achieve the permanence of the students, all of this supported by empirical analysis. Thus, we can conclude by stating that:

- The use of a semantic web based on ontology for the management of the control of the PDE promotion indicators in Ecuadorian higher education student cohorts can be viewed as a mechanism that allows correcting deviations of the promotion indicators through quantitative and qualitative indicators within the social context in which they are working, obtained from diagnoses made in the teaching-educational process, to achieve the fulfillment
- The importance of control in these terms of complexity lies in the impact it has on promotion indicators since its application can reverse or adapt the system of training objectives in the efficiency of the teaching-educational process.
- The goal is to mediate the teaching-educational process by ontology-based semantic web technologies and the control of promotion indicators in student cohorts, to diagnose, predict, and intervene on the major causes affecting the training process.

References

1. Altamirano, M., et al.: Usability and implementation of a semantic web for the website of Santa Elena Peninsula University. Rev. Am. J. Eng. Res. **7**(8), 52–61 (2018)
2. Amilburu, M.G., Gutiérrez, J.G.: Filosofía de la educación: Cuestiones de hoy y de siempre (2012)
3. Astorga, A. et al.: Educación de calidad para todos. Un asunto de derechos humanos. Red Iberoamericana de Investigación sobre Cambio y Eficacia Escolar (RINACE) (2007)
4. Benítez, N.G., et al.: La integración de las tecnologías de la información y las comunicaciones al control de indicadores de promoción en cohortes estudiantiles de la educación superior cubana. Rev. Ref. Pedag. **2**(1), 2–29 (2014)
5. Berners-Lee, T., et al.: The semantic web (2001). https://doi.org/10.1038/scientificamerican0501-34
6. Calleja, J.M.R.: Dirección y gestión educativa. Fundación Educativa Esumer (2004)
7. Codina, L., Rovira, C.: Web Semántica: visión global y análisis comparativo. Tendencias en (2006)
8. Curras, E.: Ontologías, taxonomía y tesauros: manual de construcción y uso (2005)
9. Decker, S., et al.: The semantic web: the roles of XML and RDF. IEEE Internet Comput. **4**(5), 63–73 (2000)
10. Gómez, D.: OASEARCH: Modelo de aplicación basado en web semántica para la búsqueda de objetos de aprendizaje mediante perfilado de consultas
11. Gruber, T.R.: Toward principles for the design of ontologies used for knowledge sharing. Int. J. Hum. - Comput. Stud. **43**(5–6), 907–928 (1995). https://doi.org/10.1006/ijhc.1995.1081

12. Hayes, D.: Leading technologies: a mid-term analysis of a longitudinal study into the integration of learning technologies into NSW public schools. In: Combined Proceedings of the Australian and New Zealand Associations for Research in Education (2003)
13. Juca Maldonado, F., Burgo Bencomo, O.B.: Blended learning as a model for universities use moodle. Investig. Tecnol. Innov. **8**, EE SE-Article, 27–34 (2016). https://doi.org/10.53591/iti.v8iEE.140
14. Laborde, J., et al.: Teaching process for learning probability analysis based on its application in real life cases with the programming language R and RStudio. Ecuadorian Sci. J. 3, 1 SE-Research Paper (2019). https://doi.org/10.46480/esj.3.1.22
15. Di Lucas, M.A., et al.: Ontología neutrosófica en la Web Semántica para disminuir la incertidumbre en la gestión de la información de los repositorios digitales. Rev. Asoc. Latinoam. Cien. Neutrosóficas. **9**(5), 53–62 (2019). ISSN 2574-1101
16. Marquès Graells, P., et al.: Algunas notas sobre el impacto de las TIC en la universidad. Educar (2001)
17. Martínez Rizo, F.: Estudio de la eficiencia en cohortes aparentes. ANUIES, Deserción, Rezago y Efic. Termin. en las IES. Propues. Metod. para su Estud. 244 (2001)
18. Tusa, F. et al.: The construction of an education of the good living from the study of the technologies of the communication and the information. Investig. Tecnol. Innov. **8**, 8 SE-Article, 97–106 (2016). https://doi.org/10.53591/iti.v8i8.141
19. Yépez, S.T., et al.: An approach to teacher training and ICT as a teaching and learning process. Ecuad. Sci. J. **4**, 1 SE-Research Paper (2020). https://doi.org/10.46480/esj.4.1.55

Sensitivity Analysis to the Evidence in Bayesian Networks to Analyze the Elements of Humanized Childbirth Care

Hector Lara Gavilanez(✉), Carlos Banguera Díaz, and Juan Carlos Cedeño Rodríguez

University of Guayaquil, Guayaquil, Ecuador
{hector.larag,carlos.banguerad,juan.cedenor}@ug.edu.ec

Abstract. The recognition of the plurinational, intercultural, pluricultural, and multiethnic condition of the country makes it necessary to seek coordination mechanisms between institutional health care and the traditional practices of the different communities of the country. Culturally appropriate childbirth care involves the care of the mother and the newborn and seeks to incorporate into its practice not only the classic characteristics of care in free position, but also a set of actions and attitudes aimed at increasing access by communities, people, and indigenous and Afro-Ecuadorian nationalities to institutional childbirth care, as well as other demands from various social movements that demand humanized childbirth care. For this reason, in the present work, a sensitivity analysis was carried out on the evidence in Bayesian Networks of the elements of humanized childbirth care from the perspective of health personnel, which is useful to verify the standards of the application of culturally appropriate childbirth in areas of support decision-making for continuous improvement in childbirth care processes.

Keywords: Sensitivity analysis · Bayesian Network · Humanized childbirth · Decision making · Delivery care · Maternal and newborn care

1 Introduction

Labor from another perspective of care, such as raising awareness of the health team based on managing the experiences of pregnant women in a sensitive manner and focusing on their emotional sphere and the adaptation of the institution, is considered in Latin America, childbirth humanized. From the perspective of health personnel, delivery with humanized characteristics will be carried out according to the needs of the pregnant woman.

Humanized childbirth requires an environment of tranquility and security where the role of health personnel is immersed. These personnel play a primordial role in relation to humanized childbirth. Due to their training, they must have an active listening focused on managing the emotions of the pregnant woman. Humanized childbirth is currently a model of childbirth care that considers the opinions, needs, and personal spheres of the pregnant woman and her family, in which the satisfaction of the woman in her spiritual, psychological, and social spheres prevails [4, 12].

© The Author(s), under exclusive license to Springer Nature Switzerland AG 2023
M. Zambrano Vizuete et al. (Eds.): RITAM 2021, LNNS 512, pp. 369–378, 2023.
https://doi.org/10.1007/978-3-031-11295-9_28

The author refers to the fact that the environment required for humanized childbirth must be warm, comfortable, and non-medicalized. In the intervention of the professional, it is proportional to the needs that occur, to avoid the appearance of adverse events due to the administration of medications or environmental stressors.

The humanized care of childbirth includes the care of the pregnant woman from the observation of a series of attributes to allow a satisfactory experience of labor and delivery, which prevents the pregnant woman from generating feelings of loss of autonomy, loneliness, misunderstanding, and perception of danger during or at the time of labor. In this process, different alternatives are carried out, such as maneuvers, positions, the implementation of music in childbirth, and even the adaptation of rooms for labor by providing comfort to the pregnant woman [15].

The accompaniment in labor constitutes a permanent education to understand the importance of humanized childbirth, and it is the health personnel, in particular the nursing personnel, who require continuous training so that this process is effective and pleasant for the pregnant woman. Humanized childbirth is a gradual and continuous process that acts in the transformation of the care model of childbirth through the behaviors and attitudes of the health team and family members. Permanent education constitutes a different practice that considers the ethics and benefits of the pregnant woman in humanized childbirth in an accurate way. By articulating scientific knowledge with the practices and rights of the pregnant woman, it generates and settles new knowledge according to personal and institutional needs for good maternal health [8, 25].

Regarding health personnel, and in particular nursing personnel, humanized childbirth consists of special care for the pregnant woman to convey confidence and security in the delivery process. In this regard, it should be noted that nursing has had the responsibility of care over time [1, 6, 14, 19, 22] where attitudes and care practices distinguish nursing staff from contributions from other disciplines [18].

Not being clear about this mission and the relevance of this task means not understanding the purpose of nursing as a profession. There are now more and more places for professionals to play a role in people's well-being, including in humanized childbirth, disease prevention, and health recovery. The most important thing is that people now know that professionals help people who are sick or at risk not only to cure them, but also to comfort them, take charge of the effects of the disease on them, and help them improve their abilities [2].

Humanism as a vital attitude based on an integrating conception of human values means holistically valuing the human being and the human condition. That is why humanism is related to generosity, compassion, and concern for the valuation of attributes and human relationships [7, 10]. When analyzing the meaning of the word "human" is to be compassionate, pious, tender, and understanding, and that the act of humanizing is the action of softening, softening, taking pity, according to Sanz [21], humanized childbirth carries with it the particularity that pregnant women are unique, different, and unrepeatable, and, therefore, their individualities must be considered.

On humanized childbirth, the World Health Organization (WHO) proposed recommended practices for the humanization of childbirth, where it is proposed to allow women to make decisions about their care, continuous monitoring and freedom of movement and position during labor and delivery, not perform electronic fetal monitoring, episiotomy, shaving and enema on a routine basis, allow fluid and food intake in labor, restrict the use of oxytocin, analgesia and anesthesia, and limit the use of caesarean section rate to 10–15%. They are inherent to all members of the health care team in labor and delivery care [13, 17].

The birth process represents one of the most paradoxical experiences that women experience. On the one hand, it creates life and constitutes for some the best thing that could happen after pregnancy, but at the same time, it can be one of the most painful events that she experiences, as it involves a deep psychosocial experience that puts her femininity and personal skills to the test., limits her functional abilities, mainly by reducing the control she can maintain over her own physiology [20, 16].

Therefore, in the present study, the elements of humanized childbirth care are highlighted from the perspective of health personnel, which are analyzed using a Bayesian Network, as an artificial intelligence technique frequently used in the medical area. Since the 1950s, AI techniques have been used and applied in various areas common to the daily performance of people, making them capable of helping, replacing, or simulating the actions or decisions made by individuals with certain characteristics. As one of its main areas of application, medicine can be particularly highlighted, given that AI achieved its greatest initial impact on it through expert systems and specifically through diagnostic systems [5]. The elements with the highest incidence in humanized childbirth care by health personnel are:

- Professional and companion care
- Personalized attention
- Mobilization and adoption of various labor positions
- Place of birth
- Analgesia, pain relief, and maternal satisfaction during childbirth
- Non-pharmacological methods of pain relief

From the perspective of health personnel, a Bayesian Network is built to analyze the incidence of the elements in humanized childbirth care from the perspective of health personnel. It is useful to know those that must frequently be applied to eradicate the stigmatization of women in a process as important as the birth of a new being, by also assuming cultural elements in the conception of the birth process in Cuban women. Obtaining results confirms the need to address the care of women in labor and delivery in a comprehensive manner by the entire health team, without the pre-establishment of protocols, treatments, care plans, education, and even responses. expected, built only from the cognitive and unilateral perspective of the professional.

Bayesian networks are a very popular type of probabilistic network [3, 24], which provides information on the conditional dependency and independence relationships between variables. This makes Bayesian networks good tools for representing knowledge in a small amount of space because the number of parameters needed is less. This artificial intelligence technique has been used to carry out classification tasks, in particular prediction tasks, even when there is only one variable contained in databases, whose variable acts as a classifier and in turn represents the problem to be predicted. While all the other variables are the data stored in the database, forming a data set, to treat them as cases in different processes [9]. In general, a Bayesian network seeks to model some phenomenon of interest, considering the random variables involved in the problem and the dependency structure between them. Thus, the main objective is to obtain the conditional probability distribution of the variables that are not known, mainly of some of them defined as response variables, based on the variables that are (evidential variables). Many times, the observable variables are fixed a priori. However, other times, they can be defined during the network modeling process itself.

2 Methodology

An analysis of sensitivity to evidence in Bayesian networks to understand how information introduced into the network produces effects or fundamental changes in the conditioned distribution of variable response, useful for health-care personnel decision-making for the improvement of the humanized birth process. The information on the elements to consider for an efficient humanized birth may vary in accordance with the characteristics of the mother, resulting in changes in the parameters considered in the conditional probability distribution, or in the specific values assigned to the evidence-based variables that occur in the elements related to the humanized birth and consider the patient's personal health.

The methodology to be used for the analysis of sensitivity to the evidence in Bayesian networks to analyze the elements of humanized childbirth care is that described by Kjaerulff and Madsen [11] for discrete Bayesian networks. This methodology analyzes the value of information (value of information analysis), step by step, to quantify changes in the distribution of the response variable by incorporating an additional variable into the network as evidence.

In this regard, entropy is used as a measure of uncertainty in the distribution of the response variable. The methodology is based on using this measure to determine an order of priority when incorporating new evidence. The proposed procedure consists of the variable X, as the variable of interest of the discrete Bayesian network (humanized delivery), and the variable Y, which characterizes the set of all the remaining variables (elements of humanized childbirth care) that are characterized by being discreet and are involved in the network (initially not observed), facilitating:

1. Determine the value function $V(X) = -H(X)$.
2. Determine $I(X; Y)$ for all unobserved Y.
3. Incorporate into the network as evidence (e) the variable Y that resulted in a higher $I(X; Y)$ in 2.
4. Determine the increase in $V(X) = -(H(X) - I(X; Y = y)) = -H(X \mid Y = y)$.
5. Recalculate $I(X; Y)$ for every $Y / = e$ and embedded in 3.

If the variable with the largest $I(X; Y)$ is not observable, it is considered the second largest. The variables with $I(X; Y) = 0$ do not need to be observed because they do not contribute information to the response variable. It should be noted that the value function $V(X) = - H(X)$ is proposed as a decision measure, that is, the negative value of the entropy, instead of the entropy directly.

To justify this choice, Kjaerulff and Madsen [11] propose considering the variable of interest X to be binary, with possible true and false states. The distribution of X corresponds to a Bernoulli distribution with parameter (p). Then Prob (X = true, X = false) = (p, 1 − p) and the maximum entropy will be reached at p = 0.5. However, the analysis is feasible by obtaining as much information about the distribution of the response variable as possible rather than reducing entropy (although the same goal is achieved in both cases), so we choose to work with the value function, which will be minimum when p = 0.5 and maximum at the extremes. Therefore, this methodology generates a priority order to incorporate evidential variables into a discrete Bayesian network.

3 Results and Discussions

To analyze the elements of care for humanized childbirth, the Bayesian Network is built (Fig. 1), which represents the elements of care for humanized childbirth through the nodes (X 1, … X 6) where; X1, corresponds to the care of professionals and companions, X2, corresponds to individualized care, X3, corresponds to the mobilization and adoption of different positions during labor, X4, corresponds to the position of childbirth, X5, corresponds to pain, analgesia, and maternal satisfaction during childbirth, and X6, corresponds to non-pharmacological methods of pain relief. The variable X7 is considered the response of interest, and we will work under the assumption that initially there are no evidential variables determined.

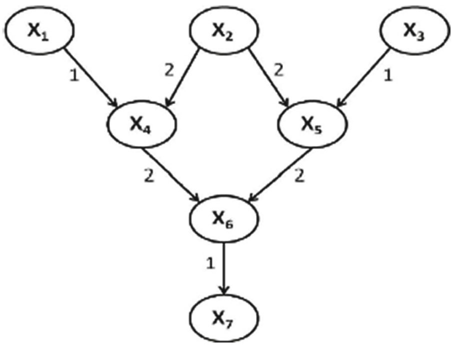

Fig. 1. Bayesian network with the elements of humanized childbirth care.

Steps 1 and 2 of the proposed methodology are calculated using Eq. 1 and the definition of entropy for the normal case, Eq. 2 and Normal Multivariate, Eq. 3, to obtain the differential entropy of the response variable X7, h(X7) = 3.7165, and the mutual information values for each of the non-evidential variables with the response variable.

$$\begin{aligned} I\ (X;Y) &= h\ (X|Y) \\ &= h\ (X|Y) \\ &= h\ (X)\ +\ h(Y)\ -\ h(X,Y) \end{aligned} \tag{1}$$

Fulfilling that:

$$h(X) = \frac{1}{2}\ln\left(2\pi e\sigma^2\right) \tag{2}$$

$$h(X_1, X_2, \ldots, X_2) = \frac{1}{2}\ln(2\pi e)^n|| \tag{3}$$

The calculations were made with the free distribution statistical software R [23], the results obtained are shown in Table 1.

Table 1. Sensitivity analysis by calculating I (X; Y) for all unobserved Y.

$Y - i$	$h(Y_{-i})$	$h(X7, Y_{-i})$	$I(X7; Y_{-i})$
x1	1.4190	5.1149	0.0207
x2	1.4990	4.6156	0.5201
x3	1.7656	5.4401	0.0422
X4	2.3149	5.4719	0.5596
x5	2.5703	5.5019	0.7850
X6	3.7064	5.4719	1.9510

From the Bayesian Network (Fig. 1), related to the seven elements of humanized childbirth care, connected as shown in the graph of Fig. 1, the joint distribution of X was obtained, corresponding to a multivalent normal distribution with parameters μ and Σ. From these parameters, it is obtained that the marginal distribution of the variable X7 corresponds to a normal distribution X7 ~ N (8, 99). This value shows that the associated distribution has a high variability, which is reflected in a high entropy that denotes the existence of uncertainty with the elements to be considered in humanized childbirth by health personnel.

To reduce this uncertainty, which affects the efficiency of the work of health personnel, it is necessary to look for the elements that are not considered for an effective humanized delivery, considering these elements as variables that have not been observable up to now. According to the results shown in Table 1, it is possible to obtain a priority order to decrease the entropy of X7 (humanized delivery). Variable X6 (non-pharmacological methods of pain relief) is the most important one for X7. Then variable X5 (pain, analgesia, and maternal satisfaction during childbirth) is the next one.

To show how the choice of the variable to be observed affects the decrease in the uncertainty of the response variable X7, the conditioned variance of X7 and its conditioned differential entropy were calculated, considering the assumed case that each of the evidential variables were observed. The result obtained is shown in Table 2.

The results obtained do not depend on the value that the observed variable takes, but only on the set of evidential variables considered. Given that the initial distribution of X7 (Humanized Parthian) is N (8, 99) with a differential entropy of h(X7) = 3.7166, it is clear that X6 is the most informative variable for X7. In fact, if this variable could be incorporated as evidence, the variance of X7 would decrease to 2 and its entropy to 1.77; that is, it would be enough to observe X6 for the problem to be solved with high precision. X1 and X3 are two of the variables that were used as evidence, but they don't seem to have a big impact on X7's uncertainty level on their own.

Table 2. Sensitivity analysis of X7 (Humanized childbirth) to the evidence.

$Y - i$	Var $(X7 \mid Y_{-i})$	h $(X7 \mid Y_{-i})$
x1	96	3.6960
x2	36	3.1967
x3	92	3.6744
X4	32.4	3.1565
x5	20.7	2.9317
X6 2 1.7655	3	1.7656

Therefore, to reduce uncertainty, it is assumed that variable X6 is not available, but that information is available for variable X5, which is the one that produces the next largest effect. If this variable is used as evidence in the network (step 3 of the proposed procedure), the new distribution of X7|X5 is N (8, 20.7), and from step 4 a conditioned differential entropy h(X7|X5) = 2.9317 is obtained, implying a significant reduction in uncertainty.

According to steps 5 and 6, respectively, of the proposed procedure, through X5 ϵ E and the conditional mutual information of the rest of the variables $Y - i$ with X7, is calculated. Calculate the Multivariate Normal distribution conditioned by the rest of the variables when propagating X5, that is, with a distribution of (X1, X2, X3, X4, X6, X7 | X5), and then carry out the calculations in a manner analogous to that performed for Table 1. The results obtained are shown in Table 3.

Table 3. Sensitivity analysis, conditioned on X5.

$Y - i$	$h(Y_{-i} \mid X5)$	$h(X7, Y_{-i} \mid X5)$	$I(X7; Y_{-i} \mid X5)$
x1	1.4190	4.2427	0.1080
x2	1.1636	3.7815	0.3138
x3	1.6540	4.5452	0.0405
X4	2.1598	4.1280	0.9634
X6	2.8806	4.6461	1.1662

The results shown in Table 3 show that the variable X6 is the one that allows the most significant reduction in the uncertainty of X7, but since it has been considered that this variable cannot be observed, the second most informative variable will be incorporated as evidence for X7, the variable X4. So, in step 3, after propagating X4, we get the new Var (x7|x5, x4) = 3, which means that we can now get a result with a high level of precision.

Finally, the conditioned differential entropy that has been obtained for X7 | X5, X4 is h (X7 | X5, X4) = 1.969. In Table 4, the new values of entropy and mutual information of the variables that are left as non-obvious are shown. On the one hand, the variables X1, X2, and X3 have mutual information values with X7 of zero, indicating that they are independent of X7 given X4 and X5, as shown in the DAG.

Table 4. Sensitivity analysis, conditioned on X4 and X5.

$Y-i$	h(Y_{-i} | X5, X4)	h(X7, Y_{-i} | X5, X4)	I(X7; Y_{-i} | X5, X4)
x1	1.2884	3.2566	0
x2	0.7644	2.7326	0
x3	1.6048	3.5730	0
X6	1.4190	3.1845	0.2028

4 Conclusions

- In the present work, an approach was made to the elements of humanized childbirth care related to health personnel and nursing personnel. According to the pregnant woman's personal and psychosocial characteristics, the distinguishing elements for a satisfactory and comfortable humanized childbirth were demonstrated.
- According to the identified elements, a Bayesian network is built to analyze the elements that carry greater weight and that cause greater satisfaction to pregnant women in humanized childbirth. For this purpose, a sensitivity analysis was carried out on the evidence of the elements identified for an effective humanized childbirth. A sensitivity analysis was carried out on the results obtained a priori through the Bayesian Network, where the elements of humanized childbirth care were interrelated from the perspective of health personnel.
- The result obtained is useful since it contributes to supporting decision-making by health personnel. The analysis of sensitivity to the evidence in Bayesian Networks constitutes a useful methodology to verify the standards of the application of culturally appropriate delivery and for the continuous improvement in delivery care processes to be considered in intercultural and humanized obstetric care from the perspective of health personnel.

References

1. Afanador, N.P.: El cuidado como objeto del conocimiento de enfermería. Av. en enfermería. **20**(1), 43–51 (2002)
2. Álvarez, C.V., García, J.H.V.: El cuidado en enfermería, perspectiva fenomenológica. Hacia la Promoción la Salud. **16**(2), 175–189 (2011)
3. Analytics, C.R.: About Bayesian belief networks. Cambridge Charles River Anal. (2004)
4. Benítez, N.G., et al.: Bayesian factor to estimate the presence of diarrheas in children by rotavirus in front of condition climatic. Ecuad. Sci. J. **5**, 2 SE-Research Paper (2021). https://doi.org/10.46480/esj.5.2.54
5. Bernal, E.A.: Sistema prototipo de entrenamiento pediatra para el proceso de adaptación neonatal. Tesis de Maestría en Ingeniería de Sistemas y Computación, Línea de (2014)
6. de Caballero, R., Medina, L.S.: Significado del cuidado de Enfermería desde la perspectiva de los profesionales de una institución hospitalaria de tercer nivel en Santafé de Bogotá, Colombia. Cult. los Cuid. año X, n^{o}19, 1er Semest. 2006; pp. 55–62 (2006)
7. Coello, A. et al.: Bayesian statistics to measure HIV mortality in the city of Guayaquil-Ecuador year 2017. Ecuad. Sci. J. **4**, 1 SE-Research Paper (2020). https://doi.org/10.46480/esj.4.1.48
8. Espinoza, D.C., et al.: Bayesian decision theory to find similarity of qualitative and quantitative variables used in maternal deaths. Ecuad. Sci. J. **3**, 2 SE-Research Paper (2019). https://doi.org/10.46480/esj.3.2.27
9. González Benítez, N., et al.: Estudio y selección de las técnicas de Inteligencia Artificial para el diagnóstico de enfermedades. Rev. Cienc. Médicas Pinar del Río. **22**(3), 131–141 (2018)
10. Izquierdo Medina, R.: La comunicación interpersonal en la familia con un miembro consumidor de sustancias ilícitas (2012)
11. Kjærulff, U.B., Madsen, A.L.: Probabilistic networks for practitioners-a guide to construction and analysis of Bayesian networks and influence diagrams. Department of Computer Science, Aalborg University. HUGIN Expert A/S (2006)
12. Laako, H.: Human rights in social movements: the case of autonomous midwives in Mexico. Rev. Mex. Cienc. Polit. Soc. **61**(227), 167–194 (2016). https://doi.org/10.1016/S0185-1918(16)30025-3
13. Lutz, L., Misol, S.: Parto Humanizado: Recopilación de folletos y artículos, Material de apoyo para los talleres de capacitación. Red Latinoamericana y del Caribe para la Humanización del Parto y el Nacimiento (RELACAHUPAN), Uruguay (2007). [citado 2014 Mayo 22]: 3–5
14. Malvárez, S.: El reto de cuidar en un mundo globalizado. Texto Context. **16**(3), 520–530 (2007)
15. de Maria Caceres-Manrique, F., Nieves-Cuervo, G.M.: Atención humanizada del parto. Diferencial según condición clínica y social de la materna. Rev. Colomb. Obstet. Ginecol. **68**(2), 128–134 (2017). https://doi.org/10.18597/rcog.3022
16. de Martins, J., et al.: Resignificando la humanización desde el cuidado en el curso de vivir humano. Rev. enferm. UERJ. 276–281 (2008)
17. Martis, R.: Apoyo continuo para las mujeres durante el parto. La Bibl. Salud Reprod. la OMS (2007)
18. McFarland, M., Leininger, M.: Teoría de la diversidad y de la universalidad de los cuidados culturales. Marrier A, Raile M. Model. y teorías en enfermería, 6th edn., pp. 472–493. Madrid MOSBY-Elsevier (2007)
19. Muñoz Hernández, Y., et al.: Significado de cuidado humanizado en egresadas de la facultad de enfermería. Rev. Repert. Med. y Cirugía. **18**(4), 246–250 (2009). https://doi.org/10.31260/repertmedcir.v18.n4.2009.561

20. Paulina Bravo, V., et al.: El cuidado percibido durante el proceso de parto: Una mirada desde las madres. Rev. Chil. Obstet. Ginecol. **73**(3), 179–184 (2008). https://doi.org/10.4067/s0717-75262008000300007
21. de Robles, F.C.: Diccionario español de sinónimos y antónimos. Aguilar SA (1995)
22. Salazar, M., Gutiérrez, A.: La responsabilidad de la Enfermería ante la indicación de transfundir sangre y hemoderivados: la experiencia en Costa Rica. Rev. Latinoam. Der. Méd. Medic. Leg. **96**(1), 1 (1995)
23. Team, R.C., et al.: R: a language and environment for statistical computing (2013)
24. Tumbaco, G.M.V., et al.: Statistical analysis to measure the linear by using a Bayesian approach. Ecuad. Sci. J. **4**, 1 SE-Research Paper (2020). https://doi.org/10.46480/esj.4.1.53
25. Vela Coral, G.P.: Percepción de la paciente sobre la atención del parto humanizado en el Servicio de Centro Obstétrico del Instituto Nacional Materno Perinatal durante el periodo marzo-abril de 2015 (2015)

Author Index

© The Editor(s) (if applicable) and The Author(s), under exclusive license
to Springer Nature Switzerland AG 2023

M. Zambrano Vizuete et al. (Eds.): RITAM 2021, LNNS 512, pp. 379–380, 2023.
https://doi.org/10.1007/978-3-031-11295-9